Understanding NAC Transcription Factor Mediated Signaling in the Regulation of Growth and Abiotic Stress Tolerance in Cowpea

A

Thesis

submitted for the degree of

DOCTOR OF PHILOSOPHY

by

RICHA SRIVASTAVA
(Roll No. 156106015)

supervised by

Prof. Lingaraj Sahoo

Department of Biosciences and Bioengineering
INDIAN INSTITUTE OF TECHNOLOGY GUWAHATI
Guwahati -781 039, India

October 2021

DECLARATION

This is to declare that the thesis entitled "***Understanding NAC Transcription Factor-Mediated Signaling in the Regulation of Growth and Abiotic Stress Tolerance in Cowpea,***" submitted to the Indian Institute of Technology Guwahati (IITG), for awarding the degree of Doctor of Philosophy, is a bonafide work carried out by me under the supervision of Prof. Lingaraj Sahoo. The content of this thesis, in whole or in parts, has not been submitted to any other university/institute for the award of any degree/diploma. I also wish to state that nothing in this report amounts to plagiarism to the best of my knowledge.

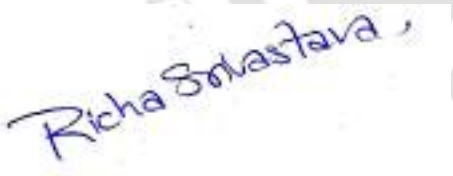

RICHA SRIVASTAVA
(Enrollment ID: 156106015)
Department of Biosciences and Bioengineering,
Indian Institute of Technology Guwahati,
Guwahati-781039, Assam, India.
Date: 09-10-2021

CERTIFICATE

This is to certify that the thesis entitled **" *Understanding NAC Transcription Factor-mediated Signaling in the Regulation of Growth and Abiotic-Stress Tolerance in Cowpea,*"** submitted by **RICHA SRIVASTAVA**, a Ph.D. student enrolled in the Department of Biosciences and Bioengineering (BSBE), Indian Institute of Technology Guwahati (**Enrollment ID: 156106015**), for the award of the degree of Doctor of Philosophy, is a record of an original research work carried out by her under my supervision and guidance. The thesis has fulfilled all requirements as per the institute's regulations and, in my opinion, comply the standards required for submission. The work embodied in the thesis has not been submitted to any other university/institute to award any degree or diploma.

Prof. Lingaraj Sahoo

(Ph.D. Supervisor)

Department of Biosciences and Bioengineering,

Indian Institute of Technology Guwahati,

Guwahati-781039, Assam, India.

Date: 08-06-2021

ACKNOWLEDGMENT

It has been a wondrous journey since I came to the DBT Support Facility, Centre of Excellence (COE) in IIT Guwahati. It was a privilege to work at such an eminent institute. Completing this thesis was impossible without the support and guidance of many people, and I am indebted to all of them. Firstly, I want to express my gratitude and appreciation for my Ph.D. Supervisor, Prof. Lingaraj Sahoo, for his extreme support and undue guidance. I thank him for believing in my credentials and encouraging the experimental ideas that helped me growing as a researcher. He maintained a peaceful work environment and surplus lab resources readily accessible to all. Besides, I would like to thank my doctoral committee, Dr. Biplab Bose (chairperson), Dr. Shankar P. Kanuajia, and Dr. Laishram B. Singh, for their insightful suggestions and critical questions that motivated me to polish my research. I express my sincere thanks to Dr. Siddharth S. Ghosh, our collaborator, for his generous support during my Ph.D. journey.

I convey my special thanks to Prof. Hiroyuki Koyama for allowing me to visit his prestigious lab in Japan that exposed me to a global perspective of research. His aspiration to serve the science community through novel contributions swayed me. I am grateful to Dr. Takua Enomoto and Dr. Ayan Sadhukan for guiding me through my experimental work during my stay there. I am obliged to Dr. Yasufumi Kobayashi and Dr. Moses Abiala, who shared their expertise while visiting our lab for post-doctoral research. I can never forget the support that I received from my lab members throughout the tenure of my Ph.D. I truly admire my seniors Dr. Sanjeev Kumar and Dr. Devender Kumar, who inspired me with their intellect to work meticulously. I owe my batchmates Muthu and Prabeen, whom I shared every phase of the Ph.D. journey, and my juniors Mahesh and Kiran, who assisted me in my work. I extend my acknowledgment to the Department of Biosciences and Bioengineering (BSBE), the faculty members, and the staff for their constant support. I am highly thankful to the Central Instrument Facility (CIF) of IITG for providing high-end facilities to improve my work quality.

I am lucky to have mentors like Dr. Ramesh V. Sonti, Dr. Shakunthala Pillai, and Dr. Shafaq Rasool earlier who recognized my potential and found the researcher in me. Needless to say, but this project would never have been a success without the blessings and encouragement of my parents, who constantly supported me in their best positive way. Lastly, I thank the almighty for providing me with the strength and wisdom to endure the difficulties of my work.

Richa Srivastava

SYNOPSIS

Abiotic stresses such as drought, salinity, and high temperatures impose severe threats to crop productivity, accounting for more than 50% of yield loss in food legumes. Stabilizing grain legume production is crucial to ensure food and nutritional security for a growing population. NAC transcription factors (TFs) have emerged as a powerful genetic engineering tool to manipulate central stress regulatory networks. However, the functional conservation of orthologous NAC members is unpredictable, hence not suitable for legume improvement. Besides, transcriptional reprogramming of stress signaling often comes with a yield penalty. Thus, it is important to identify native NAC stress factors that can harmonize the balance between growth and stress responses without trading off biomass growth and seed production. Many non-commercial genotypes of cowpea, a crucial food legume, are resilient to drought, heat, and nutrient limitation, hence ideal for exploring NAC-mediated signaling that unifies stress tolerance and growth *via* a beneficial cross-talk. However, no information on NAC genes is available for cowpea. This study performed a genome-wide analysis to annotate the cowpea NAC family (VuNAC) and cloned two potential genes from a drought-resilience genotype to improve abiotic stresses tolerance and growth simultaneously.

First, we carried out a comprehensive *in-silico* study to identify the NAC TF family in cowpea. We found around 130 VuNAC proteins classified into eight phylogenetic groups encoded by 90 distinct genes. Their promoter analysis and interactome study were performed to illuminate the regulation of the unique cowpea TF family. The data suggested their regulation by light, ABA, auxin, sugar, micronutrient, and stress-responsive transcription factors (MYB/WRKY), indicating their role in both stress and growth signaling. Out of 130, two potential genes, namely *VuNAC1* and *VuNAC2* exhibiting prominent induction by multiple stressors such as dehydration, osmotic stress, salinity, aluminum toxicity, heat, cold, and ABA, were chosen for functional characterization. Their subcellular localization in the nucleus, binding to MYC-like DNA motifs, expression of yeast-based reporter genes, and protein-protein interactions demonstrated the transactivation and dimerization abilities of the proteins. The heterologous expression in yeast conferred tolerance to multiple stresses, cell proliferation, longevity, and biomolecule composition *via* metabolic remodeling of vital energy-generating metabolic pathways such as biosynthesis of nucleotides, vitamin B complex, aspartate derivatives, methionine, glutathione, and carbohydrate. These studies anticipated the role of VuNAC1/2 TFs as a positive transcriptional regulator of abiotic stress signaling as well as

growth-associated processes. For further functional validation, these TFs were characterized by generating transgenic Arabidopsis in response to drought and salt stress under carbon sufficient and deficit conditions. The transgenic seedlings showed better growth under different stresses induced by PEG, NaCl, aluminum, cadmium, and H_2O_2. The transgenic plant also displayed adequate tolerance to dehydration and high salinity by modulating relative water content, preventing membrane damage, and producing ROS scavengers such as proline, ascorbate, and glutathione. Besides, the VuNAC1/2 TFs promoted plant growth by efficient carbon assimilation through improved photosynthetic activity and stomatal abundance and reduced ABA sensitivity that regulates dormancy and carbon starvation.

To establish the functional aspect of VuNAC1/2 in the native species, the genes were overexpressed and transiently silenced to find the gain- and loss-of-function phenotypes in a commercial cowpea variety. The gain of function manifested early seedling emergence, accelerated post-embryonic growth with increased biomass in transgenic seedlings. The mature plants exhibited improved physiological, agronomic, and stress-tolerance traits such as enhanced shoot and root biomass, nodule density, CO_2 assimilation rate, flower induction and pod development, and seed production. Whereas the loss of function by virus-induced gene silencing of the TFs impaired both vegetative growth and reproductive growth, indicating the indispensability of VuNAC1 and VuNAC2 for basal plant development. The transgenic plants exhibited improved tolerance to persistent drought, salinity, heat, and cold stress imposed during the terminal growth phase and retained the yield potential by maintaining tissue water-status, Na^+/K^+ ion-homeostasis, photosynthesis, membrane integrity, reducing power, and nutrient availability. The transcriptome analysis of the transgenic plants indicated activation of a large set of chloroplastic and chromosomal genes forming the photosynthetic components, stress-response machinery, carbohydrate metabolism, nutrient-uptake, cell division, meristem-initiation, cell-wall biogenesis, ABA, and auxin signaling, indicating consolidation of diverse plant processes.

In conclusion, unlike their orthologs, the bifunctional VuNAC1/2 TFs mediate favorable transcriptional cross-talk to regulate multiple stress tolerance and beneficial agronomic traits. These cowpea NAC genes are promising biotechnological tools for sustainable legume genetic engineering without yield trade-off.

CONTENT

LIST OF FIGURES

LIST OF TABLES

ABBREVIATIONS

ABA	Abscisic Acid
ABRE	ABA Responsive Element
ATAF	Arabidopsis Transcription Activation Factor
DAM	Differentially Accumulated Metabolite
DEG	Differentially Expressed Gene
DRE	Endoplasmic Reticulum
ER	Dehydration Responsive Element
GA	Gibberellic Acid
JA	Jasmonic Acid
NAC	NAM/ATAF1/2/CUC2
NACBS	NAC Binding Site
NLS	Nuclear Localisation Signal
PEG	Polyethylene Glycol
PLM	Preferentially Located Motif
ROS	Reactive Oxygen Species
SA	Salicylic Acid
SAM	Shoot Apical Meristem
SNAC	Stress-responsive NAC
TF	Transcription Factor
TAR	Transactivation Region
TMM	Transmembrane Motif
UTR	Un-translated Region
VuNAC	Vigna unguiculata NAC

1. INTRODUCTION

Climate change has adversely impacted agricultural productivity worldwide. Yields of major crops, particularly legumes, have risen steadily over the past decades. The loss caused by abiotic stresses currently accounts for 50-70%, whereas approximately 35% decline is estimated to be implicated by biotic constraints [1, 2]. The productivity is primarily circumvented by environmental constraints in the form of abiotic and biotic stresses [3, 4]. Pulses are usually cultivated under un-irrigated conditions on marginal drylands with low rainfall and poor soil fertility, therefore, more prone to climatic challenges like drought, high salinity, heat, and soil acidity. The degree of damage depends on the crop, genotype, stress duration, and the phenological stage. Terminal drought and heat stress are predominant in most legumes, reducing flowering and pod development by more than 70% [5]. Salinity is damaging throughout the life cycle, however, the effect is more prevalent in the reproductive stage, reducing metabolite partitioning, causing up to 80% yield loss when paired with insect/pest infestation [6]. Chilling temperature retards growth by impairing photosynthetic efficiency and inflicting oxidative injury. In addition, extreme conditions imposed by drought, salinity, heat, water-logging, heavy metals, and soil alkalinity may generate nutrition deficiency by declining the nutrient availability or impairing the plant's ability to assimilate the available nutrition [7].

As per the predicted elevation in atmospheric CO_2 level by 2050, future legume agriculture is at the stake of downturn [8]. Although the increase in CO_2 alone has been predicted to increase carbon gain in plants, the accompanying elevation in ambient temperatures, water scarcity, and evaporation is expected to cut down nutritional content and yield potential, risking the future legume agriculture [8, 9]. High temperatures reduce the yield by shortening the reproductive span of indeterminate crops and cause inadequate pollination, pollen sterility, and degenerated seed quality [10]. Frequent drought events decline the photosynthetic efficiency, impair reproductive organ development, and increase flower abortion [11]. The elevated atmospheric CO_2 reduces iron and zinc content in C3 legumes [12]. As the regional productivity depends on the local manifestation of interacting climatic factors, the yield of dry pea, chickpea, broad bean, and lentil is projected to decrease in tropical and sub-tropical countries like India, Ethiopia, Africa [13].

Currently, in Africa, the gap between the genetic yield of cowpea and farmer's yield is reported to be more than 300%, producing only 10–20% of the genetic potential [14]. In India,

a wide yield gap exists in the production of soybean (850-1320 kg/ha), groundnut (1180-2010 kg/ha), pigeon pea (550-770 kg/ha), and chickpea (610-1150 kg/ha) depending on the production zones, indicating an overall low production of major legumes [15]. In India, a wide yield gap exists in the production of soybean (850-1320 kg/ha), groundnut (1180-2010 kg/ha), pigeon pea (550-770 kg/ha), and chickpea (610-1150 kg/ha) depending on the production zones, indicating an overall low production of major legumes [15]. India is the largest producer as well as consumer of legumes contributing with 25-28% of the world's production (>73 mmt), about 33% acreage of cultivation (~85 million ha), and 27% of consumption, as per 2019-20 [16]. Ironically, India also is the largest importer of pulses to fulfill domestic demand, far from achieving self-sufficiency in pulse production [17]. The Food and Agricultural Organization (FAO) had declared 2016 as the "International Year of Pulses (IYP)," emphasizing the impact of pulses on human health, asking for immediate attention on these orphan crops to ensure food and nutritional security [14]. Despite breeding-assisted crop improvement, good agronomic practices, and efficient water and nutrient management, the decline in crop yield raises severe concerns. Biotechnological intervention is urgently needed to develop and adopt climate-resilient legume crops to overcome.

However, stress adaptation often comes with a yield penalty. The endeavor to survive adverse conditions customarily does not resonate with plant development and yield, compromising beneficial agronomic traits [18]. Many stress-tolerant varieties trade-off biomass growth and yield by a concomitant obstruction in cell division and photosynthesis to conserve energy and avoid metabolic burden during stress. The unwanted cross-talk of stress signaling with growth-associated pathways causes phenotypic aberrations, such as hormonal perturbations and metabolic imbalance [19]. Given the complexity of field stresses that often occur in combinatory events (heat and drought) or in succession (salinity followed by drought) to mount a unique concomitant effect, extrapolating the tolerance mechanisms against multiple or combined stress is much complicated [20, 21]. It is comprehensible that a number of traits need to be manipulated to exert stress tolerance against multiple stresses without compromising crop yield in the process. Molecular breeding in legumes has met with limited success in combining the polygenic genetic determinants of stress tolerance. Biotechnological intervention could therefore serve as the faster solution to overcome the technical shortcomings of breeding in achieving durable crop plasticity for a wide range of stress.

The overload of constitutively overexpressing stress machinery can be alleviated to some extent by employing stress-inducible expression. However, the strategy is only effective during intermittent or short-duration stress. Persistent and terminal field stresses may inflict detrimental effects that are beyond recovery. Approaches like gene-stacking involving co-expression of stress-responsive and growth-regulating genes to compensate for growth arrest are complex [22]. To combat multiple stress without growth trade-offs, it is necessary to identify stress regulators that integrate stress tolerance and growth improvement through a single gene. As yield is linearly related to plant fitness and proliferation, the ubiquitous expression of such a gene is desirable to translate stress adaptation into yield improvement.

Transcription factors (TFs) are the most versatile stress regulators and act as molecular switches to control diverse cellular processes, such as stress signaling, cell division, phase transitions, and development, unlike transporters, enzymes, chaperones, *etc.* [23]. As a central player in stress-signaling, transcription factors (TFs) have emerged as powerful tools to strengthen stress adaptation networks by manipulating the native stress regulatory network [24, 25]. NAC (NAM/ATAF1/2/CUC2) proteins belong to a stress-responsive TF family regulating multiple stresses and growth responses [26]. Mining suitable NAC genes from wild cowpea germplasms that are inherently drought-hardy and deciphering the underlying molecular mechanisms, is indispensable for the genetic improvement of cowpea and related legumes for improving the agronomic traits and stress resilience.

1.1 MOTIVATION AND OBJECTIVES

Stress adaptation often comes with a yield penalty. Mitigation efforts can be inadequate for the absolute restoration of biomass growth and reproductive recovery. Lack of strategic tools to develop stress tolerance overcoming the growth while trade-off defeats the purpose of sustainable crop improvement. To rescue and improve the existing agricultural yield potential, it is imperative to investigate the stress-associated physiological, biochemical, and metabolic signaling that overlap with the genetic controls contributed by the plant's developmental stages.

NAC transcription factors (TFs) have emerged as crucial regulators of plant growth and stress response. The members of the ATAF subgroup are the most studied NAC genes in several plant species due to their ability to regulate multiple stress nature [27-33]. Despite being a multifaceted stress regulator, ATAF-like TFs can cause growth retardation [27, 30]. However, the overexpressor phenotype and the targeted gene-set can vary in different species [27, 28]. The divergent C-terminal part of the NAC proteins, carrying the crucial regulatory signals that determine transcription activity (activation/repression), makes it hard to anticipate the function of orthologous members in legumes. As the regulatory signals of a NAC TF in non-native species are unpredictable, members from native or related species will be more suitable for legume improvement. Although, the information of legume NAC TFs is very limited, particularly for cowpea, which is emerging as a 21st-century food legume, rich in robust growth and nutritional traits, complying with sustainability principles [34]. Wild cowpea germplasms, being drought-hardy, serve as a suitable source for screening NAC/ATAF-mediated stress tolerance mechanisms and employ them to improve traits of susceptible cultivars [5]. This present study aims to identify novel NAC TFs from cowpea regulating multiple abiotic stresses harmonized with growth and yield *via* beneficial cross-talk or pleiotropy. The objectives of the doctoral research are listed below.

- Genome-wide analysis of NAC transcription factor family in cowpea (VuNAC TF)
- Cloning and characterization of promising TFs (VuNAC1 & VuNAC2) by heterologous expression in yeast system
- Functional characterization of the VuNAC TFs in Arabidopsis to understand growth and stress regulation
- Genetic manipulation of cowpea for multiple stress tolerance and improved agronomic traits through VuNAC-mediated regulation

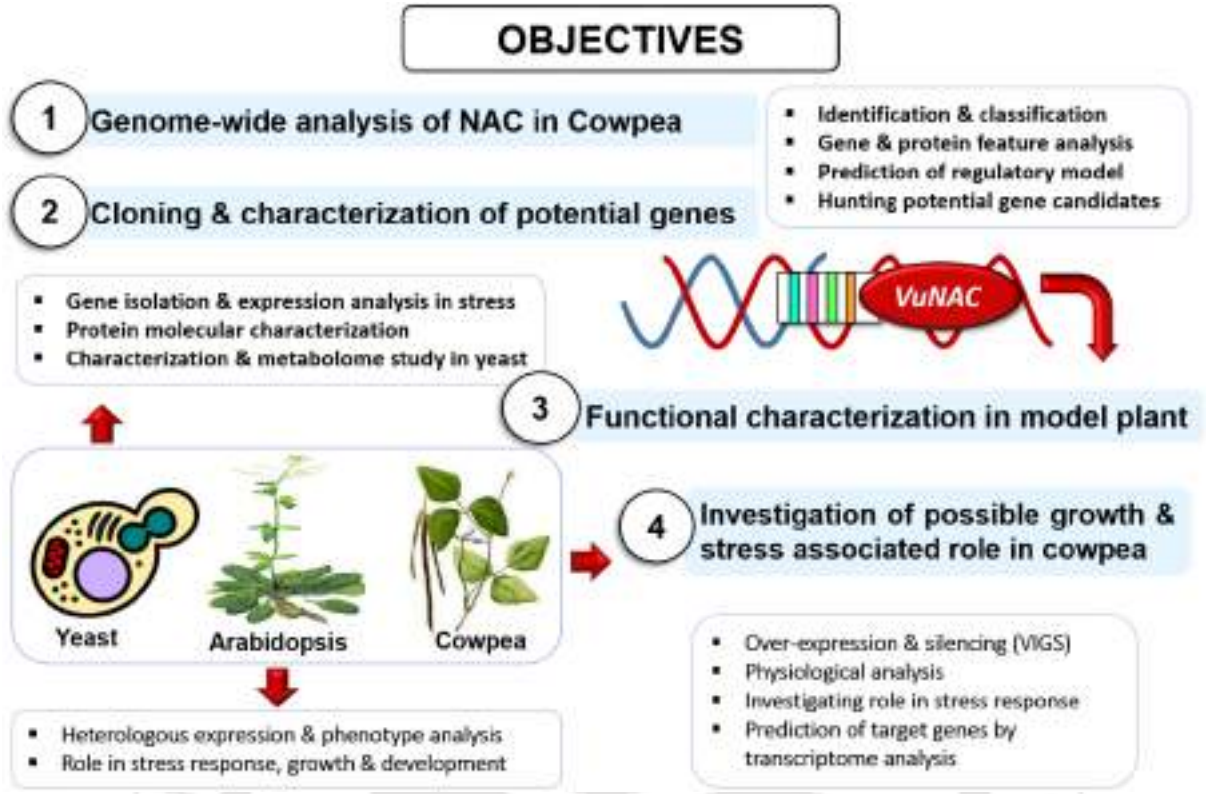

Fig. 1.1 Graphical illustration of experimental objectives

1.2 THESIS OUTLINE

Based on the above experimental objectives, the thesis is sectioned into five chapters. The brief outline of the content discussed in each chapter is given as follows:

- **CHAPTER 1**

This chapter discussed the major abiotic stresses declining the legume yield, the tolerance strategies to mitigate the damage, and the traits targeted for improving yield and stress resilience. The role and function of NAC TFs in various stress and developmental processes studied since the last decade and their shortcomings in the implication of legume crop improvement were critically reviewed. Additionally, drought-hardy cowpea germplasms were proposed as a suitable model for exploring native NAC-mediated signaling regulating both growth and stress responses to improve legume productivity.

- **CHAPTER 2**

This chapter discussed a genome-wide *in-silico* study to identify and annotate the NAC family in cowpea (VuNAC), analyzing the sequence and structure of the genes, proteins, and

promoters to identify the unique features and anticipate the functional role of the TF family in various growth, developmental, and stress signaling. The knowledge of orthologous species was used to predict the potential regulators, co-expressed and/or interacting partners of the VuNAC family.

- **CHAPTER 3**

In this chapter, two potential NAC TFs (VuNAC1 and VuNAC2), cloned from a drought-hardy genotype, were examined for their response in various abiotic stresses, followed by the molecular characterization of the proteins to assess their transcriptional activity. The TFs were heterologously expressed in the yeast system to anticipate their physiological and stress-responsive phenotypes. The metabolic alterations in the transgenic strains were studied to identify various nucleotides, vitamins, and amino acid biosynthetic pathways regulated by the VuNAC1/2 TFs.

- **CHAPTER 4**

This chapter is dedicated to exploring the possible roles of VuNAC1/2 TFs in growth and stress tolerance under nutrition-sufficient and deficit conditions in transgenic Arabidopsis. The constitutive expression of the TFs improved multiple stress tolerance as well as vegetative and reproductive growth in nutrition limiting conditions, indicating the better energy status of the transgenic lines. Moreover, the plants exhibited enhanced production of anti-oxidants, stomatal density, and photosynthetic activity, playing an essential role in stress recovery and plant fitness.

- **CHAPTER 5**

This chapter is focused on the functional characterization of the VuNAC1/2 TFs in native species by studying their gain/loss-of-phenotype in cowpea. The phenotype evaluation of the overexpressor transgenic lines and gene-silencing showed the indispensability of both the TFs for seedling development, biomass growth, floral transition, and pod yield of cowpea. The transgenic cowpea lines exhibited tolerance to persistent drought, salinity, heat, and cold stress. Subsequently, the transcriptome study revealed the potential gene targets expressed by VuNAC1/2 TFs integrating disparate plant processes.

The conclusions drawn from the above-mentioned experimental objectives and the future perspectives of the work are described at the end.

Chapter 1

CHAPTER 1

2. LITERATURE REVIEW

This chapter discussed strategies to improve legume yield by transcriptional reprogramming *via* NAC transcription factors, which are the bonafide regulators of growth and stress-signaling. Disparate signals converge at the molecular level that launch NAC-mediated transcriptional reprogramming to initiate a stress response. Like other stress regulators such as DREB, DDF1, bZIP, PYL, NAC-mediated stress adaptation often compromises beneficial agronomic traits causing yield-penalty. Their overexpression can cause metabolic and hormonal perturbations that exert growth-retardation by activating ABA-hypersensitivity, chloroplast-degradation, or carbon-starvation, resulting in growth arrest and decline in photosynthetic activity. In addition, due to the non-conserved C-terminal of NAC proteins, functional conservation of non-native members is unpredictable, limiting the utilization of well-studied orthologous NAC genes in legume crops. The co-occurrence of multiple stresses further perplexes the broad-range stress improvement of legume crops. To achieve a sustainable stress adaptation by overcoming the trade-offs, we need to understand the cross talk and growth checkpoints mediated by the stress-responsive gene candidate. Indeed, a versatile NAC member regulating both growth and stress signals simultaneously through benefitting and synergistic crosstalk in a harmonized mode, may hold the key for sustainable improvement of stress tolerance and plant yield. The successful manipulation of stress responses depends on controlled ABA homeostasis and strengthening carbon assimilation during various growth stages. Besides, improved light perception, metabolic adjustments, and their mobilization to pay the energy costs for growth and reproductive yield are other traits that need to be aimed for sustainable stress tolerance without compromised plant fitness.

Keywords: Cross-talk, cowpea, growth trade-off, legume improvement, multiple stress tolerance, NAC transcription factor

2. INTRODUCTION

Grain legumes are a vital component of sustainable agricultural practices that provide a cheap and affordable source of dietary protein essential for sustaining food and nutritional security [35]. They support non-leguminous crops and the environment by fixing the atmospheric nitrogen fixation to enrich the soil [36]. Dry seeds and green pods of grain legumes are a healthy source of high protein content, fiber, and certain functional components that can prevent cardiovascular disease risk factors and carcinogenic effects, whereas the forage legumes serve as livestock feed to support dairy and meat production for centuries [37]. Grain legumes offer immense opportunities to improve the socio-economy of subsistence farming by uplifting the livelihoods of farmers with small landholding. However, in India, where the diet habits are cereal-centric to satisfy hunger through calorie intake, pulses share only a small share of the staple food. Fewer market opportunities and consumer preference push the farmers to grow pulses on marginal agricultural lands with low rainfall and poor soil fertility, limiting the pulse yield. Poor storage and milling facilities cause additional risks, as unshelled pulses have a low shelf life. Consequently, pulses turned out neglected and underutilized in agriculture, despite their well-documented significance. Although, with a large section of the malnourished population, more attention needs to be sought on cultivating legumes to meet protein nourishment. Moreover, stress-resilient cultivars are required to achieve sustainable pulse production, ensuring food security.

Cowpea (*Vigna unguiculata* L. Walp) is a major grain legume of semi-arid regions of Sub-Saharan Africa, grown in every continent except Antarctica, and consumed as pulse seed, vegetable, fodder, and green manure, reflecting its desirability [3]. The protein content of the dry grain ranges from 23-32%, serving as a major source of cheap and quality protein for rural and urban dwellers [38]. Cowpea is a crop for challenging environments, usually grown in nutrient-poor soil, mainly under un-irrigated conditions [39]. Among grain legumes, cowpea is considered relatively more tolerant to drought, heat, and shade, thriving in annual rainfall of even 300 mm or less, owing to their deep taproot system, making it a choice for the dryland agriculture and hot habitats, though cultivars that flourish in the moist soil are also available [40]. Thus, emerging as the 21st-century legume, cowpea offers immense opportunities for socio-economic, agricultural, and environmental improvement complying with sustainability principles [41].

Although legume crops consistently encounter multiple stresses such as water deficit, extreme temperature, soil salinity, low pH, Al toxicity, and biotic stresses under field conditions, making it challenging to extrapolate the tolerance mechanisms for the combined effects [20]. Diverse breeding strategies have been employed but achieved only partial success due to the polygenic trait of the tolerance mechanism [42]. Moreover, the inherent adaptive endeavors of plants to survive these environmental challenges inevitably compromise their fitness and genetic yield due to hormonal and metabolic perturbations [19]. For instance, ABA is a key mediator of multiple stress responses, mainly desiccation tolerance, nevertheless, it can cause growth retardation by increasing seed dormancy, inhibiting shoot and flower bud induction. The hormonal homeostasis and signaling of stress hormones are controlled by transcription factors, imbalance in which invites unwanted growth phenotypes [43, 44]. To avoid salt-induced ion toxicity, plants restrict the ion uptake by maintaining the osmotic potential, cell turgor, and membrane stability by accumulating compatible solutes and anti-oxidants. Besides, plants sequester the excess ions in cell-vacuoles to perpetuate the cytosolic K^+/Na^+ ratio. Regardless, vital metabolic processes are hampered under high salinity, affecting cell expansion and division [45]. Harnessing these mechanisms to refine crop stress response does not necessarily synchronize with agronomic traits. For instance, overloading of *NCED/PYL* mediated ABA signaling perturbed the vegetative growth in barley [46]. The constitutive overexpression of *AtDREB1A* and *OsDREB1A* improved freezing and dehydration tolerance in transgenic Arabidopsis but showed severe growth retardation depending on the number of differentially expressed target genes [47]. Overexpression of salinity responsive gene *DDF1* caused dwarfism by attenuating gibberellin (GA) signaling in transgenic Arabidopsis [48].

Thus, a comprehensive understanding of the underlying molecular mechanism and its possible cross-talk with other physiological, biochemical and metabolic processes is mandatory for sustainable stress development of food crops. We need a unified mechanism to improve stress tolerance and agronomic traits of cowpea. However, the greatest challenge is finding suitable candidate genes that simultaneously improve stress responses and growth through favorable cross-talk or pleiotropic effect. The key to sustainable stress tolerance by overcoming the tolerance/growth trade-off lies in the genetic diversity of the varieties inhabiting harsh geography. Crops encounter adverse situations by exercising plasticity as part of their genetic and/or epigenetic makeup. Some wild genotypes can thrive in the drier habitats receiving annual rainfall of even less than 300 mm, and tolerate much hotter temperatures than maize

[40]. Genes involved in growth and yield sustenance in adverse conditions are usually not present in the farmed cultivars owing to their loss during domestication, germplasm improvement, and linkage drag when produced in optimal environments. Thus, efforts are being made to make the hardy crop even tougher to deliver better yield under harsh conditions by unifying the heat and drought tolerant attributes of wild relatives with the agronomic traits of cultivated genotypes. Using the natural variations holds great promise to mine specific causal genes and associated molecular, cellular, and physiological processes that are integral to environmental adaptation and yield acclimation. As the degree of the stress damage and the plant's ability to cope, adapt, and recover depends on the plant growth stages and fitness, identifying the genes determining trait of interests such as forage growth, vigor, biomass, and water-use efficiency, together with multiple stress-tolerance, brings insights into novel stress-regulatory mechanisms. Identifying stress regulators through reverse genetics approaches by testing their roles in regulating growth-associated traits through overexpression, knockout/knockdown in model crop species, can be a helpful strategy [49]. Transferring such genes to modern cultivars and related species by biotechnological means can uplift yield, as well as stress tolerance.

Plants use intricate molecular networks to fight unfavorable situations. The secondary stress signals from diverse stresses such as ABA, reactive oxidative species (ROS), nitrogen oxide (NO), polyamines, phytochrome B, and Ca^{2+} ions synergistically or antagonistically to transduce the signal towards the downstream effectors, *i.e.*, transcription factors (TFs). TFs are DNA-binding proteins that launch stress-signaling by activating or repressing the expression of enzymes, ion channels, hormones, kinase cascades, TFs, and other stress-responsive genes, in a specific, temporal and spatial manner to launch stress-response [50]. Being the central molecular switches of cell fates, developmental programs, and responses to various biotic and abiotic stresses, TFs have emerged as potential candidates for developing stress-resilient crops [23, 24]. Genetic engineering of stress-associated TFs offers smart options to develop climate-smart food crops [25, 51]. The discovery of more than 50 stress-responsive TF families in plants has opened up new opportunities for crop manipulation [52]. NAC (NAM/ATAF1/2/CUC2) proteins belong to one such family implicated in multiple abiotic and biotic stress, senescence, and growth processes [53]. TFs offer considerable opportunities to generate complex and multiple stress tolerance [26].

2.1 NAC transcription factor: a potential integrator of stress tolerance, growth, and yield traits in cowpea

Plant genomes dedicate a large portion of the genome (~7%) to encode TF proteins. Extensive sequencing of the cDNA pool and genomes revealed that legumes encode more than 2,000 TFs per genome [54]. To date, more than 80 stress-responsive TF families have been identified, such as AP2/ERF, bZIP, NAC, CBF/DREB, MYB, MYC, C2H2, WRKY, *etc.*, each having a dedicated regulatory binding site to recognize their targets and perceive stress signal to manipulate the expression of specific target gene-clusters. Despite their seminal participation in growth, differentiation, development, and central role in stress-signaling, less than 1% of TFs have been characterized genetically, even in model crops [54].

The last two decades have seen a resurgence of plant stress-responsive TF families, claiming immense potential for crop improvement [51]. NAC (ATAF1/NAM/CUC2) is one of the key families, which has been identified and ascribed for improved stress responses in several edible crops [55]. Mainly, the ATAF-like members have been widely studied in Arabidopsis, rice, soybean, wheat, and other crops to confer tolerance to various abiotic and biotic stresses and influence vital developmental processes [27, 30, 56-58]. Despite their seminal role, the function of NAC TFs is still unknown in many important orphan legumes like cowpea, pigeon pea, mung bean, chickpea, *etc*. To date, no Cowpea NAC gene has been reported and functionally annotated. Identification and functional characterization of NAC family members in this valuable drought-hardy legume crop could unravel novel mechanisms for multiple stress response, growth, and development. The knowledge can be of immense importance for translational application in legumes for abiotic stress tolerance and yield improvement. The recent availability of a comprehensive draft genome of cowpea has enabled the investigation of the NAC family in this crop [59].

2.1.1 NAC: a multifarious TF family regulating basal developmental as well as stress-responses in plants

2.1.1.1 Evolutionary history and identification of NAC family

NAC is one of the largest and diverse plant-specific families. The acronym NAC was derived from the earliest three genes carrying the unique domain, *no apical meristem* (*NAM*), *Arabidopsis transcription activation factor 1,2* (*ATAF1,2*), and *cup-shaped cotyledon 2* (*CUC2*), identified in petunia and Arabidopsis, primarily involved in the formation of shoot

apical meristem (SAM) and post-embryonic organ separation [60, 61]. Although the primary purpose of the emergence of the NAC family was speculated to support plant life in terrestrial form, their diverse nature allows the activation/repression of a diverse cluster of downstream genes regulating complex and interlinked cellular functions, including stress signaling, thus establishing them as critical stress-responsive plant TF family.

The genome sequencing of plant species revealed that the NAC family was exclusively present in the land plants, including monocots, eudicots, mosses, and conifers. The subsequent identification of NAC genes in streptophytic green algae consisting of both fresh water and terrestrial members, suggested that the origination of NAC TFs predates the emergence of land plants [62]. The evolutionary studied revealed that NAC genes were originated 725-1200 million years ago (mya) from the diversification pre-vascular streptophyte ancestors, which further evolved in vascular plants in two discrete steps. The first expansion of the NAC family occurred 470 mya, intended to adapt the land plants, *i.e.*, bryophytes, to facilitate the transition from aquatic to land habitat by activating DNA damage responses, differentiation of cells involved in water-conduction and mechanical support in vascular tissues, and formation of secondary cell-wall formation [63]. The second major expansion is thought to occur during the early Cretaceous period parallel with the evolution of flowers in angiosperms [64], rising one of the largest plant TF family expanded through duplication events to give redundant members. Phylogenetic analyses revealed both the conserved and lineage-specific NAC subfamilies in angiosperms, proposing two evolutionary pathways, the first ancient duplication occurred before the divergence of dicots and monocots, followed by second recent duplications in a particular lineage to give distinct features between monocots and dicots, as well as, among NAC subfamilies [65, 66]. The duplication of NAC TFs and high evolutionary rates drove the versatile function of the family, conferring beneficial characteristics to provide fitness advantage in higher complex plants.

The recent advancements in the sequencing of plant genomes facilitated genome-wide research of NAC families in several cereals, vegetables, fruits, and legumes, as listed in Table 2.1. A large number of NAC members have been reported in several model plants and legumes, such as Arabidopsis (117) [67], rice (151) [68], tobacco (152) [69], barrel clover (97) [70], soybean (180) [71], common bean (106) [72], chickpea (180) [73], pigeon pea (88) [74], peanut (132) [75], maize (152) [76], wheat (488) [77], millet (147) [78], *etc*.

Table 2.1 NAC gene distribution in model plants, legumes, cereals, fruits, and vegetable

Common name	Species	Number of NAC genes	Genome size (Mb)	Chromosome number	Category	Reference
Arabidopsis	*Arabidopsis thaliana*	117	135	5	Model plant	[67]
Rice	*Oryza sativa*	151	389	12	Model plant	[68]
Tobacco	*Nicotiana tabacum*	152	450	12	Model plant	[69]
Barrel clover	*Medicago truncatula*	97	390	8	Model plant	[70]
Soybean	*Glycine max*	180	1150	20	Grain legume	[71]
Common bean	*Phaseolus vulgaris*	106	587	11	Grain legume	[72]
Chickpea	*Cicer arietinum*	180	738	16	Grain legume	[73]
Pigeon bean	*Cajanus cajan*	88	852	22	Grain legume	[74]
Peanut	*Arachis hypogaea*	132	2556	20	Grain legume	[75]
Mung bean*	*Vigna radiata*	82	579	22	Grain legume	[52]
Adzuki bean*	*Vigna angularis*	115	500	11	Grain legume	[52]
Maize	*Zea mays*	152	2365	10	Cereal	[76]
Barley	*Hordeum vulgare*	167	5100	7	Cereal	[79]
Sorghum	*Sorghum bicolor*	145	730	10	Cereal	[80]
Wheat	*Triticum aestivum*	488	16000	46	Cereal	[77]
Foxtail millet	*Setaria italica*	147	490	18	Cereal	[78]
Proso millet	*Panicum miliaceum*	151	923	18	Cereal	[81]
Buck wheat	*Fagopyrum tataricum*	80	489	16	Cereal	[82]
Chinese cabbage	*Brassica rapa*	204	405	20	Vegetable	[83]
Cassava	*Manihot esculenta*	96	750	36	Vegetable	[84]
Potato	*Solanum tuberosum*	110	840	12	Vegetable	[85]
Radish	*Raphanus sativus*	172	387	18	Vegetable	[86]
Tomato	*Solanum lycopersicum*	104	950	12	Fruit	[87]
Water melon	*Citrullus lanatus*	80	425	22	Fruit	[88]
Cucumber	*Cucumis sativus*	91	454	12	Fruit	[89]
Grape vine	*Vitis vinifera*	74	500	19	Fruit	[88]
Banana	*Musa acuminate*	181	523	11	Fruit	[90]
Apple	*Malus domestica*	180	750	17	Fruit	[91]

*Note: NAC family in these crops has not been annotated yet. The number of genes was predicted by sequence study.

2.1.1.2 Phylogeny and classification of the NAC TFs

Earlier, Zhu *et al.* (2011) performed the clustering analyses of nine different plant lineages of land plants to categorize NAC TFs into 21 subfamilies, out of which 15 were found exclusively in angiosperms consisting of more than 100 members per species. According to the most recent phylogenetic classification of NAC TFs in angiosperms, including 24 different species, the proteins were re-categorized into six major orthologous groups (Group I-VI) [66], as shown in Fig. 2.1. Group I is considered the basal group consisting of VND/SND members involved in xylem development essential for water conduction and mechanical support. Group II consists of NAM/CUC members involved in developmental pathways like organ separation, SAM formation, and other ethylene and auxin-associated pathways. Group III accommodates TMM (transmembrane motif) proteins anchored to bio-membranes, especially in the endoplasmic reticulum (ER) membrane. Group IV proteins are involved in diverse

developmental processes in Arabidopsis, such as flowering time (*ANAC034/LOV1*), cell division (*FEZ*), and longevity (*JUB1*). Group V consists TFs that are mainly involved in stress responses (SNAC) and senescence. The last Group VI contains species-specific proteins evolved by neo- and/or sub-functionalization *via* whole-genome duplication (WGD) events.

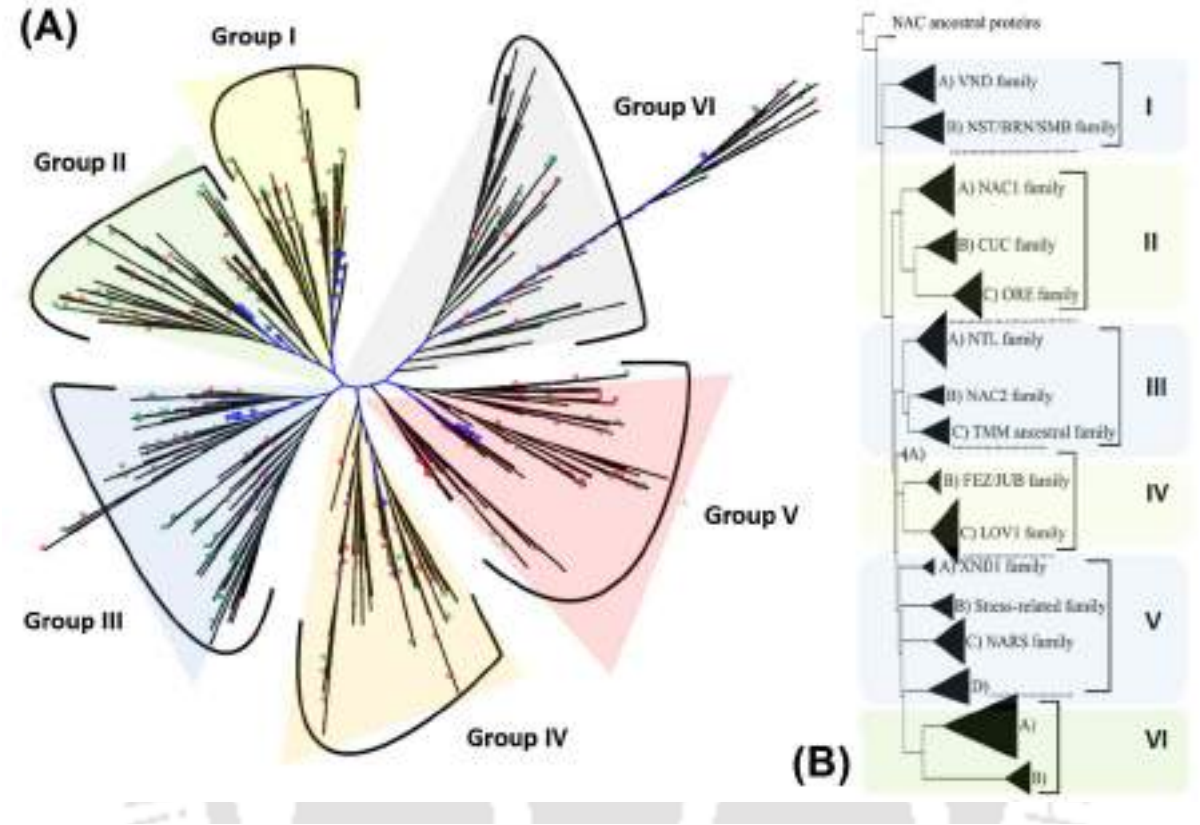

Fig. 2.1 Evolutionary and phylogenetic classification of NAC TF. (A) The unrooted phylogenetic tree derived from the alignment of the 2106 NAC domains from 24 plant species clustered into six major groups. **(B)** Schematic depiction of the NAC family classification into six groups and 16 subgroups (graphic adapted from Pereira-Santana *et al.*, 2015.

2.1.1.3 NAC domains structure

A typical NAC protein carries a tightly conserved N-terminal domain (~150 amino acid) which is further divided into five subdomains (A-E) responsible for DNA-binding and dimerization, and a variable C-terminal transcriptional activation region (TAR), playing either activator or repressor, as shown in Fig. 2.2 [92, 93]. Regarding the additional features, the N-terminal contains a monopartite or bipartite lysine-rich nuclear localization signal (NLS), and the C-terminal of ~10% NAC proteins exhibit a transmembrane motif (TMM) or even a protein-binding domain, crucial for interaction with other co-regulatory partners and stress responses [94, 95]. Subdomain A is involved in dimerization. The subdomains C and D are highly conserved and rich in positively charged amino acid residues, and involved in DNA

binding and nuclear shuttling. However, the subdomain B and E exhibit less conservation, probably involved in developmental regulation in a tissue-specific manner, indicating the variable degree of conservation within the conserved N-terminal domain. Whereas the C-terminal is characterized by the frequent occurrence of amino acid repeats and regions rich in serine, threonine, proline, and glutamine. [53, 96].

The X-ray crystallography of Arabidopsis ANAC revealed the first three-dimensional (3D) structure of NAC proteins, serving as a template to study NAC-mediated molecular interactions (Fig. 2.2). The N-terminal DNA-binding domain (DBD) lacks the classical helix-turn-helix motif. It possesses a unique fold consisting of seven twisted anti-parallel β-sheet surrounded by few α-helical elements [97]. Mutation studies showed that two areas with positive charged Lys123 and Lys126 (positioned between β4 and β5 in subdomain D) and Lys79, Arg85, and Arg88 (residing between β1 and β2 in subdomain C), are biochemically crucial for ANAC DNA binding. Interestingly, Arg88 is conserved in all NAC proteins. The functional dimer involving the N-terminal DBDs of two NAC proteins, folds into a butterfly-like shape, also sharing structural similarity with ANAC019 and rice NAC TF (SNAC1) [96, 98]. The dimerization is modulated by Leu14–Thr23 and Glu26–Tyr31 residues in subdomain A, forming a short anti-parallel β-sheet at the dimer interface stabilized by salt bridges formed by Arg19 and Glu26. In contrast, the TRR regions of the C-terminal part containing low complexity sequences failed to self-fold into an ordered 3D structure with a propensity for flexible protein segments.

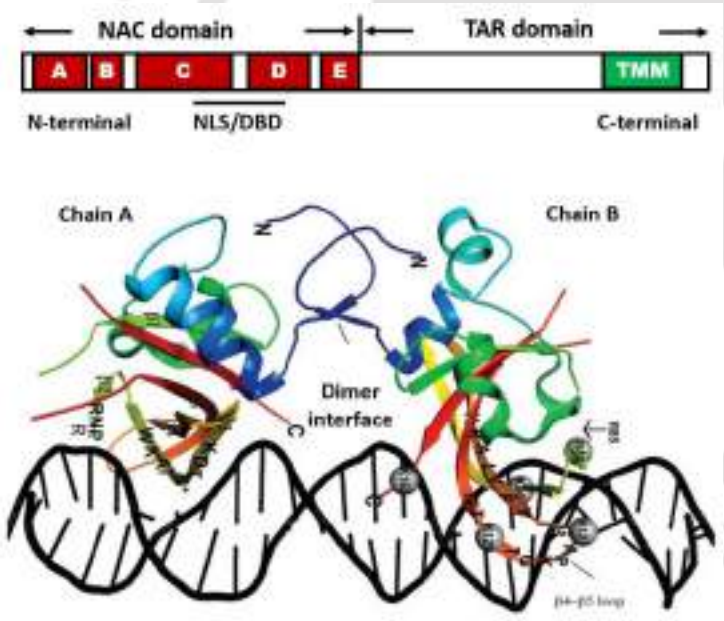

Fig. 2.2 NAC protein structure. (A) Five subdomains (A-E) at the N-terminal part and TAR region in the C-terminal part. **(B)** The butterfly-like 3D structure of NAC dimer binding to DNA major groove using the 'WKATGtDK' DBD and in the β4 and β5 loop (graphic adapted from Welner *et al.*, 2016 with printable license).

A DBD sequence WKATGtDK is conserved in subdomain C of most of the NAC TFs and binds DNA major groove, responsible for the specificity of NAC proteins, whereas other portions enhance the TF binding [99]. This sequence specifically recognizes CGT(G/A) core present in the target gene promoters of many stress-responsive NAC TFs such as *ANAC019/055/072*, *ANAC092*, and *ANAC069*, also known as NAC binding Sites (NACBS), however variation in preferential NACBS exists [100]. The DBD in some NAC proteins contains highly hydrophobic NAC Repression Domains (NARDs), consisting of the residue 'LVFY' imposing structural interference for DNA binding or nuclear import. They suppress the transcriptional activity of NAC proteins, such as GmNAC20 and TaNAC69, and even members of other TF families like Dof, WRKY, and AP2/DREB [101]. However, the repressive action of NARD can be compensated by the C-terminal activation domains. Thus, NAC TFs can have dual properties causing the same protein to manifest opposite behavior depending on the circumstances (*AtNAP/OsNAP*, *ANAC083/VNI2*, *ONAC20*, and *ONAC26*), or either as an activator (*ATAF1*, *OsNAC5*, and *TaNAC29*) or repressor (*CBNAC/NTL9* and *ANAC050*).

2.1.1.4 Diverse functions of the multifaceted NAC: one gene many functions

The first comprehensive review of NAC TFs was published in 2005 [92]. Several reports have evident the pivotal role of NAC TFs in plant growth and stress response modulated through hormone signaling [26, 51, 102, 103]. Being diverse in nature, they are extensively involved in transcriptional reprogramming of distinct plant processes by serving as both activators and repressors of transcription (Fig. 2.3A), orchestrating cascades of gene regulatory networks. The growth and developmental processes governed by NAC TFs includes seed germination and morphogenesis [104, 105], formation of shoot apical meristem (SAM) [106], cell division, expansion and cell-cycle [107, 108], programmed cell death (PCD), senescence [109-111], xylem vessel and wood formation [95, 112, 113], secondary wall synthesis [114, 115], lateral root development [116], organ development, and boundary maintenance [117], flowering and floral organ development [118], fiber development [114, 119], and nutrient remobilization from leaves to seeds [120]. Also, NAC genes intimately regulate plant adaptation to diverse pathogen infection [121, 122], and various environmental stresses, such as drought [31, 123, 124], salinity [28, 125], cold [126], heat [127], oxidative stress [128], water-logging [129], aluminum stress [130, 131], boron deficiency [132], high light, phosphate deprivation [133, 134], and hormone signaling [50]. Furthermore, the NAC TFs also regulate intricate processes like miRNA-mediated cleavage of mRNAs [125, 135] and ubiquitin-

dependent proteolysis [136]. Whether the role of NAC is limited to stress and plant development is still debatable.

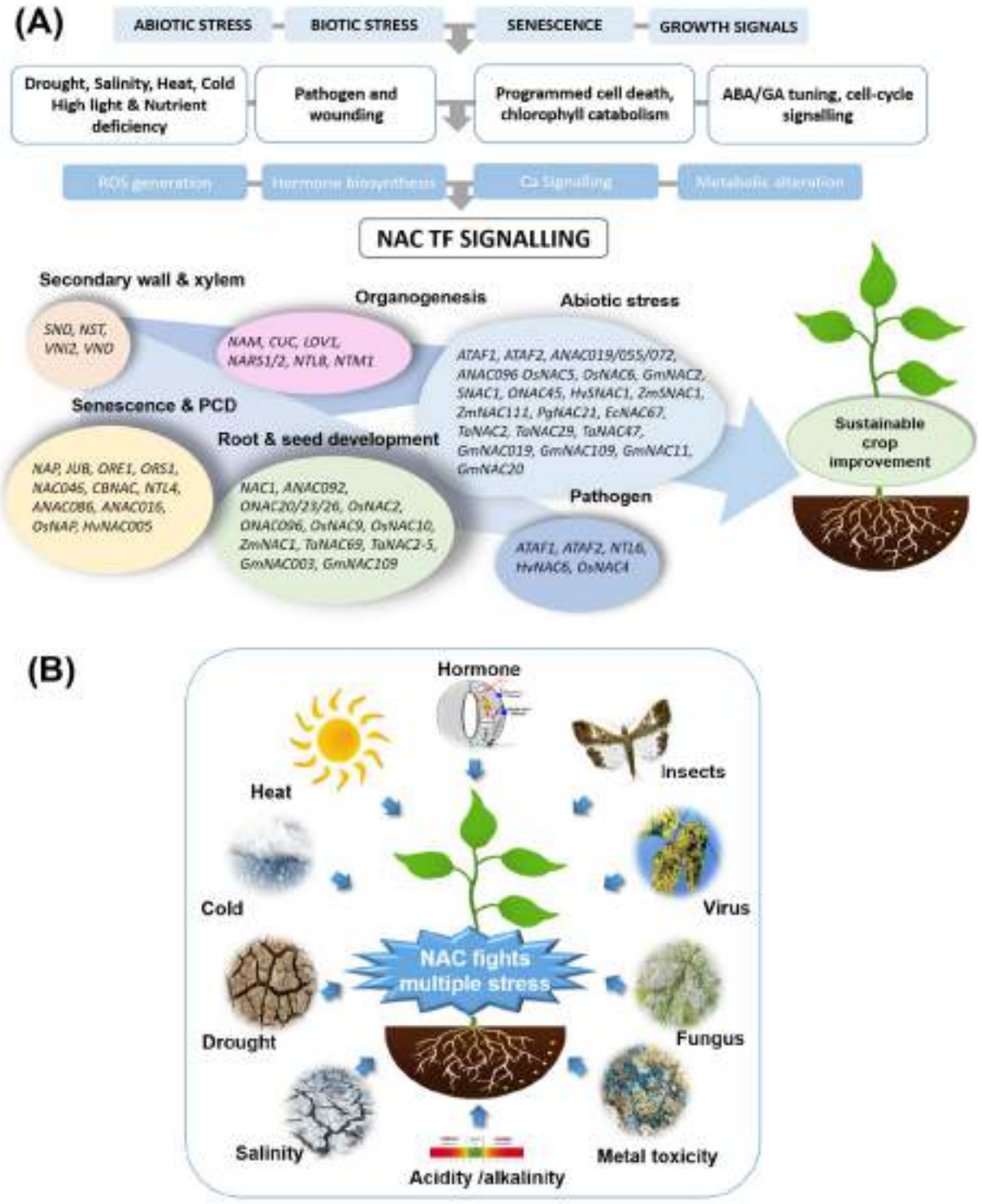

Fig. 2.3 Multifaceted nature of NAC TFs. (A) Overlapping NAC-mediated signaling in abiotic/biotic stress, senescence, and growth. **(B)** Single ATAF-like NAC gene-many functions.

Moreover, a single NAC TF can serve multiple conglomerate processes. For instance, ATAF1, a *bona fide* regulator of abiotic and biotic stress, controls chloroplast maintenance, senescence cascades, ABA biosynthesis, and plant development mediated by *SnRK1* signaling [27, 28, 56, 57]. Similarly, a rice NAC TF *Os04g0477300* regulates three different processes, such as biotic stress, senescence, and phosphate and boron deficiency [132, 133]. Thus, the NAC gene can control several different functions and mediate the cross-talk between different signaling pathways such as abiotic and biotic stress response, senescence, metabolic and developmental programs, as depicted in Fig. 2.3B.

2.1.2 NAC gene expression in the developmental and stress responses in legume crops

NAC TFs were primarily known to regulate basal plant development. In the last decade, their involvement in stress responses and other metabolisms has been uncovered. The bioinformatic analysis and expression profile of several species, including Arabidopsis, rice, and other cereals and legumes, revealed that a significant proportion of the NAC family (~20-25%) are extensively involved in the regulation of diverse biotic and abiotic stresses such as drought, salinity, cold, high temperature, oxidative stress, *etc*. through a complex pathway. The phylogenetic analysis indicated that stress-responsive NAC TFs exist in large homologous groups, which are somewhat functionally redundant, exhibiting sequence conservation in the NAC domain. Such members are expressed differentially under adverse conditions and are tightly regulated at transcriptional levels. Nevertheless, they also exhibit preferential tissue-specific and/or temporal expression at various life cycle stages, or development, indicating an overlapping regulation of NAC TFs in stress and growth.

For instance, barrel clover (*Medicago truncatula*), close to most food and forage legumes, serves as a genomic and functional research model. The genome-wide expression study revealed that 40 out 97 *MtNAC* genes were expressed in all the six tissue, roots, nodules, blades, buds, pods, and flowers. In contrast, nine genes were preferentially expressed in roots, 13 genes in pods, and 3 genes in buds. Moreover, out of the 44 stress-induced genes, *17 MtNAC* genes were highly expressed in all five stresses, *i.e.*, drought, salt, ABA, cold and freezing stress. However, 33 *MtNAC* genes showed exclusive expression in drought, 33 genes in the cold, 36 genes in freezing stress, and 6, 8, and 8 *MtNAC* repressed in the respective stresses [70]. In soybean (*Glycine max*), 28 out of the 139 *GmNAC* genes were predicted to be drought-responsive [123]. A recent study disclosed that 40% of the *GmNAC* genes were differentially regulated by natural leaf senescence. Moreover, the expression profile of *GmNAC* in

endoplasmic-reticulum (ER) stress, osmotic stress, and salicylic acid (SA) treatment corroborated their phylogenetic classification [71]. In chickpea (*Cicer arietinum*), out of the 71 *CaNAC* genes identified, 23 genes were dedicated to dehydration response, with 19 genes showing differential expression in shoots and /or roots in either ABA-dependent or independent manner [73]. In common bean (*Phaseolus vulgaris*), most NAC genes displayed specific temporal and spatial expression patterns, with 20 *PvNAC* members dedicated to drought [72]. Recently in peanut (*Arachis hypogaea*), out of the 132 *AhNAC* genes, 20 genes were significantly induced by drought and ABA in roots and/or leaves [75]. However, the functional exploration and characterization of the NAC superfamily in these major food legumes are still undetermined.

2.1.3 Potential utilization of NAC genes for abiotic stress tolerance in food crops

Several NAC genes from Arabidopsis, staple cereal crops (rice, wheat, maize, millet, *etc.*), legumes (soybean, chickpea, and peanut), vegetables, and fruits, have been characterized by overexpression or knockdown to identify their functional roles (Table 2.2). The studies present substantial evidence to support the potential of NAC TF as a crop improvement tool. The utilization of suitable NAC genes may potentially rescue crop yield from loss due to environmental stress. However, the functional conservation of NAC TFs across species and their response to a particular stress type is still debatable, mainly due to the partial divergent structure of NAC proteins and their complex regulation. Though enough information is available for the soybean NAC family, unlike cereal crops, the functional study of NAC in legume species is still preliminary.

Table 2.2 NAC role in stress response of food crops and model plants

NAC TF	Function	Reference
ATAF1 (Arabidopsis)	Overexpression enhanced tolerance to drought, ABA biosynthesis, sensitivity to ABA, salt, oxidative stress, and necrotrophic fungus, and promoted senescence in Arabidopsis; Overexpression increased salt and cold tolerance and ABA insensitivity in rice;	[27, 28, 56, 57]
ATAF2	Overexpression increased age-dependent and dark-induced senescence	[137]
ANAC032	Overexpression enhanced age-dependent and stress-induced senescence, repressed anthocyanin accumulation in stress in Arabidopsis	[138, 139]
ANAC102	Overexpression promoted seed germination under hypoxia-stress	[128]
ANAC019, ANAC055, ANAC072	Overexpression of ANAC019/055/072 increased drought tolerance and chlorophyll degradation during senescence in Arabidopsis; Overexpression of ANAC019 improved reproductive recovery in drought stress	[140] [141]
ANAC096	Mutation decreased tolerance to dehydration and osmotic stress;	[142]
ANAC016	Mutation delayed senescence and improved drought tolerance in Arabidopsis	[143, 144]
ANAC047/SHYG	Overexpression increased water-logging tolerance by inducing hyponastic leaf movement	[129]

ANAC029/AtNAP	Overexpression promoted leaf and fruit senescence and reduced salt tolerance in Arabidopsis	[145-147]
ANAC092/AtNAC2	Overexpression promoted senescence, lateral root development under salt stress in Arabidopsis, and improved tolerance to drought and salt in peanut	[148-150]
ANAC046	Overexpression promoted senescence and chlorophyll degradation	[151]
NTL9/CBNAC	Overexpression promoted senescence in Arabidopsis	[152]
ANAC042/JUB1	Overexpression delayed senescence to extend longevity and enhanced tolerance to heat stress in Arabidopsis	[153, 154]
OsNAC14 (Rice)	Overexpression improved drought tolerance in rice	[155]
ONAC066	Overexpression increased tolerance to drought, oxidative stress, and ABA sensitivity in rice	[126]
ONAC095	Overexpression increases drought susceptibility and cold tolerance in rice	[156]
ONAC096	Mutation increased panicle number and delayed senescence in rice	[157]
ONAC022	Overexpression increased tolerance to drought, salinity stress, and ABA sensitivity in rice	[158]
ONAC106	Overexpression inhibited leaf senescence and increased salt tolerance in rice	[159]
ONAC011	Overexpression promoted leaf senescence in rice	[160]
OsNAP	Overexpression promoted leaf senescence in rice	[109]
OsNAC45	Overexpression increased salt tolerance in rice, whereas the knockout had the opposite effect	[161, 162]
OsNAC2	Overexpression reduced tolerance to drought and salinity; promoted leaf senescence *via* ABA biosynthesis in rice	[163, 164]
OsNAC3	Overexpression improved tolerance to drought and heat through ROS scavenging	[165]
OsNAC5	Overexpression improved tolerance drought, salt, and cold stress in rice and root diameter	[166]
OsNAC10	Overexpression increased tolerance to drought and grain yield in rice	[167]
OsNAC6/SNAC2	Overexpression improved salt and cold tolerance and reduced growth in rice	[30, 168]
OsNAC9/SNAC1	Overexpression enhanced tolerance to drought and salt stress in rice, wheat, and cotton	[169-171]
TaRNAC1 (Wheat)	Overexpression enhanced tolerance to drought in wheat	[172]
TaNAC47	Overexpression enhanced tolerance to drought, salt, and freezing stresses and ABA hypersensitivity in Arabidopsis	[173]
TaNAC29	Overexpression enhanced drought and salt tolerance in Arabidopsis	[174, 175]
TaNAC2L	Overexpression enhanced heat tolerance in Arabidopsis	[176]
TaNAC2	Overexpression enhanced tolerance to drought, salt, and freezing stresses in Arabidopsis; enhanced drought tolerance in tobacco and wild wheat;	[177-179]
TaNAC69	Overexpression enhanced tolerance to drought and water-use efficiency in wheat	[179, 180]
ZmNAC55 (Maize)	Overexpression enhanced dehydration tolerance in Arabidopsis	[181]
ZmNAC111	Overexpression enhanced tolerance to drought and water-use efficiency in maize and Arabidopsis	[182]
ZmSNAC1	Overexpression enhanced drought tolerance in Arabidopsis	[183]
PgNAC21 (Millet)	Overexpression enhanced salt stress tolerance in Arabidopsis	[184]
EcNAC67 (Millet)	Overexpression enhanced tolerance to dehydration and salt stress in rice	[185]
HvSNAC1 (Barley)	Overexpression enhanced dehydration tolerance in barley	[186]
HvNAC005 (Barley)	Overexpression resulted in stunted growth and early senescence in barley	[187]
GmNAC109 (Soybean)	Overexpression improved drought and salt tolerance in Arabidopsis	[116, 188]
GmNAC019	Overexpression improved drought tolerance in Arabidopsis	[189]
GmSNAC49	Overexpression improved drought tolerance in Arabidopsis	[190]
GmNAC085	Overexpression improved drought tolerance in Arabidopsis	[124, 191]
GmSNAC1	Overexpression improved drought tolerance in Arabidopsis	[190]
GmNTL1	Overexpression improved drought tolerance in Arabidopsis	[192]
GmNAC20, GmNAC11	Overexpression of *GmNAC20* improved salt and freezing tolerance, and *GmNAC11* improved salt tolerance in Arabidopsis	[166]
GmNAC2	Overexpression increased hypersensitivity towards drought, salt, and cold in tobacco	[33]

GmNAC1, GmNAC5, GmNAC6	Transient expression in enhanced senescence in tobacco	[193]
AhNAC2 (Peanut)	Overexpression enhanced salt and drought resistance in Arabidopsis	[194]
AhNAC3	Overexpression enhanced drought tolerance in tobacco	[195]
AhNAC4	Overexpression enhanced drought tolerance in tobacco	[196]
MuNAC4 (Horse gram)	Overexpression enhanced drought tolerance in peanut	[197]
CarNAC6 (Chickpea)	Overexpression enhanced drought tolerance in Arabidopsis	[198]
CarNAC4	Overexpression enhanced drought and salt tolerance in Arabidopsis	[199]
CarNAC3	Overexpression enhanced drought and salt tolerance in poplar	[200]
SlNAC11 (Tomato)	Silencing reduced drought and salt tolerance in tomato	[201]
SlNAM1	Overexpression enhanced chilling stress in tobacco	[202]
SlJUB1	Silencing reduced drought tolerance in tomato	[203]

2.1.3.1 NAC-mediated stress-response in the developmental model: Arabidopsis

Arabidopsis, a dicotyledonous species from the mustard family, serves as a developmental biology model. Most of the knowledge of NAC TFs has been stemmed from reverse genetics and genome-wide expression study in this model. In this species, the ATAF group is discovered as a *bona fide* regulator of various biotic and abiotic stress responses, consisting of four genes, *ATAF1*, *ATAF2*, *ANAC032,* and *ANAC102*. Numerous gene expression surveys have implicated *ATAF*-like members as wide-range stress regulators. The early studies reported early and local induction of *ATAF1/2* (*Arabidopsis transcription activation Factor 2*) in wound response [204]. Later, it was found that *ATAF2/ANAC081* is involved in auxin biosynthesis through *NIT2* (*nitrlase2*) expression [205]. It also regulates photo-morphogenesis and brassinosteroids (BR) deficiency-mediated dwarfism by suppressing BR catabolic genes like *BAS1* (*CYP734A1*) and *SOB7* (*CYP72C1*) that control hypocotyl elongation and root growth *via* transcriptional feed-back regulation and DNA-protein and protein-protein interaction with *CCA1* (*circadian clock associated 1*) [29, 206]. In addition, *ATAF2* regulates age-dependent and dark-induced leaf senescence by expressing *ANAC092/ORE1* [137]. Similarly, *ATAF1/ANAC002* is also a negative regulator of various pathogenic responses, but it plays a positive role in abiotic stress tolerance through the ABA-dependent pathway. *ATAF1* overexpression led to dwarf and short primary root phenotypes, increasing sensitivity to ABA, salt, and oxidative stress but enhanced tolerance towards drought response correlated with enhanced expression of stress-responsive marker genes such as *ADH1*(*alcohol dehydrogenase 1*), *RD22/RD29A* (*responsive to desiccation 22/29A*), *COR47* (*cold regulated 47*), and genes involved in ABA biosynthesis and transport, such as *NCED3* (*nine-cis-epoxycarotenoid dioxygenase 3*), and *ABCG40* (*ABC transporter G family member 40*) [27, 56]. *ATAF1* positively regulates chloroplast maintenance and senescence cascade by expressing *GLK1* (*golden2-like 1*) and *ORE1* (*ORESARA1/ANAC092*) [57]. At the protein level, ATAF1 interacts

with AKIN10 and AKIN11, catalytic subunits of SnRK1 protein (SNF1-related protein kinase 1), a key integrator in stress and glucose signal transduction, to coordinate metabolic, hormonal, and developmental signaling pathways [58]. Contrary to the behavior in Arabidopsis, *ATAF1* overexpression in rice increased salt tolerance and ABA insensitivity [28]. Whereas, *ANAC102* regulates stage-specific hypoxia stress by enhancing the viability of seed germination under low-oxygen [128]. *ANAC032* has been characterized as a positive regulator of age-dependent and stress-induced leaf senescence by promoting the production of H_2O_2 under high light, sucrose, auxin and salt stress, and expression of *AtNYE1* (*non-yellowing 1*), *SAG113,* and *SAUR36* (*small auxin-up RNA genes/SAG201*), involved in chlorophyll degradation, auxin and ABA-mediated onset of senescence [138]. Moreover, *ANAC032* represses the production of anthocyanin pigment under various stress by downregulating *DFR* (*dihydroflavonol 4-reductase*), *ANS* (*anthocyanidin synthase*)/*LDOX*, *TT8* (*transparent testa 8*), *AtMYBL2*, and *SPL9* (*squamosa promoter-binding-like protein 9*) [139]. *ANAC032* inhibits ROS-mediated root cell elongation through *MYB30* regulation [207]. *ATAF1* and *ANAC032* are induced in carbon starvation [57, 58]. The transcriptome and physiological analysis revealed that *ANAC032* inhibits photosynthetic genes, induces ROS accumulation and carbon starvation by directing expression of *TRE1* (*trehalase1*) that triggers sugar and amino acid catabolism to maintain energy supply [208].

Three closely related genes, *ANAC019*, *ANAC055/AtNAC3,* and *ANAC072/RD26*, that bind to *ERD1* gene promoter, respond to diverse stress and hormone stimulus such as dehydration, high salinity, freezing, wounding, ABA, JA, *etc.* through an overlapping network. Overexpression of these homologous genes significantly improved drought tolerance, possibly by regulating the expression of *glyoxalase I* involved in glutathione-based detoxification but played an antagonist role in ABA signaling and ionic osmotic stress [140]. Y1H study identified potential overlapping upstream regulators, such as ABA-responsive genes (*ABF3*, *ABF4*, and *ABI4*) and a cluster of MYB TFs (*MYB2*, *MYB21*, *MYB108*, *MYB112*, and *MYB116*), implicated in stress responses and ABA/JA signaling, interacting with the promoters of *ANAC019*, *ANAC055*, and *ANAC072*, whereas *CBF1-4* (*C-repeat binding factor 1-4*) binds *ANAC072* promoter only [111]. Finally, it was found that *MYC2* and *ANAC019* interact physically and synergistically to regulate the *NYE1* involved in degreening through chlorophyll catabolism [209]. In addition, the distinct regulators justify the differential role of the gene set, *i.e.*, the involvement of *ANAC072* in cold, desiccation, and *ANAC019* and *ANAC055* in JA and/or ethylene mediated pathogen response.

ANAC092/AtNAC2, preferentially expressed in roots and flowers, regulates salt stress tolerance through modulation of lateral root architecture, serving as a downstream target of auxin and ethylene signaling [148]. When expressed in peanut (*Arachis hypogaea*), *AtNAC2* showed enhanced tolerance to drought and salinity with improved yield [149]. In contrast, *ANAC029/AtNAP*, a senescence regulator induced by NaCl, mannitol, and ABA treatments, negatively regulates salt-response by repressing genes such as *AREB1(ABA-responsive element binding protein 1)*, *RD20*, and *RD29B* [147]. In addition, *ANAC016*, a senescence regulator, negatively regulates drought tolerance by repressing *AREB1* [144]. In addition, *ANAC096* cooperates with the bZIP type TFs encoded by *ABF2* and *ABF4* synergistically to activate *RD29A* and many other ABA-responsive genes. Mutation of *ANAC096* resulted in ABA hyposensitivity displaying impaired ABA-induced stomatal closure and increased transpiration and sensitivity to dehydration and osmotic [142]. In contrast to senescence, *ANAC042/JUB1* regulates longevity, also imparting thermo-tolerance by tuning *DREB2A*, *HFSFA2*, and Glutathione S-transferases, resulting in lower H_2O_2 level and elevated proline and trehalose content [154].

2.1.3.2 NAC-mediated stress-response in cereal model: Rice

Fang *et al.*, 2008 reported that 20 out of 140 *ONAC* genes were significantly induced in drought and/or salt, with five genes induced by drought only, 19 genes by salt only, and 16 genes by cold [210]. The SNAC (stress-responsive NAC) group of rice is well documented for its involvement in stress regulation. Overexpression of NAM-like *SNAC1/OsNAC1* significantly enhanced drought tolerance and higher seed setting (22–34%) under severe dehydration imposed at the reproductive stage and improved salt tolerance at the vegetative stage [169]. Also, the gene ameliorated drought and salt tolerance and elevated ABA sensitivity in wheat by tuning stress-related genes such as *FAB1B* (*1-phosphatidylinositol-3-phosphate-5-kinase*), *SPS* (*sucrose phosphate synthase*), type 2C protein phosphatases, and regulatory components of ABA receptors, resulting in higher leaf-water and chlorophyll content [170]. In addition, *SNAC1* expression improved tolerance to drought and high salinity in cotton through vigorous root development and reduced transpiration rate [171]. Whereas, *OsNAC2*, also belonging to the NAM subfamily, negatively regulated drought and tolerance, probably by downregulating stress marker genes, such as *OsLEA3* (*late embryogenesis abundant 3*) and *OsSAPK1* (*stress-activated protein kinases 1*) [163].

Two rice genes, *OsNAC6/SNAC2* and *OsNAC5*, belonging to the ATAF family, are induced by cold, salt, drought, wounding, ABA and JA, integrating signals from abiotic and biotic stresses in rice. The transgenic plants overexpressing *OsNAC6* exhibited tolerance to drought, high salinity, cold, and blast disease. *OsNAC6* overexpression improved plant vigor during freezing conditions and enhanced germination and growth rate under salt stress. Although the constitutive expression of *OsNAC6* retarded growth and caused yield penalty, which was compensated by using stress-inducible *LIP9* and *OsNAC6* promoters were used [32, 168]. However, *OsNAC5* expression not only improved drought tolerance but also improved and root diameter and grain yield under both drought (22-63%) and normal conditions (9-23%), when expressed in roots, regulating genes implicated in root growth and development such as *GLP (germin-like protein 3-5), PDX1-like protein 4, MERI5* (*meristem protein 5*) *and OMT* (*O-methyl transferase*) [30, 31]. Microarray analysis of the transgenic plants showed upregulation of genes such as *PRX46* (*peroxidase 46*), *OsOAT* (*ornithine aminotransferase*), *HMA* (*heavy metal-associated protein*), *NHE3* (*sodium/hydrogen exchanger 3*), *HSP* (*heat shock protein*), *GDSL-like lipase*, and *OsPAL* (*phenylalanine ammonia lyase*) [168]. Like *OsNAC5, OsNAC10* and *OsNAC9* also increased drought endurance through improved root architecture. Root specific expression of *OsNAC10* increased tolerance and grain yield under drought (by 22-42%) and normal conditions (4-14%), while the constitutive expression gave a similar yield to that of control [167]. Similarly, root-specific expression of *OsNAC9* (similar to *SNAC1*) increased yield under drought (28-72%) and normal conditions (13-18%), and the constitutive expression increased 13-12% yield under normal conditions [211].

Furthermore, *ONAC022* is a positive regulator of drought and salt tolerance that control transcriptional water loss, Na^+ accumulation, and contents of proline and soluble sugars through increased ABA biosynthesis and signaling mediated by target genes such as *OsNCED, OsPSY, OsPP2C02, OsPP2C49, OsPP2C68, OsbZIP23, OsAP37, OsDREB2a, OsMYB2, OsRAB21, OsLEA3* and *OsP5CS1* [158]. Recently, *ONAC66* was reported to be induced by PEG, NaCl, H_2O_2, and ABA treatment to improve drought and oxidative stress tolerance by increasing ABA sensitivity and decreasing ROS accumulation [126]. Another *SNAC* gene, *SNAC3/ONAC003*, induced by multiple abiotic stress and ABA treatment, enhanced tolerance to high temperature, drought, and oxidative stress when overexpressed in rice by modulating ROS homeostasis through increased expression of ROS scavengers like *OsCATA, OsAPX8*, and *OsRbohF*. The overexpressor and silenced lines exhibited no change in ABA signaling genes, indicating that *SNAC3* exerts its function through an ABA-independent mechanism,

unlike most NAC TFs [165]. A rice gene *OsNAC14*, predominantly expressed at the meiosis stage, resulted in the vegetative stage drought endurance, higher panicle count, and filling rate, by interacting with *OsRAD51A1*, a vital component of the DNA repair system, when overexpressed [155]. *OsNAP*, a senescence-associated gene, conferred ABA-dependent tolerance to high salinity, drought, and cold during the vegetative stage and improved yield under drought stress at the flowering stage [212]. *ONAC106*, a negative regulator of senescence, positively regulated salt-stress response by tuning salt-signaling through *OsBREB2A*, *OsLEA3*, and *OsbZIP23* [159].

2.1.3.3 NAC-mediated responses in other cereals and legumes

In wheat (*Triticum aestivum)*, a staple cereal food, several NAC TFs have been identified to regulate disparate stress responses. The expression of two NAC genes, *TaNAC2* and *TaNAC47*, resulted in enhanced tolerance to drought, salt, and freezing in Arabidopsis by inducing *DREB2A*, *RD22*, *RD29A/B*, *ABI1/2/5*, and *Rab18* [173, 178]. Another gene, *TaNAC2L*, similar to *TaNAC2*, activated the heat tolerance in Arabidopsis [176]. *TaNAC29*, predominantly expressed in senesced leaves, boosted drought and salt tolerance, accompanied with ABA hypersensitivity, delayed bolting, and flowering in transgenic Arabidopsis [174]. Overexpression of *TaNAC69* improved drought adaptation and biomass in wheat [180]. *HvSNAC1*, a close homolog of *TaNAC2*, enhanced drought tolerance and photosynthetic activity in barley (*Hordeum vulgare*) [186]. *SbSNAC1* of sorghum (*Sorghum bicolor*), induced by dehydration, salinity, and ABA, improved drought tolerance in Arabidopsis [213]. In maize (*Zea mays*), two genes *ZmSNAC1* and *ZmNAC55* conferred dehydration tolerance when expressed in Arabidopsis, but increased hypersensitivity to ABA and osmotic stress at the germination stage [181, 183]. *ZmNAC111* overexpression enhanced drought endurance in maize seedlings [182]. *EcNAC67* from Finger millet (*Eleusine coracana*) improved drought and salt endurance in rice by retaining grain yield and biomass under exhibiting better post-stress recovery [185]. Another millet gene, *PgNAC21* from Pearl millet (*Pennisetum glaucum*), conferred salt tolerance in transgenic Arabidopsis by expressing *COR47*, *RD20*, and *GSTF6* (*Glutathione S-transferase F6*) [184].

In soybean (*Glycine max*), a vital legume, 31 *GmNAC* genes were cloned and analyzed for response in drought, salinity, cold, and ABA, indicating their diverse role, as per early reports [214]. *GmNAC2*, an *ATAF*-like gene, is a negative regulator of major abiotic stresses in tobacco, repressing the ROS scavenging genes [33]. Two genes *GmNAC11* and *GmNAC20*,

differentially regulate stress response. *GmNAC11* overexpression imparts salt tolerance, whereas *GmNAC20* confers salt and freezing tolerance in transgenic soybean through *DREB/CBF-COR* pathway [166]. As per recent reports, ectopic expression of *GmNAC109* augmented drought tolerance in Arabidopsis, probably through stronger superoxide mutase and catalase activities and increased ABA sensitivity, displaying a 20-54% greater recovery rate [188]. Similarly, *GmNAC085* positively regulates drought tolerance by elevating GSH/GSSG (reduced/oxidized glutathione) ratio in transgenic Arabidopsis *via* glutathione-dependent detoxification of ROS and methylglyoxal, however, caused growth retardation [191]. Also, *GmSNAC49* expression increased drought tolerance in Arabidopsis [190].

Three drought-responsive genes have been isolated from peanut (*Arachis hypogaea*) and characterized in model plants. An *ATAF*-like gene, *AhNAC4*, isolated from immature peanut seeds, conferred drought tolerance in tobacco by regulating stomatal closure and improving water-use-efficiency [196]. Another gene, *AhNAC3*, showed hyper-resistance to dehydration in tobacco by accumulating osmoprotectants and ROS scavengers due to induction of mainly four genes, *i.e.*, *SOD*, *LEA*, *ERD10C*, and *P5SC* [195]. *AhNAC2*, when expressed in Arabidopsis, resulted in ABA hypersensitivity to attenuate root growth, seed germination, and stomatal closure, implying a role in positive ABA signaling [194]. Moreover, the expression of horse gram *MuNAC4*, improved long-term desiccation tolerance in peanut, accompanied by increased lateral root and improved osmotic adjustment and antioxidant activity [197]. *CarNAC3*, an *AtNAP* like gene from chickpea (*Cicer arietinum)*, conferred drought and salt tolerance in poplar, but reduced plant height [200]. Two other genes, *CarNAC4* and *CarNAC6*, improved drought and salt endurance along with root growth in Arabidopsis [198, 199].

2.1.4 Potential utilization of NAC genes to improve seed quality, pod-yield, and growth

There are several agronomic traits, which indirectly or directly influence crop yield potential and productivity. Factors such as biomass growth, plant architecture, prolific root system, prolonged grain-filling duration, efficient nutrient uptake and mobilization, affect the yield indirectly, whereas seed development, seed size, pod/panicle length, *etc.*, are directly related to yield traits. In major cereal crops, quantitative trait loci (QTLs) influencing the grain yield, nitrogen assimilation, and lateral root formation co-localizes [215]. Nitrogen supply is crucial for crop productivity, a limitation of which can cause a yield penalty. In addition, a prolific root system is required to acquire nitrogen and water under adverse conditions. Several

studies have implicated NAC TFs in yield improvement, holding great potential for crop improvement, listed in Table 2.3 [120, 216, 217].

Table 2.3 NAC role in growth and development of food crops and model plants

NAC TF	Function	Reference
ATAF2	Overexpression increased auxin biosynthesis, suppressed BR catabolism, hypocotyl elongation, lateral root formation in Arabidopsis	[29, 205, 206]
ANAC032	Overexpression inhibited root growth and induced carbon starvation in Arabidopsis	[207, 208]
ANAC102	Overexpression suppress BR catabolism in Arabidopsis	[218]
ANAC012/SND1	Overexpression repressed secondary wall formation and increased callose deposition in Arabidopsis	[219]
ANAC017	Overexpression enhanced mitochondrial retrograde signaling inhibiting the growth	[220]
ANAC021/022/NAC1	Overexpression increased lateral root formation in Arabidopsis	[221]
ANAC035/LOV1	Overexpression increased the vegetative phase by delaying flowering in Arabidopsis	[222]
FEZ, SMB	Overexpression of FEZ induced cell division, while SMB repressed FEZ activity in Arabidopsis	[107]
ANAC083/VNI2	Overexpression repressed xylem vessel formation in Arabidopsis	[95]
NARS1, NARS2	Knockout produced abnormal seeds in Arabidopsis	[104]
NST1, NST3	Overexpression induced secondary wall thickening in Arabidopsis	[223]
ANAC068/NTM1	Mutation reduced cell proliferation in Arabidopsis	[108]
GmNAC109	Overexpression improved lateral root formation in Arabidopsis	[188]
GmNAC11, GmNAC20	Overexpression improved lateral root formation in Arabidopsis	[166]
OsNAC20, OsNAC26	Mutation decreased starch and storage protein content in rice	[216, 224]
OsNAC2	Overexpression decreased plant height and delayed flowering by repressing the GA pathway, increased panicle length to improve yield	[225, 226]
OsNAC5	Overexpression enlarged root diameter and grain yield	[31]
OsNAC9	Root-specific expression improved root architecture	[211]
TaNAC2-5A	Overexpression enhanced grain nitrate content and seed vigor	[215, 227]
TaNAC69	Overexpression enhanced root length and biomass in wheat	[228]
TaRNAC1	Overexpression enhanced root length and biomass in wheat	[172]
ZmNAC34	Overexpression negatively regulated starch accumulation in rice	[229]
ZmNAC126	Overexpression positively regulated starch synthesis in Maize	[230]
ZmNAC1	Overexpression enhanced lateral root development	[231]

2.1.4.1 Role of NAC in yield potential, seed size, and plant architecture

Several NAC TFs have been reported to improve yield potential and productivity by regulating seed development, nutrient remobilization, and improved crop architecture. In rice, three NAC TF, namely *ONAC020*, *ONAC026*, and *ONAC023*, exhibit strong endosperm-specific expression during seed development. *ONAC020* and *ONAC023* are targeted to ER and cytoplasm, respectively, and hetero-dimerize with nuclear localizing *ONAC026*, suggesting an overlapping as well as an independent association with the regulation of seed size/weight [224]. Later, it was reported that *ONAC20* and *ONAC26* play redundant roles in starch and seed storage protein biosynthesis by directing the expression of *SSI (starch synthase I*, *Pul*

(pullulanase), GluA1 (glutelin A1), GluB4/5 (glutelin B4/5), a-globulin, 16 kD prolamin, AGPS2b (*ADP-Glc pyrophosphorylase small subunit 2b*), *AGPL2* (*ADP-Glc pyrophosphorylase large subunit 2*), *SBE1 (starch branching enzyme I)*, and plastidial *DPE1 (disproportionating enzyme 1)* [216]. Another rice gene, *ONAC096*, enhanced grain yield by increasing panicle number (15%) without altering grain weight or fertility by repressing *OsCKX2* (*cytokinin oxidase/dehydrogenase 2*) in the mutated lines, and delaying the leaf senescence by controlling chlorophyll degradation, thus extending their photosynthetic capacity [157]. Also, repression of *OsNAP*, a regulator of ABA-mediated senescence, improved grain yield by extending the grain filling period [232]. An endosperm-specific maize gene *ZmNAC34* negatively regulates starch synthesis, causing abnormal seed morphology and increased amylose fraction in rice by tuning 17 starch-associated genes [229]. Moreover, another maize gene, *ZmNAC126* expressing in endosperm and maize kernel, interacts with starch biosynthetic genes, *ZmGBSSI*, *ZmSSIIa*, *ZmSSIV*, *ZmISA1*, and *ZmISA2*, proposing the crucial role of *ZmNAC126* in starch synthesis in maize [230].

Besides regulation of seed development by endosperm-expressing NAC TFs, efficient nutrient uptake is another attribute controlled by NAC TFs to improve the yield potential. In Arabidopsis, *AtNAC4/ANAC080* was the principal target downstream of *AtFB3*-mediated auxin signaling regulating nitrate response [217]. In wheat, *NAM-B1*, identified through positional cloning of Gpc-B1, a QTL associated with increased grain protein, zinc, and iron content, accelerated the flag leaf senescence, allowing efficient nutrient remobilization from leaves to developing grains [233]. A nitrate inducible NAC TF, *TaNAC2-5A*, directs the expression of nitrate transporters and glutamine synthetase. Its overexpression in wheat enhanced root growth and nitrate influx rate, thereby nitrogen accumulation in aerial parts leading to improved seed vigor and nitrogen allocation in grains [215, 227].

Moreover, NAC TFs may regulate plant architecture to improve yield potential indirectly. *OsNAC2* reduces plant height and delays flowering time by suppressing GA biosynthetic genes, *OsKO2 (rice ent-Kaurene oxidase 2)* and *OsKAO* (*rice kaurenne acid oxidase*), flowering-time related gene *Hd3A (heading date 3a)*, and directing the expression of GA signaling repressors such as *OsSLRL* (*rice SLR1-like*) and *OsEATB (rice ERF protein associated with tillering and panicle branching*) [225]. However, expression of an *OsNAC2* mutant (OErN), which was resistant to miR164b cleavage, improved grain number, panicle length, and plant architecture through the expression of *IPA1* (*ideal plant architecture 1)* and *DEP1* (*dense and erecticle*

panicle 1) [226]. Furthermore, *ONAC106* regulates tiller angle, an important architectural component affecting photosynthesis rice yield potential, by interacting with *LPA1* (*loose plant architecture 1*) [159].

2.1.4.2 Role of NAC in embryonic, floral, and vegetative architecture development

NAM (*no apical meristem*), isolated from petunia, was the first NAC gene to be characterized, followed by Arabidopsis *CUC1/2* (*cup-shaped cotyledon 1,2*), establishing the importance of NAC genes in plant development [60, 61]. Mutation of these genes caused fusion of cotyledons leading to failure in shoot apical meristem (SAM) formation in the seedlings during early embryonic development, whereas the overexpression induced adventitious shoots due to expression of genes crucial for embryonic SAM formation and maintenance such as *STM* (*shoot meristemless*), *AS1* (*asymmetric 1*), and *AS2* [106]. *CUC3*, a functional homolog, is required to initiate axillary meristems in rosette leaf axils. Plants having *cuc1*/*cuc2* double-mutation showed organ fusions between sepals and stamens in flowers [61]. In addition, *CUC* genes regulate leaf serration and leaflet separation. They redundantly induce SAM formation, regulate boundary specification, and floral organ patterning, both during embryonic and post-embryonic development. Similar roles of *NAM/CUC* genes are conserved in other angiosperms such barrel clover, maize, and tomato.

Besides, the senescence-associated *AtNAP* serves as an immediate target of AP3/PI heterodimer, which is essential to specify floral organ identities [234]. Two genes, *ANAC056/NAC2/NARS1* (*NAC-regulated seed morphology 1*) and *ANAC018/NAM/NARS2*, regulate seed shape and embryogenesis *via* degeneration of ovule integuments [104]. *ANAC068/NTM1* (*NAC with transmembrane motif 1*) regulates cell division mediated by cytokinin signaling in Arabidopsis by tuning a subset of genes that inhibit *CDKs* (*cyclin-dependent kinases*) and *histone H4* [108]. Two genes, *ANAC009/FEZ* and *ANAC033/SMB* (*SOMBRERO*), control the reorientation and timing of cell division in root cap stem cells in a feed-back loop [107]. Another membrane-bound gene, *ANAC078/NTL11 (NTM- like),* regulates cell proliferation and leaf development by attenuating auxin signaling [235]. Overexpression of A*NAC040/NTL8* delayed flowering and reduced growth to produce small curled leaves under salt stress by directly repressing *FT* (*flowering locus T*) and its targets [118]. Also, the gene mediates ABA-independent and GA-mediated delayed germination by repressing the GA biosynthetic gene (*GA3Ox1*), probably as an adaptive trait to survive [236]. In addition, *LOV1* (*Long Vegetative Phase 1*), a cold-responsive NAC gene, extends the

vegetative phase by negatively regulating the expression of *CO* (*CONSTANS*), a gene controlling flowering time under long-day conditions [222].

2.1.4.3 Role of NAC in xylem vessel formation and secondary cell wall synthesis

Xylem vessels are the conducting component of the tracheary elements in the vascular tissues involved in water and mineral uptake, whereas secondary cell walls (SCW) are also an integral component of tracheary elements and fibers, contributing to a significant portion of plant biomass. The NAC subgroups such as NST (*NAC secondary wall thickening promoting factor*), SND (*secondary wall-associated* NAC *domain*), and VND (*Vascular-related NAC domains*) are the master transcriptional switches of xylem cell-fate and SCW deposition. In Arabidopsis, the gene group comprises *ANAC043/NST1*, *ANAC066/NST2*, *ANAC012/NST3/SND1*, *ANAC073/SND2*, *ANAC010/SND3*, *ANAC101/VND6*, and *ANAC030/VND7* [223]. These genes are tuned by auxin and GA signaling to direct xylem and wood formation [115]. Both *SND2* and *SND3* serve as downstream targets of *NST1/3*, which in turn express genes associated with cellulose, biosynthesis of mannan, xylan, and lignin, and increased fiber cell area. Conversely, *SND1* acts as a negative regulator of SCW formation in xylary fibers [219]. Two *VND* genes, *VND6* and *VND7*, regulate xylem vessel differentiation, along with increasing SCW formation and PCD, in coordination with other *VND* members (*VND1-5*) [112, 237]. Similarly, in rice, *OsSND2* is associated with SCW biosynthesis and increased cellulose content when overexpressed [238].

2.1.4.4 Lateral root development by NAC TF

Promoting root elongation is a well-known physiological adaptation trait of plants to achieve water balance in dry and saline soil. NAC TFs are the central molecular regulator of lateral root formation with concomitant stress tolerance and/or yield improvement (Table 2.3). Several NAC TFs in Arabidopsis, soybean, maize, and wheat regulate root development *via* auxin-mediated pathways or an interlinked ABA/GA signaling. In Arabidopsis, *AtNAC1/ANAC021* regulates auxin transduced lateral root formation by activating two downstream targets, *DBP* (*B3-type DNA binding protein*) and *AIR3* (*auxin-induced in root cultures 3*) [221]. *ANAC092/AtNAC2*, a regulator of abiotic stress tolerance and senescence, is also involved in lateral root promotion under salt and heavy metal stress [148]. In maize, *ZmNAC1*, a homolog of *AtNAC1*, showed enhanced root formation in Arabidopsis, whereas *miRNA164* mediated cleavage of endogenous *ZmNAC1* negatively influenced the lateral root density [231]. In wheat, root-specific and root-predominant overexpression of drought-

responsive *TaNAC69-1* showed a marked increase in root length and shoot biomass (32-35%) by transcriptionally repressing auxin-inhibitory signals perceived by *TaSHY2* and *TaIAA7* [228]. Similarly, root predominant overexpression of *TaRNAC1* exhibited increased root length at early growth stage and >70% dry root weight after maturity, probably through modulation of *GA2OX2*-mediated GA metabolism, also producing more grain yield under water-limiting conditions [172]. In soybean, dehydration inducible *GmNAC004* promoted lateral root formation in Arabidopsis under normal and mild stress conditions when overexpressed. The transgenic plants showed resistance to ABA-induced root-growth inhibition while 2,4-D treatment promoted the root growth, indicating *GmNAC004* exerts its function through auxin-mediated mode [239]. Similarly, *GmNAC20*, a salt and frost stress-regulating gene, expressing abundantly in roots and cotyledons, promoted lateral root formation through auxin signaling [166]. Recently, it was reported that drought and salt-responsive *GmNAC109* regulates lateral root formation by differential tuning the expression of auxin signaling genes such as *AIR3* and *ARF2* (*Auxin Response Factor 2*) in Arabidopsis [116].

Apart from phytohormone signaling, NAC TFs also target genes directly involved in stress mitigation, biogenesis, and cell expansion/division to promote root growth. For instance, in rice, the root-specific expression of three rice genes, *OsNAC10*, *OsNAC9*, and *OsNAC5*, improved grain yield and root diameter, especially under drought conditions [31, 167, 211]. However, the microarray analysis of the transgenic plants suggested independent regulatory mechanisms of the genes. 32 target genes were differentially regulated in both root-specific and constitutive *OsNAC10* expressing transgenic, including *cytochrome P450*, *OsNCED4*, *2-OGX* (*2-oxoglutarate oxidase*), and potassium transporters (*HAK5 and HAK17*), kinases, and several stress-regulating TFs from AP2, WRKY, LRR, and NAC family [167]. In addition, *OsNAC10* and *OsNAC9* shared 32 targets, along with 53 uncommon targets. *OsNAC9/SNAC1* also exhibited altered root architecture by tuning *CCR1*, *WAK3/5*, and *MERI5* involved in lignin formation and cell elongation [211]. Whereas, in the case of *OsNAC5*, out of 62 targets, 17 overlapped with *OsNAC10*. However, their expression specificities were different, suggesting that *OsNAC10*, *OsNAC9*, and *OsNAC5* are novel regulators of drought stress in rice, enhancing root thickness and grain yield through independent mechanisms [31].

2.1.4.5 NAC-mediated senescence, ROS signaling, and PCD

Age-induced leaf senescence of flag leaves is crucial for nutrient translocation to the newly developing tissues and storage organs. NAC TFs can act as either positive or negative

regulators of senescence. In Arabidopsis, *ANAC029* (*AtNAP/ NAC-like, activated by AP3/PI*), *ANAC092/AtNAC2/ORE1* (*ORESARA1*), *ANAC059/ORS1* (*ORE1 sister1*), *ANAC016,* and *ANAC046* are positive regulators of senescence [143, 146, 150, 151, 240], while the negative regulators include *ANAC042/JUB1* (*Jungbrunnen1*) and *ANAC083/VNI2* (*VND-interacting 2*) [153, 241]. *ANAC029/AtNAP* regulates leaf senescence through ABA-meditated stomatal water-loss and chlorophyll degradation by activating genes such as *SAG113* (*senescence-associated gene 113*) and *AAO3* (*abscisic aldehyde oxidase 3*) [147]. Similarly, *ANAC046* exerts its role of senescence acceleration by expressing senescence-associated genes (*SAGs*) and chlorophyll catabolic genes, namely, *NYC1* (*non-yellow coloring1*), *SGR1/2* (*stay green 1, 2*), and *PAO* (*pheophorbide A oxygenase*) [151]. The salt-responsive *ANAC092/ORE1* upregulated 39 SAGs, such as *BFN1 (bifunctional nuclease 1), SAG29* (*senescence-associated gene29/SWEET15*), *SINA1* (*seven-inabsentia 1*), and *ribonuclease 3*, most of which were also expressed in the later stage of seed maturation, demonstrating overlap of network regulating senescence and seed development [150, 242]. ANAC016 promotes dark-induced senescence (DIS) by expressing SAG-like genes, *NYC1, SGR1, PPH (pheophytinase),* and *WRKY22* along with other NAC genes like *ANAC042/JUB1, ANAC029/NAP, ANAC092/ORE1, ANAC059/ORS1,* and *ANAC083/VNI2* [143]. In contrast, *ANAC042/JUB1*, induced by H_2O_2, serves as the central longevity regulator, delaying the onset of senescence by prolonging the transition of juvenility to aging *via DREB2A* expression [153]. Similarly, *ANAC083/VNI2*, also induced by abiotic stresses, maintains leaf longevity by regulating a subset of *COR/RD (cold-regulated/ responsive to dehydration*) genes to postpone senescence [241].

In rice, *OsNAP/PS1 (prematurely senile 1)*, named after *AtNAP,* accelerates leaf senescence by elevating JA biosynthesis through *LOX2* (*lysyl oxidase 2*) and *AOC1 (amine oxidase Copper containing 1)* during the grain filling stage [109]. In addition, *OsNAC2,* a negative regulator of drought and salt-response, accelerated ABA-induced leaf senescence by directly activating chlorophyll degrading genes, *OsSGR (rice stay green)* and *OsNYC3 (rice non-yellow coloring 3*), and participated in ABA biosynthesis *via* expression of *OsNCED3* and *OsZEP1* (*rice zeaxanthin epoxidase 1*). and *OsABA8ox1 (rice ABA 8'-Hydroxylase 1*) [243]. *ONAC11/OsY37* (*Oryza sativa yellow 37*) showed early heading and precocious senescence when overexpressed in rice. In contrast, its chimeric suppression delayed both heading time and leaf senescence but resulted in reduced grain yield irrespective of the onset of senescence [160]. *ONAC106* is a negative regulator of leaf senescence, controls the expression of *SAG* such as *SGR, NYC1, OsNAP, OsEIN3,* and *OsS3H*, and regulates tiller angle due to its interaction with *LPA1* [159].

In barley (*Hordeum vulgare*), *HvNAC005* overexpression resulted in stunted and delayed development due to transcriptional reprogramming of several genes involved with secondary metabolism, hormone metabolism, stress, signaling, development, and transport [187]. In Foxtail millet (*Setaria italica*), a homolog of *AtNAP*, *i.e.*, *SiNAC1*, promotes natural and DIS senescence by increasing ABA biosynthesis through *NCED2/3* in Arabidopsis [244].

Like senescence, programmed cell death (PCD) is another cellular phenomenon required to survive under compromised and normal environments. In Arabidopsis, a membrane-tethered NAC, *NTL4* (*NAC with transmembrane motif1-like 4*), promotes PCD through H_2O_2-mediated positive feedback during heat stress [245]. *OsNAC2* promotes salt-induced PCD by targeting ROS scavengers such as *OsCOX11* (*rice cytochrome c oxidase copper chaperone*), cell-death regulating *OsAP37* (*rice aspartic protease 37*), and K^+ efflux channels encoded by *OsGORK* and *OsSKOR*, resulting in DNA degradation and reduced cell wall integrity [164]. In soybean, *GmNAC81*, a downstream effector of *DCD/NRP*-mediated cell death, promotes PCD by expressing *VPE* (*vacuolar processing enzyme*), accompanied by early flowering and senescence [246].

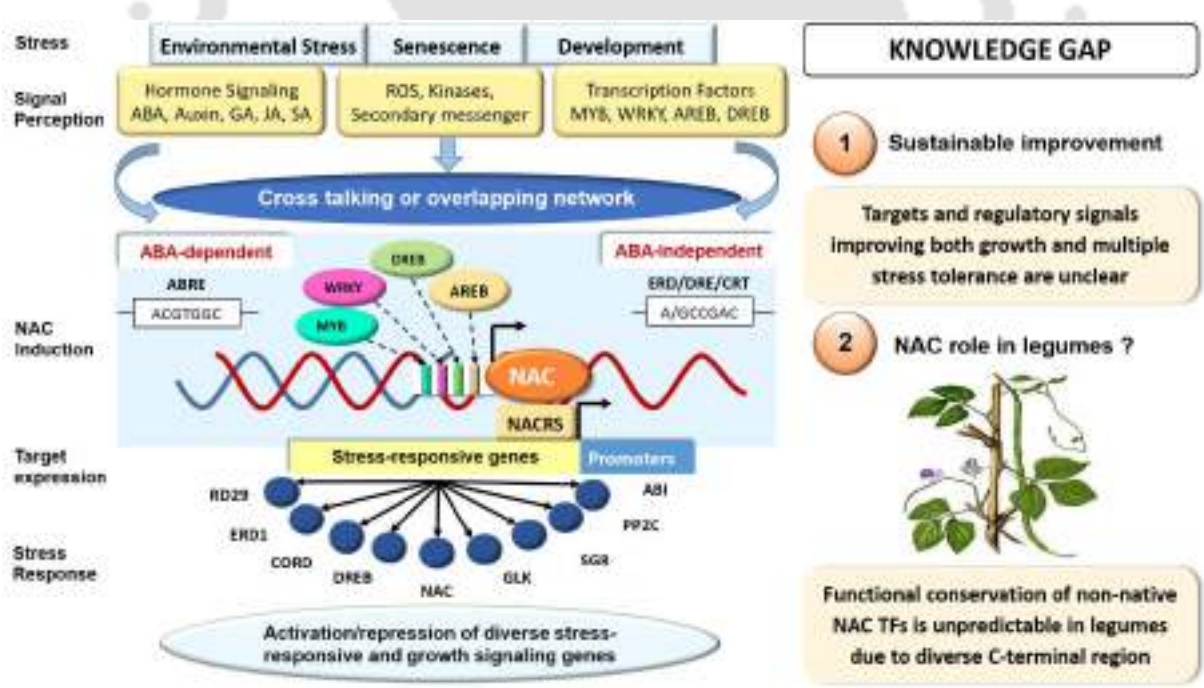

Fig. 2.4 NAC TF is a biotechnological tool for legume improvement.

2.1.5 NAC regulatory network and targets

NAC TFs are undoubtedly the master upstream regulators of basal stress responses. The signals of various abiotic, biotic stress, and senescence, cross-talk and transduced in the form of phytohormonal alteration, ROS, and secondary messengers, induce NAC TFs that execute transcriptional reprogramming of downstream stress-regulators to make necessary adaptation in the metabolism and express functional proteins to improve stress endurance, growth, and crop yield (Fig. 2.4) [53]. The NAC TFs can act as either activators or repressors to execute positive or negative stress tolerance. The functional versatility of NAC proteins is accounted by their diverse upstream regulators, fine-tuned transcriptional properties, and non-conserved motifs in the C-terminal NAC protein. In addition, NAC TFs are tightly and specifically regulated at DNA, RNA, and protein levels [64, 93].

2.1.5.1 Transcriptional regulation

NAC TFs, the transcriptional regulators of stress-response, are themselves tightly regulated at the DNA level by upstream NAC and non-NAC proteins through the over-represented TF binding sites (TFBS) and other regulatory elements in the gene promoters. The ABREs (ABA-responsive elements) recognized by AREB/ABF are present in *OsNAC5/6* promoters [30], *OsNAC3* and *SNAC1* consist of DRE (dehydration-responsive elements) recognized by DREB/CBF [162], whereas LTRE (low-temperature responsive element), JA/SA-responsive elements, and core binding sites for MYB/MYC and WRKY are present in *ONAC045*. *ANAC066/NST2* and *ANAC092*/*ORE1* are regulated by AtWRKY12 and EIN2 (ETHYLENE-INSENSITIVE 2). All seven VND members can induce *VND7*, whereas *ANAC012/SND1* is auto-regulatory.

2.1.5.2 Post-Transcriptional regulation

A complex post-transcriptional regulatory check is involved in optimizing the adequate level of NAC transcripts for their downstream functions. For instance, miR164 targets *CUC1*, *OsNAC2*, *ZmNAC1*, *SlNAM2*, *TaNAC21/22*, and *RhNAC100*, for miRNA-mediated cleavage [226, 231]. *PtrWND1B*, involved in SCW and fiber cell differentiation in poplar, is regulated by intron-mediated alternative splicing, giving antagonist functions to the two isoforms *PtrWND1B-s* and *PtrWND1B-l*. Also, functional *PtrSND1* can bind with its splice-variant lacking DNA binding ability to form a non-functional dimer. Further, trans-splicing can give rise to isoforms with varying transactivational properties, like in *ONAC20* and *OsNAC26* [224].

2.1.5.3 Post-translational regulation

The protein-level regulation includes ubiquitin-mediated degradation, dimerization, and interaction with other non-NAC proteins. The post-translational regulation ensures that NAC protein is available in the nucleus in its active form, only in conducive conditions, an absolute requirement for its transcriptional activity, which is fulfilled by the NLS sequences recognized by importins and cargo molecules. However, the membrane-bound NAC TFs like NTM1/2 and NTL6/8/9 require a proteolytic cleavage mediated by abiotic stresses such as cold, salt, and heat for activation [127, 152]. Furthermore, hetero-dimerization of ONAC020 and ONAC023 localized in cytoplasm and ER, respectively, with ONAC026, is necessary for nuclear import [224]. The nuclear localization of OsNAC4 is not possible without phosphorylation. Dephosphorylation of ANAC019 by RCF2 and phosphorylation of NTL6 by SnRK2.8 are crucial for their role in thermal resistance and drought tolerance. SLR1 (SLENDER RICE 1) represses NAC29 and NAC31 to control cellulose synthesis. In addition, ubiquitin-mediated proteolysis of NAC1 and TaNAC2L tune the respective signaling by varying the protein abundance with the corresponding transcripts [176]. ATAF1-SnRK1 protein-protein interaction may play a role in the proteasomal degradation or stress signaling of ATAF1 [58]. Other possible regulatory mechanisms are protease or kinase-mediated modification and sequestration of NAC proteins in other organelles before nuclear import.

2.1.5.4 Downstream targets of NAC TFs

A single NAC TF can express/repress targets involved in diverse functions to cooperatively achieve a phenotype. For instance, during senescence, ATAF1 activates the expression of senescence-associated genes (*SAGs*), with parallel repression of genes involved in chloroplast maintenance and photosynthesis, such as *GLK2* (a crucial marker for senescence-onset) to decline photosynthetic activity [57]. Despite the knowledge of functional roles, the understanding of downstream targets of NAC TFs is limited. The inducers, upstream regulators, and downstream targets of crucial NAC TFs are listed in Table 2.4.

Table 2.4 Upstream regulators, interacting partners, and downstream targets of NAC

NAC TF	Inducer	Upstream regulators	Downstream targets/ Interacting TF	References
ATAF1	ABA, H_2O_2, Wounding	-	*ADH1, RD22, RD29A, COR47, SnRK1, ERD10, ABCG40, NCED3, GLK1, ANAC092/ORE1, OsLEA3, OsSalT1*, and *OsPM1*	[27, 28, 57, 58]
ATAF2	Wounding	CCA1	*ORE1, NIT2, BAS1*, and *SOB7*	[29, 137, 205, 206]
ANAC032	High light, Sucrose	-	*AtNYE1, SAG113, SAUR36/SAG201, DFR, TT8, MYB30,* and *TRE1*	[138, 139, 207, 208]
ANAC102	Hypoxia	-	*ADH, SUS1,* and *ETR2*	[128]
ANAC019/055/ 072	Age, drought, salt, ABA, JA	MYC2/3/4, MYB2, MYB21, MYB108 MYB112, ABF3/4, ABI4	*ERD1, VSP1, BSMT1, ICS1, COR47, RD29b, FER1, ERD11,* and *Glyoxalase I*	[111, 209]
ANAC029	Age, ABA, salt, mannitol	ANAC016	*AREB1, RD20, RD29, SAG113*, and *AAO3*	[147, 247]
ANAC092	Age, salt, ABA	ATAF1, EIN3, ABI5, EEL, PIF4, PIF5	*ANAC083, ANAC041, ANAC054, ANAC084,NYE1, NYC1, PAO, ACS2, BFN1, SAG29, SINA1, GLK1,* and *GLK2*	[150, 242]
ANAC046	Age and dark	-	*NYC1, SGR1, SGR2,* and *PAO*	[151]
ANAC042/JUB1	H_2O_2	-	*DREB2A* and *HSFA2*	[153]
ANAC016	Drought	-	*AREB1, NYC1, PPH, SGR1/NYE1, WRKY22, JUB1, NAP, ORE1, ORS1,* and *VNI2*	[143, 144]
ANAC083/VNI2	Age, salt, ABA	-	*COR15, RD29A,* and *VND7*	[95, 241]
ANAC096	ABA, Drought, osmotic-stress	-	*RD29A, ABF2,* and *ABF4*	[142]
AtNAC2	Auxin	TIR1	*DBP* and *AIR3*	[221]
OsNAC10	Drought, Salt, ABA	-	*P450, OsNCED4, 2-OGX,* and *HAK5/17*	[167]
OsNAC5	Drought, Cold	-	*OsNCED, CCR1, OsLEA3, GLP, PDX, MERI5,* and *OMT*	[30, 31]
OsNAC9	-	-	*CCR1, Ca^{2+} ATPase, WAK3,5, 2-OGX,* and *OMT*	[211]
OsNAC2	Osmotic stress and ABA	-	*OsKO2, OsKAO, OsEATB, OsSLRL, Hd3a, OsLEA3, OsSAPK1, OsSGR, OsNYC3, OsNCED3, OsZEP1, OsABA8ox1, IPA1, DEP1, OsAP37,* and *OsCOX11*	[163, 164, 225, 226, 243]
ONAC022		-	*OsNCED, OsPSY, OsPP2C02, OsPP2C49, OsPP2C68, OsbZIP23, OsAP37, OsDREB2a, OsMYB2, OsRAB21, OsLEA3* and *OsP5CS1*	[158]
OsNAP	JA, MeJA, Senescence	-	*OsABI2, OsPP2C09, OsPP2C68,* and *OsSAIT OsDREB1A, OsMYB2, OsAP37, OsAP39, LOX2, AOC1, AOS2,* and *OPR7*	[109, 212]
ONAC106	Salt, age, dark	-	*SGR, NYC1, OsNAC5, OsNAP, OsEIN3, OsS3H, OsDREB2A, OsLEA3,* and *OsbZIP23*	[159]
TaNAC69-1	Drought	-	*TaSHY2* and *TaIAA7*	[228]
GmNAC20	Dehydration, Salt, Cold, NAA	-	*DREB1A/CBF3, KIN2/COR6.6,* and *DREB1C/CBF2*	[166]
GmNAC11	Salt, dehydration, ABA, NAA	-	*DREB1A, ERD11, cor15A, ERF5, RAB18,* and *KAT2*	[166]
GmNAC109	Drought	-	*DREB1A, DREB2A, AREB2, RD29A, COR15A, ABI1, ARF2,* and *AIR3*	[116]

2.1.6 NAC TFs can balance the trade-off between stress growth and stress tolerance

Different stress signals converge at the transmission components, such as Ca^{2+} sensors, ROS, phytohormones, and stress-responsive TFs like NAC, which overlap with growth signal perception, hinting at a potential harmonized cross-talk favoring both stress adaptation and plant fitness. As discussed in section 2.1.4, NAC TFs are the interface of multiple stress-signaling and basal growth (plant architecture, seed production, and senescence), connected *via* cross-talking phytohormones. Besides, their versatile gene targets regulate disparate signaling pathways. In addition, NAC promoters contain both ABRE (A/G)CCGACNT) and DRE (ACGTGGC) elements, regulating ABA-dependent as well as ABA- independent expression, indicating a multi-tier regulation, like *RD29A, COR78, LTI78, etc*., induced by drought, high salinity, and cold [248]. There are several NAC-mediated ways to compensate for growth retardation and hormonal and metabolic perturbations during stress adaptation (Fig. 2.5). A stress-tolerance conferring NAC TF can (a) induce flowering to enhance yield, (b) activate photosynthetic genes to promote biomass, (c) negatively regulate growth-inhibitory ABA signaling, (d) induce energy-generating pathways, (e) trigger root proliferation, and (f) regulate cell wall biogenesis to maintain the cellular integrity and infrastructure against pathogenic invasion and unfavorable climate. A *NAC2c* gene in pepper balances the growth/defense trade-off by avoiding the cross-talk of heat and pathogen response [249].

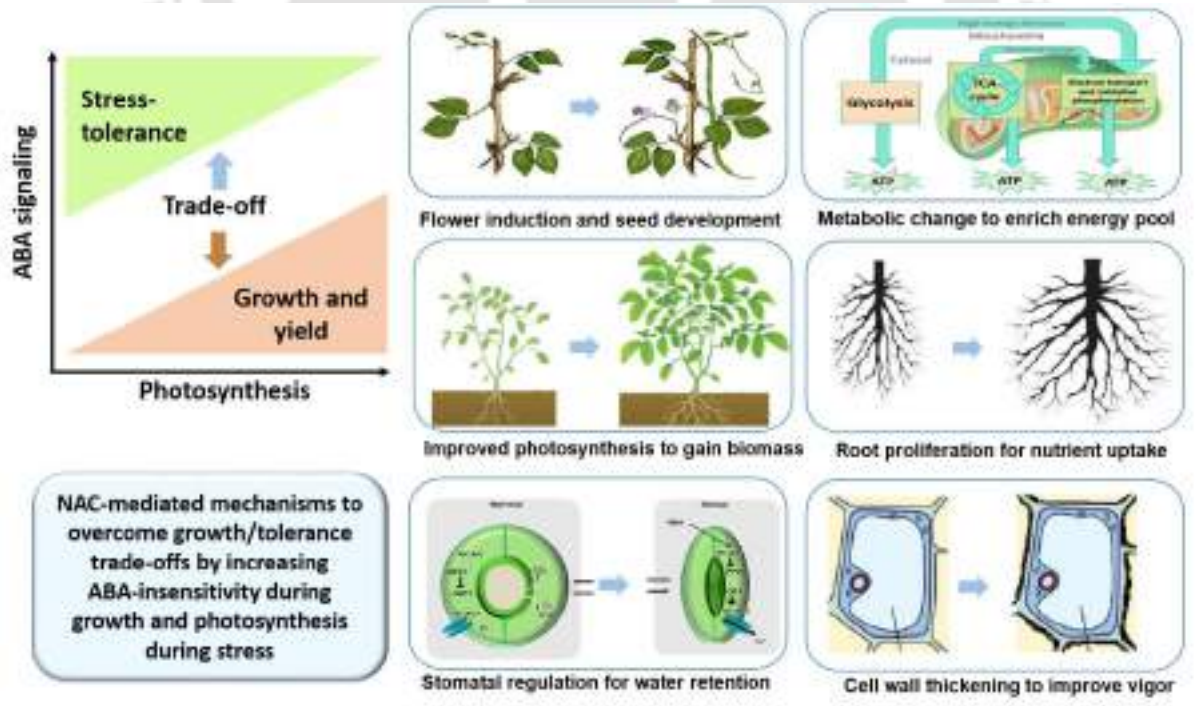

Fig. 2.5 NAC TFs can harmonize stress and growth responses to balance the trade-off.

2.2 Cowpea: a biotechnological model for legume improvement research

Cowpea (*Vigna unguiculata*, (L.) Walp) is a tropical food legume belonging to the *Fabaceae* family. It is indigenous to Africa but consumed worldwide in the arid and semi-arid regions of Sub-Saharan Africa, Asia, Southern Europe, Central, and South America, the Middle East, and the United States, using low input production systems [3]. It is also known as southern pea, crowder pea, black eye pea, or lobia. It is cultivated in warm to hot regions over ~14.5 million ha, with an annual production of 6.5 mmt (million metric tons) [250]. African produces ~85% of the world's overall production, owning 87% of the harvest area (12.3 million ha). Nigeria alone produces one-third of the African cowpea yield, while other leading producers include Myanmar, United States of America, Peru, Serbia, Sri Lanka, and China (FAOSTAT, 2017) [251].

Fig. 2.6 Kannanado white, drought hardy cowpea genotype

Several features make cowpea as ideal legume research model: (a) drought and heat resilience, (b) shade tolerance, (c) rapid growth and short life-cycle, (d) availability of genetic manipulation techniques, (e) genetic closeness to the major legume crops, and (f) accessible genetic material. For instance, a drought-hardy variety Kannanado White (IITA, Nigeria), can serve as a suitable genetic material for gene mining [252]. The variety is featured with 8-10 feet plant height, dense and vigorous vegetative growth, big and rough leaves, producing curly pods, each containing about six to seven white and globular seeds (Fig. 2.6).

2.2.1 Ideal genetic source to explore traits for nutritional benefits as well as stress-resilience

In cowpea, the whole aerial portion is rich in nutritional values holding immense health benefits. Mature can grain contains 23-32%

protein (equivalent to meat), 50-60% starch, B vitamins such as folic acid, essential amino acids like lysine and tryptophan, phenolic compounds, and micronutrients such as iron, calcium, and zinc, but less fat content (1%) [38]. Besides nutritional value, the legume possesses immense potential for exploring stress-tolerance mechanisms. Cowpea is usually robust to drought and high temperatures because of its naturally drier habitat, making it one of the most drought-hardy food legumes, which easily survive non-irrigated and low light conditions [253]. In addition, cowpea can withstand both acidic and alkaline soil conditions as long as they are well-drained [254]. It is recalcitrant to the low nitrogen soil. Due to its lofty nitrogen-fixation and intensive symbiont relationships with mycorrhizae, the natural soil reserves restores, making cowpea ideal for crop rotation [255]. However, phosphorus deficiency, an element required for nitrogen fixation, may lower productivity [250].

2.2.2 Production constraints in cowpea

Despite its climate-resilient nature and favored choice for arid and semi-arid cultivation, the cowpea seed yield and quality are adversely affected by numerous biotic and abiotic challenges [3]. Although cowpea is ideal for dryland agriculture under high temperatures, its yield can be susceptible to climatic challenges. Many early-maturing cultivars with a growth cycle of only 60-80 days are suitable for escaping the seasonal drought but unable to deliver the genetic yield potential. Several varieties are drought-tolerant if exposed for a short duration. However, the seed yield is severely compromised by terminal drought, causing water deficiency prior to and during the anthesis period [18, 256]. Cowpea yield is also sensitive to salinity, and the severity depends on the growth stage. Pod-filling and seed yield were significantly reduced when the salinity was inflicted in the vegetative stage [257]. Also, cowpea can take the heat, but night temperatures around 35°C or higher lead to pollen sterility, flower abortion, preventing pod formation [258]. Soils deficient in phosphorous, an element required for nitrogen- fixation, further lower the productivity [250].

The available stress-tolerance measures do not maintain yield under extreme, composite, and sequential field stress, especially during reproductive development, which is the desired definition of stress tolerance in food legumes like cowpea. Under an aggravated unfavorable environment, tolerance to stress is generally associated with the arrest of growth and photosynthesis, pollen sterility, and aborted seed development to conserve energy, which may never recover [259]. Thus, stress adaptation does not necessarily resonate with productivity due to growth trade-offs.

Considering the current trend in production, area expansion, and cowpea yield, the global supply is predicted to reach 12.3 mmt in 2030, against the projected global demand of nearly 11.2 mmt. However, the consumer preference of this vital pulse crop may change the predicted demand, which may impose a possible deficit. On top of that, the current productivity does not reach its genetic potential, which is limited by several abiotic and biotic cues. For instance, in Sub-Saharan Africa, the gap between potential and farmer's yields is reported to be more than 300%, yielding only 10–20% of the genetic potential of cowpea [14]. When environmental stress attacks the reproductive stage, the output yield may shrink to 600 kg/ha from the 2000 kg/ha of yield potential [40]. The biotic stresses that damage the harvest include pests, diseases, nematodes, parasites, and weeds, affecting almost every stage of the life cycle with varying degrees of damage [3]. Aphids (*Aphis craccivora*) mainly damage cowpea seedlings, bean flower thrips (*Megalurothrips sjostedti*) destroys flowers before pod-formation, pod borers (*Maruca vitrata*) attack young shoots and green pods, pod-sucking bugs penetrate the seeds in pods, whereas cowpea weevil destroys pulse grains in storage. The abiotic constraints are discussed in detail in section 2.3 [3].

2.3 Major abiotic challenges and their effect in cowpea and related legumes

Drought, heat, and salinity are the major production constraints declining the cowpea yield more than all the pathogens combined [3, 6]. Drought is one of the most deleterious climatic challenges, adversely affecting the growth and yield, ranging from morphological, physiological, and biochemical alterations, evident at all phenological and developmental stages [260]. Salinity is another brutal abiotic threat to crop productivity, jeopardizing agricultural potential [261].

2.3.1 Terminal drought impair vegetative proliferation and seed development

In general, drought causes a decline in biomass, grain yield, photosynthesis, and nutrient partitioning, leading to wilting and impairment of metabolic functions. The foremost effect of drought is impaired germination and poor stand establishment. Water deficiency inhibits growth determining cellular events such as mitosis, cell elongation, and expansion by reducing cell turgor, causing reduced plant height, smaller leaves, and overall growth retardation. The cellular processes determining the yield are deleteriously affected by water deficiency. Most edible cowpea and other legumes varieties are susceptible to the pre-anthesis and terminal (post-anthesis) drought. The pre-anthesis water-stress shrinks the anthesis period, while the post-anthesis (terminal) stress shortens the grain-filling phase by curbing the enzymatic

activities that synthesize starch, hence detrimental to seed yield. Drought influences plant water relations by reducing relative water content (RWC), leaf water potential, stomatal resistance, and transpiration rate, with a concomitant increase in leaf and canopy temperature. Diminished water availability also limits nutrient acquisition and transportation. It also hampers photosynthetic activity mediated by decreased leaf area, impaired photosynthetic machinery, and pigments to invite premature leaf senescence. Drought alters stomatal oscillations in an ABA-dependent manner to prevent water loss in evapotranspiration, subsequently limiting CO_2 influx in leaves. In addition, the low tissue water potential shrinks the cell volume, making the cellular components more viscous, which hampers the enzymatic activity of Rubisco and the photosynthetic machinery due to disrupted NADP-dependent linear electron flow [262, 263]. Consequently, the impaired carbohydrate metabolism affects the translocation of assimilates to that reproductive sinks, hampering seed-set and filling [264]. Moreover, drought increases susceptibility to photo-damage by disturbing the homeostasis of ROS levels and antioxidants [265].

Drought susceptibility of a genotype is often measured as a function of yield-reduction that depends on the timing, duration, and severity of the water deficit. As mentioned earlier, early maturing cowpea varieties can escape drought by completing their life cycle before the occurrence of terminal drought [266]. Also, intermittent moisture stress during vegetative and reproductive stage cause detrimental effects on many cultivars [267]. The most drought-sensitive growth stage in cowpea is just before and during the bloom, followed by pod-filling, vegetative, flowering, and fruiting [268]. Due to water deficiency, the flowering period terminates early, formation of new floral organs delays or aborted, leading to low productivity. As mentioned earlier, in Sub-Saharan Africa, the productivity of cowpea can curb from 2000 kg/ha (yield potential) to 600 kg/ha when drought attacks the flowering stage [40]. Drought can result in up to 60% yield loss during the pod-filling and pod-setting stage [268, 269].

2.3.2 Terminal heat and freezing stress impair flowering and fertilization

Cowpea is somewhat adapted to dry conditions and high temperatures. However, night heat injury caused by 30°C can lead to complete floral bud abortion, pollen sterility, and indehiscence of anthers to prevent pod formation [258]. Some cultivars can exhibit a 4–14% reduction in grain yield per °C increase in minimum night temperature during the reproductive phase. The combination of prevailing drought, heat, and long days can impede floral bud development and reduce grain filling by hampering assimilate partitioning. Furthermore, being

a warm-season crop, cowpea cannot thrive in cold temperatures and be killed by frost [270]. Chilling temperatures reduce seedling emergence by disrupting membrane organization in the embryo, degrades photosynthetic activity in the vegetative stage, which subsequently impair reproductive growth [271]. Cold tolerance can be traced in some sub-tropical varieties. Early sowing can benefit indeterminate crops like cowpea, enabling a longer growing period to compensate yield due to a second flush of fruit initiation and development [272]. However, this may invite imbibitional chilling injury leading to early seedling emergence with poor stand and low vigor.

2.3.3 High salinity cause lethal toxicity

Sub-lethal salinity reversibly retards growth without indicating any injury. However, high concentrations (100-200 mM NaCl) diminish yield, severely inhibit growth, or even kill the plants [273]. High salt levels in soil exert ionic stress in plants, individually, or in composite to drought. Indeed, irrigation can induce an accumulation of salt at the soil surface to negatively affect seed germination, seedling stand, vegetative development, and yield. In cowpea, high salinity can cause water deficiency, ion toxicity, nutritional imbalance, oxidative damage [274, 275]. Salt sensitivity varies with the plant's developmental stage. Pod and seed yield is significantly reduced when the salinity is applied in the vegetative stage, producing fewer or smaller seeds. In contrast, only biomass growth was hampered by salt stress imposed during the flowering and pod-filling stage [257]. Thus, the vegetative stage of cowpea is most severely susceptible to salt stress, and the sensitivity decreases later with development.

Salinity affects plants in two phases, resulting in disturbed physiological and biochemical interactions that affect almost all the developmental stages [276]. In the first phase, the roots deplete water-extraction, exerting osmotic imbalance, which is expressed as reduced leaf area and stunted growth due to loss in cell-turgor, water-content, and limited cell-expansion and stomatal closure. The second phase is characterized by the cytotoxicity caused by the accumulation of Na^+ and Cl^- ions in the leaf blade, resulting in the death of sensitive, old, and non-expanding leaves, while the new leaves cope by diluting the ions. The ion toxicity destroys water interactions *via* kosmotropic as well as chaotropic effects. The influx of Na^+ disturbs the K^+/Na^+ ratio, which is further aggravated by K^+ efflux mediated by ion transporters or leakage due to increased membrane permeability. K^+ ions are the most abundant cation in the cytosol, an essential nutrient and cofactors for many enzymes (such as pyruvate kinase) required to maintain adequate membrane potential and ionic and pH homeostasis [277]. The higher charge

density of Na^+ compared to K^+ makes it a weaker kosmotrope, affecting the biochemistry of enzymes, other proteins, and DNA. Na^+ cannot compensate for the biochemical requirement of K^+ in enzymatic and polysome activity, which can also lead to K^+ associated programmed cell death (PCD) [278]. Salinity also transiently arrests cell-cycle by diminishing the activity of cyclins and cyclin-dependent kinases (CDKs) to conserve energy and augment defense and repair cellular systems [279]. Despite osmotic stress and ion toxicity, salinity also imposes oxidative damage, photosynthetic degradation, nutrient deficiency, and deteriorates the water-uptake ability to induce water deficiency. High salt levels upset the nutrient balance by interfering with the uptake of nitrogen, phosphorus, calcium, potassium, *etc*. [280, 281]. Salinity declines photosynthesis efficiency mainly through shrinking leaf area, chlorophyll content, and stomatal conductance [282]. Salinity adversely affects reproductive development by inhibiting microsporogenesis, ovule abortion, and senescence of fertilized embryos [283, 284].

2.3.4 Nutrition deficiency and oxidative stress inhibit growth and survival

Dehydration and salt stress often impose nutrition deficiency in the stressed plants. The physiological damage caused by the stress degrades the plant's ability to assimilate and transport the available sources of nutrition. Besides channeling of plant energy towards defense and repair, nutrition starvation can also be one of the factors leading to growth retardation during stress. Moreover, oxidative stress may also occur as a concomitant effect, resulting in the generation of reactive oxygen species (ROS) such as superoxide anion radicals (O_2^-), hydroxyl radicals (OH^-), hydrogen peroxide (H_2O_2), alkoxy radicals (RO), and singlet oxygen (O_2^1) [285]. Chloroplasts are the primary source of strong oxidants generated due to excited pigments in thylakoid membranes. Their excess accumulation can react with cellular biomolecules, leading to lipid peroxidation, membrane injuries, protein degradation, and enzyme inactivation.

2.4 Potential strategies to combat the climatic challenges

Diverse breeding strategies have been employed but achieved only partial success due to the polygenic trait of the tolerance mechanism [42]. One approach to confer tolerance to multiple stress tolerances would be genetic engineering of transcriptional programs and incorporating a desired phenotypic trait to execute climate resilience.

2.4.1 Life-span and phenotypic flexibility

Crop stress tolerance is defined as maintaining the shoot growth and yield under prolonged terminal stress. When the phenological development is compatible with the available soil-moisture and seasonal temperature, the plant may escape drought and heat by cutting its life-cycle short and induce early flowering and seed-setting, facilitating the completion of reproductive span, or even delaying the reproductive phase until the unfavorable conditions. Adjusting flowering time is helpful for short-term stress mitigation in crops with indeterminate growth habits like cowpea and chickpea. However, under terminal stress conditions, the plants employ avoidance strategies involving adjustment in morphological features of shoot and root, such as controlling water loss through stomatal transpiration, increasing water-use efficiency (WUE) by developing glacousness and waxy bloom on leaves, and improving water uptake through a deeper rooting system. Plants generally limit water consumption through xeromorphic traits like adjusting leaf number, area, and pubescence. To retain the water potential and improve water-use efficiency, plants undergo leaf shedding and produce smaller leaves. The production of leaf hairs and trichomes protects plants from transpiration, radiation, and excessive heat. Although tolerance is defined as the plant's ability to rescue the shoot growth, the root is the only medium that can acquire available water to maintain a favorable water status [286]. Developing an extensive, prolific, and thicker root architecture improves drought adaption by constitutive water uptake. Drought-induced rhizogenesis occurring in *Brassicaceae* and related families is associated with the formation of short, tuberized, hairless roots capable of retaining turgor pressure to withstand prolonged drought. As crop yield is linearly related to the duration of crop, growth, and biomass production, most of the above-stated adaptive strategies mitigate stress, but at the cost of yield penalty.

2.4.2 Osmotic adjustment, osmoprotectant, and maintenance of membrane-integrity

A more progressive drought tolerance mechanism includes physiological mechanisms such as osmotic adjustment, production of osmolytes, and strengthening of the cell membrane [287]. Although cell or tissue water potential is not a defining feature for drought sensitivity, osmotic adjustment and cell wall elasticity can elevate the tissue water status [288]. Osmotic adjustment can be achieved by the active accumulation of various compatible solutes such as proline, glutamate, carnitine, glycine betaine, organic acids, sugar derivatives like sorbitol, mannitol, trehalose, Ca^{+}, Na^{+}, and Cl^{-} ions, *etc.* The compatible solutes are highly soluble, non-toxic at high concentrations, and do not interfere with cellular macromolecules. Their accumulation

decreases the internal water-potential, allowing the water-influx to maintain the high turgor and water-status for a prolonged period. This can delay dehydrative and osmotic damage and support cell-turgor, photosynthesis, nutrient translocation, and other physiological functioning crucial for growth.

Besides, the compatible solutes also serve as osmoprotectants to detoxify ROS, stabilize membranes, and retain the native conformation of cellular enzymes and biomolecules. Free proline serves as cytosolute to lower cytosolic water potential, a ROS scavenger, molecular chaperone, pH buffer, and store for carbon and nitrogen assimilation [289]. Similarly, glycinebetaine also plays a vital role in multiple stress tolerance. Citrulline is the most effective OH^- scavenger, also guarding DNA and enzymes against oxidative injuries. Trehalose, a non-reducing sugar, functions by stabilizing dehydrated biomolecules under desiccation, even at a small amount. Apart from stress adaptation, the compatible solutes also participate in stress-induced signal transduction pathways. In grain legumes, osmotic adjustment is achieved by increasing the sugar alcohols like mannitol, sorbitol, and inositol with a parallel decline in sugar.

Biological membrane integrity is a primary physiological index to measure drought, salt, and heat tolerance. The cell and organelle membrane may be injured by dehydration, salt-induced ionic imbalance, or temperature-induced deformation of membrane proteins. The increased permeability of the membrane leaves them exposed to the risk of membrane fusion, protein denaturation, and solute leakage. The membrane stability may be strengthened by osmotic adjustment by accumulating compatible solutes. Another way of adapting is increasing polar lipids to refine the biochemical composition of the membrane.

2.4.3 Increased production of anti-oxidants and ROS scavengers

To mitigate the deleterious effects, plants employ a ROS scavenging system consisting of the non-enzymatic components like cysteine, reduced glutathione, reduced ascorbate, carotenoids, tocopherols, flavonoids, di-terpenes, *etc.*, and the enzymatic components such as ascorbate peroxidase (APX), dehydroascorbate reductase (DHAR), monodehydroascorbate reductase (MDHAR), glutathione reductase (GR), glutathione S-transferase (GST), superoxide dismutase (SOD), catalase (CAT), and peroxiredoxin (PRX) [285]. In the photosynthetic tissue, the ROS scavengers are crucial for sustaining photochemical processes and chloroplast functioning. As stress tolerance is itself a cost-intensive phenomenon, it involves spending a considerable amount of energy on root growth, maintenance, and dry matter production,

resulting in ATP depletion. ATP synthesis accompanies ROS generation. Plants use alternative oxidase (AOX) as the terminal electron acceptor to circumvent the mitochondrial ROS level. Boosting the synthesis of antioxidants and ROS scavenging molecules can mitigate oxidative damage, and supporting the cellular energy pool, can be a more efficient strategy.

2.4.4 Tuning the balance between growth regulators and stress hormones

Plant growth regulators (PGRs), also referred to as phytohormones, such as auxins, gibberellins (GAs), cytokinins (CKs), ethylene, and abscisic acid (ABA), jasmonic acid (JA), that control diverse aspects of plant growth and development, endogenously as well as when applied externally. They act both under normal and stressed conditions, although differentially. Generally, under drought stress, the endogenous concentration of growth hormones (auxin and cytokinin) decreases, while the content of stress hormones such as ABA and ethylene elevates [290]. Auxin, CKs, and GAs are mandatory for the induction of cell division to regulate growth and flower development. Auxins induce new root formation by breaking the root apical dominance induced by CKs. Besides, the two hormones cross-talk between the growth and ROS signaling [291], and regulate stomatal opening by counteracting the action of ABA, a key mediator of stress signaling [43]. Under water-deficit conditions, ABA biosynthesis is induced, and its catabolism is suppressed. ABA regulates stomatal aperture to control water loss, enhances anti-oxidant enzymatic activities, orchestrates cascades of stress signaling (mainly desiccation), and expression of ABA-induced genes, usually in coordination with JA [292, 293]. Nevertheless, being a growth inhibitor, ABA retards growth by increasing seed dormancy, limiting the formation of leaf area and deep root system. Though, its effect can be antagonized by GAs and CKs [44]. Similarly, ethylene signal the onset of senescence and optimizes the vegetative growth to survive abiotic stresses [294]. However, a balance in stress and growth hormone signaling such as ABA/GA ratio and its homeostasis is required to avoid growth retardation under stress.

2.4.5 Overexpressing the molecular regulators of stress tolerance

Plants employ ubiquitously available functional and regulatory proteins to mitigate stress. The functional stress molecules include water channels/transporters, protection factors (LEA, chaperones), antioxidants, osmolytes, biosynthetic enzymes, and proteases. In contrast, transcription factors (TFs), protein kinases, hormones, and other signaling molecules, are the regulatory molecules.

2.4.5.1 Upregulating stress-mitigating functional proteins

Aquaporins are transmembrane intrinsic proteins (IPs), forming channels in plasma membranes (PIPs), tonoplast (TIPs), or nodulin (NIPs) to facilitate the passive movement of water in either direction across the water channel pore. In addition to water, some major intrinsic proteins (MIPs) can also transport glycerol, CO_2, urea, ammonia, hydrogen peroxide, boron, lactic acid, and O_2 [295]. Several reports are available that support overexpression of aquaporins to improve hydraulic conductivity of membranes and enhance the water uptake by more than 10-fold, resulting in increased plant vigor, water-use efficiency, and water retention, to cope with dehydration, ion toxicity, and osmotic stress [296-298]. For instance, the expression of *VfPIP1* in Arabidopsis improved drought resistance by reducing transpiration rates. Over-expression of *RWC3* in rice showed increased resistance to osmotic stress by enhancing root hydraulic conductivity [296]. In tobacco, overexpression of *AtPIP1b* increased stomatal density and transpiration rates. Synthesis of stress proteins, molecular chaperones, and antioxidant enzymes is exclusively implicated in abiotic stress tolerance [297, 298]. Late embryogenesis abundant (LEA)/dehydrin-type proteins and heat-shock proteins are induced in drought, extreme temperatures, and even at hypoxia conditions to stabilize and protect the vital cellular enzymes and proteins from denaturation. Dehydrins confer stress tolerance by increasing water-binding capacity through hydrophobic interactions and sequestering ions concentrated under a desiccated environment [297]. Heat-shock proteins (chaperones) prevent irreversible misfolding and aggregation of proteins and guide the correct refolding of denatured proteins [298].

2.4.5.2 Transcriptional reprogramming of stress-responsive genes

TFs monitors stress-specific gene expression by binding to *cis*-regulatory elements (TFBS) in the promoter of their target genes to mediate ABA-dependent and ABA-independent stress transduction. AREB/ABF family regulates ABA-mediated drought and salt stress signal signaling by binding to the ABRE motif (ACGTGGC) present in bZIP proteins encoded by genes, such as *RD29A*, *RD20A*, *RD22*, *RD26*, *etc* [299]. Another drought-responsive family of MYB/MYC/MYBR proteins like MYB2 and MYC2 recognizes stress marker genes like *RD22 via* MYBRS/MYCRS motifs (YAACR/CANNTG) to confer ABA-dependent tolerance [300-302]. In contrast, DREB1/CBF family uses the DRE motif ((A/G)CCGACNT) to effectively improve drought, cold, and salinity tolerance ability in several crops, including groundnut and rice, by an ABA-independent mechanism [303, 304]. Another gene, *ERD1*, induced by dehydration and senescence, but not by cold or ABA, is also a crucial part of ABA-independent

stress response, involving interaction with novel transcriptional proteins, later identified as ANAC019 and ANAC055 [140].

2.4.5.3 Amplifying the stress-signal perception

The sensing of stress signal and resultant activation of acclimation pathways is mediated by complex signaling events orchestrated by ROS, Ca^{2+}-regulated proteins, a cascade of mitogen-activated protein kinases (MAPKs), and cross-talking TF-mediated signaling. Increased cytosolic Ca^{2+} has been established as a ubiquitous secondary messenger in plants during various abiotic stresses, which interacts with downstream Ca^{2+}-dependent sensors comprising calcium-dependent protein kinases (CDPKs), salt-overly sensitive proteins (SOS), voltage-gated calcium channels, *etc*. A group of SNF1-related protein kinase (SnRKs) serves as an essential bridge between abiotic stress and metabolic responses to govern the energy balance. Some lipid-signaling mechanisms are also activated by stress to generate an array of secondary messengers through the phosphoinositide pathway. Additionally, stress signals are mediated by DNA-damage induced repair processes and cell-cycle checkpoints. Overexpressing the key signal mediators improve stress tolerance.

2.5 Traits to be screened or improved in cowpea and related legumes

Several agronomic, morphological, and stress-associated traits of interest regarding genetic improvement for cowpea and other legumes are listed in Table 2.5. Agronomic traits such as forage growth, pod yield, seed weight, seed size, maturity period, and qualities associated with processing, like seed coat and recovery, are the significant traits for agronomic research interests that need to be improved in cultivated cowpea varieties [41, 305]. Short-life cycles resulting in early flowering and pod maturity may be helpful for drought escaping in cowpea, chickpea, and pigeon pea. The onset of delayed senescence may be utilized to improve grain and biomass yields indirectly. Enhancement in sugar and amino acid content can enrich nutritional qualities. Further, fortification of phosphorus and iron by improving assimilation or metabolism can enrich nutritional attributes and prevent Iron Deficiency Chlorosis (IDC).

In terms of morphological characteristics, plants with erect growth and more canopy height may effectively suppress weeds and improve light harvest for photosynthesis rather than semi-prostate habit [306]. Highly branched and rich foliage biomass may translate into a higher seed yield [307]. In legumes, roots and nodules are key morphological features strongly associated with drought and salt stress. Moreover, in cowpea, soybean, chickpea, and common bean,

certain root traits important for efficient water uptake, such as root length, density, and depth, are crucial for drought avoidance and can be targeted to improve water-mining from drier and deeper soil layers [308, 309]. Root traits also have a core relationship with reproductive growth. Reduction in rooting biomass and length also declines pod set and pod weight.

Table 2.5 Potential traits to be improved for drought tolerance in legume

Legume	Trait	Function	Reference
	MORPHOLOGICAL TRAITS		
Soybean, Chickpea, Pigeonpea, Fababean, Lentil	Prolific root system with deeper, primary and vigorous, and thicker lateral roots	Improved water conduction under the limitation	[308, 310-313]
Chickpea, Mungbean, Fababean, Pigeonpea	Vigorous shoot biomass, smaller leaf area, canopy coverage	Better dry matter accumulation and light perception	[314, 315]
Cowpea	Erect morphology and short stature	Weed resistance	[306]
	AGRONOMIC TRAITS		
Chickpea, Cowpea, Pigeonpea	Early maturity or short life-cycle	Terminal drought escape	[316]
Pigeonpea, chickpea	Short stature and smaller leaf area index	Water conservation	
Soybean, Chickpea	Seed size and 100 seed weight	Yield	[317]
Common bean	Pod partitioning and pod harvest index	Yield	
Mungbean	100 seed weight, carbohydrate storage remobilization, or dry matter partitioning	Seed/grain size and quality	[315]
Cowpea	Delayed senescence	Biomass and seed yield	[309]
	STRESS-ADAPTATION TRAITS		
Chickpea, Mungbean, Fababean, Pigeonpea	Shoot traits such as improved photosynthetic efficiency, chlorophyll content	Drought and salt tolerance	[314, 315]
Soybean	More water-use efficiency, proline accumulation, ABA content, stomatal conductance	Drought and salt tolerance	
Common bean	Canopy temperature decrease	Avoids heat damage	[318]

To confer stress-resilience, traits such as high relative water content (RWC), membrane stability index (MSI), proline content, leaf area, and plant height, like drought-tolerant mungbean varieties [314, 315]. Likewise, high chlorophyll content and pod harvest index are exploited as primary traits for high yield in drier regions. Furthermore, water use efficiency (WUE) is critical in determining crop yield and drought tolerance in many crops. High stomatal conductance and photosynthetic efficiency have often translated into higher grain yield under stress. Canopy size is proportional to carbon assimilation and biomass accumulation, whereas canopy temperature is associated with heat conductance during vegetative growth, reflecting plant water status and thermo-tolerance [318]. Utilizing traits related to both stress tolerance and development in legumes could be a promising way for positive yield gain through genetic engineering.

2.6 Conclusion

The yield potential of cowpea and other related food legumes is severely declined by abiotic challenges like terminal drought, high night temperatures, and salinity. Indeed, stress-tolerance approaches often trade-off plant growth and fitness, resulting in compromised yield potential. To overcome the adverse effects of constitutively overexpressed stress machinery, growth-associated traits such as photosynthetic activity, energy balance, or nutrition fortification must be uplifted simultaneously to achieve a sustainable stress tolerance and improved seed yield. Polygenic strategies to manipulate multiple traits can be complex. Even stress-inducible overexpression of the gene candidate cannot compensate for the damage of aggravated and persistent stress field stresses, causing unrecoverable detrimental effects. As the central molecular switch for basal stress and growth signaling, NAC transcription factors can provide a unified mechanism to achieve the dual benefits. Single and versatile NAC gene from a stress-resilience non-cultivated cowpea genetic resource can be a suitable biotechnological tool to constitutively confer multiple stress tolerance and improved growth in legume crops.

Chapter 2

CHAPTER 2

3. GENOME-WIDE ANALYSIS OF NAC TRANSCRIPTION FACTOR FAMILY IN COWPEA

The chapter discusses the genome-wide identification and annotation of the NAC family in cowpea and elucidation of the genetic and molecular relationships indicating their role in basal growth and stress response. We identified 130 N AC proteins, namely VuNAC1-130, encoded by 90 distinct genes. The family was classified into eight phylogenetic groups, including a cowpea-specific group (GVII) with 27 members with no close orthologs from other species. The VuNAC proteins carried multipartite nuclear signals and unique transactivation regions with conserved patterns. Several proteins also consisted of non-NAC domains, exhibiting chimerism. The genes owned a unique promoter architecture encompassing pyrimidine-rich elements. The family manifested prominent segmental and tandem chromosomal duplication resulting in numerous stress-responsive members and large paralogous groups. The promoter and interactome analysis revealed multi-tier regulation through light, hormone, and transcription factors (NAC/MYB/WRKY/ERF and Dof/TCP), suggesting a cross-talk between stress and growth-regulating signals. Besides, the TFs were associated with metabolic processes like trehalose and folate synthesis, carbohydrate transport, lipid signaling, and electron transfer. In conclusion, the study predicted that a versatile NAC family in cowpea regulates stress tolerance and physiological growth, holding great potential for the genetic engineering of legume crops.

Keywords: Cowpea NAC family, gene-annotation, transcription factor, VuNAC

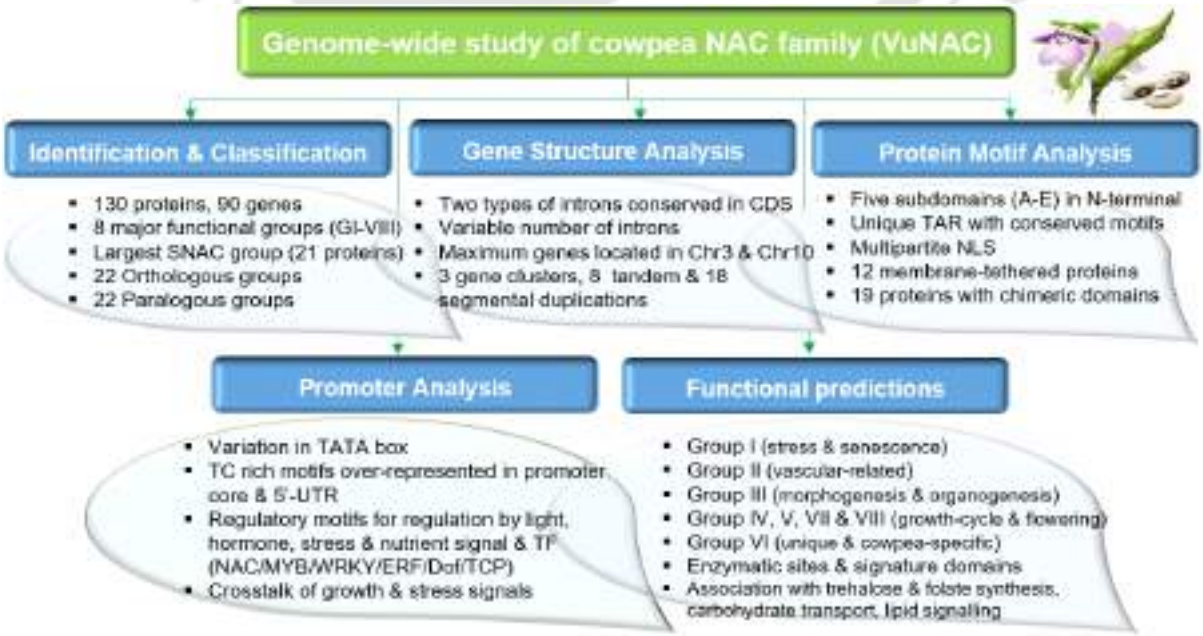

3.1 INTRODUCTION

NAC (NAM/ATAF1/2/CUC2) is one of the largest and versatile plant TF families, besides MYB, MYC, ERF, bZIP, and WRKY, which offers considerable potential to manipulate native stress adaptation networks to improve multiple stress tolerance [51]. A typical NAC protein carries a unique and tightly conserved signature N-terminal domain (~160 aa), forming a butterfly-like dimerized structure responsible for the DNA-binding [98], which is further divided into five subdomains (A–E). In contrast, the C-terminal transcriptional activation region (TAR), carrying crucial regulatory motifs, is highly divergent, bearing no fixed structure. The protein consists of nuclear localization signals (NLSs), while some membrane-tethered members also possess a transmembrane motif (TMM). Although the emergence and evolution of the NAC gene family have been reasoned to favor the adaptation of plant life from an aquatic to a terrestrial form [64], their peculiar features allow them to activate or repress diverse clusters of downstream genes regulating multiple and interlinked cellular or molecular processes including environmental stresses, for instance, development of shoot apical meristem [319], seed germination [104], cell division, expansion, and cell cycle [107], hormone signaling [50], nutrient remobilization [233], flowering time and development [118], lateral root formation [221], leaf senescence [110], secondary cell wall biosynthesis and fiber development [237]. In addition, they regulate the plant response against pathogens and abiotic stresses, including drought, high salinity, and cold [103, 122].

Being the control switch of cell fates, developmental programs, phase transitions, metabolic processes, and stress responses, NAC TFs offer smart options for developing stress-resilient crops, complying with growth and yield sustainability. Several NAC members, mainly from the ATAF subgroup, have been identified and ascribed for stress tolerance in several edible crops such as rice, soybean, wheat, and other crops [27, 30, 56-58]. The gene family have been reported in several cereals, legumes, and model plants such as Arabidopsis (117) [68], rice (151) [68], wheat (488) [77], maize (152) [76], millet (147) [78], barrel clover (65), and, soybean (180) [71], common bean (106) [66], and pigeon pea (88) [74]. However, the indispensable NAC family is still unexplored in many important orphan legumes like cowpea, pigeon pea, mung bean, chickpea, *etc*., with absolutely no information available for cowpea.

Among grain legumes, cowpea is considered relatively more stress-resilience than soybean and mung bean, usually well adapted to nutrient-deficit soil, grown mainly under un-irrigated conditions, thriving the dry and hot habitat, to yield even in under 300 mm of rainfall, due to

their deeper root system [320]. The plant has a short life-cycle, indeterminate vegetative growth under favorable conditions with extensive primary and lateral root systems rich in nodules, diverse growth forms varying from erect, climbing, and bushy. The recent availability of a comprehensive draft genome of cowpea has paved the way for high throughput genomic and functional studies [59]. The investigation of the vital NAC family in this valuable drought-hardy legume crop could unravel novel mechanisms for the sustainable improvement of multiple stress responses, growth, and yield.

In this chapter, we reported the identification, annotation, and *in-silico* characterization of the cowpea NAC TF (VuNAC) family to assess their functional role and significance. The study aimed to (i) annotate the VuNAC TF family, (ii) explore the conserved signatures and novel features associated with protein and gene sequences, (iii) predict the VuNAC TFs involved in stress signaling, developmental programs, and metabolic pathways, and (iv) provide promising candidates for genetic manipulation of legume crops. Our study identified a subset of potential VuNAC TFs to improve agronomic traits and stress tolerance in commercially grown cowpea cultivars, as well as in related grain legumes.

3.2 METHODOLOGY

3.2.1 Identification of VuNAC TF family

The BLASTP search (e-value ≤ 0.05) was conducted against the cowpea proteome (taxid: 3917) seeded with six distinct NAC domains from Arabidopsis and rice *i.e.*, *AtNAM* (AT1G52880), *ATAF1* (AT1G01720), *CUC1* (AT3G15170), *AtNAC1* (AT1G56010), *AtNAC2* (AT5G04410), and *OsNAC003* (AK061716), downloaded from the NCBI database (https://www.ncbi.nlm.nih.gov/). The non-overlapping hits were subjected to a hidden markov model (HMM) search by Pfam (http://pfam.xfam.or/) and SMART database (http://smart.embl-heidelberg.de/), to examine the presence of NAC and other associated domains [321, 322]. The corresponding protein, CDS, gene, and promoter sequences of identified VuNAC TFs were retrieved from the NCBI database for further analysis [59, 323]. To estimate the theoretical pI and molecular weight of the proteins, Compute pI/Mw tool (http://web.expasy.org/compute_pi/) was used with an 'average' resolution setting [324]. The sequences of the Arabidopsis NAC proteins (AtNAC) used in this study were downloaded from the Plant Transcription Factor Database 5.0 (http://planttfdb.gao-lab.org/).

3.2.2 Alignment and classification

To classify the VuNAC proteins into functionally distinct groups, a combination of two approaches, *i.e.*, multiple sequence alignment and phylogenetic analysis, were employed. First, the domain sequences were aligned by Clustal Omega (https://www.ebi.ac.uk/Tools/msa/clustalo/) using the default settings, and the representation of conserved amino acid residues was generated with GeneDoc software. The conserved NAC sub-domains were screened and classified into respective groups and subgroups based on their sequence similarity. Subsequently, the phylogenetic clustering of 130 VuNAC proteins, seeded with 75 reference AtNAC proteins, was conducted by MEGA 6.0, using the Neighbour-Joining (NJ) method (Poisson correction, pairwise deletion, and 1000 bootstrap replicate) to achieve an outcome similar to the former approach [325].

3.2.3 Motif detection, NLS, and TMM in VuNAC TFs

NAC proteins were subjected to motif discovery analysis using MEME suite v. 5.3.1 (http://meme-suite.org/tools/meme/), to identify conserved motifs, with the optimum search parameters (motif width range: 6-50; maximum number of motif = 50; minimum sites per motif = 2; maximum sites per motif-600) [326]. The presence of nuclear localization signals (NLS) was examined in proteins, using NLStradamus software, which used a 4-state HMM model suitable to find the multipartite NLS (prediction cut-off 0.3) [327]. To identify the transmembrane regions, we used TMHMM server v. 2.0 (https://services.healthtech.dtu.dk/service.php?TMHMM-2.0) [328].

3.2.4 Gene structure and chromosome location and duplication

To illustrate the exon-intron organization within the coding region of the *VuNAC* genes, Gene Structure Display Server 2.0 (http://gsds.gao-lab.org/) was used [329]. The gene phylogenetic tree generated by MEGA 6.0 and the CDS/gene sequences were used as input. The physical chromosomal location was graphically documented, indicating the paralogous and orthologous gene duplications. A chromosome region with two or more genes located 200 kb apart was defined as a gene cluster. The occurrence of two or more genes from the same phylogenetic group, locating within 100 kb distance on the same chromosome were denoted as tandem duplications, while the genes located on the different chromosomes were defined as segmental duplication [330].

3.2.5 Promoter analysis and study of regulatory elements

The 1.5 kb upstream sequences from the transcription start site (TSS) of the VuNAC genes were retrieved from NCBI to perform the promoter analysis. To investigate the presence of regulatory *cis*-elements, two promoter analysis tools, PlantCare (http://bioinformatics.psb.ugent.be/webtools/plantcare/html/) and PLACE (https://www.dna.affrc.go.jp/PLACE/? action=newplace) were used [331, 332]. The heat map of over-represented cis-elements was generated using the Multiple Experiment Viewer (MEV) tool.

3.2.6 RNA-sequencing and analysis

The healthy seeds of a drought-resilient cowpea genotype (Kannanado, IITA) were germinated for four days and then grown in soil pots for six weeks, under long-day *photoperiod* condition (*16 hr* light/ 8 hr *dark)* at 28 °C, with white light illumination (110 µmol photons $m^{-2}s^{-1}$) to attain the mature vegetative stage. Some germinated seedlings were cultured in hydroponic conditions and supplied with modified Hoagland media for 15 days (until the first trifoliate leaves were fully expanded) [333]. The mature leaves from soil plants and seedlings roots (5g of each) were sampled for the RNA sequencing, followed by the library preparation. The expression patterns of the *VuNAC* genes in leaf and root tissues of different growth stages were analyzed separately. The initial quality assessment on raw reads was carried out to remove the low-quality reads (quality phred score <30) using FastQC v0.11.7 [334] and the adapter sequences using NGSQC Toolkit v. 2.3.3 [335]. The high-quality reads were mapped on the cowpea genome available at NCBI Genome database under the BioProject ID PRJNA381312, using HiSAT2 separately for all samples, followed by reconstruction of the transcriptome from the RNA seq reads using StringTie [336, 337]. The expression of the *VuNAC* transcripts was calculated as fragments per kilobase of exon per million fragments mapped (FPKM), using the cuffdiff v2.2.1 program.

3.2.7 Gene-interactome analysis

The orthologous Arabidopsis NAC TFs were used as a model to predict the gene interactome, using ATTED II v. 10.1 tool (https://atted.jp/) [338]. The *VuNAC* genes were grouped into the co-expressing clusters. The genes in the constructed network were subjected to ontology analysis using the Panther tool (http://go.pantherdb.org/geneListAnalysis.do) to predict the associated role and regulatory genes [339].

3.3 RESULTS

3.3.1 Cowpea attributed a large family of NAC transcription factors (VuNAC)

3.3.1.1 Identification, nomenclature, and classification

Based on the protein-protein blast search (BlastP) throughout the cowpea proteome, we identified 130 NAC proteins in the family, encoded from 90 distinct genes, including the splice-variant isoforms, namely VuNAC1-90 (Table 3.1). The proteins harbored a conserved NAC domain similar to at least one of the six query sequences (bit-score ≥150). The HMM analysis carried by SMART and Pfam further revealed the domain architecture, verifying the 126 proteins to possess a single full-length NAC domain (~160 aa) (IPR003441), except the four truncated isoforms (VuNAC57.3, VuNAC59.3, VuNAC67.4, and VuNAC67.6) of the *VuNAC57/59/67* genes. Interestingly, we found a correlation between the size of the NAC family and genome when four widely studied legume species, cowpea (*V. unguiculata*), kidney bean (*P. vulgaris*) [72], soybean (*G. max*) [71], barrel clover (*M. truncatula*) [70], were analyzed, including Arabidopsis (*A. thaliana*) [67] as dicot model (Fig. 3.1A). In general, the size of the NAC gene family depends on the degree of whole-genome duplication (WGD) events underwent by the species, suggesting evolution being the primary force expanding NAC genes in plant lineage, regardless of the genome size, as in Arabidopsis [66]. However, the abundance of NAC genes was proportionate with the chromosome number and genome size in cowpea, similar to the other three legume species, being *P. vulgaris* the closest.

There are no consistent criteria for classifying the NAC proteins as the C-terminal region do not witness reasonable conservation, resulting in varying phylogenetic groups among species. To classify the VuNAC family in discrete functional groups, first, we grouped the proteins based on the conserved N-terminal subdomains found by sequence alignment (Fig. 3.2), followed by a comparative phylogenetic study of full-length NAC proteins consisting of 130 VuNAC proteins and 75 reference AtNAC proteins (Fig. A1.1, Appendix 1). Combining the two approaches, the 130 VuNAC proteins were clustered into eight major groups (I-VIII) and 21 subgroups (bootstrap support ≥ 85%). The distribution of VuNAC proteins in each group was depicted in Fig. 3.1B. The subgroups were named after the widely studied NAC members clustered together (Table A1.2, Appendix 1) [67].

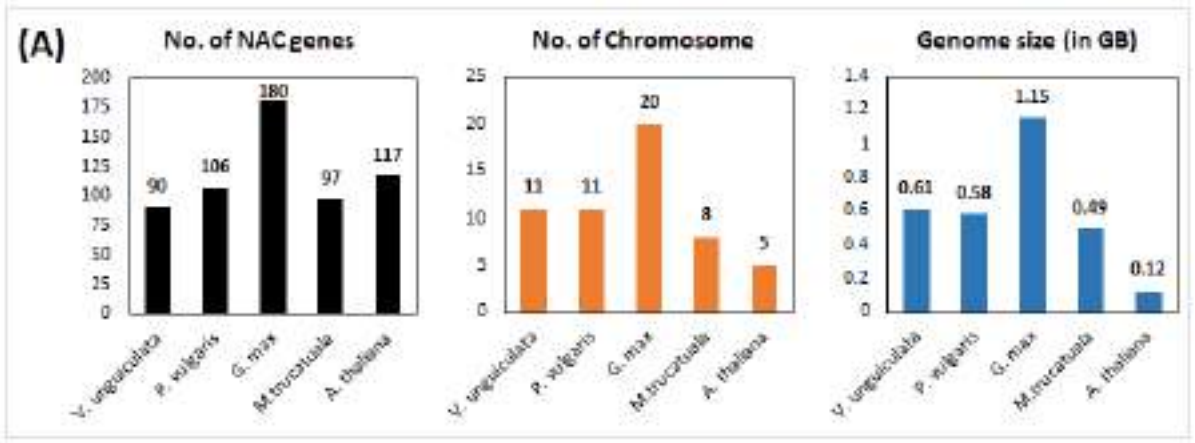

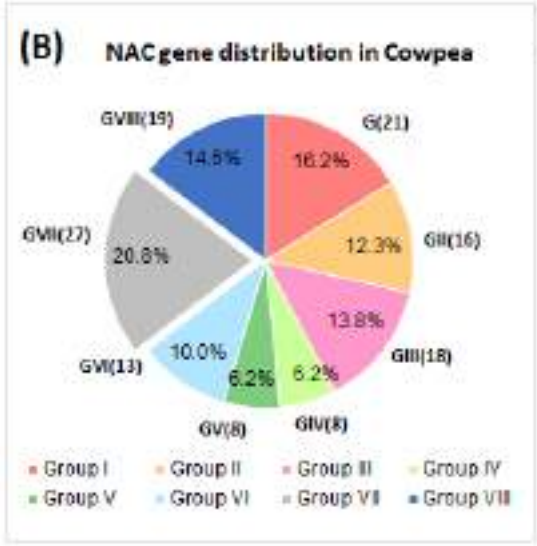

Group	Subgroup	Group name	# VuNAC Genes	# VuNAC Proteins
Group I	GIa	ATAF-like	5	5
	GIb	AtNAC3-like	2	2
	GIc	NAP-like	10	11
	GId	VNI2-like	3	3
Group II	GIIa	SMB/NST-like	2	4
	GIIb	VND-like	7	12
Group III	GIIIa	NAC1-like	3	3
	GIIIb	NAM-like	4	4
	GIIIc	CUC-like	7	11
Group IV	GIVa	TIP-like	1	1
	GIVb	NTL8-like	1	1
	GIVc	ANAC011-like	5	6
Group V	GVa	TERN-like	3	5
	GVb	FEZ/JUB1-like	3	3
Group VI	GVIa	XND1-like	3	7
	GVIb		4	4
	GVIc		2	2
Group VII	GVII	Cowpea- specific	17	27
Group VIII	GVIIIa	SND-like	2	12
	GVIIIb		4	5
	GVIIIc		2	2
		Total	90	130

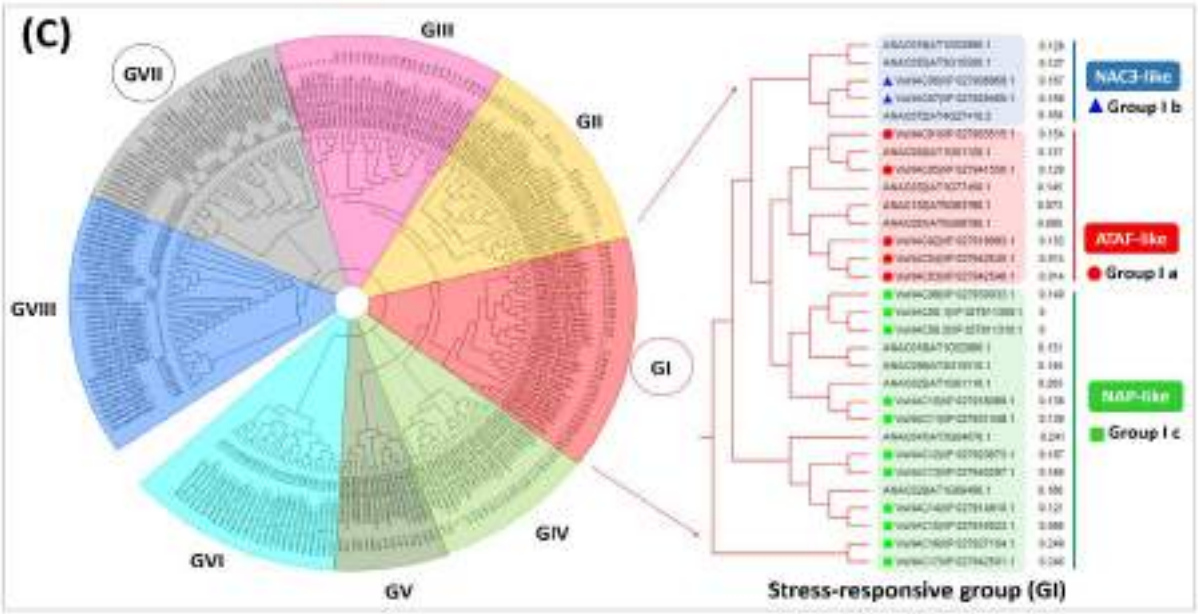

Fig. 3.1 Classification and distribution of proteins. (A) Comparative study of NAC gene distribution in legume crops. **(B**) Distribution of VuNAC members in the respective functional groups (I-VIII) and their annotation. **(C)** Phylogenetic classification (GI-GVIII) of VuNAC proteins corroborated the domain clustering. The stress-responsive group (GI) and were shown as an enlarged view (right panel).

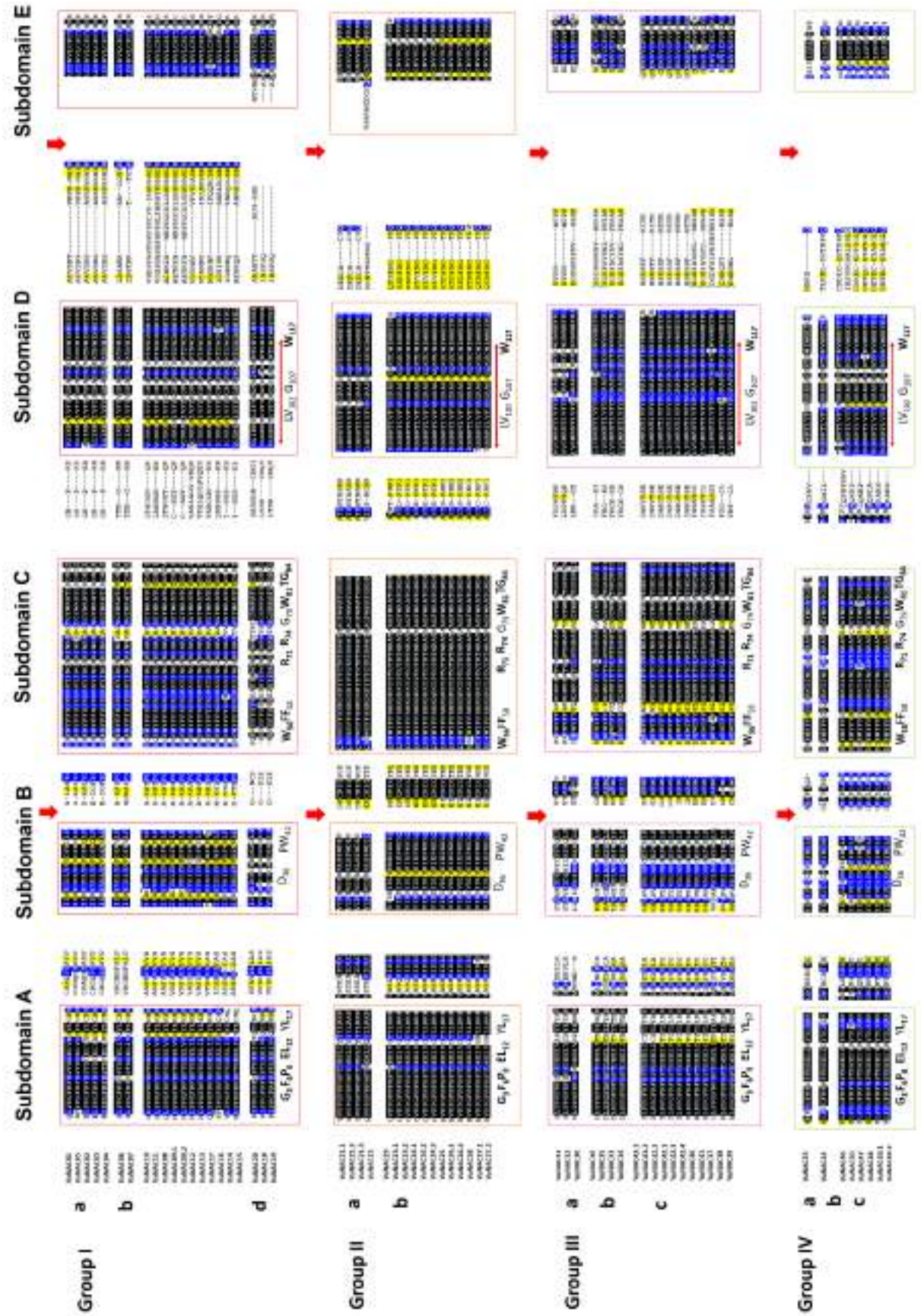

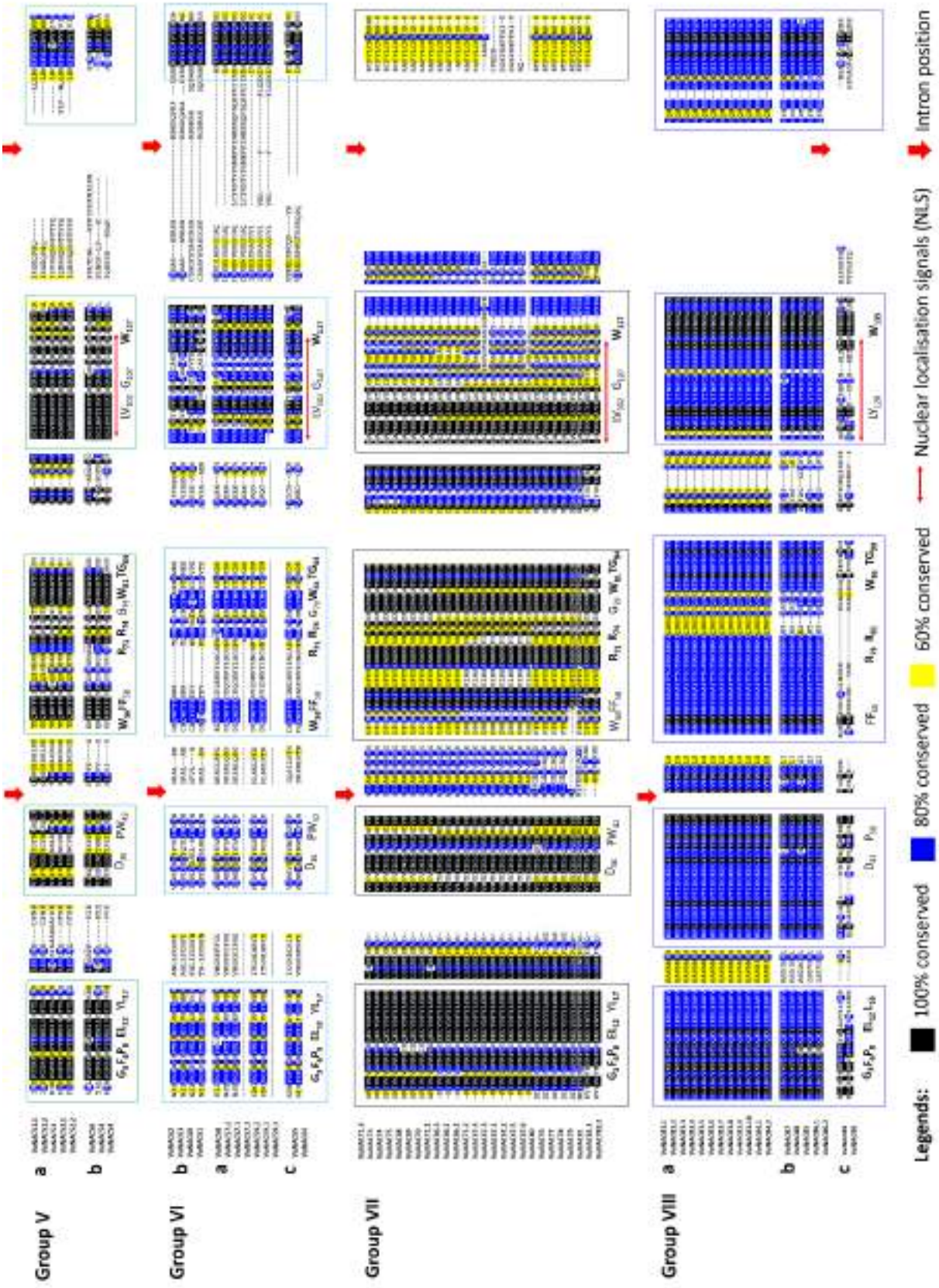

Fig. 3.2 Structural analysis of VuNAC domain. Sequence alignment of the N-terminal NAC domains of VuNAC functional groups (I-VIII) indicating the conserved intron positions, protein sub-domains, amino acid residues, and the potential nuclear localization signals (NLSs).

Group I consisted of 21 SNAC-like proteins encoded by 20 distinct genes, potentially associated with stress-signaling, making it the largest group (Fig. 3.1C). This group was subdivided into four subgroups, namely ATAF-like (Group Ia), AtNAC3-like (Group IIb), NAP-like (Group Ic), and VNI2-like (Group Id). Group II consisted of 16 xylem-associated proteins, named as NST-like (Group IIa) and VND-like (Group IIb) encoded by 9 *VuNAC* genes. Group III was dedicated to organogenesis, having 18 VuNAC proteins (14 genes), classified as NAC1-like (Group IIIa), NAM-like (Group IIIb), and CUC-like (Group IIIc). Group IV (8 proteins, 7 genes) belonged to TIP-like proteins (Group IVa), NTL8-like proteins (Group IVb), and ANAC011-like (Group IVc) proteins. Group V (8 proteins, 6 genes), namely TERN-like (Group Va) and FEZ/JUB1-like (Group Vb), seemed to be associated with cell division and growth cycle. Group VI (13 proteins, 9 genes) was named as XND1-like, consisting of three cell-death associated sub-groups. Group VII was the second largest group consisting of 27 proteins encoded by 17 *VuNAC* genes. This group was unique to cowpea, with no AtNAC sharing this phylogenetic clade (Fig. 3.1C). Group VIII was assigned 19 proteins and 8 genes, divided into three sub-groups, named as SND-like.

Table 3.1. List of 130 VuNAC proteins encoded by 90 distinct genes

Protein name	Protein ID	Subgroup	Group	Protein size (aa)	mRNA (bp)	Domain Span*	pI	M.W. (kDa)	VuNAC domain (aa)	Arabidopsis Homolog
VuNAC01	XP_027903515	ATAF-like	**Ia**	295	1491	8..131	6.5	33.7	152	ANAC002 (ATAF1), ANAC032
VuNAC02	XP_027919983	ATAF-like	**Ia**	295	1306	8..131	5.9	34.0	153	ANAC081, ANAC102
VuNAC03	XP_027942546	ATAF-like	**Ia**	281	1034	8..131	6.6	32.4	153	ANAC081, ANAC102
VuNAC04	XP_027942545	ATAF-like	**Ia**	281	1400	8..131	6.6	32.5	153	ANAC081, ANAC102
VuNAC05	XP_027941556	ATAF-like	**Ia**	271	1149	10..133	7.6	30.7	153	ANAC002 (ATAF1), ANAC032
VuNAC06	XP_027908969	AtNAC3-like	**Ib**	335	1455	15..139	6.1	37.7	152	ANAC055 (AtNAC3),
VuNAC07	XP_027929469	AtNAC3-like	**Ib**	340	1480	15..139	8.2	38.2	151	ANAC072 (RD26)
VuNAC08	XP_027930033	NAP-like	**Ic**	376	1864	18..142	8.6	41.8	162	NA
VuNAC09.1	XP_027911309	NAP-like	**Ic**	357	1583	18..142	6.8	39.7	160	NA
VuNAC09.2	XP_027911310	NAP-like	**Ic**	355	1753	18..142	6.8	39.5	160	NA
VuNAC10	XP_027918089	NAP-like	**Ic**	360	1506	16..142	7.9	40.1	164	ANAC025
VuNAC11	XP_027931348	NAP-like	**Ic**	352	1435	19..145	9.0	39.3	165	ANAC025
VuNAC12	XP_027923673	NAP-like	**Ic**	345	1706	10..139	7.8	31.1	158	NA
VuNAC13$_m$	XP_027940297	NAP-like	**Ic**	386	1622	45..175	9.2	43.3	159	NA
VuNAC14	XP_027914810	NAP-like	**Ic**	286	1231	10..134	8.9	32.9	154	ANAC029 (NAP), ANAC047
VuNAC15	XP_027916523	NAP-like	**Ic**	257	1263	10..134	8.2	29.4	154	ANAC029 (NAP), ANAC047
VuNAC16	XP_027942501	NAP-like	**Ic**	329	1267	12..138	6.1	39.3	155	NA
VuNAC17	XP_027927104	NAP-like	**Ic**	345	1546	13..139	6.7	37.6	155	NA
VuNAC18	XP_027930186	VNI-like	**Id**	232	1166	15..138	9.5	26.7	145	ANAC083(VNI2)
VuNAC19	XP_027928673	VNI-like	**Id**	232	1196	15..138	9.5	26.6	145	ANAC083(VNI2)
VuNAC20	XP_027920859	VNI-like	**Id**	234	892	15..141	8.7	26.3	157	NA
VuNAC21.1	XP_027920590	SMB-like	**IIa**	325	1373	11..139	6.8	37.4	150	ANAC033(SMB)
VuNAC21.2	XP_027920598	SMB-like	**IIa**	325	1476	11..139	6.8	37.4	150	ANAC033(SMB)
VuNAC21.3	XP_027920605	SMB-like	**IIa**	325	1344	11..139	6.8	37.4	150	ANAC033(SMB)
VuNAC22	XP_027906834	SMB-like	**IIa**	425	1685	16..143	6.0	47.4	161	ANAC033(SMB)
VuNAC23.1	XP_027913243	VND-like	**IIb**	377	1515	45..172	5.2	43.3	150	ANAC037(VND1), ANAC076(VND2)
VuNAC23.2	XP_027913244	VND-like	**IIb**	342	1531	10..137	5.1	39.2	150	ANAC037(VND1), ANAC076(VND2)
VuNAC24.1	XP_027917722	VND-like	**IIb**	335	1264	7..134	7.1	38.9	150	ANAC037(VND1), ANAC076(VND2)
VuNAC24.2	XP_027917723	VND-like	**IIb**	335	1447	7..134	7.1	38.9	150	ANAC037(VND1), ANAC076(VND2)
VuNAC24.3	XP_027917724	VND-like	**IIb**	335	1293	7..134	7.1	38.9	150	ANAC037(VND1), ANAC076(VND2)
VuNAC25	XP_027909884	VND-like	**IIb**	349	2232	8..135	6.0	40.6	150	ANAC007(VND4), ANAC026(VND5)
VuNAC26.1	XP_027922140	VND-like	**IIb**	349	1982	8..135	5.9	40.7	150	ANAC007(VND4), ANAC026(VND5)
VuNAC26.2	XP_027922148	VND-like	**IIb**	349	1411	8..135	5.9	40.7	150	ANAC007(VND4), ANAC026(VND5)
VuNAC27.1	XP_027913369	VND-like	**IIb**	355	1342	30..157	8.0	41.0	150	ANAC007(VND4), ANAC026(VND5)
VuNAC27.2	XP_027913370	VND-like	**IIb**	333	1552	8..135	7.3	38.5	150	ANAC007(VND4), ANAC026(VND5)

VuNAC28	XP_027918169	VND-like	**IIb**	362	2330	8..135	6.5	41.9	150	ANAC007(VND4), ANAC026(VND5)
VuNAC29	XP_027934534	VND-like	**IIb**	341	1524	19..145	6.5	39.4	150	NA
VuNAC30	XP_027902620	NAC1-like	**IIIa**	301	1227	45..175	8.3	34.0	148	NA
VuNAC31	XP_027934266	NAC1-like	**IIIa**	290	1142	11..137	6.5	33.4	149	NA
VuNAC32	XP_027920779	NAC1-like	**IIIa**	286	1339	11..137	6.0	33.0	149	NA
VuNAC33	XP_027923069	NAM-like	**IIIb**	390	1794	18..143	6.6	44.3	152	ANAC087, ANAC046
VuNAC34	XP_027939901	NAM-like	**IIIb**	396	1727	17..142	6.2	44.9	152	NA
VuNAC35	XP_027915454	NAM-like	**IIIb**	352	1544	17..141	8.2	39.7	151	ANAC100, ANAC080
VuNAC36	XP_027924014	NAM-like	**IIIb**	329	1292	29..153	5.8	37.4	151	ANAC100, ANAC080
VuNAC37	XP_027905363	CUC-like	**IIIc**	363	1268	23..149	6.7	41.0	155	NA
VuNAC38	XP_027918474	CUC-like	**IIIc**	311	1639	6..130	8.8	27.0	147	NA
VuNAC39	XP_027923742	CUC-like	**IIIc**	324	1357	6..130	7.0	36.4	147	ANAC058
VuNAC40	XP_027911896	CUC-like	**IIIc**	364	1500	23..149	6.9	40.3	153	ANAC098(CUC2), ANAC054(CUC1)
VuNAC41	XP_027929418	CUC-like	**IIIc**	351	1986	16..142	8.2	39.3	153	ANAC098(CUC2), ANAC054(CUC1)
VuNAC42.1	XP_027902107	CUC-like	**IIIc**	382	1539	62..188	8.2	42.5	151	NA
VuNAC42.2	XP_027902108	CUC-like	**IIIc**	381	1539	62..188	8.2	42.4	151	NA
VuNAC42.3	XP_027902109	CUC-like	**IIIc**	348	1340	28..154	8.8	38.7	150	NA
VuNAC42.4	XP_027902110	CUC-like	**IIIc**	348	1340	28..154	8.8	38.7	150	NA
VuNAC43.1	XP_027940684	CUC-like	**IIIc**	357	1074	28..153	8.8	39.9	150	NA
VuNAC43.2	XP_027940685	CUC-like	**IIIc**	357	1074	28..153	8.8	39.9	150	NA
VuNAC44$_m$	XP_027903156	TIP-like	**IVa**	599	2263	23..148	5.5	67.5	151	NA
VuNAC45$_m$	XP_027927859	NTL8-like	**IVb**	474	2105	19..143	6.6	53.4	142	NA
VuNAC46	XP_027920378	ANAC011-like	**IVc**	344	2095	7..136	5.3	38.6	154	NA
VuNAC47	XP_027923139	ANAC011-like	**IVc**	237	1071	7..133	4.9	27.2	151	ANAC057
VuNAC48$_m$	XP_027931539	ANAC011-like	**IVc**	663	2481	9..135	5.6	75.2	151	NA
VuNAC49.1$_m$	XP_027939593	ANAC011-like	**IVc**	653	2237	6..132	5.1	74.2	151	NA
VuNAC49.2$_m$	XP_027939594	ANAC011-like	**IVc**	653	2280	6..132	5.1	74.2	151	NA
VuNAC50	XP_027902039	ANAC011-like	**IVc**	346	1426	7..133	5.0	39.7	152	ANAC020
VuNAC51.1	XP_027921862	TERN-like	**Va**	260	1245	5..134	5.6	30.0	154	NA
VuNAC51.2	XP_027921868	TERN-like	**Va**	258	1239	5..134	5.6	29.8	152	NA
VuNAC52.1	XP_027927348	TERN-like	**Va**	253	1157	5..133	6.8	28.7	163	ANAC090
VuNAC52.2	XP_027927350	TERN-like	**Va**	248	1141	5..133	6.8	28.0	158	ANAC090
VuNAC53	XP_027909833	TERN-like	**Va**	239	1180	6..139	6.1	27.1	161	ANAC090
VuNAC54	XP_027909063	FEZ/JUB1-like	**Vb**	303	1277	16..142	8.2	34.5	146	ANAC036
VuNAC55	XP_027918398	FEZ/JUB1-like	**Vb**	412	1650	57..181	6.7	46.7	146	NA
VuNAC56	XP_027914711	FEZ/JUB1-like	**Vb**	409	1628	18..143	6.0	46.4	158	NA
VuNAC57.1	XP_027904869	XND-like	**VIa**	517	2320	8..133	4.9	56.5	177	NA
VuNAC57.2	XP_027904870	XND-like	**VIa**	489	2236	8..133	4.8	53.2	149	NA
VuNAC57.3	XP_027904871	XND-like	**VIa**	438	2144	8..133	4.6	47.3	105	NA
VuNAC58	XP_027920595	XND-like	**VIa**	335	1912	8..133	5.0	37.4	149	NA
VuNAC59.1$_m$	XP_027936856	XND-like	**VIa**	620	2441	6..129	4.6	67.9	158	NA
VuNAC59.2$_m$	XP_027936857	XND-like	**VIa**	611	2412	6..129	4.5	66.8	149	NA
VuNAC59.3$_m$	XP_027936858	XND-like	**VIa**	516	2465	2..25	4.3	55.9	59	NA
VuNAC60	XP_027904951	XND-like	**VIb**	199	830	9..124	4.9	23.3	151	ANAC104(XND1)
VuNAC61	XP_027921386	XND-like	**VIb**	203	957	10..125	5.5	23.0	151	ANAC104(XND1)
VuNAC62	XP_027918201	XND-like	**VIb**	190	1282	9..127	4.9	22.1	151	ANAC104(XND1)
VuNAC63	XP_027931410	XND-like	**VIb**	189	902	9..127	5.8	21.8	151	ANAC104(XND1)
VuNAC64	XP_027936859	XND-like	**VIc**	462	1850	35..159	6.7	51.6	153	ANAC050
VuNAC65$_m$	XP_027935892	XND-like	**VIc**	559	2323	21..145	4.7	63.1	149	NA
VuNAC66.1	XP_027908500	NA	**VII**	550	2457	10..139	4.8	62.9	150	NA
VuNAC66.2	XP_027908501	NA	**VII**	549	2464	10..139	4.8	62.8	150	NA
VuNAC66.3	XP_027908502	NA	**VII**	522	2370	10..139	4.9	59.7	150	NA
VuNAC67.1	XP_027907828	NA	**VII**	155	961	4..133	9.4	18.0	132	NA
VuNAC67.2	XP_027907829	NA	**VII**	155	957	4..133	9.4	18.0	132	NA
VuNAC67.3	XP_027907830	NA	**VII**	146	3651	4..133	9.2	17.0	132	NA
VuNAC67.4	XP_027907831	NA	**VII**	146	825	4..>40	9.8	16.9	46	NA
VuNAC67.5	XP_027907832	NA	**VII**	143	883	4..133	9.5	16.8	132	NA
VuNAC67.6	XP_027907833	NA	**VII**	128	3592	4..>40	10.2	15.0	46	NA
VuNAC68	XP_027906703	NA	**VII**	561	2443	21..150	4.7	64.0	150	NA
VuNAC69	XP_027908222	NA	**VII**	561	2445	21..150	4.7	64.0	150	NA
VuNAC70	XP_027912578	NA	**VII**	561	2444	21..150	4.7	64.0	150	NA
VuNAC71.1	XP_027908219	NA	**VII**	564	2207	21..150	4.6	64.2	150	NA
VuNAC71.2	XP_027908220	NA	**VII**	547	2131	4..133	4.6	62.4	150	NA
VuNAC71.3	XP_027908221	NA	**VII**	313	1020	21..150	5.2	41.9	150	NA
VuNAC72	XP_027912585	NA	**VII**	192	699	4..133	8.8	21.8	150	NA
VuNAC73	XP_027912579	NA	**VII**	370	1727	21..150	5.1	42.1	150	NA
VuNAC74	XP_027912580	NA	**VII**	370	1778	21..150	5.1	42.1	150	NA
VuNAC75	XP_027906014	NA	**VII**	339	1020	5..134	5.0	38.4	150	NA
VuNAC76	XP_027908225	NA	**VII**	328	1562	5..135	5.1	37.9	151	NA
VuNAC77	XP_027912582	NA	**VII**	328	1397	5..135	5.1	37.9	151	NA
VuNAC78	XP_027912583	NA	**VII**	328	1562	5..135	5.1	37.9	151	NA
VuNAC79	XP_027908227	NA	**VII**	313	1543	5..120	5.4	36.0	135	NA
VuNAC80	XP_027906015	NA	**VII**	316	951	5..134	5.1	36.5	149	NA
VuNAC81	XP_027907627	NA	**VII**	282	1564	5..133	5.1	32.7	149	NA
VuNAC82.1$_m$	XP_027908223	NA	**VII**	481	2023	12..139	5.4	54.2	148	NA

VuNAC82.2$_m$	XP_027908224	NA	**VII**	480	2021	12..139	5.4	54.1	147	NA
VuNAC83.1	XP_027923078	SND-like	**VIIIa**	458	2212	48..189	6.7	51.9	163	ANAC075
VuNAC83.2	XP_027923079	SND-like	**VIIIa**	458	2280	48..189	6.7	51.9	163	ANAC075
VuNAC83.3	XP_027923080	SND-like	**VIIIa**	458	2204	48..189	6.7	51.9	163	ANAC075
VuNAC83.4	XP_027923081	SND-like	**VIIIa**	458	2299	48..189	6.7	51.9	163	ANAC075
VuNAC83.5	XP_027923082	SND-like	**VIIIa**	458	2208	48..189	6.7	51.9	163	ANAC075
VuNAC83.6	XP_027923083	SND-like	**VIIIa**	458	2227	48..189	6.7	51.9	163	ANAC075
VuNAC83.7	XP_027923084	SND-like	**VIIIa**	458	2278	48..189	6.7	51.9	163	ANAC075
VuNAC83.8	XP_027923086	SND-like	**VIIIa**	458	2324	48..189	6.7	51.9	163	ANAC075
VuNAC83.9	XP_027923087	SND-like	**VIIIa**	458	2328	48..189	6.7	51.9	163	ANAC075
VuNAC83.10	XP_027923088	SND-like	**VIIIa**	458	2236	48..189	6.7	51.9	163	ANAC075
VuNAC84.1	XP_027917437	SND-like	**VIIIa**	446	2183	48..189	6.7	50.5	163	ANAC075
VuNAC84.2	XP_027917439	SND-like	**VIIIa**	446	2183	48..189	6.7	50.5	163	ANAC075
VuNAC85	XP_027931119	SND-like	**VIIIb**	323	1513	64..205	8.1	36.4	165	ANAC073(SND2)
VuNAC86.1	XP_027917265	SND-like	**VIIIb**	314	1368	60..199	6.4	35.6	161	ANAC073(SND2)
VuNAC86.2	XP_027917266	SND-like	**VIIIb**	314	1358	60..199	6.4	35.6	161	ANAC073(SND2)
VuNAC87	XP_027929257	SND-like	**VIIIb**	279	1637	49..188	8.7	31.9	161	ANAC073(SND2)
VuNAC88	XP_027909536	SND-like	**VIIIb**	281	1805	45..184	8.6	32.0	161	ANAC073(SND2)
VuNAC89	XP_027920185	SND-like	**VIIIc**	204	920	15..139	8.7	23.2	145	NA
VuNAC90	XP_027923726	SND-like	**VIIIc**	211	887	17..132	9.1	24.0	137	NA

*NAC domain (IPR003441), 'm' stands for membrane The names 'VuNACx.1, VuNACx.2' and so on indicated splice variants encoded by the VuNACx gene.

3.3.1.2 Investigation of the salient protein features

When the VuNAC proteins were screened for salient features, several other functional motifs were found within the TF, besides the DNA-binding sites and nuclear localization signals. In 19 members, the signature NAC domains were associated with non-NAC functional domains making them chimeric proteins, as listed in Table 3.2. The associated domains were involved in cell division (CEP19, SHE3), signaling (GIT_CC), cell death (BIRC6), cytoskeleton synthesis (RPEL, FPP), respiration (Oxired_q4, Pex26, V_TPase, VKOR), and gene transcription (TFIIA, bZIP_1). The detailed information of the associated domain was listed in Table A1.3.1, Appendix 1. The presence of these domains indicated possible co-regulation of cell function directly by non-transcriptional activities, indicating the versatility of VuNAC proteins actions. Such chimeric nature was also reported in the WRKY TF family [340]. Furthermore, VuNAC proteins consisted of a multi-repeat assembly of internal sequences (*VuNAC57*, *VuNAC58*, *VuNAC59*, *VuNAC70,* and *VuNAC71*). This might have resulted from the evolutionary events intended to enlarge the available binding surface area of protein.

Besides the chimeric domains, NAC also harbored binding motifs for other proteins and the enzymatic activity sites (Table A1.3.2, Appendix 1). Most of the VuNAC proteins were rich in phosphorylation, glycosylation, myristoylation, and amidation sites. However, several VuNAC proteins possessed unconventional motifs. VuNAC66 (GVII) had '*ATP/GTP binding site motif A'* and '*leucine-rich repeat (LRR)'* involved in the immune response. VuNAC72 (GVII) contained the '*PTS EIIB domain profile',* found in *the* phosphotransferase system involved in sugar transport. '*7,8-dihydro-6-hydroxymethylpterin-pyrophosphokinase*

signature', associated with folate synthesis enzyme, were found in VuNAC24 and VuNAC25 (Group II). VuNAC87 (GVIII) possessed '*Cytochrome c oxidase subunit Vb'*, involved in electron transfer. VuNAC73 and VuNAC74 (GVII) embodied the '*NHL repeat profile'* found in growth regulatory protein. '*C-CAP/cofactor C-like domain profile'*, of cytoskeleton-related protein, was found in VuNAC55 (GVI), VuNAC67, and VuNAC72 (GVII). The '*LDL-receptor class B (LDLRB) repeat profile'* associated with lipid signaling was found in VuNAC34, VuNAC47, and VuNAC55. '*Cell attachment sequence'* was found in VuNAC44 (GIV), VuNAC51, and VuNAC52 (GV), along with '*cell wall-binding repeat profile* 'in VuNAC45 (GIV). The presence of these functional sites and signature motifs associated with miscellaneous roles suggesting the involvement of VuNAC TFs in versatile cellular and metabolic pathways, in addition to growth and stress response.

Table 3.2 List of chimeric VuNAC TFs

Role	Associated domain	Genes	Description*
Cell division	CEP19	VuNAC49	CEP19-like protein
	SHE3	VuNAC68-70	SWI5-dependent HO expression protein 3
Cell-death regulation	BIRC6	VuNAC55	Baculoviral IAP repeat-containing protein
Cell-signalling	GIT_CC	VuNAC58, VuNAC64	GIT coiled-coil Rho guanine nucleotide exchange factor
Cytoskeleton synthesis	RPEL	VuNAC56	RPEL repeat
	FH2	VuNAC68-70	Formin Homology 2 Domain
	FPP	VuNAC68-71	Filament-like plant protein, long coiled protein
Mitosis	DASH_Dad4	VuNAC45	DASH complex subunit Dad4
	HAUS6_N	VuNAC64	HAUS augmin-like complex subunit 6 N-terminus
	CENP-F_leu_zip	VuNAC68-71	Leucine-rich repeats of kinetochore protein Cenp-F/LEK1
Gene expression	TFIIA	VuNAC39	Transcription factor IIA, alpha/beta subunit
	bZIP_1	VuNAC64	bZIP transcription factor
	THOC7	VuNAC68-70	Tho complex subunit 7
DNA repair	MutS_V	VuNAC83	MutS domain V
Iron uptake	ExbD	VuNAC45	Biopolymer transport protein ExbD/TolR
Respiratory complex	Oxidored_q4	VuNAC45	NADH-ubiquinone/plastoquinone oxidoreductase
	Pex26	VuNAC83	Pex26 protein
Electron transfer	V_ATPase_I	VuNAC07	V-type ATPase 116kDa subunit family
	VKOR	VuNAC45	Vitamin K epoxide reductase family
Unknown	DUF4562	VuNAC20	Domain of unknown function (DUF4562)
	PT-VENN	VuNAC41	Pre-toxin domain with VENN motif
	Pdase_C33_assoc	VuNAC51	Peptidase_C33-associated domain
	DUF5082	VuNAC64	Domain of unknown function (DUF5082)
	YycC	VuNAC68-70	YycC-like protein
	DUF1664	VuNAC45, VuNAC68-70	Protein of unknown function (DUF1664)
	zinc_ribbon_4	VuNAC85	zinc-ribbon domain
	zf-ribbon_3	VuNAC85, VuNAC86	zinc-ribbon domain
	RB_B	VuNAC87	Retinoblastoma-associated protein B domain

***Source: Pfam database**

3.3.1.3 Analysis of VuNAC domain structure and biochemical features

The length, domain span, theoretical pI, and molecular weight of the VuNAC proteins were indicated in Table 3.1. The shortest protein was VuNAC67 (145 aa, 16.9 kDa), and VuNAC48 was the largest (663 aa, 75.2 kDa). The length of the protein was associated with the phylogenetic groups. On average, Group VIb constituted the shortest VuNAC proteins (195 aa, 22.6), and Group VIc constituted the largest protein (510 aa, 57.4 kDa). Further, the average size of the conserved N-terminal VuNAC domain was 152 aa residues, unlike the 160 aa domain found in most plants, which varied among the subgroups. The unique cowpea-specific group (Group VII) consisted of the shortest domain (~146 aa), whereas, the SND-like (Group VIIIa and Group VIIIb) contained the largest domains (~162 aa). Also, the isoelectric point (pI) is a crucial biochemical property required for protein transport, solubility, and sub-cellular localization. The pI value ranged from 4.5 (VuNAC59) to 9.6 (VuNAC67). Group VIa comprised the most acidic proteins (average pI, 4.7), while Group Id constituted the most basic proteins (average pI, 9.2). 67.7% of the VuNAC proteins had acidic pI, suggesting their positively charged nature at physiological pH favoring the transport to negatively charged nuclear membranes, whereas, 27.7% of the VuNAC proteins had basic pI, difficult for nuclear import, hence might be tethered to organelle membrane or reside in the cytosol.

The VuNAC proteins contained five subdomains (A-E), except the VuNAC67 isoforms lacking the subdomain E (Fig. 3.2). Unlike in other species where subdomains A, C, and D are tightly conserved, the subdomains in VuNAC proteins (except A) were divergent. When examined closely, the sequences varied among the phylogenetic groups. The diversity in subdomain B, generally involved in dimerization, and subdomain C containing the DNA binding sites indicated assorted modes of regulation of different VuNAC members, depending on the developmental stage or tissue specificity. Moreover, the sequence alignment revealed conserved amino acid residues and positions, as indicated in Fig. 3.2. The residues G_3, F_6, P_8 E_{12}, and YL_{17} residues were completely conserved in subdomain A, except the Group VIII members, which did not conserve YL_{17} residues. Similarly, in all the groups (except group VIII), D_{36} and PW_{42} (subdomain B), W_{56}, FF_{58}, R_{71}, R_{74}, W_{81}, and TG_{99} (subdomain C) and W_{117} (subdomain D) were conserved. However, many residues were conserved but shifted in Group VIII members (FF_{65}, R_{78}, R_{81}, W_{96}, TG_{84}, and W_{135}). Further, several major conserved consensus sequences were found such as, -D[DE]L[IV]- (subdomain A), -DLxKx_2PW[DE]LP- (subdomain B), -EWYFFS-,-G[YF]WK[AT]TGxD[RK]x_{1-2}[IV]- (subdomain C), -

GxKKxLVFY-, -TxWxMHEY- (subdomain D), and -[WF]V[LV]CR[ILV][FY]x[KR]K- (subdomain E). The presence of the -D[DE]L[IV]- motif, associated with several calcium-dependent kinases, suggested involvement in cell signaling. The sequences -G[YF]WK[AT]TGxD[RK]x_{1-2}[IV]- (subdomain C) and -GxKKxLVFY were rich in positive amino acids suggesting their role in DNA binding activity, as reported previously [99]. The hydrophobic -GxKKxLVFY- were similar to the NAC repression domains (NARD), negatively regulating the transcription of WRKY, Dof, and APETALA 2 proteins [101]. Although the subdomain E was not tightly conserved, -E[DE]GWVVCRxKK- was conserved in the NST/VND-like (Group II) and CUC-like (Group IIIc) members, whereas, -LDDWVLCR- motif was conserved in SNAC-like Group I members.

3.3.2 The *VuNAC* genes exhibit prominent chromosomal duplication resulting in large paralogous groups

3.3.2.1 Intron/exon arrangement

The 90 *VuNAC* genes encoding the cowpea NAC family, their size, and locus were listed in Table 3.3. The average gene size was 3.1 kb, which varied from 1.1 kb (*VuNAC60*) to 16.4 kb (*VuNAC67*). The entire Group I genes were the shortest with an average size of 1.6 kb, whereas Group IIIa accommodated the largest genes, having an average length of 4.7 kb, followed by Group IIb (4.5 kb). To understand the structural similarity or diversity in the *VuNAC* genes of different functional groups, we generated an exon-intron map representing the coding sequences (CDS) and the 5'-untranslated regions (UTR) (Fig. 3.3A). The CDSs were interrupted by the introns varying in position and count, resulted from the genomic rearrangement and evolution. The highest intron count was witnessed in Group VI (*TIP*, *NTL8,* and *ANAC011*-like) and subgroup VIIIa (*SND*-like) members, which carried 5-6 introns in the CDS (6-7 introns in the whole gene). Most of the groups, like Group 1 (*SNAC*-like), Group 2 (*NST*/*VND*-like), Group III (*AtNAC1*/*NAM*/*CUC*-like), and Group V (*TERN*/*JUB1*-like), carried only two introns.

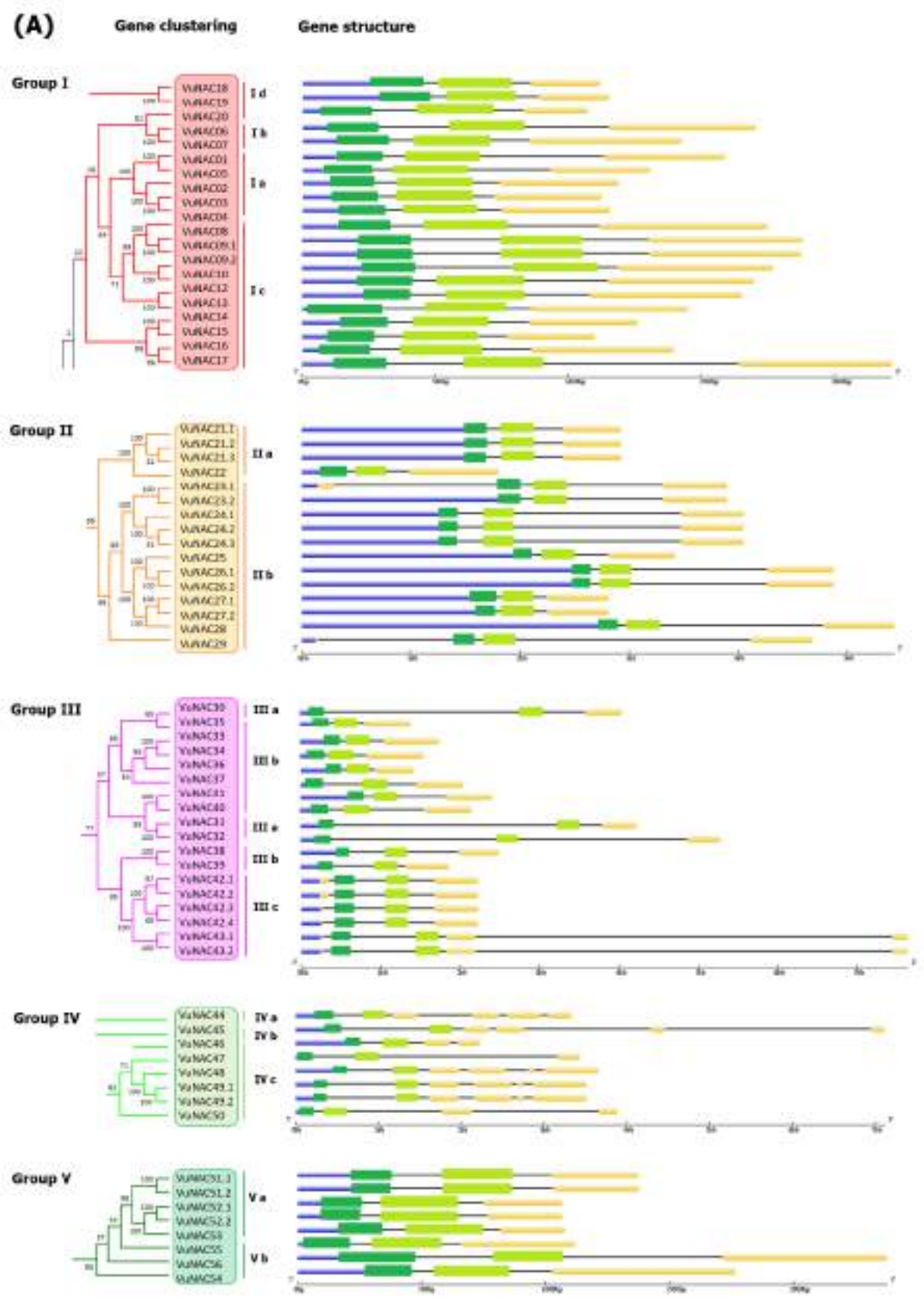

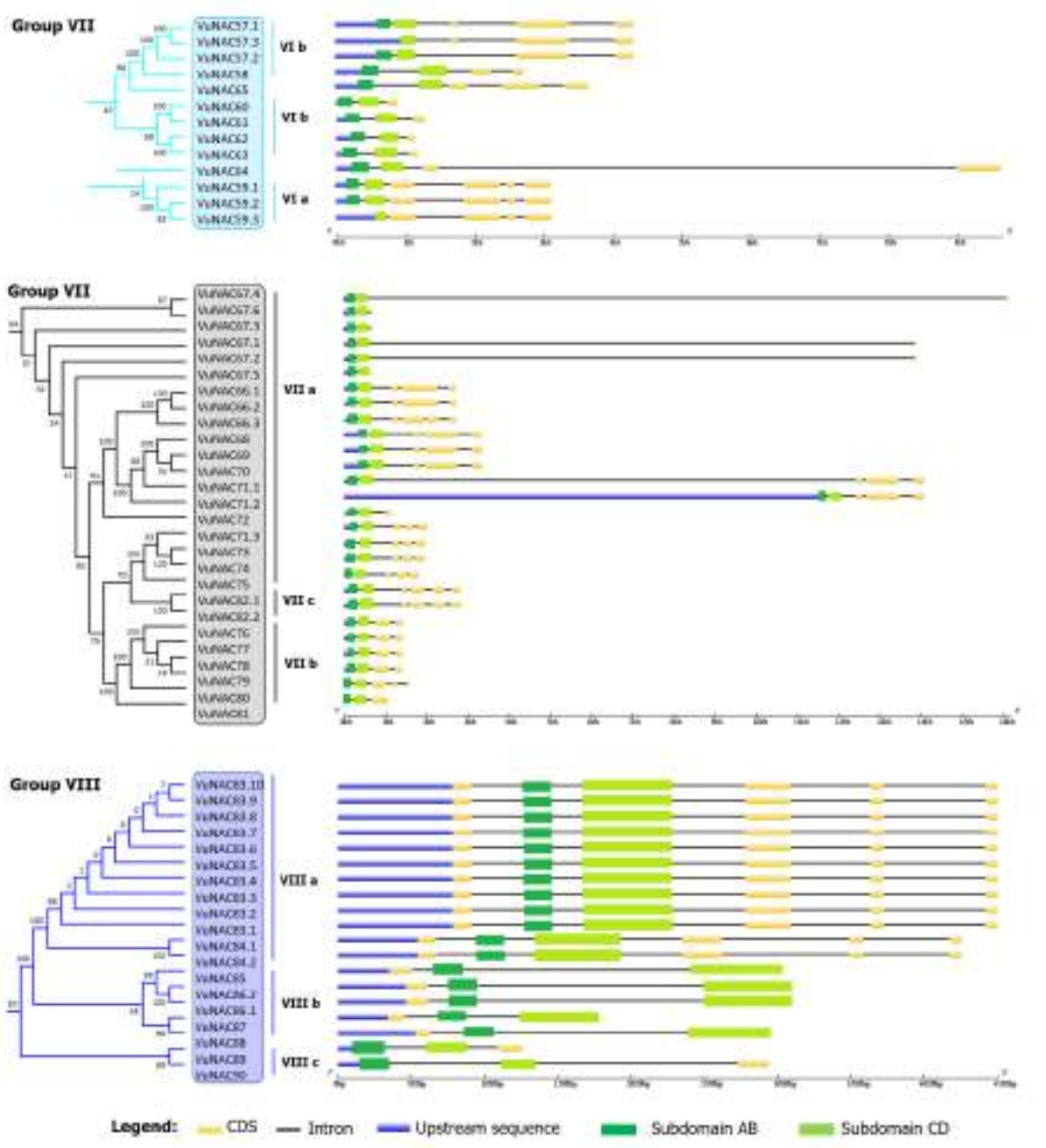

Fig. 3.3 Gene structure. (A) Intron/exon arrangement of VuNAC genes generated by GSDS 2.0 tool.

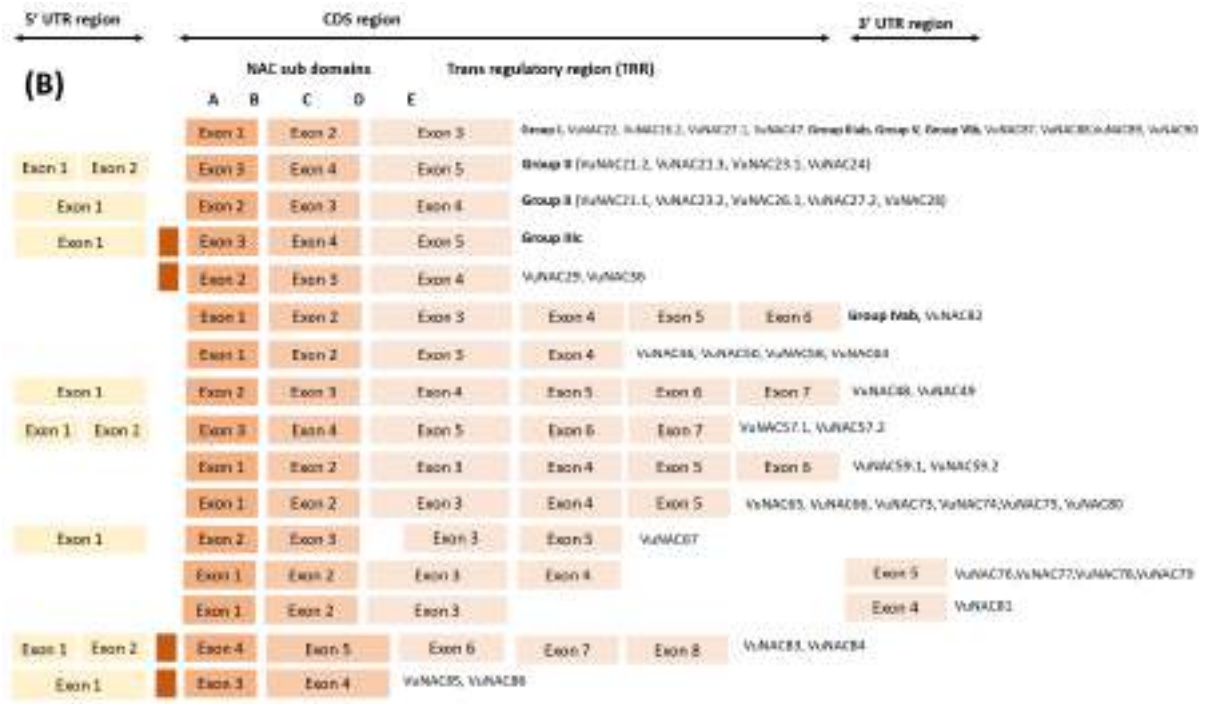

Fig. 3.3 Exon distribution. (B) Types of exons distribution over NAC domain, trans-activational regions (TAR), and untranslated regions (UTR).

Besides, the intron count varied in genes within the same group, such as Group VII (cowpea-specific) and Group VIII (*SND*-like). This variable distribution of introns in these groups indicated both exon loss and gain during the evolution to acquire the desired function. However, two types of introns were conserved in terms of position in most of the genes, the LP\x type (occurring after the LP residue), splitting the subdomain B and C, while the other intron type dividing subdomain D and E, but having no conserved residues (except in Group I with conserved [K/R]\LD). Nevertheless, the SND-like members of Group VIIIa and Group VIIIb lacked the second intron. The residues conserved in both *VuNAC* genes and their *AtNAC* homologs were highlighted in bold (Table 3.3). In addition, a schematic of the exon arrangement was illustrated in Fig. 3.3B. The exon count varied from 3-8 throughout the genes, with the N-terminal domain sharing 2-4 exons.

Table 3.3 List of VuNAC genes and their features

Name	Gene ID	Gene span	Strand	Size (bp)	Group	Introns (CDS)	Conserved intron positions	
							B/C domain	D/E domain
VuNAC01	114163399	Chr9::33300089...33302149	(-)	2061	**Ia**	2	**LP/G**	**R/LD**
VuNAC02	114178342	Chr3:4945775...4947276	(-)	1502	**Ia**	2	**LP/D**	**R/LD**
VuNAC03	114196185	Chr9:26464007...26465020	(+)	1202	**Ia**	2	**LP/E**	**R/LD**
VuNAC04	114196184	Chr9:26453906...26454919	(+)	1568	**Ia**	2	**LP/E**	**R/LD**
VuNAC05	114195332	Chr8:13486162...13487724	(+)	1563	**Ia**	2	**LP/G**	**R/LD**
VuNAC06	114168383	Chr11:16461521...16463576	(+)	2056	**Ib**	2	**LP/A**	**K/LD**
VuNAC07	114185763	Chr5:38122572...38123861	(+)	1747	**Ib**	2	**LP/S**	**K/LD**
VuNAC08	114186191	Chr5:38169866...38172210	(+)	2345	**Ic**	2	**LP/A**	**K/LD**
VuNAC09	114170041	Chr11:14743567...14745919	(+)	2353	**Ic**	2-3	**LP/A**	**K/LD**
VuNAC10	114177058	Chr3:10221122...10223084	(+)	1963	**Ic**	2	**LP/S**	**K/LD**
VuNAC11	114187328	Chr6:31924177...31926042	(+)	1866	**Ic**	2	**LP/S**	**K/LD**
VuNAC12	114181421	Chr4:27447443...27449529	(+)	2087	**Ic**	2	**LP/A**	**K/LD**
VuNAC13	114194335	Chr1:24039970...24041860	(+)	1891	**Ic**	2	**LP/E**	**K/LD**
VuNAC14	114174217	Chr2:20264548...20266034	(+)	1487	**Ic**	2	**LP/D**	**K/LD**
VuNAC15	114175881	Chr3:33676977...33678467	(+)	1491	**Ic**	2	**LP/D**	**K/LD**
VuNAC16	114196146	Chr1:34039212...34040797	(-)	1586	**Ic**	2	**LP/N**	**K/LD**
VuNAC17	114184067	Chr5:44383357...44385959	(+)	2603	**Ic**	2	**LQ/S**	**K/LD**
VuNAC18	114186324	Chr5:97829...99159	(-)	1331	**Id**	2	LP/G	H/N
VuNAC19	114185250	Chr5:90905...92265	(-)	1361	**Id**	2	LP/G	Q/A
VuNAC20	114178911	Chr3:4078831...4080020	(+)	1190	**Id**	2	LP/G	Q/A
VuNAC21	114178728	Chr1:7557707...7560526	(-)	3080	**IIa**	2	LK/D	**Q/ED**
VuNAC22	114166321	Chr10:37065813...37067838	(-)	2026	**IIa**	2	IQ/E	I/VS
VuNAC23	114173187	Chr2:27622897...27627169	(-)	4273	**IIb**	2-3	LQ/D	**Q/EE**
VuNAC24	114176769	Chr3:42697313...42701453	(-)	4141	**IIb**	2	**LQ/E**	**Q/EE**
VuNAC25	114169063	Chr11:41298448...41302298	(-)	3851	**IIb**	2	**LQ/E**	**Q/EE**
VuNAC26	114179857	Chr1:1000216...1005436	(+)	5221	**IIb**	2	**LQ/E**	**Q/EE**
VuNAC27	114173283	Chr2:31205839...31208915	(-)	3077	**IIb**	2	**LQ/E**	**Q/EE**
VuNAC28	114177117	Chr3:49676234...49682116	(-)	5883	**IIb**	2	**LQ/E**	P/EE
VuNAC29	114189997	Chr7:32869460...32874520	(+)	5061	**IIb**	3	LQ/D	**Q/EE**
VuNAC30	114162839	Chr1:12677500...12681754	(+)	4255	**IIIa**	2	IP/E	**K/ED**
VuNAC31	114189778	Chr7:18090097...18094361	(-)	4265	**IIIa**	2	**LP/E**	**K/ED**
VuNAC32	114178852	Chr1:32489855...32495432	(-)	5578	**IIIa**	2	**LP/E**	**K/ED**
VuNAC33	114180967	Chr4:27713365...27715433	(+)	2069	**IIIb**	2	**LP/K**	**K/DE**
VuNAC34	114194056	Chr1:24102998...24104991	(+)	1994	**IIIb**	2	**LP/K**	**K/DE**
VuNAC35	114174921	Chr3:53536846...53538554	(+)	1709	**IIIb**	2	**LP/W**	**K/DE**
VuNAC36	114181690	Chr4:5131276...5132850	(-)	1575	**IIIb**	2	**LP/C**	M/ND
VuNAC37	114164798	Chr9:42750395...42752551	(-)	2157	**IIIb**	2	**LP/D**	K/DE
VuNAC38	114177363	Chr3:1224105...1226855	(-)	2751	**IIIb**	2	**LP/G**	K/EE
VuNAC39	114181473	Chr4:1707815...1709829	(+)	2015	**IIIb**	2	**LP/G**	**K/DE**
VuNAC40	114170586	Chr11:12643122...12645544	(+)	2423	**IIIb**	2	**LP/E**	**K/DE**
VuNAC41	114185732	Chr5:36963430...36966174	(+)	2745	**IIIb**	2	**LP/E**	**K/DE**
VuNAC42	114162425	Chr9:37290224...37292661	(+)	2438	**IIIc**	3	**LP/G**	R/QD
VuNAC43	114194562	Chr8:9627264...9635079	(+)	7816	**IIIc**	4	**LP/G**	K/QD
VuNAC44	114163198	Chr9:30033650...30037216	(+)	3567	**IVa**	5	MP/D	Q/NA
VuNAC45	114184747	Chr5:42786452...42793889	(-)	7438	**IVb**	5	**LP/A**	Q/DS
VuNAC46	114178578	Chr3:47848076...47850747	(-)	2672	**IVc**	3	**LP/E**	Q/GG
VuNAC47	114181023	Chr4:3479486...3483250	(-)	3765	**IVc**	2	LA/E	Q/DT
VuNAC48	114187476	Chr6:22802804...22806589	(+)	3786	**IVc**	5	**LP/G**	**Q/DA**
VuNAC49	114193845	Chr8:31257369...31261040	(-)	3672	**IVc**	6	**LP/G**	**Q/DA**
VuNAC50	114162369	Chr1:11308220...11312430	(-)	4211	**IVc**	3	**LP/D**	K/DS
VuNAC51	114179648	Chr1:35724730...35726351	(+)	1622	**Va**	2	LP/Q	Q/LR
VuNAC52	114184259	Chr5:42838225...42839587	(-)	1363	**Va**	2	LP/S	**K**/(FL/**LR**)
VuNAC53	114169023	Chr11:33272503...33273871	(-)	1369	**Va**	2	LP/T	Q/LR
VuNAC54	114168448	Chr11:39749198...39750659	(+)	1462	**Vb**	2	LP/D	K/EI
VuNAC55	114177310	Chr3:63907468...63910090	(-)	2623	**Vb**	2	**LP/A**	**K/AE**
VuNAC56	114174141	Chr2:20683641...20685538	(-)	1898	**Vb**	2	**LP/K**	N/ES
VuNAC57	114164401	Chr9:27465669...27470240	(-)	4572	**VIa**	3-4	**LP/D**	Q/(LI/DS)
VuNAC58	114178735	Chr3:5228252...5231490	(-)	3239	**VIa**	3	LP/A	Q/HS
VuNAC59	114191703	Chr7:30733818...30737355	(+)	3538	**VIa**	4-5	LP/P	L/(VR/DV)
VuNAC60	114164463	Chr9:25352552...25353640	(-)	1089	**VIb**	2	LN/G	H/DQ
VuNAC61	114179297	Chr3:5136355...5137852	(+)	1498	**VIb**	2	LN/G	S/DQ
VuNAC62	114177146	Chr3:13165272...13166898	(+)	1627	**VIb**	2	LH/G	A/DY
VuNAC63	114187367	Chr6:33442316...33443725	(+)	1410	**VIb**	2	LH/G	A/DH
VuNAC64	114191704	Chr7:30718969...30728844	(+)	9876	**VIc**	3	LA/D	Q/DA
VuNAC65	114190985	Chr7:33239015...33243002	(-)	3988	**VIc**	4	**LP/G**	**K/DY**
VuNAC66	114167597	Chr10:37412180...37415600	(-)	3421	**VIIa**	4-5	VP/A	Q/(KA/AF)
VuNAC67	114167089	Chr10:2401257...2417694	(+)	16438	**VIIa**	2	VP/V	(Q/S)/(DG/CV/SA/NQ)
VuNAC68	114166210	Chr10:37420985...37424727	(-)	3743	**VIIa**	4	VP/G	E/NA
VuNAC69	114167350	Chr10:37458729...37462474	(-)	3746	**VIIa**	4	VP/G	E/NA

VuNAC70	114172047	NA:24231…27975	(-)	3745	**VIIa**	4	VP/G	E/NA
VuNAC71	114167348	Chr10:37477738…37492219	(-)	14482	**VIIa**	4	VP/G	(E/Q)/(NA/RC)
VuNAC72	114172054	NA:45134…46296	(-)	1163	**VIIa**	2	VP/G	Q/NA
VuNAC73	114172048	NA:34871…37394	(-)	2524	**VIIa**	4	VP/G	E/RC
VuNAC74	114172049	NA:16422…18331	(-)	2575	**VIIa**	4	VP/G	E/RC
VuNAC75	114165639	Chr10:37469895…37471753	(-)	1859	**VIIa**	4	VP/G	Q/RT
VuNAC76	114167352	Chr10:37464699…37466722	(-)	2024	**VIIb**	3	VP/M	Q/RT
VuNAC77	114172052	NA:11384…13240	(-)	1857	**VIIb**	3	VP/M	Q/RT
VuNAC78	114172053	NA:30200…32223	(-)	2024	**VIIb**	3	VP/M	Q/RT
VuNAC79	114167353	Chr10:37485056…37487114	(-)	2059	**VIIb**	3	VP/M	Q/RT
VuNAC80	114165640	Chr10:37473460…37475034	(-)	1575	**VIIb**	4	VP/M	Q/RT
VuNAC81	114166939	Chr10:2396767…2398655	(+)	1889	**VIIc**	2	VP/M	Q/RT
VuNAC82	114167351	Chr10:37493130…37496409	(-)	3280	**VIIc**	5	VP/A	Q/(KT/KF)
VuNAC83	114180975	Chr4:333751…338854	(+)	5104	**VIIIa**	5	**LP/G**	-
VuNAC84	114176561	Chr3:2034088…2038887	(-)	4800	**VIIIa**	5	**LP/G**	-
VuNAC85	114187164	Chr6:31262634…31265962	(-)	3329	**VIIIb**	2	**LP/G**	-
VuNAC86	114176422	Chr3:8920043…8923188	(-)	3146	**VIIIb**	2	**LP/G**	-
VuNAC87	114185617	Chr5:40313578…40315813	(-)	2236	**VIIIb**	2	**LP/G**	-
VuNAC88	114168788	Chr11:29140079…29143447	(-)	3369	**VIIIb**	2	**LP/G**	-
VuNAC89	114178462	Chr1:20856718…20858172	(+)	1455	**VIIIc**	2	**LP/G**	K/MS
VuNAC90	114181461	Chr4:20370129…20373167	(+)	3039	**VIIIc**	2	**LP/G**	Q/MA

3.3.2.2 Chromosome location, duplication, and orthologous groups

An illustration of the *VuNAC* genes mapped throughout the eleven cowpea chromosomes was shown in Fig. 3.4A (the locus of six genes could not be determined). The genes were scattered over different chromosomes, showing no correlation between the functional groups and location, except the Group VII (Cowpea-specific) members located on VuChr10. The most considerable portion of the genes (15 genes) was shared by VuChr3, followed by VuChr10 harboring 12 genes. The distribution of the rest of the gene was as follows: VuChr1 (10 genes), VuChr5 (nine genes), VuChr9 (eight genes), VuChr4 and VuChr11 (seven genes each), VuChr7 (five genes), VuChr2 and VuChr6 (four genes each), and VuChr8 (three genes). In addition, the VuNAC family was rich in tandem and segmental duplications. Overall, 54 *VuNAC* genes (60% of total abundance) were involved in duplications. Total 11 gene clusters were found, out of which eight gene pairs/groups of the same functional groups were found to be tandemly duplicated, lying <100 kb apart, *i.e.*, (*VuNAC03*, *VuNAC04*, Chr9), (*VuNAC07*, *VuNAC08*, Chr5), (*VuNAC18*, *VuNAC19*, Chr5), (*VuNAC58*, *VuNAC61*, Chr3), (*VuNAC61*, *VuNAC62*, Chr3), (*VuNAC59*, *VuNAC64*, Chr7), (*VuNAC67*, *VuNAC81*, Chr10) and (*VuNAC66*, *VuNAC68*, *VuNAC69*, *VuNAC71*, *VuNAC75*, *VuNAC76*, *VuNAC79* and *VuNAC80*, Chr10), as indicated in Fig. 3.4A. In addition, 18 segmental duplicates with ≥70% similarity were found, as depicted in Fig. 3.4B and Table A1.4. Overall, there were 22 paralogous groups within the VuNAC family based on phylogenetic closeness, regardless of the chromosomal locations, including the five tandem duplications and nine segmental duplications.

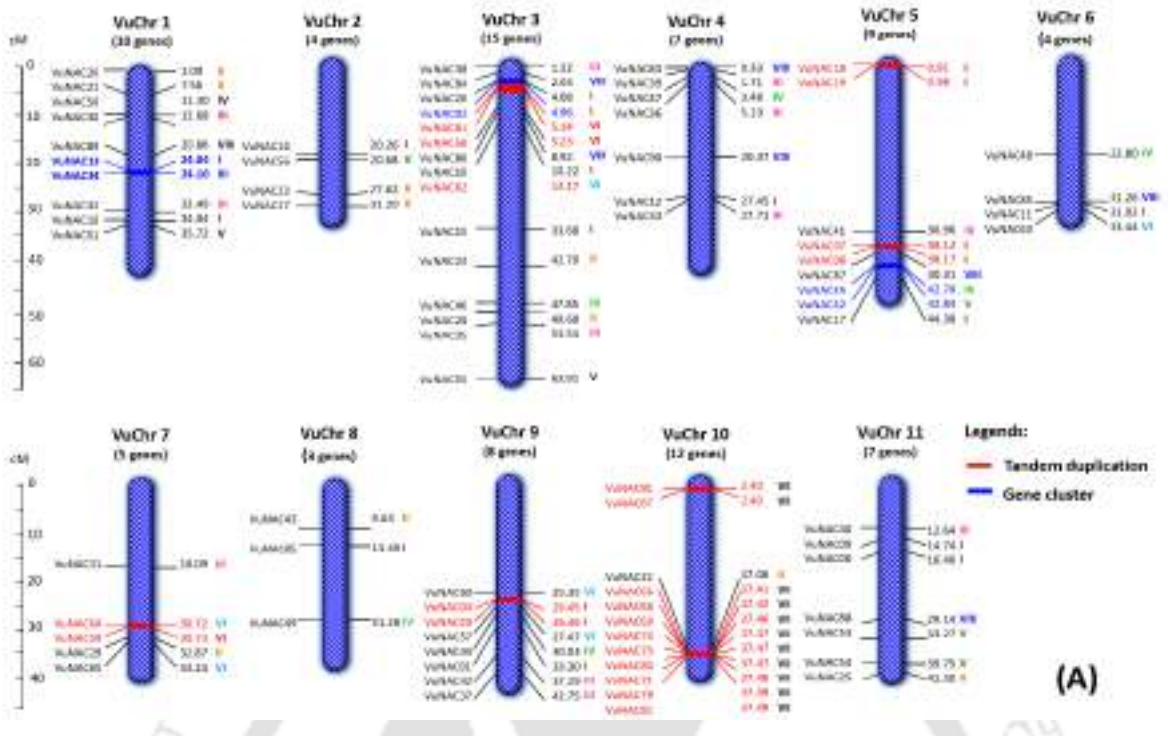

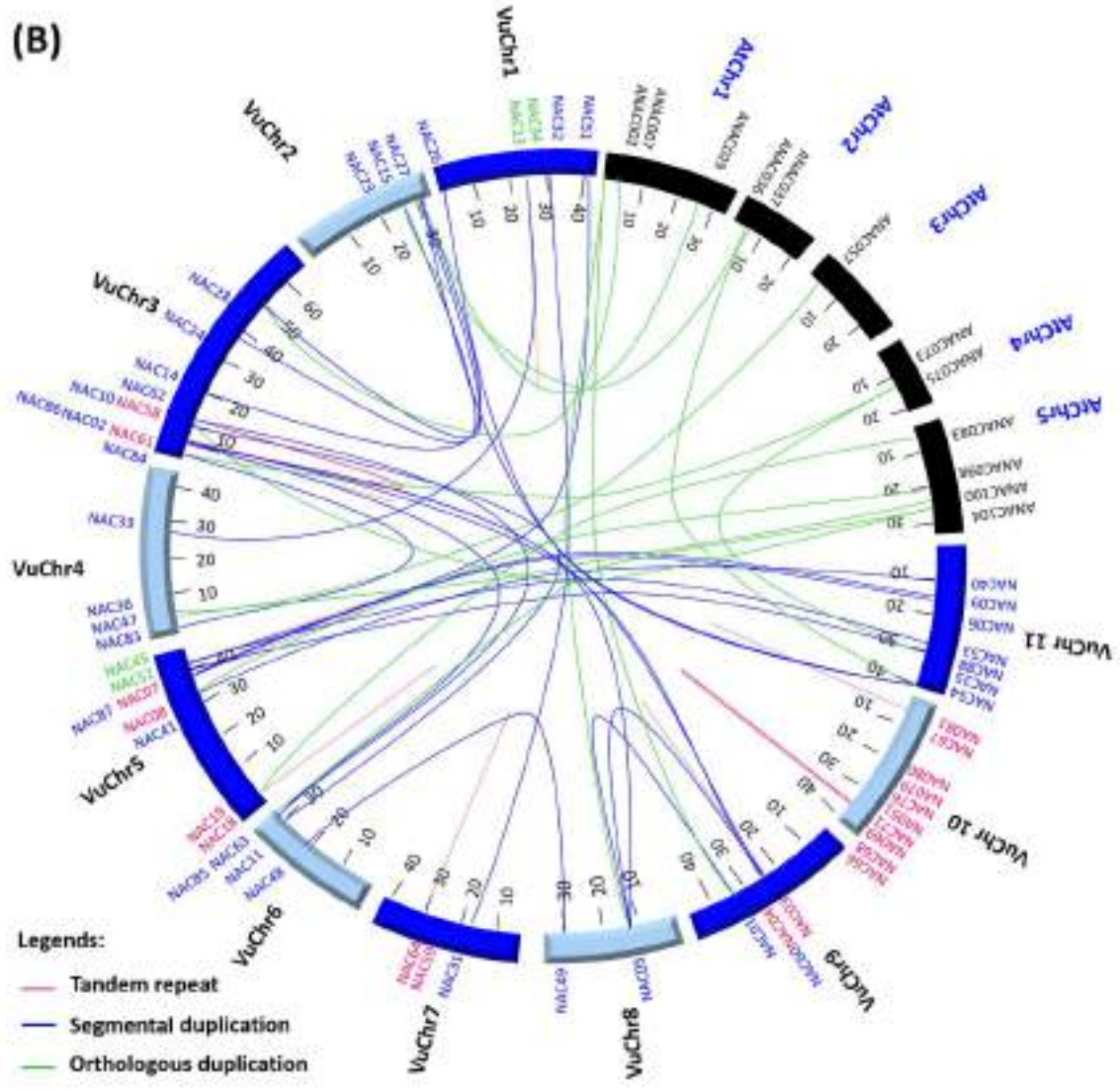

Fig. 3.4 Gene location and duplication. (A) Chromosomal distribution of the VuNAC genes over eleven cowpea chromosomes. **(B)** Representation of the tandem and segmental duplications (≥ 70% protein similarity) and the orthologous groups from Arabidopsis (≥ 70 % protein similarity).

This study indicated that the VuNAC family expanded through large-scale chromosomal duplication events due to selective pressures. We also identified 22 orthologous groups using comparative analysis between cowpea and arabidopsis NAC family. The 12 orthologous groups with ≥70% similarity were (*VuNAC01*, *VuNAC05*, *ANAC002*/*ATAF1*), (*VuNAC14*, *VuNAC15*, *ANAC029*/*NAP*), (*VuNAC18*, *VuNAC19*, *ANAC083*/*VNI2*), (*VuNAC23*, *VuNAC24*, *ANAC037*/*VND1*), (*VuNAC25*, *VuNAC26*, *VuNAC27*, *VuNAC28*, *ANAC007*/*VND4*), (*VuNAC35*, *VuNAC36*, *VuNAC100*), (*VuNAC40*, *VuNAC41*, *ANAC098*/*CUC2*), (*VuNAC47*, *ANAC057*), (*VuNAC54*, *ANAC036*), (*VuNAC60*, *VuNAC61*, *VuNAC62*, *VuNAC63*, *ANAC104*/*XND1*), (*VuNAC83*, *VuNAC84*, *ANAC075*) and (*VuNAC85*, *VuNAC86*, *VuNAC87*, *VuNAC88*, *ANAC073*/*SND2*), as depicted in Fig. 3.4.B.

3.3.3 Detection of conserved motifs in TAR region, transmembrane motifs (TMM), and nuclear localization signals (NLS)

Apart from the N-terminal VuNAC domains, as shown in Fig. 3.2, the C-terminal transcriptional activation region (TAR) consisted of short stretches of conserved patterns that may be crucial for protein activity. To inspect conservation throughout the protein, including the TAR, we performed a motif hunt by MEME analysis that identified signature sequences associated with different functional groups (Fig. 3.5). We found 50 conserved motifs occurring in at least three proteins, listed in Table A1.5, Appendix 1. In Group II proteins, we found motif 21 and motif 20, *i.e.,* QLPQL[EF]SP and QVTDWR[AV]LDK[FL]VASQLS, which resembled the LP box and WQ-box, known for transcriptional activity in NST-like proteins (Group II) [341]. In Group VIII, serine-rich motif 30 (NLSSVSSSDLIDAKL) and motif 12 (NNSSRRDSGSGSCSS) were detected along with the glutamine-rich motif 7 (QQHQQHQQHQQHAHHQ). The function of these motifs could not be understood. Cowpea-specific conserved patterns were also detected in Group VII members, like motif 43 (VHEGVCM[PS]SPIHEKKQEKKKKKKS[IK]FSFF), which was rich in lysine residues at the C-terminal end. Besides, we also detected some conserved motifs by sequence alignment, as shown in Fig. 3.6. The serine-rich regions SDS[IVM]x[KR]Lxx[TS]xSSxSeQVVSP and [EQ]xSNGSSxSSSSH[VL]xD[MV][VL]ES were found in the stress-responsive Group I.

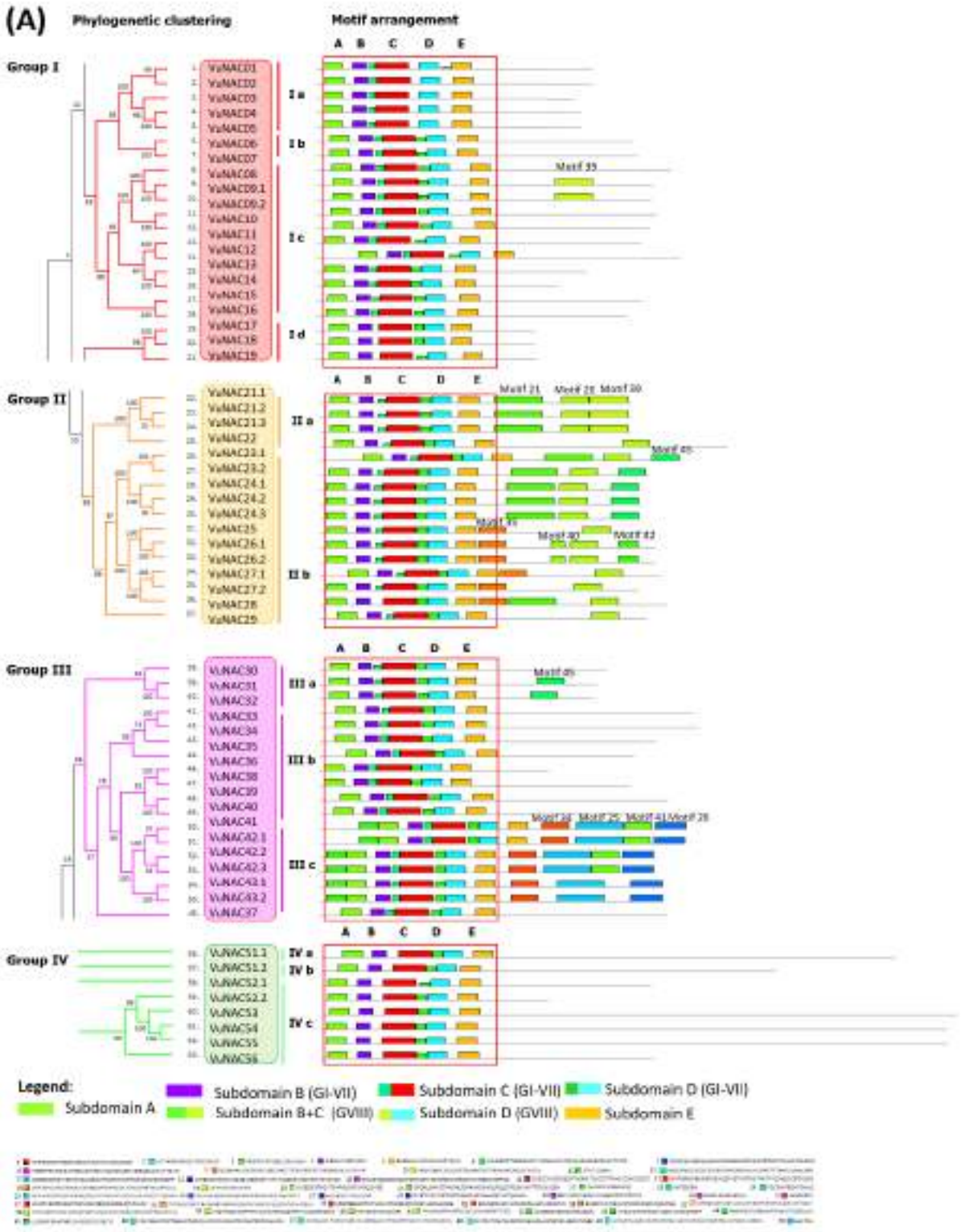

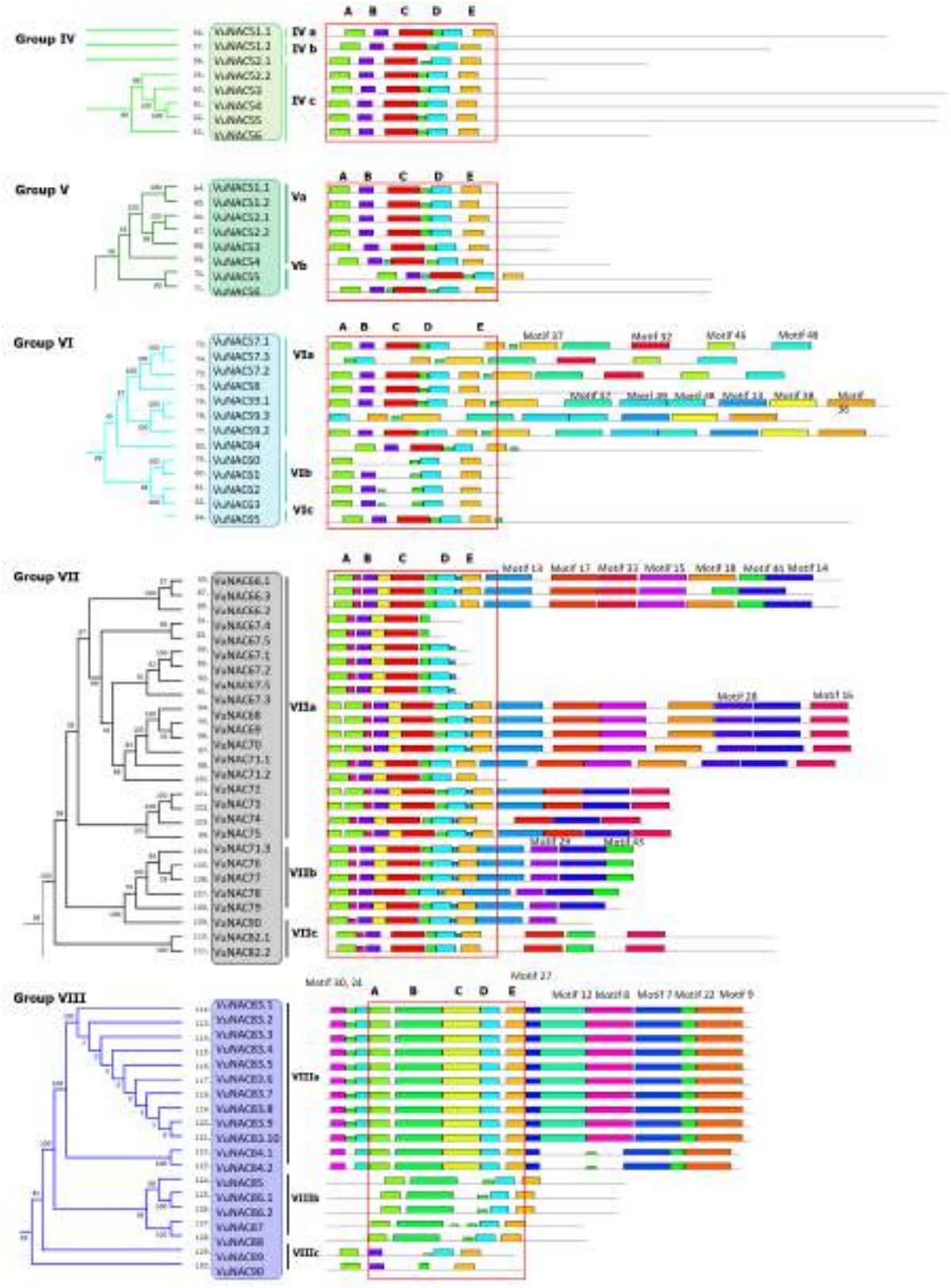

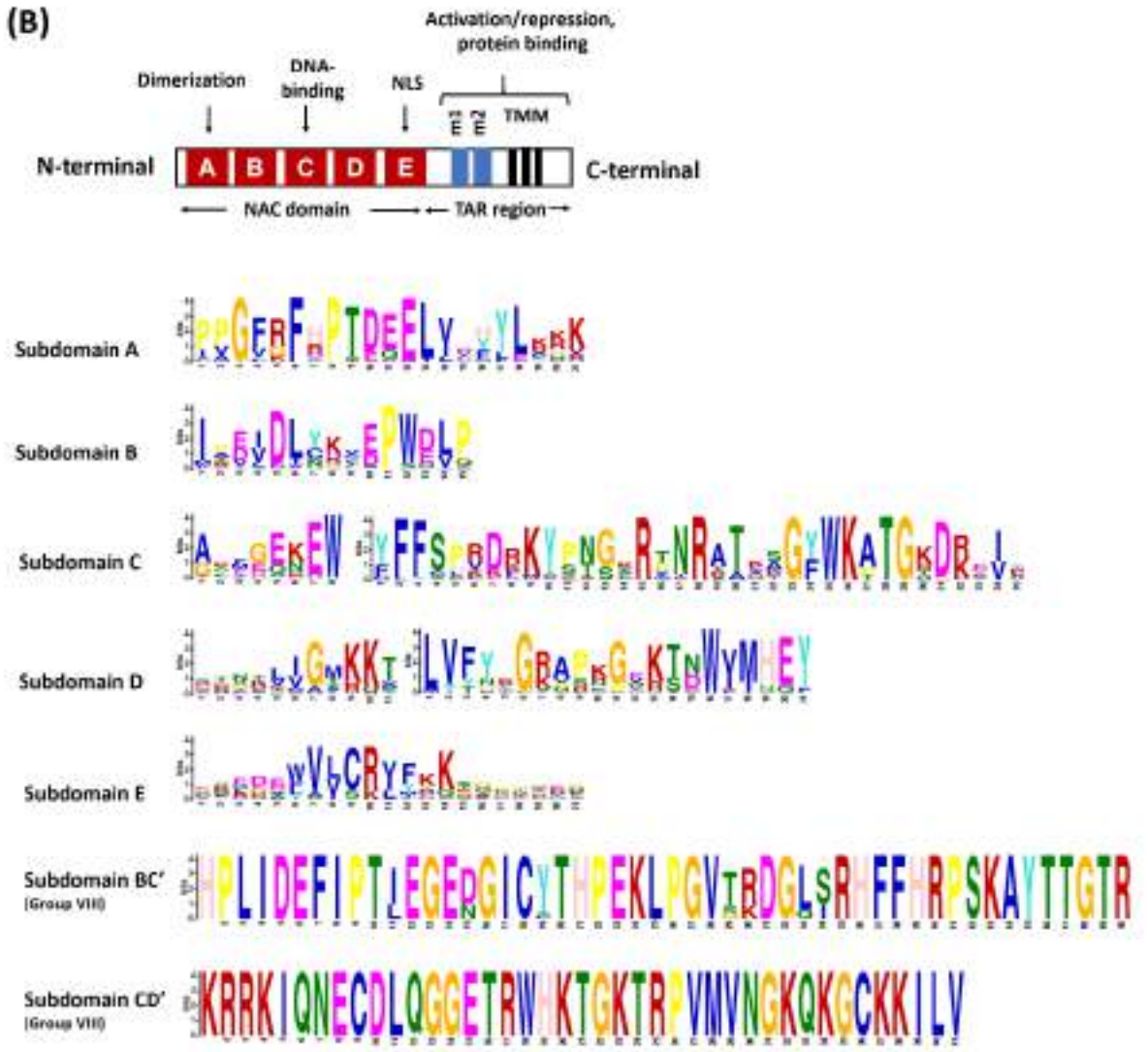

Fig. 3.5 Conserved motif detection. (A) Analysis of conserved motifs in VuNAC protein (including the TAR regions) by MEME tool. **(B)** Schematic representation of protein domain architecture (top) and sequence logo of the N-terminal sub-domains generated from the position-specific scoring matrices (below) 130 VuNAC proteins. Group I-VII proteins had a similar architecture of subdomains (A-E), except for the Group VIII members. The height of each symbol is proportional to the relative frequency of the amino acid residue, indicating its conservation at each position. The color denoted the chemical properties: green for polar, non-charged, and non-aliphatic residues (N, Q, S, and T), magenta for acidic residues (D, E), blue for hydrophobic residues (A, C, F, I, L, V, W, and M), red for positively charged residues (K, R), pink for histidine (H), orange for glycine (G), yellow for proline (P), and turquoise for tyrosine (Y).

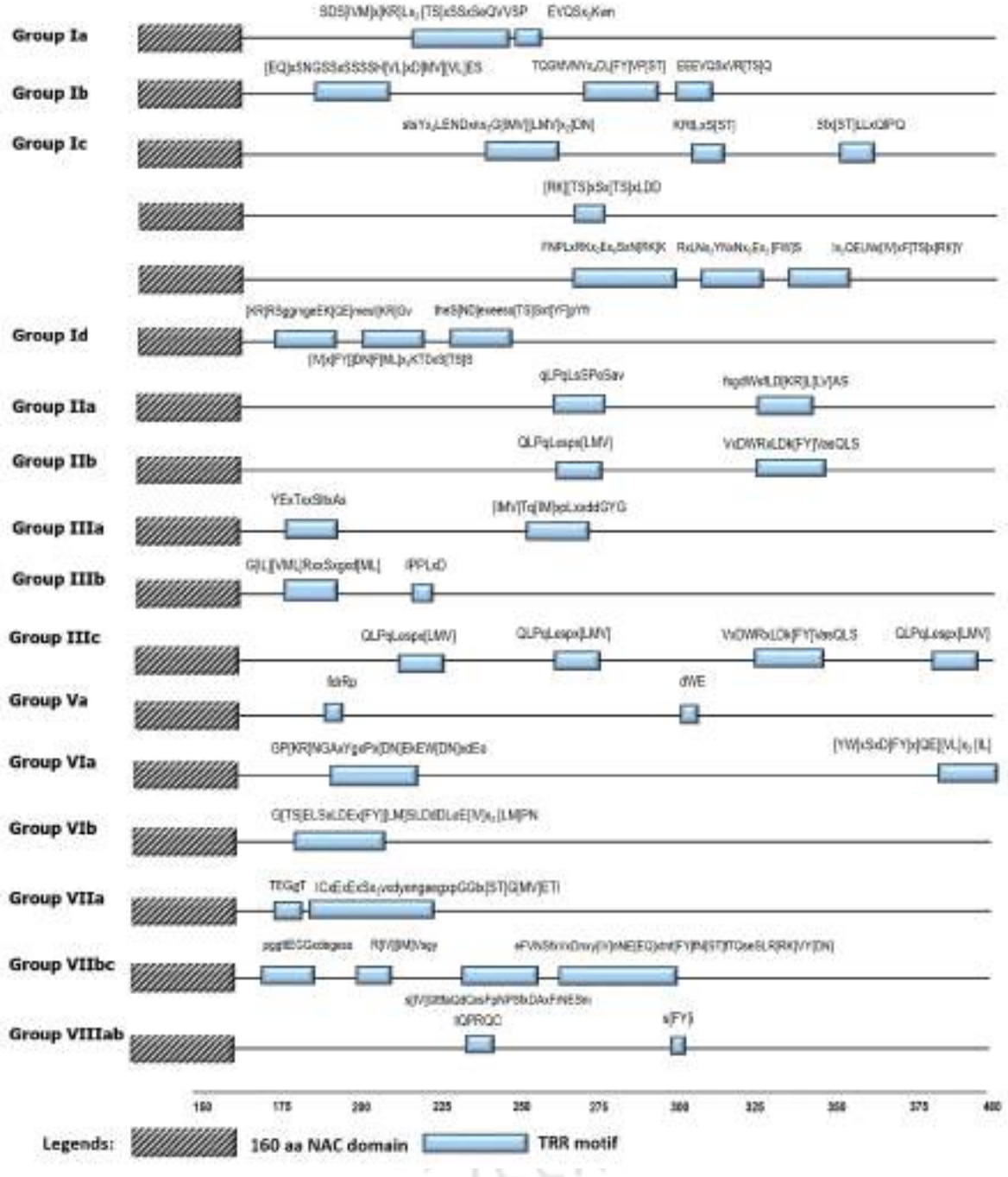

Fig. 3.6 Conserved motif detection in the TAR region. Identification of conserved motifs in TAR by sequence alignment.

The signature motif present of XND protein, *i.e.*, G[TS]ELSxLDEx[FY][LM]SLDdDLeE[IV]xx[LM]PN, was detected in Group VIb members. These findings suggested that, besides the N-terminal domain, the TAR regions of paralogous proteins also manifested conservation, hence crucial for the functional determination of the protein. Moreover, no notable similarity was found in the TAR regions of the orthologous groups found in arabidopsis, stipulating distinct functions of the VuNAC proteins.

The NAC proteins are also regulated at post-translational levels. Many NAC TFs (~10%) are physically tethered with the membrane of sub-cellular organelles, require proteolytic cleavage for release, and non-covalent interactions for activation [342]. The examination of signaling sequences revealed that 12 VuNAC proteins carried a transmembrane motif (TMM), namely VuNTM1-VuNTM12 (VuNAC with Transmembrane Motif), shown in Supplementary Fig. 3.7A. The TMM domain was located at the C-terminal end of eleven proteins, except in the VuNTL1 (VuNAC13) case, carrying the transmembrane helix motif at the N-terminal region. Eighty percent of the TMM sequence of VuNAC proteins was made of hydrophobic residues primarily containing Leu, Ile, and Ser residues. Both the bitopic (TMMs spanning the membrane once having a single transmembrane α-helix) and polytopic (TMMs spanning the membrane multiple times containing multi α-helical motif) were detected. The functioning of such members might be inducible and act only in response to some stimuli such as environmental or endoplasmic reticulum (ER) stress response. Hence, the VuNTL proteins could be explored for the genetic engineering of stress tolerance.

After activation, all the TFs are transported to their functional sites in the nucleus *via* importins and cargo molecules, which recognize the nuclear localization signals (NLS). The NLSs detected in the VuNAC proteins were listed in Table A1.6, Appendix 1. The majority of the proteins contained multiple NLS located primarily in the N-terminal region. Some NLS motifs were monopartite, having a single cluster of 3-4 consecutive positive charged amino acid residues. Besides, bipartite NLSs containing two clusters separated by a linker sequence of 10-12 residues were also recognized. The distribution of NLS in Group I-III members was represented in Fig. 3.7B, showing the bipartite N-terminal NLSs R-x-R-K-x5-R-x2-R-x7-K-x5-K, K-K-x-LVFY-x2-K-x2-K-x2-K-x8-R, RKK-x3-[R/K][R/K]-x6-[R/K]-x8-R-x-R, K-x-K-K-x5-R-x2-R-x7-K-x3-R-x-K, K-K-x-LVFY-K-x-R-x5-K-x8-R, and the monopartite C-terminal NLSs, R-x2-R-K-K-x3-R and K[K/R]-x4-R-x3-K.

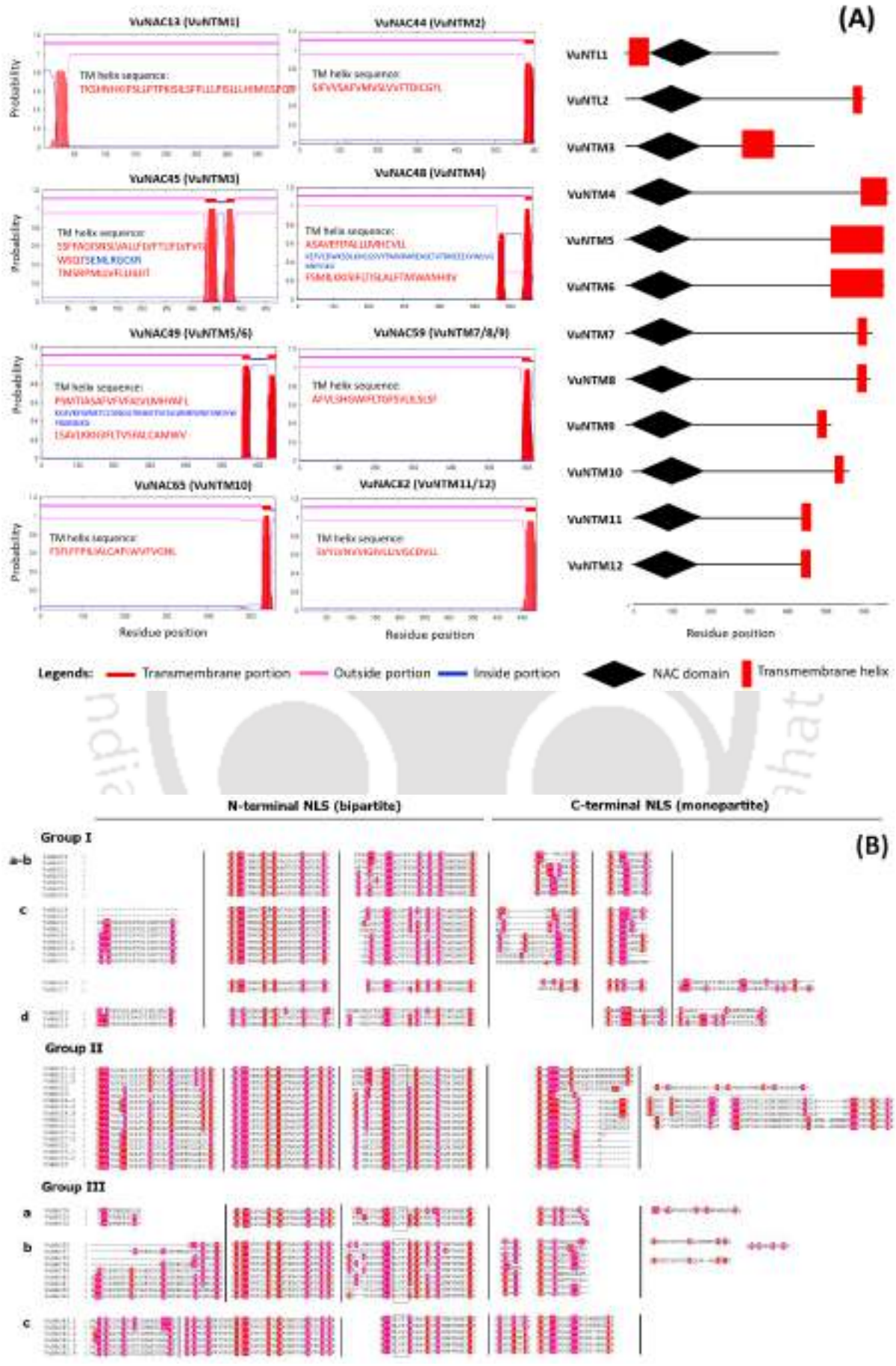

Fig. 3.7 Transmembrane motifs (TMM) and nuclear localization signals (NLS). (A) Depiction of the VuNTMs, VuNAC with transmembrane motifs (left), an illustration of their position (right). **(B)** Representation of bipartite and monopartite NLSs identified in ATAF-like Group I, VND-like Group II, and NAM-like Group III. The positively charged residues arginine and lysine were highlighted in red and pink, respectively.

3.3.4 *VuNAC* genes feature unique promoter architecture

3.3.4.1 The arrangement of preferentially located motifs (PLM) in the core region

Each promoter has unique gene-specific architecture dictating the controlled expression. The core region (typically spanning from -60 bp to +40 bp) may consist of preferentially located motifs (PLMs), such as transcription start site (TSS), YR region, an Initiator element (Inr), downstream promoter element (DPE), TATA box, TC-rich element, CAAT box, required for the binding of RNA polymerase and TFs [343]. The major PLMs identified in the 130 VuNAC coding sequences were mapped in Fig. 3.8A. The promoters of 78 genes (60%) possessed a TATA box, with its position varying from +9 to +55 bp relative to the TSS (+1). Out of those 78 TATA boxes, 18 were canonical (TATAWAWR), while 60 were non-canonical, with TATAWA consensus or other variations (TATA-variants). The TC-rich element was found in 69 promoters (53%), whose position varied from +14 to +53 bp. We found none of the TATA box or TC-rich elements in 19 promoters (14.6%) sequences (Fig. 3.8B). Depending on the presence of the TATA box or TC-rich element, the *VuNAC* promoters were classified into four classes, as listed in Table A1.7, Appendix 1. 21.5% of the promoters fell into Class I type, containing both the TATA box and TC-rich elements governing the transcription. 37.6% of the promoters were categorized as Class II types, having only TATA box (canonical or variant) but no TC-rich element. 26% of the promoters were Class III types, which were TATA-less but had the TC-rich element in the positions of the TATA box. The promoters not possessing any PLMs (TATA box and TC-rich elements) were categorized as Class IV type. The TSS was associated with a 'YR' sequence, CA(44.6% promoters), CG(13% promoters), TG (22.3% promoters), and TA(0.76% promoters), defining the (+1) position (TSS). 19% of the TSS did not follow the YR rule. In addition, we found that the core promoter region (-100 bp to +1) and the 5'-UTR (+1 to +200 bp) were rich in pyrimidines (TC-rich regions), as shown in Fig. 3.8C. The genes encoding Group I, Group II, Group VII, and Group VIII proteins were rich in distinctive TC-rich repeats with 60-70 % pyrimidine composition in the promoter core and 5'-UTR region. As per previous reports, the presence of TC-repeats in

the 5-UTR regions ensures high-level gene expression., whereas the TC-repeats in core regions may facilitate defense mechanisms and stress induction [344].

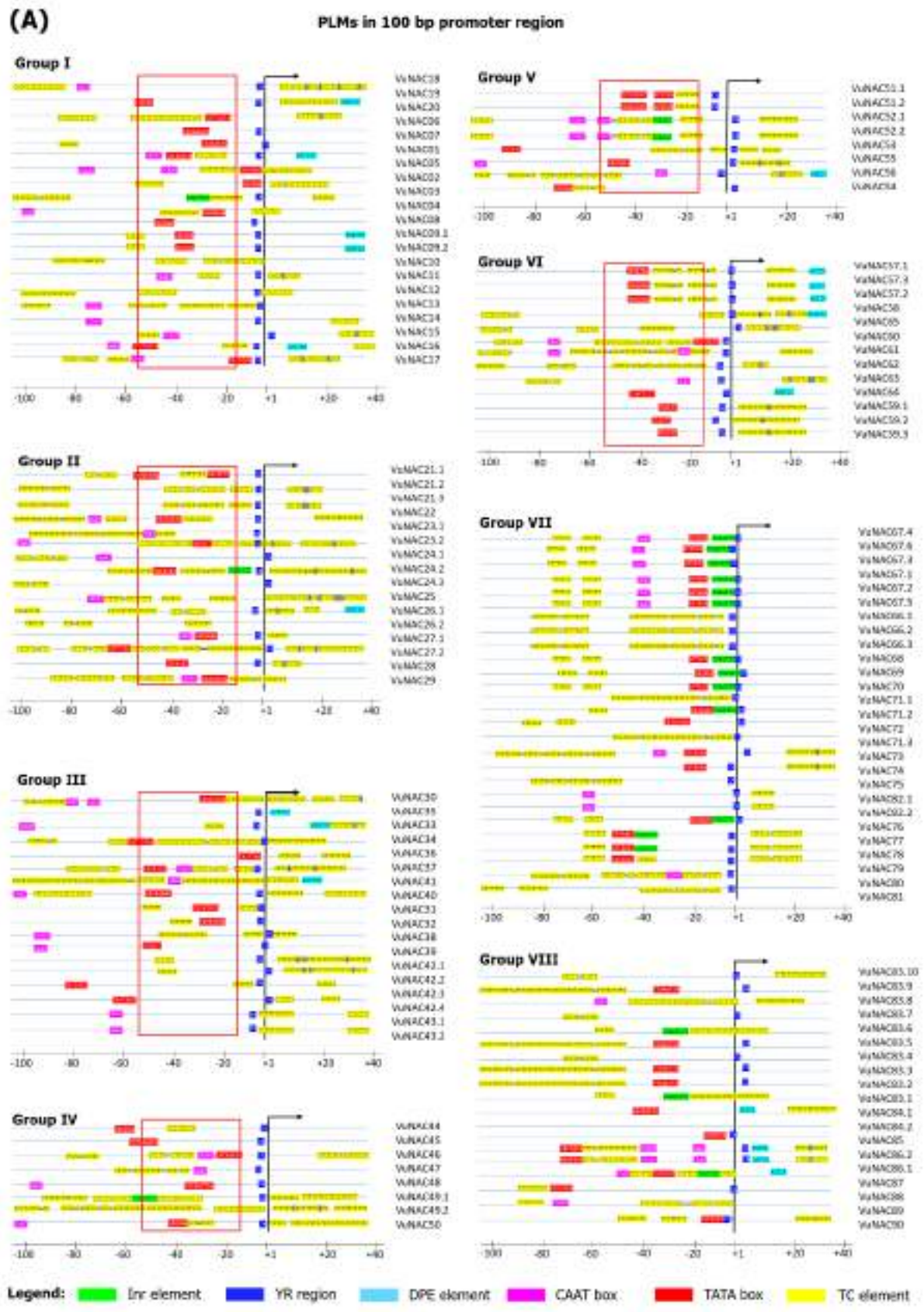

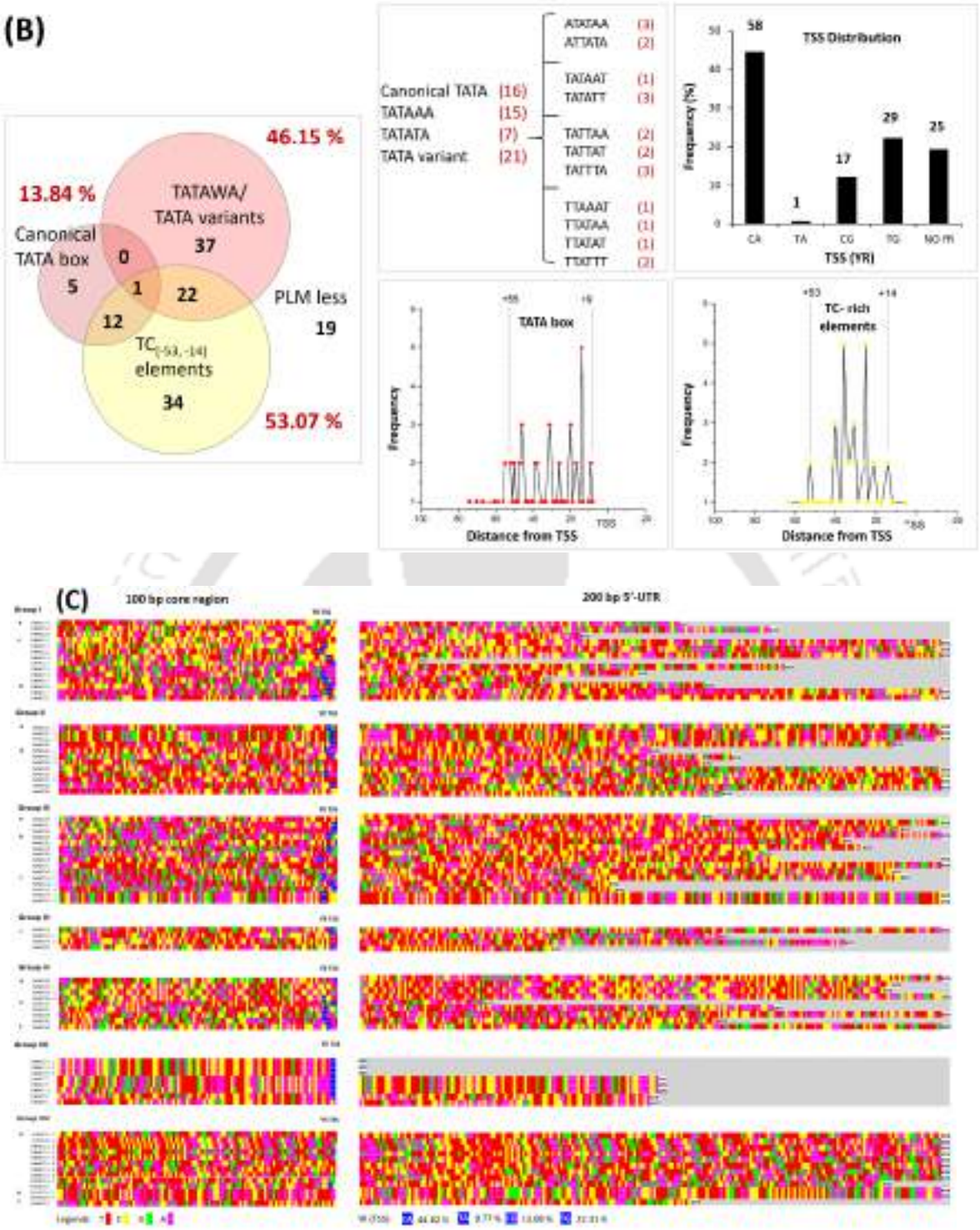

Fig. 3.8 Identification of preferentially located motifs (PLMs) in core promoter regions. (A) Illustration of PLMs (TATA box, TC-rich elements, DPE, CAAT, and Inr). **(B)** Sequence and positional analysis of TATA box, TC-rich elements, and TSS. (C) Pyrimidine composition, T(red) and C (pink) in the 100 bp core and 5'-UTR region. The group I, II, VII, and VIII members were abundant with ≥ 60% 'T' and 'C' bases.

3.3.4.2 The promoters were over-represented with stress and light regulatory elements

Each promoter consists of a unique arrangement of 6-10 bp TF binding sites (TFBSs) recognized by the regulatory TFs. We identified the *cis*-regulatory elements overrepresented in the proximal and distal promoter to determine the inducers, elicitors, and transcriptional regulators governing the underlying gene expression (Table A1.8, Appendix 1). The elements associated with abiotic stress, hormonal response, light, and TF binding were mapped in Fig. 3.9A. The elements involved in hormone signaling, detected primarily in SNAC Group I gene promoter, were as follows: ABRE element (ABA-responsive), TGA-element, AuxRR-core (auxin-responsive), CGTCA-motif (JA-responsive), GARE-motif, P-box, TATC-box (GA-responsive), and TCA-element (SA-responsive). The auxin-responsive element was also abundant in Group VIII genes. The elements associated with meristem expression (CAT-box), endosperm expression (GCN4_motif), and seed-specific expression (RY-element) were also found in several Group I and Group V genes promoters. Most promoter sequences were rich in light-responsive elements like G-Box, GT1-motif, GATA-motif, TCT-motif, TCCC-motif, and LAMP elements. The anaerobic response elements (ARE) were also found in most of the promoter sequences. This suggested that *VuNAC* genes may facilitate plant response to submergence or waterlogging, generating anoxia in root tissues, making the plants switch their energy-producing pathways from Kreb's cycle respiration to fermentation [345].

The binding sites for many stress-responsive TFs (MYB, MYC, ERF, bZIP, and WRKY were abundant in most promoters, especially in the ATAF-like genes (Group Ia), suggesting the regulation of *VuNAC* genes *via* other TF groups (Fig. 3.9B). The promoters were detected with over-representation of elements crucial for stress induction, for instance, ACGTATERD1, DRECRTCOREAT (recognized by dehydration responsive ERD1), TAAAGSTKST1 (regulating K^+ influx channel in stomata), LTRECOREATCOR15, CRTDREHVCBF2 (cold-responsive element), GT1GMSCAM4 (pathogen and salt-responsive element). The Group Ia genes were also rich in the elements involved in nutrition deficiency, like P1BS (regulating phosphate-starvation) and IRO2OS (regulating iron deficiency). Moreover, the presence of elements like PYRIMIDINEBOX- OSRAMY1A, SREATMSD, TATCCAYMOTIF-OSRAMY3D suggested that the gene group was apparently involved in the sugar-mediated expression, which may impact the plant metabolism and development (Table A1.8.3, Appendix 1).

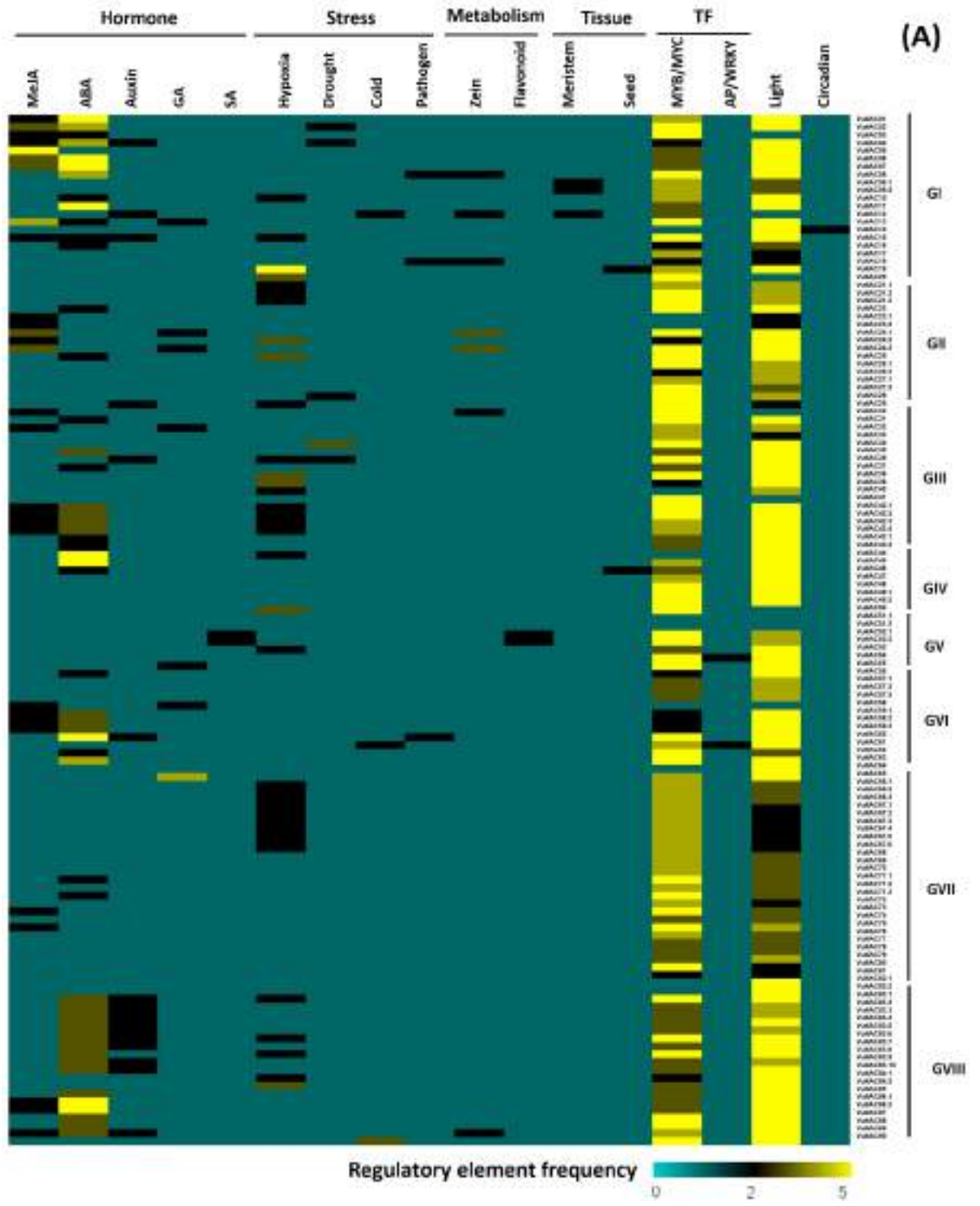

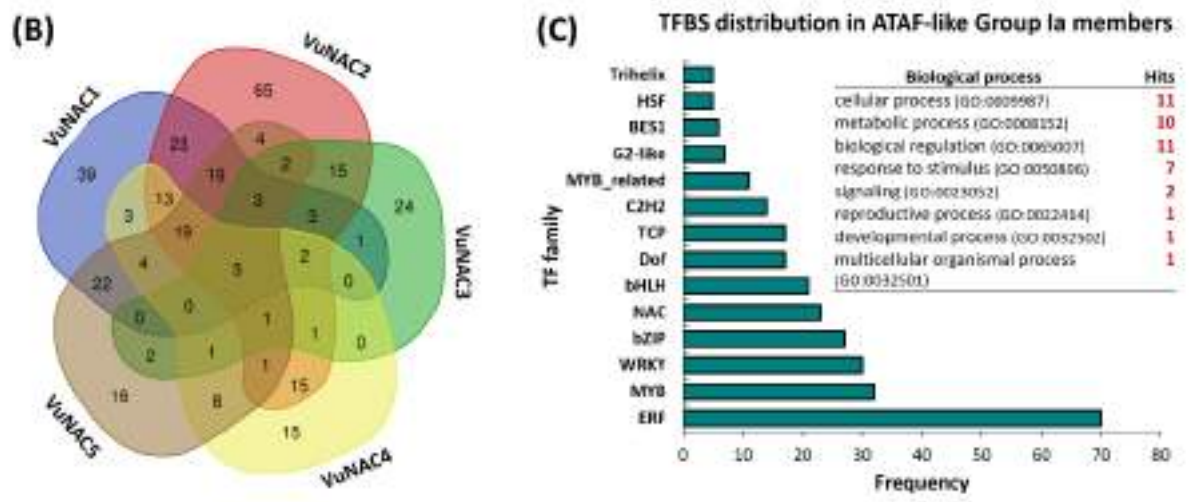

Fig. 3.9 Analysis of cis-regulatory elements and TF binding sites (TFBSs) in the promoter. (A) Heatmap depicting the over-representation (≥2) of cis-regulatory elements involved in light, TF binding, abiotic stress, pathogen response, metabolism, and tissue-specific roles. **(B)** Distribution of TFBS identified in ATAF-like VuNAC genes (top) and frequency of TFBS of different protein families and their biological process annotation (bottom).

3.3.5 Prediction of biological functions associated with VuNAC proteins

The phylogenetically close proteins may have the same function as suggested by the lineage-specific expansion of NAC genes after divergence from their common ancestors. The comparative study of cowpea and Arabidopsis disclosed the presence of many orthologous groups. The relationship between their conserved NAC domains can predict the role and function of the cowpea NAC family, using the acquired knowledge of model species, as mentioned in Table 3.4. Exceptionally, no orthologous AtNAC could be found for the cowpea-specific VuNAC proteins, clustered in Group VII.

3.3.5.1 Stress and senescence-associated

There were six orthologous groups in Group I, comprising 13 stress-responsive NAC (SNAC)-like members. Group Ia shared tight sequence similarity with the ATAF members of Arabidopsis (VuNAC01, VuNAC05, ANAC002/ATAF1) and (VuNAC02, VuNAC03, ANAC081/ATAF2, ANAC102), whose role in stress is conserved among rice, soybean, barley, and cotton [27, 28, 30, 31, 56, 166, 346, 347]. Group Ib was shared by VuNAC06, VuNAC07, ANAC055/AtNAC3, and ANAC072/RD26 involved in dehydration response [299]. Group Ic grouped VuNAC10, VuNAC11, VuNAC14, and VuNAC15 with ANAC025, ANAC029/NAP, ANAC018/NAM, and ANAC056/NARS1, known to regulate leaf senescence, seed embryogenesis, and pathogen resistance in Arabidopsis and rice [104, 109, 146]. The Group Id

consisted of VuNAC18 and VuNAC19, similar to VNI2 (ANAC083) that regulate xylem vessel formation in association with VNDs (Vascular NAC domains) [95]. Altogether, Group I (VuNAC1-20) was the stress-responsive cluster of the VuNAC family, protecting against various abiotic and biotic stresses, like their Arabidopsis orthologs, putatively functioning *via* ABA-mediated network, also supported by the promoter elements.

3.3.5.2 Vascular-related VuNAC proteins

Group II comprised three orthologous groups (VuNAC21, VuNAC22, ANAC033/SMB), (VuNAC23, VuNAC24, ANAC037/VND1), and (VuNAC25, VuNAC26, VuNAC27, VuNAC28, ANAC007/VND4). Group IIa members were associated with ANAC033/SMB and secondary cell wall thickening factors, ANAC063, ANAC066/NST2, which controls stem cell division, secondary cell-wall modification in woody tissues [107, 223]. The Group IIb VuNAC members were homologous to Vascular NAC domains (VND) proteins (ANAC037, ANAC076, ANAC007, ANAC026, and ANAC030), involved in the biosynthesis of xylem vessel and wood formation [237]. Previous reports have suggested that VND members have contributed to the evolution of the water-conduction system and cell support in land plants [63]. *NST and VND are functionally redundant, and their role is conserved through angiosperms as transcriptional regulators of the secondary cell wall and lignin formation [348, 349]. Thus, Group II was the basal functional group, given their indispensability.*

3.3.5.3 Morphogenesis and Organ development related

Group III was associated with four orthologous groups (VuNAC33, VuNAC34, ANAC087), (VuNAC35, VuNAC36, ANAC100), and (VuNAC38, VuNAC39, ANAC058/CUC3) and (VuNAC40, VuNAC41, ANAC098/CUC2). The Group IIIa proteins shared similarity with ANAC021/AtNAC1 involved in auxin signaling and lateral root development [221], and ANAC074, regulating flower senescence and programmed cell death [350]. Whereas Group IIIb consisted of ANAC087, ANAC046, and ANA100, controlling cell death *via* chlorophyll catabolism and ethylene response in association with SMB [351]. Group IIIc was shared by CUC proteins (ANAC054, ANAC098, and ANAC031), which are involved in the shoot apical meristem formation, embryogenesis [319]. Hence, Group III VuNAC members were speculated to be responsible for morphogenesis and development of different organs, such as leaf, root, and flower, through hormone-regulated pathways.

3.3.5.4 Growth-cycle and flowering regulating VuNAC

Group IV clustered together three orthologous groups, (VuNAC46, ANAC096), (VuNAC47, ANAC057) and (VuNAC50, ANAC020) along with ANAC091/TIP involved in viral protection [142], and ANAC040/NTL8, regulating flowering time [118], and ANAC096 involved in dehydration and osmotic stress [142]. Rest of the six orthologous clusters were grouped as follows: (VuNAC51, VuNAC52, VuNAC53, ANAC090/TERN) and (VuNAC54, ANAC035/LOV1) in Group V, (VuNAC60, VuNAC61, VuNAC62, VuNAC63, ANAC104/XND1) and (VuNAC64, ANAC050) in Group VI, and (VuNAC83, VuNAC84, ANAC075) and (VuNAC85, VuNAC86, VuNAC87, VuNAC88, ANAC073/SND2) in Group VIII. The Group V members shared similarity with ANAC090/TERN and ANAC035/LOV1 prolonging vegetative phase by controlling flowering time [222], ANAC009/FEZ, controlling cell division [107], and ANAC042/JUB1 known to regulate longevity and stress tolerance *via* GA/BR metabolism [352]. Group VI included ANAC082, regulating ribosomal stress and growth [353], ANAC053 controlling anther dehiscence [354], ANAC104/XND1 regulating lignin synthesis, and programmed cell death [119], and ANAC103 that interacts with VND proteins. Group VIII clustered ANAC075 regulating vegetative phase transition [355], ANAC073/SND2, and ANAC010/SND3 regulating secondary cell-wall biogenesis [114]. Taken together, the VuNAC members falling in the groups as mentioned above might be crucial for vegetative and reproductive growth regulation.

3.3.6 Expression analysis and elucidation of co-expressed network

3.3.6.1 RNA-seq study

The transcriptomic study of two different tissues, shoot (vegetative stage) and root (seedling stage), validated the expression of more than 90% of the predicted *VuNAC* genes (the information about nine genes could not be obtained). The FPKM values were listed in Table A1.9, Appendix 1. Although the gene expression did not manifest any tissue-specificity, most of the genes showed higher expression in seedling root rather than the shoot tissue of the vegetative stage (Fig. 3.10A). Exceptionally, four genes *VuNAC86*, *VuNAC89*, and *VuNAC90* (Group VIII), along with *VuNAC63* (Group VI), showed 2-10 times more FPKM values in the shoot sample. The genes having FPKM more than the average value of 5.2 were defined as high expressing genes. In the shoot tissue, we found 18 high-expressing genes, mainly clustered in Group I and Group IV, while 39 high-expressing genes in the root tissue fell in Group I, Group II, and Group III (Fig. 3.10B). The analysis of the promoter type in these genes revealed that a significant proportion of the high-expressing genes carried the Class I type promoter with

both TATA box and TC-rich element in their core (Fig. 3.10B). The distribution of promoter type in the shoot was as follows: Class I (44.44%), Class II (33.33%), Class III (16.67%), and Class IV (5.56%). Whereas in the root tissue, the distribution was Class I (30.77%), Class II (28.21%), Class III (23.08%), and Class IV (17.95%). The results showed that the TC-rich elements were crucial for the high expression of the *VuNAC* genes.

Table 3.4 Prediction of functions associated with VuNAC TFs based on orthologous proteins in Arabidopsis

Orthologous groups			Similarity	Predicted Function
S.N.	Protein	Closest Arabidopsis homolog		
1	**VuNAC01**	**ANAC002** (ATAF1), ANAC032	78.4%	Involved in ABA & auxin signaling [56]
	VuNAC05	**ANAC002** (ATAF1), ANAC032	78.4%	Involved in senescence [139], response to hypoxia, salinity, drought, and pathogen [28], involved in glutathione metabolism, toxin catabolism, carbohydrate metabolism, and chlorophyll degradation [139]
2	**VuNAC02**	**ANAC081,** ANAC102	68.1%	Response to ABA, auxin, light, and hypoxia [128, 205]
	VuNAC03	**ANAC081,** ANAC102	64.4%	Involved in seed germination, root hair elongation, leaf senescence [128]
	VuNAC04	**ANAC081,** ANAC102	60.9%	Involved in glucosinolate metabolism and brassinosteroid catabolism
3	**VuNAC06**	**ANAC055**(AtNAC3), ANAC072(RD26)	65.5%	Response to ABA and JA
	VuNAC07	**ANAC055**(AtNAC3)	68.4%	Response to dehydration [299]
4	**VuNAC10**	**ANAC025**	63.6%	Involved in seed dormancy and cell-wall expansion [104]
	VuNAC11	**ANAC025**	66.4%	
5	**VuNAC14**	**ANAC029** (NAP), ANAC047	60.8%	Response to ABA
	VuNAC15	**ANAC029** (NAP), ANAC047	**72.4%**	Involved in cell growth, seed development, flower development, fruit ripening, and leaf senescence [146], involved in ethylene biosynthesis
6	**VuNAC18**	**ANAC083**(VNI2)	**73.3%**	Involved in xylem development [95]
	VuNAC19	**ANAC083**(VNI2)	70.3%	Involved in salinity and leaf senescence
7	**VuNAC21**	ANAC033(SMB)	64.4%	Regulates cell fate commitment
	VuNAC22	ANAC043(NST1)	62.5%	Involved in root cap development and secondary cell wall biogenesis [356]
8	**VuNAC23**	**ANAC037**(VND1), ANAC076(VND2)	**70.9%**	Involved in seed dormancy, cell-wall biogenesis, and xylem vessel member cell differentiation [237]
	VuNAC24	**ANAC037**(VND1), ANAC076(VND2)	69.5%	
9	**VuNAC25**	**ANAC007**(VND4), ANAC026(VND5)	67.0%	
	VuNAC26	**ANAC007**(VND4), ANAC026(VND5)	65.4%	
	VuNAC27	**ANAC007**(VND4), ANAC026(VND5)	61.1%	
	VuNAC28	**ANAC007**(VND4), ANAC026(VND5)	**71.0%**	
10	**VuNAC33**	ANAC087, ANAC046	60.4%	Involved in leaf senescence and chlorophyll catabolism [351]
11	**VuNAC35**	**ANAC100**, ANAC080	69.5%	
	VuNAC36	**ANAC100,** ANAC080	**73.0%**	
12	**VuNAC39**	ANAC058	67.2%	-
13	**VuNAC40**	**ANAC098**(CUC2), ANAC054(CUC1)	63.2%	Regulates meristem initiation, organ separation, leaf development [319]
	VuNAC41	**ANAC098**(CUC2), ANAC054(CUC1)	66.9%	
14	**VuNAC46**	ANAC096	**59.6%**	Involved in dehydration and osmotic stress [142]
15	**VuNAC47**	ANAC057	**82.7%**	-
16	**VuNAC50**	ANAC020	62.1%	-
17	**VuNAC52**	ANAC090	62.4%	-
18	**VuNAC54**	ANAC036	69.6%	Regulates cell-size and leaf morphogenesis [357]
19	**VuNAC60**	ANAC104(XND1)	65.7%	Involved in xylem development and programmed cell death [119]
	VuNAC61	ANAC104(XND1)	63.8%	
	VuNAC62	ANAC104(XND1)	**81.7%**	
	VuNAC63	ANAC104(XND1)	**78.8%**	
20	**VuNAC64**	ANAC050	63.8%	Involved in photoperiodism and reproductive phase transition
21	**VuNAC83**	ANAC075	68.9%	Involved in tracheary element differentiation and vegetative transition [355]
	VuNAC84	ANAC075	**70.9%**	
22	**VuNAC85**	ANAC073(SND2)	62.8%	Involved in secondary cell-wall biogenesis [114]
	VuNAC86	ANAC073(SND2)	66.0%	
	VuNAC87	ANAC073(SND2)	66.6%	
	VuNAC88	ANAC073(SND2)	**69.6%**	

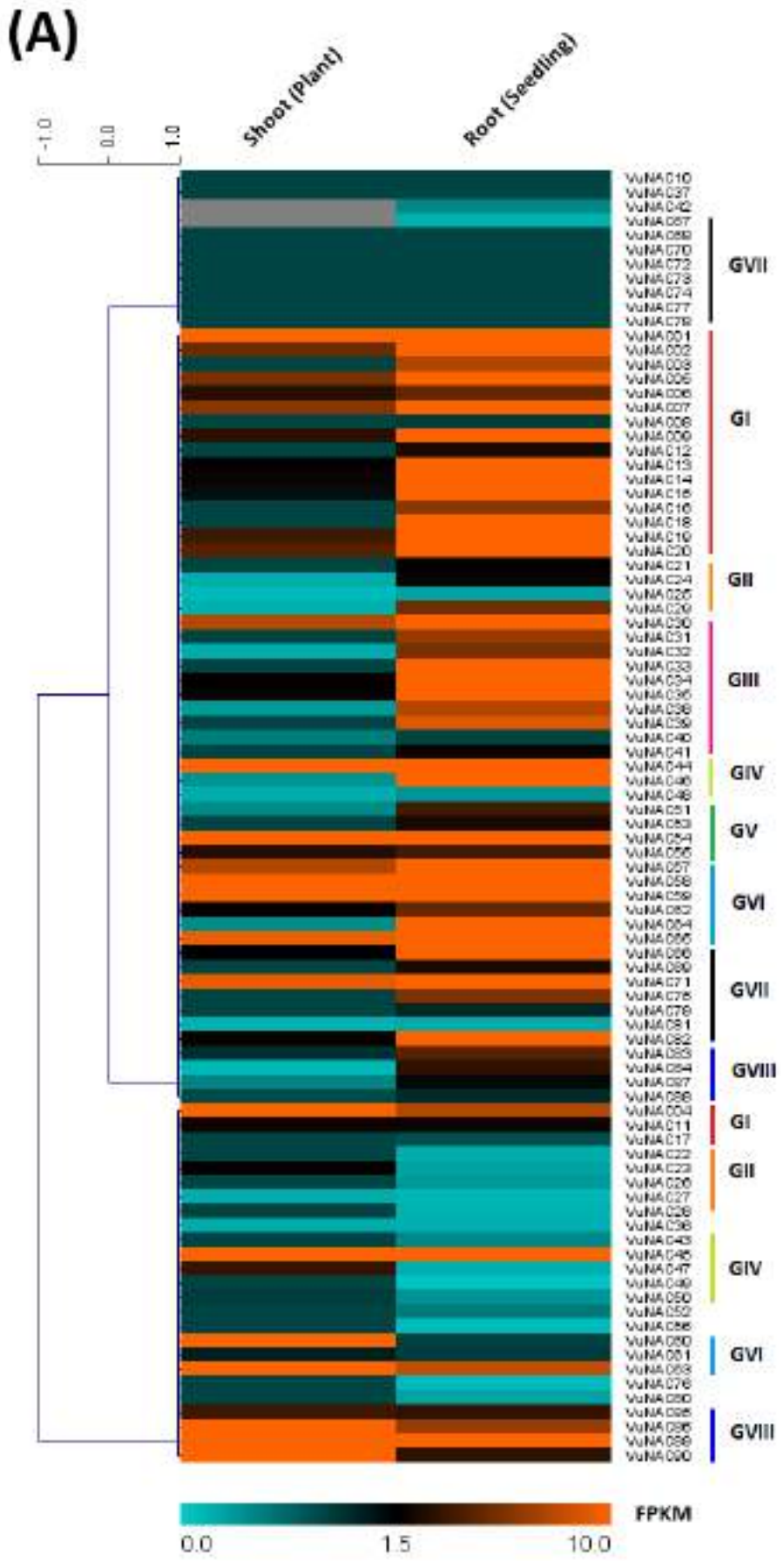

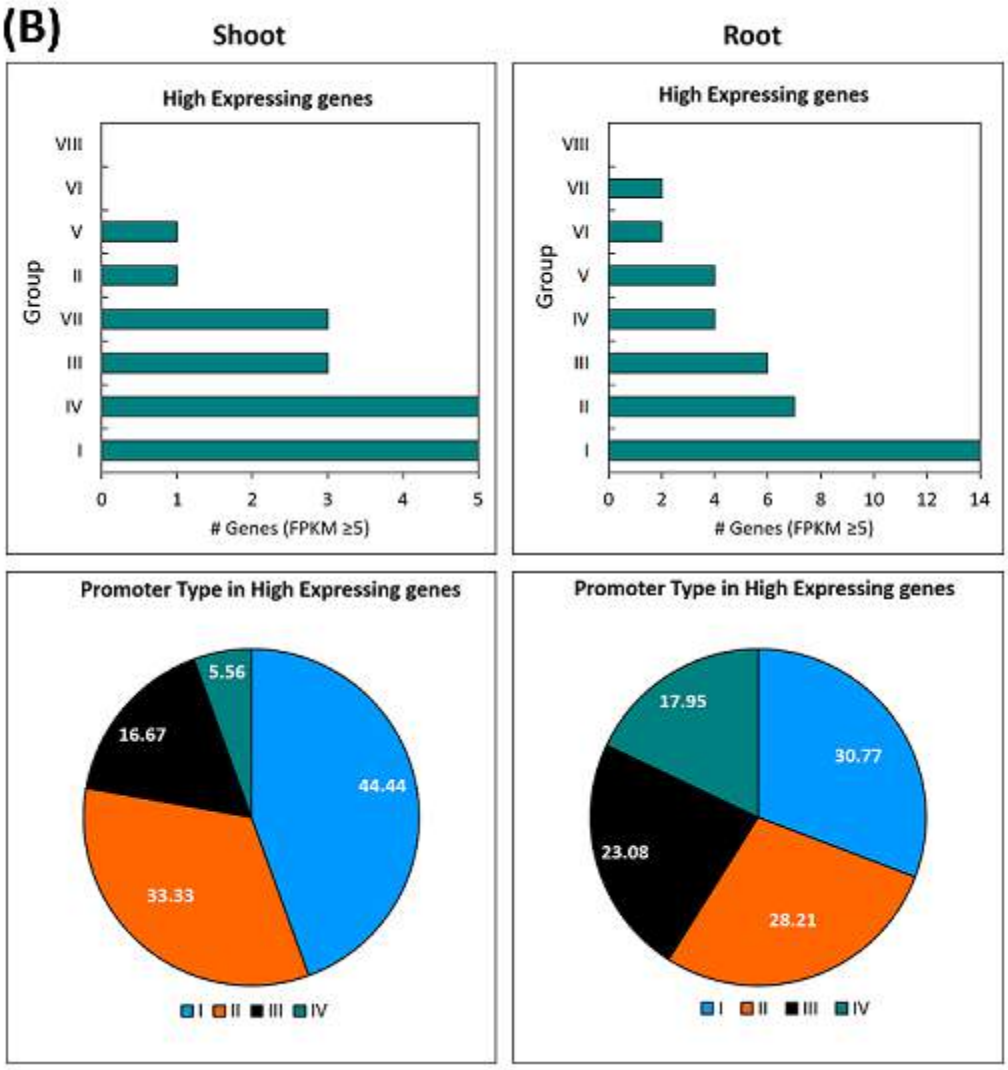

Fig. 3.10 RNA-sequencing analysis. (A) Heatmap of VuNAC genes expressing in mature leaves and seedling roots. **(B)** Group-wise (top) and promoter class-wise (bottom) distribution of high expression genes (FPKM value ≥ 5).

3.3.6.2 Interactome of VuNAC TF

NAC TFs interact with other genes, including the NAC members, to co-regulate a function. We carried out the co-expression study of AtNAC orthologous to the VuNAC TFs, to predict the co-expressing/interacting clusters in cowpea proteome to reveal additional homologous co-proteins in the network. The VuNAC family could be grouped into four co-expression clusters based on the interactome analysis (Fig. 3.11 and Table 3.5). Cluster 1 consisted mainly of Group I members (10 proteins), speculated to be involved in stress responses, hormone signaling, cellular metabolism, growth, and developmental processes. These VuNAC TFs may interact with other proteins sharing the network or regulate their gene expression. For instance, hormone signaling associated proteins like ABI1 (ABA INSENSITIVE 1), PYL7HAI2

(HIGHLY ABA-INDUCED PP2C PROTEIN 2), HAB1 (HYPERSENSITIVE TO ABA1), NCED3, SAUR-like auxin-responsive proteins, ACS2 (1-AMINO-CYCLOPROPANE-1-CARBOXYLATE SYNTHASE 2), ERF4 (ETHYLENE RESPONSIVE ELEMENT BINDING FACTOR 4), GA2OX6 (GIBBERELLIN 2-OXIDASE 6), JRG21 (JASMONATE-REGULATED GENE 21), shared the network. Many drought and salt-responsive proteins, LEA4-5, DREB2A, GBF3, HSFB2A, MYB74, and STZ (SALT TOLERANCE ZINC FINGER), pathogen resistance-related proteins like Avr9/Cf-9, WRKY6, WRKY40, and WRKY75, and stress-signaling proteins, MAPKK9, MAPKKK18, A20/AN1, and CYSTEINE-RICH TM MODULE, were found in the interactome. Cluster 1 was also speculated to be involved in ion homeostasis, amino acid, and carbohydrate secondary metabolism *via* interaction with proteins like MSS1 (MAJOR FACILITATOR SUPERFAMILY PROTEIN), SODIUM/CALCIUM EXCHANGER family protein, ADC2 (ARGININE DECARBOXYLASE 2), DHFR (DIHYDROFOLATE REDUCTASE), BAM1 (BETA-AMYLASE 1), BGLU11 (BETA GLUCOSIDASE 11), NSP5 (NITRILE SPECIFIER PROTEIN 5), GRX480 (THIOREDOXIN SUPERFAMILY PROTEIN), GSTU1/4/7/9/24 (GLUTATHIONE S-TRANSFERASE TAU 1 PROTEIN).

Cluster 2 included four NAP-like TFs from Group I and two SMB like TFs belonging to Group III, potentially involved in stress and age-dependent senescence. This cluster was rich in auxin signaling proteins like SAUR36, AUXIN EFFLUX CARRIER, WES1, and senescence regulating proteins (NYE1, SRG1, and TPS), in addition to proteins involved in cell detoxification, such as HIPP22 (heavy metal transporter), ZF15 (MATE efflux gene), CATION/H^+ EXCHANGER 17, K^+ UPTAKE PERMEASE 6, GRXS13, and DOX1). Seven VND-like TFs from Group II build the third co-expression (Cluster 3), responsible for cell wall and xylem development. The network involved mainly enzymes regulating cellulose and chitin metabolism (CESA4, IRX1/33, and CTL2), pectin lyases, and pectin invertases regulating cell-wall pectin metabolism. It also included proteins like TRACHEARY ELEMENT DIFFERENTIATION-RELATED 6/7, and TRICHOME BIREFRINGENCE-LIKE 33/34, involved in secondary cell-wall biogenesis. Other proteins included glycosyl hydrolases (RXF12, MAN6, and SUCROSE SYNTHASE 5/6), laccase (LAC2, LAC10, LAC11, LAC17, and IRX12), xylem cysteine peptidases, and HSP20-like chaperones (AT2G27140, AT5G20970, AT3G10680, and RTM2). Five VuNAC TFs distributed in Group IV, V, and Group VIII formed Cluster 4. Although the precise orthologous function of this cluster could not be predicted, the interactome analysis suggested their involvement in cell signaling and

pathogen resistance. The network included calcium-binding EF-hand family proteins and cysteine-rich RECEPTOR-like kinases regulating cell signaling (CRK4-7, CRK14/15, CRK23/24, and CRK41), ankyrin repeat family proteins controlling growth and stress, and defense-related proteins (TIR-NBS, HR3, PR1/5, WRKY30, WRKY46, WRKY53, and WRKY70).

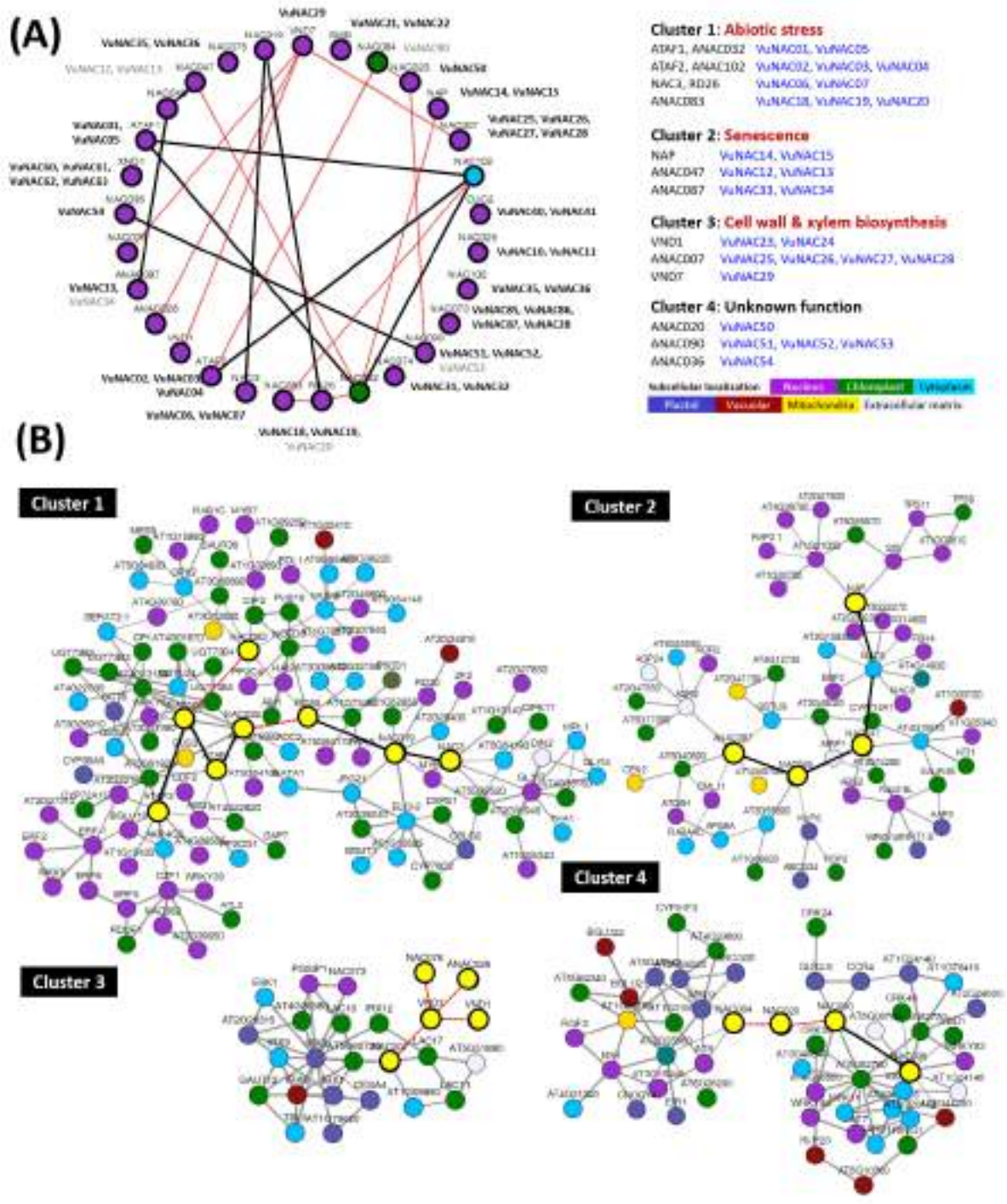

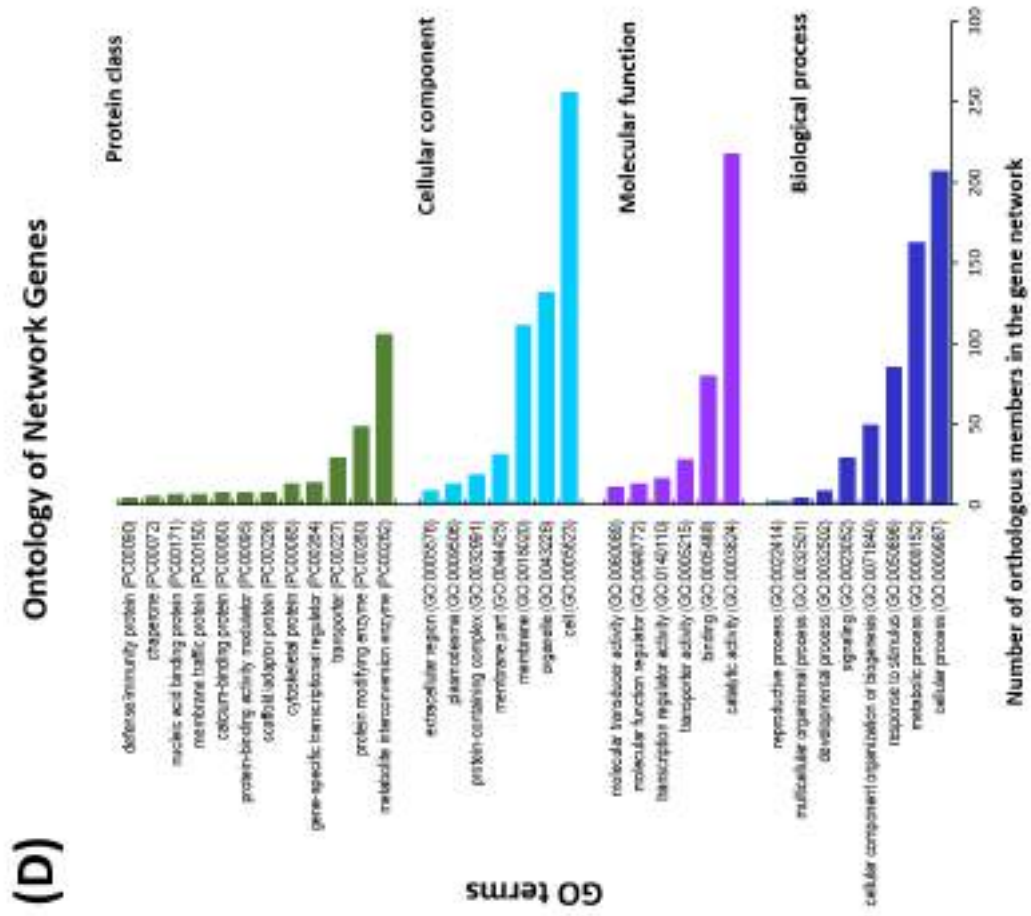

(C) Pathway Annotation of Network Genes

KEGG ID	Pathway	# Genes	Link to the KEGG map
ath04075	Plant hormone signal transduction	15	
ath00500	Starch and sucrose metabolism	9	
ath04016	MAPK signaling pathway - plant	7	
ath00940	Phenylpropanoid biosynthesis	7	
ath04626	Plant-pathogen interaction	5	

Gene	Function	Entrez ID	Link to the KEGG map
TPS11	trehalose phosphatase/synthase 11	816385	
TPS8	trehalose-6-phosphatase synthase 58	843365	
DIN2	Glycosyl hydrolase superfamily protein	825184	
SUS3	sucrose synthase 3	820281	
BGLU10	beta glucosidase 10	828896	
BGLU21	Glycosyl hydrolase superfamily protein	842944	
BGLU22	Glycosyl hydrolase superfamily protein	842945	
ATA27	Glycosyl hydrolase superfamily protein	843927	
cwINV4	cell wall invertase 4	838191	
SAUR36	SAUR-like auxin-responsive protein family	819129	
AT2G46690	SAUR-like auxin responsive protein family	819281	
AT3G60690	SAUR-like auxin-responsive protein family	825240	
AT5G53590	SAUR-like auxin-responsive protein family	835441	
AT3G12830	SAUR-like auxin-responsive protein family	820465	
AT4G31320	SAUR-like auxin-responsive protein family	829259	
AT5G13380	Aswin-responsive GH3 family protein	831179	
TGA4	TGACG motif-binding factor 4	830866	
TGA1	bZIP transcription factor family protein	836646	
PP2CA	protein phosphatase 2CA	820314	
ABI1	Protein phosphatase 2C family protein	828714	
HAI2	highly ABA-induced PP2C protein 2	837255	
EBF2	EIN3-binding F box protein 2	832607	
ERF2	ethylene responsive element binding factor 2	834768	
SNRK2.7	SNF1-related protein kinase 2.7	830162	
MKK9	MAP kinase kinase 9	843685	
AT5G51890	Peroxidase superfamily protein	835264	
AT1G68850	Peroxidase superfamily protein	843218	
WRKY33	WRKY DNA-binding protein 33	818429	
CNGC14	cyclic nucleotide-gated channel 14	816997	
CML11	calmodulin-like 11	821865	
CEN2	centrin 2	829855	
AT1G73610	EF hand calcium-binding protein family	843697	

Fig. 3.11 Interactome analysis (A) Clustering VuNAC genes into co-expression groups (top) and their interaction network predicted using the orthologous AtNAC as reference. **(B)** The associated KEGG pathways **(C)** GO annotation of the genes fabricating the VuNAC interactome.

Table 3.5 Prediction of interacting/co-expressing partners based on orthologous network in Arabidopsis

Gene ID	Description	Rank	Function
	CLUSTER 1:STRESS RESPONSE RELATED		
AT5G64230	1,8-cineole synthase	2.98	Terpene biosynthesis
ACS2	1-amino-cyclopropane-1-carboxylate synthase 2	2.72	Ethylene biosynthesis
AT5G05600	2-oxoglutarate (2OG) and Fe(II)-dependent oxygenase superfamily protein	2.98	DNA repair, secondary metabolite synthesis
AT4G22820	A20/AN1-like zinc finger family protein	3.41	Stress response
AFP1	ABI five binding protein	3.91	ABA signaling
ACX1	acyl-CoA oxidase 1	3.1	Perixosomal Beta oxidation
ADC2	arginine decarboxylase 2	2.43	Arginine metabolism
AT5G54165	Avr9/Cf-9 rapidly elicited protein	3.12	Pathogen resistance
BGLU10	beta glucosidase 10	2.54	Sugar metabolism
BGLU11	beta glucosidase 11	2.53	Sugar metabolism
BAM1	beta-amylase 1	3.17	Leaf starch breakdown
AT1G05340	cysteine-rich TM module stress tolerance protein	3.52	Stress response
CYP81D11	Cytochrome P450 superfamily protein	3.56	Monooxygenase
AT5G42050	DCD (Development and Cell Death) domain protein	3.09	Stress-responsive asparagine-rich protein
AT4G24380	dihydrofolate reductase	2.41	Folate metabolism
DREB2A	DRE-binding protein 2A	3.37	Drought, cold
EDL3	EID1-like 3	3.45	ABA, Germination
ESL1	ERD (early response to dehydration) six-like 1	2.45	Stress response
ERF-1	ethylene-responsive element-binding factor 1	3.76	Ethylene signaling
ERF4	ethylene-responsive element-binding factor 4	3.16	Ethylene signaling
GBF3	G-box binding factor 3	3.13	Drought, cold
GA2OX6	gibberellin 2-oxidase 6	2.86	GA metabolism
GSTU1	glutathione S-transferase TAU 1	3.47	Reseveratrol metabolism
GSTU19	glutathione S-transferase TAU 19	3.02	Reseveratrol metabolism
GSTU24	glutathione S-transferase TAU 24	3.12	Reseveratrol metabolism
GSTU4	glutathione S-transferase tau 4	3.05	Reseveratrol metabolism
GSTU7	glutathione S-transferase tau 7	4.29	Reseveratrol metabolism
AT4G39670	Glycolipid transfer protein (GLTP) family protein	3.01	Lipid transfer
AT5G13200	GRAM domain family protein	3.1	Seed germination/dormancy
HSFB2A	heat shock transcription factor B2A	3.38	Heat stress
HAI2	highly ABA-induced PP2C protein 2	3.04	ABA signaling
AT1G63720	hydroxyproline-rich glycoprotein family protein	3.45	Plant cell-wall protein
HAB1	HYPERSENSITIVE TO ABA1	2.97	ABA signaling
JRG21	jasmonate-regulated gene 21	3.1	JA signaling
JAZ1	jasmonate-zim-domain protein 1	3.43	JA signalling
GLYI7	Lactoylglutathione lyase/glyoxalase I family protein	2.48	Methylglyoxal metabolism
LEA4-5	Late Embryogenesis Abundant 4-5	2.58	Dessiaction response
MSS1	Major facilitator superfamily protein	2.66	Ion transporter
AT3G53960	Major facilitator superfamily protein	2.34	Ion transporter
MKK9	MAP kinase kinase 9	3.38	Senescence
MAPKKK18	mitogen-activated protein kinase kinase kinase 18	3.72	Senescence and Growth
MYB2	myb domain protein 2	2.91	Nitrogen assimilation
MYB74	myb domain protein 74	3.41	Salt response
NCED3	nine-cis-epoxycarotenoid dioxygenase 3	3.47	Auxin biosynthesis
NSP5	nitrile specifier protein 5	3.04	Nitrile formation
HAI1	PP2C protein (Clade A protein phosphatases type 2C)	3.69	ABA signaling
ABI1	Protein phosphatase 2C family protein	4.1	ABA signaling
AT3G62260	Protein phosphatase 2C family protein	3.53	ABA signaling
ABI2	Protein phosphatase 2C family protein	3.07	ABA signaling
PYL7	PYR1-like 7	2.52	ABA signaling
STZ	salt tolerance zinc finger	3.18	Salt stress
AT3G60690	SAUR-like auxin-responsive protein family	2.53	Auxin signaling
AT2G28400	senescence regulator (Protein of unknown function, DUF584)	3.98	Senescence
SERAT2;1	serine acetyltransferase 2;1	3.42	Cysteine biosynthesis
AT5G17850	Sodium/calcium exchanger family protein	2.59	Ion transporter
AT5G61820	stress up-regulated Nod 19 protein	4.66	Uncharacterized
GRX480	Thioredoxin superfamily protein	2.89	Redox reaction
UGT73B5	UDP-glucosyl transferase 73B5	3.61	Stress response
UGT74E2	Uridine diphosphate glycosyltransferase 74E2	3.17	Auxin-mediated stress response
AT3G22160	VQ motif-containing protein	3.39	Seed development, abiotic stress
WRKY40	WRKY DNA-binding protein 40	3.21	Pathogen resistance
WRKY6	WRKY family transcription factor	3.56	Pathogen resistance
	CLUSTER 2: SENESCENCE RELATED		
ACX2	acyl-CoA oxidase 2	2.99	Perixosomal Beta oxidation
ALIS5	ALA-interacting subunit 5	3.2	Lipid transport

AGP2	arabinogalactan protein 2	2.95	Cell-wall glycoprotein
AT3G22600	Bifunctional inhibitor/lipid-transfer protein/seed storage 2S albumin superfamily protein	2.82	Lipid transport
AT4G26470	Calcium-binding EF-hand family protein	2.77	
CHX17	cation/H+ exchanger 17	3.1	Ion transporter
CEN2	centrin 2	3.24	DNA repair
AT1G05340	cysteine-rich TM module stress tolerance protein	3.6	Stress response
CYP710A1	cytochrome P450, family 710, subfamily A, polypeptide 1	2.84	Mooxygenase
ESL1	ERD (early response to dehydration) six-like 1	2.81	Desiccation response
GLR1.3	glutamate receptor 1.3	3.32	Light and calcium homeostasis
GLR2.5	glutamate receptor 2.5	2.82	Light and calcium homeostasis
GRXS13	Glutaredoxin family protein	2.78	Redox reaction
HIPP22	Heavy metal transport/detoxification superfamily protein	2.86	Detoxification
AT1G23040	hydroxyproline-rich glycoprotein family protein	3.13	Plant cell-wall protein
AT1G63720	hydroxyproline-rich glycoprotein family protein	3.02	Plant cell-wall protein
AT5G54870	inositol-1,4,5-trisphosphate 5-phosphatase	2.82	Messenger
KUP6	K+ uptake permease 6	2.82	Ion transporter
GLYI7	Lactoylglutathione lyase/glyoxalase I family protein	3	Glyoxalase metabolism
AT1G65690	Late embryogenesis abundant (LEA) hydroxyproline-rich glycoprotein family	2.94	Desiccation response
AT3G14280	LL-diaminopimelate aminotransferase	3.1	Lysine biosynthesis
AT4G33150	lysine-ketoglutarate reductase/saccharopine dehydrogenase bifunctional enzyme	3.09	Lysine biosynthesis
MAP18	microtubule-associated protein 18	2.84	Cytoskeletal synthesis
MYB2	myb domain protein 2	2.92	Nitrogen assimilation
UMAMIT33	nodulin MtN21 /EamA-like transporter family protein	2.75	Carbohydrate transport
NYE1	non-yellowing 1	2.89	Senescence response
AT3G49210	O-acyltransferase (WSD1-like) family protein	3.3	Wax biosynthesis
DOX1	Peroxidase superfamily protein	3.25	Oxidative stress
AT4G37520	Peroxidase superfamily protein	2.81	Oxidative stress
AT2G45220	Plant invertase/pectin methylesterase inhibitor superfamily	3.06	Pectin biosynthesis
ABI1	Protein phosphatase 2C family protein	2.85	ABA signaling
RLP22	receptor-like protein 22	3.17	Plant immunity
ARSK1	root-specific kinase 1	3	Root hair growth
SAUR36	SAUR-like auxin-responsive protein family	2.92	Auxin metabolism
SRG1	senescence-related gene 1	3.48	Senescence response
PDE337	VQ motif-containing protein	2.96	Stress response
WRKY45	WRKY DNA-binding protein 45	3.76	Pathogen resistance
WRKY61	WRKY DNA-binding protein 61	3.25	Pathogen resistance
WRKY75	WRKY DNA-binding protein 75	4.1	Pathogen resistance
AT2G17500	Auxin efflux carrier family protein	2.57	Auxin signaling
WES1	Auxin-responsive GH3 family protein	2.3	Auxin signaling
COBL2	COBRA-like protein 2 precursor	2.17	Cell-wall biogenesis
DREB2A	DRE-binding protein 2A	2.25	Drought, cold
HSF4	heat shock factor 4	2.58	Heat shock response
GLYI4	Lactoylglutathione lyase/glyoxalase I family protein	2.44	Methylglyoxal metabolism
MSS1	Major facilitator superfamily protein	2.54	Ion transporter
AT5G14940	Major facilitator superfamily protein	2.38	Ion transporter
ZF14	MATE efflux family protein	2.65	Detoxification
AT3G26470	Powdery mildew resistance protein, RPW8 domain-containing protein	2.3	Pathogen resistance
AT5G50760	SAUR-like auxin-responsive protein family	2.74	Auxin signaling
	CLUSTER 3: CELL WALL AND XYLEM BIOSYNTHESIS		
APX5	ascorbate peroxidase 5	1.11	Redox reaction
AT1G29380	Carbohydrate-binding X8 domain superfamily protein	1.2	Structural support
CESA4	cellulose synthase A4	1.61	Cellulose biosynthesis
IRX3	Cellulose synthase family protein	1.95	Cellulose biosynthesis
IRX1	cellulose synthase family protein	1.77	Cellulose biosynthesis
CTL2	chitinase-like protein	1.6	Cellulose biosynthesis
IRX6	COBRA-like extracellular glycosyl-phosphatidyl inositol-anchored protein family	1.88	Cell-wall protein
GulLO3	D-arabinono-1,4-lactone oxidase family protein	1.23	Redox reaction
FLA11	FASCICLIN-like arabinogalactan-protein 11	1.45	Cell wall protein
AT5G07800	Flavin-binding monooxygenase family protein	1.34	Redox reaction
AT1G54790	GDSL-like Lipase/Acylhydrolase superfamily protein	1.77	Lipase
GLP10	germin-like protein 10	1.53	Pathogen resistance
GL22	germin-like protein subfamily 2 member 2 precursor	1.71	Pathogen resistance
AT5G59845	Gibberellin-regulated family protein	1.12	GA signaling
GSTF4	glutathione S-transferase F4	1.13	Reseveratrol metabolism
AT4G08160	glycosyl hydrolase family 10 protein / carbohydrate-binding domain-containing protein	1.65	Sugar metabolism
RXF12	glycosyl hydrolase family 10 protein / carbohydrate-binding domain-containing protein	1.57	Sugar metabolism
AT4G33810	Glycosyl hydrolase superfamily protein	1.57	Sugar metabolism
MAN6	Glycosyl hydrolase superfamily protein	1.18	Sugar metabolism
AT3G15800	Glycosyl hydrolase superfamily protein	1.16	Sugar metabolism
AT2G27140	HSP20-like chaperones superfamily protein	1.34	Heat protection
RTM2	HSP20-like chaperones superfamily protein	1.24	Heat protection
AT5G20970	HSP20-like chaperones superfamily protein	1.21	Heat protection
AT3G10680	HSP20-like chaperones superfamily protein	1.21	Heat protection
KP1	kinesin-like protein 1	1.05	Microtubule synthesis
LAC10	laccase 10	1.81	Oxidation reaction

LAC11	laccase 11	1.86	Oxidation reaction
LAC17	laccase 17	1.89	Oxidation reaction
LAC2	laccase 2	1.05	Oxidation reaction
IRX12	Laccase/Diphenol oxidase family protein	1.81	Oxidation reaction
AT1G08160	Late embryogenesis abundant (LEA) hydroxyproline-rich glycoprotein family	1.13	Desiccation response
JLO	Lateral organ boundaries (LOB) domain family protein	1.42	Organ development
MRH1	Leucine-rich repeat protein kinase family protein	1.21	Pathogen resistance
AT1G79620	Leucine-rich repeat protein kinase family protein	1.11	Pathogen resistance
AT5G42210	Major facilitator superfamily protein	1.14	Ion transporter
NAC073	NAC domain-containing protein 73	1.88	Cell wall biogenesis
AT2G28315	Nucleotide/sugar transporter family protein	1.55	Sugar transport
IRX9	Nucleotide-diphospho-sugar transferases superfamily protein	1.7	Sugar transport
AT5G67460	O-Glycosyl hydrolases family 17 protein	1.03	Sugar metabolism
AT1G70500	Pectin lyase-like superfamily protein	1.49	Pectin metabolism
AT1G23460	Pectin lyase-like superfamily protein	1.23	Pectin metabolism
AT1G05310	Pectin lyase-like superfamily protein	1.16	Pectin metabolism
AT3G47400	Plant invertase/pectin methylesterase inhibitor superfamily	1.04	Pectin metabolism
AT5G38610	Plant invertase/pectin methylesterase inhibitor superfamily protein	1.45	Pectin metabolism
AT3G49330	Plant invertase/pectin methylesterase inhibitor superfamily protein	1.01	Pectin metabolism
SUS5	sucrose synthase 5	1.14	Sugar metabolism
SUS6	sucrose synthase 6	1.34	Sugar metabolism
TED6	tracheary element differentiation-related 6	1.54	Secondary cell wall modification
TED7	tracheary element differentiation-related 7	1.66	Secondary cell wall modification
TBL33	TRICHOME BIREFRINGENCE-LIKE 33	1.31	Secondary cell wall modification
TBL34	TRICHOME BIREFRINGENCE-LIKE 34	1.8	Secondary cell wall modification
ESK1	trichome birefringence-like protein (DUF828)	1.6	Secondary cell wall modification
TBL3	trichome birefringence-like protein (DUF828)	1.53	Secondary cell wall modification
XCP1	xylem cysteine peptidase 1	1.65	Xylem-specific peptidase
XCP2	xylem cysteine peptidase 2	1.88	Xylem-specific peptidase
XSP1	xylem serine peptidase 1	1.32	Xylem-specific peptidase
	CLUSTER 4: UNKNOWN FUNCTION		
ANK	ankyrin	2.69	Growth and stress
AT4G11000	Ankyrin repeat family protein	2.96	Growth and stress
AT4G03450	Ankyrin repeat family protein	2.94	Growth and stress
AT2G24600	Ankyrin repeat family protein	2.8	Growth and stress
AT1G10340	Ankyrin repeat family protein	2.42	Growth and stress
AGP5	arabinogalactan protein 5	2.46	Cell wall protein
PBS3	Auxin-responsive GH3 family protein	2.46	Auxin signaling
BGL2	beta-1,3-glucanase 2	3.34	Glucan metabolism
AT2G44290	Bifunctional inhibitor/lipid-transfer protein/seed storage 2S albumin superfamily protein	2.41	Lipid transport
AT5G39670	Calcium-binding EF-hand family protein	3.24	Calcium signaling
AT3G47480	Calcium-binding EF-hand family protein	2.99	Calcium signaling
AT3G01830	Calcium-binding EF-hand family protein	2.91	Calcium signaling
AT2G46600	Calcium-binding EF-hand family protein	2.37	Calcium signaling
WAK1	cell wall-associated kinase	2.66	Pectin metabolism
AT5G52760	Copper transport protein family	5.28	Metal transporter
CCR4	CRINKLY4 related 4	3.17	Growth and development
CRK14	cysteine-rich RECEPTOR-like kinase	2.87	Cell signaling
CRK15	cysteine-rich RECEPTOR-like kinase	2.39	Cell signaling
CRK23	cysteine-rich RLK (RECEPTOR-like protein kinase) 23	3.06	Cell signaling
CRK24	cysteine-rich RLK (RECEPTOR-like protein kinase) 24	3.12	Cell signaling
CRK37	cysteine-rich RLK (RECEPTOR-like protein kinase) 37	3.02	Cell signaling
CRK4	cysteine-rich RLK (RECEPTOR-like protein kinase) 4	2.65	Cell signaling
CRK41	cysteine-rich RLK (RECEPTOR-like protein kinase) 41	2.47	Cell signaling
CRK5	cysteine-rich RLK (RECEPTOR-like protein kinase) 5	2.66	Cell signaling
CRK6	cysteine-rich RLK (RECEPTOR-like protein kinase) 6	3.08	Cell signaling
CRK7	cysteine-rich RLK (RECEPTOR-like protein kinase) 7	3.45	Cell signaling
BCS1	cytochrome BC1 synthesis	2.48	Cell-death, SA signaling
AT1G66090	Disease resistance protein (TIR-NBS class)	2.46	Pathogen resistance
GLR2.8	glutamate receptor 2.8	3.5	Light and calcium homeostasis
AT5G52750	Heavy metal transport/detoxification superfamily protein	4.31	Detoxification
AT5G26690	Heavy metal transport/detoxification superfamily protein	2.54	Detoxification
HO3	heme oxygenase 3	2.49	Heme catabolism
HR3	homolog of RPW8 3	2.5	Pathogen resistance
SOBIR1	Leucine-rich repeat protein kinase family protein	3.19	Plant defense
AT3G47090	Leucine-rich repeat protein kinase family protein	2.37	Plant defense
PR1	pathogenesis-related protein 1	2.5	Pathogen resistance
PR5	pathogenesis-related protein 5	2.51	Pathogen resistance
AT3G60415	phosphoglycerate mutase family protein	3.33	Glycolytic enzyme
PCR1	PLANT CADMIUM RESISTANCE 1	2.79	Ion transporter
RLK1	receptor-like protein kinase 1	3.6	Cell signaling
AT1G78410	VQ motif-containing protein	2.95	Stress response
WRKY30	WRKY DNA-binding protein 30	2.45	Pathogen resistance
WRKY46	WRKY DNA-binding protein 46	3.39	Pathogen resistance
WRKY70	WRKY DNA-binding protein 70	2.81	Pathogen resistance
WRKY53	WRKY family transcription factor	3.79	Pathogen resistance

3.4 DISCUSSION

NAC is a versatile TF family, functioning at the center of crucial transcriptional signaling regulating growth and stress responses. The divergent C-terminal part of the NAC proteins, carry crucial regulatory signals that determine transcriptional activity (activation/repression), making it hard to anticipate the function of orthologous proteins in legumes. Cowpea holds salient traits like short life-cycle, fastidious vegetative growth, convenient genetic manipulation, closeness to commercial legumes, and ability to survive the strenuous environment, stepped up as a potential model for the pulse-research [39]. However, no systematic study of the NAC family is available in cowpea. This knowledge of the VuNAC family in cowpea could be of immense importance for translational application in legumes for abiotic stress tolerance and yield improvement.

3.4.1 The eccentric VuNAC family comprehends unique members, and the largest paralogous group expanded by extensive gene duplication

Chromosomal duplication, accounting evolution of genetic systems, is a prime mechanism establishing new gene functions vital for adaptation [358]. Segmental duplication occurs in slowly evolving gene families like MYB, while in the case of a quickly evolving NBS-LRR gene family, tandem duplications in local genomic clusters. Our analysis revealed eight clusters of tandem duplicates, including 15.3% genes and 18 clusters of segmental duplicates comprising 22.3% of the genes, formed the paralogous groups of cowpea NAC TFs (Fig. 3.4 and Table A1.4). Tandem duplication was most evident in Group IId (VNI2-like), Group II (SMB/VND-like) members, Group VII (cowpea-specific), suggesting their rapid evolution. While, the phenomenon of segmental duplication was observed, primarily in Group I (SNAC-like) and Group VIII (SND-like). Due to a substantial number of paralogous members in cowpea, we stipulated that the number of VuNAC genes might have increased during the course of evolution, and both segmental and tandem duplications of chromosomal regions may be the driving force in the expansion of this family in the lineage. Although the cowpea-specific Group VII manifested the most considerable amount of paralogous duplication, suggesting functional redundancy, the most prominent orthologous duplication was noticed in the stress-responsive Group I, giving the largest SNAC group of 21 proteins followed by Arabidopsis having 17 members (Fig. 3.1C). This homology indicated that SNAC members of cowpea and Arabidopsis have eventually evolved from a common ancestor.

However, the variable distribution of introns within the same phylogenetic groups (IV, VI, VII, and VIII) suggests both loss and gain of introns during gene rearrangement and duplication (Fig. 3.3A and Table 3.4). The membrane-tethered NTM-like genes are known to integrate biotic and abiotic stress signaling [359]. The presence of substantial membrane-tethered NAC members (12 proteins) suggested the potential involvement of these groups in the cross-talk (Fig. 3.7A). Most importantly, the high divergence of the C-terminal TAR sequences imparted novelty to the cowpea NAC family (Fig. 3.6). The presence of 27 species-specific members and 21 stress-responsive members suggested that the evolution of the cowpea NAC family occurred under unique environmental pressure (Fig. 3.1B). The promoters of these members (Group VII) were rich in ARE elements suggesting their expansion to fight anaerobic conditions like submergence (Fig. 3.9A). The over-representation of MYB/MYC binding elements specified their transcriptional regulation.

3.4.2 Multi-tier regulatory network of VuNAC TF

3.4.2.1 Unique promoter arrangement

The promoter analysis revealed the unconventional structure of the *VuNAC* promoters. The position of the TATA box was highly variable from +10 to +55 bp. The 5'-UTR and core region were rich in rare TC-rich elements (Fig. 3.8C). The high-expressing genes showed an inclination towards bearing the TC-rich elements, irrespective of the presence of the TATA box (Fig. 3.10B). At the same time, the presence of binding sites for NAC TFs and other multiple stress-responsive TFs like MYB/MYC, WRKY, ERF, bZIP, bHLH, *etc*. (Fig. 3.9B) and *cis*-regulatory elements regulating versatile cellular functions makes the *VuNAC* promoters typically unique (Table A1.8, Appendix 1). Furthermore, the protein sequences were rich in post-translational modification sites like methylation, glycosylation, and phosphorylation, along with the landscapes of amino acid repeats (Table A1.3, Appendix 1). Our analysis gave the insight that the *VuNAC* genes undergo a multi-tier regulation at the level of promoter-mediated expression, protein modification as well as protein-protein interaction

3.4.2.2 Transcriptome analysis and co-expression network

Recently, the comprehensive genome draft for cowpea was made available [59]. Still, the reports for the RNA-seq study of cowpea disclosing the annotation aspects of cowpea are rare. Our study presented the first report annotating the cowpea NAC family under two different growth stages, *i.e.*, seedling and vegetative stage, and elucidating the relationship between their

expression, promoter nature, and functional group (Fig. 3.9). NAC proteins being a TF, works together with innumerable partners. For instance, the overexpression of one of the co-expressing AtNAC TFs ANAC019/ANAC055/ANAC072) alone could not induce the *ERD1* gene because the induction of *ERD1* depends on the co-expression of ZFHD1 as well [94]. Thus knowing the interaction partner is crucial for the functional study of cell response in a broader way keeping the interlinked signaling cascade in consideration. Therefore, the interactome network of VuNAC TFs was explored based on the information available for Arabidopsis (Fig. 3.11). The co-expression Cluster 1 (stress-responsive) and Cluster 2 (senescence-related) were interlinked *via* RD26, ANAC019, DREB2A, and the other 12 genes in the network. The analysis suggested that the NAC-mediated stress response and growth processes are entangled by overlapping hormone and cell-signaling networks involved in abiotic stress, energy metabolism, and cell expansion. The senescence-associated *VuNAC* gene cluster potentially interacts with peroxidases (*DOX1*), regulating redox balance and trehalose biosynthetic genes like *TPS8*/*TPS11*, required for the onset of leaf senescence when high content of carbon is available [360]. Cluster 3 and Cluster 4 did not seem connected (Fig. 3.11B), suggesting independent regulation of the speculated basal and architectural functions.

3.4.3 Cowpea NAC family is multifarious in function

3.4.3.1 Versatile domains of VuNAC TFs

Cowpea NAC TFs harbored chimeric domains that are functional trademarks for other proteins involved in cell division, cell death, cytoskeleton synthesis, respiration, and cell signaling apart from the transcriptional motifs (Table 3.2). Furthermore, many VuNAC proteins owned the functional sequence profiles of proteins involved in pivotal processes, like folate synthesis, carbohydrate transport, lipid signaling, cell-wall binding, electron transfer, and growth regulation (Table A1.3.2, Appendix 1). This suggested that the NAC TFs have the propensity to undertake diverse cellular processes directly. In addition, the motif analysis in TAR regions and the noteworthy conservation and redundancy in the paralogous proteins advocate their functional and evolutionary importance (Fig. 3.5). Clearly, VuNAC TFs genes play crucial roles in plant processes integrating stress and growth-associated cellular metabolic phenomena. Our study revealed that 16.2% of the VuNAC TF fraction was dedicated to stress responses exclusively. 26.9% and 13.9% proteins were dedicated to cell-wall and xylem development and basal organogenesis, respectively. 22.3% of the portion was speculated to be involved in other developmental processes like flowering and aging. 20.8% of the family

having no similarity to any other species were novel to cowpea, hence a prominent candidate for further research in plant science (Table 3.5).

3.4.3.2 ATAF-like Group I members signified potential tools for crop improvement

Plants continuously evolve the intricate stress-signaling pathways and their genetic determinants to sustain tolerance to the changing adverse environments by tuning innumerable biochemical, metabolic, and molecular mechanisms. Our finding regarding functional clustering of cowpea NAC TF might elaborate on understanding NAC response in development and stress response over a broad scale. The five ATAF-like members clustered in subgroup Ia held the immense potential to serve as a genetic manipulation tool to combat stress and improve crop yield (Fig. 3.1C). Because they seemed to function in coordination with other stress-responsive TFs (NAC/MYB/ERF/WRKY) and genes crucial for growth such as Dof (regulator of seed-storage protein) and TCP (cell proliferation), possibly integrated by glutathione and starch/sucrose metabolism, thus, the members could potentially boost the plant defense and basal development (Fig. 3.9B and Fig. 3.11C).

Chapter 3

CHAPTER 3

4. CLONING OF NOVEL COWPEA TRANSCRIPTION FACTORS AND THEIR FUNCTIONAL CHARACTERIZATION IN YEAST

This chapter discussed the cloning of two unique ATAF-like TFs (VuNAC1 and VuNAC2), isolated from a drought-hardy wild cowpea genotype, which were induced by multiple abiotic stresses, abscisic acid, and light. The GFP-fused proteins were localized to the nucleus. Y2H and reporter assay demonstrated the dimerization and transactivation abilities of VuNAC proteins having structural folds similar to rice SNAC1. The gel-shift assay indicated that the TFs recognize an "ATGCGTG" motif for DNA-binding shared by several native TFs in yeast. The heterologous expression of VuNAC1/2 in yeast improved growth, biomass, lifespan, fermentation efficiency, and altered cellular composition of biomolecules. The transgenic strains conferred tolerance to multiple stresses such as high salinity, osmotic stress, freezing, and aluminum toxicity. The LCMS-based analysis of the metabolome revealed reprogramming of major pathways synthesizing nucleotides, vitamin B complex, amino acids, antioxidants, flavonoids, and other energy currencies and cofactors. Our results suggested that VuNAC1 and VuNAC2 TFs are positive transcriptional regulators of abiotic stress signaling and growth-associated processes acting through metabolic remodeling to maintain the energy status, hence improving stress recovery and nutrition balance of the transgenic strains. These findings laid the foundation for further study of the functional role of VuNAC1/2 TFs in the stress and growth signaling of plants.

Keywords: Cowpea NAC transcription factor, multiple stress-tolerance, metabolic reprogramming, energy homeostasis, improved growth, LCMS, Saccharomyces cerevisiae

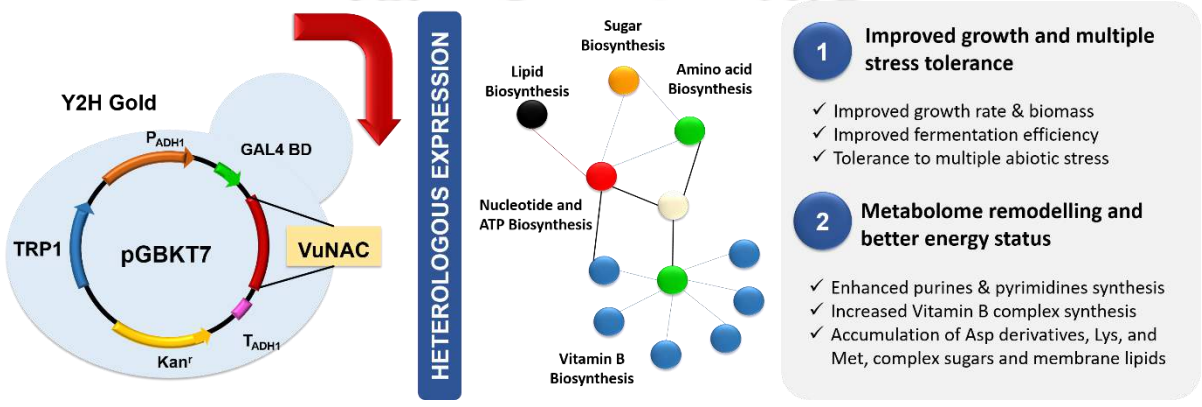

4.1 INTRODUCTION

NAC TFs are the central regulators of stress responses and development in plants. However, functional conservation of orthologous NAC TFs can be unpredictable, hence not suitable for legume genetic engineering. Cowpea (*Vigna unguiculata* L. Walp) is emerging as a 21st-century food legume, holding immense nutritional and economic value [361]. It is an inexpensive grain legume providing a cheap protein source to rural and urban populations. The hay left after the grain harvest serves as high-value nutritious forage to farm animals. The genetic diversity in cowpea is greater than that of any other crop in the dry African Savannah [362]. The wide genetic variability, robustness, and phenotypic plasticity of cowpea have enabled its adaptation to adverse soil and climatic conditions to acquire the peculiar features of stress resilience. Such natural variants in crop plants mainly resulted from spontaneous mutations in their wild progenitors, with crop domestication and breeding. Understanding the genetic basis of phenotypic variation and identifying the genetic variants underlying natural variation of tolerance can help us understand the adaptive potential of wild plant populations and efficiently utilize these diverse genetic resources for crop improvement. Enormous germplasm resources, whole-genome sequencing combined with genome-wide analysis, and large-scale transcriptome and metabolome analysis have enabled extensive and rapid exploration of the natural variations and associated phenotype variants and the underlying sequence alterations and exploiting that for crop design through transformation tools.

Thus, studying stress-resilience and non-commercial cowpea varieties like *Kannanado white* [252] to explore native untapped and versatile NAC TFs balancing the growth and stress regulating, and characterizing the functional roles in research models offers viable means to deal with legume stresses and secure yield potential by a more effective approach. However, NAC TFs can function as both transcriptional activators and repressors to execute stress tolerance as well as sensitivity [27, 58]. Besides, no NAC genes have been cloned in cowpea, and their role in abiotic stresses and plant development is largely unknown. Thus, it is imperative to anticipate their physiological and stress-responsive phenotypes by characterizing the genes in a simpler model before being used as candidates for the genetic improvement of plants under fragile environments and yield traits.

Yeast serves as a crucial eukaryotic model for cell and molecular biology research to study fundamental biological processes, including cell cycle, aging, and stress response. According to Zhu *et al.*, yeast's core stress signaling pathways are the foundation for the evolution of plant

stress sensing components [363]. For instance, SnRK1 (sucrose non-fermenting 1-related) kinase family of plants is similar to yeast SNF1 (**S**ucrose **N**on-**f**ermenting-1), a mediator of stress signaling and energy status controlling sugar metabolism and growth arrest under glucose deprivation through extensive transcriptional and metabolic reprogramming to restore homeostasis [364]. Previously, it has been reported that heterologous expression of plant genes such as *AtMED15*, *AtOxR*, and *AtSOS* can alter cellular phenotype, improve fermentation efficiency and confer stress tolerance in yeast [365-367]. *ATAF1, ANAC032, and ANAC102* encoding stress-responsive plant TFs belonging to the ATAF subgroup have been found to successfully regulate orthologous gene expression in yeast using their native activation domain [368]. As many basal metabolic and biosynthetic pathways are conserved in eukaryotes, yeast can be a convenient system for the functional characterization of untapped plant stress factors. The heterologous NAC TFs can retain their protein fold, biological activity, and cellular functions when expressed. Further, the OMIC tools and well-elaborated metabolic and functional relationships of yeast can be used as a model to understand the potential regulatory mechanism. The deduced preliminary knowledge may lay the foundation for further validation in complex native system.

This chapter discusses the characterization of stress-induction, protein characterization, and possible growth and stress-related role of novel ATAF-like TFs, VuNAC1, and VuNAC2, isolated from drought hardy cowpea variety by heterologous expression in a yeast model. The transformed yeast strains exhibited tolerance to multiple environmental stresses complemented with ameliorated growth characteristics. In addition, the accumulation of cellular antioxidants such as glutathione and flavonoids aided stress tolerance. Our study identified suitable NAC candidates for sustainable stress improvement, compensating the energy depletion and remodeling vital cellular metabolism for better growth and maintenance under nutrient-limited or surplus conditions.

4.2 MATERIALS AND METHODS

4.2.1 Gene isolation and construction of expression vectors

The trifoliate leaves from 15-day-old healthy cowpea seedlings of Kannanado White (IITA, Nigeria), a drought hardy genotype [252], were subjected to PEG 6000 (20% w/v) and NaCl (200 mM) stress for 24 h and sampled for RNA extraction to prepare the cDNA library. Nested PCR was performed to isolate two partial NAC encoding gene sequences from the library, using a set of degenerate primers targeting conserved regions of previously reported stress-responsive NAC genes [27, 31, 33]. The full-length ORFs were retrieved by the 5' and 3'-RACE PCR (Invitrogen), mentioned in Table A2.10, Appendix 2. For their phylogenetic clustering, the ESTs available for cowpea NAC family and Arabidopsis NAC genes were downloaded from Plant TFDB 4.0 database (http://planttfdb.gao-lab.org/index.php) [52]. The promoter sequences were retrieved from the NCBI database (https://www.ncbi.nlm.nih.gov), and the regulatory elements were identified using the PLACE tool (https://www.dna.affrc.go.jp/PLACE/?action=newplace) [332].

For the localization study, the 35S:VuNAC1/2:GFP constructs were generated by fusing an eGFP sequence (isolated from pBI221) at the 3'-end of the VuNAC ORFs lacking the stop codon, by overlapping PCR, followed by cloning in pBEAB plant binary expression vector (provided from Gifu University, Japan) at the SfiI sites. The constructs were transformed in the EHA105 Agrobacterium strain. For protein expression, the full-length ORFs were cloned in the pET28a (+) vector (GE Healthcare) to fuse the 6×His tag at the N'-end, using BamH1/SalI site (VuNAC1) and BamH1/XhoI sites, followed by the transformation in BL21(DE3) bacterial strain (GE Healthcare). For the yeast-based reporter assay, GAL4BD was fused with the full-length VuNAC ORFs (GAL4BD:VuNAC1/2) and with the VuNAC ORFs having truncated C'-part (GAL4BD:VuNAC1/2ΔAD) and cloned in pGBKT7 vector (Clontech) at NdeI/BamHI sites. All the constructs were individually transformed in the Y2H Gold yeast strain, as described in the Yeast transformation manual (Clontech). The transformants were screened on SD-/Trp plates incubated at 30ºC for 3-4 days. The GAL4BD:VuNAC1/2ΔAD constructs were also used as bait plasmids for the yeast two-hybrid (Y2H) assay. To generate the prey plasmids, GAL4AD was fused with the full-length VuNAC ORFs (GAL4AD:VuNAC1/2) and cloned in pGADT7 vector (Clontech) at NdeI/BamHI sites. The constructs were transformed in the Y187 yeast strain (Clontech). The transformants were screened on SD-/Leu plates incubated at 30 ºC for 3-4 days. The primer sequences used in this study are listed in Table A2.11, Appendix 2.

4.2.2 Expression analysis and stress treatment

Healthy cowpea seeds (*Kannando White*) were germinated by soaking in water for two days in the dark followed by a long-day photoperiod condition (16 hr of light, 8 hr of dark) at 28°C, with white light illumination (110 µmol photons $m^{-2}s^{-1}$). Four-day-old germinated seedlings were transferred to gauzed hydroponics container supplied with modified Hoagland hydroponics media for approximately ten days until the first trifoliate leaves expanded [333]. For various stress treatments, the hydroponics media was supplemented with 20% PEG 6000, 200 mM NaCl, 50 µM of $AlCl_3$ (pH 5.0), 50 µM (±) ABA, and 50 µM methyl jasmonate (MeJA), individually. For heat and cold treatments, the plants were transferred to the respective growth chambers maintained at 45°C and 4°C. For dehydration stress, the leaves were dried at 26°C until 10% fresh weight loss. The trifoliate leaves from the stressed and the control plants were sampled at the indicated time intervals for RNA extraction using the RNeasy mini kit (Qiagen), followed by cDNA synthesis (Applied Biosystems, USA). The semi-quantitative and quantitative real-time PCR was performed in triplicates for each sample on Thermocycler Dice, Real-time system II (Takara, Japan). *VuUbiquitin2* was used as a reference to determine the relative expression. The experiments were repeated three times with similar results.

4.2.3 Localization, transactivation, and dimerization

To determine the subcellular localization of GFP-tagged VuNAC1 and VuNAC2 proteins, healthy onion epidermis was transiently transformed by infiltration method, with the Agrobacterium strain carrying the 35S:VuNAC1/2:GFP constructs ($O.D._{600}$ ~0.8), suspended in the infiltration buffer (41.65 mM D-glucose, 10 mM $MgCl_2$, 10 mM MES-KOH (pH 5.6), and 100 µM Acetosyringone). The strain expressing the eGFP alone driven by a 35S promoter was used as the positive control. After three days of co-cultivation, the infiltrated section was stained with 1 µg/mL DAPI (4',6-diamidino-2-phenylindole) in 10% glycerol and kept in darkness for 10 min. The fluorescence was captured by Zeiss Axio (Germany) under the excitation filters 470 nm (for eGFP) and 400 nm (for DAPI). For the yeast-based reporter assay, the 10-fold serial dilutions of the overnight cultures (O.D. ~0.6) of Y2H transformants carrying the pGKT7 plasmid (negative control), GAL4BD:VuNAC1/2, and GAL4BD:VuNAC1/2ΔAD constructs were spotted on agar plates with appropriate selection media, SD/-Trp, SD-Trp + 40 µg/ml of X α-gal (SD/-Trp +X) and SD/-Trp + 40 µg/ml of X α-gal + 2 µg/ml of Aureobasidin A (SD/-Trp + XA), and incubated at 30 ºC for 2-3 days. The formation of blue colonies and growth in the presence of Aureobasidin A antibiotic indicated the expression of *MEL1* and *AUR1C* reporter genes, respectively, through transactivation. For the Y2H assay, Y2H gold

strain harboring the bait plasmid, *i.e.*, pGBKT7-53 (positive control), pGBKT7-Lam (negative control), and GAL4BD:VuNAC1/2ΔAD constructs and Y187 strain carrying the prey plasmid, *i.e.*, pGADT7-T (positive control) and GAL4AD:VuNAC1/2 constructs, were mated as described in the Y2H manual (Clontech), and the colonies were screened in the double drop-out media (SD/-Trp-Leu) for the presence of both bait and prey plasmids. The 10-fold serial dilutions of the overnight cultures (O.D. ~0.6) of selected colonies were spotted on agar plates with appropriate selection media SD/-Trp-Leu, SD/-Trp-Leu-Ade-His (quadruple drop out), SD/-Trp-Leu + 40 µg/ml of X α-gal (SD/-Trp-Leu + XA), and incubated at 30 ºC for 2-3 days. The formation of blue colonies on SD/-Trp-Leu-Ade-His media in the presence of Aureobasidin A indicated the expression of *MEL1, HIS3, ADE2,* and *AUR1C* reporter genes, due to prey-bait interaction. To avoid the false reporter expression due to the transactivation ability of VuNAC1/2, the bait plasmids with truncated C'-part (GAL4BD:VuNAC1/2ΔAD) were used for the Y2H assay.

4.2.4 Protein purification, EMSA assay, and structure prediction

The BL21 (DE3) strains harboring the His-tagged VuNAC ORFs were grown in LB media + 50 µg/ml Kanamycin ($O.D._{600}$ ~0.4). The culture was induced with 1mM IPTG followed by incubation for 16 hours at 30 ˚C, 180 rpm. The cells were harvested, the pellet was re-suspended in 50 ml of suspension buffer (50 mM Na_2HPO_4, 50 mM NaH_2PO_4, 300 mM NaCl, and 1 mM PMSF), added with 0.5 mg/ml lysozyme, pH 7.4), and incubated on a rocker at 4 ˚C for 1 hour. The lysate was homogenized by sonication and centrifuged at 11000 rpm at 4 ˚C for 30 min to separate the soluble and insoluble fractions. The His-tagged protein was purified from both the fractions by Ni-NTA affinity chromatography and eluted in suspension buffer supplemented with 250 mM imidazole. The eluted protein was diluted in 50 ml of dialysis buffer (5 mM Tris-HCl and 15 mM NaCl, pH 7.4) and dialyzed overnight to purify and regenerate the native structure. The protein was further concentrated with a centrifugal filter (10 kDa MWCO). The concentration of the purified protein was estimated using Bradford's assay to be around 20 mg/ml. 20 µl of the protein was electrophoresed on 12% SDS-PAGE gel at 120 V to evaluate the purity and molecular weight. The purified VuNAC proteins were tested for their ability to bind 40 bp NACBS probe made of 4X repeats of 5'-CATGTCCACG-3' motifs NACBS using electrophoretic mobility shift assay (EMSA) [369]. The HPLC-purified oligonucleotide and its reverse complementary strands were annealed by heating at 70 ºC for 5 min and gradual cooling at room temperature in 50 mM NaCl solution to form a double-stranded DNA probe. The NACBS motif was substituted with polyAs to generate the mutated

probe to serve as a negative control. The different concentrations of the protein sample were incubated with 0.01 nmol of DNA probes at 25 ˚C for 30 min in 1 X binding buffer (20 mM Tris–HCl, pH 8.0, 100 mM KCl, 5 mM $MgCl_2$, 5% glycerol, and 1 mM DTT) in a 25 µl reaction volume. After incubation at 25˚C for 30 min, the reaction mixture was electrophoresed in 1% agarose gel in 0.5X TBE buffer at 110 V, and the DNA shift was visualized in the UV light after ethidium bromide staining. Furthermore, the secondary structures and 3D protein folds were predicted using Phyre v 2.0 (http://www.sbg.bio.ic.ac.uk/phyre2/html/page.cgi?id=index)

4.2.5 HPLC analysis

The Y2H Gold strains expressing GAL4BD:VuNAC1/2 (transgenic) and pGBKT (wild type) were cultured in a shaking flask (200 rpm) at 30ºC in YPD media. The supernatant was collected followed by 10000 rpm spin for 30 s at the indicated time-intervals and filtered through a 0.2 µm membrane filter. 20 µl of the sample was injected in a Shimadzu Prominence HPLC System with SPD-M20A DAD (Shimadzu, Japan), equipped with an automatic injector. The Aminex HPX-87H column (300 χ 7.8 mm) (Bio-Rad Labs, CA) was used at the oven temperature of 50°C, and the sample and reference cells were maintained at 25°C. The isocratic elution was done in a de-gassed mobile-phase solvent of 3.0 mM of sulfuric acid in water at a flow rate of 0.6 ml/min. The analytes were detected by an RI detector (Model 410). The serial dilutions of ethanol, glycerol, and glucose were run as standard for quantitative estimation.

4.2.6 FTIR spectroscopy

The yeast strains were cultured in a shaking flask (200 rpm) at 30ºC in YPD media. The samples were collected at two different growth phases, the late-log phase (OD_{600} ~1.2) and late- stationary phase ($O.D._{600}$ ~2.0), in biological replicates. The metabolism was cold-arrested in ice. The cells were harvested, washed in PBS buffer, and then dried to powder using the Scanvac Coolsafe Freeze dryer (Electronex, Mumbai). The ATR-FTIR spectra for the powdered sample were recorded with an ATR unit (Specac, U.K.) combined with an IRAffinity 1-S spectrophotometer (Shimadzu, Japan) with a resolution of 4 cm^{-1} and 64 scans in the range of 4500-400 cm^{-1}. The acquired spectra were analyzed using OMNIC software. The absorption spectra of the wild type strain were subtracted from that of the transgenic strains and plotted to project variations between the two samples.

4.2.7 FESEM and Light microscopy

The yeast cells were fixed with 1.0% (v/v) glutaraldehyde solution for 3 h [370]. After fixation, the cells were spotted on an aluminum surface mounted on carbon tape and gradually air-dried. The specimen was coated with gold and analyzed at 2000X magnification using GeminiSEM 300 (Zeiss, Germany), operating under an accelerating voltage of 2 kV. For light microscopy, the yeast culture was spotted on a glass slide and visualized under Nikon E100 LED Binocular Microscope (Nikon, Japan) under the bright field.

4.2.8 LC-MS profiling of metabolome

50 mg powder of each sample was taken, and metabolite quenching was carried out using 2 ml of methanol: water (1:1) mixture, followed by ultrasonication for 30 min and centrifugation at 14000 rpm for 3 min. The polar-phase supernatant was dried by lyophilization. The residue was re-suspended in 0.5 ml of LC mobile phase A (0.1% formic acid in water) and filtered through a 0.2 µm filter before injection [371]. The samples were analyzed by LC-MS in Agilent 1260 binary LC System (Agilent Technologies, D.E.) using Agilent Zorbax Eclipse Plus C18 column (50 x 2.1 mm, 1.8 µm). The injection volume was 2.0 µl and the flow rate was 0.3 ml/min. The LC solvents were 0.1% formic acid in water (solvent A) and acetonitrile (solvent B). The gradient elution was as follows: t = 0 min, 5% B; t = 18 min, 95% B; t = 27 min, 95% B; t = 27.1 min, 5% B; t = 30 min, 5% B. All MS acquisitions were performed in both positive and negative electrospray ionization (ESI) mode at a scan rate of 3.0 Hz in the mass range 60-1600 m/z. The capillary voltage, cone voltage, fragmentor voltage were 4 kV, 45 V, and 150 V, respectively. The gas temperature was set at 350 °C. The data were analyzed with Agilent Masshunter Qualitative Analysis v. B.06.00 and Agilent Mass Profile professional v. 12.6.1 to detect peaks and de-convolute the mass spectra. The Yeast Metabolite Database (YMD) and METLIN database were used to annotate the metabolites.

4.3 RESULTS

4.3.1 ATAF-like VuNAC1/2 TFs isolated from wild cowpea genotype were induced by light, ABA, and multiple abiotic stresses

NAC genes exhibit a differential spatiotemporal expression in response to stress. However, a significant proportion of the genes express ubiquitously, having strong expression in leaves [123]. As many growth-associated traits are coupled with the shoot, we chose leaf tissue to hunt the candidate genes having versatile roles in growth and stress responses. We isolated two NAC genes (*VuNAC1* and *VuNAC2*) from a non-commercial drought-hardy cowpea genotype (*Kannanado White*) treated with NaCl and PEG-induced stress [372], using a degenerate PCR approach seeded by the ATAF-like drought and salt-responsive genes from Arabidopsis, rice, and soybean shown in the phylogenetic tree [27, 31, 33] (Fig. 4.1A, B and Fig. A2.1, Appendix 2). When the cloned sequences were aligned with ATAF subgroup members of Arabidopsis and the ESTs available for cowpea NAC genes, a close relationship of VuNAC1/2 with the ATAF subgroup was found (Fig. 4.1C). The complete ORFs (888 bp each), retrieved by RACE-PCR, encoded a 295 aa protein with a NAC signature domain (InterPro ID: IPR036093) of 160 amino acid residues present in the N-terminal part, displaying close similarity to the ATAF1 domain [27], with a sequence identity of 93.5% and 85.8%, respectively. However, overall protein sequence identity of 70.9% and 60.6% indicated high divergence in the C-terminal regions, which carry crucial regulatory motifs, suggesting a possibly indifferent behavior from their ATAF-like homologs in other plants.

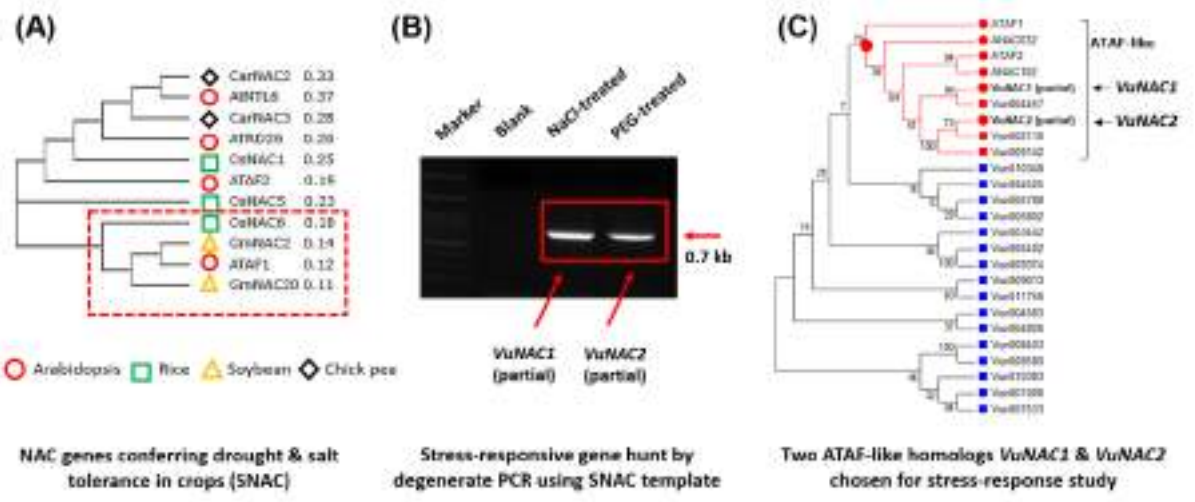

Fig. 4.1 Identification and isolation of stress-responsive *VuNAC* genes from a drought-hardy cowpea variety. (A) ATAF-like NAC genes improving drought and salt tolerance in crops used as a template to design degenerate PCR primers to isolate stress-responsive orthologs from cowpea. **(B)** Amplification of putative NAC encoding genes from cowpea seedlings (*Kannanado White*) treated with 20% of PEG and 200 mM of NaCl (separately) for 24 hours. **(C)** The clones obtained were aligned with the ESTs available for cowpea NAC genes and ATAF orthologs (ATAF1/2, ANAC032, and ANAC032) to study their phylogenetic relationships.

The analysis of the gene promoters revealed over-representation of the key *cis*-regulatory elements, identified in Arabidopsis and other model species for hormone signaling (ABA and auxin), TF binding (MYB, WRKY, and NAC), abiotic stresses (dehydration, osmotic stress, hypersalinity, and cold), nutrition signals (sugar, iron, and copper), light regulation, and expression in cytochrome and mesophyll tissues (Table 4.1). The time-course study of *VuNAC1/2* expression indicated that the genes exhibited strong induction in response to dehydration (10% loss in fresh weight), salt (200 mM NaCl), and osmotic stress (20% PEG), induced after 3 hrs, showing a marked accumulation of transcripts after 24 hrs with the maximum relative fold change recorded (Fig. 4.2 A, B). When examined in response to aluminum stress (50 µM, acidic pH 5.0) in shoot tissue, we found the strongest induction at 3 hrs, which decreased gradually with time, unlike the other dehydration and salt responses which persisted for more than 24 hrs. Whereas in the roots, the genes showed delayed induction with prominent expression after 24 hrs, indicating the different mode of signal perception in shoots and roots (Fig. A2.2, Appendix 2). In addition, the genes exhibited significant induction in response to ABA (50 µM), methyl jasmonate (50 µM), cold treatment (4 °C), and heat stress (45 °C), as shown in Fig. 4.2C. Rapid and transient induction by light exposure was also recorded, which diminished within an hour (Fig. 4.2D). This can explain the peculiar expression profile at 12 hr when *VuNAC1/2* showed induction in control conditions irrespective of the stress treatment (Fig. 4.2A). Our study of promoter regulatory elements and gene expression pattern indicated that the ATAF-like cowpea orthologs, *VuNAC1* and *VuNAC2*, regulate multiple abiotic stresses, hormones, light, and nutrition signaling to play a crucial role in both growth and stress adaptation.

Table 4.1. List of *cis*-regulatory elements in the promoter of the *VuNAC1/2* genes identified by PLACE tool

Mode of regulation		cis-element	Description	Frequency	
				VuNAC1	*VuNAC2*
Hormonal regulation	ABA	ABREATRD22, ABREATCONSENSUS	ABA responsive element	4	5
	Auxin	ASF1MOTIFCAMV, NTBBF1ARROLB, CATATGGMSAUR	Auxin/SA responsive element	5	5
	JA	CGTCA-motif	JA responsive element	2	3
	GA	GADOWNAT	GA responsive element	2	1
	Ethylene	ERELEE4	Ethylene responsive element	2	1
Transcriptional regulation	MYB	MYCCONSENSUSAT, MYB2CONSENSUSAT, MYBCORE, MYB1AT, MYBST1	MYC and MYB binding sites involved in water-stress	15	18
		MYBPZM	MYB binding site, involved in flavonoid biosynthesis	1	2
	WRKY	WRKY71OS, WBOXATNPR1, WBOXNTERF3	W-box involved in GA and SA response and wounding	12	22
	CBF	CBFHV	CBF binding site involved in dehydration-response	2	3
	EMBP	EMBP1TAEM	EMBP binding-site involved in ABA-response	1	2
	NAC	NACRS	NAC binding site	2	1
Light Regulation		GT1CORE, SORLIP1AT, GATABOX	Light-responsive element	28	30
Stress and nutritional regulation	Dehydration	ACGTATERD1, DRECRTCOREAT	Required for etiolation-induced expression of AtERD1	5	8
	Osmotic & Hyper salinity	TAAAGSTKST1	Element regulating a K(+) influx channel in stomata	5	5
		ABRERATCAL	Elements in Ca(2+)-responsive genes	5	3
	Low-temperature	LTRECOREATCOR15, CRTDREHVCBF2	Cold responsive element	1	2
	Oxygen	ANAERO2CONSENSUS	Involved in the fermentation	1	1
	Elicitor	GT1GMSCAM4	Pathogen and salt-responsive element	21	26
		EBOXBNNAPA, ARR1AT	RRE (R response element)		
	Phosphate	P1BS	Phosphate-starvation responsive element	0	1
	Sulphur	SURECOREATSULTR11	Sulphur-responsive element	0	3
	Iron	IRO2OS	Iron deficiency responsive element	1	2
	Copper	CURECORECR	Copper-responsive element	2	3
	Sugar (repression)	PYRIMIDINEBOX-OSRAMY1A, SREATMSD, TATCCAYMOTIF-OSRAMY3D	Involved in sugar repression	4	5
Others	Circadian	CIACADIANLELHC	Element involved in the circadian expression of tomato	1	0
	Enhancer	EECCRCAH1	Enhancer element	1	3
	Root-hair	RHERPATEXPA7	Root hair-specific element	1	2
	Endosperm	AACACOREOSGLUB1	Element for endosperm-specific expression	0	0
	Mesophyll	CACTFTPPCA1	Element for mesophyll-specific expression	4	17
	Cytochrome	SITEIIATCYTC	Element in cytochrome genes	4	0

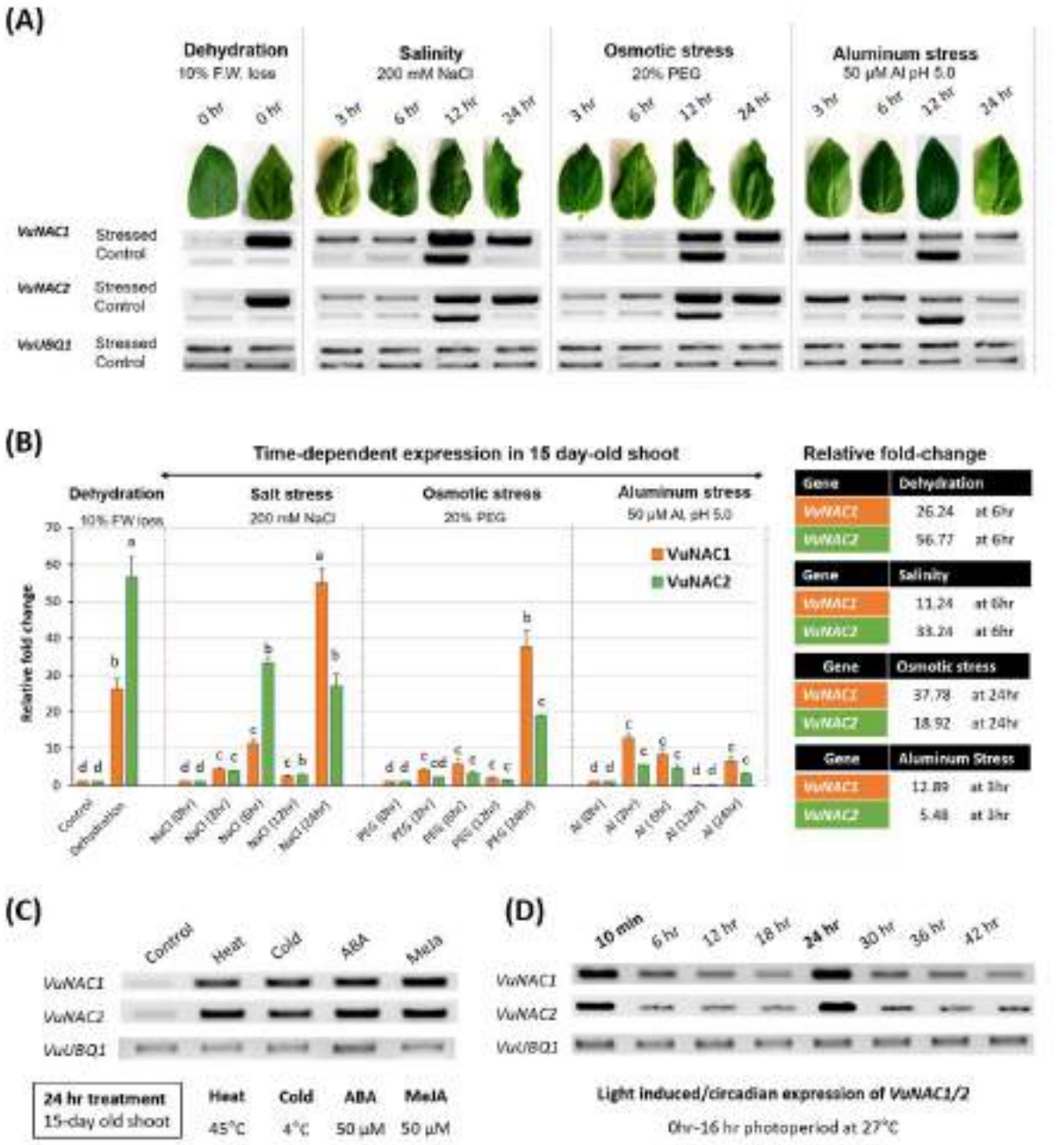

Fig. 4.2. Time-course study of *VuNAC1/2* induction under abiotic stresses, stress hormones, and light. (A) Expression analysis of *VuNAC1* and *VuNAC2* in 15-day-old cowpea seedlings showing strong induction by dehydration, PEG, NaCl, and aluminum. **(B)** The fold-change of the transcripts accumulated was determined by qRT-PCR. The experiment was repeated more than three times with triplicate samples to get similar outcomes. The letters a, b, *etc.,* indicated the significant differences between the response at $p < .05$ (Tukey's test). **(C)** Persistent induction of VuNAC1/2 by heat, freezing, abscisic acid (ABA), methyl jasmonate **(D)**, and diurnal light exposure.

4.3.2 Characterization of subcellular localization, transactivation, and dimerization abilities of VuNAC1/2 proteins

When VuNAC1/2 proteins fused with a C-terminal GFP (Fig. 4.3A) were expressed in onion epidermal cells, a localized expression of GFP was detected in the nucleus, unlike the 35S CaMV promoter-driven GFP, which was expressed in the whole cell (Fig. 4.3B). This indicated that both VuNAC1 and VuNAC2 are nuclear proteins, unlike the ~10% fraction of NAC members tethered to membrane requiring an inducible proteolytic cleavage for activation [359]. Further, a typical NAC protein is characterized by a conserved N-terminal part (N') responsible for DNA-binding, dimerization, nuclear localization, and divergent C-terminal part (C') carrying the transcriptional regulatory region (TRR) [97, 373].

To assess the transactivation activity of the VuNAC proteins, we performed a yeast-based reporter assay using two types of GAL4BD-fusion (binding domain) constructs, one with full VuNAC (both N' and C' part) sequences (GAL4BD:VuNAC) and the other construct containing partial VuNAC sequences with the truncated C'-part (GAL4BD:VuNACΔAD), as depicted in the Fig. 4.3C. The transformants expressing the GAL4BD:VuNAC constructs formed blue colonies when grown on SD/-Trp medium supplemented with X α-gal, indicating β-galactosidase activity due to *MEL1* reporter expression (Fig. 4.3D). In addition, the transformants also grew on Aureobasidin A containing medium, indicating the expression of the *AUR1C* reporter gene, whereas the transformants expressing constructs lacking the C'-region could not grow. The expression of the reporter genes governed by the GAL4-responsive promoter in the absence of GAL4AD (activation domain) demonstrated the transactivation ability of VuNAC1/2 TFs in the yeast system. The study also stipulated that the sequences necessary for the transactivation reside in the C'- region of the VuNAC proteins.

Furthermore, to test the dimerization ability of the proteins, a yeast-two hybrid (Y2H) assay was carried out using the GAL4AD:VuNAC (prey) and GAL4BD:VuNACΔAD (bait) carrying strains. When the strains were mated and grown on SD/-Trp-Leu and SD/-Trp-Leu-Ade-His (double and quadruple drop-out media), all four reporter genes (*HIS3*, *ADE2*, *MEL1*, and *AUR1C*) independently governed by GAL4-responsive promoter were expressed, manifesting strong prey-bait protein interaction. The study indicated that VuNAC1/2 TFs form dimer with self (homodimer) as well as another protein partner (heterodimer) (Fig. 4.3E). The expression of GAL4BD:VuNACΔAD was sufficient to show strong protein interactions, indicating that the domains responsible for dimerization lie in the N'-part.

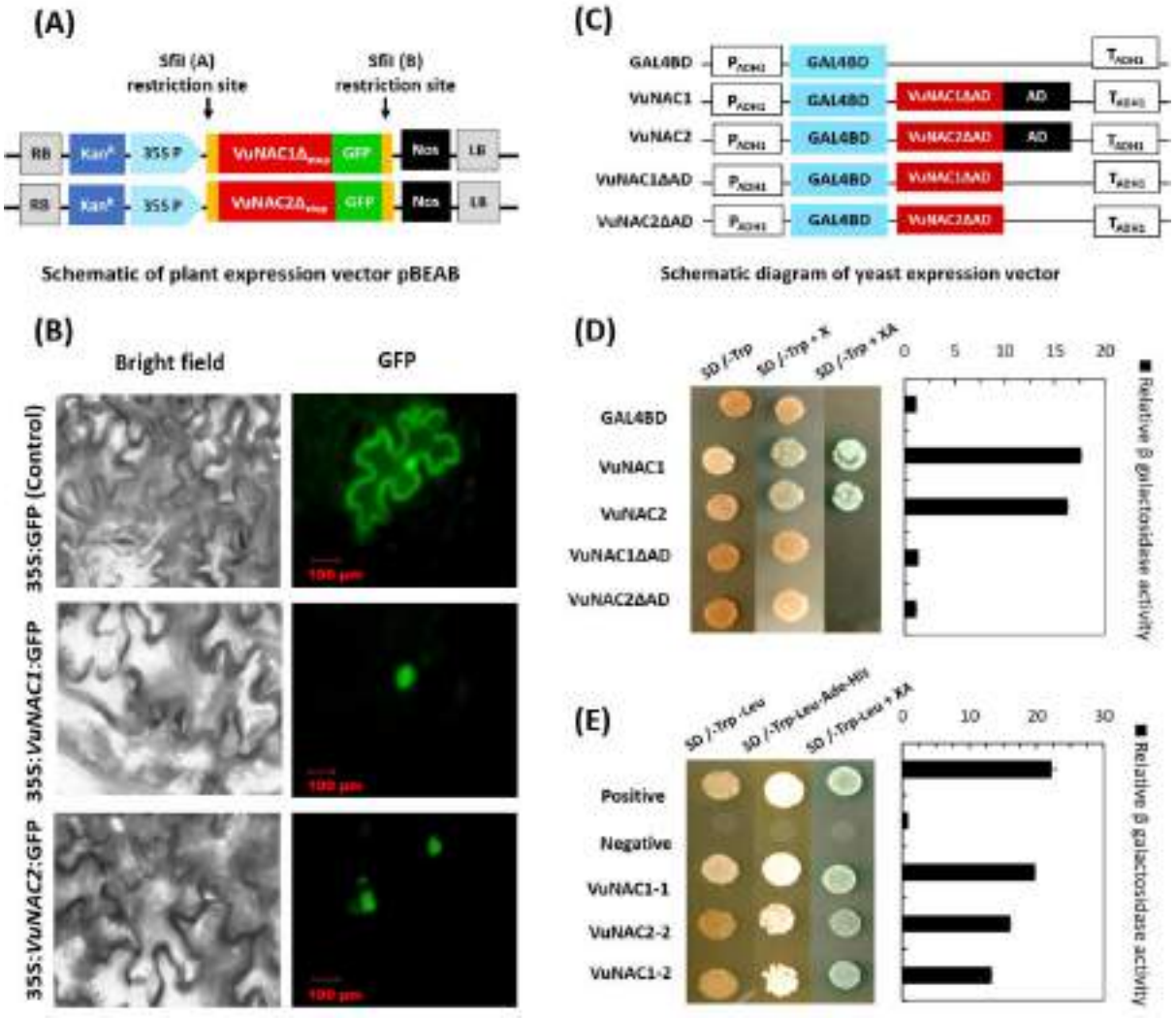

Fig. 4.3 Sub-cellular localization, transactivation, and dimerization of VuNAC1/2 proteins. **(A)** Schematic diagram of 35S:VuNAC1/2:GFP constructs in pBEAB, a plant expression vector. **(B)** Sub-cellular localization of the GFP-fused VuNAC1/2 proteins in tobacco leaf epidermis. **(C)** Schematic of GAL4BD:VuNAC1/2 and GAL4BD:VuNAC1/2ΔAD with truncated C'-part carrying potential activation domain (AD) cloned in pGBKT (bait), and GAL4AD:VuNAC1/2 (prey). **(D)** Yeast-based reporter assay showing the transactivation ability of VuNAC1/2 proteins. **(E)** Yeast two-hybrid assay indicating dimerization of VuNAC1/2 proteins.

4.3.3 Protein purification, DNA-binding activity, and prediction of 3D folding and secondary structures

When the His-tagged VuNAC1/2 proteins were expressed in an inducible bacterial system, we found significant induction of the protein in the insoluble fractions of cell lysate, as predicted by the high instability index of the proteins (Fig.4.4A), in the presence of 1 mM IPTG after 16 h incubation at 30ºC, showing two prominent bands near 34 kDa and 50 kDa (Fig. 4.4B). The former band corresponds to the monomeric form, while the latter stipulates the oligomeric conformation due to incomplete denaturation of the protein structure. To isolate

the protein, the cells were lysed by a combination of enzymatic treatment and sonication, followed by Ni-NTA affinity chromatography. When the proteins were purified further by dialysis, we found a single prominent band close to the theoretical size (68 kDa) of the VuNAC1/2 dimer. This showed that the VuNAC1/2 proteins exist in the dimeric form in solutions, possibly formed by salt-bridges and hydrophobic interactions, which do not dissociate even at high denaturing conditions, like in ANAC (Arabidopsis) and SNAC1 (rice) proteins [98].

NAC TFs recognize their targets using various NACBS [100, 374]. Previously, it has been shown that drought controlling ANAC019/055/072 cluster binds to a MYC-like 'CATGT' sequence with a 'CACG' core [140]. ATAF1 and ANAC019/55/72 also have a binding preference for a 'TACGT' model [100]. Hence, the purified VuNAC1/2 proteins were tested for their ability to bind a 40 bp double-stranded DNA probe containing 4X-repeats of 'CATGTCCACG' sequence derived from an NACBS (TGCGTG) by the electrophoretic mobility shift assay (EMSA). The DNA:protein concentration was optimized to find a visible shift at 1:40 molar ratio (0.01 nmol probe and 50 µg VuNAC1/2 protein). Fig. 4.4C showed that the dimeric proteins displayed band-shift indicating the formation of DNA-protein complex between VuNAC and NACBS probe, whereas no binding was observed with the polyA containing mutated DNA probe. Also, the undialyzed protein containing the monomeric or improperly folded protein conformations did not show any shift. The gel-shift assay indicated that VuNAC1/2 proteins specifically bind the DRE/CRT-like 'CACG' core and the 'CATGT' element, which is recognized by several drought-responsive genes and MYC TFs, respectively. Moreover, the dimerization of VuNAC proteins is necessary for their DNA binding activity.

The VuNAC N'-domain was further divided into five sub-domains (A-E) as mapped in Fig. 4.4D. As a whole, the N'-domain was rich in positively charged amino acids (R and K), mainly the sub-domains C and D. In contrast, the sub-domain B contained a high proportion of negatively charged amino acids (D, E, and N). The putative NLS signals were identified in the sub-domain D. The divergent C'- part possessed the 'EVQSEPKW' motif conserved in ATAF-like proteins. The secondary structures and three-dimensional (3D) protein folding were predicted by the Phyre 2.0 tool, using the crystal structure of rice SNAC1 as the template, having 100% confidence, 49% coverage, (N'-part), and overall sequence identity of 75.5% (VuNAC1) and 76.3% (VuNAC2), as shown in Fig. 4.4E and Fig. A2.3, Appendix 2 [98]. The N'-part consisted of α-helices and β-strands, as mapped in the figure.

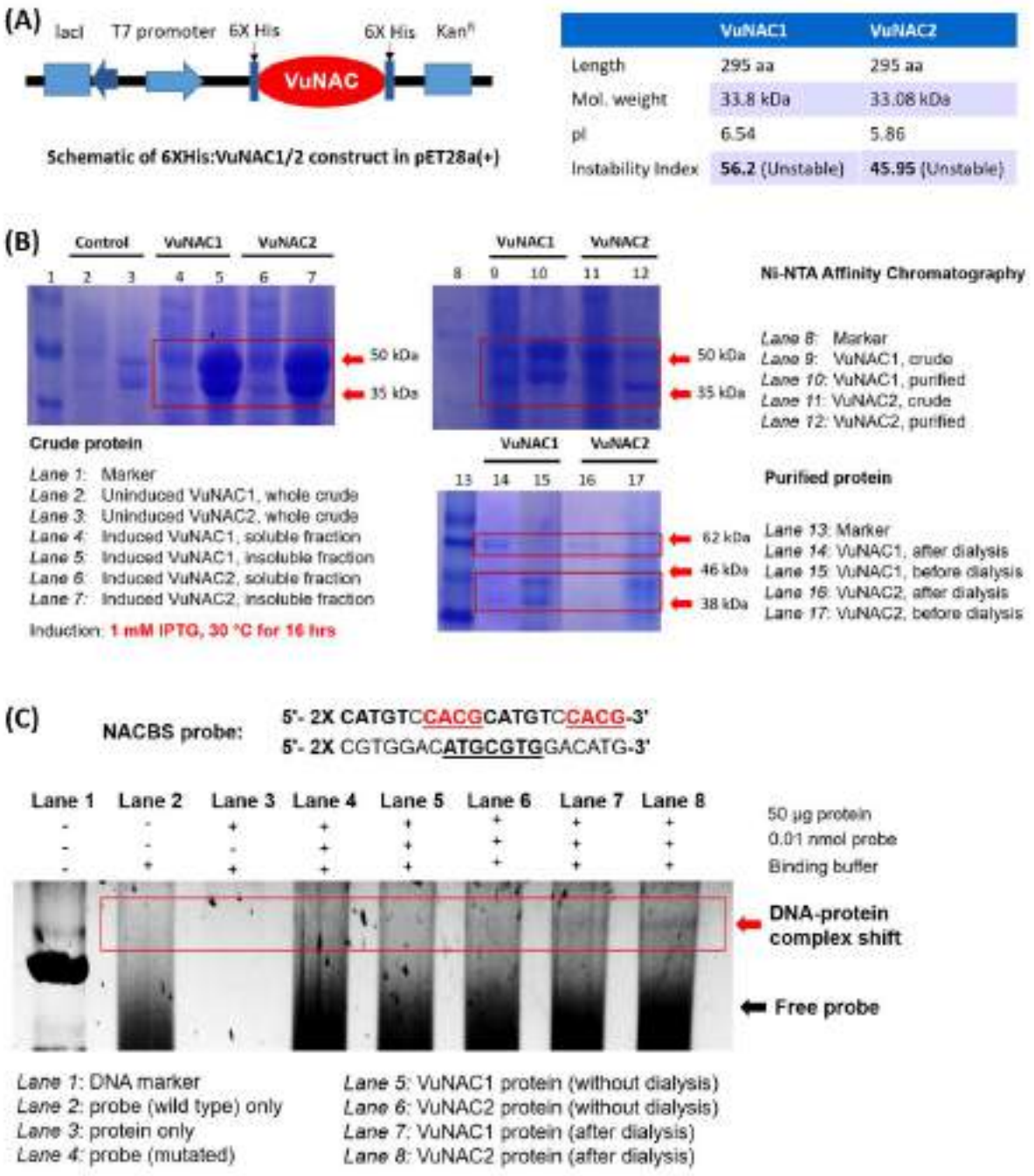

Fig. 4.4 Protein purification and DNA-binding assay. (A) Schematic diagram of 6XHis:VuNAC1/2 construct in IPTG-inducible bacterial expression vector pET28a (left) and biochemical parameters (right). **(B)** Expression of VuNAC1/2 proteins in IPTG-inducible bacterial system (pET28a) and their purification using Ni-NTA Agarose affinity chromatography followed by dialysis. **(C)** Gel-shift assay (EMSA) to determine the binding of VuNAC1/2 proteins to 4X repeat of 'CATGTCCACG' DNA dimer derived from NAC binding site (NACBS).

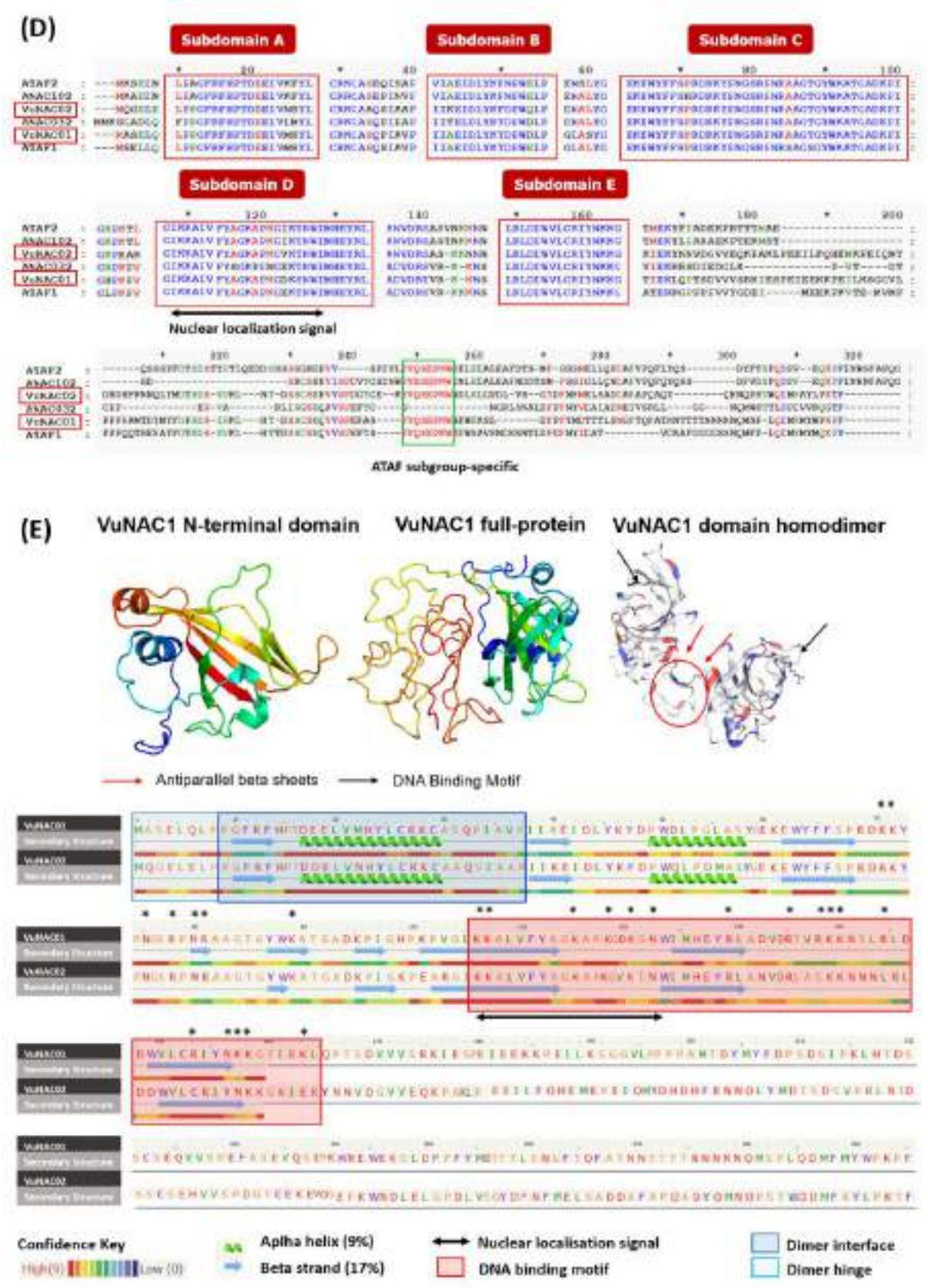

Fig. 4.4 Structure prediction of VuNAC1/2 proteins. (D) Identification of structural sub-domains by aligning the VuNAC1/2 proteins with their Arabidopsis homologs (ATAF1/2, ANAC032, and ANAC102). **(E)** Secondary structures and 3D protein fold of VuNAC1/2 proteins predicted by Pyre 2.0 tool.

The 3D model consisted of a barrel-like central structure formed by seven twisted anti-parallel β strands, sandwiched between two α-helices, one at the N'-end and a shorter helix on the other side. The rest of the structure contained loops. No secondary structure could be predicted for the divergent C'-parts. However, they were rich in polar and acidic amino acid residues like aspartate (D), glutamate (E), asparagine (N), and glutamine and (Q). In the dimeric state, VuNAC1/2 TFs seemed to acquire the unique butterfly-like architecture forming the DNA-binding face [98]. The positions of the amino acid residues likely to participate in the formation of the dimer hinge (1-8) and the dimer interface (9-37) were shaded in blue. The conserved Arg27 and Glu32 may form the salt bridge. The region Val110-Lys165 lying in subdomain D and E containing the β strands (shaded in red) may be involved in the DNA-binding through their positively charged amino acid residues, mainly Lys 118 and Lys 121(indicated by asterisks). Like in ANAC, the Lys72, Arg78, and Arg81 amino acid residues in the sub-domain C may also be significant for binding the DNA substrate [375].

4.3.4 Potential conservation of NAC-like signaling in yeast

NAC is a stress-responsive TF family of plants bearing a unique DNA-binding fold consisting of twisted β-sheets surrounded by α-helical elements rather than the classical helix-turn-helix motif. The members recognize their targets for transcriptional activation or repression through specific binding to the NAC binding sequence (NACBS) in promoter DNA, consisting of a CGT[G/A] core flanked with bases that determine the binding affinity [100, 374]. On investigation, we found that several TF members in yeast, belonging to ATF/CREB, AP-1, and bZIP families, regulating functions such as nutrition assimilation, detoxification, and stress responses, use NACBS-like motif [T/A][T/G]NCGT[G/A] to identify their target genes, as listed in Table 4.2. For instance, ACA1 and ACA2, transcriptional activators stimulated by osmotic shock, regulate yeast growth on non-fermentable carbon sources by binding to the 'TTACGTAA' motif in their dimeric form [376]. Whereas, Sko1p is a transcriptional repressor that regulates gene cascade protecting from oxidative damage [377]. Cad1p, an AP-1 like TF, regulates pleiotropic drug resistance through ABC transporters [378], while Cin5p regulates osmotic stress, metabolism of sugars, glycerol, alcohol, and trehalose, and their transport [379]. Furthermore, Gcn4p is a master transcriptional regulator of amino acid and purine biosynthesis under starvation and stress in yeast [380]. Our study suggested the conservation of NAC-like TF/target network in yeast, corroborating that basal cellular machinery regulating stress responses and primary metabolism in plants evolved from yeast [363].

Table 4.2 List of yeast (S288c) TFs having DNA binding sites similar to NACBS

Yeast TFs	Family	Binding site	Function
ACA1	ATF/CREB	TTACGTAA	utilization of non-optimal carbon sources [376]
ACA2(Cst6p)	ATF/CREB	TTACGTAA	utilization of non-optimal carbon sources, regulates oleate responsive genes [376]
Sko1p	ATF/CREB	ATGACGTA	osmotic & oxidative stress responses [377]
Cad1p (YAP2)	AP-1	TTACgTAAt	stress responses, iron metabolism, and pleiotropic drug resistance [378]
Cin5p (YAP4)	AP-1	gMTTAcgTaA	pleiotropic drug resistance and salt tolerance [379]
Gcn4p	bZIP	TTGCGTGA	amino acid biosynthetic genes in response to amino acid starvation [380]
YAP1	bZIP	ATGACGTA	oxidative and cadmium stress tolerance [378]
YAP6	bZIP	gtctgMTTAcgTaAgcgac	sodium and lithium tolerance [379]

The NAC binding sequence (NACBS) [T/A][T/G]NCGT[G/A] is underlined.

4.3.5 Characterization of growth and stress response of VuNAC1/2 TFs in yeast system

4.3.5.1 Phenotype study of the transgenic yeast strains.

Saccharomyces cerevisiae cells divide asymmetrically into large parent and smaller daughter cells after attaining the critical cell size [381]. When the strains expressing the VuNAC TFs (VuNAC1-ox and VuNAC2-ox) were visualized under field emission scanning electron microscopy (FESEM) in their late-logarithmic phase, a larger fraction of daughter cells was observed than the wild type strain, which had a higher fraction of the parent population instead. Also, fewer dead cells were observed in the transgenic strain during the late-stationary phase than the wild type counterpart (Fig. 4.5A). This suggested that the transgenic strains were more proliferating and viable. Furthermore, their enhanced growth rate and biomass indicated faster cell division and longer lifespan. (Fig. 4.5B). There could be several factors determining the cell size, budding time, lifespan under the nutrition-limiting conditions. One of them is the proportion of quiescent cells which acquire resistance to starvation and preserve their ability to proliferate [382]. In addition, the transgenic strains showed lesser self-aggregation and slower sedimentation (Fig. 4.5C and Fig. 4.5D), suggesting altered cell-surface properties.

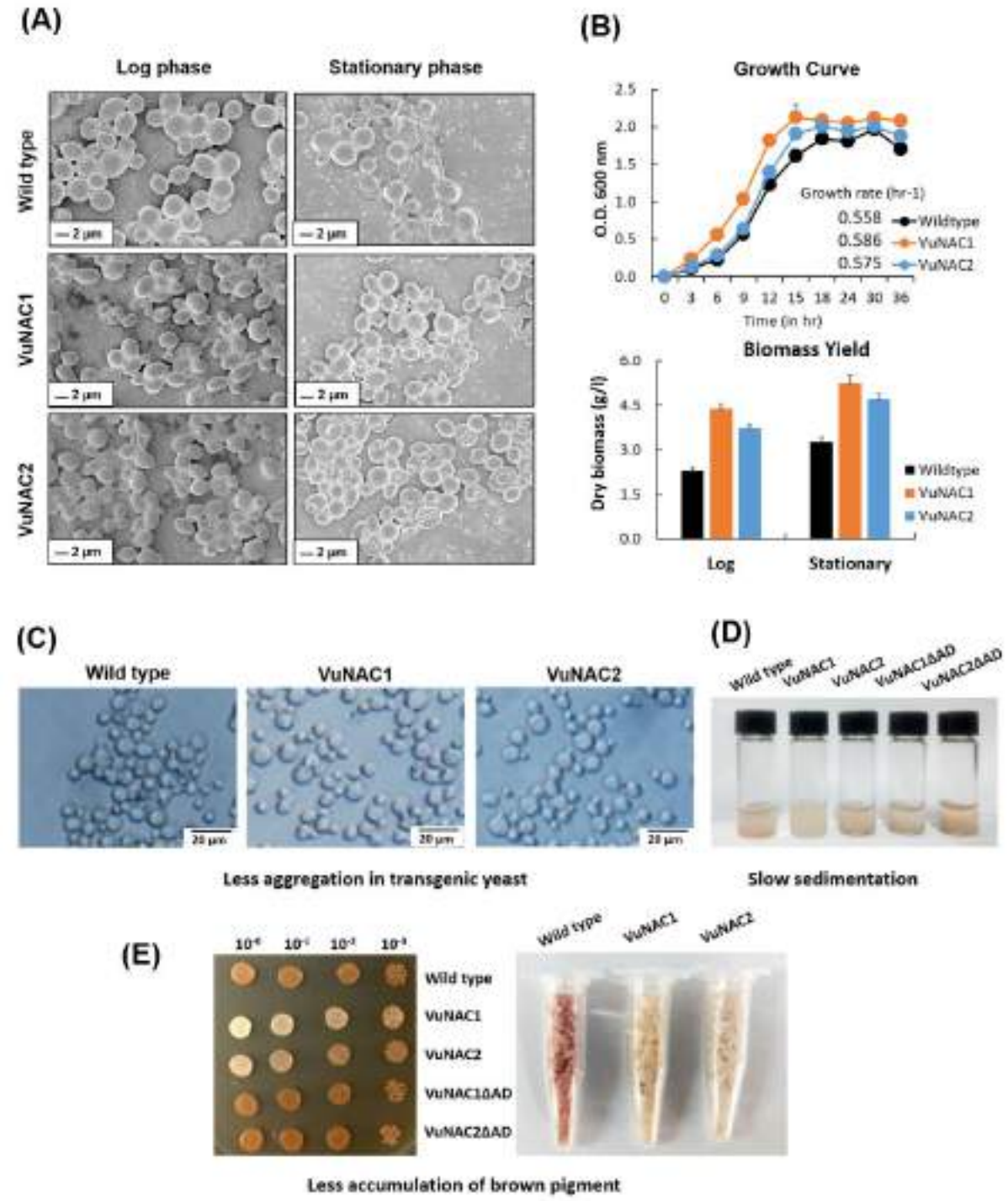

Fig. 4.5 Growth and phenotype characterization of the transgenic strains expressing VuNAC1 and VuNAC2 TFs. (A) Cell morphology in late-log and late-stationary growth phases visualized by FESEM, showing more fraction of dividing daughter cells (small) in the transgenic strains than the mature parent cells (large). **(B)** Growth curve and biomass yield of the strains in different growth phases. **(C, D)** Lesser cell aggregation and slower sedimentation were observed in the transgenic strains.

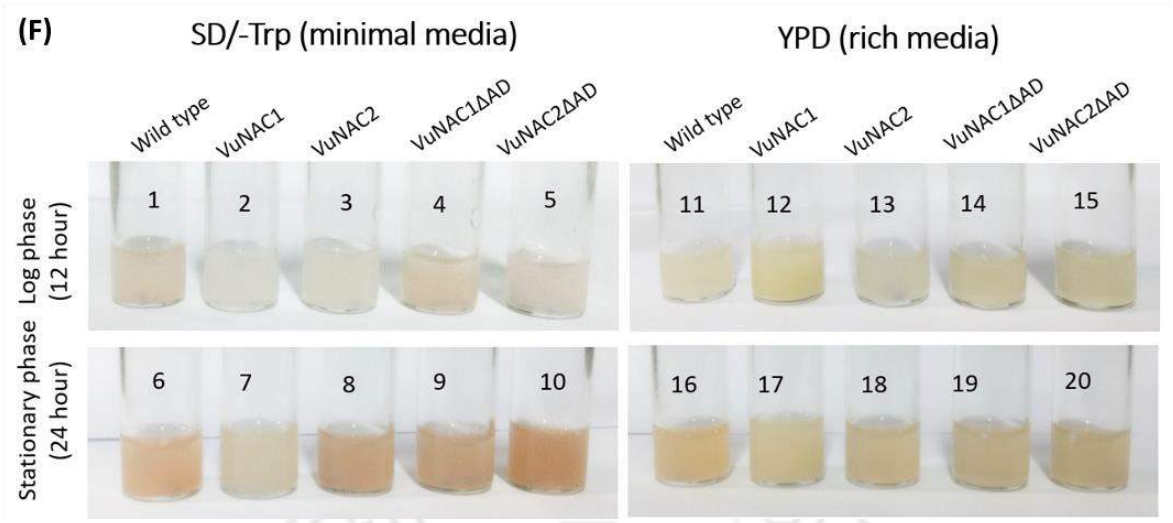

Fig. 4.5 Phenotype under nutrient-limited vs. rich growth conditions. (E, F) Less accumulation of brown pigment (residual adenine substrate) was observed in the transgenic strains expressing full VuNAC1/2 proteins (mainly VuNAC1-ox) when grown in minimal media SD/-Trp (containing limited adenine) and YPD growth media (rich in adenine) after the nutrient was exhausted during the late-stationary phase. The strains expressing the truncated proteins (VuNAC1/2ΔAD) appeared like the wild type.

The wild type Y2H Gold strain was defective in the *Ade2* gene, hence appeared reddish-brown due to the accumulation of the substrate involved in its *de novo* biosynthesis, *i.e.*, P-ribosylaminoimidazole carboxylate (AICAR), during the limiting adenine availability in SD/-Trp, mainly in stationary phase [383]. The transgenic strains showed lesser accumulation of the brown pigment when grown in the minimal synthetic defined (SD) media (Fig. 4.5E). However, the pigment was further reduced when YPD media, rich in adenine supply, was used (Fig. 4.5F). The results suggested that VuNAC1/2 TFs might have a role in adenine salvage to ensure availability, hence avoiding the activation of the *de novo* pathway during the limiting conditions.

4.3.5.2 Evaluation of fermentation efficiency and composition of cellular biomolecules

To proliferate, cells must meet the energy urges inflicted by cellular processes like metabolic biosynthesis, DNA replication, generation of gradients, and cell structure sustentation. Yeast employs a mixed respiro-fermentative pathway to generate ATP and CO_2 from glucose substrate, also producing ethanol, a by-product of commercial interest. A high but optimum amount of glucose aids fermentation to produce maximum ethanol. However, excess glucose may not only repress the respiratory growth *via* the crab-tree effect but also reduce the fermentation efficiency [384, 385]. We analyzed the growth and ethanol production

of the transgenic strains at different glucose concentrations (10%, 20%, and 30%). Compared to the wild type strain, the VuNAC1/2-ox strains manifested a higher growth rate, suggesting endurance to growth suppression. Overall, the growth was highest in 20% glucose, which slowed significantly in 30% glucose until 24 h but was restored eventually in the stationary phase (Fig. A2.4, Appendix 2). The ethanol production was measured the highest, 9.0% (VuNAC1) and 7.8% (VuNAC2) in 20% glucose after 48 h, followed by 10% glucose (Fig. 4.6A). However, the highest fold change *w.r.t.* wild type strain, 3.76 (VuNAC1) and 3.46 (VuNAC2), was observed after 36 h. Glycerol, a major by-product of fermentation, as well as one of the compatible solutes, was also measured. At 10% glucose, the transgenic strains accumulated more glycerol than the wild type. Also, at higher glucose concentrations (log phase), the strains did not show a significant drop in glycerol production like the wild type strain. The results indicated that the transgenic strains exhibited tolerance to glucose-mediated growth repression and improved fermentation efficiency even at high glucose concentrations. This phenomenon may be helpful to ensure ATP synthesis at high substrate concentrations without a trade-off between respiratory growth and fermentation efficiency.

Apparently, there are major alterations in the biochemical composition of the VuNAC1/2-ox strains compared to the wild type. To gain further insight, we used vibrational spectroscopy (FTIR) to study the absorption spectrum of dried cells harvested in the late-log and stationary phases. The differential spectra, divided into five spectral windows (I-V) was shown in Fig. 4.6B, indicating a striking difference between the chemical profile of the transgenic and wild type strains. The prominent absorption bands and their assignment were listed in Table A2.5, Appendix 2 [386, 387]. The region I (3500-3000 cm^{-1}) was wide and convoluted. It included mainly –OH stretching of polysaccharides at around 3400-3300 cm^{-1}, -NH stretching of proteins and peptides at around 3350-3310 cm^{-1}, and amide II overtone near 3100 cm^{-1}. This variation in this region suggested significant modification in the cell-wall polysaccharides and proteins. Region II (3000-2820 cm^{-1}) included absorptions assigned to the stretches in -CH2 and -CH3 bonds of lipids. The variations in this zone suggested an enhanced membrane lipid or β-oxidation of fatty acids in the stationary phase. The region III (2820-1800 cm^{-1}) corresponds to triple bond functional groups like isocyanate (2275-2250 cm^{-1}) and azide (2160-2120 cm^{-1}). Region IV (1800-1325 cm^{-1}) was rich in the amide I and amide II bands of proteins along with lipid ester –C=O peak near 1740 cm^{-1}. The increased absorbance in this zone proposed an increase in the α helix and β sheets form of proteins. The neat increase in spectral absorption indicated more lipid and protein accumulation, especially during the stationary

phase. The region V (1325-750 cm^{-1}) constituted the phosphate ion band of DNA, RNA, and various phospholipids near 1250 cm^{-1}. The marked increase in the carbohydrate region (1135-858 cm^{-1}) indicated the accumulation of mannan oligosaccharides and other complex sugars in the transgenic strain in both the growth phases. Overall, the differential FTIR spectra advocated the role of VuNAC1 and VuNAC2 TFs in regulating the structural and/or cellular lipid/protein, polysaccharides, and nucleotide content.

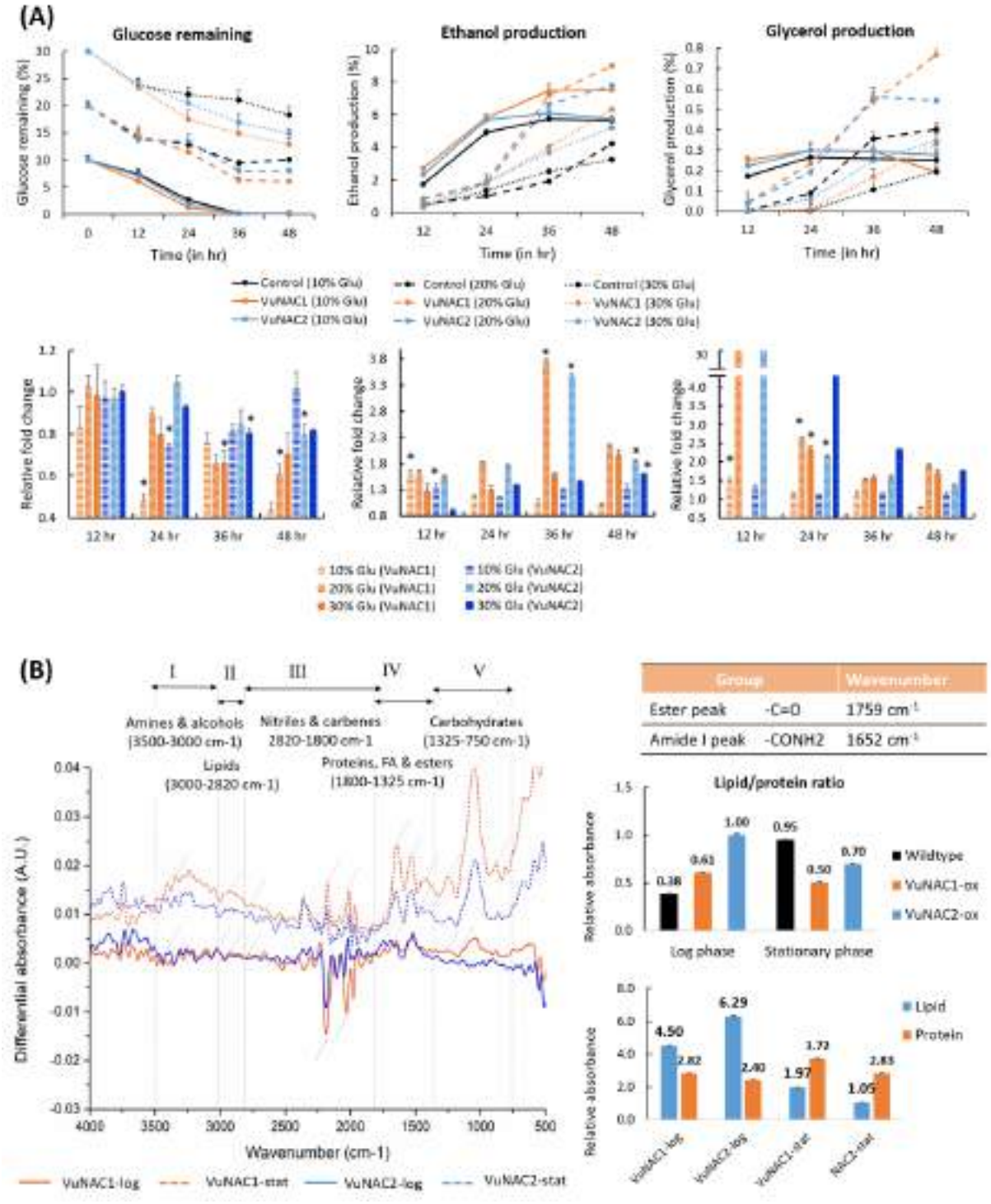

Fig. 4.6 Evaluation of fermentation efficiency under high glucose levels and cellular composition of biomolecules. (A) Estimation of ethanol and glycerol produced (%) at different concentrations of glucose (10%, 20%, and 30%) using HPLC (top), the fold change w.r.t. to the wild type strain (bottom) indicated increased fermentation efficiency of the transgenic strains. **(B)** Differential ATR-FTIR spectra indicate enhanced lipids, proteins, polysaccharides, and nucleotides in the transgenic strains during log and stationary phases.

4.3.5.3 Investigation of stress-responsive roles of VuNAC1/2 TFs

Interestingly, we discovered that the VuNAC1 and VuNAC2 TFs improved yeast growth. We further investigated their role in stress response by subjecting the strains to various environmental stresses and examining their growth and phenotypic changes. The VuNAC1 and VuNAC2 expressing strains could sustain high salinity, up to 1.0 M NaCl and 0.75 M $MgCl_2$, unlike the wild type strain, which almost ceased to form colonies at higher dilutions (Fig. 4.7A). In addition, less cell rupturing was observed in the transgenic strains indicating reduced salt-induced cell death (Fig. A2.6, Appendix 2). The strains could tolerate the osmotic stress induced by sorbitol up to 1.25 M, as indicated by less cell lysis (Fig. 4.7B). However, in response to metal toxicity, only the VuNAC1-expressing strain showed distinguishable tolerance to cadmium and aluminum stress under both normal and acidic pH. At the same time, the VuNAC2-expressing strain behaved similar to the wild type strain in aluminum stress and sustained the cadmium toxicity up to 50 µM. However, at higher concentrations, *i.e.*, 75 µM, the strain showed sensitivity, displaying severe cell death.

We also studied the recovery of strains after treating with heat (45º C, 4hr, 8hr) and cold (0º C, 24 hr, 48 hr). Both the transgenic strains recovered their growth and showed less cell shrinking after the cold arrest, indicating tolerance to the freezing stress (Fig. 4.7B and Fig. A2.6). While, in the case of heat stress, the VuNAC2-expressing strain grew similar to the wild type strain. The VuNAC1-ox strain could not tolerate the heat treatment beyond 8 h, showing decreased growth and severe cell lysis (Fig. 4.7B). The growth and phenotype analysis showed that both the VuNAC TFs improved tolerance to high salinity, osmotic pressure, and freezing. However, only VuNAC1 conferred tolerance to aluminum and cadmium toxicity. The differential response of the two transgenic strains to cadmium and heat suggested that VuNAC1 and VuNAC2 regulate a different set of gene targets in these stresses.

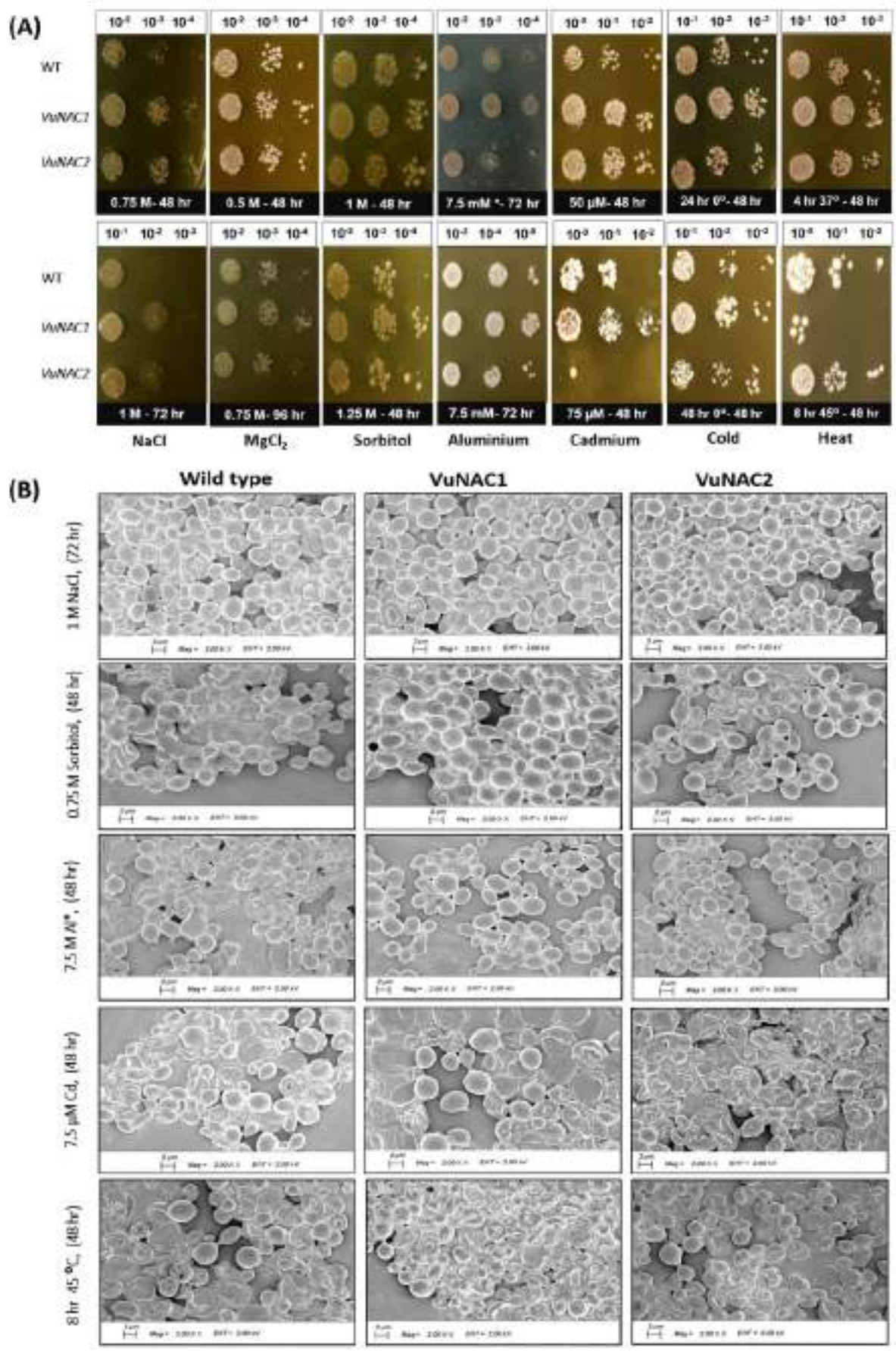

Fig. 4.7 Behavior in response to various environmental stresses. Study of growth **(A)** and cellular morphology **(B)** indicated lesser cell shrinking and/or rupturing in response to the imposed stress conditions in the transgenic strains w.r.t. wild type strains (* indicates no adjustment of pH up to 5.8).

4.3.6 LCMS-based profiling of differentially accumulated metabolites (DAMs)

We studied the metabolic reprogramming in the transgenic strains resulted from VuNAC1/2 mediated transcriptional tuning by analyzing the whole-cell metabolome detected by LC-MS. The statistical analysis of the spectra (Fig. A2.7, Appendix 2) showed that a total of 2588 metabolites were detected in the log phase, whereas 2233 metabolites were found in the stationary phase (p-value ≤0.05), out of which 210 metabolites were commonly detected in both phases. The distribution of differentially accumulated metabolites (DAMs) having fold change (FC) ≥ 2.0 (increase), FC ≤0.5 (decrease), and variable importance in projection (VIP) ≥1.0 was represented in the venn-diagrams (Fig. 4.8A) and scatter plots (Fig. 4.8B). In the VuNAC1-expressing strain, 858 (log) and 848 (stationary) metabolites significantly increased, whereas 1084 (log) and 995 (stationary) metabolites decreased. A similar trend was perceived for the VuNAC2-ox strain. The histograms depicting mass distributions (Fig. 4.8C) indicated variations in metabolic profile. The increase in peak width and standard deviation (S.D.) of histograms indicated that the metabolome of the transgenic strains was spread over a larger range of m/z ratio during the log phase. The left shift in the mean values suggested the presence of simpler compounds with lower molecular weight rather than complex compounds, mainly in the stationary phase. The heatmap representation of relative ion-abundance implied a contrasting difference in the metabolome of the strain expressing VuNAC1 and VuNAC2 compared to the wild type in the two different growth phases (Fig 4.8D), and the graphs depicting the fold change in peak intensities further indicated a change in metabolic compositions (Fig. A2.8, Appendix 2). The phylogenetic clustering suggested a close relationship between the stationary-phase metabolome of transgenic strains and the log-phase metabolome, indicating prolongation of the log-phase due to VuNAC1/2 (Fig. 4.8E). The top 50 DAMs were depicted based on their VIP score in Fig. 4.8F. The annotated DAMs were comprehensively listed in Table 4.3 and Table 2.9, Appendix 2. The metabolites belonged to various classes of biomolecules such as nucleotides, vitamins cofactors, amino acids, TCA cycle intermediates, sugars, fatty acids, lipids, *etc.*, showing significant accumulation as well as exhaustion (Fig. 4.9). As a result, major metabolic pathways were affected as mapped in order of degree of impact (Fig. 4.10). The remodeled pathways in the log phase of the VuNAC1-ox strain were pictorially illustrated in Fig. 4.11.

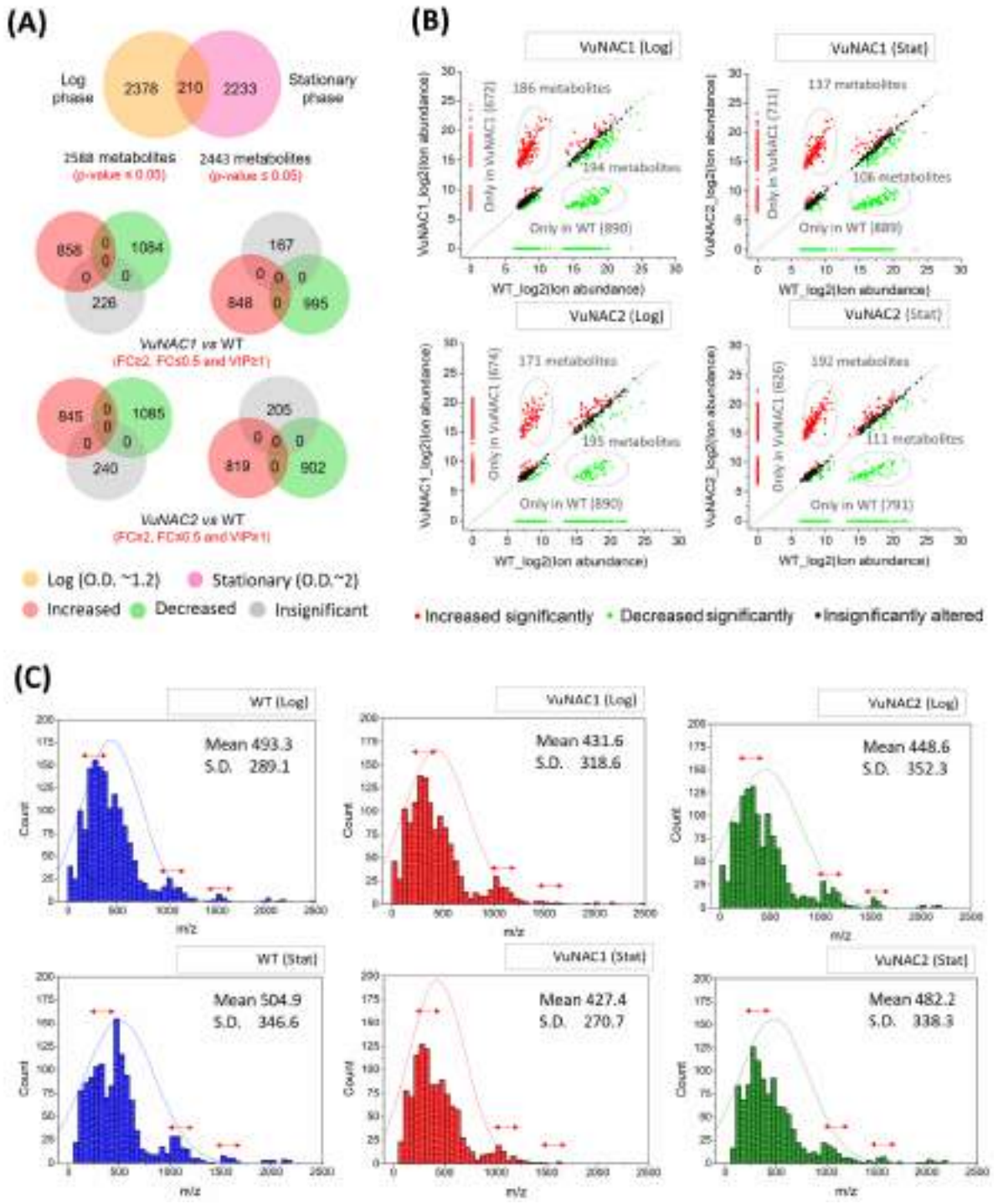

Fig. 4.8 Metabolic profiling by LC-MS detection. (A) Venn diagram depicting the distribution of the metabolites detected in late log and stationary phases (top) and differentially accumulated metabolites (DAMs) in the transgenic strains *w.r.t.* wild type (bottom). **(B)** Scatter plot of log_2 ion abundance indicating significant increase (red) and decrease (green) of the metabolic signals in the LC-MS spectra of the transgenic strains. **(C)** Histograms showing variation in the mass distribution in the transgenic strains. The change in peak height and standard deviation indicated that the metabolite profile spread out over a large range of m/z ratio in the transgenic strains in the log phase. The shift in the mean values suggests the conversion of high molecular weight metabolites to lighter weight metabolites in the stationary phase.

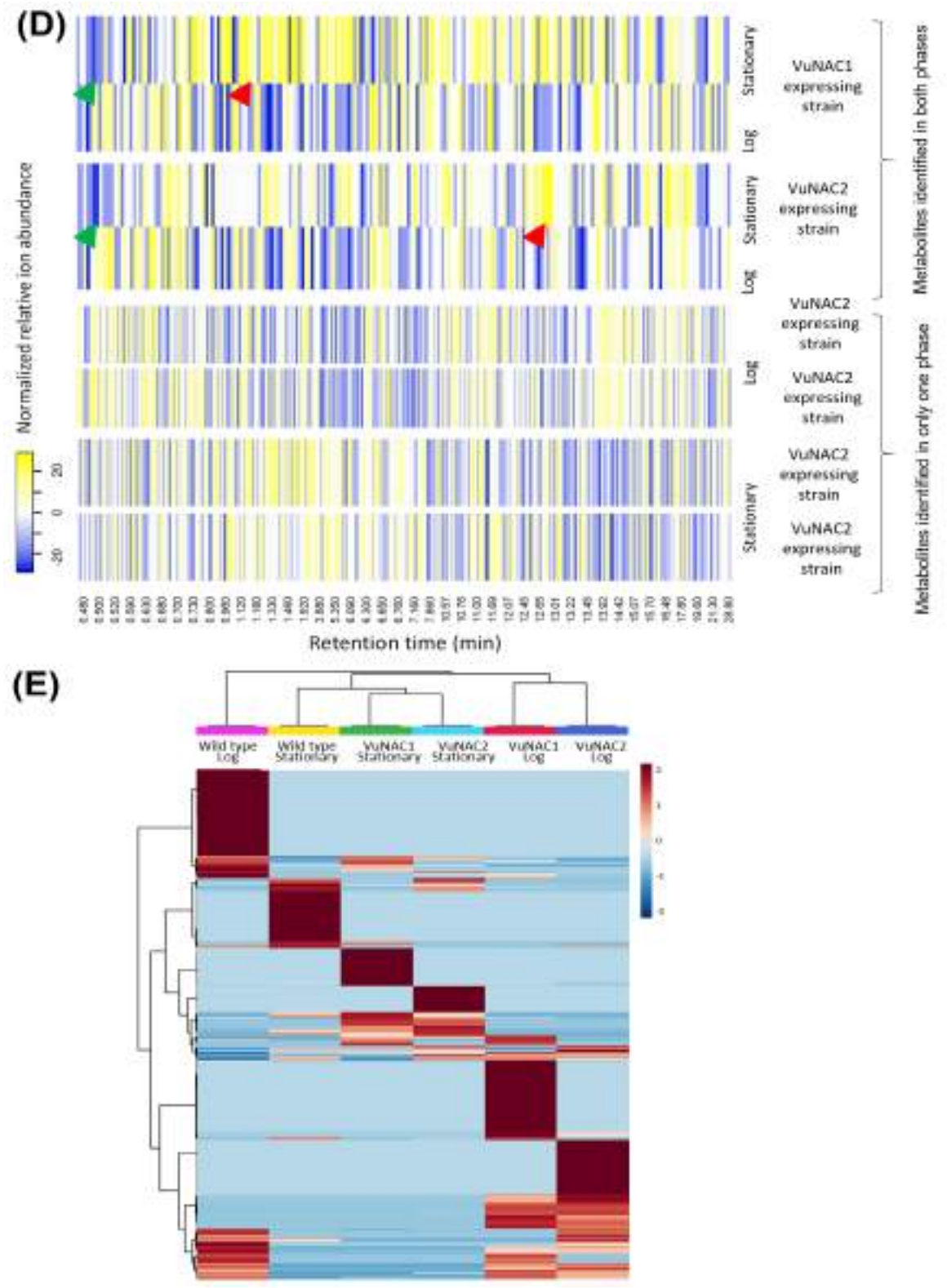

Fig. 4.8 Metabolite clustering. (D) Heatmap representing the relative ion abundance (transgenic *vs*. wild type strain) in the late-log and late-stationary phases, indicating altered regions in the LCMS spectra, increase (red arrow), and decrease (green arrow). **(E)** Metabolome clustering revealed a close relationship between the profiles of VuNAC1 and VuNAC2 expressing strains. Also, a significant alteration in the log phase profiles of transgenic strains indicated that metabolic remodeling plays a vital role in conferring the phenotype of delayed aging and longer lifespan.

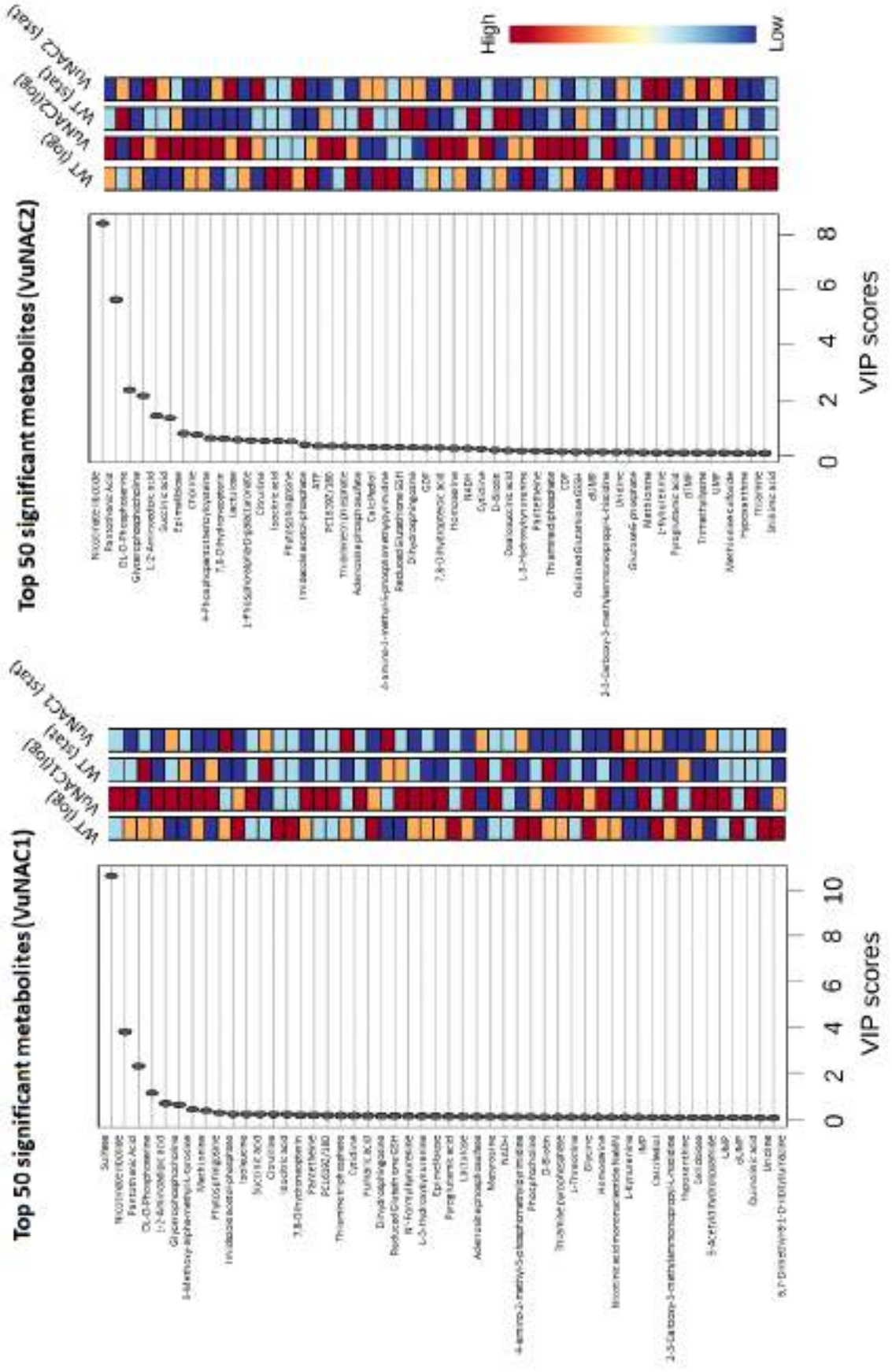

Fig. 4.8 Statistically significant DAMs. (F) The top 50 DAMs are listed in the order of VIP scores.

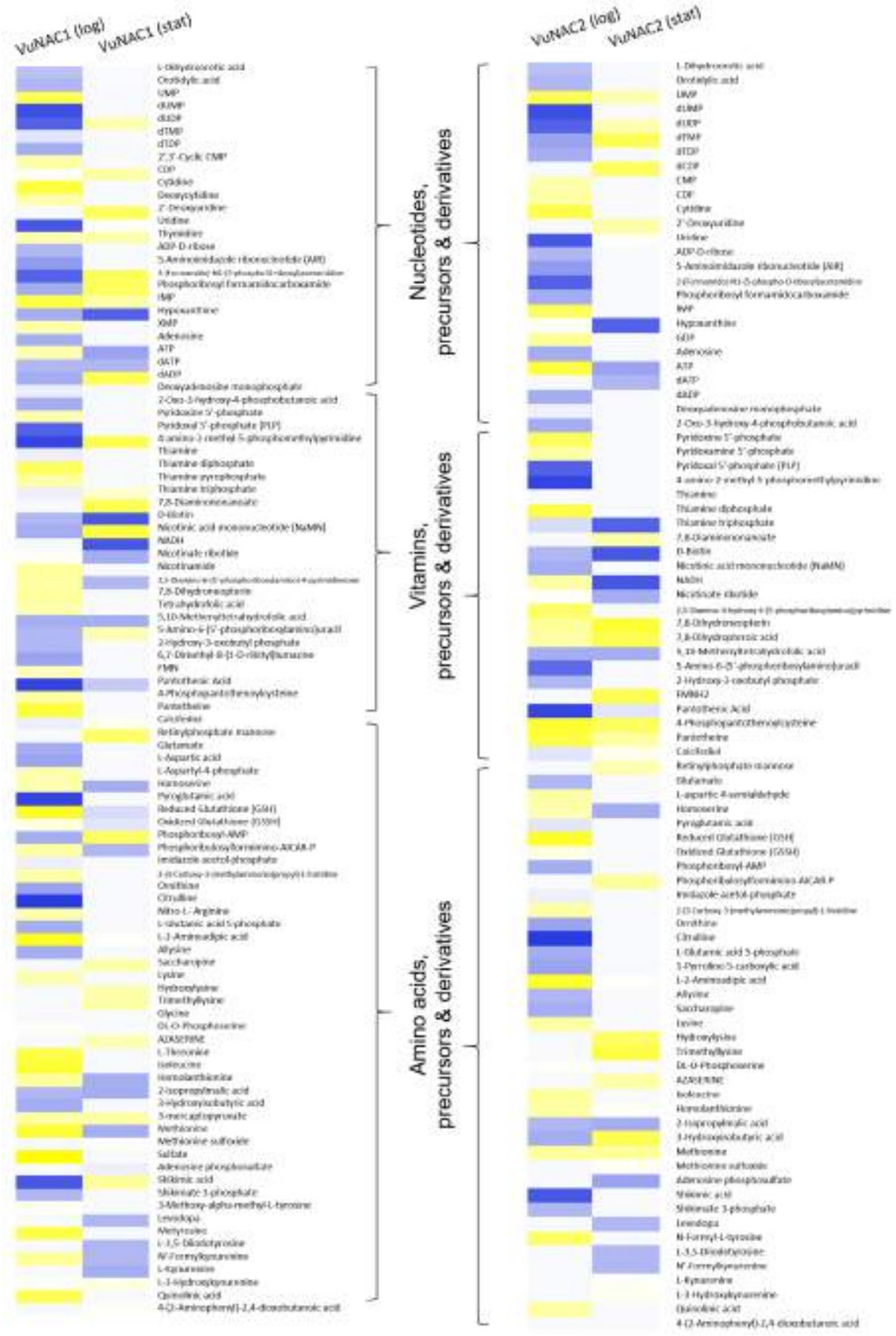

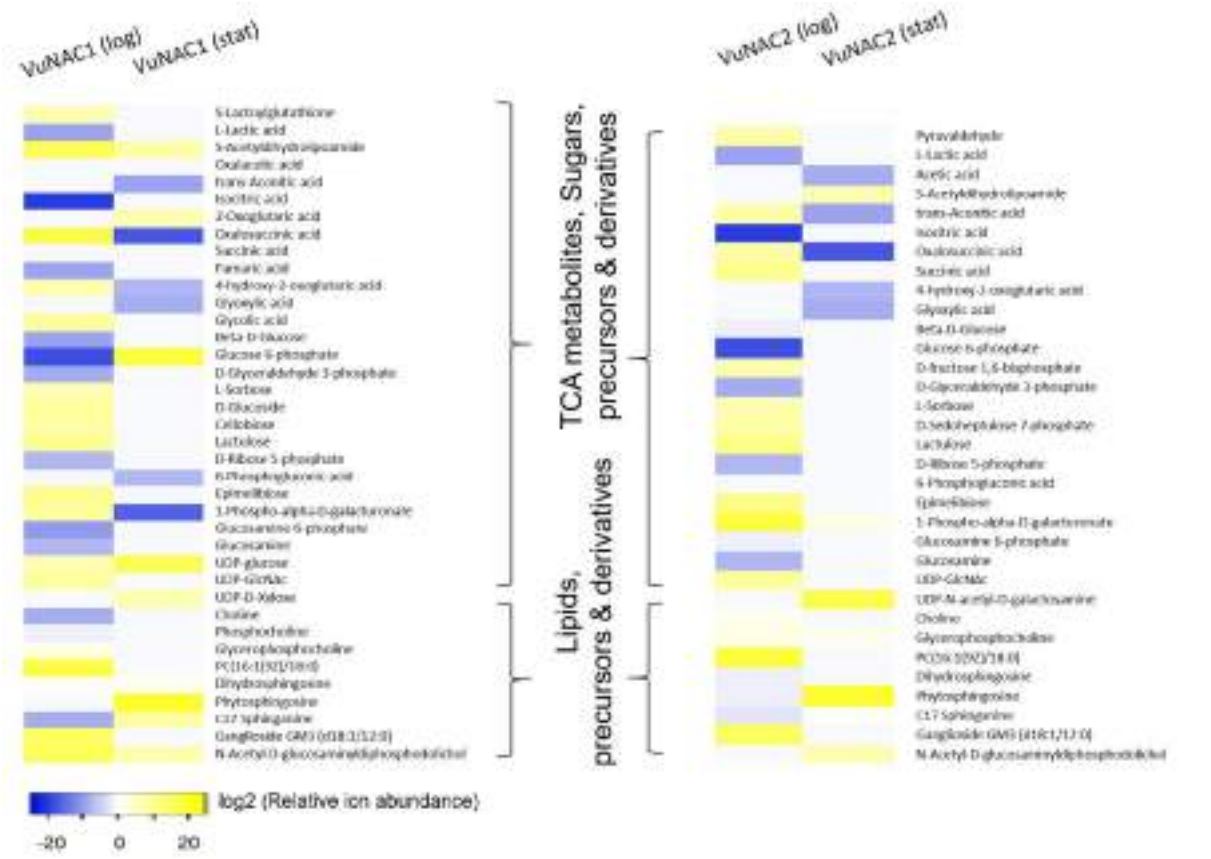

Fig. 4.9. **Heatmap representing the significantly altered content of biomolecules.** Relative ion abundance of the annotated DAMs was plotted for the transgenic strains expressing VuNAC1 (left) and VuNAC2 (right). The yellow color indicates accumulation, whereas the blue color indicates exhaustion of metabolites.

4.3.6.1 Nucleotide biosynthesis pathway

Nucleotides are major biomolecules serving as precursors for DNA, RNA, energy, and signaling molecules essential for cell function and growth. In transgenic strains, the *de novo* precursors of both the purines and pyrimidine dropped along with a simultaneous accumulation of the end products, *i.e.*, CMP, CDP, GDP, and ATP, indicating the flux of pathways toward biosynthesis (Figure 8, Figure 9A, Table 2, and Supplementary Table S11). In addition, the strains indicated an abundance of the salvage precursors (UMP, IMP, and XMP), which may aid in maintaining the nucleotide pool even in nutrient-limited conditions. However, the deoxynucleotides were less abundant in the log phase suggesting their faster consumption in the DNA synthesis of proliferating cells. Also, the adenine substrates like 5-Aminoimidazole-4-carboxamide ribonucleotide (AICAR) and 5-Formamidoimidazole-4-carboxamide ribotide (FAICAR) were not cumulated, explaining the whitish color of the transgenic strains [383].

4.3.6.2 Vitamin B and cofactor biosynthesis pathway

The second prominently altered pathway was the vitamin B complex biosynthesis, which is crucial for growth rate and biomass generation (Figure 8, Figure 9B, Table 2, and Supplementary Table S11). We observed the accumulation of vitamin B1, B2, B3, B5, B6, and B9 and/or its derivatives in the transgenic strains. We found reduced thiamine (vitamin B1) content and its precursor, 4-amino-2-methyl-5-pyrimidyl diphosphate (HMP-PP), however high content of the active form, *i.e.*, thiamine diphosphate (TDP) and thiamine pyrophosphate (TPP), coenzymes required for glucose metabolism other crucial biochemical reactions [388]. The intermediates in riboflavin (Vitamin B2) biosynthesis, including 2-Hydroxy-3-oxobutyl phosphate and 6,7-Dimethyl-8-(1-D-ribityl) lumazine, were exhausted, accompanied by an accumulation of the FMN and FMNH2 products [389]. Furthermore, both *de novo* and salvage precursors of nicotinamide (Vitamin B3), *i.e.*, quinolinate and nicotinate ribotide, were accumulated in the transgenic strains, which could be used to generate NADH/NADPH, an essential redox cofactor and substrate for several lifespan-regulating enzymes by calorie restriction, even in anaerobic conditions [390]. The content of pantothenate (Vitamin B5), the precursor for coenzyme A involved in fatty acid biosynthesis, was exhausted, but its derivatives, 4-phosphopantothenoylcysteine, and pantetheine were accumulated [391]. Pyridoxine phosphate (vitamin B6 phosphate) was significantly accumulated, while its active coenzyme form, *i.e.*, pyridoxal phosphate (PLP) required for the biosynthesis of amino acids, carbohydrates, and lipids, seemed to be exhausted. However, these B6 vitamers can salvage through interconversion [392]. Tetrahydrofolate (THF), a vitamin B9 derivative and the cofactor involved in one-carbon (1C) metabolism, was found accumulated in the transgenic strains, whereas its precursor 7,8-dihydroneopterin and derivative 5,10-methenyltetrahydrofolic acid, were depleted.

4.3.6.3 Amino acid biosynthesis pathway

Amino acids are the building blocks of proteins, precursors of nucleotides, and non-essential amino acids, the pool of which varied significantly in the VuNAC-expressing strains (Figure 8, Figure 9C, Table 2, and Supplementary Table S11). The acidic amino acids such as glutamate and aspartate decreased. The depletion may be justified by the increased biosynthesis of associated products like purines, pyrimidines, vitamin B complexes, and TCA cycle intermediates. Moreover, the aspartate derivatives, such as homoserine, a key intermediate in synthesis essential amino acids (lysine and leucine), were piled up. Both the oxidized and

reduced forms of glutathione, an antioxidant, were enhanced [393]. However, the derivatives of basic amino acids accumulated. 2-(3-Carboxy-3(methylammonio)propyl)- L-histidine, a post-translationally modified histidine residue shot up. Lysine, a crucial nitrogen reservoir, precursor L-2-aminoadipic acid, and the derivatives hydroxylysine (lysine analog) and trimethyllysine involved in carnitine synthesis were increased [394]. Nitro-L- Arginine, an arginine derivative which detoxifies cellular nitrogen oxide (NO), also increased. Glycine, the starting ingredient of thiamine and other amino acids, seemed to be exhausted. Phosphoserine, an intermediate in serine and cysteine biosynthesis, branched amino acids such as threonine and isoleucine, which also aid in the fermentation process, were piled up [395]. Further, we found a significant accumulation of methionine and sulfate ions, a marker for amino acid sufficiency [396]. This explained the prolongation of the logarithmic phase of transgenic strains, probably *via* inhibition of autophagy signaling [397]. In addition, methionine sulfoxide, which increases lifespan by regulating the aging process, was increased significantly in the stationary phase. Shikimic acid and shikimic 3-phosphate were reduced with a concomitant increase in their aromatic acid derivatives. L-kynurenine and L-3-hydroxykynurenine and catabolites of tryptophan were accumulated, possibly fuelling the Vitamin B3 producing kynurenine pathway. Moreover, levodopa, a dopamine precursor that inhibits respiratory growth in yeast, was reduced during the stationary phase [398].

4.3.6.4 Energy generating and secondary metabolic pathways

Pathways such as pyruvate metabolism, TCA cycle, glycolysis, *etc*., involved in energy conversion were also impacted in the transgenic strains (Table 2, and Supplementary Table S11). Pyruvaldehyde and lactoylglutathione, intermediates of pyruvate metabolism, were accumulated. Acetyldihydrolipoamide, oxidizing pyruvate into acetyl-CoA to enter the TCA cycle, increased. The oxalosuccinate and glycolate, products of the TCA and glyoxylate cycle, respectively, accumulated. Glucose, glucose 6-phosphate, and glyceraldehyde 3-phosphate, the key metabolites in glycolysis and pentose phosphate pathway, were exhausted in the transgenic strain, indicating the improved glycolytic flux. Nevertheless, the cells were rich in other sugars like sorbose, cellobiose, and lactulose, along with galactose pathway metabolites such as melibitol, epimelibiose, and 1-phospho-α-galacturonate, which were not detected in the wild type strain. The glucosamine and glucosamine 6-phosphate, precursors for cell wall sugars, seemed exhausted to synthesize UDP- N-acetylglucosamine and UDP-xylose. In addition to the sugars and cellular polysaccharides, lipids, fatty acids, and other metabolites regulating membrane homeostasis and stress tolerance such as carnitine, glycerophosphocholine, *etc*.

[399, 400], were also enhanced in the transgenic strain, as listed in Table 2. Flavonoids like kaempferol and catechin, responsible for the antioxidant activity and alcohol tolerance, respectively, were increased. N-(3-oxo-hexanoyl)-homoserine lactone involved in quorum sensing and stress tolerance was also enhanced. In contrast, metabolites having anti-growth effects such as 5-hydroxydopamine and miglitol *via* inhibiting respiration and carbohydrate metabolism, respectively, decreased. Sialic acids like N-Acetyl-9-O-lactoyl neuraminic acid and their precursors were accumulated in transgenic strain, which could increase cell-negative charge, hence explaining the reduced aggregation in the VuNAC- expressing cells [401].

Table 4.3. Annotation of metabolites detected by LC-MS

S.N.	Compounds	Description	m/z	RT	log FC (log phase)		log FC (stationary)	
					VuNAC 1	VuNAC 2	VuNAC 1	VuNAC 2
		PYRIMIDINE METABOLISM						
1	Orotidylic acid	*de novo* pyrimidine precursors	390.2	5.9	-7.74	-7.74	-	-
2	UMP	salvage pyrimidine and RNA precursors	307.2	10.7	16.23	15.60	0.00	7.69
3	CMP	RNA precursors	345.0	0.7	0.00	7.64	-	-
4	2',3'-Cyclic CMP	secondary messengers	343.1	0.8	8.22	0.00	-	-
5	CDP	DNA and RNA precursors	445.0	0.7	0.55	8.12	8.14	0.00
6	dUDP	thymidine precursors	388.2	6.5	-15.80	-15.80	7.04	6.95
7	dTMP	DNA precursors (thymidine)	342.2	0.7	-1.99	-9.51	15.68	0.00
8	Cytidine	salvage pyrimidine precursors	281.2	7.3	18.09	17.25	-	-
9	2'-Deoxyuridine		270.2	14.4	-	-	15.52	7.87
10	Thymidine		288.2	12.5	6.94	0.00	7.12	0.00
		PURINE METABOLISM						
11	AICAR	*do novo* purine precursor	321.2	0.7	-7.16	-7.16	-	-
12	FAICAR		317.2	6.7	-16.54	-16.54	15.15	0.00
13	IMP	salvage purine precursor	408.2	13.7	16.75	15.19	7.83	0.00
14	XMP		363.2	14.9	7.35	-0.04	-	-
15	Hypoxanthine		136.0	0.8	-8.60	0.23	-15.69	-15.69
16	GDP	RNA precursor	465.2	5.1	0.17	8.99	-	-
17	ATP	RNA precursor, energy currency	489.2	0.5	7.47	17.89	-9.00	-9.00
18	dATP	DNA precursor	508.2	6.2	-7.75	-0.62	-7.35	-7.35
19	dAMP	secondary messengers	333.2	2.9	-1.42	-1.31	-	-
		VITAMIN B6 AND THIAMINE METABOLISM						
20	Pyridoxine 5'-phosphate	vitamin B6	269.1	9.6	7.76	14.90	-	-
21	Pyridoxal 5'-phosphate (PLP)		246.2	5.4	-16.47	-16.47	-	-
22	HMP-P	thiamine precursor	218.1	1.2	-19.21	-19.21	16.84	0.00
23	Thiamine	TPP co-enzyme precursor	264.1	0.5	-1.30	-0.72	-	-
24	Thiamine diphosphate (TDP)	thiamine derivative, cofactor	423.3	11.6	15.49	16.55	-	-
25	Thiamine pyrophosphate (TPP)	coenzyme	442.3	16.8	8.42	-0.09	-	-
		FOLIC ACID AND PTERIN METABOLISM						
26	2,5-Diamino-6-(5'-phosphoribosylamino)-4-pyrimidineone	biopterin and flavin precursor	336.2	16.4	8.71	0.00	-7.41	-0.08
27	2,5-Diamino-4-hydroxy-6-(5-phosphoribosylamino) pyrimidine		335.2	12.5	0.00	14.14	-	-
28	7,8-Dihydroneopterin	biopterin precursor	254.2	16.5	9.12	9.07	0.00	18.58
29	Tetrahydrofolic acid (THF)	folate derivative	467.4	15.8	7.28	0.00	-	-
30	5,10-Methenyltetra-hydrofolic acid		460.4	18.3	-7.90	-7.90	-8.47	-8.47
		RIBOFLAVIN METABOLISM						
31	6,7-Dimethyl-8-(1-D-ribityl) lumazine	riboflavin intermediate	325.3	17.2	-9.04	-0.25	-	-
32	FMN	cofactor, riboflavin derivative	456.4	11.3	6.79	0.00	-	-

33	FMNH2		462.3	13.0	-	-	0.00	15.90
		PANTOTHENATE AND COENZYME A METABOLISM						
34	Pantothenic Acid	coenzyme A precursor	218.1	1.2	-19.21	-19.21	-5.05	-2.24
35	4-Phosphopantothenoyl cysteine	coenzyme A intermediate	406.1	3.4	9.22	18.78	0.00	14.70
36	Pantetheine		278.1	6.2	18.31	16.71	0.00	8.46
		NAD/NADH METABOLISM						
37	NaMN	vitamin B3/NAD precursor	374.2	5.3	-8.65	-8.65	18.39	0.00
38	NADH	cofactor	665.1	0.8	0.00	8.02	-17.38	-17.38
39	Nicotinate ribotide	vitamin B3/NAD salvage precursor	273.3	10.6	0.51	0.33	-7.80	-7.80
40	Nicotinamide	vitamin B3	103.1	0.5	9.06	0.00	-	-
		GLUTAMATE, ASPARTATE AND ALANINE METABOLISM						
41	Glutamate	TCA intermediate, nucleotides and amino acid precursor	147.1	0.6	-8.42	-7.32	-	-
42	L-Aspartic acid		132.1	17.0	-8.88	-0.23	-	-
43	L-Aspartyl-4-phosphate	aspartate derivative, amino acid precursor	273.1	0.5	7.53	0.00	-	-
44	Homoserine	lysine, threonine and cysteine precursor	119.1	0.5	7.03	7.62	-8.76	-8.76
		GLUTATHIONE METABOLISM						
45	Pyroglutamic acid	glutathione precursor	167.1	0.8	-19.27	-2.00	-	-
46	Reduced Glutathione (GSH)	anti-oxidant	307.1	0.7	20.68	20.27	-2.96	-0.17
47	Oxidized Glutathione (GSSH)		612.2	0.7	2.32	2.34	-2.06	-0.44
		HISTIDINE, ARGININE AND LYSINE METABOLISM						
48	Imidazole acetol-phosphate		201.1	1.5	-1.03	-1.18	-	-
49	2-(3-Carboxy-3(methylammonio)propyl)- L-histidine	histidine derivative	251.1	11.7	8.25	7.96	-	-
50	Nitro-L- Arginine	arginine derivative, NO inhibitor	236.1	1.9	8.30	0.00	-	-
51	L-2-Aminoadipic acid	lysine precursor	143.1	0.7	20.65	20.32	0.29	0.78
52	Lysine	nitrogen nutrient, histone component	146.1	0.5	7.46	8.44	-	-
53	Hydroxylysine	lysine analog, collagen biosynthesis	222.1	10.9	-	-	7.20	14.44
54	Trimethyllysine	histone component, carnitine biosynthesis	188.2	0.5	-	-	8.47	17.21
		LINEAR AND BRANCHED AMINO ACID METABOLISM						
55	Glycine	thiamine and amino acid precursor	103.1	0.5	-0.59	0.05	-	-
56	DL-O-Phosphoserine	serine intermediate, cysteine precursor	207.1	0.7	0.79	0.54	-	-
57	L-Threonine	isoleucine precursor	157.1	1.4	16.94	0.00	-	-
58	Isoleucine	promotes fermentation duration	113.1	2.7	18.61	9.24	-	-
59	2-Isopropylmalic acid	eucine precursor	204.1	0.5	-7.38	-7.38	-8.39	-8.39
60	3-Hydroxyisobutyric acid	valine metabolite	86.0	0.6	-8.16	-8.20	0.00	16.50
		SULFUR AMINO ACID METABOLISM						
61	3-mercaptopyruvate	cysteine metabolite	124.0	28.9	7.87	0.00	8.40	0.00
62	Methionine	amino acid, prolongs log phase	148.1	4.7	19.42	9.28	-8.50	8.91
63	Methionine sulfoxide	anti-oxidant, effects lifespan	165.1	0.7	-	-	0.41	0.75
64	Adenosine phosphosulfate	sulfur reduction pathway	427.0	0.6	-	-	-1.28	-9.41
		AROMATIC AMINO ACID METABOLISM						
65	Levodopa	dopamine precursor	243.1	0.5	-	-	-7.09	-7.09
66	Metyrosine	tyrosine derivative	177.1	3.1	17.45	0.00	-	-
67	N-Formyl-L-tyrosine		231.2	9.0	0.00	14.01	-	-
68	N'-Formylkynurenine	tryptophan catabolite	217.2	7.6	9.06	-0.16	-7.05	-7.05
69	L-3-Hydroxykynurenine		223.2	9.7	0.08	-0.51	2.03	1.57
70	Quinolinic acid	folate and pterin precursor	187.1	0.5	16.21	8.35	-	-
		PYRUVATE METABOLISM						
71	Pyruvaldehyde	pyruvate intermediate	71.1	2.7	0.00	8.37	-	-
72	S-Lactoylglutathione		401.4	14.4	7.01	0.00	-	-
73	S-Acetyldihydrolipoamide	converts pyruvate into acetyl-CoA	248.1	0.6	16.24	0.00	7.98	7.56
		TCA AND GLYOXYLATE CYCLE						
74	Isocitric acid	TCA cycle intermediates	174.1	0.4	-20.16	-20.16	-	-
75	Oxalosuccinic acid		189.1	1.0	16.76	8.22	-16.83	-16.83
76	Succinic acid		117.1	0.6	-0.28	10.44	-0.39	-0.65
77	Fumaric acid		115.1	0.6	-9.52	0.13	-	-
78	Glycolic acid	glyoxalate derivative	118.1	1.9	9.34	0.00	-	-
		GLYCOLYSIS/ GLUCONEOGENESIS AND PENTOSE PHOSPHATE PATHWAY						
79	Beta-D-Glucose	hexose sugar	202.1	1.4	-9.11	-1.94	-	-
80	D-Glyceraldehyde 3-phosphate	glycolsysis end product	151.0	5.1	-8.63	-8.63	-	-
81	D-Ribose 5-phosphate	pentose sugar, purine precursor	276.1	6.6	-7.16	-7.16	-	-
82	L-Sorbose	hexose sugar	222.2	12.0	7.50	7.26	-	-

83	D-Sedoheptulose 7-phosphate	heptose sugar derivative	328.0	12.0	0.00	7.93	-	-
84	Cellobiose	disaccharides	342.3	11.2	8.10	-0.16	-	-
85	Lactulose	disaccharides, synthetic sugar	342.1	0.5	9.92	11.01	-	-
		GALACTOSE METABOLISM						
86	Melibitol	disaccharide, galactose metabolism	361.2	1.1	9.07	0.00	-	-
87	Epimelibiose		388.1	0.5	9.82	11.26	-9.69	-9.69
88	1-Phospho-alpha-D-galacturonate	galactose derivative	216.1	0.6	9.41	18.29	-15.84	2.85
		AMINO AND NUCLEOTIDE SUGAR METABOLISM						
89	Glucosamine 6-phosphate	lipid and nucleoside sugar precursor	259.2	1.3	-10.10	-1.53	-	-
90	UDP-GlcNAc	cell wall precursor	607.1	0.6	9.44	9.37	-	-
91	UDP-D-Xylose		596.1	0.7	-	-	7.67	0.00
92	UDP-N-acetyl-D-galactosamine		653.1	0.7	-	-	0.00	16.57
		LIPID AND FATTY ACID METABOLISM						
93	Phosphocholine	represses phospholipid biosynthesis	183.1	13.0	-1.66	-0.25	-0.73	0.08
94	Glycerophosphocholine	membrane lipid homeostasis, salt tolerance	257.1	0.6	2.84	2.31	-0.26	1.89
95	GPCho(O-16:0/2:0)	membrane phospholipid, activator	523.4	15.9	10.71	0.78	8.78	9.64
97	GPEtn(18:0/0:0)	glycerophosphorylethanolamine	541.3	14.4	8.11	8.08	-7.73	-7.73
98	GPEtn(16:0/0:0)		513.3	13.2	8.88	8.13	-10.30	-0.73
99	GPSer(18:1(9Z)/0:0)	glycerophosphoserine	497.3	14.4	-7.88	0.60	-8.58	-8.42
100	Hexadecanedioic acid	membrane lipid precursor	285.2	13.8	8.40	8.74	-	-
101	7-palmitoleic acid	unsaturated FA	236.2	16.5	8.26	0.00	16.65	8.35
102	2-methyl-tridecanedioic acid	methyl FA, C13	257.2	12.1	10.07	10.15	0.00	15.35
103	3-Hydroxydodecanedioic acid	hydroxy FA, C12	268.1	13.6	8.56	-0.07	8.13	8.09
104	Carnitine	carnitine, FA oxidation	143.1	1.0	7.81	8.62	-16.49	-16.49
		OTHER METABOLITES						
104	N-Acetyl-D-mannosamine 6-phosphate	sialic acid precursor	347.1	0.5	8.42	7.71	-	-
105	N-Acetyl-9-O-lactoyl neuraminic acid	reduces cell-adhesion	363.1	5.2	8.43	0.00	1.17	0.45
106	Peonidin	anthocyanin	305.2	9.3	-6.88	-6.88	16.49	8.37
107	Alloxanthin	carotenoid, anti-oxidant and vitamin precursor	584.3	17.0	7.94	7.55	-	-
108	Kaempferol	flavonols, anti-inflammatory and antioxidant	324.2	13.4	9.55	9.68	-	-
109	Catechin	flavanols, alcohol and toxin resistance	289.3	10.8	-0.07	-0.51	1.66	1.30
110	Piceatannol	stilbenes	272.2	14.2	16.05	15.83	-	-
111	Epinephrine-like	promotes glycogen break	165.1	1.2	22.23	22.02	0.90	0.42
112	Indole-3-carboxylic acid-like	promotes sporulation	143.0	3.9	0.65	-8.80	18.18	8.20
113	Kinetin riboside-like	promotes cell proliferation	347.1	5.9	8.06	7.97	-	-
114	5-Hydroxydopamine	drug inhibiting respiratory growth	151.1	0.7	-8.99	-8.89	-	-
115	Miglitol	drug inhibiting complex carbohydrate catabolism	189.1	1.2	-	-	-10.17	-0.63
116	Sulfasalazine	drug inhibiting biopterin biosynthesis	440.1	0.5	-	-	-3.05	-1.74
117	Sulfamerazine	drug inhibiting the folic acid synthesis	246.1	0.5	-	-	-9.98	-9.98
118	Flumequine	drug, anti-lipase, growth inhibition	307.1	0.7	-	-	-8.14	-8.14
119	N-(3-oxo-hexanoyl)-homoserine lactone	quorum sensing, oxidative stress tolerance	212.1	0.7	8.35	16.27	-	-
120	Metergoline	Alkaloid inducing cell death	423.2	1.9	-8.62	-9.48	-	-

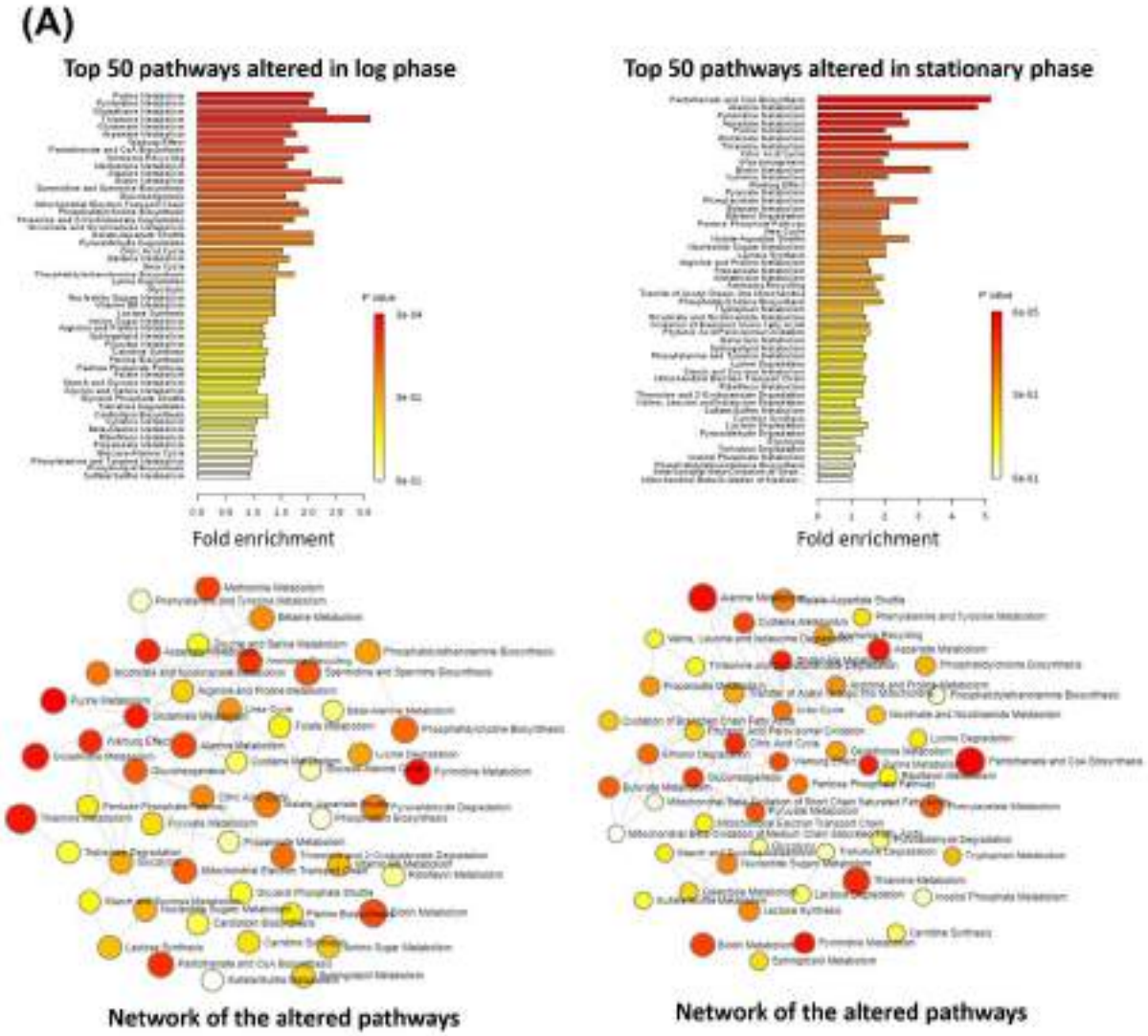

Fig. 4.10 Pathway Enrichment Analysis. (A) Major altered pathways and their networks resulted from the differential accumulation of metabolites in the VuNAC1/2 expressing strains in different growth phases.

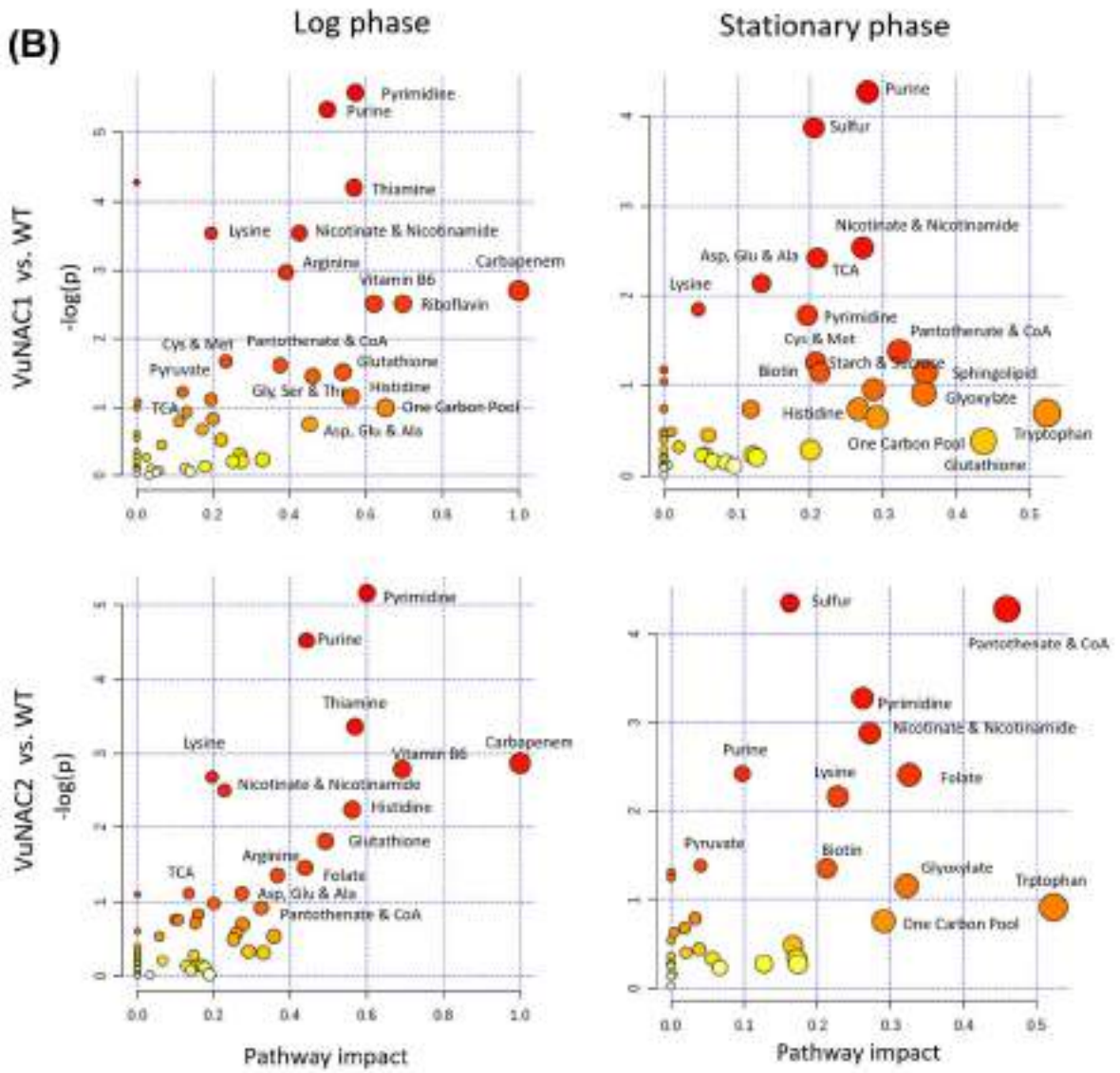

Fig. 4.10. Pathways impact analysis. (B) The bubble plot indicated alterations in the primary metabolic pathways in the order of the impact resulting from the differential accumulation of the metabolites due to transcriptional tuning of the genes/enzymes involved in the biosynthesis or metabolic conversions. The bubble size was proportional to the impact, and the color denoted statistical significance from highest (red) to lowest (white).

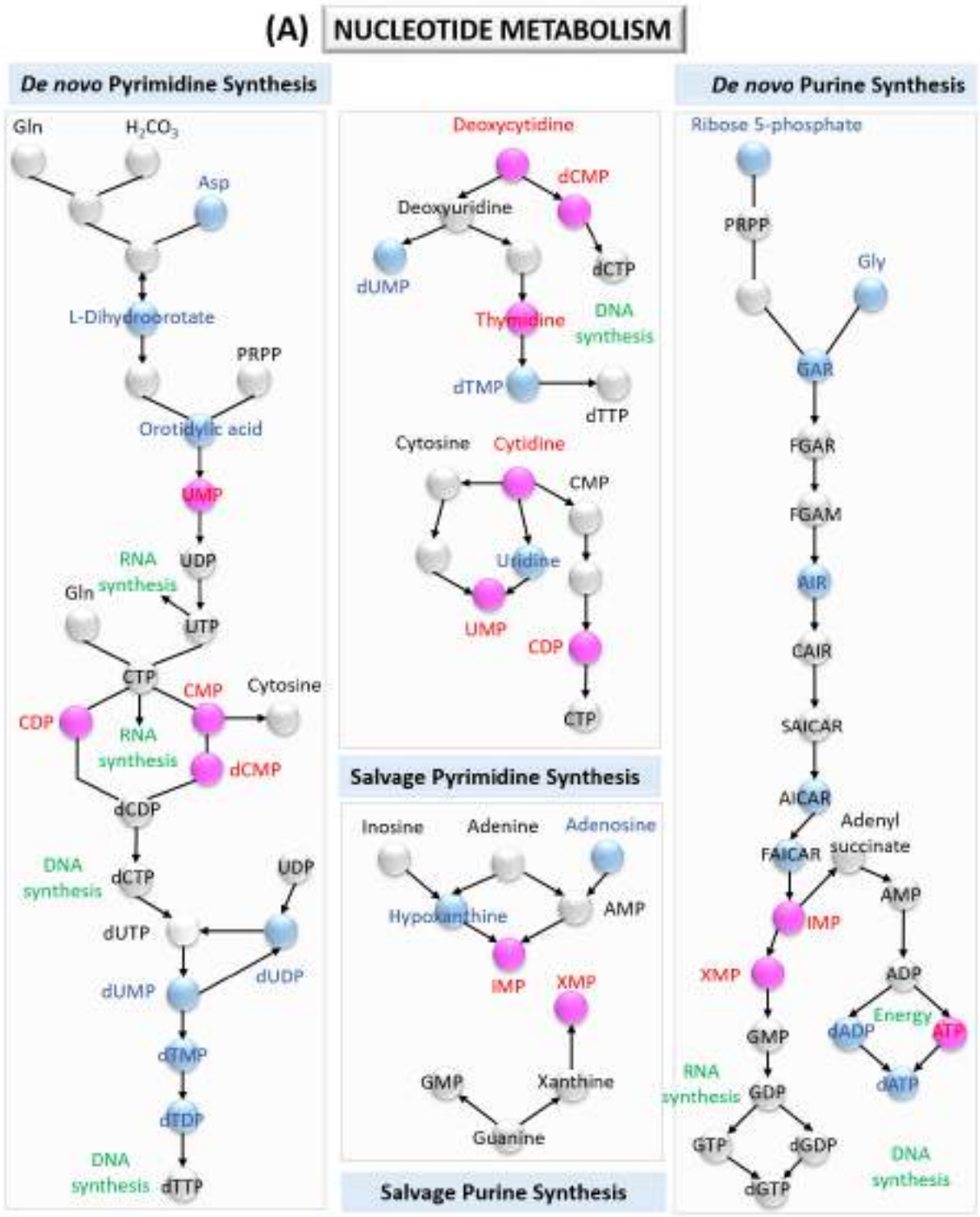

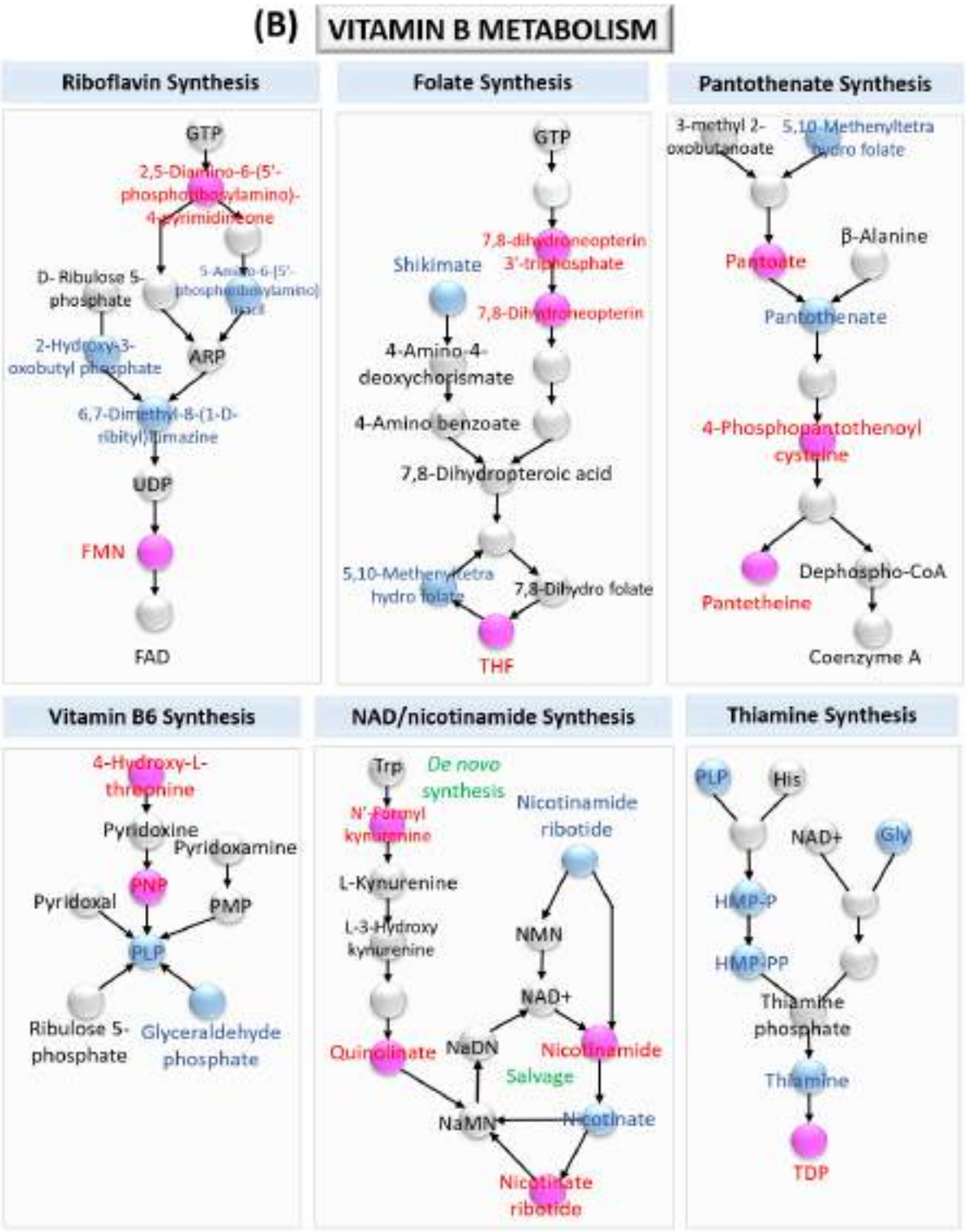

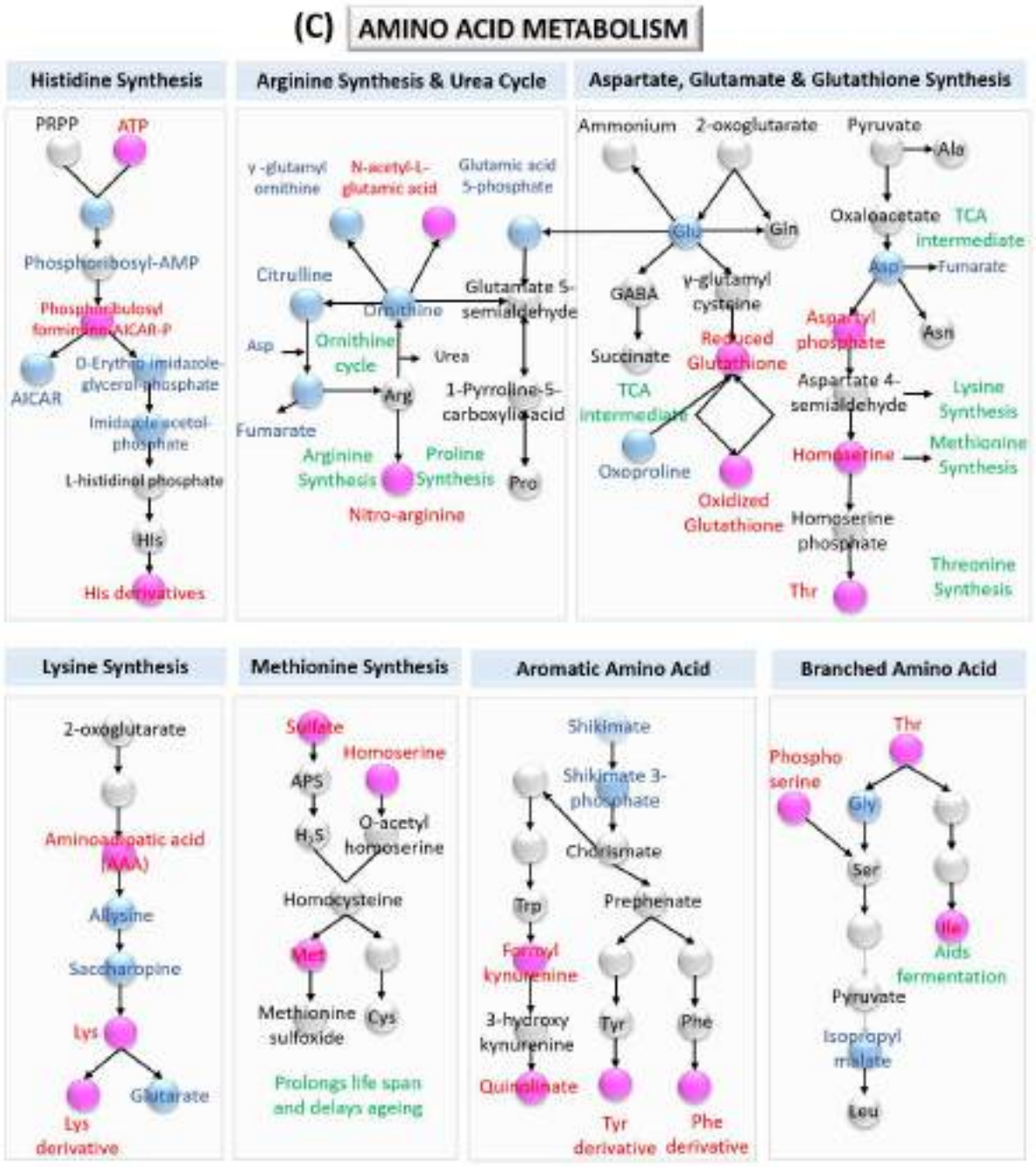

Fig. 4.11 Pictorial illustration of the remodeled pathways in VuNAC1-expressing strain in log phase. (A) Nucleotide biosynthesis, **(B)** Vitamin biosynthesis, and **(C)** Amino acid biosynthesis. The pink spheres indicated accumulated metabolites, the blue spheres indicated exhausted metabolites, and the grey color indicated either no change or unavailability of information.

4.4 DISCUSSION

4.4.1 VuNAC1 and VuNAC2 are multi-faceted TF undergoing multilayer regulation

The remarkable induction of cowpea *VuNAC1* and *VuNAC2* genes, in response to crucial abiotic stresses like dehydration, high salt, extreme temperature, and cold along with stress regulatory hormones, *i.e.,* ABA and MeJA, proposed that VuNAC1/2 TFs converge multiple stress responses directly or indirectly *via* hormone signaling or other target genes (Fig. 4.2). NAC functional homologs are co-expressed and are compensatory in actions [218]. The similar gene expression pattern and phenotype of VuNAC1 and VuNAC2 implied that the two homologous TFs might function complementarily or coordinately in multiple stress responses at a time or even at different stages of the same stress response (Fig. 4.2, Fig. 4.5, and Fig. 4.8). Furthermore, the analysis of *cis*-regulatory elements in the promoter region revealed that *VuNAC* genes are regulated by a multilayer mode mediated by hormone signaling (ABA, auxin, GA, JA, *etc*.), TF-based regulation (MYB, WRKY, and CBF), light induction, and direct stress signals (Table 4.1). The over-representation of elements like GT1GMSCAM4 and response regulators like EBOXBNNAPA and ARR1AT, suggested their participation in biotic stress as well as cell-signaling [402-404]. Drought tolerance is regulated by ABA-dependent pathways *via* ABA-responsive factors (ARFs), which recognize stress-regulatory elements like ABREATRD22 and ABREATCONSENSUS in the promoter regions of target genes. In addition, the ABA- independent pathways employ a DRE/CRT element (DRECRTCOREAT) to regulate dehydration-related genes [248]. Interestingly, both the elements were found in the promoter of *VuNAC1/2* genes, indicating ABA-mediated as well as independent growth and stress signaling.

4.4.2 The VuNAC TFs remodeled the primary biomolecule synthetic pathways in yeast

The heterologous expression of VuNAC1/2 TFs led to differential accumulation of key metabolites in yeast (Fig. 4.8 and Fig. 4.9), which impacted critical metabolic pathways (Fig. 4.10), resulting in their remodeling (Fig. 4.11). Like its homologs in other plant species, VuNAC1/2 TFs may tune the genes involved in reprogramming crucial metabolic pathways [27, 58, 208, 405]. As the basal pathways and signaling mechanisms are conserved, probably the VuNAC1/2 TFs execute their transcriptional function by targeting the genes set shared by the yeast native TFs, ACA1/2, Cad1p, Sko1p, and Gcn4p, which function in dimer using the DNA binding sites similar to the NACBS to regulate various stress-responses and metabolic functions in yeast [376-380] (Table 4.2).

The metabolic remodeling indicated efficient securing of carbon and nitrogen in the transgenic strains *via* reprogrammed carbohydrate and nucleotide biosynthetic pathways (Fig. 4.9). The strains were affluent in purines, pyrimidines, and their salvage precursors [406]. The transgenic strains gathered ample ATP mainly in the log phase, indicating high energy status, supporting cell replication, DNA synthesis, and other biochemical processes in the growing cells. The accumulation of the vitamin B and derived cofactors that are critical for biomass growth, conversion of various biomolecules into energy currencies, and fuelling other biosynthetic pathways (TDP, TPP, THF, pantethine, pterine intermediates, carnitine) may support the cell proliferation and energy homeostasis during starved conditions. Furthermore, the improvement in growth characteristics can be speculated as an index of commendable protein synthesis. Evidently, the VuNAC-expressing strains indicated a rich amino acid pool due to the activation of the biosynthesis of sulfur-containing and branched-chain amino acids, also favoring longevity and fermentation process. The enhanced accumulation of complex polysaccharides, medium-chain fatty acids (MCFAs), like palmitic and stearic acid derivatives, and some vital class of membrane lipids derived from the MCFAs, glycerophosphocholines (GPCs), glycerophosphoserines (GPSers), and glycerophosphoethanolamine (GPEs) in the transgenic strains, might further stimulate lipogenesis, mitochondrial energy processes and provide the structural framework to the cell (Table 4.3). Overall, the accumulation of products and exhaustion of precursors and intermediates suggested the inclination of the metabolic pathways towards biosynthesis. Also, the abundance of salvage precursors indicated efficient metabolic interconversions to restore the balance during limiting or surplus conditions.

4.4.3 VuNAC1/2 TFs exhibited dual functions of multiple stress tolerance and growth benefits

Being the central transcriptional regulator, NAC TFs are known to play versatile roles [53]. A single NAC TF can cross-talk with disparate pathways to reprogram the whole-cell signaling regulating growth processes and/or stress responses. The unique VuNAC1/2 TFs played dual roles in yeast, *i.e.*, improving growth and tolerance to major environmental stressors when expressed heterologously. The TFs rendered noteworthy changes such as longer lifespan, faster proliferation, and enhanced biomass than the wild type strain (Fig. 4.5B). In addition, the healthy survival under limiting nutrients indicated the sufficiency of purines and other critical nutrients in the transgenic strains (Fig. 4.5F). The improved fermentation efficiency overcame the glucose repression, showing balance in the aerobic and anaerobic energy scope, even at high glucose levels (Fig. 4.6A). The FTIR profile comprehends increased cell-wall

polysaccharides, structural lipids, and glycoproteins (Fig. 4.6B). More importantly, the transgenic strains sustained multiple abiotic stresses (Fig. 4.7). The activation of genes regulating the synthesis of essential redox factors and antioxidants (FMN, NAD, and glutathione) and flavonoids may be the factors bridging the growth and stress-tolerant roles of the VuNAC1/2 TFs (Table 4.3). However, the detailed mechanism of the versatile VuNAC1/2 functioning at the transcriptional level still needs to be explored.

Taken together, our study showed that the VuNAC1 and VuNAC2 transcription factors play a crucial role in the regulation of cell energetics and signaling to uplift growth and viability. Moreover, they can intricately regulate multiple abiotic stress challenges to improve stress perception. Unlike most structural genes like transporters, chaperones, enzymes, or cell-wall components, the VuNAC TFs signify great potential to control and integrate disparate metabolic and cellular signaling pathways to accomplish multi-cooperative objectives. Furthermore, the versatile but dual behavior of the VuNAC1/2 TFs in yeast makes them distinctive from their homolog found in plant species, which do not harmonize growth with the stress response. Thus, our study in the yeast model upraised the possibility that these TFs may overcome the detrimental trade-off between tolerance and growth when overexpressed in plants, unlike their homologs [30, 33]. Hence making a promising candidate for improving agronomic traits when expressed in cowpea or other related legume crops like mung bean and soybean.

Chapter 4

CHAPTER 4

5. CHARACTERIZATION OF VUNAC1/2 TFS IN RESPONSE TO ABIOTIC STRESSES UNDER STARVATION

ATAF-like NAC transcription factors are bonafide regulators of stress-signaling. However, their overexpression exerts growth-retardation by activating ABA-hypersensitivity, chloroplast-degradation, or carbon-starvation, despite the stress-adaptation. This chapter studied the two cowpea ATAF orthologs induced by multiple abiotic stress and light, *VuNAC1* and *VuNAC2*, to examine their harmonized role to improve stress tolerance complying with growth sustainability. Their constitutive overexpression in Arabidopsis conferred tolerance to severe drought, high-salinity, aluminum, cadmium, and H_2O_2 toxicity, without any phenotypic defects, showing improved water status, membrane stability, and accumulation of glutathione, proline, and ascorbate. The transgenic lines manifested improved growth (embryonic, rosette, and inflorescence), yielding more siliques, under both normal and nutrition-deficit conditions, with simultaneous augmentation in photosynthetic activity and stomatal-density, besides tolerance to nutrition and abiotic stresses. Moreover, the seedlings displayed tolerance to ABA-promoted dormancy and hypersensitivity. The interactome analysis deduced from orthologous proteins proposed a multi-tier regulatory network integrating hormonal, stress, and developmental signals, sugar metabolism (glucose, sucrose, trehalose, starch, and lignin), lipid, phosphate, and nitrogen. Our study identified unique NAC TFs conferring drought, salt, oxidative, and metal stress tolerance with synchronous growth enhancement *via* tuning of photosynthetic controls, ABA insensitivity, and nutritional-homeostasis, unlike their orthologs. Being the transcriptional activator of both growth and stress responses, these genes can be ideal biotechnological tools for translating stress tolerance into improved yield.

Keywords: ABA insensitivity, ATAF ortholog, growth trade-off, multiple stress tolerance, photosynthetic activity, stomatal density

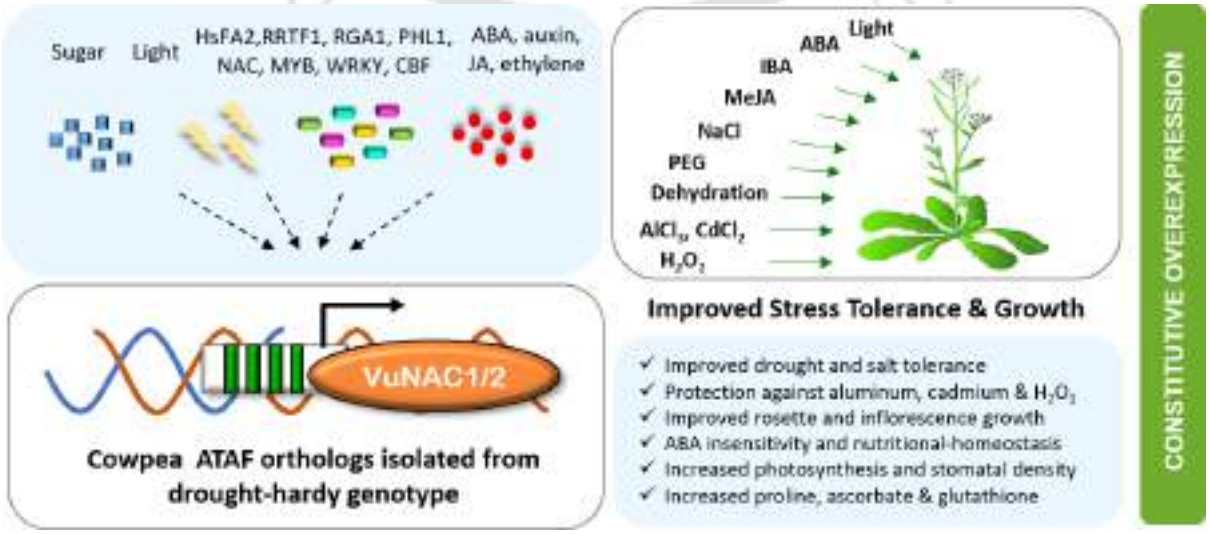

5.1 INTRODUCTION

Plants encounter multiple stresses under field conditions making it challenging to extrapolate the tolerance mechanisms for the combined effects [20]. Diverse breeding strategies have been employed but achieved only partial success due to the polygenic trait of the tolerance mechanism [42]. One approach to confer tolerance to multiple stress tolerances would be genetic engineering of transcriptional programs that play a crucial role in stress tolerance in plants. Recent studies uncovered that several transcription factors (TFs) regulate multiple stress tolerance together [407]. For example, STOP1 regulating proton and aluminum tolerance can also control biotic and abiotic stress responses by exerting pleiotropic effects through target genes such as *PGIP1, HsfA2, GDHs, ALMT1, etc.* [408] Many other TF families, such as MYB, bZIP, DREB, NAC, *etc*., are also emerging as central regulators of stress responses, hence ideal biotechnological tools for developing multiple stress tolerance in crops [25, 51, 55]. For instance, overexpression of OsHBP1b, a bZIP TF, controls diverse abiotic stresses in rice through enhanced antioxidant and photosynthesis [409]. The ectopic expression of OsMYBR1 TF, a member of the rice MYB family, conferred tolerance to drought and chromium stress in Arabidopsis [301]. Genetic engineering, including overexpression of such TFs, would be one useful approach to confer multiple stress tolerance of plants.

The ATAF (Arabidopsis Transcription Activation Factor) members of the NAC family have been identified and ascribed for their role in various abiotic and biotic stress responses in the Arabidopsis model and edible crops such as rice and soybean [27, 30, 33]. A single ATAF member can serve multiple roles, *e.g.,* ATAF1 controls drought tolerance, chloroplast maintenance, senescence cascades, photosynthesis, ABA biosynthesis, carbon starvation, and developmental processes in Arabidopsis, mediated by proteins such as RD22/RD29A (RESPONSIVE TO DESICCATION 22/29A), COR47 (cold regulated 47), NCED3 (NINE-CIS-EPOXYCAROTENOID DIOXYGENASE 3), GLK1 (GOLDEN2-LIKE 1), SnRK1 (SNF1-Related Protein Kinase 1), *etc.* [57, 405] This suggests that genetic engineering of ATAF would be one promising approach in molecular breeding of stress tolerance. The nature of the NAC TF is majorly dictated by the conserved NAC subdomains, determining the set of target genes and the interacting TF co-partners. However, perturbation in ABA-signalling can lead to detrimental crosstalk between stress responses and growth. For instance, authentic *ATAF1* overexpression in Arabidopsis enhanced tolerance towards drought response but led to dwarf and short primary root phenotypes, increasing sensitivity to ABA, salt, and oxidative stress in Arabidopsis [27]. Moreover, the ABA signal may activate the carbon starvation signal

due to the ATAF1-SnRK interaction [57]. Similarly, overexpression of *ATAF* homolog in rice (*OsNAC6*) improved tolerance to high salinity but retarded the growth of transgenic rice [30]. These results suggest that genetic engineering of ATAF-like proteins would require establishing procedures that escape overexpression's adverse effects, including cross-talk of ABA signaling.

There are several strategies to minimize the adverse effects caused by overexpression of stress-responsive genes. For example, substituting the constitutive 35S CaMV promoter with an inducible RD29A promoter improved drought tolerance by alleviating the growth anomalies associated with DREB1A expression [304]. This strategy might be suitable for improving tolerance to short-duration intermittent stress treatment, but the growth may never recover after persistent and aggravated stress conditions in fields, resulting in massive yield penalties [259]. Approaches like gene-stacking involving co-expression of stress-responsive and growth-regulating genes to compensate for the trade-offs are complex [22]. Another suitable approach would be the overexpression of versatile TFs, playing dual roles by amalgamating transcriptional networks of stress tolerance with growth improvement. Our previous studies found two ATAF-like NAC TFs encoded by *VuNAC1* and *VuNAC2* cloned from drought-resilience cowpea (*Vigna unguiculata* L. Walp) genotype improved both growth and stress tolerance by reprogramming energy-producing biosynthetic pathways when expressed heterologously in yeast system [372]. Such ATAF homologs isolated from robust genetic sources hold potential for sustainable improvement of stress tolerance in plants without growth penalty [410].

In this study, we examined the functional roles of *VuNAC1* and *VuNAC2* in the signaling of plant stress and growth processes. When overexpressed constitutively in Arabidopsis, the orthologs showed tolerance to various abiotic stresses limiting crop productivity, such as drought, salinity, and metal toxicity. Moreover, the transgenic lines did not show any growth penalties and sustained nutrition-deficient conditions. This harmonized phenotype conferred by VuNAC1/2 could be accounted for by several possible factors such as improved photosynthetic activity or suppression of chloroplast degradation, carbon starvation signals, hormonal perturbation, *etc*., unlike their Arabidopsis homolog ATAF1 [57, 405]. To investigate that, we characterized the photosynthetic parameters, ABA-sensitivity, and the relationship of stress response with the availability of nutrition. The ubiquitous and constitutive expression of such unique regulatory mechanisms may bring favorable and multiple functional benefits during the long term and broad-spectrum stress, opposed to their temporal or stress-

inducible gene expression. This study in Arabidopsis and the inference thereof laid the foundation of implementing the strategy legumes to accomplish dual objectives, *i.e.*, multi-stress resilience and yield improvement. Further understanding the underlying molecular mechanisms can bring new insights to cross-talk between stress adaptation and growth.

5.2 METHODOLOGY

5.2.1 Vector preparation

The *VuNAC1/2* genes were cloned from a drought-hardy cowpea genotype (*Kannando White*) [252], as described in our previous work [372]. The 35S:VuNAC1/2 constructs used to generate the constitutive overexpressor Arabidopsis lines were prepared by cloning the complete ORF (888 bp each) at the *Sfi*I site of pBEAB, a T-DNA vector (provided from Gifu University, Japan). The constructs were mobilized in the EHA105 strain of *Agrobacterium tumefaciens*, independently using tri-parental mating through pRK2013 helper plasmid.

5.2.2 Floral-dip transformation

The wild type Arabidopsis seeds (Col-0 variety) were imbibed in water at 4˚C for two days. Around 50 seeds were sprinkled per pot containing soilrite mix supplemented with MS media. The plants were grown at 24˚C, 16/8 light/dark photoperiod conditions at 85% relative humidity, for around five weeks until the bolting stage arrived with the maximum number of unopened buds. The agrobacterium strain harboring the 35S:*VuNAC1* and 35S:*VuNAC2* plasmid were grown till $O.D._{600}$ reached 0.8 in LB media. The cells were harvested and suspended in 10 mM $MgCl_2$, 5% sucrose, and 0.02 % Silwet-L-77 [411]. The plants were dipped in the agrobacterium suspension for 10 seconds with gentle swirling and incubated in the dark for one day, followed by transfer in the growth chamber. The T_0 generation seeds were harvested upon maturation. The seeds were sterilized in 1% (v/v) sodium hypochlorite for 10 minutes with vigorous vortexing followed by washing with de-ionized water (5X, 2 min each). For screening, the seeds were germinated in ½X MS supplemented with 0.8% agar, 0.5% sucrose, and 50 µg/ml kanamycin. After seven days of selection, the green seedlings were transferred to soil to further analyze the transgene insertion.

5.2.3 Growth conditions for stress analysis

For the study in the seedling stage, healthy seeds of wild type (Col-0) and T_2 generation transgenic seeds were sterilized in 1% (v/v) sodium hypochlorite for 10 minutes followed by washing with de-ionized water and kept for stratification at 4°C for 48 hrs. The seeds were

transferred to plates containing ½ X MS media supplemented with 1% (w/v) sucrose (added as indicated), 0.8% agar, (pH 5.8) and grown in long-day photoperiod condition (16 hr of light, 8 hr of dark) at 25 °C, with white light illumination (110 µmol photons $m^{-2}s^{-1}$). For various stress treatments, the growth media was supplemented with the chemicals as per the indicated concentration. For stress analysis of soil-grown plants, 1-week old germinated seedlings were transferred to soilrite mix and grown for four weeks while supplementing MS media every week. For imposing nutrient stress, only water was supplied throughout the vegetative growth of 4 weeks. For drought assay, water was withdrawn, and plants were maintained at 40% humidity for a week until recovery. To inflict high salinity, 400 mM of NaCl solution was supplied twice for a week.

5.2.4 Physiological parameters and biochemical assays

5.2.4.1 Determination of photosynthetic parameters

To determine chlorophyll fluorescence and gas exchange, we chose the fourth fully expanded trifoliate from the top to record the associated parameters using a portable infrared gas analyzer photosynthetic system Li-COR 6800 (Li-COR, U. S. A). To measure attributes such as net photosynthetic rate (A), stomatal conductance (Gsw), internal CO_2 concentration (Ci), quantum-yield of photosystem II (ϕ PSII) and electron transport rate (ETR), the air-temperature, relative-humidity, CO_2 concentration, fan-speed, light-intensity, and color-spectrum were maintained at 25° C, 50%, 400 µmol mol^{-1}, 10000 rpm, 100 µmol m^{-2} s^{-1}, red/blue 0.9/0.1 respectively.

5.2.4.2 Determination of relative water content

Fresh leaves taken from mid-canopy were cut into 3x3 cm segments. Ten segments were weighed together to record the fresh weight (FW). The turgid weight (TW) was determined by measuring fully hydrated leaf segment weight, kept immersed in the sealed flask at 10 ^{0} C for 4 hours. The dry weight (DW) was determined by drying the leaf segments at 70^0 C in an oven for 36 hrs to obtain consistent weight. Finally, the relative water content (RWC) was calculated for each sample using the formula [412]:

$$RWC\ (\%) = \{(FW-DW) / (TW-DW)\} \times 100$$

5.2.4.3 Determination of electrolyte leakage rate

The leaf samples were cut into 1 cm discs and dipped in de-ionized water. The electrical conductivity (ECa) was determined in terms of µS at 25°C using a conductivity meter (CON 700, Eutech). Next, the samples were incubated at 50° C water bath for 30 min in sealed test tubes, and the electrical conductivity (ECb) was measured. The samples were then boiled at 100° C for 10 min to measure the electrical conductivity (ECc). The electrolytic leakage was calculated as [413]:

$$\text{Electrolyte leakage (\%)} = \{(ECb - ECa) \times 100\} / ECc$$

5.2.4.4 Determination of lipid peroxidation

The level of membrane lipid peroxidation was estimated by the method described by Heath and Packer (1968) in terms of malondialdehyde (MDA) content [414]. 200 mg leaf tissue was homogenized in 5 ml of TBA reagent: 0.25% (v/v) thiobarbituric acid and 10% (v/v) trichloroacetic acid. The homogenate mixture was boiled for 30 min in a water bath at 95° C and cooled to RT. After centrifugation (10,000 g, 10 min), the absorbance of the clear supernatant was measured at 532 nm and 600 nm. The lipid peroxidation rate equivalents were as:

$$\text{MDA equivalent nmol/gFW} = [(A532-A600)/155000] \times 1000000$$

5.2.4.5 Determination of proline content and non-enzymatic ROS scavengers (glutathione and ascorbate)

Proline concentration was determined following the method of Bates *et al.* (1973) [415]. 100 mg of each leaf sample was homogenized in 5 ml of 3% aqueous sulfosalicylic acid (v/v) and left for 3 hrs for extraction. The mixture was centrifuged (3000 g, 10 min) to separate the supernatant. To the 0.5 ml supernatant, 0.5 ml glacial acetic acid and 0.5 ml acidic ninhydrin was added and boiled in a 90° C water bath for 30 min. After cooling, 1.5 ml of toluene was added and mixed vigorously. The absorbance was read at 520 nm. The proline concentration was determined in terms of µg/ml from a standard curve. Total glutathione and ascorbate contents were determined as per the method Griffith (1980) and Oser (1979), respectively [416, 417]. 200 mg of each leaf sample was homogenized in 5% (w/v) sulphosalicylic acid and centrifuged (10000 g, 15 min at 4º C) to collect the supernatant. To determine ascorbate content, 0.2 ml of plant extract was mixed with 0.4 ml of 2% sodium molybdate, 0.4 ml 0.15

N H_2SO_4 and 0.2 ml 1.5 mM Na_2HPO_4, and incubated at 60 ºC for 40 minutes. The mixture was centrifuged at 3000 g, and the clear supernatant was collected to record the absorbance at 660 nm. For the determination of total glutathione content, plant extract was neutralised with 0.1 M phosphate buffer. The 0.4 ml neutralised extract was mixed with 0.25 µl of 0.1 M phosphate buffer, 80 µl of 6 mM 5,5´-dithiobis (2-nitrobenzoic acid). The absorbance was recorded at 412 nm. The concentration was determined from the standard curve.

5.2.5 Visualization of stomata by FESEM

The plant tissue was pre-fixed with 2.5 % glutaraldehyde solution overnight. The sample was then dehydrated with an ethanol gradient (10%, 20%, 30%, 50%, and 70%, once for 10 min at each step), and then immersed in 100% ethanol (twice, 30 minutes each step). One-cm-sections were mounted on carbon tape. The specimen was coated with gold and analyzed at 2000X magnification using FESEM (Gemini 300, Zeiss, Germany), operating under an accelerating voltage of 3 kV.

5.2.6 Gene regulatory models

The orthologous Arabidopsis NAC TFs were used to predict the VuNAC1/2 coexpression network generated by ATTED II v. 10.1 (https://atted.jp/) [338]. The genes in the constructed network were subjected to ontology analysis to annotate the ATAF-like VuNAC TFs using the panther tool (http://go.pantherdb.org/genelistanalysis.do) [339]. The upstream regulators were predicted using the RnR (Regulatory Network Research) database of Arabidopsis T87 culture cells (http://webs2.kazusa.or.jp/kagiana/rnr0912/indexff.html).

5.3 RESULTS

5.3.1 ATAF-like VuNAC1/2 TFs improved embryonic, rosette, and inflorescence growth in transgenic Arabidopsis under limited nutrition availability

We generated at least three independent lines, ectopically expressing the *VuNAC1/2* TFs in Arabidopsis, governed by a 35S CaMV promoter (Fig. 5.1B). The quantification of RNA transcripts by qRT-PCR showed a significant accumulation of the transgene under controlled growth conditions (Fig. 5.1C). As indicated by their promoter analysis, VuNAC1/2 TFs were stipulated to play indispensable roles in plant growth regulation and nutrient assimilation (Table 4.1).

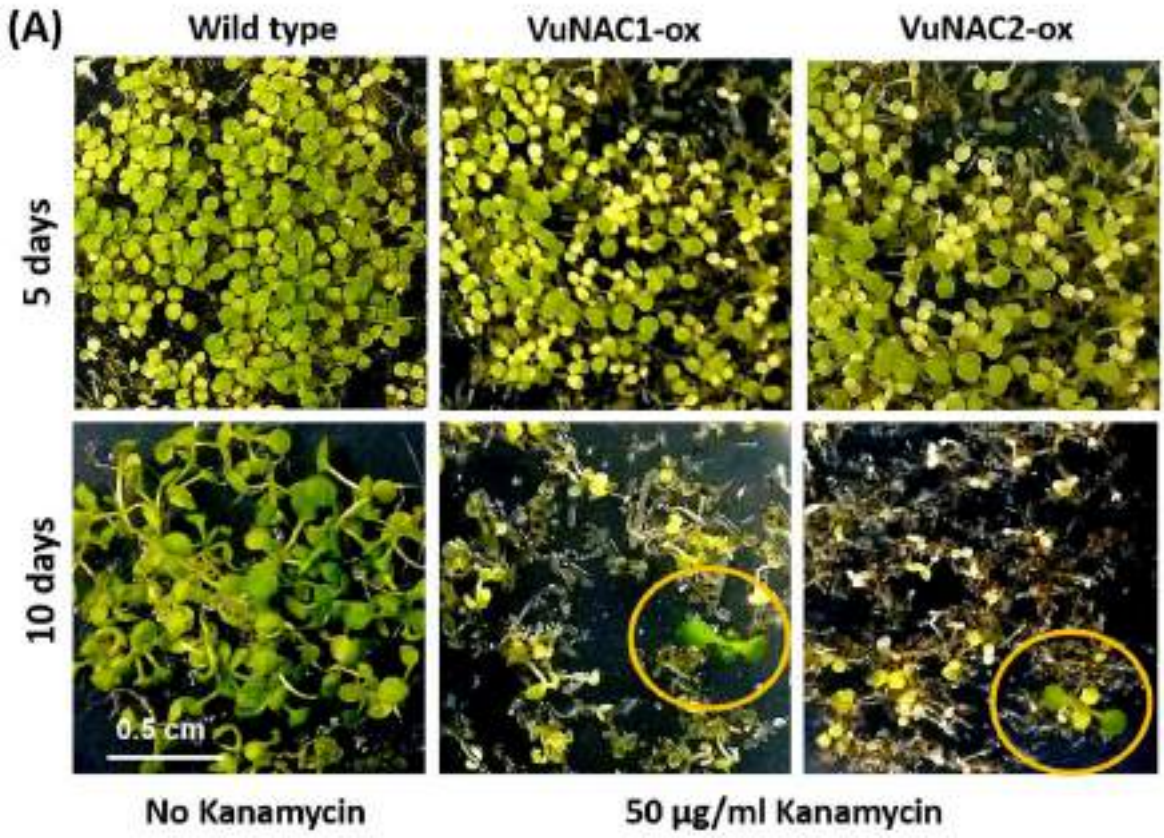

Fig. 5.1 Screening of VuNAC1/2 expressing Arabidopsis lines. (A) The seeds produced after floral dip transformation (T_0 generation) were screened in the presence of 50 µg/ml kanamycin supplied in the ½X MS media. The seedlings with successful gene integration (VuNAC1-ox and VuNAC2-ox) germinated to grow into mature seedlings (encircled) after ten days of selection, exhibiting kanamycin resistance, while the non-transformed seedlings displayed bleached leaves after five days of growth and died eventually.

To characterize the growth-associated roles, we studied the phenotypes of the transgenic lines under both embryonic, rosette, and flowering stages. In the presence of sucrose, all the germinated seedlings displayed emerging green primary leaves after one week (Fig. 5.2A and Fig. A3.1A, Appendix 3). But, the VuNAC1/2-ox seedlings showed early sprouting, the maximal leaf-blade size and root length increased, displaying more expanded cotyledonary leaves and emerging juvenile leaves. In contrast, in the absence of sucrose, all the seedlings showed a lighter green appearance with less expanded leaf after one week (Fig. 5.2B). However, the VuNAC1/2-ox seedlings reached their post-germination stage with expanded leaves and roots, despite the limited growth, whereas, in the wild type seedlings, the primary leaves and roots were still not fully emerged. Even so, after four weeks, the VuNAC1/2-ox seedlings displayed increased leaf size and primary root length, in addition to more number of newly emerging leaves and denser lateral roots, as compared to the wild type counterparts (Fig. 5.2C). The study indicated impeded seed-dormancy and accelerated post-embryonic growth in Arabidopsis due to VuNAC expression under both sucrose-rich as well as sucrose deficient conditions, suggesting better photosynthetic sequestration in the transgenic seedlings.

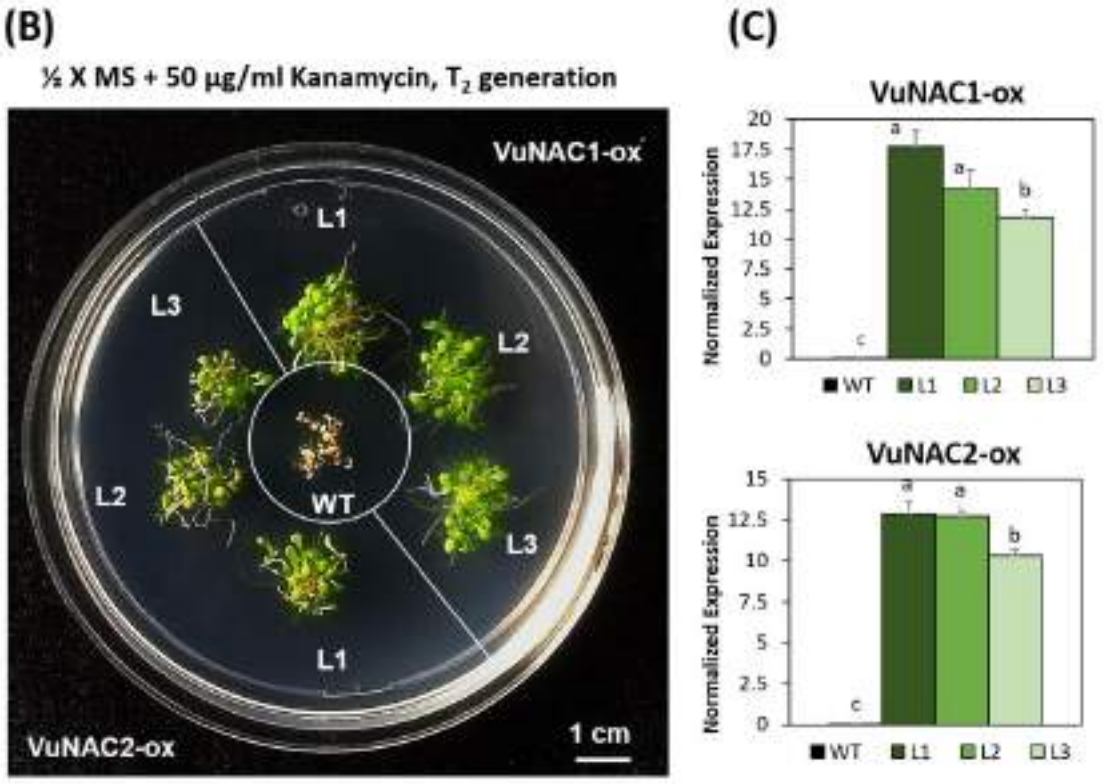

Fig. 5.1 Screening of VuNAC1/2 expressing Arabidopsis lines. (B) Selection of T_2 transgenic seeds of three independent transgenic lines (L1, L2, and L3) for the kanamycin resistance. (C) Quantification of the VuNAC1/2 transcripts normalized by the housekeeping actin2 in T_2 transgenic lines (VuNAC1-ox and VuNAC2-ox).

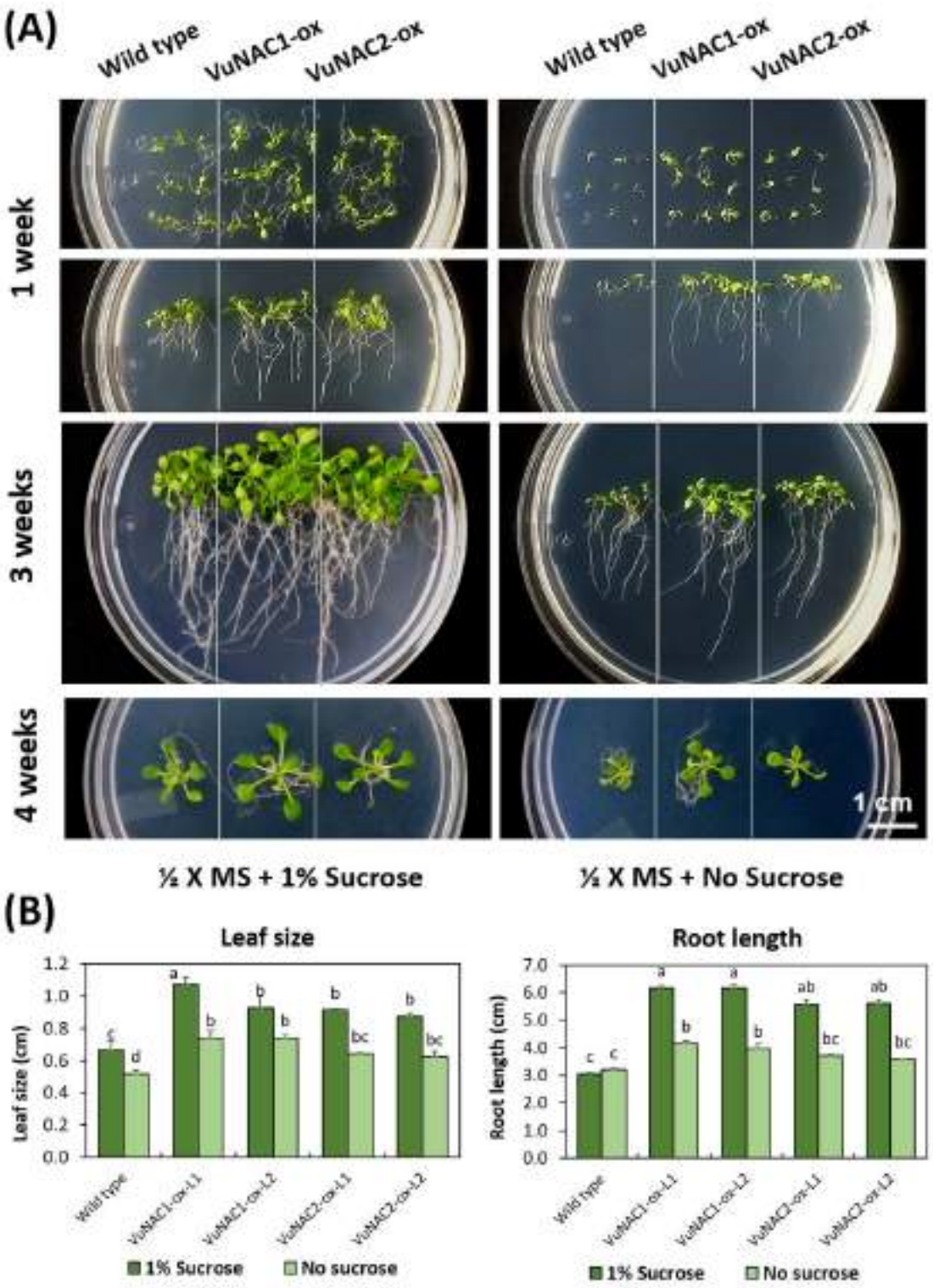

Fig. 5.2 Characterization of seedling phenotypes in normal and carbon-deficient conditions. (A) Embryonic (one week after germination) and juvenile (3-4 weeks after germination) phenotypes were studied under two different nutritional conditions, media with 1% (w/v) sucrose and the growth media lacking any carbon source. **(B)** The relatively increased growth parameters such as maximal leaf blade size (cm) and primary root length (cm) in the 4-week-old VuNAC1/2-ox seedlings indicated improved growth under both normal and nutritional stress conditions.

When the gain-of-function phenotype was studied in the mature stage under normal conditions, the VuNAC1/2-ox plants displayed richer rosette growth with increased plant height, leaf count, leaf area, and rosette diameter (Fig. 5.3 and Table 5.1). The plants exhibited more branched inflorescence with a thicker flowering axis, producing more siliques, and improving seed yield (Fig. 5.3B).

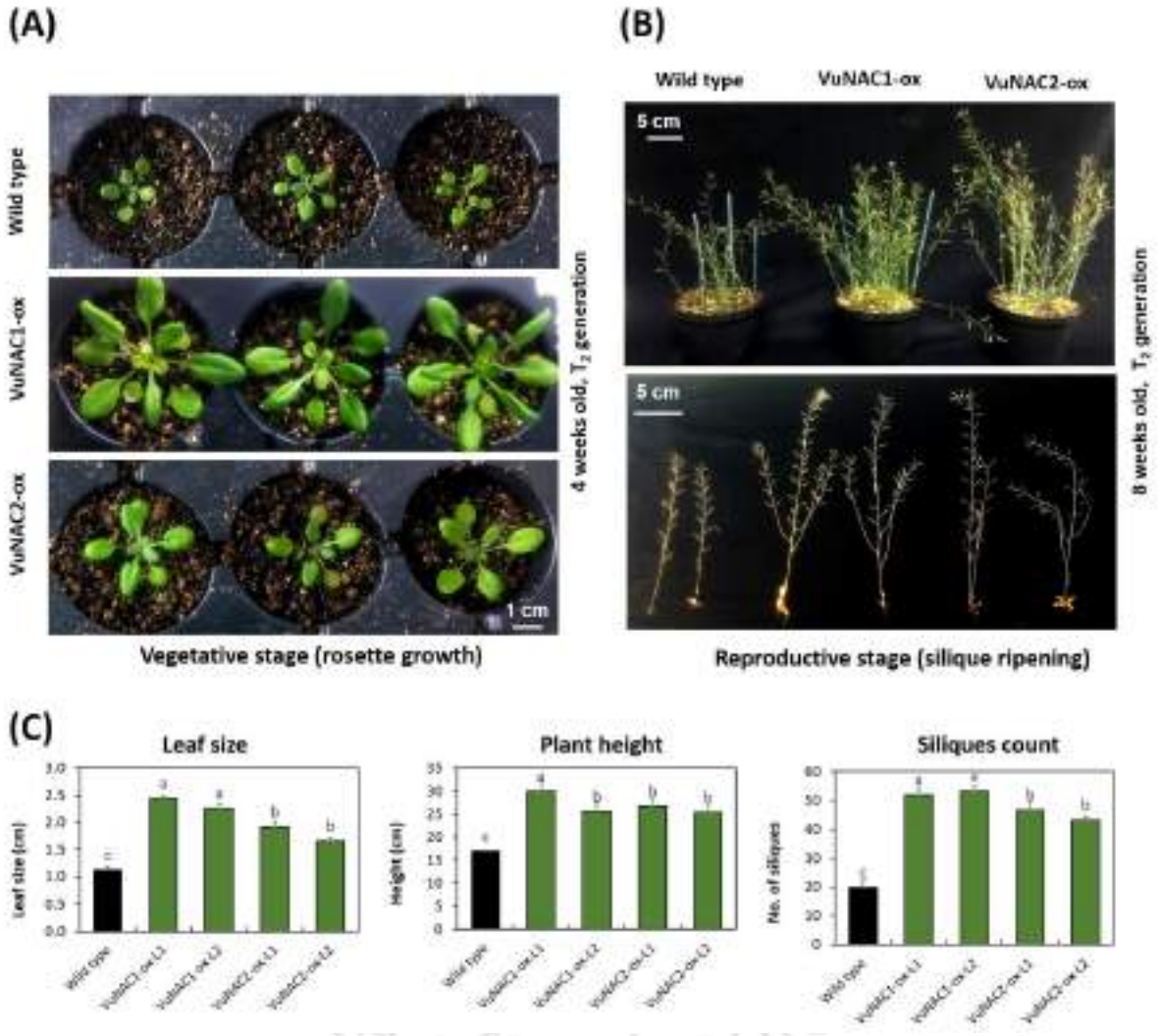

Fig. 5.3 Analysis of vegetative and reproductive growth traits under normal conditions. (A) The VuNAC1/2-ox lines displayed greater rosette biomass in 4-week old soil-grown plants. **(B)** Richer inflorescence growth in 8-week old plants (top), resulting in higher silique production and seed yield (bottom). **(C)** The rosette leaf size (cm), inflorescence height (cm), and siliques count were evaluated to find better growth and yield attributes of VuNAC1/2-ox plants.

Table 5.1. Evaluation of growth, photosynthetic and yield parameters of the transgenic lines under normal and nutrition-deficient conditions

		Growth Parameter				Photosynthetic Parameter		Yield parameter
		4 week-old seedling in plate		8 week-old plant in soil		8 week-old plant in soil		12 week-old plant
		Germination Rate (%)	Seedling Size (in cm)	Rosette Size (in cm)	Plant Height (in cm)	CO2 assimilation rate (in µmol m^{-2} s^{-1})	Chlorophyll (a+b) (in ug/ml)	Siliques per plant
Normal Condition	**Wild type**	98.3 ± 1.5	3.1 ± 0.05	2.3 ± 0.15	16.9 ± 0.15	11.5 ± 0.39	259.2 ± 20.3	20.0 ± 2.0
	VuNAC1-L1	99.4 ± 1.2	6.2 ± 0.11	4.9 ± 0.10	30.0 ± 2.00	22.7 ± 0.41	336.3 ± 3.8	52.0 ± 2.5
	VuNAC1-L2	98.3 ± 1.6	6.1 ± 0.18	4.5 ± 0.12	25.6 ± 2.00	22.6 ± 0.25	341.7 ± 15.7	53.3 ± 1.5
	VuNAC2-L1	99.4 ± 1.1	5.6 ± 0.05	3.8 ± 0.21	26.7 ±1.53	19.3 ± 0.29	357.1 ± 7.1	46.6 ± 3.1
	VuNAC2-L2	99.5 ± 1.1	5.6 ± 0.01	3.3 ± 0.10	25.3 ±1.15	16.9 ± 0.52	347.0 ± 25.5	43.3 ± 1.2
Nutrition Stress	**Wild type**	83.6 ± 2.4	3.2 ± 0.06	1.4 ± 0.10	12.6 ± 0.57	4.4 ± 0.29	199.6 ± 6.8	11.3 ± 1.2
	VuNAC1-L1	97.4 ± 1.1	4.2 ± 0.12	3.8 ± 0.21	25.3 ± 0.80	16.5 ± 0.41	281.5 ± 20.5	42.5 ± 2.5
	VuNAC1-L2	98.4 ± 1.5	4.0 ± 0.13	3.3 ± 0.10	24.0 ± 0.58	17.8 ± 0.25	310.5 ± 8.1	43.3 ± 2.8
	VuNAC2-L1	97.8 ± 1.1	3.7 ± 0.14	3.6 ± 0.06	22.7 ± 1.66	15.4 ± 0.29	296.1 ± 2.1	36.6 ± 2.9
	VuNAC2-L2	98.6 ± 1.3	3.6 ± 0.12	3.1 ± 0.12	23.3 ± 0.76	14.0 ± 0.52	293.1 ± 10.8	38.7 ± 3.2

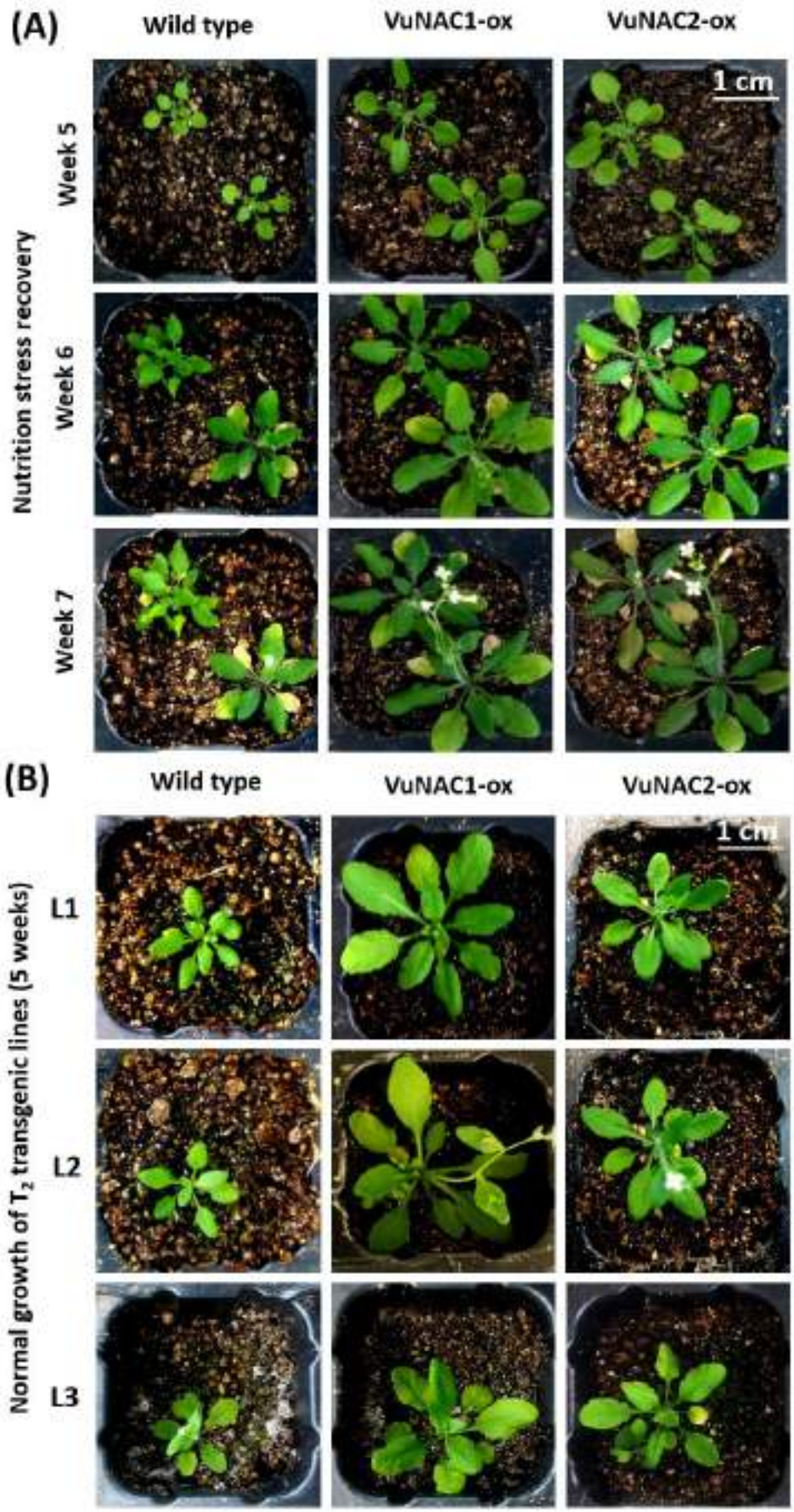

Fig. 5.4 Analysis of growth traits under nutrient deficit conditions. (A) The better growth recovery of VuNAC1/2-ox lines after 4-weeklong nutritional stress indicated tolerance to nutrition deficiency. **(B)** Three independent transgenic lines (L1, L2, and L3) showing enhanced rosette growth under nutrient-sufficient conditions.

To study response to the nutritional stress, two-week-old healthy plants were grown under nutrition-deficit conditions for a month, followed by restoration of nutrition supply. Although, all the plants displayed chlorosis as a symptom of nutrition deficiency, which was recovered by nutritional supplements post-stress. The VuNAC1/2-ox plants grew expanded rosette leaves and healthy reproductive growth. In contrast, the wild type plants showed poor growth and impeded development, having smaller rosette base and delayed emergence of the floral axis (Fig. 5.4A). Our result indicated that the expression of VuNAC1/2 TFs refined both vegetative and reproductive growth under normal and nutrition-deficit conditions. As indicated by the promoter regulatory elements, the VuNAC1/2 TFs may be involved in nutrition assimilation by signaling sugar metabolism, phosphate starvation, and ion uptake.

5.3.2 VuNAC1/2 TF overexpressing lines exhibited improved photosynthetic efficiency

The induction of *VuNAC1/2* under controlled growth conditions, and the promoter elements suggested circadian or light-mediated regulation, indicating a role in photosynthesis, nutrition metabolism, and other developmental programs. Moreover, the transgenic plants showed improved growth and thrived in limited supplied nutrition. One of the possible reasons for nutrition sufficiency can be improved photosynthetic activity. Photosynthesis fixes carbon (C) in the form of CO_2 in the leaf, which is metabolized to produce energy currencies as well as provide the organic C-skeleton for assimilating nitrogen (NO_3^-, NH_4^+) taken by the roots [418]. Moreover, the sink regulation of photosynthesis determines the optimal biomass growth by maintaining the C/N balance [419]. To assess the photosynthetic activity, the gas exchange and chlorophyll fluorescence parameters were recorded in at least three independent VuNAC1/2-ox lines after two weeks of the nutritional stress (Fig. 5.5). The higher CO_2 assimilation rate (A), stomatal conductance (Gsw), quantum yield of photosystem II (φ PSII), and electron transport rate (ETR) were noted in the VuNAC1/2-ox plants, as compared to the wild type. The results indicated enhanced photosynthetic activity in transgenic plants *via* activating genes forming with the photosynthetic components, particularly the light-harvesting chlorophyll–protein complexes (LHCP), electron transport, and $NADP^+$-reducing components of thylakoids, and the enzymes protecting against photo-damage [420]. The photosynthetic efficiency not only dictates the biomass growth but also the crop yield potential [421].

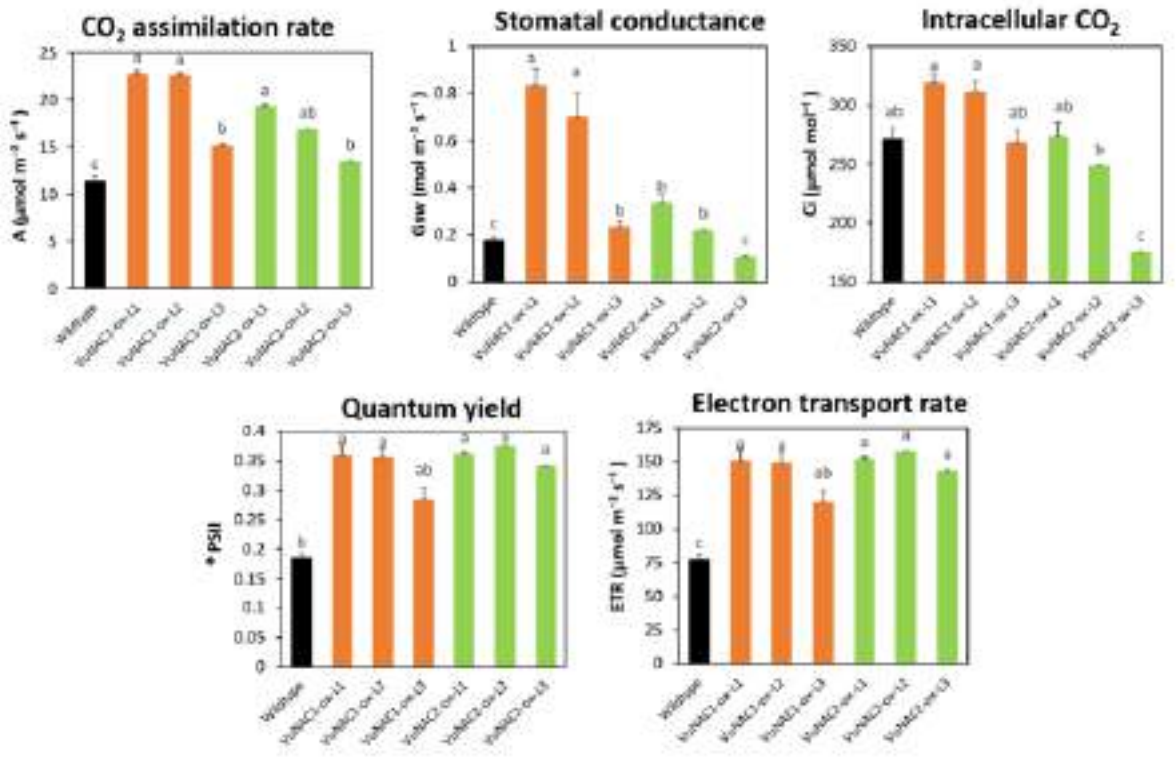

Fig. 5.5 Evaluation of photosynthetic efficiency under nutritional stress. The enhanced gas exchange and chlorophyll fluorescence parameters such as carbon assimilation rate (A), stomatal conductance (Gsw), photosystem II quantum yield (ϕ PSII), and electron transport rate (ETR), indicated improved photosynthetic activity under nutrition stress (data for normal conditions not shown).

5.3.3 The transgenic seedlings displayed ABA and auxin insensitivity at germination and post-germination stage

ABA plays a pivotal part in the maintenance and release of seed dormancy. Dynamic changes in ABA level or sensitivity can elicit signaling perceived by TFs like ABI5 to regulate developmental checkpoints transitioning dormancy to germination through radicle emergence and post germinative seedling establishment [422], which can be counteracted by antagonist actions of gibberellins (GA) [423]. ABA can also suppress growth in germinated seedlings by inhibiting the expression of enzymes required for cell-wall loosening, expansion, cell-wall biosynthesis, and other structural proteins. Besides, the post-germinative growth is finely tuned by auxin. A somewhat lower range of auxin concentrations accelerates root growth, but the application of high concentrations can retard both shoot and root growth, probably due to pathological toxicity [424]. The transgenic seedlings manifested improved germination rates under normal and stressed conditions (Fig. 5.2), and their promoter analysis indicated ABA and auxin-mediated regulation (Table 4.1).

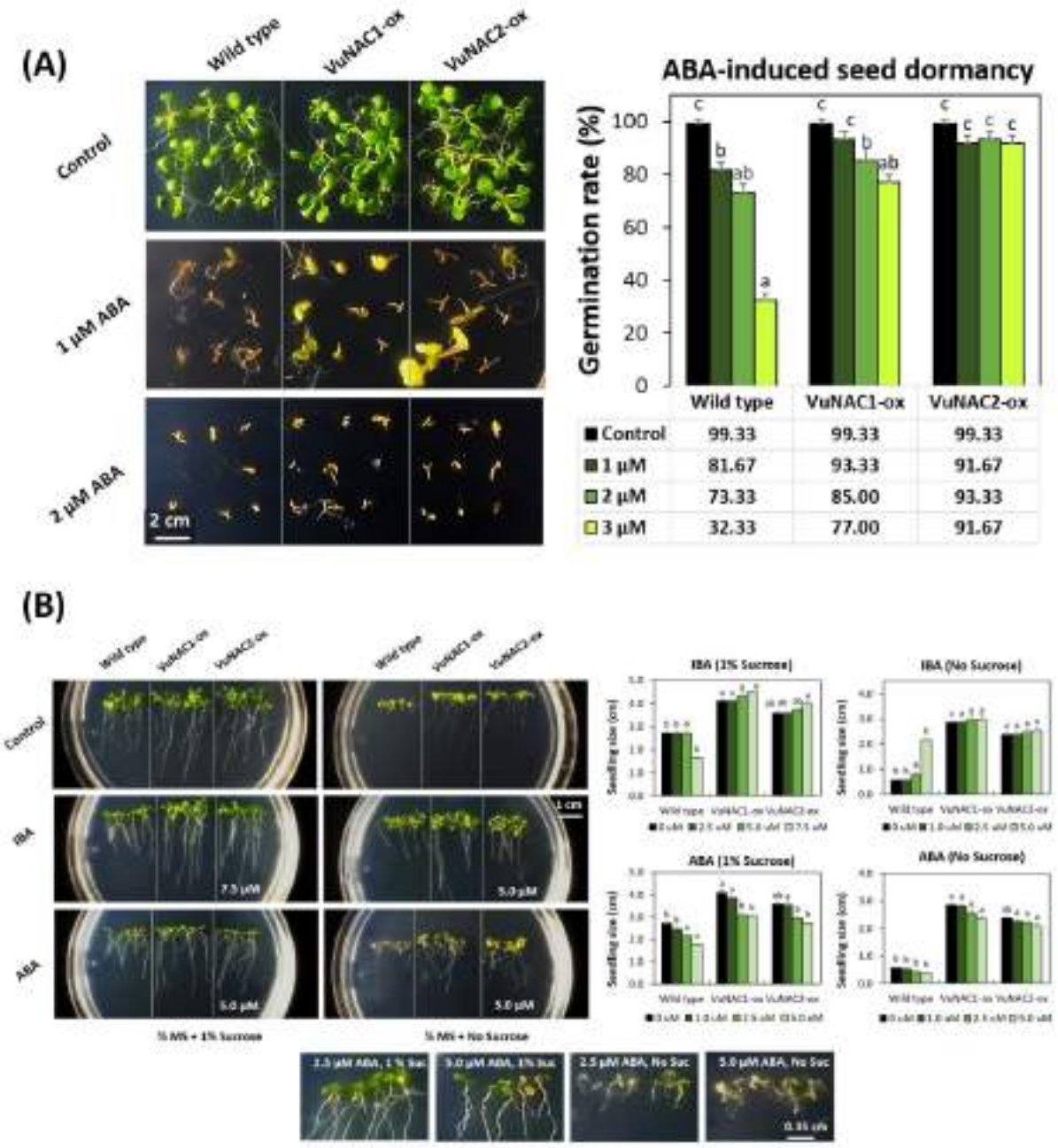

Fig. 5.6 Study of ABA and auxin response on the germination rate and post-germinative growth of the transgenic seedlings. (A) The VuNAC1/2-ox seedlings indicated ABA insensitivity resulting in greater germination rates, whereas the wild type seedlings displayed ABA-induced dormancy. **(B)** VuNAC1/2-ox seedlings showed less toxicity caused by high ABA and auxin levels.

Thus, to examine the role of ABA-inducible VuNAC1/2 TF in breaking seed dormancy, we studied germination rate under high exogenous ABA levels, 1.0 µM, 2.0 µM, and 3.0 µM (Fig. 5.6A). The transgenic seeds displayed a higher germination rate indicating counteraction of the inhibitory effects of ABA, while the wild type seeds showed dormancy with increasing ABA levels. However, at 3.0 µM ABA, the post-germinative seedling establishment was affected in

transgenic lines. Further, to study the post-germinative sensitivity of transgenic seedlings, we examined the growth phenotype at different concentrations of ABA and Indole-3-butyric acid (IBA) under both availability/lack of sucrose (Fig. 5.6B). The high levels of ABA imposed growth inhibition and induced senescence in the wild type seedlings, more apparently in the sucrose deficit conditions. In contrast, the VuNAC1/2-ox seedlings showed tolerance to ABA sensitivity. Moreover, in the presence of sucrose, 2.5 µM and 5.0 µM of IBA triggered lateral root formation in all seedlings but no substantial change in the primary root length. However, at higher levels (7.5 µM), the shoot and root growth of wild type seedlings exhibited inhibition, whereas the VuNAC1/2-ox seedlings continued growth, suggesting auxin insensitivity. Without sucrose, IBA triggered thicker root formation in all seedlings. 5.0 µM IBA induced the primary root length of the wild type seedlings but no significant increase in the VuNAC1/2-ox seedlings. In fact, the VuNAC1/2-ox seedlings produced lengthier roots with/without any IBA supply.

5.3.4 The ectopic expressing of *VuNAC1/2* conferred tolerance to multiple abiotic stress such as drought, salinity, aluminum, cadmium, and H_2O_2 stress in Arabidopsis

Both VuNAC1 and VuNAC2 showed prominent induction in abiotic stress in cowpea (Fig 4.2), and regulated yeast response to dehydration (PEG, sorbitol), salinity (NaCl, $MgCl_2$), and metal toxicity ($AlCl_3$, $CdCl_2$), oxidative stress (H_2O_2), heat and cold (Fig 4.7), hence indicating promising involvement in plant stress responses. To validate their functional roles in the Arabidopsis model, we examined the growth phenotype of the transgenic seedlings under varying doses of stress inducers under both nutrition-sufficient and limiting conditions imposed by the presence/absence of sucrose supply. The VuNAC1/2-ox seedlings exhibited a better germination rate and seedling growth under NaCl and PEG-induced stress (Fig. 5.7). When severe stress was imposed during the post-germinative stage, the VuNAC1/2-ox seedlings exhibited tolerance to dehydration, NaCl, aluminum, cadmium, metal toxicity, and oxidative stress, depending on the degree and duration of stress, showing increased seedling size than the wild-type (Fig. 5.8). The one-week-old transgenic seedlings could survive up to 5.0% PEG, 150 mM NaCl, 15.0 µM $AlCl_3$, 10.0 µM $CdCl_2$, 7.5 µM H_2O_2, whereas the wild type seedlings showed severe inhibition in the growth of shoot and root, and failed to survive after 3-4 days of stress. Interestingly, the stress tolerance phenotype was more prominent under the nutrient-deficit conditions (Fig 5.8B). The results indicated that *VuNAC1/2* overexpression conferred

tolerance to multiple abiotic stresses in transgenic lines, and their ability to maintain growth under starvation favors stress mitigation and recovery.

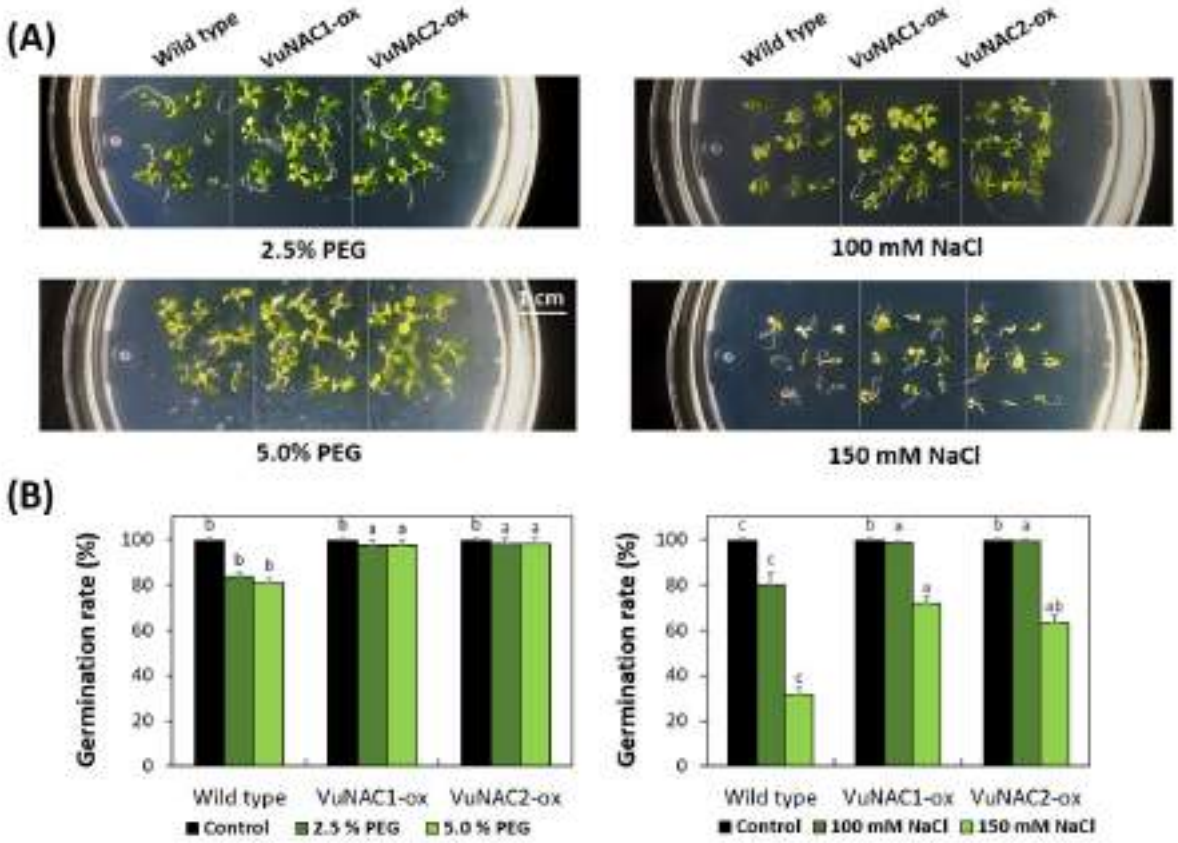

Fig. 5.7. Study of germination efficiency under drought and salt stress. (A) Phenotype analysis of the transgenic seedlings exhibiting improved growth under PEG and NaCl-induced stress, whereas the wild type seedlings showed severe root inhibition under high PEG concentration (5%) and ion toxicity under 150 mM of NaCl. **(B)** The germination rate (%) indicating less stress-induced inhibition of embryonic growth in the transgenic seedlings.

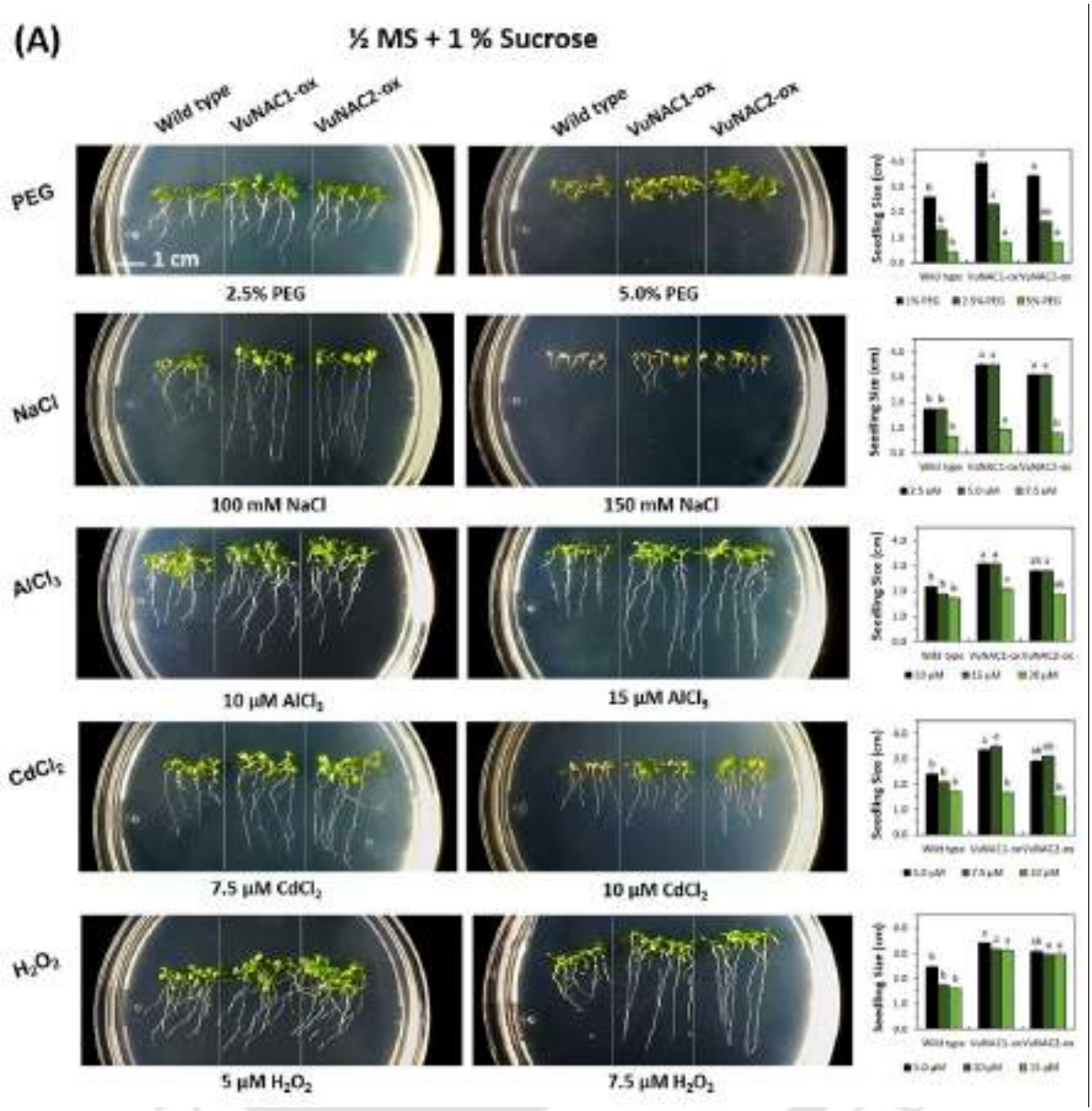

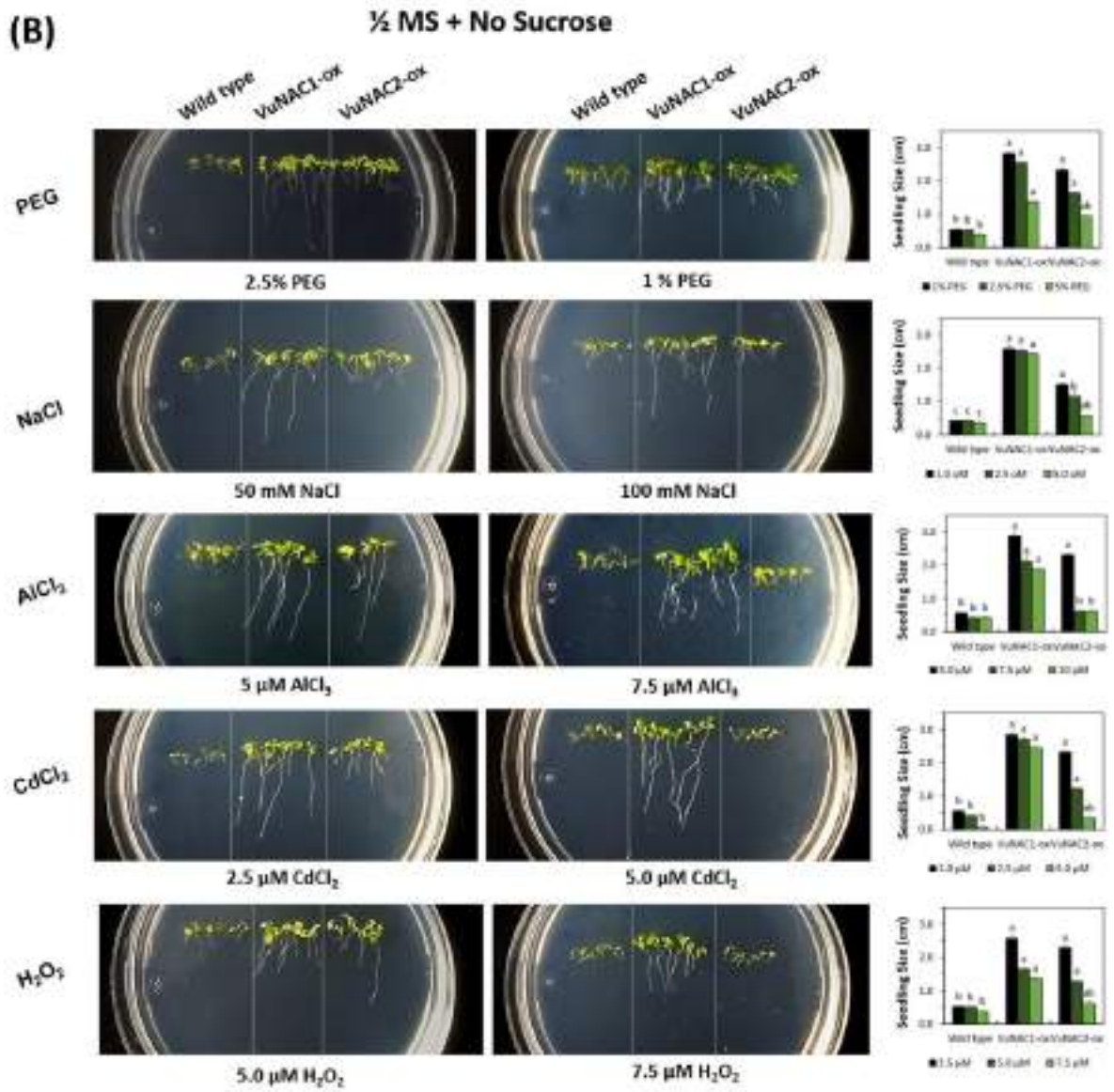

Fig. 5.8. Examining role of VuNAC1/2 in stress tolerance. The one-week-old Arabidopsis seedlings were characterized in dehydration, salinity, metal toxicity, and oxidative stress imposed by PEG, NaCl, $AlCl_3$, $CdCl_2$, and H_2O_2, in **(A)** normal and **(B)** carbon-deficient growth media, showing better tolerance to multiple abiotic stresses as well as growth sustenance in the VuNAC1/2-ox lines.

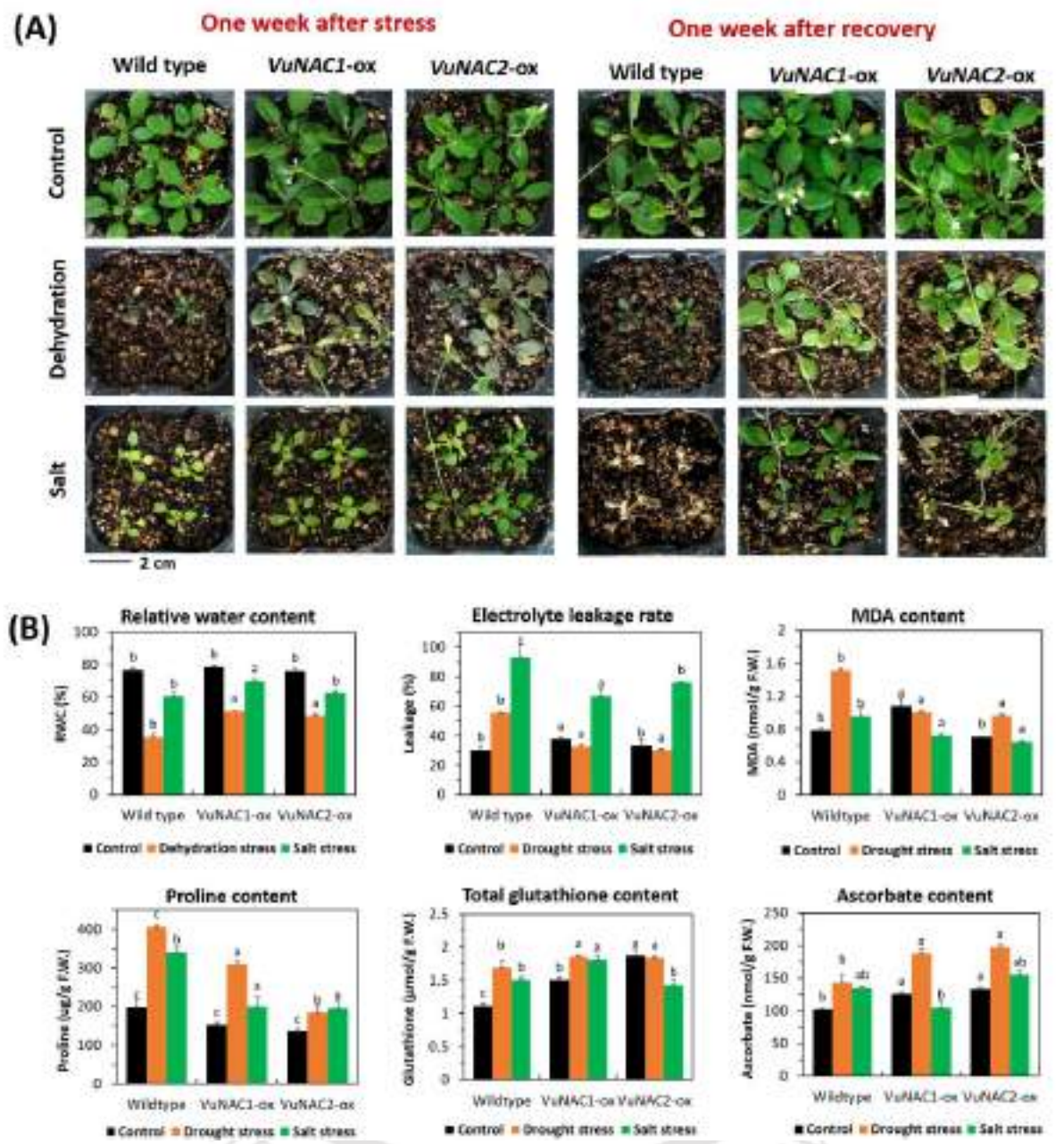

Fig. 5.9. Recovery from severe drought and salinity and the associated physiological and biochemical changes. (A) One-week desiccation and high-salinity were imposed in five-week-old soil-grown plants, manifesting recovery of vegetative and inflorescence growth in VuNAC1/2-ox lines, whereas the wild-type plants could not survive. **(B)** Higher relative-water content (RWC %), lesser electrolyte leakage rate (%) and malondialdehyde (MDA) content, and accumulation of proline, glutathione, and ascorbate in the VuNAC1/2-ox lines, indicated their better stress-adaptation.

5.3.5 The transgenic plants displayed increased stomatal density

We had already demonstrated that transgenic plants exhibited better photosynthetic parameters (Fig. 5.5). One of the possible factors that can be directly translated into increased photosynthetic activity and biomass growth can be the stomatal abundance [425]. As per the reports, NAC TFs such as *ZmNAC49* and *VvNAC17* regulate stomatal density in maize and grapevine [426, 427]. The field emission scanning electron microscopy (FESEM) visualization of the adaxial (upper) surface of leaf epidermis revealed a noteworthy higher stomatal density in the VuNAC1/2-ox plants (Fig. 5.10). The results suggested that increased CO_2 assimilation rate and stomatal conductance were dictated by stomatal density in the transgenic plants.

However, under drought conditions, the regulation of stomatal aperture is crucial to control transpiration rate to maintain leaf water potential to sustain the water-deficit conditions [428, 429]. Thus, stomata have to strike a balance between carbon gain and water-use efficiency. We noticed that the stomatal pores were closed under drought stress in both VuNAC1/2-ox and wild type leaves with a slight reduction in the density (Fig. 5.10). Even so, the increased stomatal density in the transgenic leaves indicated improved and optimized photosynthetic activity under drought stress *via* optimization and maintenance of CO_2 uptake. Several genes, such as *FAMA* and *MUTE*, regulate stomatal density and patterning by regulating cell division and differentiation and altered patterns of stomata and epidermal cells. VuNAC TFs may be directly involved in the direct expression of the genes associated with stomatal development like *ZmNAC49* and *VvNAC17*.

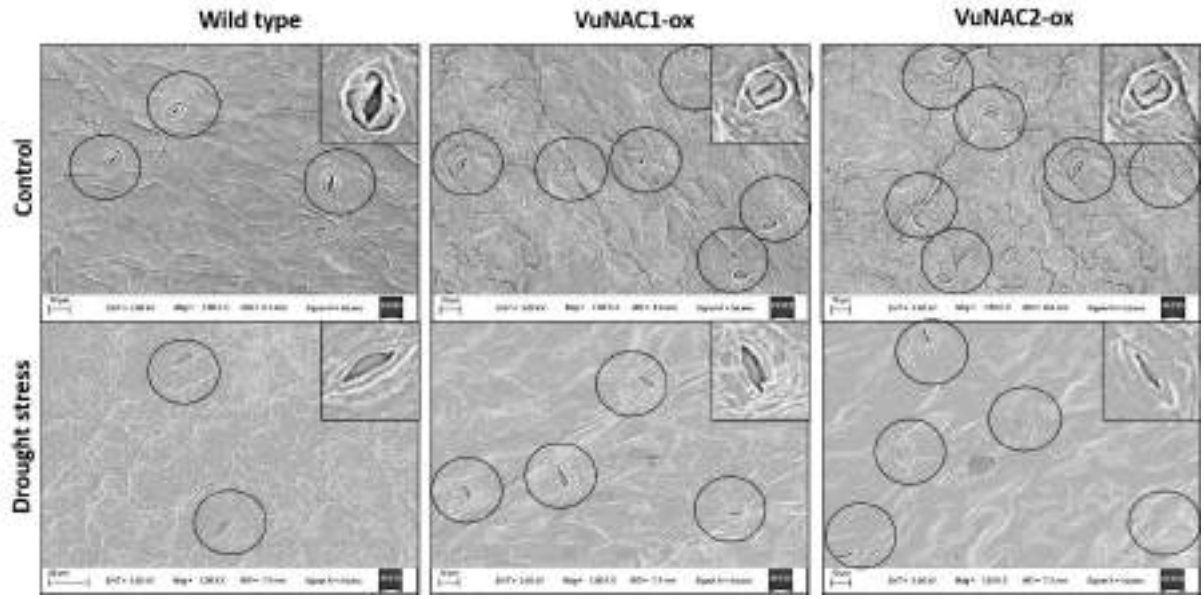

Fig. 5.10 Examining of the stomatal density in the transgenic plants and their regulation under drought stress. The increased stomatal density normal conditions indicated improved photosynthetic gas exchange in VuNAC1/2-ox. Whereas under drought stress, the stomatal aperture was closed, indicating less evapotranspiration in the transgenic lines.

5.3.6 Elucidation of orthologous interactome indicated VuNAC1/2 interaction with regulators of stress responses, hormone balance, metabolism, and growth

Integrative gene regulatory networks (iGRN) covering orthologous genes of model plants can provide a foundational framework for understanding and inferring the gene regulation of plants with unknown mechanisms [430]. The upstream regulators of the VuNAC1/2 TFs predicted based on the Arabidopsis homologs indicated that they perceive the signal of several other proteins such as HSFA2 (combined stress-response and ascorbate signaling) [431], RRTF1 (oxidative stress response) [432], COBRA (cell-expansion), MYB21 (photo-morphogenesis), ANAC025 (pollen and seed development) [104], flower development (PISTILLATA) [433], and PHL1 and HRS1 (nitrogen, phosphate and iron starvation and breaking of ABA-mediated seed dormancy) [434-436] (Table 5.2). Further, we generated a gene interactome for ATAF subgroups of Arabidopsis, bearing close homology with the VuNAC1/2 TFs, by convoluting experimental data of multiple co-expression studies under different developmental and environmental conditions, including PPIs (protein-protein interactions). The analysis predicted possible interacting partners of the VuNAC TFs (Fig. 5.11, Table 5.3, and Table A3.2), corroborating with the functional phenotypes of the transgenic plants and providing supporting evidence. As discussed below, the orthologous interactome suggested the interaction of VuNAC1/2 TFs with many stress and hormone signaling proteins, transporters, and metabolic enzymes. Combining the upstream regulatory model and coordinating gene network, suggested that *VuNAC1/2* might be induced by stress, hormone, nutrition, light, and developmental signals in a feedback loop.

5.3.1.1 Interaction with signaling proteins

The protein network comprised PROTEIN PHOSPHATASES TYPE 2C (PP2Cs), ABA INSENSITIVE (ABIs), and HYPERSENSITIVE TO ABA1 (HAB1) that negatively regulates ABA signaling by inhibiting SNF1-RELATED PROTEIN KINASE1 (SnRK1). PP2CG1 signals salt tolerance, HIGHLY ABA-INDUCED 1 (HA1) regulates drought acclimatization *via* dehydrins and LEA proteins, ZINC-INDUCED FACILITATOR PROTEIN (ZIFL1) controls polar auxin transport and drought tolerance, UDP GLYCOSYLTRANSFERASE

74E2 (UGT74E2) and GH3 protein (Gh3.15) regulate plant architecture by perturbing auxin homeostasis. The interactome also included NAC and other family TFs involved in the developmental and stress-associated processes, such as NAC2, RD26, NAC062, DREB2A, GBF3, regulating drought response [299, 437, 438], NAP and NAC047 tuning senescence and ethylene biosynthesis during hypoxia, Ras-related proteins (RAP2.4 and RAP2.6L), and ERF members (ERF1, ERF4, and ERF6) modulating cross-talk between ethylene, auxin, and ABA responses [129, 439-442]. Proteins like MYB74, CCX2, and CFZ1 regulating salt-response and osmo-tolerance also co-expressed, suggesting possible interaction. Other stress-responsive proteins in the network were bZIP60 and NAC062, mitigating ER stress, DJ1A activating cytosolic superoxide dismutase, G2-like flavonoid regulator (GFR) involved in cold response and flavonoid metabolism, NAP and MKK9 playing a crucial role in senescence regulation and several proteins from MATE family regulating detoxification processes.

5.3.1.2 Interaction with stress-responsive proteins

The interactome included NAC and other TFs involved in the developmental and stress-responses, such as NAC2, RD26, NAC062, DREB2A, GBF3, regulating drought response [148, 299, 437, 438]. Proteins like MYB74, CCX2, and CFZ1 regulating salt-response and osmo-tolerance also co-expressed, suggesting possible interaction [443-445]. Other stress-responsive proteins in the network were bZIP60 and NAC062, mitigating endoplasmic reticulum (ER) stress [446], DJ1A activating cytosolic superoxide dismutase, G2-like flavonoid regulator (GFR) involved in cold response and flavonoid metabolism, NAP and MKK9 regulating senescence [146, 447-449], and several proteins from MATE (Multidrug And Toxic Compound Extrusion) family regulating detoxification [450].

5.3.1.3 Interaction with growth-regulating proteins

Several signaling proteins associated with growth and developmental processes were found in the network, such as Carbon/Nitrogen Insensitive 1 (CNI1/ATL31) ligase controlling post-germination nutrient signaling [451], ZAT6 regulating germination under salt and osmotic stress, as well as cadmium tolerance [452], ERF6/11 stimulating growth through GA-mediated responses [453]. MADS-box proteins (AGL12/16) and CYCLIC DOF FACTOR 2 (CDF2) controls flowering time and floral transition [454, 455]. TCP proteins TCP7/14/15/23 are involved in perceiving endogenous signals (circadian clock, plant hormones) and environmental (pathogens, light, nutrients), forming an interface between environmental cues and plant growth [456-458]. Moreover, proteins like BBX18 regulate seedling photo-

morphogenesis by preventing hypocotyl inhibition [459], ALTERNATIVE OXIDASE 1A (AOX1A) protecting against oxidative damage by intense light [460], BCS1 and CYTC-2 forming the mitochondrial electron transport chain, were also included.

5.3.1.4 Interaction with metabolism-associated and signaling proteins

Metabolic enzymes such as CINNAMOYL COA REDUCTASE (CCR), CINNAMYL-ALCOHOL DEHYDROGENASE (CCD), FRK1, and BAM1 synthesizing structural components (cellulose, starch, and lignin), ARABINOGALACTAN POLYSACCHARIDES 1 (AGP1), and GAT6 synthesizing arabinogalactan polysaccharides essential for foliage growth were also found in the interactome [461, 462]. ADENOSINE 5'-PHOSPHOSULFATE REDUCTASE (APR3) and serine acetyltransferase (SAT1) catalyzing sulfur assimilation in cysteine and methionine, THIAMINE PYROPHOSPHATE KINASE 1 (TPK1) kinase controlling TPP activity required for fuelling photosynthesis and cellular metabolism [463], DEHYDROASCORBATE REDUCTASE (DHAR2) involved in ascorbate recycling to maintain redox homeostasis [464], PAP1, ADT4, and ADT5 regulating anthocyanin production and radical scavenging, GLUTATHIONE S-TRANSFERASES (GSTs) mediating cellular detoxification and stress tolerance through flavonoid metabolism [465], and PHL2 mediating phosphate starvation comprising the network, indicated cross-talk between growth and stress signaling [466]. Transporters regulating nucleotide, folate, carnitine, and other solute transport [467, 468], and calcium signaling proteins (CBL1, CPK32, CML37), and other signal transducers like MAPKKK14/18, PERK9, LYK5 linked the interactome nodes [469].

Table 5.2 Upstream regulators of VuNAC1/2 TFs predicted by RnR database

Gene ID	Gene ID	P.R. Score	Function
COBRA	At5g60920	99.4	necessary for oriented cell expansion
MYB103	At1g63910	99.2	involved in tapetum development and exine formation in anthers
MYB28	At5g61420	98.7	major regulator glucosinolate biosynthesis protects against insects
PISTILLATA	At5g20240	98.4	required for petals and stamen development
ANAC025	At1g61110	98.3	anther, pollen and seed development
HsFA2	At2g26150	98.2	heat-stress recovery
PHL1	At5g29000	98.2	involved phosphate starvation response;
RGA1	At2g01570	97.8	represses GA-induced vegetative growth and floral initiation
MYB48	At3g46130	97.8	regulate flavonol biosynthesis primarily in cotyledons
DIV2	At5g04760	96.7	negatively regulates salt response
RRTF1	At4g34410	100	regulates redox homeostasis
SAP6	At3g52800	99.4	stress response
ATHB-8	At4g32880	99.2	involved in the regulation of vascular development
ATMYB21	At3g27810	99.1	involved in photomorphogenesis in the light
HRS1	At1g13300	97.3	nitrate and phosphate starvation responses and adaptation of root architecture
CYP79B2	At4g39950	99.5	a precursor for tryptophan-derived glucosinolates and indole-3-acetic acid (IAA)

Source: http://webs2.kazusa.or.jp/kagiana/rnr0912/indexff.html

Table 5.3 List of orthologous proteins in the putative VuNAC1/2 interactome

	Gene ID	Description	Supportability	Rank	Function
Hormone	**AFP1**	ABI five binding protein	3	7.1	ABA signaling
	HAB1	HYPERSENSITIVE TO ABA1	2	5.6	ABA signaling [470]
	PP2CG1	Protein phosphatase 2C family protein	1	5.5	ABA signalling [440]
	ABI2	Protein phosphatase 2C family protein	2	5	ABA signaling
	HAI1	PP2C protein (Clade A protein phosphatases type 2C)	3	6.4	ABA signaling [471]
	MAPKKK18	mitogen-activated protein kinase kinase kinase 18	1	6	ABA signaling
	IAGLU	indole-3-acetate beta-D-glucosyltransferase	2	5.4	Auxin metabolism
	SAUR-like	SAUR-like auxin-responsive protein family	1	5.2	Auxin signaling
	ZIFL1	zinc induced facilitator-like 1	2	5.8	Auxin signaling [441]
	ACS6	1-aminocyclopropane-1-carboxylic acid (acc) synthase 6	3	5	Ethylene biosynthesis [472]
	RAP2-13	Integrase-type DNA-binding superfamily protein	1	5.7	Ethylene biosynthesis [472]
	ERF1	ethylene-responsive element binding factor 1	3	8.1	Ethylene signaling [442]
	JAZ1	jasmonate-zim-domain protein 1	3	5	JA signalling
Abiotic Stress	**MYB74**	myb domain protein 74	0	6.7	Salt stress response [443]
	STZ	salt tolerance zinc finger	3	5.6	Salt stress response
	SZF1	salt-inducible zinc finger 1	3	5.3	Salt stress response
	CZF1	zinc finger (CCCH-type) family protein	3	8	Salt stress response
	TSPO	TSPO (outer membrane tryptophan-rich sensory protein)-like protein	3	5.5	Salt stress response [444]
	GBF3	G-box binding factor 3	2	5.7	Drought response
	RDUF1	zinc finger (C3HC4-type RING finger) family protein	3	5.9	Drought response
	LEA4-5	Late Embryogenesis Abundant 4-5	3	5.8	Desiccation
	BZIP60	basic region/leucine zipper motif 60	3	6	ER stress
	NAC062	NAC domain containing protein 62	3	7.7	ER Stress tolerance [446]
	HSFB2A	heat shock transcription factor B2A	3	6	Heat stress
	RHL41	C2H2-type zinc finger family protein	3	6	Light stress
	DJ1A	Class I glutamine amidotransferase-like superfamily protein	3	6	Oxidative stress [447]
	PMSR1	peptidemethionine sulfoxide reductase 1	1	5	Oxidative stress
	OPR2	12-oxophytodienoate reductase 2	2	5.1	Detoxification
	MKK9	MAP kinase kinase 9	3	5	Senescence [449]
	AT2G28400	senescence regulator (Protein of unknown function: DUF584)	2	5.4	Senescence
	SAP9	A20/AN1-like zinc finger family protein	1	6.1	Stress response
	DREB2A	DRE-binding protein 2A	0	5.9	Stress response
	UGT73B3	UDP-glucosyl transferase 73B3	3	5.5	Stress response
	AGC2-1	AGC (cAMP-dependent: cGMP-dependent and protein kinase C) kinase family protein	3	5.6	Stress signaling
	S6K2	serine/threonine protein kinase 2	0	5.3	Stress signaling
	CAD1	MAC/Perforin domain-containing protein	3	5.1	PCD
Biotic Stress	**BAP1**	BON association protein 1	2	5.7	Defense signaling
	EXO70B1	exocyst subunit exo70 family protein B1	3	5.4	Defense signaling
	NHL3	NDR1/HIN1-like 3	3	5.2	Defense signaling
	NPR3	NPR1-like protein 3	2	5.8	Defense signaling
	TIP	TCV-interacting protein	3	5.3	Defense signaling
	RIPK	Protein kinase superfamily protein	3	5.1	Disease resistance
	AT5G54165	Avr9/Cf-9 rapidly elicited protein	2	5.2	Pathogen resistance
	WRKY33	WRKY DNA-binding protein 33	3	6.5	Pathogen resistance
	WRKY40	WRKY DNA-binding protein 40	3	6.3	Pathogen resistance
Growth & Development	**ZAT6**	C2H2-type zinc finger family protein	3	5	Phospahte homeostasis [452]
	OCT5	organic cation/carnitine transporter5	0	5	Lateral root development [467]
	ZF2	zinc-finger protein 2	3	5.8	Flower abscission
	CYP81D8	cytochrome P450: family 81: subfamily D: polypeptide 8	2	5.1	Photosynthesis
	BCS1	cytochrome BC1 synthesis	3	5.7	Photosynthesis
	CNI1	carbon/nitrogen insensitive 1	3	5	C/N tolerance [451]
	VQ22	VQ motif-containing protein	2	7.2	Growth regulator
	TET8	tetraspanin8	3	5.5	Cell differentiation
Metabolism	**ADC2**	arginine decarboxylase 2	1	5.8	Arginine metabolism
	SUS3	sucrose synthase 3	3	5	Sugar Metabolism
	BAM1	beta-amylase 1	2	6.5	Sugar Metabolism
	BGLU11	beta glucosidase 11	2	5.6	Sugar Metabolism
	GPX2	glutathione peroxidase 2	1	5.2	Glutathione metabolism
	FC1	ferrochelatase 1	3	5.5	Heme biosynthesis

	GATL10	galacturonosyltransferase-like 10	3	5	Pectin metabolism
	GSTU24	glutathione S-transferase TAU 24	3	7	Reseveratrol metabolism
	CGS1	CDP-diacylglycerol-glycerol-3-phosphate 3-phosphatidyltransferase	3	5.6	Phospholipid metabolism
	GLTP	Glycolipid transfer protein (GLTP) family protein	3	5.7	Lipid transfer

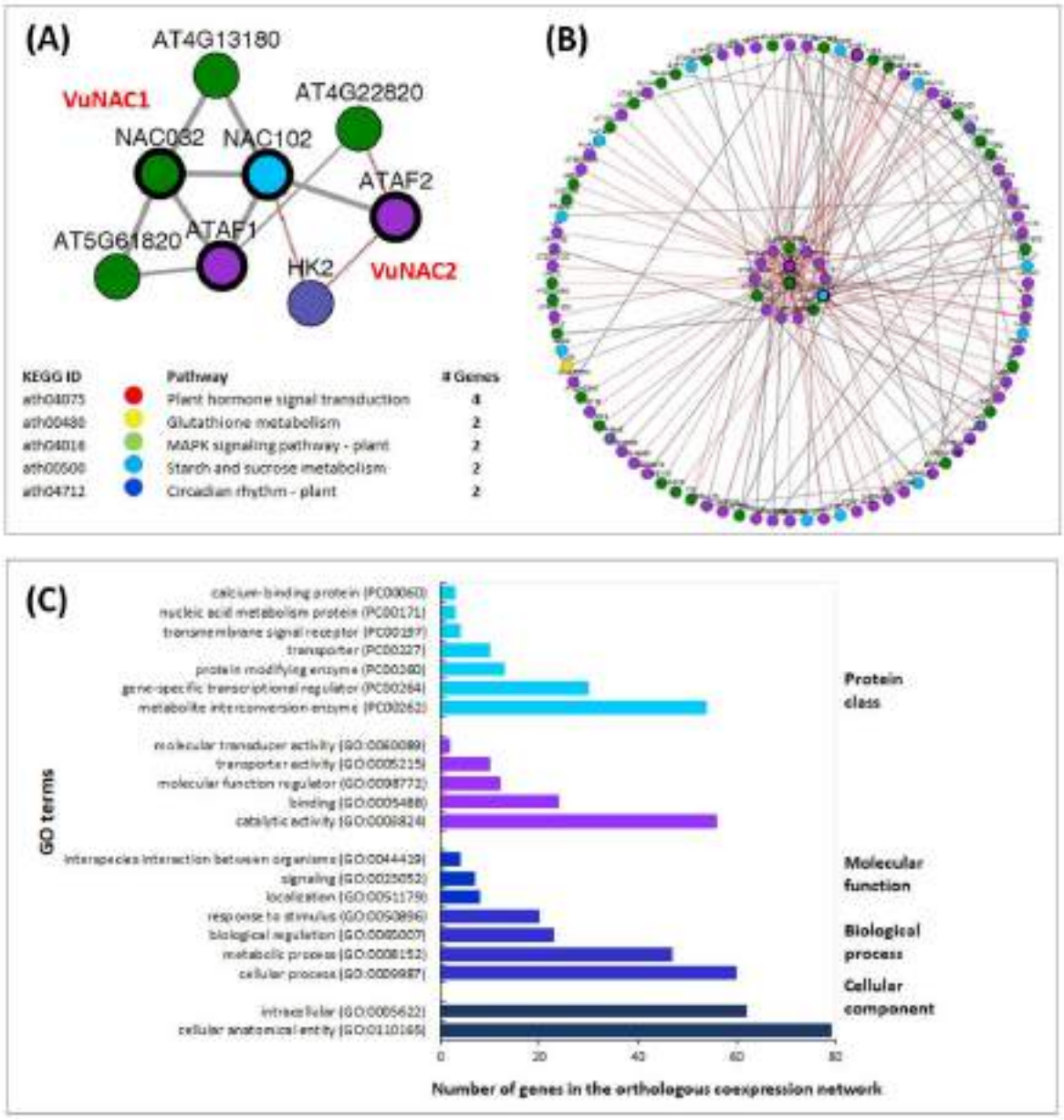

Fig. 5.11. Proposed regulatory network (A) The orthologous (ATAF-subgroup network). **(B)** The interactome of co-expressing genes (connected by grey lines) and protein-protein interactions (connected by red lines), predicted the regulon for VuNAC1 and VuNAC2 (C) The gene ontology (GO) analysis of the network annotated the cellular, molecular and biological function associated with VuNAC1/2 TFs.

5.4 DISCUSSION

Several NAC TFs, such as ATAF in Arabidopsis and their orthologs in rice, soybean, *etc.*, are induced by diverse stress-related signals and improve crop stress tolerance [27, 30, 33]. However, the constitutive overexpression of critical stress-regulating NAC proteins compromised the plant growth due to perturbations in an intertwined hormonal signaling or metabolic rerouting to affect beneficial growth processes [27, 30, 473, 474]. Our study of untapped cowpea ATAF orthologs (VuNAC1 and VuNAC2), cloned from a drought-resilience genotype (*Kannanado White*), showed that their ectopic expression in Arabidopsis (governed by 35S CaMV promoter), conferred drought and salt tolerance, with simultaneous improvement of rosette growth and seed-yield, under both normal and nutrition-deficit conditions (Table 5.1). Hence, constitutive overexpression of functional ATAF orthologs from cowpea conferred multiple stress tolerance harmonized with plant growth, overcoming the growth aberrations, unlike their orthologs in Arabidopsis and rice. Thus, these unique and multifaceted NAC genes could be promising biotechnological tools for the sustainable engineering of stress tolerance in crops.

5.4.1 The VuNAC1/2 TFs improved stress tolerance without growth trade-off by modulating photosynthetic activity and sugar metabolism

Cowpea ATAF orthologs converge multiple stress responses and growth signaling. Both *VuNAC1* and *VuNAC2* genes were inducible by various abiotic stimuli, including dehydration, salinity, osmotic stress, ABA, showing persistent expression characteristics similar to *ATAF1*. Moreover, these cowpea TFs were also induced by aluminum and light (Fig. 4.2). Their ectopic overexpression in Arabidopsis conferred tolerance to drought, salinity, aluminum, cadmium, and H_2O_2 stress (Fig. 5.7, Fig. 5.8, and Fig. 5.8). In fact, it also improved embryonic, rosette, and inflorescence growth resulting in enhanced seed yield in Arabidopsis (Fig. 5.2, Fig. 5.3, and Table 5.1). These overexpression characteristics suggested that VuNAC1/2 TFs might be involved in the central transcriptional tuning of the growth-controlling entities in the transgenic lines influencing cell proliferation, developmental fates, and floral transition, besides the stress machinery, to secure the tolerance/growth trade-off (Table 5.32 and Fig. 5.11). The concomitant increase in photosynthetic activity, stomatal abundance, and ABA insensitivity, seemed to play a pivotal part in the stress tolerance without growth-inhibiting (Fig. 5.5, Fig. 5.10 and Fig. 5.6).

Previous studies reported that ATAF1 coupled stress-signaling with photosynthesis-related transcriptional cascades, executing repression of the *GLK* genes required for chloroplast development resulting in photosynthetic suppression [57]. Unlike ATAF1, the overexpression of VuNAC1/2 increased rosette size and boosted photosynthetic activity (Fig. 5.3, Fig. 5.4, and Fig. 7). This suggested that the *VuNAC1/2* lack the ability to suppress photosynthesis-associated genes (PAGs), like ATAF1. The concomitant improved photosynthetic activity might support the energy requirements due to efficient sequestration of photosynthates such as sucrose even when no exogenous carbon (Fig. 5.2 and Fig. 5.4). In addition, VuNAC1/2 overexpression yielded an enhanced stomatal density in Arabidopsis (Fig. 5.10), one of the possible factors resulting in increased photosynthetic activity and biomass growth [425]. The TFs may be rather involved in activating genes that control the stomatal development, unlike the *ZmNAC49*, which repressed *ZmMUTE*, *ZmSDD1*, *ZmFAMA*, *etc*., leading to reduced stomatal density in maize [426]. Also, some unknown mechanisms, like the ABA-dependent reduction of stomatal density in *VvNAC17* overexpressing in grapevine, can be involved [427]. Further studies are needed to investigate the role of VuNAC1/2 in controlling photosynthesis and stomatal development. Moreover, the VuNAC1/2 overexpression did not exert carbon starvation and ABA hypersensitivity phenotypes, like ATAF1 [405]. Instead, the transgenic plants exhibited tolerance to nutrition starvation imposed at seedling and mature stages (Fig. 5.2 and Fig. 5.4A). In contrast, the transgenic seedlings showed insensitivity to ABA-induced seed dormancy and post-embryonic growth inhibition due to ABA, NaCl, and PEG-induced stress (Fig. 5.8). In our earlier studies in yeast, we have found that *VuNAC1/2* triggered the biosynthesis of ATP, vitamin B complex, methionine, and glucose metabolism (Fig. 4.10) [372]. Similarly, this study in Arabidopsis indicated that the nutrition sufficiency of the transgenic plants could possibly be due to improved uptake of phosphate and nitrogen [133], *via* regulation by *PHL1* and *HRS1* implied by the predicted regulators and promoter elements (Table 5.2 and Table 4.1). Taken together, our study indicated that VuNAC1/2 also plays a crucial role in boosting growth and nutrition assimilation, besides improving stress tolerance and recovery, unlike other ATAF1 orthologs. One of the major factors accounting for this dissimilar behavior could be the different regulatory domains present in the VuNAC1/2 protein.

The conserved N-terminal domains of VuNAC1/2 TF hold significant similarity with Arabidopsis ATAF1 (≥ 85%), implying similar target gene sets. But the mode of transcriptional tuning (activation/repression) and functional versatility also depend on the transcriptional regulatory regions (TRR) residing in the divergent C-terminal regions. The uniqueness of the

C-terminal regions of VuNAC1/2 TFs (~30% protein length) may be responsible for the indifferent behavior from their orthologous counterparts through dissimilar protein interactions. Besides, the over-representation of both ABA-responsive elements (ABRE) as well as ACGTATERD1, DRECRTCOREAT, and CBFHV in the promoters indicated both ABA-dependent and/or ABA-independent modes of regulation of the VuNAC1/2 TFs. The mixed ABA signaling can be responsible for the pleiotropic responses in the transgenic lines due to execution of ABA-dependent stress tolerance cross-talking with ABA-independent growth functions, counteracting growth penalty, despite constitution expression throughout different developmental stages [475].

5.4.2 The multifaceted VuNAC1/2 TFs are associated with a network of proteins regulating stress responses, hormonal flux, and growth signals

The functional versatility of NAC genes is accounted by the tight regulation at the transcriptional, post-transcriptional, and post-translational levels. Their specificity can be determined by the set of target genes recruited by the TFs and their coordinating partners, melding disparate biological processes at different developmental stages. Our study of co-expressed protein networks and upstream regulators suggested that the *VuNAC1/2* genes might be induced and regulated by stress, nutritional and metabolic signals in a feedback loop. Combining our findings, several modes of VuNAC regulation can be proposed (i) key stress-regulating transcription factors, (ii) ABA, auxin, and ethylene signal and homeostasis, (iii) cellular metabolism, (iv) stress stimuli, and (v) developmental signals. Thus, the plant responses can be dissected into disparate regulatory networks involving NAC TFs as central signaling molecules.

We found a cluster of TFs belonging to the NAC family and other stress-responsive groups (DREB, ERF, TCP, and WRKY), co-expressing with ATAF-subgroup (ATAF1/2, ANAC032, and ANAC102), probably involved in the co-binding to the target gene promoter. Their interaction may amalgamate diverse processes such as ethylene biosynthesis (NAC047), ABA-mediated drought response (RD26), ethylene, auxin and salt response (MYB74), cold (DREB2A), lateral root formation (NAC2), leaf senescence (NAP), ER stress response (NAC062). Multiple hormones signaling and their metabolism (ABA, ethylene, auxin, and GA) seemed intertwined with VuNAC signaling *via* various proteins PP2Cs, ABIs, HAB1, Aux/IAA, ERFs, and RGA1. Primary metabolites such as carbohydrates (glucose, sucrose, trehalose) and lipid, nitrate and phosphate, also seemed to undergo regulation *via* proteins like

CNI1, ADC2, SUS3, TPPG, *etc*., signaling C/N balance signal, carbon starvation, and nitrogen assimilation. The proposed upstream regulatory TFs also indicated signaling of VuNAC1/2 TF perceived by proteins like HSFA2 (heat-response), RRTF1 (oxidative stress response), COBRA (cell-expansion), MYB21 (photo-morphogenesis), ANAC025 (pollen and seed development), and flower development (PISTILLATA) (Table 5.2).

The interactome and regulator prediction stipulated the coordinated changes in the stress response, metabolic and hormone signaling underlying seed germination, seed establishment, vegetative and reproductive growth in the transgenic Arabidopsis plants. As indicated by the interactome analysis, the VuNAC1/2 TFs may interact with proteins like ABI1/2, HAB1, and PP2C49, negatively regulating the ABA signaling, UGT74E2, and Gh3.15, controlling the auxin flux, and ZAT6 regulating seed germination under stress [439, 470]. Moreover, the SnRK kinases triggering the carbon starvation response seemed to be attenuated by trehalose signaling *via* TPPG. After germination, the successful seedling establishment depends on the transition to autotrophic nutrition assimilation, from the heterotrophic acquire from the seed reserve. Proteins like Carbon/Nitrogen Insensitive 1 (CNI1/ATL31) ligase controlling the post-germination nutrient-signal transduction may be associated with VuNAC signaling.

Later, several proteins promoting biogenesis of structural components and cell division, such as FORMIN7, PLIM2a, GAT6, AGP1, TET8, *etc*., and TFs like TCP, ERF11, and ZAT6 tuning hormonal responses, may involve. Photoreceptors perceiving light can also indirectly contribute to growth by regulating metabolic programs *via* stem elongation, leaf expansion, seed germination, flower initiation, chloroplast development, endogenous hormone levels, and transport. Co-expressed proteins like FC1, BCS1, CYTC-2, and AOX1A regulating heme-biosynthesis, electron transfer, and photo-damage control might improve photosynthetic efficiency through better light perception by the transgenic plants. VuNAC1/2 TFs may also regulate shade tolerance under low-light conditions *via* BBX18 and AtMYB21. The co-expression studies implied VuNAC1/2 interaction with enzymes catalyzing the synthesis of cell-wall polysaccharides and energy generation through glycolysis, FA oxidation, and cofactor biosynthesis. APR3 and SAT1 regulating the synthesis of cysteine and PHL2 might improve sulfur and phosphate assimilation in transgenic plants. The transgenic tissues accumulated proline, glutathione, and ascorbate, even under normal conditions, indicating direct regulation of proline, glutathione, and ascorbate metabolism *via* VuNAC1/2 TFs. The coexpression network suggested DHAR2 and GSTs enzymes involved in ascorbate recycling and

detoxification and PAP1, ADT4, and ADT5 regulating anthocyanin production and MATE transporters [450, 464, 465].

In conclusion, our study indicated that VuNAC1/2 TFs regulate stress responses, hormonal and nutritional homeostasis, and plant development through cross-talk of photosynthesis, carbon metabolism, and ABA signaling. However, the detailed model for VuNAC1/2 regulation is still unknown. Genes like *VuNAC1/2* that confer tolerance to multiple abiotic stresses and ameliorate the shrinking vegetative growth and reproductive yield should be used for sustainable drought and salinity tolerance in cash crops to accomplish dual objectives, *i.e.*, multi-stress resilience and yield improvement. They might also play a crucial role in protection against pH-dependent phytotoxicity of aluminum and other toxic metals, which are significant constraints for root development in acidic soil [131]. As the unfavorable climatic conditions are becoming persistent, ubiquitous and constitutive expression of unique VuNAC1/2 TFs may avoid the trade-off and secure yield potential of crops. Further understanding of the underlying molecular mechanisms can bring new insights to harmonized cross-talk between stress adaptation and growth. The functional role of these TFs in native Cowpea species and related legume crops needs to be explored.

Chapter 5

CHAPTER 5

6. IMPROVING AGRONOMIC TRAITS AND STRESS RESPONSE IN COWPEA BY VUNAC1/2-OVEREXPRESSION

The functional conservation and gene targets of NAC transcription factors (TFs) are unpredictable in non-native species, hence orthologous stress-regulating genes are not suitable for legume genetic engineering. The drought and heat tolerance of the non-commercial cowpea germplasms makes it exemplary to explore native NAC-signaling attributes to blend with the agronomic traits of cultivated varieties. Overexpression of *VuNAC1* and *VuNAC2*, cloned from a drought-hardy genotype, improved growth, yield, and tolerance to multiple yield-declining abiotic stresses in an edible variety. The gain-of-function manifested improved seedling development, richer shoot biomass with bigger leaves, thicker stem, and denser root system rich in nodules. The transgenic plants produced more pods (~2-fold and ~1.4-fold) with increased seed weight (10.3% and 6.0%), accompanied by improved photosynthetic activity and stomatal density, whereas loss-of-function severely retarded growth and impaired flower initiation. In addition, the transgenic lines showed remarkable recovery from persistent drought, salinity, heat, cold, and nutritional stresses and restored their reproductive development through improved CO_2 exchange, membrane-integrity, water status, Na^+/K^+ ion-homeostasis, and reducing power. The transcriptome analysis indicated activating a large set of chloroplastic and chromosomal genes forming photosynthetic components, stress-regulating machinery, carbohydrate metabolism, nutrient-uptake, meristem-initiation, cell-wall biogenesis, ABA, and auxin signaling, indicating consolidation of diverse plant processes. Unlike their orthologs, bifunctional VuNAC1/2 TFs mediate favorable transcriptional crosstalk to regulate multiple stress-tolerance and beneficial agronomic traits without yield trade-off, hence useful biotechnological tool for legume improvement.

Keywords: Cowpea NAC, growth trade-off, multiple stress-tolerance, photosynthesis, yield

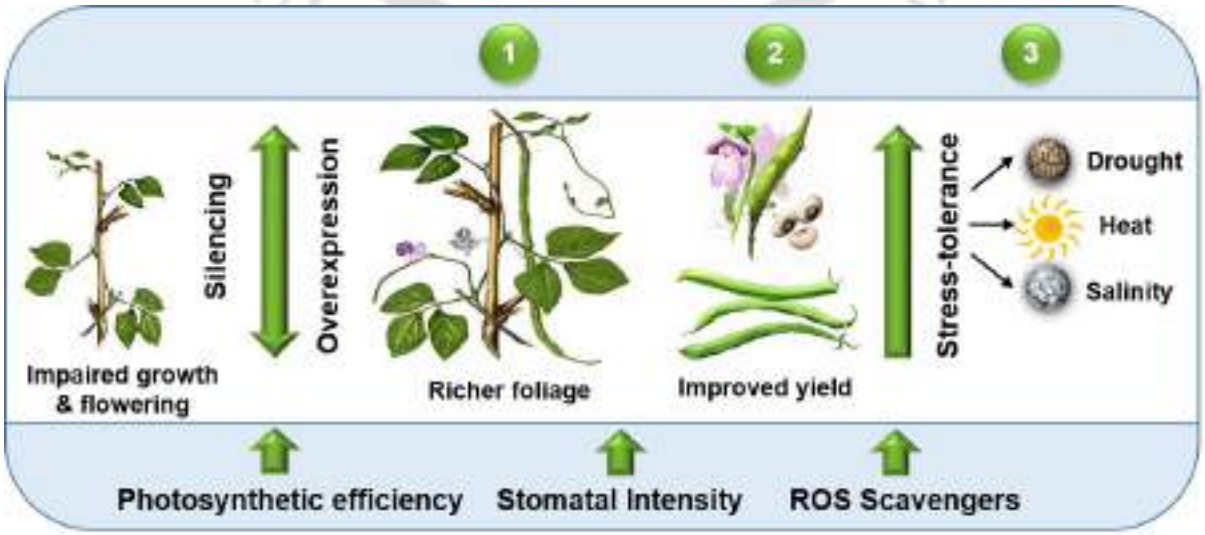

6.1 INTRODUCTION

Cowpea (*Vigna unguiculata* (L.) Walp.) is an annual food legume indigenous to Sub Saharan Africa, also cultivated and consumed worldwide in Asia, Southern Europe, Central, and South America, Middle East, and the United States, and consumed as pulse seed, vegetable, fodder, and green manure, reflecting its desirability [3]. In addition, it is grown as a niche crop to replenish soil nitrogen between wheat-rice rotations, owing to its nitrogen fixation, short life-cycle, and shade tolerance [476]. Moreover, it is usually grown in nutrient-poor soil, mainly under non-irrigated conditions. Cowpea grains, as well as foliage, are rich in nutritional values, holding immense health benefits. Mature grain may contain 23-32% protein, serving as a source of cheap and quality protein (23-32%) for both rural and urban dwellers. It is also rich in 50-60% starch, vitamin B such as folic acid, essential amino acids like lysine and tryptophan, phenolic compounds, and essential micronutrients such as iron, calcium, and zinc, starch but less fat content (1%) [38]. Thus, emerging as the 21st-century legume, cowpea offers immense opportunities for socio-economic, agricultural, and environmental improvement complying with sustainability principles [41].

Although cowpea is ideal for dryland agriculture under high temperatures, its yield can be susceptible to climatic challenges. Many early-maturing cultivars with a growth cycle of only 60-80 days are suitable for escaping the seasonal drought but unable to deliver the genetic yield potential. Several varieties are drought-tolerant if exposed for a short duration. However, the seed yield is greatly compromised by terminal drought, causing water deficiency prior to and during the anthesis period [18, 256]. Salt sensitivity in cowpea is also dependent on the growth stage. Pod-filling and seed yield reduced most significantly when the stress was inflicted in the vegetative stage [257]. Cowpea can take the heat, but night temperatures around 35°C or higher lead to pollen sterility, flower abortion, preventing pod formation [258]. Soils deficient in phosphorous, an element required for nitrogen- fixation, further lower the productivity [250]. Drought, heat, and salinity are the major production constraints declining the cowpea yield more than all the pathogens combined. Apart from stress tolerance, there are several morphological and agronomic traits of interest regarding improvement for cowpea, such as forage growth, pod yield, seed weight, seed size, and maturity period [305]. Plants with erect growth and having more canopy height may effectively suppress weeds and improve light harvest for photosynthesis rather than semi-prostate habit [306]. High branching and foliage biomass may translate into a high seed yield [307]. Further, boosting phosphorus and iron assimilation or biosynthesis can fortify nutritional qualities other than the protein content and

prevent Iron Deficiency Chlorosis (IDC) in cowpea. Thus we need a unified mechanism to improve stress tolerance and agronomic traits of cowpea.

The available stress-tolerance measures do not maintain yield under extreme, composite, and sequential field stress, especially during reproductive development, which is the desired definition of stress tolerance in food legumes like cowpea. Under an aggravated unfavorable environment, tolerance to stress is generally associated with the arrest of growth and photosynthesis, pollen sterility, and aborted seed development to conserve energy, which may never recover [259]. Hence, stress adaptation does not necessarily resonate with productivity. The key to sustainable stress tolerance by overcoming the tolerance/growth trade-off lies in the genetic diversity of the traditional varieties inhabiting harsh geography. Some wild genotypes can thrive in the drier habitats receiving annual rainfall of even less than 300 mm, and tolerate much hotter temperatures than maize [40]. Genes involved in growth and yield sustenance in adverse conditions are usually not present in the farmed cultivars owing to their loss during domestication, germplasm improvement, and linkage drag when produced in optimal environments. Thus efforts are being made to make the hardy crop even tougher to deliver better yield under harsh conditions by unifying the heat and drought tolerant attributes of wild relatives with the agronomic traits of cultivated genotypes. In addition, the degree of the stress damage and the plant's ability to cope, adapt, and recover depends on the plant growth stages and fitness. Boosting growth-based traits such as forage growth, vigor, biomass, and water-use efficiency, together with multiple stress-tolerance, can yield higher.

The last ten years have been a resurgence discovering more than 50 stress-responsive transcription factor (TF) families in plants [52]. NAC (NAM/ATAF1/2/CUC2) family have been reported as central transcriptional regulators orchestrating cascades of gene regulatory networks involved in growth, development, and complex stress signaling, claimed as ideal candidates for genetic manipulation to acquire food security [26, 53, 102]. Many NAC members have been studied for stress responses, such as drought [31, 123, 124], salinity [28, 125], cold [126], heat [127], oxidative stress [128], water-logging [129], boron deficiency [132], high light, phosphate deprivation [133, 134]. Moreover, a single NAC TF can serve multiple conglomerate processes. For instance, ATAF1, a *bona fide* regulator of both abiotic and pathogen stress, also controls chloroplast maintenance, senescence cascades, ABA biosynthesis, and plant development mediated by *SnRK1* signaling [27, 28, 56, 57]. Similarly, a rice NAC *Os04g0477300*, regulates three different processes biotic stress, senescence, and

phosphate and boron deficiency [132, 133]. NAC TF can mediate the cross-talk between different signaling pathways such as abiotic and biotic stress response, senescence, and developmental programs. Despite a crucial role in stress response, the orthologous candidates are not suitable for cowpea genetic engineering, as the behavior of non-conserved C-terminal protein region and the set of target genes is difficult to anticipate in non-native species. To date, no NAC gene has been studied in cowpea. Mining suitable NAC genes from a robust cowpea genotype and deciphering the underlying molecular targets are indispensable for the genetic improvement of cowpea and related legumes.

This chapter characterized two unique cowpea NAC transcription factors (VuNAC1 and VuNAC2), isolated from a drought-hardy genotype to improve tolerance to multiple stresses such as drought, salt, heat, and cold tolerance with a concomitant increase in vegetative growth and reproductive yield in a commercial cowpea variety, by activating stress signaling, growth, and photosynthetic activity without any trade-off in yield. In countries like India, where the diet habits are cereal-centric to satisfy calorie intake, a slight increase in cowpea yield can improve protein nourishment to benefit millions of people. Our findings can address the challenges in cowpea production by improving abiotic stress tolerance and agronomic traits simultaneously through a unified single-gene mechanism.

6.2 METHODOLOGY

6.2.1 Construct preparation

The 888 bp open reading frames (ORF) sequences were cloned at the *Sfi*I site in the pBEAB vector (provided from Gifu University, Japan) to generate the 35S:VuNAC1 and 35S:VuNAC2 constructs for overexpression (Fig. A4.1, Appendix)[372]. The VuNAC1/2-si constructs were prepared by cloning the 300 bp non-conserved gene region from the 3'-end were cloned at the *BamH*1 and *Kpn*I sites in the pTRV2 vector (provided from NIPGR, India) for VIGS-based silencing (Fig. A4.1, Appendix 4). All the constructs were mobilized in the EHA105 Agrobacterium strain. The primers used were listed in Table A4.2, Appendix 4.

6.2.2 Genetic transformation

The healthy cowpea seeds of Pusa komal variety were sterilized in 0.2% $HgCl_2$ (w/v) for 2 mins, followed by washing with deionized water (5X, 2 minutes each). After blot drying, the seeds were transferred to germination medium (1X MSB_5 basal salt, 0.8 % Agar, 10.0 µM Thidiazuron, pH 5.8) and incubated at 27˚C in the dark for two days, followed by long-day

photoperiod condition (*16 hr* of light, 8 hr of *dark)* at 28°C, with white light illumination (110 µmol photons $m^{-2}s^{-1}$). 1-cm sections of cotyledonary nodes were excised from the four-day-old seedlings and dipped in LPGM medium (1X MSB_5 basal salt, 1.0 µM BAP, 3% (w/v) sucrose, pH 5.5). The explants were injured at the node and dipped in the Agrobacterium strains carrying the 35S:VuNAC1/2 constructs (pre-cultured in AB minimal media + 50 µg/ml Kanamycin until the $O.D._{600}$ reaches up to 0.6) suspended in co-cultivation media (LPGM, with freshly added 100 µM Acetosyringone). The explants were infected with the empty vector carrying strains to generate wild type control plants, whereas explants without the infection served as a negative transformation control. The co-cultivation suspensions were shaken at 90 rpm for 30 minutes at 22˚C, blot dried, and co-cultivated further at 22˚C under dark conditions on Whatman paper soaked with the co-cultivation medium. After three days, the explants were washed in 500 mg/l Cefatoxime for 10 minutes, followed by washing in de-ionized water (5X, 2 minutes each). After trimming, the explants were cultured in shoot induction media (1X MSB_5 basal salt, 0.8% Agar, 5.0 µM BAP, 0.5 µM Kinetin, 200 µg/ml Kanamycin, 500 µg/ml Cefatoxime, pH 5.8), at 27˚C for seven days. The regenerated explants were sub-cultured in shoot elongation media (1X MSB_5 basal salt, 0.8 % Agar, 2.5 µM BAP, 0.1 µM Kinetin, 200 µg/ml Kanamycin, 500 µg/ml Cefatoxime, pH 5.8) for 15 days. The elongated shoots were transferred to the rooting medium (0.5 X MSB_5 basal salt, 0.7 % Agar, 5.0 µM IBA, 500 µg/ml Cefatoxime, pH 5.7) and cultured until root induction. The seedlings were hardened in soilrite mix supplemented with ¼ MS medium for ten days and then grown in potting soil mixture in greenhouse conditions (*photoperiod* of *16/*8 hr of *light/dark*, white light illumination of 110 µmol/$m^{-2}s^{-1}$, maintained at 28 °C).

6.2.3 VIGS assay

The EHA105 Agrobacterium strain harboring pTRV1, pTRV2, pTRV2-VuNAC1-si, and pTRV2-VuNAC2-si were grown in LB media containing 50 µg/ml Kanamycin and 25 µg/ml Rifampicin up to OD_{600}=1.0. Equal volumes of cultures carrying pTRV1 and pTRV2 or its derivatives were mixed. The cells were harvested (3,000 x g for 5 min) and suspended in the agro-infiltration buffer (10 mM $MgCl_2$, 10.0 mM MES-KOH, pH 5.6, and 100 µM Acetosyringone) and kept at RT for 4 hours. The sterilized cowpea seeds were imbibed in LPGM media for 24 hours in the dark to initiate sprouting. The healthy sprouts were co-cultivated with the pTRV1 and pTRV2 constructs by immersing in 10 ml of the agro-infiltration buffer and kept for shaking (150 rpm for 1 hour, 22 °C). The sprouts treated with empty pTRV1 and pTRV2 constructs served as wild type control plants. After soaking dry, the

sprouts were further co-cultivated at 22°C for 36 hrs in the dark and then cultured at 27°C with a 16/8 light/dark photoperiod. The germinated seedlings were then transferred to the soil pots and grown under greenhouse conditions.

6.2.4 Growth conditions for stress analysis

6.2.4.1 Seedling-stage study in hydroponic culture

Healthy seeds of wild type control and T_2 generation transgenic lines were germinated for two days in the dark followed by 16/8 light/dark photoperiod conditions at 28°C. The four-day-old seedlings were grown in a gauzed hydroponics container supplied with ½ X modified Hoagland hydroponics media for approximately ten days until the first trifoliate leaves expanded [333]. The media was supplemented with 20% PEG 6000 (polyethylene glycol) and 200 mM NaCl to impose dehydration and salt stress. The trifoliate leaves from the stressed and the control plants were sampled at the indicated time intervals for RNA extraction using the RNeasy mini kit (Qiagen), followed by cDNA synthesis (Applied Biosystems, USA). The semi-quantitative and quantitative real-time PCR was performed in triplicates for each sample on Thermocycler Dice, Real-time system II (Takara, Japan). *VuUbiquitin2* was used as a reference to determine the relative expression. The experiments were repeated three times with similar outcomes. To impose nutritional deficiency, the strength of the growth media was reduced to 1/10 fold, and the seedlings were grown for four weeks by replacing the media every three days.

6.2.4.2 Greenhouse study of soil plants

Four-day-old germinated seedlings were sown in soil pots and grown under greenhouse conditions for six weeks to acquire the mid-vegetative stage. For drought assay, the water was withdrawn for six weeks, followed by re-watering for recovery. The soil was supplemented with a gradient of NaCl solution (50 mM, 100 mM, 150 mM, and 200 mM, at an interval of two days) and then kept saturated with at 200 mM NaCl aqueous solution to impose salt stress for overall four weeks. The soil was drained with tap water to leach out deposited salt and maintained under normal greenhouse conditions to recover from the high salinity. For heat and cold stress, the six-week-old plants were transferred to growth chambers maintained at max/min temperature regime of 44°C/34°C and 18°C/ 12°C, to impose heat and cold stress for four weeks, while the plants maintained 27°C/ 20°C served as unstressed control. All the plants were moved to the normal green-house temperature regime (27°C/ 20°C) for recovery.

6.2.4.3 Study under lysimeter-operated conditions

The drought assay was carried out using Drought Simulator (Spura, India) to mimic the field environment in a poly-house. A field capacity (FC) of 95% was maintained throughout the vegetative growth of the plant. The FC was ramped down to 20% over eight days and maintained to impose drought stress throughout six weeks. For recovery, the FC was reset to 95%. A real-time monitoring computational server was used to determine the amount of water supplied and evapotranspiration. However, to assess the senescence phase, the plants were grown in fields, and their phenotype and biochemical parameters such as membrane damage and chlorophyll degradation were measured.

6.2.5 Measurement of physiological parameters and biochemical assays

6.2.5.1 Determination of photosynthetic parameters, relative water content, electrolyte leakage rate, and lipid peroxidation

The experiments were performed using the similar method described in sections 5.2.4.1, 5.2.4.2, 5.2.4.3, 5.2.4.4.

6.2.5.2 Determination of chlorophyll and carotenoid content

100 mg of each tissue sample was homogenized in 2 ml of ice-cold 80 % (v/v) acetone. The extract was centrifuged (3000 rpm, 10 min), and the supernatant was collected to measure the absorbance A_{646}, A_{663}, and A_{470}. The chlorophyll and carotenoid content were estimated using the equations given by Lichtenthaler & Welburn (1983) [477]:

$$\text{Chlorophyll a } (\mu g/ml) = 12.21\ (A_{663}) - 2.81\ (A_{646})$$

$$\text{Chlorophyll b } (\mu g/ml) = 20.13\ (A_{646}) - 5.03\ (A_{663})$$

$$\text{Carotenoids x+c } (\mu g/ml) = (1000\ A_{470} - 3.27Ca - 104Cb) / 229$$

6.2.5.3 Determination of Na^+ and K^+ ion content

100 mg of oven-dried (75°C) leaf powder was digested in 1 N HCl at 90 °C water-bath for 30 minutes. The extract was cooled and centrifuged at 12000 rpm for 10 min to collect the top layer suspension. The extract was diluted 100 times using sterile de-ionized water. The ion content was estimated using Flame Photometer 128 (Systronics, India) in terms of ppm.

6.2.5.4 Histochemical Staining of H_2O_2 and O_2^- radicals

Fresh staining solutions of 1 mg/ml 3,3′-Diaminobenzidine (DAB), pH 3.8) and 0.2% (w/v) Nitrotetrazolium blue chloride (NBT) solution in 50 mM sodium phosphate buffer, pH 7.5,

were prepared to detect H_2O_2 or O_2^-, respectively. One-cm tissue sections were vacuum-infiltrated with the staining solution and left overnight at RT, wrapped in the dark. The solution was drained, and the tissue was boiled for 10 min in absolute ethanol to remove chlorophyll and immersed in 60% glycerol.

6.2.6 Visualization of stomata by FESEM

The experiment was performed using the similar method described in sections 5.2.5.

6.2.7 Transcriptome sequencing

The leaf tissues of six-week-old plants in their mid-vegetative stage were sampled from the wild type control and the T_2 generation transgenic lines for RNA isolation, followed by cDNA library preparation. The raw reads were acquired using the next-generation sequencing technique. The initial quality assessment was carried out using FastQC v0.11.7 [334]. The low-quality reads (Q<30) were trimmed out using NGSQC Toolkit v. 2.3.3 [335], followed by mapping on the cowpea reference genome downloaded from the NCBI database (BioProject ID: PRJNA381312) using HiSAT2 separately for all samples [336], followed by reconstruction of the transcriptome using StringTie [337]. The expression was measured in terms of FPKM values. The differential gene expression analysis was carried out using cuffdiff v2.2.1 [478]. The assembled transcriptome was searched against the cowpea reference proteome using diamond blastx utility. The transcripts which were failed to align were searched against the plant RefSeq protein database. The e-value cut-off for both the searches was kept as 0.00001. The obtained blast hits were then used to annotate the transcripts using the UniProt database. The transcripts were converted into the possible open reading frames (ORFs) using the 'transeq' program implemented in EMBOSS package [479], and the longest transcript was selected for the COG (Clusters of Orthologous Groups) database search [480], using eggNOG web-based API [481].

6.3 RESULTS

6.3.1 Overexpression of VuNAC1/2 TFs exhibited tolerance to salinity and hyperosmotic stress in seedlings

To study the gain-of-function phenotype, we generated more than three independent cowpea transgenic lines (L1, L2, and L3) constitutively overexpressing *VuNAC1* (VuNAC1-ox) and *VuNAC2* (VuNAC2-ox) governed by a modified CaMV 35S promoter (Fig. 6.1A). The detailed design of gene constructs in the T-DNA vector was depicted in Fig. A4.1, Appendix 4. The genomic PCR study validated the insertion of T-DNA, indicating amplification of the *VuNAC1/2* genes (Fig. 6.1B). The qRT-PCR analysis showed an increase in the VuNAC transcripts (~ 2 fold) in the transgenic lines compared to their wild type counterparts. The data for two transgenic lines was shown in Fig. 6.1C. In addition, the leaf-disc assay showed that the transgenic tissue was kanamycin-resistant, indicating the T-DNA expression, whereas the wild type tissue turned brown due to cell death (Fig. 6.1D).

To examine their dehydration and salt stress response, the transgenic seedlings were exposed to 20% PEG and 200 mM NaCl for five days (until the wild type seedlings reached their wilting point), as shown in Fig. 6.2A. The transgenic seedlings (VuNAC1/2-ox) resumed their growth after the stress conditions were withdrawn, displaying gain in fresh weight after ten days of the recovery, whereas the wild type seedlings failed to recover. Moreover, both the *VuNAC1* and *VuNAC2* genes were significantly induced in the transgenic as well as wild type seedlings under stressed conditions. However, the degree of induction was ~1.5 times higher in the transgenic seedlings (Fig. 6.2B). However, comparing the two expression patterns noted under normal (Fig. 6.1C) and stressed conditions (Fig. 6.2B), the *VuNAC* genes found to be induced (transgenic *vs.* wild type) more significantly under the stressed conditions, indicating transcriptional and/or post-transcriptional regulation of the *VuNAC1/2* transcripts by endogenous stress-responsive factors. Thus, despite constitutive expression, the activity of VuNAC TFs could be tightly modulated by the internal signals, keeping the mRNA level in check unless required by different developmental phases and environmental cues.

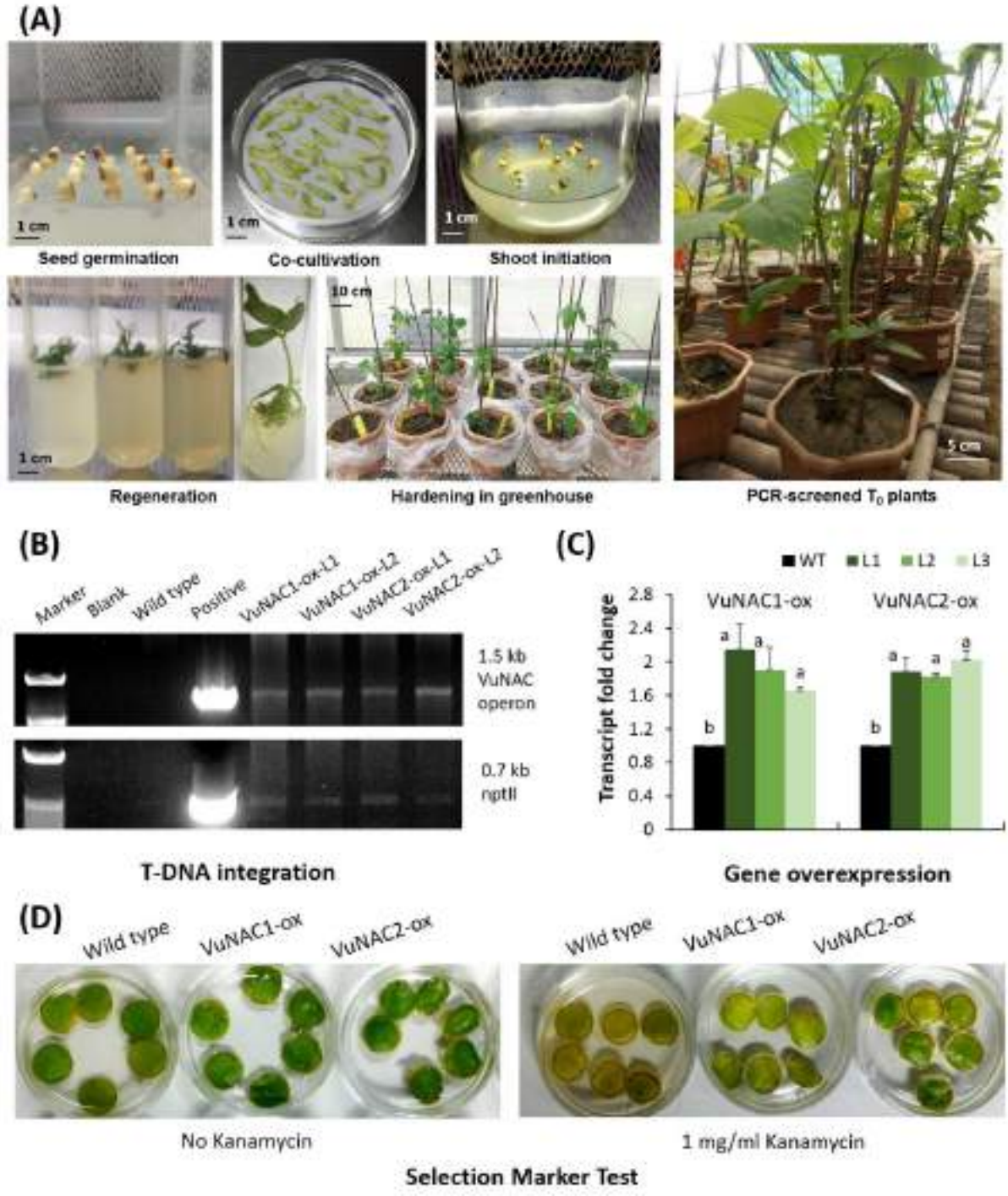

Fig. 6.1 Generation of transgenic cowpea lines overexpressing the *VuNAC1/2* genes. (A) Transformation of cowpea (Pusakomal variety) by Agrobacterium-mediated T-DNA transfer to hypocotyl explant, followed by regeneration by tissue culture and hardening of the T_0 generation plants in the greenhouse. **(B)** Schematic diagram of the T-DNA vector construct. **(C)** PCR analysis of the Agrobacterium strains used for genetic modification. **(D)** Kanamycin sensitivity assay to assess T-DNA expression. The brown leaf tissue indicates cell death.

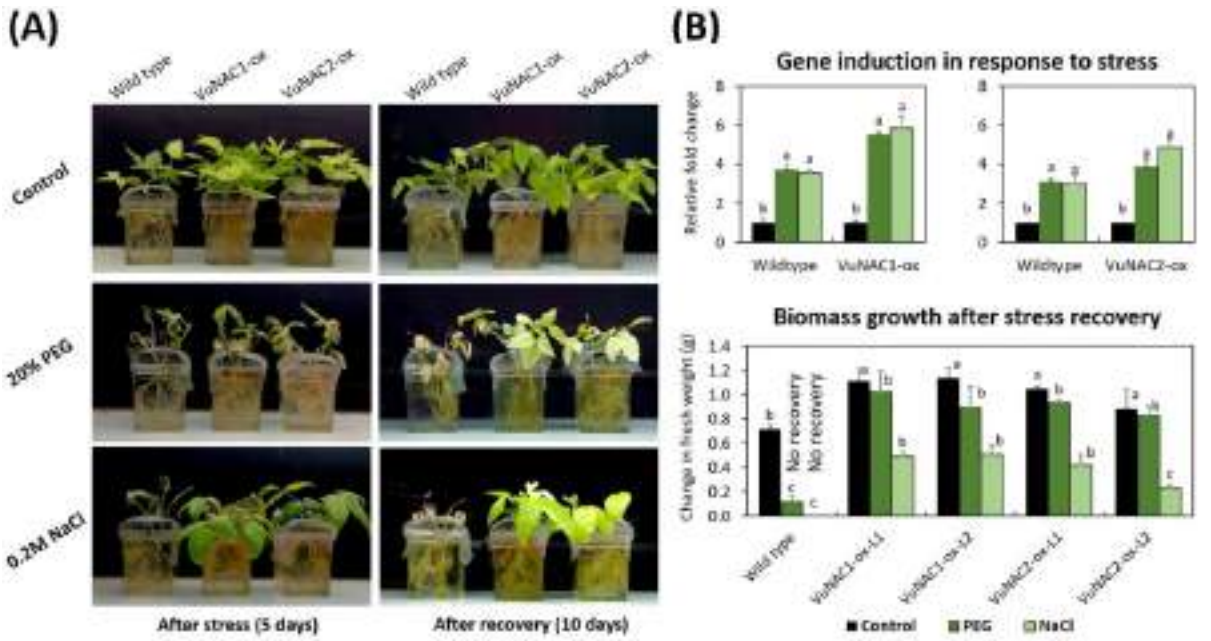

Fig. 6.2 Gene expression analysis in transgenic seedlings under PEG and NaCl-induced stress. (A) Dehydration (20% PEG) and salt stress (200 mM NaCl) were imposed in trifoliate-stage seedling for five days, followed by recovery. **(B)** Expression analysis conducted after 24 hrs of stress treatment (top) showing significant induction in transgenic lines and gain in fresh weight (bottom) after recovery.

6.3.2 The transgenic seedlings manifested accelerated germination and improved post-germinative growth under limiting nutrition

The VuNAC1/2-ox seeds burst-opened earlier to develop plumules. After five days of post-germinative growth, the transgenic seedlings produced thicker and enlarged hypocotyls bearing expanded leaves and a dense bunch of lateral roots, unlike the wild type seedlings, which only partially emerged the cotyledonary leaves (Fig. 6.3A and Fig. 6.3B). When grown further under hydroponic conditions, the trifoliate-stage seedlings (15 days old) displayed improved morphological traits such as enhanced primary root length, leaf blade size, shoot, and root biomass, as shown in Fig. 6.3A. Furthermore, when examined under a nutrient-limiting condition exerted by $1/10^{th}$ strength of the growth media, the wild type seedlings showed growth arrest and nutrition deficiency symptoms after three weeks due to starvation (Fig. 6.3C). In contrast, the transgenic seedlings pursued biomass growth, showing significant fresh-weight gain without any aberrant symptoms, indicating a better energy status. Our results suggested the role of VuNAC1/2 TFs in breaking seed dormancy and regulating post-germinative growth, possibly through improved nutrient mobilization from the seed repository or by photosynthetic assimilation enabled by phase transition during post-embryonic growth.

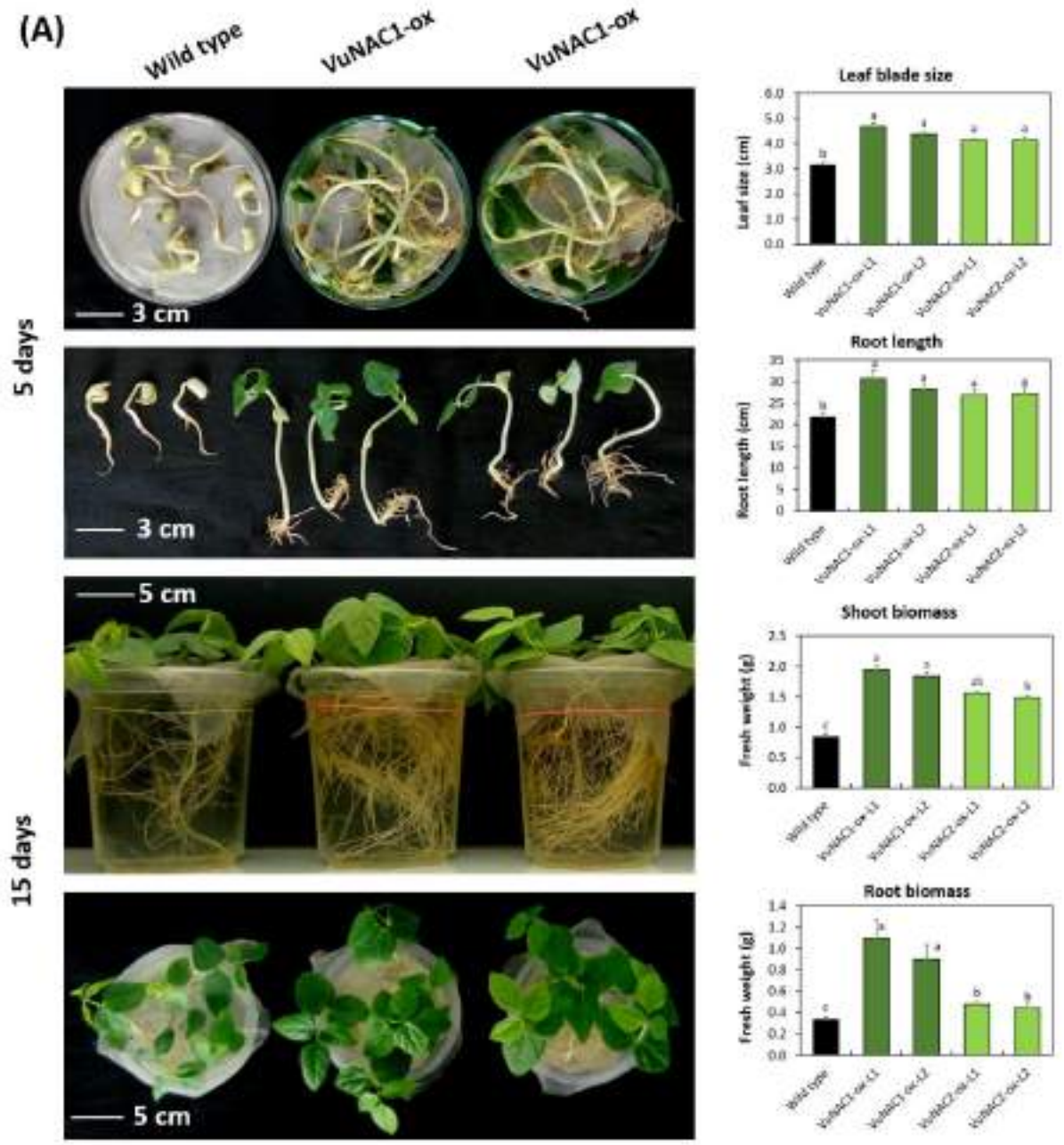

Fig. 6.3 Morphological analysis of transgenic seedlings under nutrient-sufficient conditions. (A) Growth phenotype was studied in seedlings at the post-embryonic stage (5 days) and post-germinative stage (15 days), grown in ½ X Hoagland solution. The transgenic seedlings showed increased growth-associated parameters (leaf size, root length, and fresh weight) recorded after 15 days compared to the wild type.

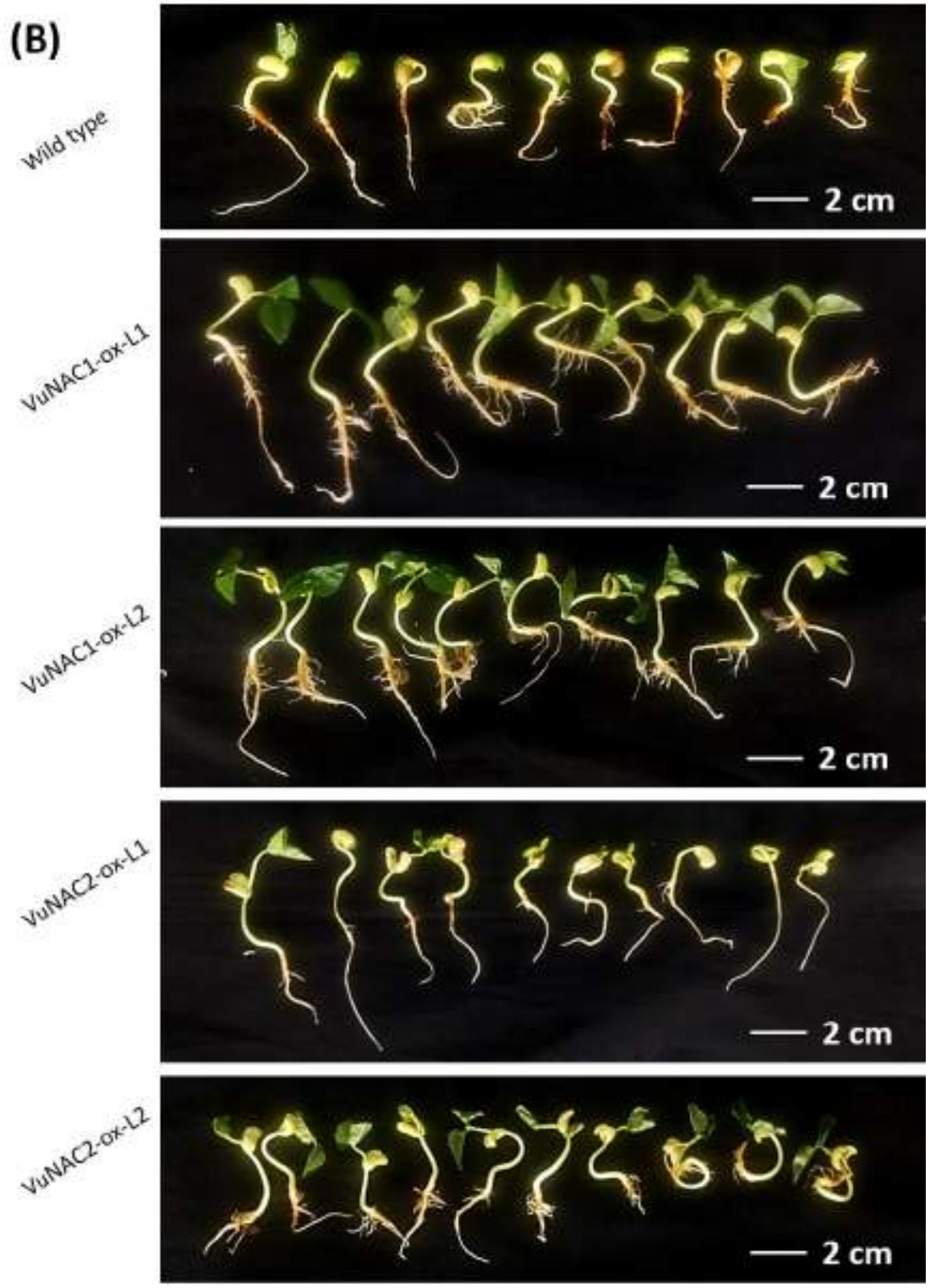

Fig. 6.3 Morphological analysis of transgenic seedlings under nutrient-sufficient conditions. (B) The seedlings were germinated in ½ X Hoagland solution for five days to analyze shoot size and root length in two transgenic lines, each expressing *VuNAC1* and *VuNAC2*. The seedlings displayed increased shoot and root parameters relative to the wild type.

Fig. 6.3 Morphological analysis of transgenic seedlings under nutrient-deficit conditions. (C) One-week-old seedlings grown in ½ X Hoagland media were transferred to 1/10 X media to impose nutrition deficiency seedlings for three weeks. The transgenic seedlings displayed healthier growth and gain in fresh weight, while the wild type seedlings showed degradation of photosynthetic pigments as a starvation symptom.

6.3.3 The transgenic plants displayed refined agronomic traits accompanied by yield improvement

The four-week-old VuNAC1/2-ox plants grown under controlled greenhouse conditions were inspected for phenotypic changes in their mid-vegetative stage. Striking differences in crucial agronomic traits were noted in the transgenic lines relative to the wild type plants (Fig. 6.4 and Table 6.1). The VuNAC1/2-ox plants exhibited increased height, thicker axial stem, more number of nodes and fully expanded leaves, bigger leaves, and canopy area. The plants produced denser and bunchier roots bearing more fresh weight than their wild type counterparts. Interestingly, the transgenic roots were also rich in nodules indicating a better symbiotic nitrogen fixation. Moreover, the transgenic plants stood out in terms of yield-associated parameters (Table 6.1). The plants initiated early flowering and produced two flushes of healthy pods with a greater size resulting in increased seed harvest. Also, the transgenic seed weight increased by at least 16%. We also analyzed the plants grown in field conditions and noted similar outcomes indicating improved growth and yield traits in the transgenic plants (Fig. 6.4 I, J). The transgenic lines produced bigger and denser leaves, more flowers and pods, and more seeds per pod than the wild type. Our study indicated that the

VuNAC1/2 TFs conferred sturdier and richer vegetative and reproductive growth in cowpea when overexpressed.

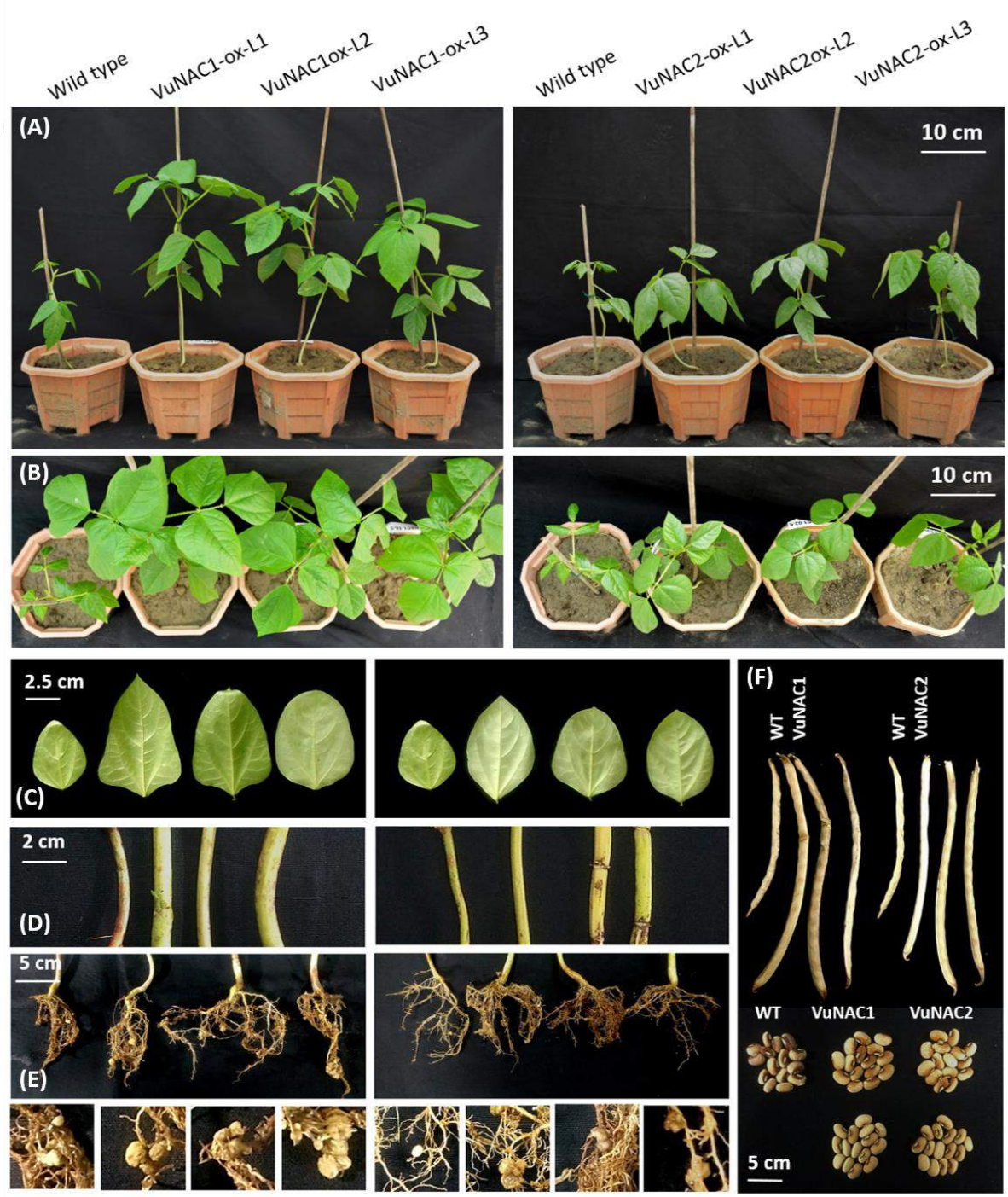

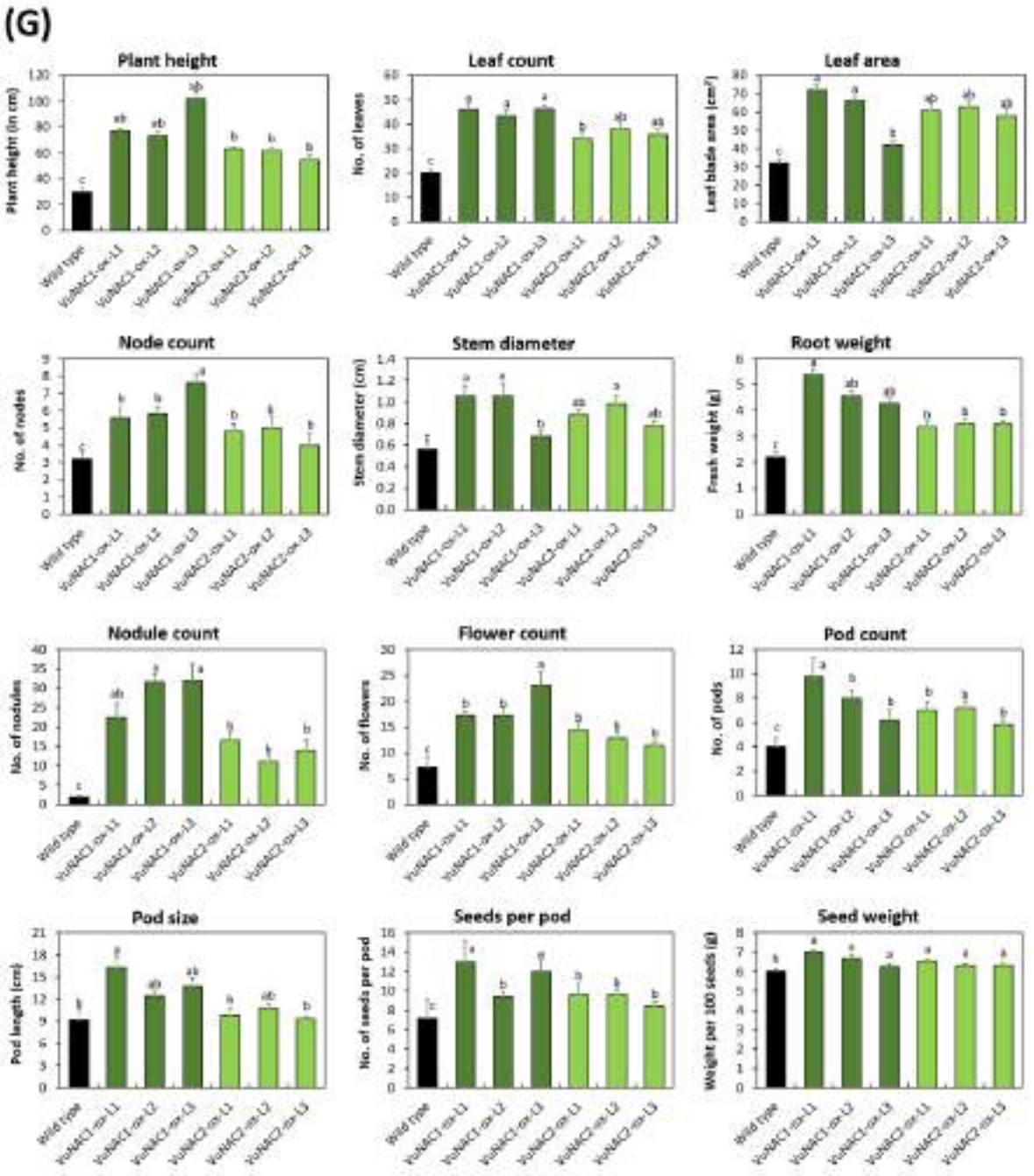

Fig. 6.4 Analysis of agronomic traits of T_2 generation transgenic plants grown under greenhouse conditions. Vegetative growth of one-month-old pot plants, **(A)** lateral view and **(B)** canopy-view, **(C)** full-expanded leaves taken from the third node down the canopy, **(D)** stem section above the first node from bottom, **(E)** root architecture bearing nodules (enlarged view, bottom). **(F)** mature-pods (top) and seed harvested (bottom). The transgenic plants exhibited two flushes of healthy flowering and mature pod harvest compared to the wild type plants showing a single bloom of healthy harvest during the interval. **(G)** Measurement of parameters associated with agronomic traits.

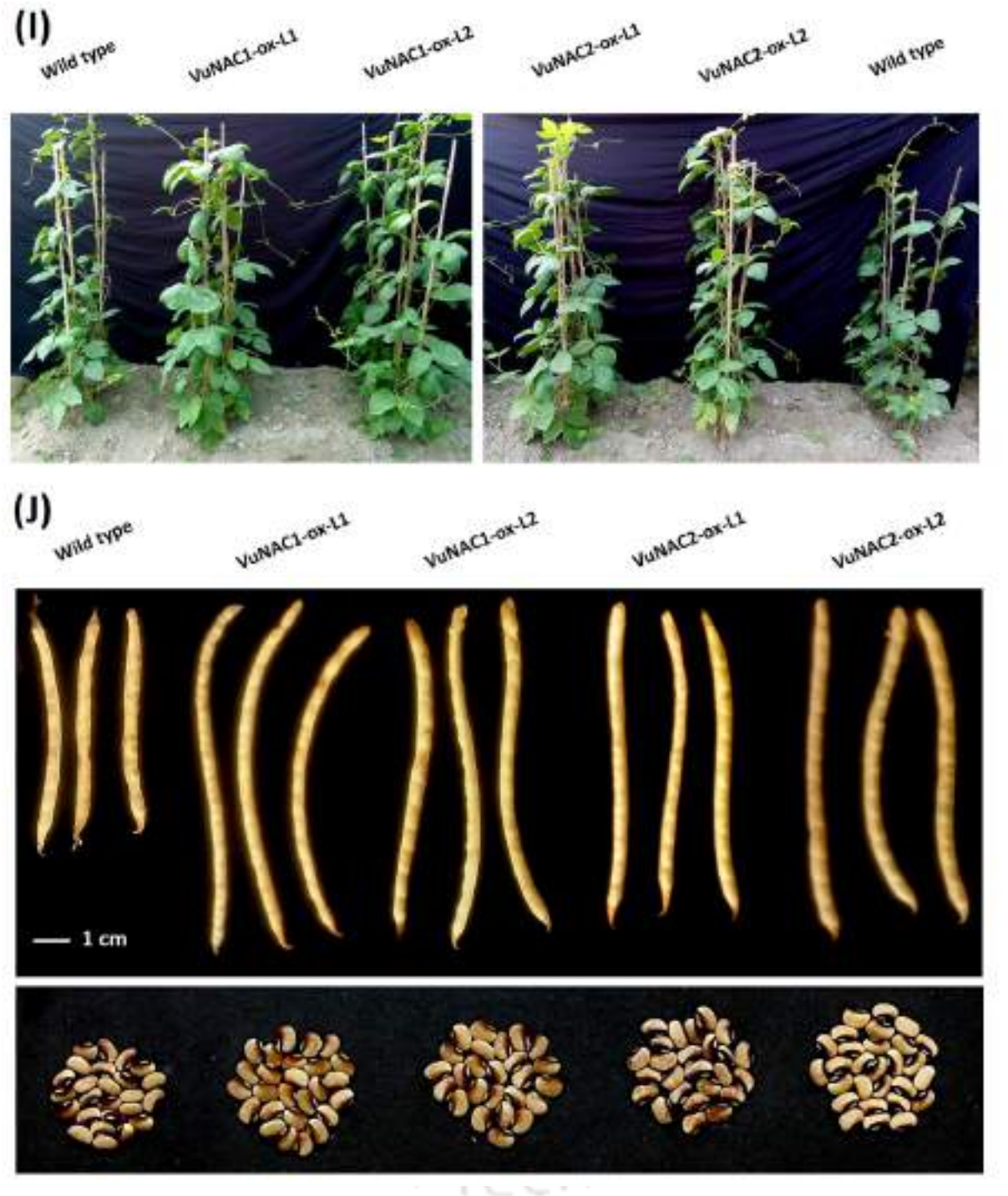

Fig. 6.4 Analysis of agronomic traits of T_2 generation plants grown under controlled field conditions **(I)** T2 generation transgenic lines (VuNAC1/2-ox-L1 and VuNAC1/2-ox-L2) expressing the cowpea NAC TFs displayed dense vegetative growth-producing leaves larger in size and count, relative to the wild type plants. **(J)** Pod and seed phenotype harvested from the field plants.

Table 6.1. Agronomic traits and yield parameters recorded for T2 generation plants grown under greenhouse conditions

	No. of nodes	Internode length (cm)	Stem diameter (in cm)	Leaf Area (in cm^2)	No. of fully expanded leaves	Plant height (in cm)	Root fresh weight (in g)	No. of nodules
Wild type	3.2 ± 0.45	5.20 ± 0.21	0.56 ± 0.05	32 ± 2.35	20.0 ± 1.41	30.0 ± 2.92	2.21 ± 0.18	1.80 ± 0.45
VuNAC1-ox-L1	5.6 ± 0.55	5.82 ± 0.58	1.06 ± 0.09	72 ± 2.74	46.0 ± 2.92	77.4 ± 1.52	5.40 ± 0.21	22.5 ± 3.54
VuNAC1-ox-L2	5.8 ± 0.45	6.08 ± 0.23	1.06 ± 0.11	66 ± 2.24	43.4 ± 2.30	73.6 ± 2.30	4.57 ± 0.19	31.5 ± 2.12
VuNAC1-ox-L3	7.6 ± 0.55	7.92 ± 0.28	0.68 ± 0.04	42 ± 2.74	46.4 ± 1.14	102 ± 5.70	4.26 ± 0.20	32.0 ± 4.24
VuNAC2-ox-L1	4.8 ± 0.45	5.70 ± 0.27	0.88 ± 0.04	61 ± 4.18	34.0 ± 3.08	63.2 ± 1.10	3.37 ± 0.18	16.5 ± 2.12
VuNAC2-ox-L2	5.0 ± 0.71	6.10 ± 0.26	0.98 ± 0.08	63 ± 2.74	38.0 ± 2.55	61.8 ± 1.92	3.49 ± 0.16	11.0 ± 1.41
VuNAC2-ox-L3	4.0 ± 0.71	5.54 ± 0.15	0.78 ± 0.04	58 ± 4.47	35.8 ± 2.05	54.8 ± 3.56	3.48 ± 0.12	14.0 ± 2.83

	Days to flower initiation	No. of flowers appeared	No. of pods	Pod-length	No. of seeds per pod	Seed weight (per 100 seed in g)	Senescence onset (in weeks)
Wild type	50.8 ± 2.59	07.2 ± 1.92	4.0 ± 0.70	09.23 ± 1.62	07.2 ± 1.92	6.02 ± 0.15	20.00
VuNAC1-ox-L1	45.4 ± 0.55	17.2 ± 0.83	9.8 ± 1.48	16.96 ± 1.20	13.0 ± 6.92	7.01 ± 0.15	17.00
VuNAC1-ox-L2	47.0 ± 1.00	17.2 ± 1.64	8.0 ± 0.70	12.45 ± 0.68	09.4 ± 6.66	6.67 ± 0.17	16.00
VuNAC1-ox-L3	35.4 ± 1.14	23.2 ± 2.38	6.2 ± 0.83	13.79 ± 1.78	12.0 ± 6.11	6.26 ± 0.14	12.00
VuNAC2-ox-L1	47.2 ± 1.64	14.4 ± 1.51	7.0 ± 0.70	09.79 ± 1.07	09.6 ± 6.32	6.51 ± 0.14	16.00
VuNAC2-ox-L2	47.8 ± 0.44	12.8 ± 1.30	7.2 ± 0.44	10.86 ± 0.55	09.6 ± 6.22	6.32 ± 0.07	16.00
VuNAC2-ox-L3	47.4 ± 1.14	11.4 ± 0.89	5.8 ± 0.44	09.39 ± 0.28	08.4 ± 6.18	6.32 ± 0.12	15.00

6.3.4 Virus-induced silencing of the *VuNAC1/2* impaired vegetative growth and flowering

The overexpression of the ATAF-like VuNAC1/2 TFs significantly improved embryonic development, seedling emergence, as well as a stress recovery in the transgenic seedlings, suggesting that the loss of function could cause a lethal phenotype. Hence, a rapid and transient virus-induced gene silencing (VIGS) method was employed to decipher the phenotype and indispensability of the post-transcriptionally silenced *VuNAC1/2* genes, using their non-conserved 3' regions [482]. The imbibed cowpea seeds were infected with the Agrobacterium strains carrying the VuNAC1-si and VuNAC2-si constructs (Fig. A1.4, Appendix 4), and the gene transcripts and growth phenotype were analyzed at various stages (Fig. 6.5). At the germination stage, the seedlings (VuNAC1/2-si) exhibited delayed plumule emergence and produced thinner radicles than the control seedlings infected with the empty vector constructs, as shown in Fig. 6.5A. After four weeks, the control plants reached the trifoliate stage bearing fully expanded leaves, while the silenced plants produced smaller leaves and continued to display poor vegetative growth after eight weeks. Later, 80% of the VuNAC1-si plants failed to initiate flower at the reproductive stage, while the VuNAC2-si plants did not flower at all (Fig. 6.5B). Consistent with the phenotype, the 4-week old plants showed a reduction in the VuNAC1/2 transcripts indicating the gene silencing. The presence of TRV2 transcripts showed that viral infection persisted for at least up to eight weeks, thereafter the VuNAC transcripts recovered (Fig. 6.5C). The 4-week-old VuNAC1-si and VuNAC2-si tissues were also examined for stress response. The leaf disc assay indicated that the tissue was sensitive to the PEG and NaCl-induced stress when VuNAC1/2 TFs were silenced. The photosynthetic pigments degraded more severely in these tissues indicating stress-induced cell death (Fig. 6.5E, F). The VIGS stud revealed that VuNAC1/2 TFs are necessary components that signal plant growth, reproduction, and stress response. They can also be crucial for expressing floral homeotic genes regulating floral transition and development [483].

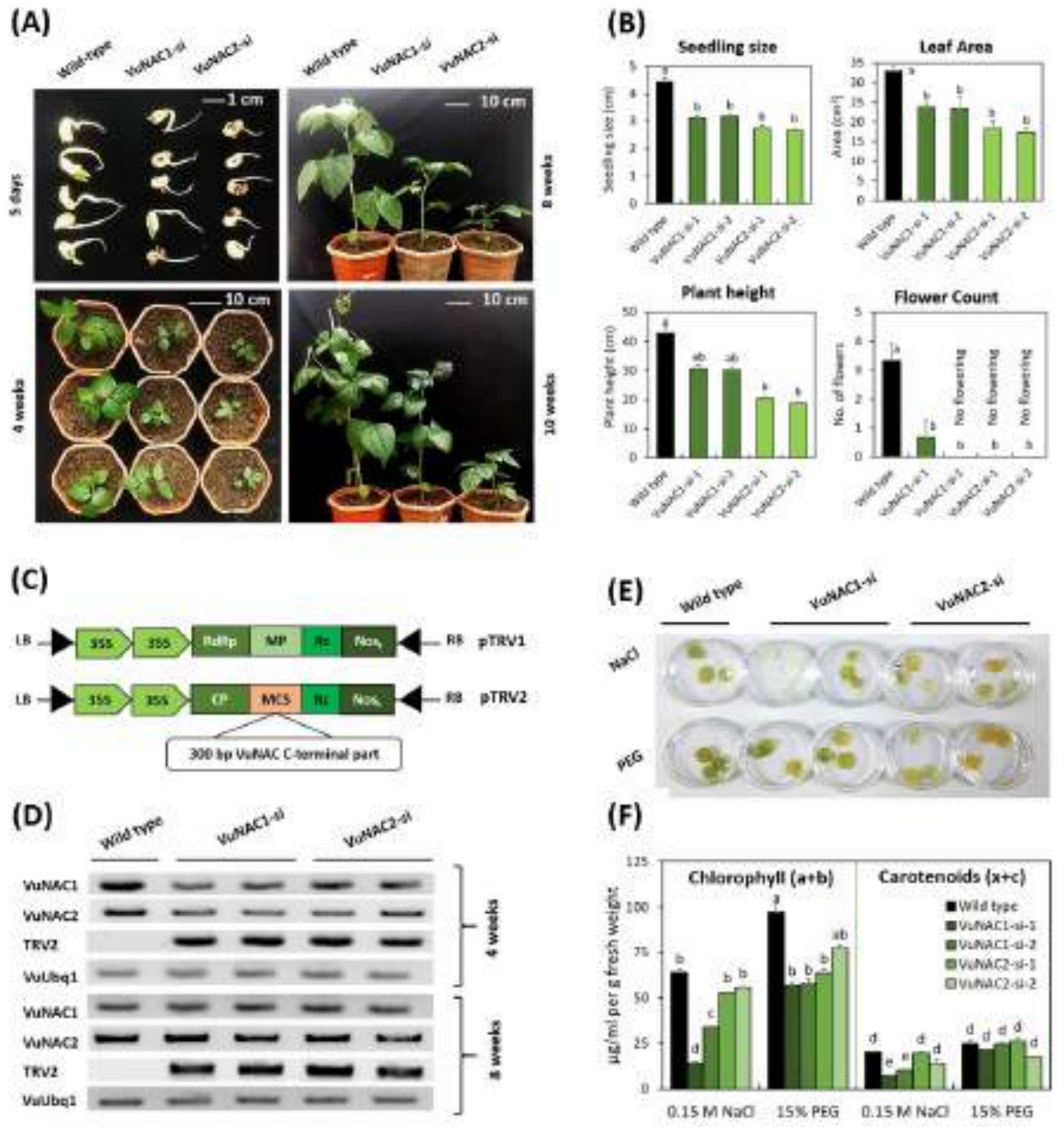

Fig. 6.5 *VuNAC1/2* suppression by virus-induced silencing (VIGS). (A) Phenotype analysis of silenced plants at different growth phases, germination, post-germination, vegetative and reproductive. **(B)** Measurement of growth and yield traits. **(C)** Schematic diagram of the pTRV1/pTRV2 construct. **(D)** Quantification of RNA transcript after silencing. **(E)** stress analysis by leaf-disc assay, **(F)** Determination of photosynthetic pigment in stressed tissue.

6.3.5 The transgenic lines exhibited tolerance to drought and salt stress displaying improved redox potential and photosynthetic activity

6.3.5.1 Evaluation of drought and salt tolerance phenotype

We imposed drought stress in a greenhouse, as well as in the field-mimicked growth conditions simulated by lysimeters in a poly house (Fig. 6.6A and Fig. 6.6B). In the greenhouse, the wild type plants started to show drought symptoms such as yellowing and scorching of the leaves after two weeks, severe leaf shedding after four weeks, and complete wilting after six weeks (Fig. 6.6A). However, the transgenic lines pursued healthier vegetative growth despite the four-week-long water withdrawal, and ~80% of the plants showed remarkable recovery of forage growth and floral transition within two weeks when the water regime was reinstated, unlike the wild type plants that failed to recover. Similarly, under the field-mimicked conditions, the transgenic lines ensued healthy and rich forage growth under water deficit (20% FC) while the wild type plants displayed drought symptoms in two weeks of drought imposition (Fig. 6.6C). After six weeks, the transgenic lines showed drought-induced leaf shedding, and the wild type plants wilted. However, the vegetative growth recovered when the 95% FC was restored after six weeks, whereas the wild type plants did not revive. Furthermore, the wild type roots showed severe wilting and degradation, while the transgenic roots were rigid and healthy, harboring a rich bunch of nodules (Fig. 6.6C).

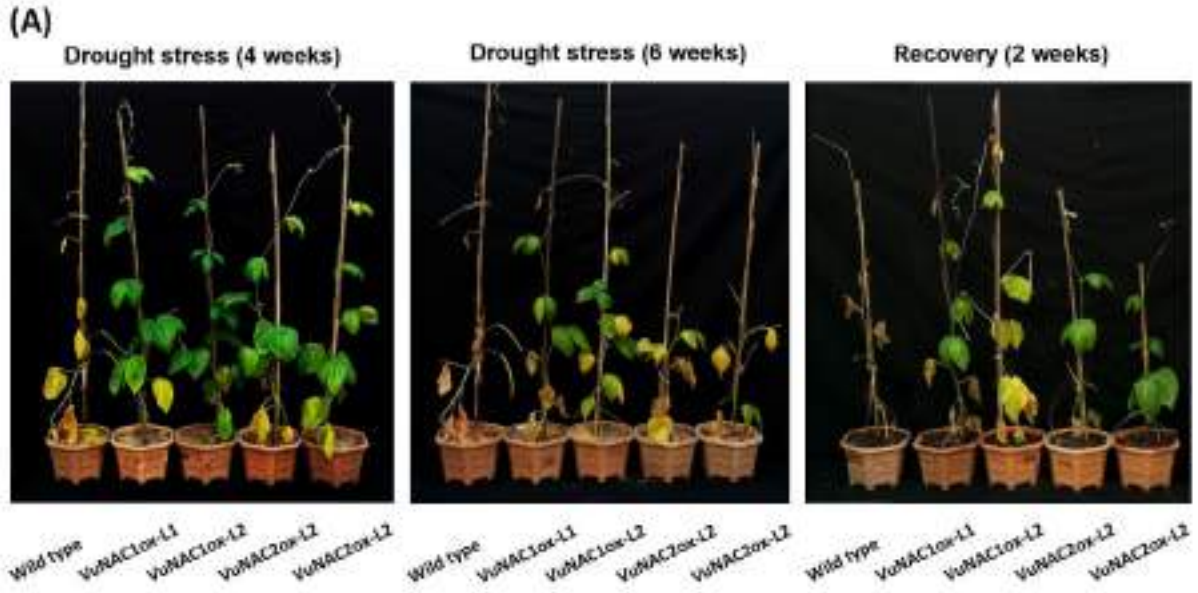

Fig. 6.6 Drought assay under greenhouse conditions. (A) The transgenic plants retained their vegetative growth when water was withdrawn to exert drought stress for six weeks while the wild type plants started wilting. The wild type plants failed to recover when the water regime was restored, whereas the transgenic plants proceeded to the reproductive growth phase.

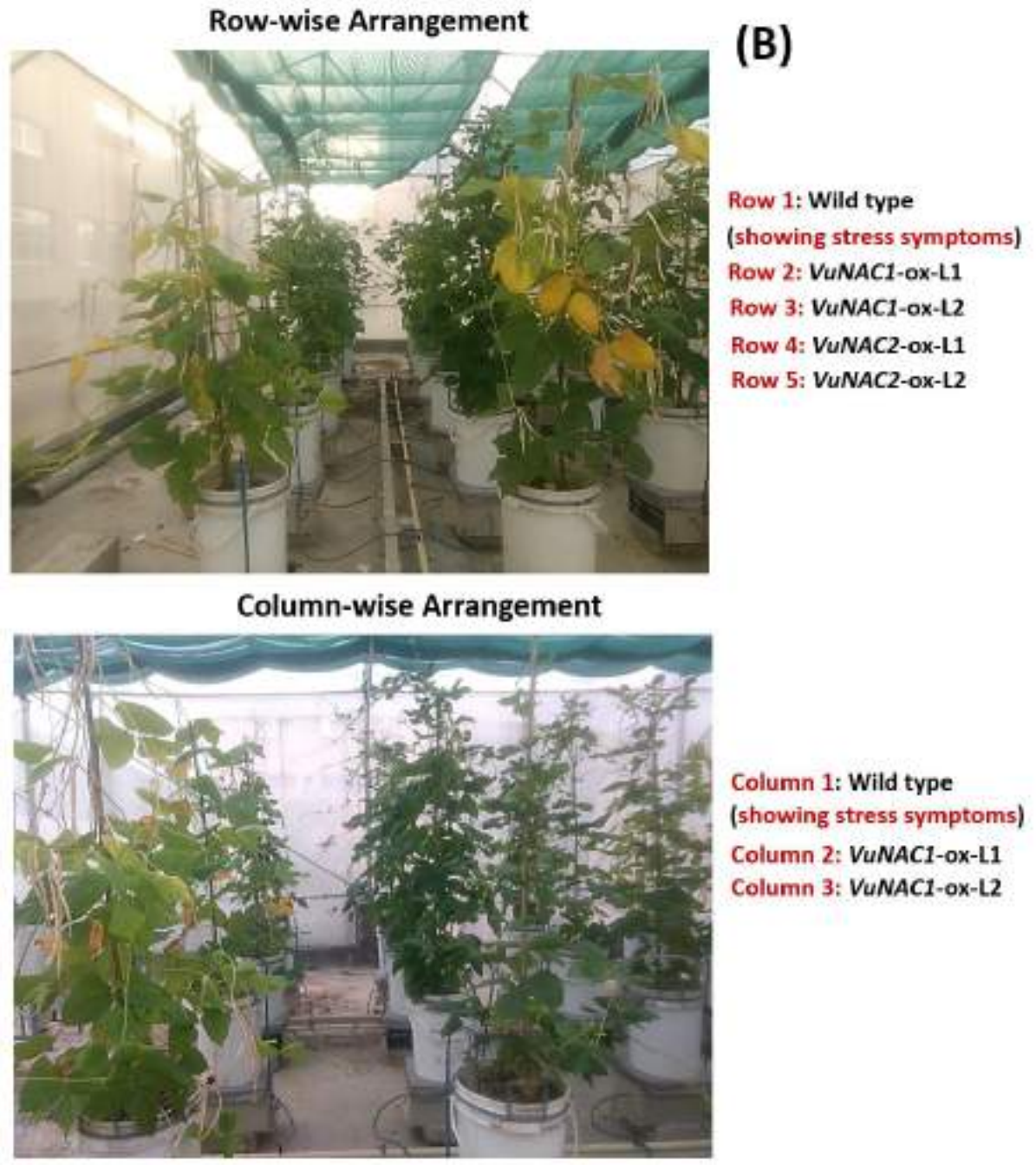

Fig. 6.6 Drought assay using drought simulator to imitate field conditions. (B) The field capacity (FC) was monitored using real-time computing servers, and the simulation devices (lysimeters) were used to maintain a water-sufficient irrigation regime (FC 90%) and water-deficit soil conditions (FC 20%).

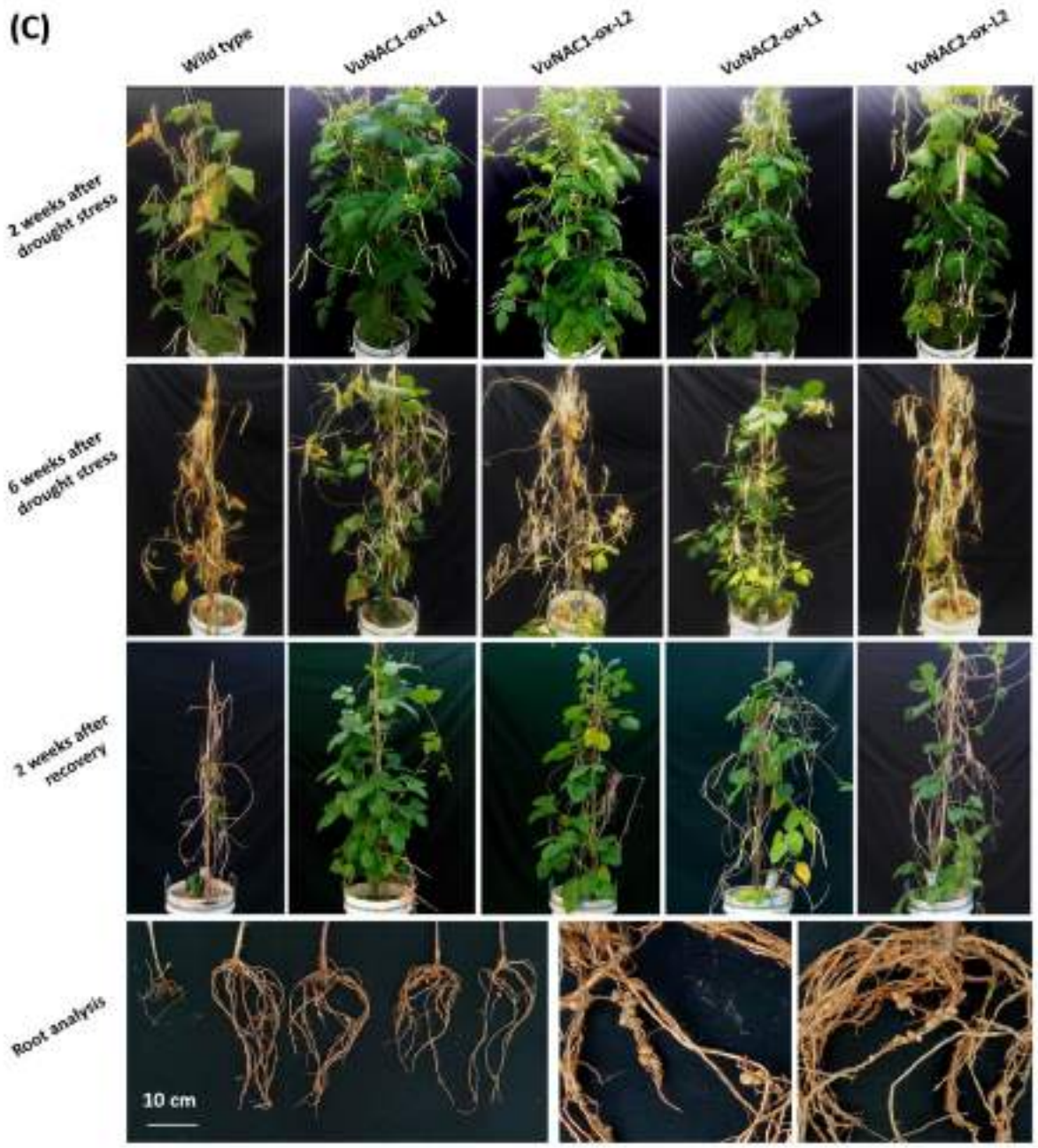

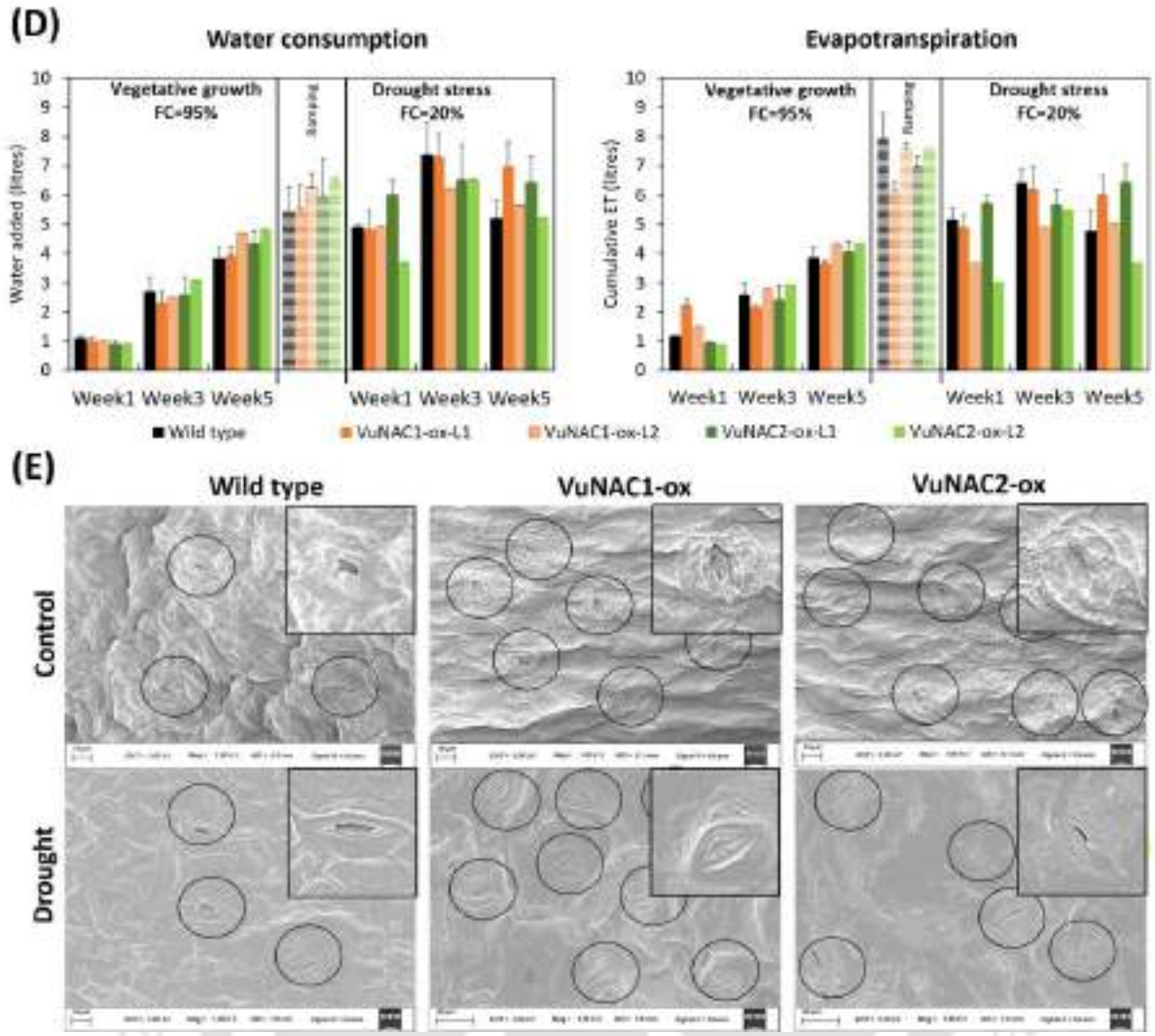

Fig. 6.6 Drought stress assay simulated by lysimeter. (C) Shoot and root phenotype under drought stress and after recovery. **(D)** Determination of water consumption and cumulative evapotranspiration. **(E)** Stomatal density and regulation before and after drought stress.

Moreover, the pod filling was adversely affected in wild type plants. Nevertheless, most of the pods were either empty or partially filled with small and discolored seeds, particularly, the pods produced in the later phase of the drought showed an elongated and curly phenotype. In contrast, the transgenic lines persisted flowering and developed healthy pods, resulting in a higher yield. The water consumption and the cumulative water-loss in evapotranspiration (ET) were recorded for five weeks, each before and after inflicting the water deficiency (Fig. 6.6D). The L2 lines of VuNAC1-ox and VuNAC2-ox plants showed a significant reduction in ET, indicating water conservation during stress. However, the increase in water uptake and evapotranspiration of the L1 lines in the later phase (3 to 5 weeks after drought stress) was justified by their rich forage biomass, unlike the wilted wild type plants. Interestingly, we found

increased stomatal abundance with a larger aperture in the transgenic leaf tissue when grown under normal conditions. However, under drought conditions, the stomatal size and aperture reduced to control water loss, especially in the VuNAC1-ox plants (Fig. 6.6E). The increased stomatal abundance might play a crucial role in the improved growth as well as stress recovery of the transgenic plants through the efficient gas exchange during photosynthesis.

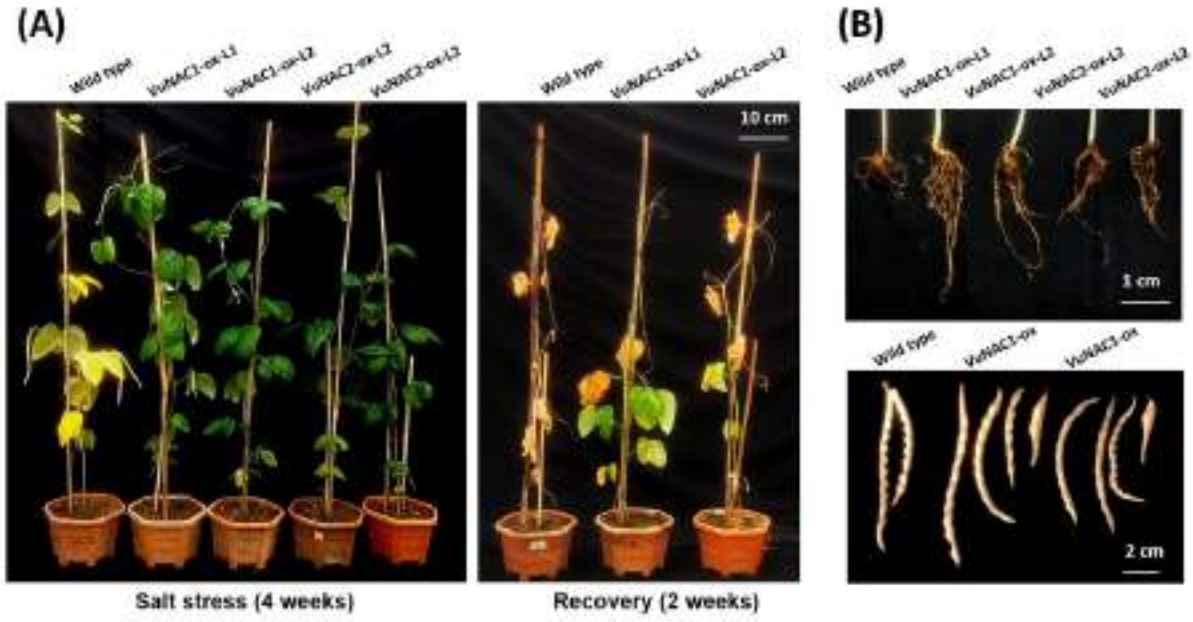

Fig. 6.7 Salt stress analysis under greenhouse conditions. (A) Shoot phenotype under salt stress and after recovery. **(B)** Root and pod phenotype after stress treatment.

Further, the transgenic plants were examined under salt stress inflicted by aqueous 200 mM NaCl in soil under greenhouse conditions. After four weeks, the wild type plants showed severe wilting, whereas 75% of the VuNAC1/2-ox plants could effectively endure the prolonged salinity, displaying green vegetative growth. However, with the progressing stress duration, the plants suffered leaf shedding to mitigate the ion toxicity (Fig. 6.7A). Nonetheless, the VuNAC1/2-ox plants recovered their reproductive growth gradually after the salt pressure was withdrawn, while the wild type plants wilted. In addition, the VuNAC1/2-ox plant developed a lengthier primary root and yielded more number of pods (Fig. 6.7B). The pods produced by the transgenic plants in the recovery phase were shorter but contained healthy and mature seeds. In contrast, the wild type pods yielded deformed seeds due to salt stress. Our study showed that the transgenic lines secured both vegetative and reproductive growth under severe and prolonged drought and salinity.

6.3.5.2 Evaluation of antioxidant activity, ion sequestration, photosynthetic gas-exchange during stress

The plants under salt and drought stress are obtruded by oxidative damage. The adaptation is attributed by the detoxification of the generated reactive oxygen species (ROS) to maintain the redox equilibrium. We performed histochemical staining of the stressed tissue to estimate the ROS level. The wild type tissue accumulated hydrogen peroxide (H_2O_2) and superoxide radicals (O_2^-), as indicated by the DBT and NBT staining (Fig. 6.8A), unlike the VuNAC1/2-ox tissue, which contained higher content of osmoprotectants and anti-oxidants such as proline, ascorbate, and glutathione (Fig. 6.8D), indicating better reducing power of the transgenic lines to detoxify the ROS. In addition, the VuNAC1/2-ox tissue contained less malondialdehyde (MDA) levels and higher content of chlorophyll a, chlorophyll b, and xanthophyll and carotenes, indicating less membrane damage and degradation of thylakoid pigments as a concomitant effect of the stress. Our results indicated that the transgenic plants employed better counter-acting mechanisms to avoid oxidative stress.

Plants combat the ion toxicity by sequestering the excess ions in cell-vacuoles to perpetuate the cytosolic K^+/Na^+ ratio or by throwing the ions out of the cell by the exclusion method [45]. We found a significantly higher endogenous content of Na^+ ions in the VuNAC1-ox shoot, along with a much higher content in VuNAC1/2-ox roots, during the salt stress indicating Na^+ sequestration (Fig. 6.8B). In addition, the content of K^+ ions was increased in both VuNAC1/2-ox shoots and roots, maintaining the K^+/Na^+ ratio. However, during stress, the Na^+ and K^+ levels reduced drastically in the wild type roots, as compared to the controlled conditions, indicating possible leakage of ions due to cell damage. The study indicated that the VuNAC1/2 TFs regulate Na^+ translocation, K^+ uptake, and their homeostasis.

Earlier, increased stomatal abundance was observed in the transgenic lines (Fig. 6.6E). When the chlorophyll fluorescence and photosynthetic gas-exchange attributes were examined, the VuNAC1/2-ox plants showed a higher CO_2 assimilation rate (A) and the stomatal conductance (Gsw) under both stressed (drought and salinity) and normal conditions, indicating improved photosynthetic activity (Fig. 6.8C). Also, the higher quantum yield for photosystem II (φ PSII) and the electron transport rate (ETR) implied improved functioning of the photosystem apparatus. The results suggested that VuNAC1/2 TFs regulate stomatal density, its development, and the synthesis of photosynthetic apparatus.

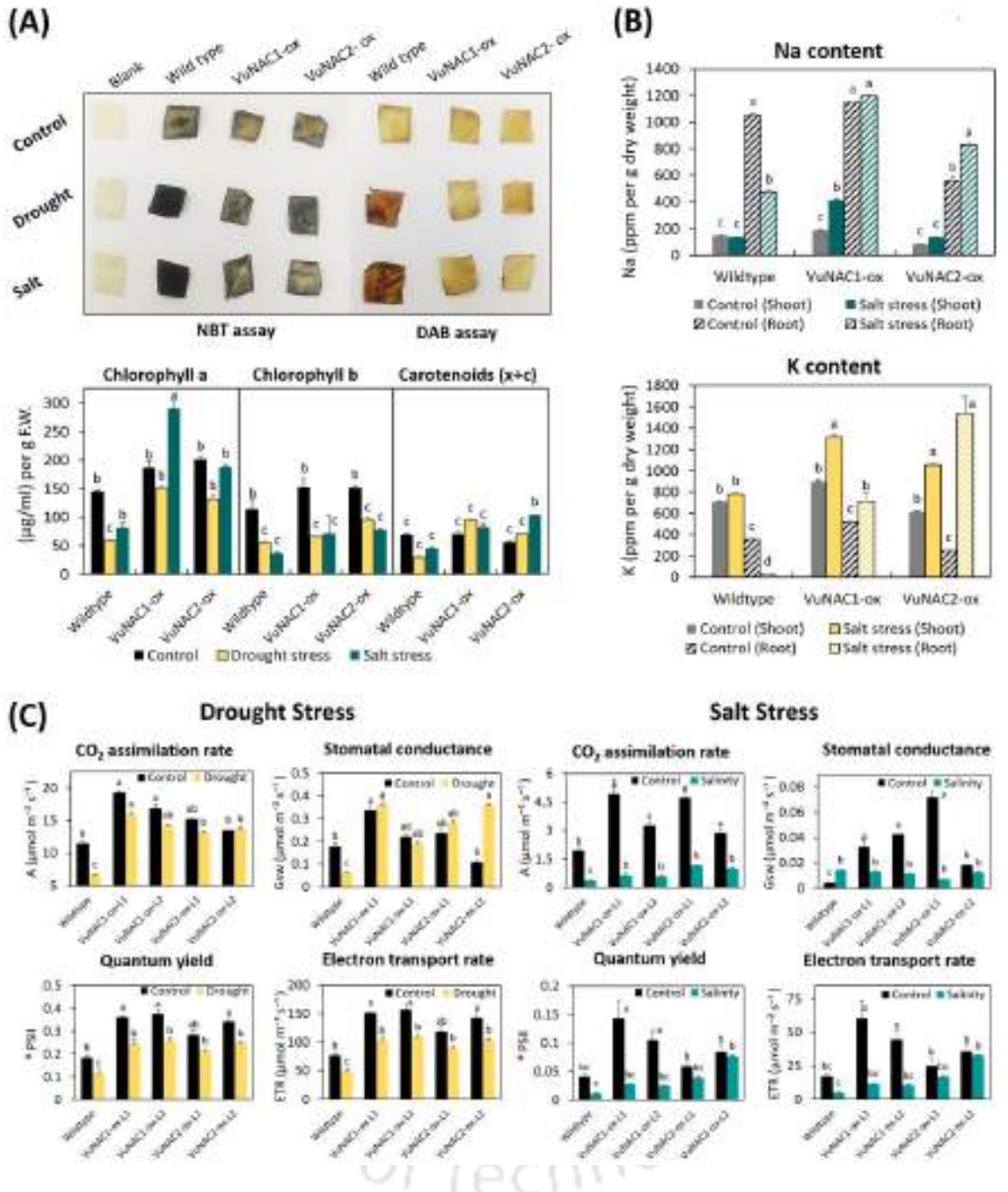

Fig. 6.8 Determination of changes in biochemical and photosynthetic parameters after stress treatment. (A) Histochemical staining of ROS species by DAB and NBT assay and estimation of photosynthetic pigments in drought and salt-stressed tissue. **(B)** Na^+ and K^+ ion content in salt-stressed shoot and root. **(C)** Determination of gas exchange and fluorescence parameters.

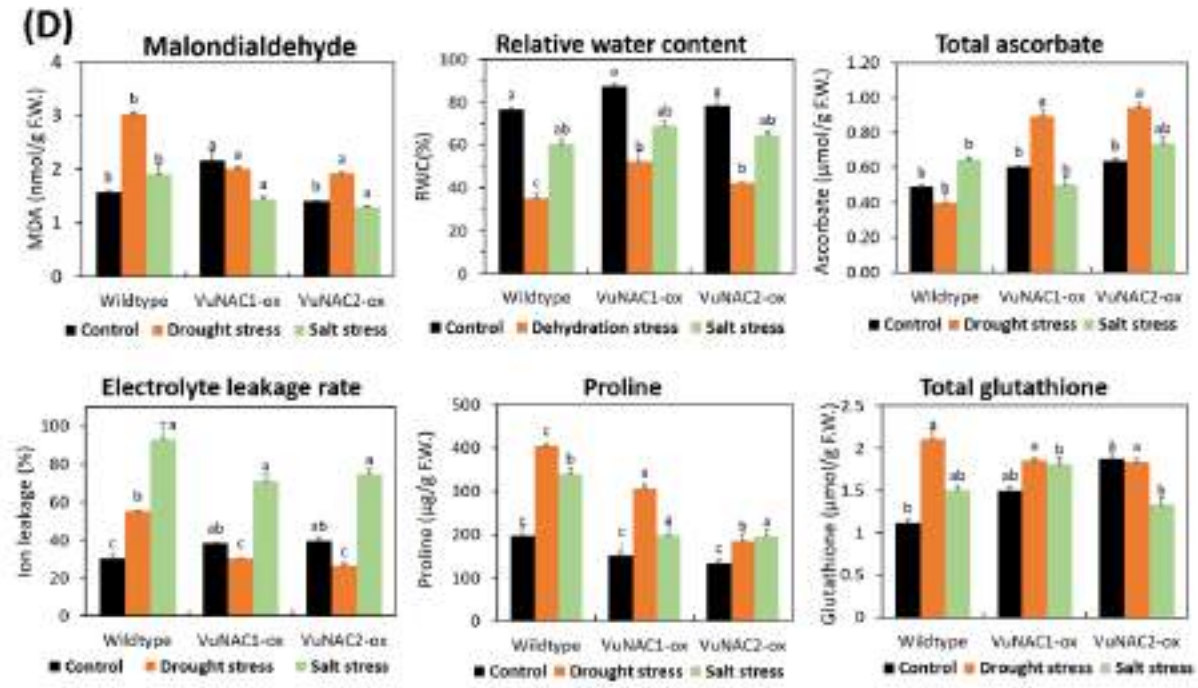

Fig. 6.8 Biochemical and physiological changes for stress response. (D) The proline, total ascorbate, and total glutathione content increased in the transgenic lines under both normal and stressed conditions indicating better ROS detoxification ability. The less MDA accumulation and more relative water content indicated that the transgenic tissue had less membrane damage and better water status under stress.

6.3.6 The transgenic plants restored flowering and pod development after prolonged heat and cold stress and exhibited early age-induced senescence

In cowpea, flower transition and pre-anthesis stages are susceptible to high temperature resulting in suppressed bud formation. In later stages, high night temperatures can impair pod setting, causing low pollen viability [258]. Additionally, freezing temperatures also affect cowpea yield by hampering the pod-setting, seed number, and seed size [484]. To analyze the effect of heat and cold stress, high and low diurnal temperature regimes were thrust upon one-month-old plants (before heading time) and ensued for a further one month throughout their early reproductive stage, followed by recovery. The VuNAC1/2-ox plants inflicted by heat stress (44°C/34°C day/night) did not show any pronounced difference in vegetative growth but produced healthy pods, despite delayed flowering (Fig. 6.9A). Nevertheless, the wild type plants failed to flower. The cold stress (18°C/12°C day/night) ceased the vegetative growth and resulted in leaf shedding in all plants. However, the VuNAC1/2-ox plants displayed better pod yield by resuming healthy blooming and pod formation, unlike the wild type plants, which showed drooping of unfertilized flowers, reduced pod-setting, and poor quality seeds.

Additionally, the CO_2 assimilation rate and electron transport rate (ETR) dropped significantly in the wild type plants and did not recover when the optimum conditions were reinstated, indicating degradation of photosynthetic activity due to heat and cold damage. (Fig. 6.9B). Our study showed that VuNAC1/2 TFs conferred tolerance to heat and cold stress.

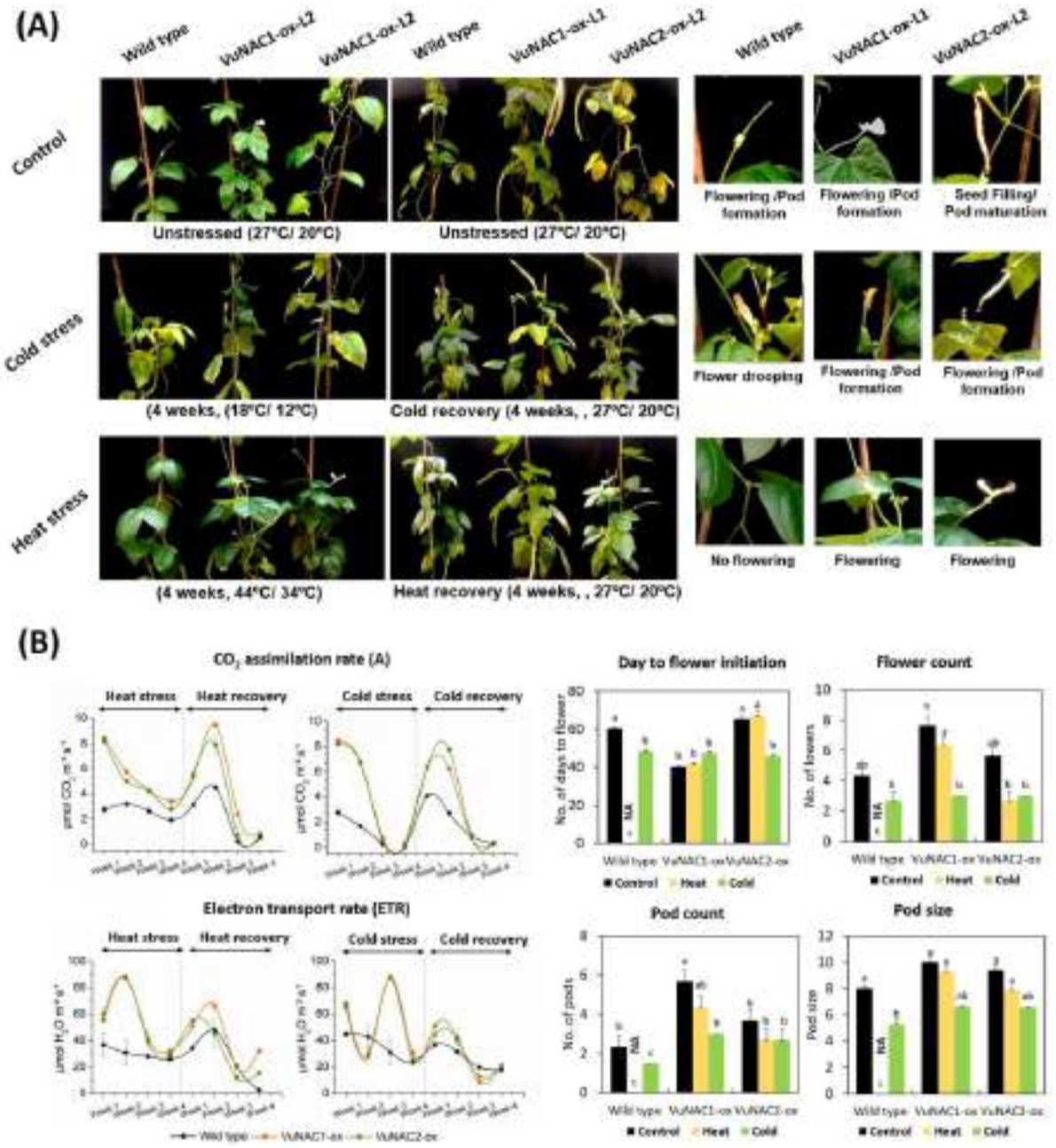

Fig. 6.9 Heat and cold stress analysis. (A) Reproductive growth phenotype under heat and cold stress and post-recovery. **(B)** Determination of photosynthetic and yield parameters in the stressed plants.

Leaf-senescence is crucial for determining seed yield and quality by allowing nutrient remobilization from the senesced tissue towards seed reserves. Thus, the onset of age-induced senescence was evaluated in the transgenic plants (Fig. 6.10). We recorded an early arrival of senescence in the VuNAC1/2-ox plants after 13 weeks, whereas the wild type plants showed aging symptoms after 15 weeks. Moreover, the enhanced electrolyte-leakage rate and degradation of photosynthetic pigments in the VuNAC1/2-ox plants recorded after 16 weeks indicated more prominent leaf-senescence in the transgenic lines. Despite early aging, the VuNAC1/2-ox plants produced more pods with higher seed count and seed weight. This indicated that VuNAC1/2 are positive regulators of age-induced senescence.

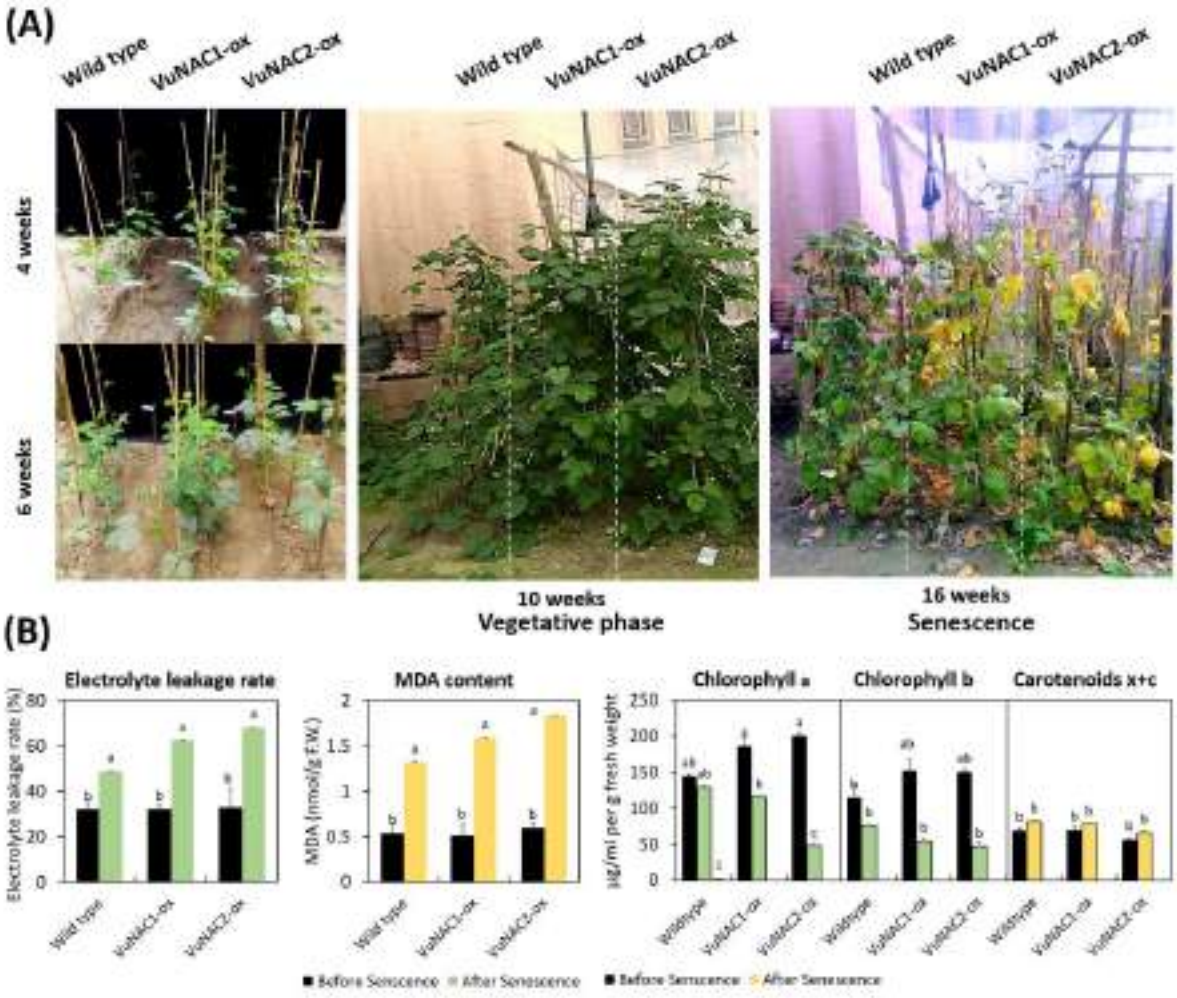

Fig. 6.10 Study of senescence onset. (A) Early leaf shedding and yellowing due to onset of age-induced senescence in the transgenic plants. **(B)** Biochemical study of senesced tissue by determining electrolyte leakage rate, lipid peroxidation, and degradation of photosynthetic pigments.

6.3.7 Study of differential gene expression in transgenic plants to identified targets of VuNAC1/2 TFs integrating disparate plant phenomena

The differential expressed (DE) transcriptome in one-month-old overexpressor transgenic lines, VuNAC1-ox (2.7 fold) and VuNAC2-ox (3.1 fold), were analyzed to identify the target genes of the TFs. The statistical distribution of the DE genes was mapped in Fig. 6.11A, indicating considerable similarity in the target gene groups tuned by VuNAC1 and VuNAC2. The GO annotations of the DE genes provided functional insight into the modified transcriptomes. The top 50 functional annotations shown in Fig. 6.11C indicated the prominent impact of VuNAC1/2 TFs on the biological processes such as: cell division [GO:0051301], cell-wall organization [GO:0071555], ATP synthesis-coupled proton transport [GO:0015986], aerobic respiration [GO:0009060], oxidative phosphorylation [GO:0006119], carbohydrate metabolic process [GO:0005975], lipid metabolic process [GO:0006629], nucleoside metabolic process [GO:0009116], cellular amino acid metabolic process [GO:0006520], response to oxidative stress [GO:0006979], transmembrane transport [GO:0055085], transcription [GO:0006351], translation [GO:0006412], and DNA repair [GO:0006281]. To predict the phylogenetic, architectural, and functional relationship of the proteome encoded by DE genes, the translated sequences were classified into Clusters of Orthologous Groups (COGs), based on the knowledge inferred from the evolutionary counterparts (Fig. 6.11D). The functional clusters for the two genes could be distributed among three major categories *viz.*, cellular processes and signaling (20.0% and 22.4 %), metabolism and metabolite transport (32.5% and 28.0%), and information storage and processing (17.8% and 14.0%). Our results advocated the crucial role of the VuNAC1/2 TFs in cell-wall/ membrane biogenesis, cell-cycle control, cell division, cytoskeleton formation, energy production and conversion, ion transport, protein turnover, and signal transduction, as shown in Fig. 6.12.

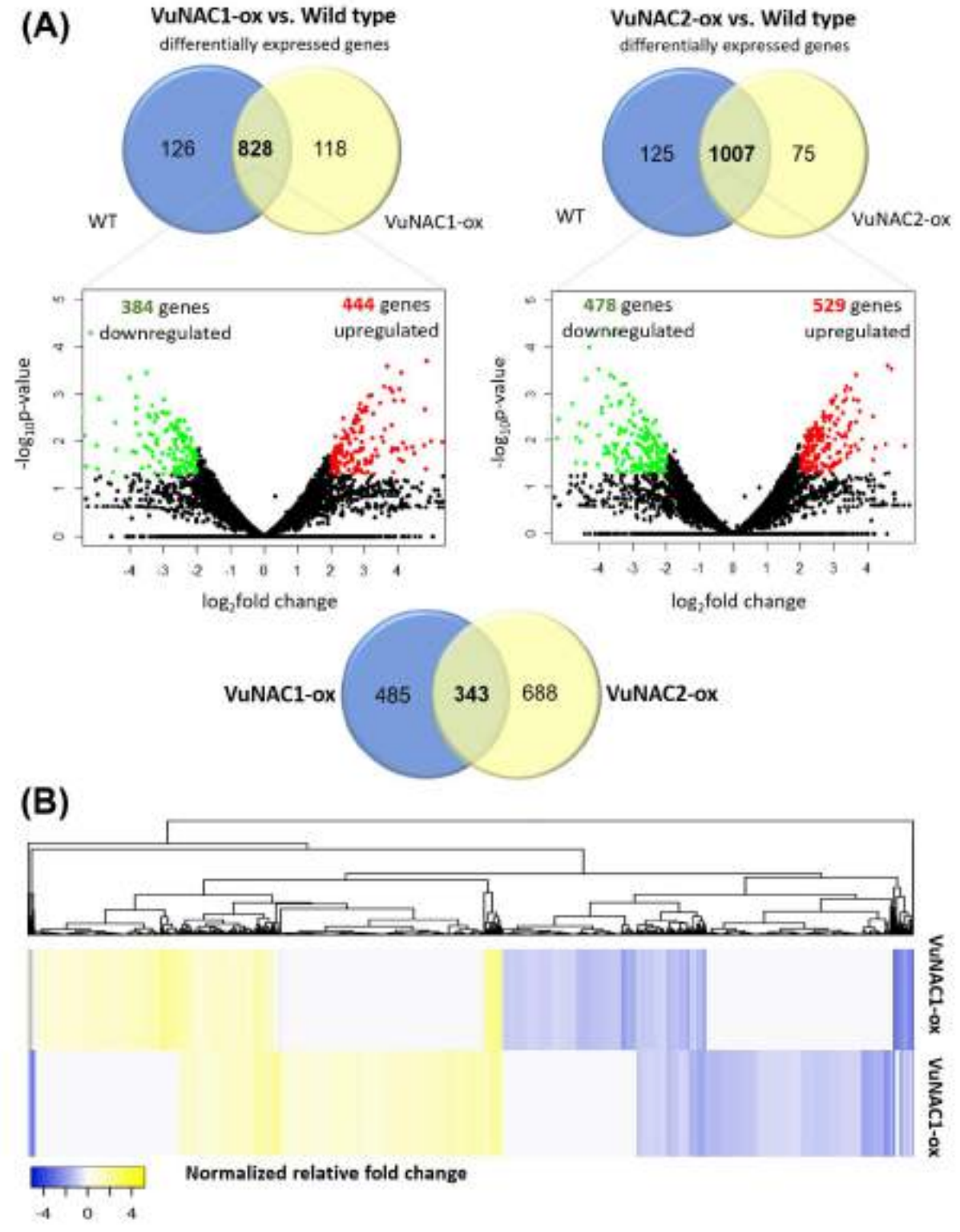

Fig. 6.11 Statistical analysis of differentially expressed genes (DEGs) in the transgenic lines. (A) 828 and 1007 *VuNAC* genes were differentially expressed (DE), showing either upregulation or downregulation in the VuNAC1 and VuNAC2 expressing transgenic plants, respectively (as mapped in the volcano plot). Out of those, 343 genes were common to both the transgenic plants. **(B)** Heat-map clustering of DE genes indicating similarity in gene targets.

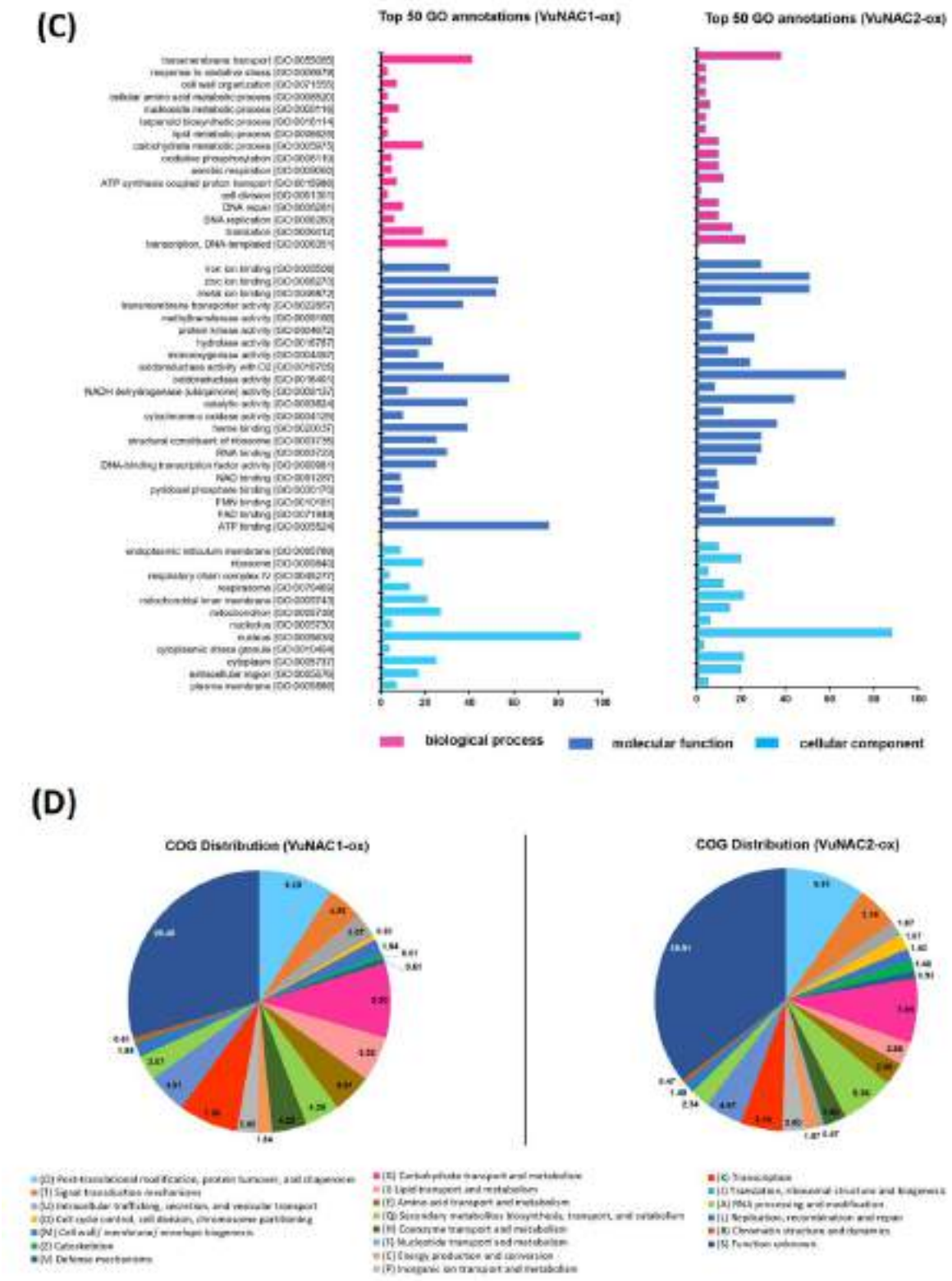

Fig. 6.11 Statistical analysis of differentially expressed genes (DEGs) in the transgenic lines. (C) Top 50 GO annotations of the DE genes associated with biological process, molecular function, and cellular content. **(D)** Functional clustering of DE genes in COGs (Clustering of Orthologous Groups) related to cellular processes and signaling, metabolism, and central dogma.

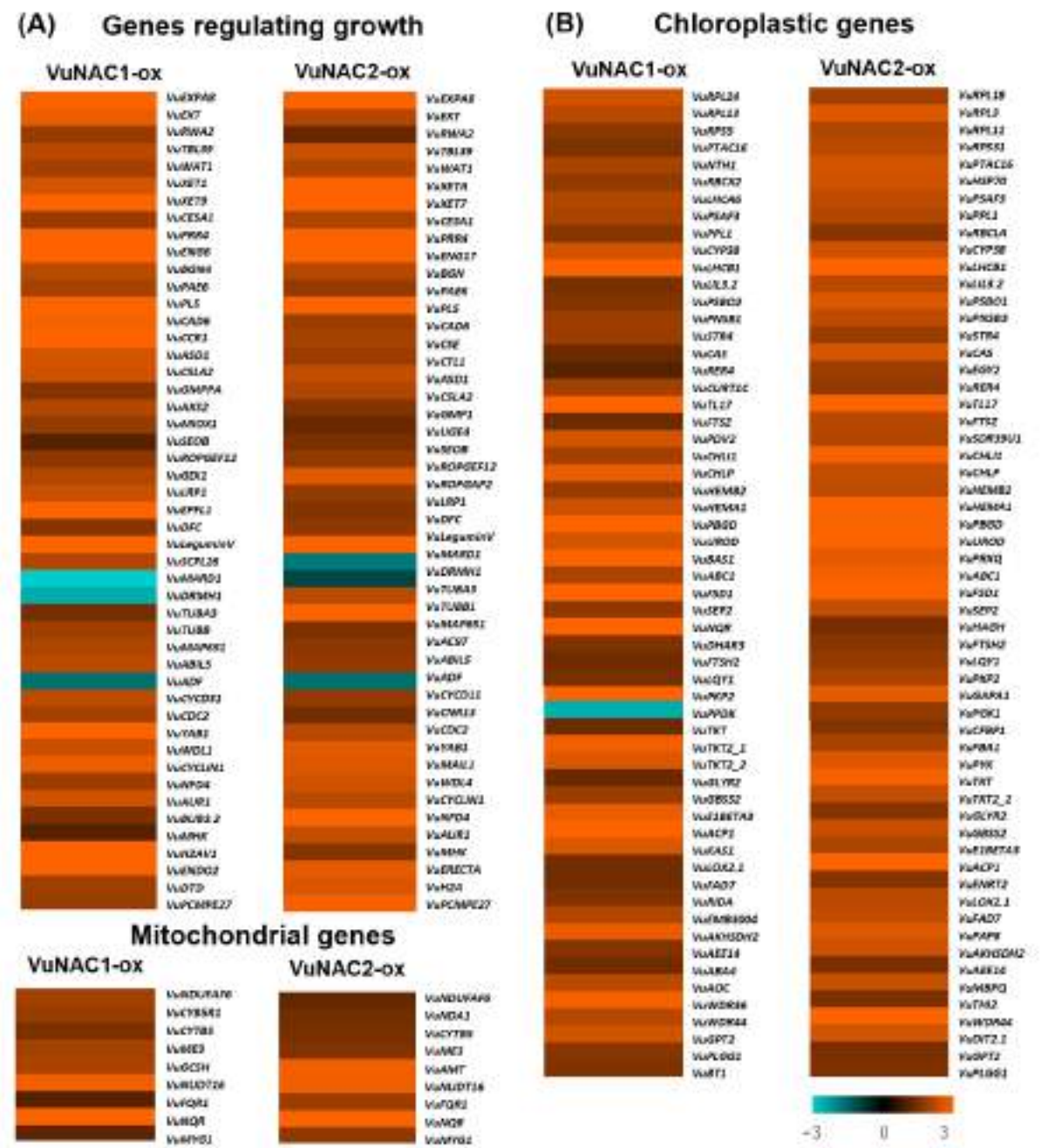

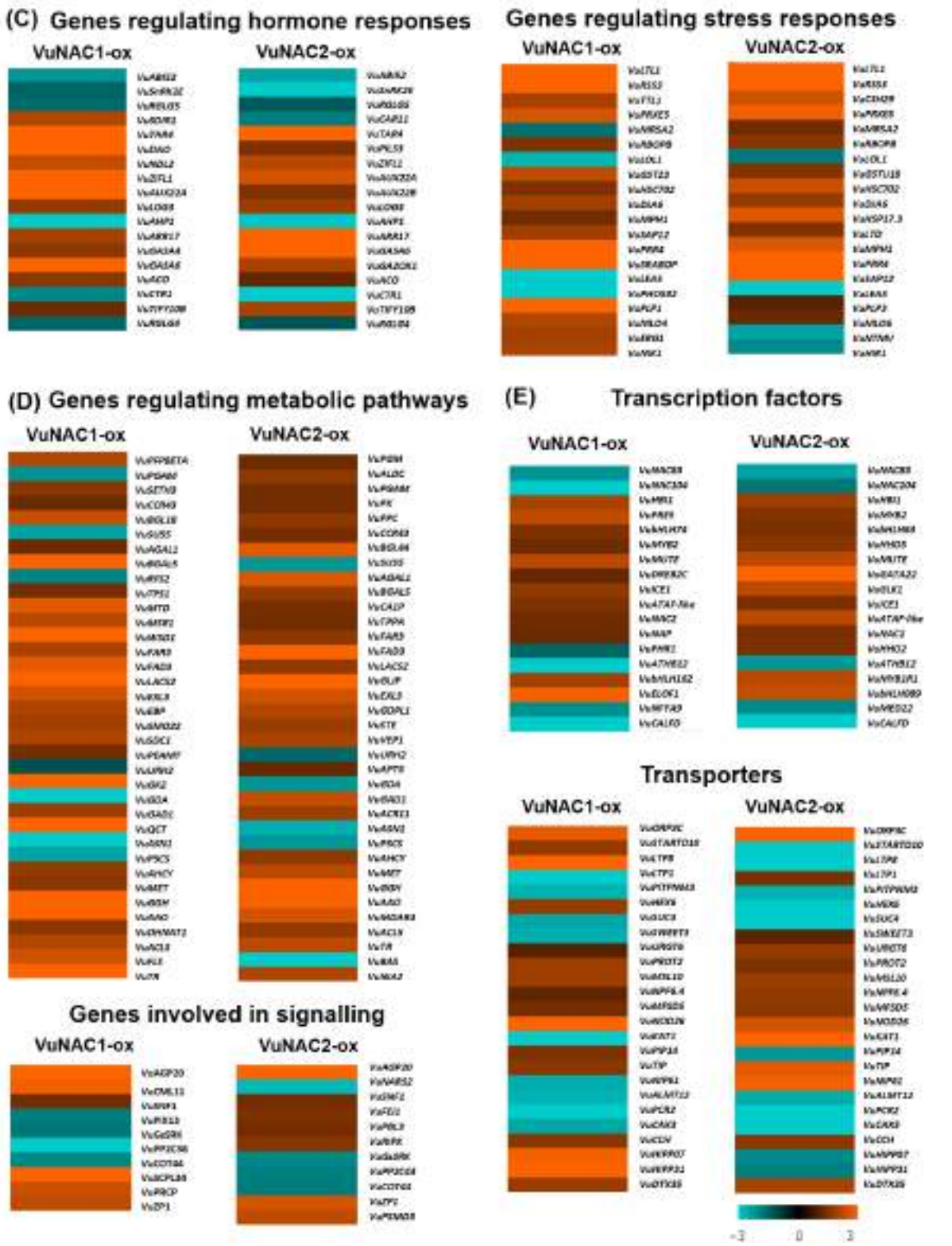

Fig. 6.12 Heat-map representation of the DEGs involved in various plant phenomena. (A) Growth and development associated genes. **(B)** Chloroplastic and mitochondrial genes. **(C)** Hormonal and stress response. **(D)** Metabolic pathways. **(E)** Transcription factors, transporters, and signaling proteins.

6.3.7.1 Cell-wall biogenesis, organogenesis, and growth-cycle regulating genes

Genes encoding cell-wall loosening enzymes such as EXPANSIN-A8 (*VuEXPA8*), XYLOGLUCAN ENDOTRANSGLUCOSYLASES (*VuXET9* and *VuXETA*), structural glycoproteins controlling cell-wall assembly and extension like EXTENSINS (*VuEXT*), proteins involved in cellulose deposition, *i.e.*, TRICHOME BIREFRINGENCE-LIKE 39 (*VuTBL39*), CELLULOSE SYNTHASE A CATALYTIC SUBUNIT 1 (*VuCESA1*) and ENDOGLUCANASE (*VuENG6*), and cell-wall modification enzymes like PECTATE LYASE 5 (*VuPL5*) and REDUCED WALL ACETYLATION 2 (*VuRWA2*), were upregulated in the transgenic lines overexpressing the VuNAC1 and VuNAC2 TFs. [485-487]. Genes encoding enzymes that synthesize nucleotide sugars and mannan proteins (*VuGMPPA* and *GMP1*) and factors involved in ROP signaling regulating cell polarity and morphogenesis (*VuROPGEF12*, *VuROPGAP2*, and *VuGDI1*) were also upregulated [488-490]. In addition, genes encoding proteins like MEDIATOR OF ABA-REGULATED DORMANCY 1 (*VuMARD1*), SERINE CARBOXYPEPTIDASE-LIKE 26 (*VuSCPL26*), and *VuLEGUMINV*, which regulate seed germination and dormancy break, were induced [491, 492]. Genes signaling cell fate by initiating shoot and root apical meristem (*VuMAIL1* and *VuYAB1*), cell-division in (*VuCYCD3-1*, *VuCYCD1-1*, *VuCDC2*, and *VuCYCLIN-1*-like), plant growth and development (*VuMHK* and *VuERECTA*) were also significantly induced in the transgenic lines [493, 494].

6.3.7.2 Chloroplastic genes encoding photosynthetic apparatus

Several mitochondrial genes involved in the assembly of electron-transport chain and chloroplastic genes encoding photosynthetic apparatus and the transcription and translation machinery required by chloroplast were significantly upregulated (Table 6.2 and Table A4.3, Appendix 4) [495]. For instance, genes encoding proteins such as PHOTOSYSTEM I CHLOROPHYLL A/B-BINDING PROTEIN 6 (*VuLHCA6*), PHOTOSYSTEM I REACTION CENTER SUBUNIT III (*VuPSAF3*), PSBP-LIKE PROTEIN 1 (*VuPPL1*), CHLOROPHYLL A-B BINDING PROTEIN OF LHCII TYPE 1-LIKE (*VuLHCB1*), and PHOTOSYNTHETIC NDH SUBUNIT OF SUBCOMPLEX B 1 (*VuPNSB1*) were induced [496-498]. Genes encoding proteins involved in chloroplast division and development (*VuCURT1C*, VuFTSZ, and *VuPDV2*) [499], chlorophyll pigment biosynthesis (*VuCHLI1*, *VuCHLP*, *VuHEMA1*, and *VuPBGD*) [500], and genes like *VuBAS1*, *VuABC1*, *VuFSD1*, and *VuFTSH2*, catalyzing the non-photochemical quenching and detoxification of ROS species were upregulated [501, 502]. Moreover, the genes regulating the energy-conversion in chloroplast through glycolysis, fatty

acid synthesis, phylloquinone, and starch biosynthesis, were also induced significantly (Table A4.3, Appendix 4).

6.3.7.3 Genes regulating energy metabolism and synthesis of carbohydrate, lipid, and other bioactive compounds

Genes encoding enzymes like PHOSPHOGLYCERATE MUTASE (*VuPGM*), PYRUVATE KINASE 1 (*VuPK1*), and PHOSPHOENOLPYRUVATE CARBOXYLASE (*VuPPC*), catalyzing key intermediate steps in energy production *via* glycolytic pathway and TCA cycle [300], CARBON CATABOLITE REPRESSOR (*VuCCR4-3*), BETA-GLUCOSIDASE (*VuBGL18/44*), GALACTOSIDASES (*VuAGAL1* and *VuBGAL5*), regulating carbohydrate metabolism, and genes like *VuTPS1*, *VuTPPA*, and *VuMTD* involved in trehalose and mannitol metabolism, were upregulated [503]. Moreover, genes encoding proteins responsible for lipid and wax synthesis like *VuWSD1*, *VuFAR3*, *VuFAD3*, and *VuLACS2*, salvage of purine nucleotides by GUANYLATE KINASE 2-LIKE (*VuGK2*) and ADENINE PHOSPHORIBOSYLTRANSFERASE 5 (*VuAPT5*), one-carbon metabolism regulated by ADENOSYLHOMOCYSTEINASE (*VuAHCY*) and METHYLTRANSFERASE (*VuMET*), were induced. Other induced genes included those encoding enzymes involved in ascorbate biosynthesis L-ASCORBATE OXIDASE (*VuAAO*) and MONODEHYDROASCORBATE REDUCTASE 4 (*VuMDAR4*), engaged in non-enzymatic anti-oxidation of ROS species, and FLAVONOL SYNTHASE (*VuFLS*) and NITRATE REDUCTASE 2 (*VuNIA2* involved in flavonoid and nitrogen metabolism (Table 6.2 and Table A4.3, Appendix 4).

6.3.7.4 Hormone and stress-signaling genes

Gene encoding E3 ubiquitin-protein ligase (*VuSDIR1*) was upregulated, suggesting a role in the modulation of ABA-mediated salt-stress response [504]. In contrast, down-regulation of genes like *VuABI5-2*, *VuSnRK2E*, and *VuRGLG5*, indicated suppression of certain ABA-dependent phenomena like inhibition of seed germination and vegetative growth [505, 506]. The accumulated transcripts for genes regulating auxin biosynthesis (*VuTAR4* and *VuDAO*) [507], their polar transport to regulate shoot meristem initiation, and drought tolerance (*VuZIFL2* and *VuNDL2*) [441, 508], indicated amplified auxin signaling in the transgenic plants. Moreover, upregulation key regulators of GA signaling like *VuGASA6* and *VuGA2OX1* stipulated their possible involvement in seed germination, flowering, and seed maturation [509]. Furthermore, genes encoding GDSL esterase (*VuLTL1*) and RICE SALT SENSITIVE 3

(*VuRSS3*), involved growth and salt tolerance, were induced [510, 511]. Genes encoding TPR repeat-containing thioredoxin (*VuTTL1*), PEROXIDASE E5 (*VuPRXE5*), METHIONINE SULFOXIDE REDUCTASE2 (*VuMRSA2*), and *VuLOL1*, regulating oxidative stress tolerance were induced in the transgenic plants [512-514]. Several other differentially regulated genes associated with various abiotic and biotic stress responses were listed in Table A4.3.

6.3.7.5 Genes encoding transporters, transcription factors, and other signaling proteins

Several genes encoding transporters responsible for the transportation of solutes, ions, and metabolites were differentially regulated in the transgenic lines. Genes involved in sugar transport (*VuSUC4/8*), as well as sugar efflux (*VuSWEET3/6*), were down-regulated [515, 516]. *VuPROT2* encoding a betaine and proline transporter was upregulated, suggesting its role in salt stress tolerance [517]. At the same time, induction of Nrt1/Ptr family protein (*NPF6.4*) indicated nitrogen assimilation *via* nitrate uptake. In contrast, *VuTIP2-1* and *VuNIP6-1* encoding aquaporins were downregulated. However, their function seemed to be compensated by upregulation of *VuNOD26* and *VuPIP1-4* like proteins transporting various uncharged solutes, including water. Several anion/cation transporters were downregulated, whereas genes encoding transporters *VuCSC1*, *VuPOT1*, and *VuSULTR2.1* responsible for calcium, potassium, and sulfate transport were upregulated [518-520]. Transporters regulating homeostasis against heavy metals and their detoxification (*VuCCH*, *VuHIPPP*, *VuDTX35*, etc.) were upregulated [521, 522]. Transcription factors encoded by *VuHBI-1*, *VuPRE5*, *VubHLH74*, and *VubHLH63* positively regulate plant growth and flowering by promoting cell expansion [523-525], and *VuMYB2* and *VuICE2*, involved in cold-response, were upregulated [300, 526]. *VuMUTE* and *VuEPFL1 r*egulating stomatal density and development were upregulated in transgenic plants [527]. Other VuNAC members like *VuVNI2* and *VuXND1*, associated with negative xylem development and secondary cell-wall biogenesis, were downregulated [95, 119]. In addition, upregulation of *ATAF* and *NAP*-like genes *VuNAC2-like* and *VuNAC29-like*, putatively involved in hypoxia, senescence, embryo development, and seed dormancy, was also observed in the transgenic lines.

Table 6.2 Differentially expressed (DE) genes regulating various basal growth and multiple stress signaling in the transgenic lines

Gene name	Protein name	Predicted Function	Category	Effect
		INCREASED CHLOROPHYLL BIOSYNTHESIS		
VuCHLI	magnesium-chelatase subunit ChlI, chloroplastic	catalyzes Mg-protoporphyrin IX synthesis	Enzyme	Up
VuCHLP	geranylgeranyl diphosphate reductase, chloroplastic	catalyzes phytol synthesis	Enzyme	Up
VuALAD	delta-aminolevulinic acid dehydratase, chloroplastic	catalyzes porphobilinogen synthesis	Enzyme	Up
VuPBGD	porphobilinogen deaminase, chloroplastic isoform X1	tetrapolymerization of monopyrrole porphobilinogen (PBG)	Enzyme	Up
VuUROD	uroporphyrinogen decarboxylase	catalyzes late steps of chlorophyll biosynthesis	Enzyme	Up
		CHLOROPLAST, PHOTOSYSTEM AND STOMATAL DEVELOPMENT		
VuRPL24	ribosomal protein L24, chloroplastic	synthesis of chloroplast genome-encoded proteins for optimal plastid performance	Functional protein	Up
VuPTAC16	plastid transcriptionally active 16, chloroplastic	involved in the regulation of plastid gene expression.	Functional protein	Up
VuCURT1C	protein curvature thylakoid 1C, chloroplastic	determines thylakoid architecture	Structural protein	Up
VuFTSZ1-like	cell division protein (CDP) FtsZ homolog 1, chloroplastic	component of plastid division machinery	Structural protein	Up
VuPDV2	plastid division protein 2	component of plastid division machinery	Structural protein	Up
VuGATA22	putative GATA transcription factor 22	involved in chloroplast development and division in cytokinin-dependent manner	Transcription factor	Up
VuGLK1	Golden2 like 1	activator of genes involved in chlorophyll biosynthesis, light harvesting, & electron transport	Transcription factor	Up
VuMUTE	transcription factor MUTE	regulates the stomata formation together with *FAMA* and *SPCH*	Transcription factor	Up
VuEPFL1	epidermal patterning factor 1-like	controls stomatal patterning	Signal peptide	Up
		PRODUCTION OF LIGHT HARVEST AND ELECTRON TRANSPORT COMPONENTS		
VuPSAF	photosystem I reaction center subunit III, chloroplastic	participates in electron transfer from plastocyanin to P700	Structural protein	Up
VuPNSB1	photosynthetic NDH subunit of subcomplex B 1, chloroplastic	shuttles electrons to quinones in the photosynthetic chain	Structural protein	Up
VuLHCB1	chlorophyll a/b binding protein of LHCII type 1	light-harvesting complex (LHC) functioning as a light receptor	Structural protein	Up
VuLHCA6	photosystem I chlorophyll a/b-binding protein 6, chloroplastic	required for NAD(P)H dehydrogenase-photosystem I supercomplex	Structural protein	Up
VuCYP38	cyclophilin CYP38, chloroplastic	required for the assembly and stabilization of PSII	Structural protein	Up
VuPPL1	psbP-like protein 1, chloroplastic	required for efficient repair of photodamaged PSII	Structural protein	Up
WDR36/44	WD repeat-containing protein 36/44	Clock proteins, essential for the proper expression phase and period length of both the oscillator and output genes known to participate in photoperiod sensing	Signal protein	Up
		VARIOUS CHLOROPLASTIC AND CYTOSOLIC STRESS RESPONSES		
VuBAS1	2-Cys peroxiredoxin BAS1, chloroplastic	reduction of H_2O_2 and organic hydroperoxides	Enzyme	Up
VuABC1-like	protein activity of BC1 complex kinase 8, chloroplastic	involved in resistance to oxidative stress, high light and heavy metals (Cd^{2+})	Enzyme	Up
VuFSD1	Fe superoxide dismutase, chloroplastic	destroys superoxide anion radicals	Enzyme	Up
VuDHAR3	dehydroascorbate reductase DHAR3, chloroplastic	involved in redox homeostasis by recycling ascorbate under oxidative stresses	Enzyme	Up
VuAAO	L-ascorbate oxidase	catalyzes ascorbate oxidation to dehydroascorbate	Enzyme	Up
VuMDAR4	monodehydroascorbate reductase 4, peroxisomal	catalyzes the conversion of monodehydroascorbate to ascorbate, oxidizing NADH in the process	Enzyme	Up
VuLQY1	low quantum yield of photosystem II 1, chloroplastic	regulate repair and reassembly of PSII complexes	Enzyme	Up
VuFTSH2	ATP-dependent zinc metalloprotease FTSH 10, mitochondrial	preventing cell death under high-intensity light conditions	Enzyme	Up
VuMPH1	maintenance of psII under high light 1	participates in the maintenance of normal PSII activity under photo-inhibitory stress	Enzyme	Up
VuPRXE5	peroxidase E5	Removal of H_2O_2, oxidation of toxic reductants	Enzyme	Up
VuLOL1-like	protein LOL1	positive regulator of reactive oxygen-induced cell death	Enzyme	Down
VuDREB2C	dehydration-responsive element binding 2C like	regulates drought and cold response	Transcription factor	Up

VuICE1	inducer of CBF expression 1	regulates *DREB1* expression and mediates stomatal differentiation *via SPCH*, *MUTE*, and *FAMA*	Transcription factor	Up
VuATAF-like	NAC domain-containing protein 2- like	response to hypoxia, embryo development ending in seed dormancy	Transcription factor	Up
VuLTL1	GDSL esterase/lipase LTL1	involved in salt tolerance	Stress protein	Up
VuRSS3	rice salt sensitive 3	regulates root cell elongation during salt stress	Stress protein	Up
VuSDIR1	salt- and drought-induced ring finger 1	regulates salt stress and ABA responses	Ligase	Up
VuPOT1	potassium transporter 1	High-affinity potassium transporter involved in K uptake	Transporter	Up
VuTTL1	TPR repeat-containing thioredoxin-like 1	responses to osmotic stress and ABA during germination and seedling development under stress	Stress protein	Up
VuPROT2	proline transporter 2-like	mediates proline and glycine betaine transport, involved in the uptake of compatible solutes	Transporter	Up
VuMTD	mannitol dehydrogenase	oxidizes mannitol to mannose, important in regulating salt tolerance	Enzyme	Up
VuTIP2-1	tonoplast intrinsic protein 2-1	channels water and small soluble solutes	Transporter	Up
VuNIP6-1	nodulin intrinsic protein 6-1	transports boric acid, glycerol, urea, and formamide	Transporter	Down
VuPCR2	plant cadmium resistance 2	involved in the detoxification of excess zinc and cadmium	Transporter	Down
VuCAX3	vacuolar cation/proton exchanger 3	translocates Ca^{2+} and other metal ions into vacuoles using the proton for ion homeostasis	Transporter	Down
VuCCH	copper transport protein CCH	involved in copper homeostasis	Transporter	Up
VuHIPP07/31	heavy metal-associated isoprenylated plant protein 7/31	heavy metal homeostasis and detoxification	Transporter	Up
VuDTX35	detoxification 35	multidrug and toxin efflux transporter involved in flavonoid metabolism and reproductive development	Transporter	Up
VuPLP1	patatin-like protein 1	dual role as a somatic storage protein and as an enzyme involved in host resistance	Storage protein	Up
		IMPROVED GROWTH AND STRESS ASSOCIATED HORMONE SIGNALING		
VuABI5-2	abscisic acid insensitive 5-like protein 2	participates in abscisic acid-regulated gene expression during seed development	Kinase	Down
VuSRK2E	serine/threonine-protein kinase SRK2E	activates ABA signaling	Kinase	Down
VuRGLG5	ring domain ligase 5	together with RGLG1, mediates degradation of PP2CA to regulate ABA signaling	Ligase	Down
VuTAR4	tryptophan aminotransferase-related protein 4	regulates auxin biosynthesis	Enzyme	Up
VuDAO	dioxygenase for auxin oxidation 1	essential for auxin catabolism and maintenance of auxin homeostasis in reproductive organs	Enzyme	Up
VuNDL2	N-MYC downregulated-like 2	regulates root auxin transport and carriers (PIN2 and AUX1) to initiate meristem and branching	Signal protein	Up
VuZIFL1	Zinc-induced facilitator 1	involved in auxin efflux and shootward transport at the root apex	Transporter	Up
VuAUX22A	auxin-induced protein 22A	represses early auxin response genes at low auxin concentrations	Signal protein	Up
VuAHP1	histidine-containing phosphotransfer protein 1	propagates cytokinin signal transduction through the multistep His-to-Asp phosphorelay	Signal protein	Down
VuARR17	two-component response regulator ARR17	response regulator involved in His-to-Asp phosphorelay	Signal protein	Up
VuGASA4	gibberellin-regulated protein 4	regulation of floral meristem and floral organ identity, and promotion of seed size and weight	Signal protein	Up
VuGASA6	gibberellin-regulated protein 6	regulates seed germination, flowering, and seed maturation	Signal protein	Up
VuACO	aminocyclopropane-1-carboxylate oxidase	involved in the ethylene biosynthesis	Enzyme	Up
VuCTR1	constitutive triple response 1	negative regulator in the ethylene response pathway	Kinase	Down
VuTIFY10B	TIFY 10B protein	repressor of jasmonate (JA) responses	Signal protein	Up
VuRGLG4	ring domain ligase 4	upstream modulator of jasmonate (JA) signaling	Ligase	Down
VuCML11	calmodulin like protein 11	calcium sensor	Signal protein	Up
		INCREASED PLANT DEVELOPMENT AND CELL DIVISION		
VuNAP	NAC transcription factor 29-like	regulates leaf senescence, cell growth, flower-development, fruit-ripening	Transcription factor	Up
NAC83-like	NAC domain-containing protein 83-like	repressor of *VND7* that regulates xylem vessel formation	Transcription factor	Down
NAC104-like	NAC domain-containing protein 104-like	repressor of SCW fiber synthesis and programmed cell death	Transcription factor	Down
VuHBI-1	transcription factor HBI1	regulator of cell elongation by activating *EXPA1* and *EXPA8*	Transcription factor	Up
VuPRE5	transcription factor PRE5	integrates multiple signaling pathways to regulate cell elongation and plant development.	Transcription factor	Up
VuMYB2-like	myb-related protein 2	involved in cell cycle progression	Transcription factor	Up

VubHLH63/74	transcription factor bHLH63/74	activates cell elongation and triggers flowering by promoting of *FT* gene	Transcription factor	Up
VuHHO5	transcription factor HHO5	regulates floral meristem homeostasis and organ number in the flower	Transcription factor	Up
VuDFC	downstream of FLC	part of a three-gene cluster (*FLC*, *UFC,* and *DFC*) regulated in response to vernalization	Functional protein	Up
VuLEGB	legumin B	protein found in the seeds and is the source of sulfur-containing amino acids in seed meals	Storage protein	Up
VuSCPL26	serine carboxypeptidase like 26	positive regulator of grain size by controlling grain size, filling, and weight	Signal protein	Up
VuMARD1	mediator of ABA-regulated dormancy 1	facilitate the interaction of SnRK1 complex with effector proteins, controls seed dormancy	Signal protein	Down
VuDRMH1	dormancy-associated protein 1	role in stress signaling	Signal protein	Down
VuSEOB	sieve element occlusion B	scaffold protein required to form the phloem filament matrix in sieve elements	Structural protein	Up
VuROPGEF12	rop guanine nucleotide exchange factor	activator of Rop GTPases to modulate root stem cell maintenance by expressing *PLT1* and *PLT2*	Signal protein	Up
VuGDI1	rho GDP-dissociation inhibitor 1	regulates the GDP/GTP exchange reaction of the Rho proteins	Signal protein	Up
VuLRP1	lateral root primordium 1	modulates root growth, stamen development, cell expansion, flowering, and SAM maintenance	Transcription factor	Up
VuEXPA8	expansin-A8	causes loosening and extension of plant cell walls	Transcription factor	Up
VuEXT	extensin	hydroxyproline-rich glycoproteins (HRGPs) of the plant cell wall	Structural protein	Up
VuRWA2	reduced wall acetylation 2	acetylation of cell wall polymers and xylan during secondary wall biosynthesis	Enzyme	Up
VuTBL39	trichome birefringence like 39	bridging protein that binds pectin and other cell wall polysaccharides	Structural protein	Up
VuWAT1	walls are thin 1	required for secondary wall formation in fibers, especially in short days conditions	Structural protein	Up
VuXET1/9	xyloglucan endotransglucosylase/hydrolase 1/9	participates in the cell wall construction of growing tissues under mechanical stress.	Enzyme	Up
VuCESA1	cellulose synthase A catalytic subunit 1	subunit of cellulose synthase terminal complexes required cell wall formation	Enzyme	Up
VuENG6	endoglucanase 6	endohydrolysis of (1->4)-beta-D-glucosidic linkages in cellulose and glucans	Enzyme	Up
VuBGN4	glucan endo-1,3-beta-glucosidase 4	Hydrolysis of (1->3)-beta-D-glucosidic linkages in (1->3)-beta-D-glucans	Enzyme	Up
VuCAD6	cinnamyl alcohol dehydrogenase 6	Involved in lignin biosynthesis	Enzyme	Up
VuCCR1	cinnamoyl-CoA reductase 1	Involved in lignin biosynthesis	Enzyme	Up
VuERECTA	LRR receptor-like serine/threonine-protein kinase	receptor kinase that, together with ERL1 and ERL2	Signal protein	Up
VuTUBA3	tubulin alpha-3 chain	a major constituent of microtubules	Structural protein	Up
VuCYCD3-1	cyclin-D3-1	activate cell cycle in the root apical meristem (RAM) and promote embryonic root	Signal protein	Up
VuCDC2	cell division control protein 2	functions in cell division and growth processes	Signal protein	Up
VuYAB1	axial regulator YABBY 1	regulates the initiation of embryonic SAM, required during flower development	Signal protein	Up
VuMAIL1	MAIN-LIKE 1-like	cell fate determination by organizing SAM and RAM and cell division in meristematic cells	Signal protein	Up
VuCYCLIN-1	G2/mitotic-specific cyclin S13-7	essential for the control of the cell cycle at the G2/M (mitosis) transition	Signal protein	Up
		IMPROVED ENERGY PRODUCTION AND METABOLITE/SOLUTE TRANSPORT		
VuHEX6	hexose carrier protein HEX6	active uptake of hexoses, such as glucose/hydrogen symport	Transporter	Up
VuSUC4	sucrose transport protein SUC4	responsible for sucrose/hydrogen symport into the cell	Transporter	Down
VuSWEET3	bidirectional sugar transporter SWEET3	mediates both low-affinity uptake and efflux of sugar across the plasma membrane	Transporter	Down
VuPFPB	pyrophosphate--fructose 6-phosphate 1-phosphotransferase	catalyzes the first committing step of glycolysis	Enzyme	Up
VuPGM	phosphoglucomutase, cytoplasmic	converts Glucose 1-phosphate to 6-phosphate	Enzyme	Up
VuPGAM	phosphoglycerate mutase	conversion of 3-phosphoglycerate to 2-phosphoglycerate	Enzyme	Up
VuPK	pyruvate kinase 1, cytosolic	catalyzes the final step of glycolysis, converting ADP and phosphoenolpyruvate (PEP) to ATP	Enzyme	Up
VuPPC	phosphoenolpyruvate carboxylase	catalyzes the formation of oxaloacetate from phosphoenolpyruvate via the TCA cycle	Enzyme	Up
VuPKP2	plastidial pyruvate kinase 2	required for plastidial pyruvate kinase activity and seed storage compounds mobilization upon germination	Enzyme	Up
VuDXS	probable 1-deoxy-D-xylulose-5-phosphate synthase 2, chloroplastic	formation of DXP for isoprenoid biosynthesis & chloroplast development	Enzyme	Up
VuGLYR2	glyoxylate/succinic semialdehyde reductase 2, chloroplastic	reduces glyoxylate to glycolate and succinic semialdehyde (SSA) to gamma-hydroxybutyrate	Enzyme	Up

VuGBSS2	granule-bound starch synthase 1, chloroplastic/amyloplastic	involved in the pathway starch biosynthesis	Enzyme	Up
VuACP1	acyl carrier protein 1, chloroplastic	carrier of the growing fatty acid chain in fatty acid biosynthesis	Enzyme	Up
VuFAD	omega-3 fatty acid desaturase, chloroplastic	biosynthesis of 16:3 and 18:3 fatty acids, important constituents of plant membranes	Enzyme	Up
VuWSD1	O-acyltransferase WSD1	Involved in cuticular wax biosynthesis	Enzyme	Up
VuFAR3	fatty acyl CoA reductase 3	catalyzes activation of FA for lipid synthesis or degradation	Enzyme	Up
VuEXL3	GDSL esterase/lipase EXL3	hydrolyzes ester bonds in lipids	Enzyme	Up
VuGPT2	glucose-6-phosphate/phosphate translocator 2, chloroplastic	transports Glc6P into plastids for starch, fatty acid biosynthesis or NADPH synthesis	Transporter	Up
VuPLGG1	plastidal glycolate/glycerate translocator 1, chloroplastic	glycolate/glycerate transporter required for photorespiration	Transporter	Up
VuBT1	adenine nucleotide transporter BT1, chloroplastic	nucleotide uniport carrier required to export newly synthesized adenylates into the cytosol	Transporter	Up
VuURH2	probable uridine nucleosidase 2	Involved in pyrimidine breakdown	Enzyme	Up
VuGK2	guanylate kinase 2	recycles GMP	Enzyme	Down
VuGDA	guanosine deaminase	catalyzes the hydrolytic deamination of guanine, producing xanthine and ammonia	Enzyme	Up
VuAHCY	adenosylhomocysteinase	synthesizes L-homocysteine from S-adenosyl-L-homocystein	Enzyme	Up
VuMET	5-methyltetrahydropteroyltriglutamate--homocysteine methyltransferase	catalyzes the transfer of a methyl group to homocysteine resulting in methionine formation	Enzyme	Up
VuRIDA	reactive intermediate deaminase A, chloroplastic	involved in isoleucine biosynthesis	Enzyme	Up
VuAKHSDH2	aspartokinase/homoserine dehydrogenase 2, chloroplastic	involved in lysine and aspartate family biosynthesis	Enzyme	Up
VuGAD1	glutamate decarboxylase 1	catalyzes the production of GABA	Enzyme	Down
VuGGH	gamma-glutamyl hydrolase	plays a role in folate stability and intracellular folate content	Enzyme	Up
VuDHNAT1	1,4-dihydroxy-2-naphthoyl-CoA thioesterase 1	catalyzes the formation of naphthoquinone ring of phylloquinone (vitamin K1)	Enzyme	Up
VuACL5	thermospermine synthase ACAULIS5	prevents premature death of the xylem vessel elements	Enzyme	Up
VuFLS	flavonol synthase/flavanone 3-hydroxylase	catalyzes the formation of flavonols from dihydroflavonols	Enzyme	Up
VuCCR4-3	carbon catabolite repressor protein 4 homolog 3	prevents the expression of genes required for the utilization of secondary *carbon* sources	Enzyme	Up
VuBGL18	beta-glucosidase 18	hydrolyzes the glycosidic bonds in beta-D-glucosides and oligosaccharides to release glucose	Enzyme	Up
VuSUS2-like	sucrose synthase 2	a sucrose-cleaving enzyme that provides UDP-glucose and fructose	Enzyme	Down
VuTPS1	alpha-trehalose-phosphate synthase	catalyzes trehalose 6-phosphate synthesis	Enzyme	Up
VuNIA2	nitrate reductase 2	the key enzyme involved in the first step of nitrate assimilation	Enzyme	Up
VuNPF6.4	NRT1/ PTR family 6.4	involved in constitutive nitrate uptake	Transporter	Up
VuNOD26	nodulin-26	transport a variety of uncharged solutes ranging from water to ammonia to glycerol	Transporter	Up
VuPIP1-4	plasma membrane intrinsic protein 1-4	facilitate the transport of water and small neutral solutes across cell membranes	Transporter	Up
VuALMT12	aluminum-activated malate transporter 12	malate-sensitive anion transporter permeable to chloride, nitrate, sulfate, and malate	Transporter	Down
CSC1	calcium-permeable stress-gated cation channel 1-like	Acts as an osmosensitive calcium-permeable cation channel for Ca^{2+}, K^{+}, and Na^{+}	Transporter	Up
SULTR2.1	sulfate transporter 2.1	Low-affinity H^{+}/sulfate cotransporter, playing a central role in sulfate assimilation	Transporter	Up

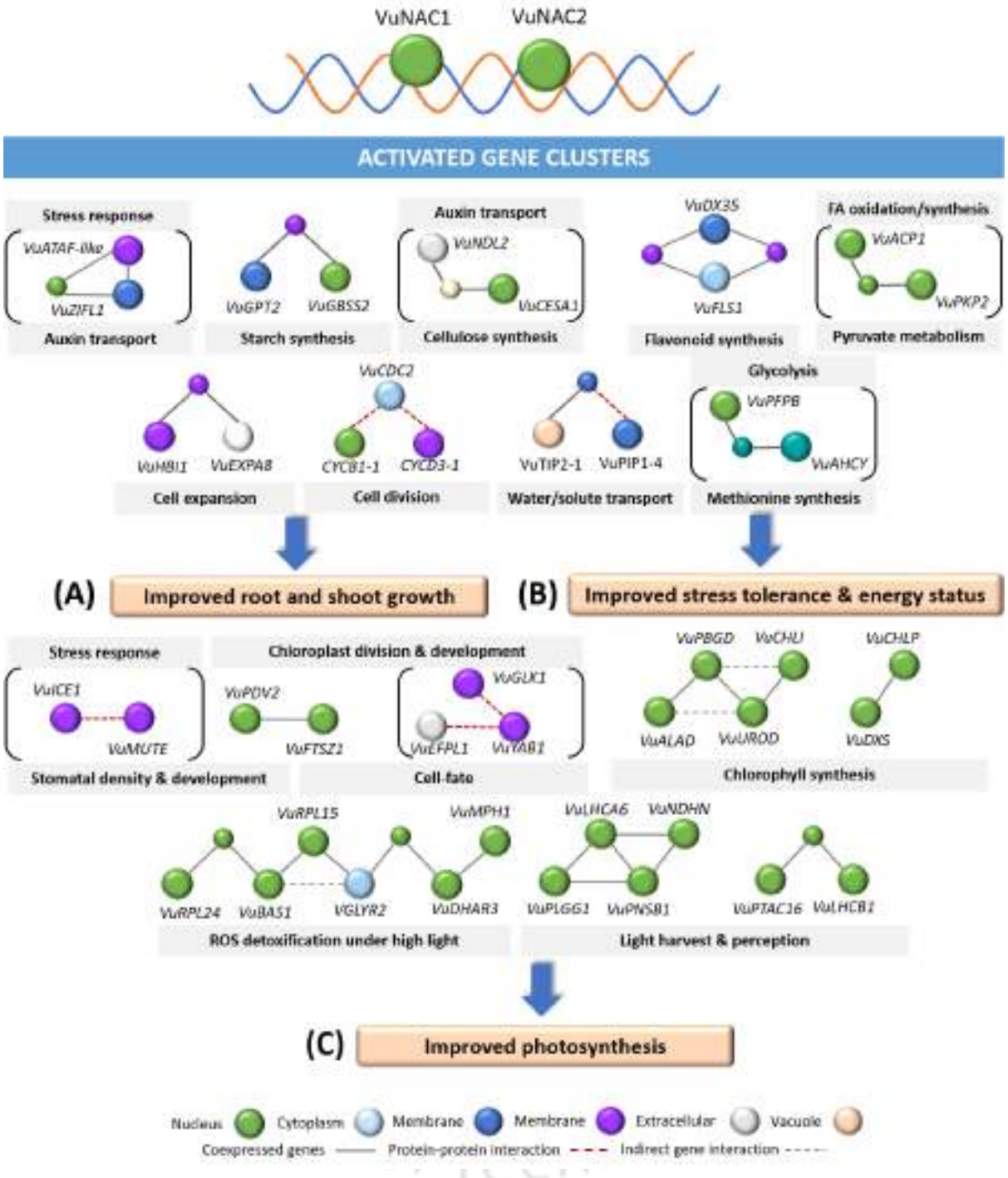

Fig. 6.13 Proposed mechanisms of VuNAC1/2-mediated signaling. (A) transcriptional reprogramming of gene targets regulating disparate plant processes. **(B)** The clusters of activated genes regulating cell proliferation, cell wall biogenesis, increased homeostasis in ROS level, water status, energy, and enhanced production of the photosynthetic machinery in the transgenic plants.

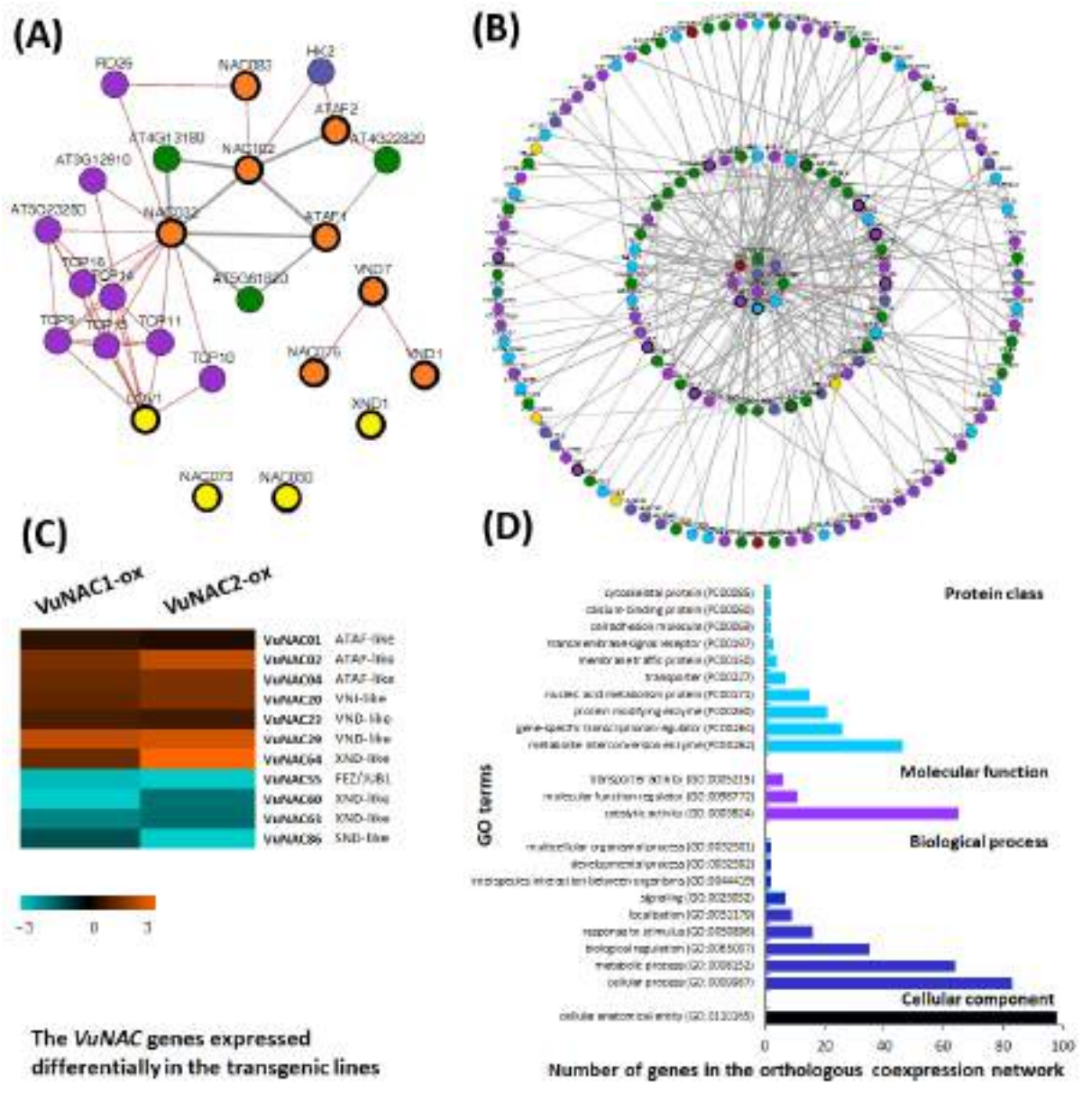

Fig. 6.14 Regulatory network of VuNAC1/2 TFs based on the homologous interactome. (A) Network of Arabidopsis NAC homologous to the VuNAC TFs up-regulated (shaded in orange) and down-regulated (shaded in yellow) in the VuNAC1/2 expressing transgenic plants. **(B)** interactome of co-expressing genes (connected by grey lines) and protein-protein interactions (denoted by red lines) (right). **(C)** Heat-map depicting the VuNAC members differentially expressed in the transgenic lines. **(D)** Gene ontology (GO) analysis of the genes comprised in the network to annotate the underlying cellular, molecular and biological function.

6.4 DISCUSSION

Drought and salt cause more yield loss in crops than all other pathogens combined. In addition, stress adaptation often comes with a yield penalty. Various physiological and metabolic adjustments can collaterally impede plant growth, degrade productivity, or both, despite stress tolerance. Cowpea is widely consumed as a pulse crop but also grown as a fodder plantation. Although the crop is somewhat drought and heat tolerant, aggravated and terminal stress can severely cause growth and yield loss. Thus, it was imperative to identify genetic determinants, which can improve tolerance to versatile climatic challenges with the simultaneous refinement of growth. In this paper, we characterized and identified functional roles of two untapped native NAC genes in cowpea, which integrated growth and stress signaling without any trade-off to manifest unique phenotype from their orthologs in Arabidopsis, rice, and soybean.

Our study showed that the constitutive overexpression of unique VuNAC1/2 TFs cloned from a drought-hardy genotype (*Kannanado White*) (Fig. 6.1) conferred accelerated embryonic, vegetative, as well as reproductive growth (Fig. 6.2, Fig. 6.3B and Fig. 6.4C), reflecting improved morphological, physiological traits and agronomic traits such as leaf area, leaf count, root density and nodule abundance (Fig. 6.4B), stomatal density, photosynthetic activity (Fig. 6.6D), chlorophyll content (Fig. 6.8A), pod count, pod-size and seed weight (Fig. 6.4 and Table 6.1), in a moderately tolerant commercial *Pusa Komal* variety (Fig. 6.1). In compliance with the gain-of-function phenotype, the silenced phenotype of VuNAC1-si and VuNAC2-si showed suppression of seedling emergence, foliage growth, and floral transition, thereby compromised the seed yield (Fig. 6.5). When exposed to prolonged drought, salinity, heat, and cold stress, the transgenic lines (VuNAC1-ox and VuNAC2-ox) recovered their vegetative growth and restored flowering to secure the yield potential (Fig. 6.6, Fig. 6.7 and Fig. 6.9). The transgenic plants produced at least two healthy flushes of healthy pods bearing mature seeds, unlike the wild type plants that stayed green while producing lesser pods (Fig. 6.10). Identifying transcriptional targets by RNA-seq analysis of VuNAC1-ox and VuNAC2-ox revealed that the TFs integrate disparate plant signaling to improve multiple-stress tolerance along with agronomic traits to mitigate yield penalty. The transcriptome study also revealed various gene-targets reprogramming organogenesis, cell-proliferation, photosynthesis, cell metabolism, and stress tolerance (Fig. 6.11, Fig.6.11, Table 6.2, and Table A4.3).

The improved post-germinative growth displayed by the transgenic seedlings (Fig. 6.3, indicated that VuNAC1/2 TFs play roles in transitioning from heterotrophic to autotrophic phase by encoding photosynthetic apparatus in the chloroplast and metabolic machinery for carbohydrate synthesis, nitrogen transport, and assimilation (*VuNIA2* and *VuNPF6.4*) to ensure C/N availability, as indicated by the transcriptome analysis [451]. Even later, the improved agronomic traits of the transgenic plants were accompanied by an enriched reserve of the root nodules and increased leaf stomatal density. Upregulation of genes involved in flavonoid biosynthesis like *VuFLS* indicated their possible involvement in increasing nodule formation and better nitrogen fixation in transgenic plants by attracting rhizobial symbionts and inducing the Nod factors required for nodule induction [528, 529]. The reproductive recovery of the transgenic lines the drought, salinity, heat, and cold stress (Fig. 6.6C, Fig. 6.7, and Fig. 6.9) and early heading time during the optimum conditions (Table 6.1) indicated the possible role of VuNAC1/2 TFs in modulating flower initiation during suitable as well as adverse environmental conditions. The induction of *VuDFC*, *VubHLH63*, *VuHHO5* in the transgenic plants and possible interaction with VuCDF2 and VuNAC052 like proteins suggested their involvement (Fig. 6.12 and Table A4.3, Appendix 4). Moreover, in contempt of the substantial improvement in the pod yield, the plants seemed to project early leaf senescence, which is crucial for nutrient remobilization in seeds. Thus VuNAC1/2 TFs control exogenous nutrient assimilation, as well as the endogenous synthesis of the organic bio-compounds *via* photosynthesis to ensure energy balance and secured yield by controlling flowering. Both of these phenomena are crucial for growth and yield recovery after stress.

The function of NAC TFs is determined by the set of target genes they recruit for the transcriptional tuning. The over-expression of VuNAC1 and VuNAC2 TFs induced and suppressed diverse genes encoding other stress-responsive TFs, ion/solute transporters, signaling kinases and proteinases, metabolic enzymes, structural and photosynthetic components (Fig. 6.11, Fig. 6.12, Table 6.2 and Table A4.3, Appendix 4, accounting for their multifaceted and unique roles from their orthologs in other plant species. According to the RNA-seq data (Fig. 6.14B), expression analysis of silenced lines (Fig. 6.5D), the paralogs VuNAC1 and VuNAC2 appeared to coexpress and co-function to execute the stress signaling and growth functions (Fig. 6.2, Fig. 6.3C, Fig. 6.6 and Fig. 6.7). Moreover, the transcript of several other VuNAC members was also altered in the transgenic lines indicating their coexpression or transcriptional tuning through VuNAC1/2. For instance, VuNAC4 (ATAF-like), VuNAC23 and VuNAC29 (VND-like), VuNAC20 (VND INTERACTING-like), and

VuNAC66 (XND-like), putatively involved in abiotic and biotic stresses and xylem vessel differentiation, like their Arabidopsis orthologs, were upregulated. In contrast, VuNAC63 and VuNAC64 (XND-like), VuNAC86 (SND-like), and VuNAC55 (JUB-like) were downregulated during the vegetative phase. This indicated negative regulation of the VuNAC members that may induce dwarfism and delay flowering time. The orthologous Arabidopsis relative to the differentially expressed VuNAC members formed a network of co-expressed genes and interacting proteins, as shown in Fig. 6.14A and Table A4.4, Appendix 4. The network also indicated the functional relationship of other NAC members, such as NAC007, NAC052, and NAC062, with the ATAF-like VuNAC1/2, to regulate growth, development, and stress-regulatory functions.

Furthermore, various target genes involved in morphogenesis, organogenesis, cell proliferation, and development were uncovered by the transcriptome analysis. The target suggested that VuNAC1/2 TFs promote growth and proliferation by activating enzymes and the proteins regulating cell wall elasticity, expansion, structural biogenesis, and cell division, as shown in Fig. 6.12 [485, 486]. The upregulation of enzymes catalyzing cell-wall acetylation and synthesis of nucleotide sugars and mannans might improve the leaf epidermis integrity and architecture of the transgenic plants [487, 488]. Genes like *VuMARD1* and *VuLEGB* might be controlling the reduced dormancy and increased seed weight of the transgenic seeds [491, 492]. Moreover, VuNAC1/2 TFs might activate genes signaling mitosis and cytoskeleton formation, cyclins, and protein kinases (such as *VuMHK* and *VuERECTA*), controlling meristem initiation and cell proliferation in the germinating seeds and other growing tissues [493, 494]. Also, components of photosystem (PSI and PSII) required for efficient light-capturing, extrinsic oxygen-evolving, electron shuttling, and protection of the photosynthetic apparatus under high-intensity light and oxidative stress were upregulated in the transgenic plants [496-498, 501, 502]. Besides, activation of genes involved in stomatal density (*VuMUTE* and *VuEPFL1*), chloroplast division, and biosynthesis of porphobilinogen (PBG) and tetrapyrrole might control photosynthetic performance under high and/or low light to boost light harvest, electron transfer, and chlorophyll biosynthesis, supporting carbon capturing and stress recovery [500]. Further, upregulation of genes regulating carbohydrate and lipid biosynthesis, less-costly salvage synthesis of purines indicated improved energy balance in the transgenic plants. Moreover, induction of genes synthesizing trehalose 6- phosphate and trehalose, which repress carbon starvation signals and carbohydrate synthesis, also served as a marker for carbon availability and energy sufficiency in the transgenic plants [503].

Additionally, multiple hormone signaling pathways, including ABA, auxin, GA, and ethylene, crucial for germination, flowering, and seed maturation, were affected in the transgenic lines [509]. Apart from growth-associated genes, several stress-responsive genes encoding TFs, transporters, and signaling proteins were also differentially regulated while constitutive expression of the VuNAC1/2 TFs. Our study indicated the multi-faceted VuNAC1/2 TFs unified growth and stress signaling to result in sustainable improvement of stress tolerance and agronomic traits in cowpea legume, without any detrimental trade-off.

7. Conclusions

7. CONCLUSIONS AND FUTURE PERSPECTIVES

7.1 Research outcomes and the challenges addressed

Abiotic challenges are the primary culprits that limit the growth and yield potential of the legume crops endangering food and nutritional security. However, the available tolerance measures are either incompetent to fight multiple cues, and/or their ubiquitous and constitutive overexpression causes detrimental effects on the normal growth, physiological, and metabolic due to energy imbalance or unwanted crosstalk of stress signaling. Energy imbalance can occur due to overexpression of stress-regulatory signaling resulting in a growth penalty. Despite continuous molecular breeding and genetic engineering endeavors, improving stress tolerance without the growth/tolerance trade-off has been challenging.

To tackle the growing challenges of legume production, exploring untapped stress regulators from the crop gene pool of a robust and relative legume model is required to improve growth and tolerance simultaneously. Moreover, a comprehensive understanding of the underlying gene network and associated signaling cascades is mandatory to avoid undesirable traits and avail multiple benefits through the ubiquitous expression of a single gene. After a thorough literature review, we found NAC transcription factors a versatile candidate to acquire sustainable legume improvement by fighting combinatorial effects of field stress. Moreover, cowpea seemed the ideal legume model to explore stress signaling, owing to its climate hardiness, ability to thrive forage growth, short-life cycle, genetic closeness to major legumes, convenient genetic manipulation, and easy-to-study morphological traits. However, no NAC members have been studied. The recent availability of a comprehensive draft genome created the headway to study the cowpea NAC family (VuNAC) that remained unexplored to date.

In the first chapter, we identified 130 VuNAC proteins that were classified into eight phylogenetic groups. Twenty-seven proteins clustered as a distinct group (GVII) with no significant similarity with known NAC proteins indicated their cowpea-specific evolution and expansion. The family exhibited prominent segmental and tandem duplication resulting in a large stress-responsive (SNAC) group and paralogous gene clusters. The cowpea NAC family possesses unique features implying their novelty and functional diversity. VuNAC proteins owned multipartite nuclear signals, unique transactivation-region with conserved motifs, and even embodied non-NAC domains to display chimeric function. The genes were associated with unique promoter architecture rich in TC elements, stipulated in stress-regulation. Further,

the promoter and interactome analysis revealed multi-tier regulation of VuNAC genes through light, hormone, and transcription factors (NAC/MYB/WRKY/ERF and Dof/TCP), suggesting cross-talk between stress and growth-regulating signals. The genes may associate with metabolic processes like trehalose and folate synthesis, carbohydrate transport, lipid signaling, and electron transfer. Our study presents potential candidates for genetic manipulation that can blend stress tolerance and physiological growth to improve crop yield through their versatile function.

In the next chapter, we isolated two novel ATAF-like VuNAC1 and VuNAC2 TFs from *Kannando White*, a robust cowpea variety, using a combination of *in-silico* and molecular biology approaches to hunt the stress-responsive candidates with unique regulatory regions. The expression analysis revealed significant induction of both the genes by dehydration, salinity, aluminum, heat, cold, light, ABA, and MeJA, suggesting their crucial role in multiple stress signaling pathways. The molecular characterization of the VuNAC1/2 proteins validated their nuclear localization, dimerization, and transactivation ability. Prediction of the protein structure revealed three-dimensional folding similar to rice SNAC1. The purified proteins formed dimeric conformation and bind to a MYC-like 'GTACACGTGC' NACBS, consisting 'CACG' core. Heterologous expression of the VuNAC proteins in the yeast system displayed elevated growth rate, enhanced biomass, and extended life span of the host strains. The strains survived nutrition exhaustion in the late stationary phase exhibiting healthy and proliferative growth. In addition, the *VuNAC* genes conferred tolerance to multiple abiotic stresses with improved fermentation efficiency and cellular composition of lipids and membrane polysaccharides. The metabolome analysis revealed reprogramming of central primary metabolisms such as nucleotide, vitamin B, cofactors, amino acid, and other energy-generating pathways. Our results suggested that VuNAC1/2 TFs maintain energy homeostasis by fuelling cellular bioenergetics *via* boosting nutritional biosynthetic and salvage pathways. The TFs are the activator of stress-tolerance signaling as well as cell proliferation processes acting through metabolic reprogramming (Fig. 7.1). These findings motivated further functional validation of the VuNAC1/2 TFs in the plant model, owing to their potential involvement in the growth, multiple stress responses, phytohormone-, and light signaling.

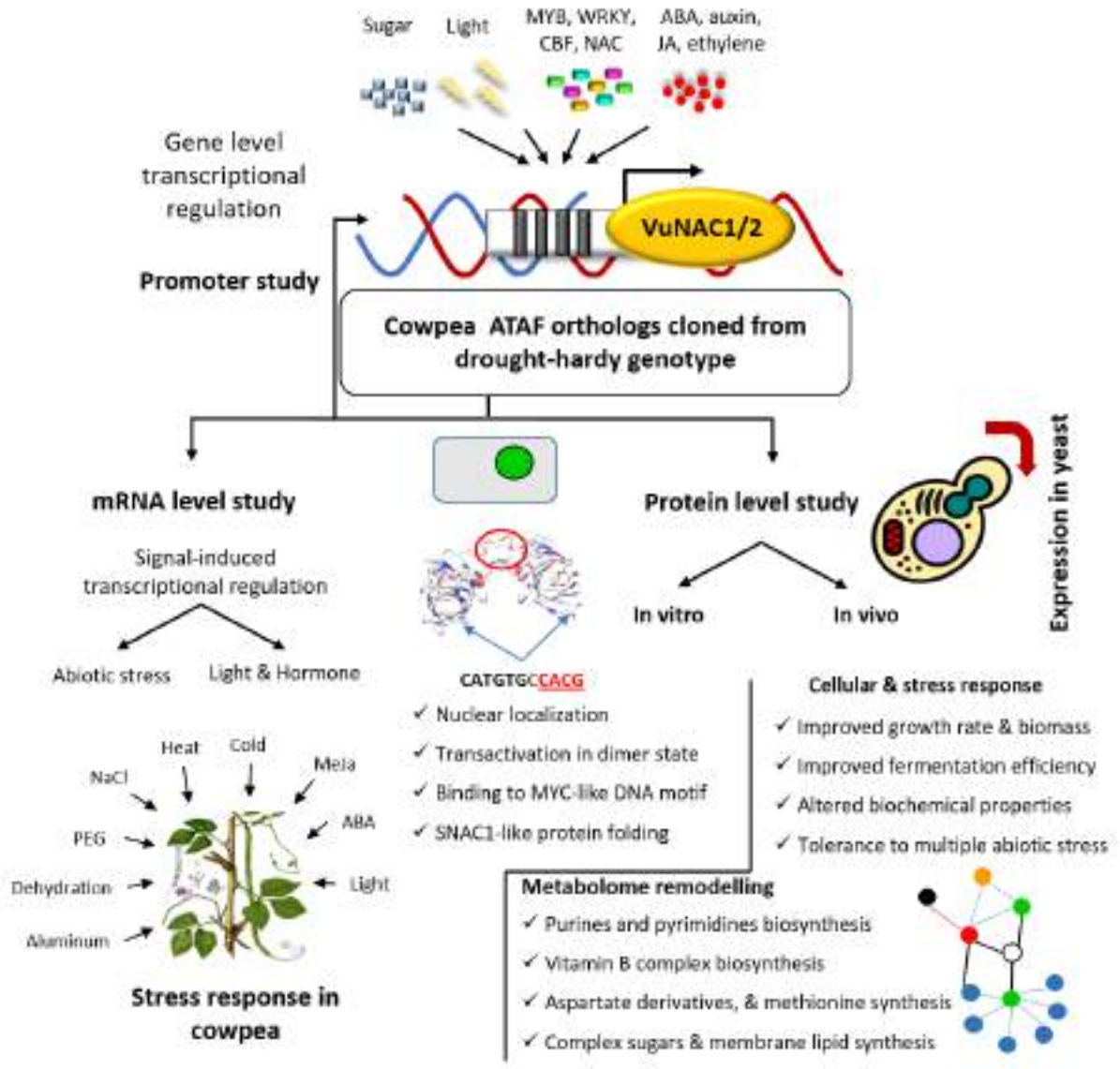

Fig. 7.1 Transcriptional model of VuNAC1/2 TFs.

The third chapter of the thesis discussed the heterologous functional study of the VuNAC1/2 TFs in Arabidopsis. The transgenic plants exhibited improved post-embryonic, rosette, and axillary growth, predominantly under the carbon-deficit conditions, along with increased stomatal density and photosynthetic parameters (CO_2 assimilation, stomatal conductance, photosystem quantum-yield, and electron transport rate). The transgenic seedlings showed reduced ABA-induced seed-dormancy and growth inhibition under a high concentration of ABA and auxin, showing better embryonic growth. Moreover, the seedlings displayed improved growth and tolerance to multiple abiotic stress stimuli such as dehydration, salinity, metal toxicity, and oxidative stress induced by PEG, NaCl, aluminum, cadmium, and H_2O_2. The plants manifested remarkable recovery of vegetative and reproductive growth from

prolonged dehydration and high salinity, displaying better water status, reduced membrane damage, and increased accumulation of proline, and glutathione, and ascorbate, forming the redox-hub. The interactome analysis indicated coexpression of the two TFs, providing a comprehensive picture of the coordinated changes in cellular metabolism, hormone, and stress signaling underlying seed development and germination associated with the VuNAC1/2 transcription factors. Moreover, like DREB TFs, the peculiar VuNAC1/2 TFs execute their functions growth and stress responses through both ABA-dependent as well as ABA-independent mechanisms. Our study in Arabidopsis validated the positive regulation stress-response and plant growth, *via* cross-talk of stress signals with photosynthesis and carbon utilization. Unlike their orthologs from other species, these cowpea TFs can overcome the growth trade-off by balancing the hormonal perturbations, nutrition availability and ROS levels (Fig. 7.2).

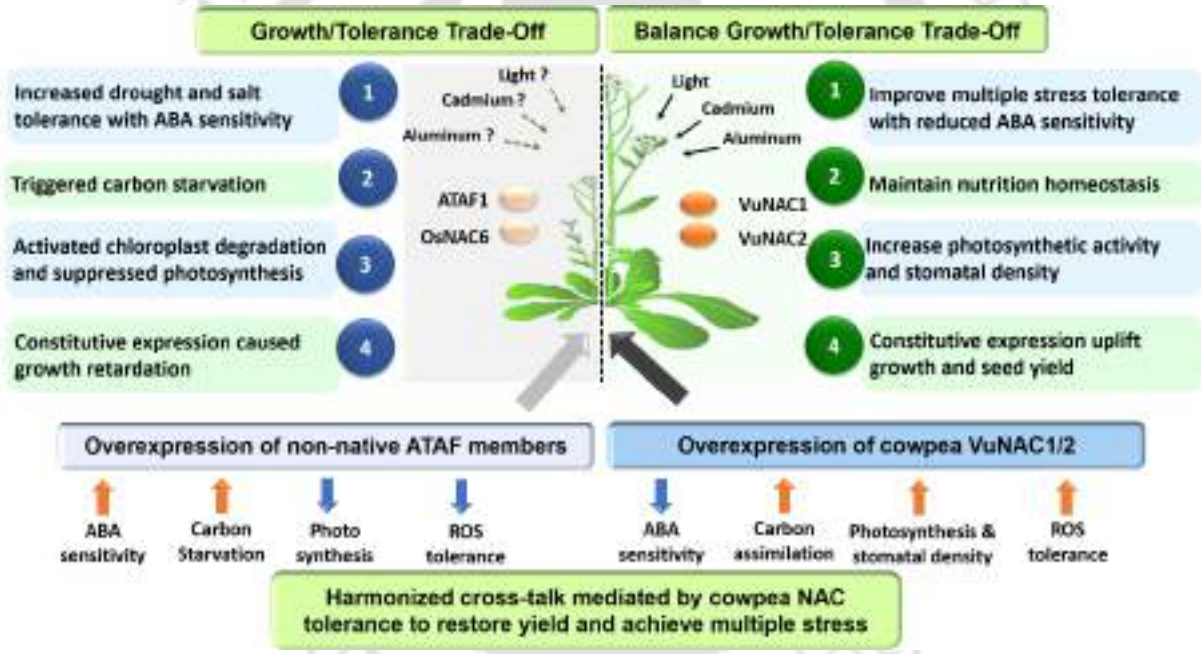

Fig. 7.2. A gene model to overcome growth trade-off. VuNAC1/2 conferred multiple stress tolerance besides constitutive overexpression by a simultaneous improvement of photosynthesis and nutrition homeostasis, in contrast to their orthologs in Arabidopsis (ATAF1) and rice (OsNAC6). Moreover, the transcription factors seemed to play a crucial role in light signaling and metal toxicity.

In the last chapter, we described overexpression of the VuNAC1/2 TFs to improve the agronomic traits, yield, and multiple stress tolerance, using the native genes. The transgenic cowpea seedlings manifested accelerated seed germination with sturdier morphology and increased biomass. The mature plants showed improved foliage growth exhibiting greater leaf area, plant height, and stem diameter, denser root rich in nodules, accompanied by increased

production of pods (~2-fold and ~1.4-fold) and seed weight (10.3% and 6.0%). The transient virus-induced silencing of the TFs impaired growth and flowering, indicating their indispensability for plant growth. In addition, the transgenic plants conferred tolerance to drought stress, implicated in the greenhouse and field-mimicked conditions, sustaining both growth and yield by reducing evapotranspiration and stomatal-regulation, efficient water use, and improved photosynthetic efficiency.

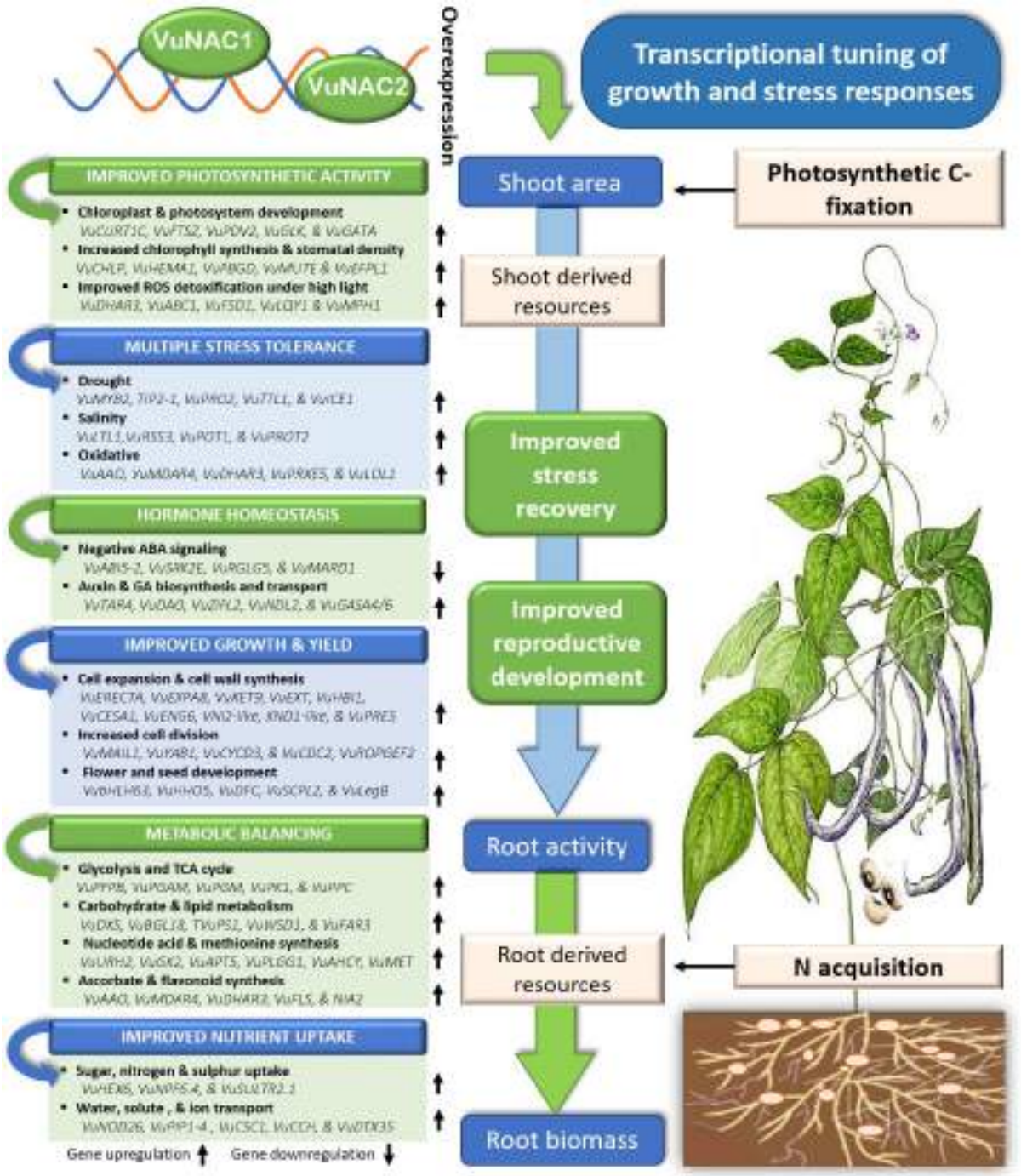

Fig. 7.3 Proposed mechanisms of VuNAC1/2-mediated signaling. Transcriptional reprogramming of gene targets regulating disparate plant processes.

The plants showed remarkable recovery of yield potential after acute salt stress by sequestration of Na^+ and K^+ in root tissue and retaining the flower initiation and seed productivity after the heat and cold stress. The early heading of age-induced leaf-senescence in the transgenic lines may be involve in the nutrient remobilization required for pod maturation and seed reserve. The transcriptome analysis revealed transcriptional-tuning of chloroplastic and genomic genes regulating growth, biogenesis, energy metabolism, hormone, and stress signaling, consolidating diverse plant processed *via* VuNAC1/2 TFs (Fig. 7.3). The study indicated potential genes of photosynthesis, carbon and nitrogen metabolism, hormone signaling and homeostasis, cell cycle, organogenesis, and stress tolerance, targeted by the VuNAC TFs.

7.2 Future Research Perspectives

The unique cowpea TFs, VuNAC1 and VuNAC2 hold great potential overcoming growth trade-off and conferring multiple stress tolerance in relative legume species. Further fundamental and applied studies can be carried out to harness the inclusive prospects of the genes for the biotechnological use (Fig. 7.4). For instance:

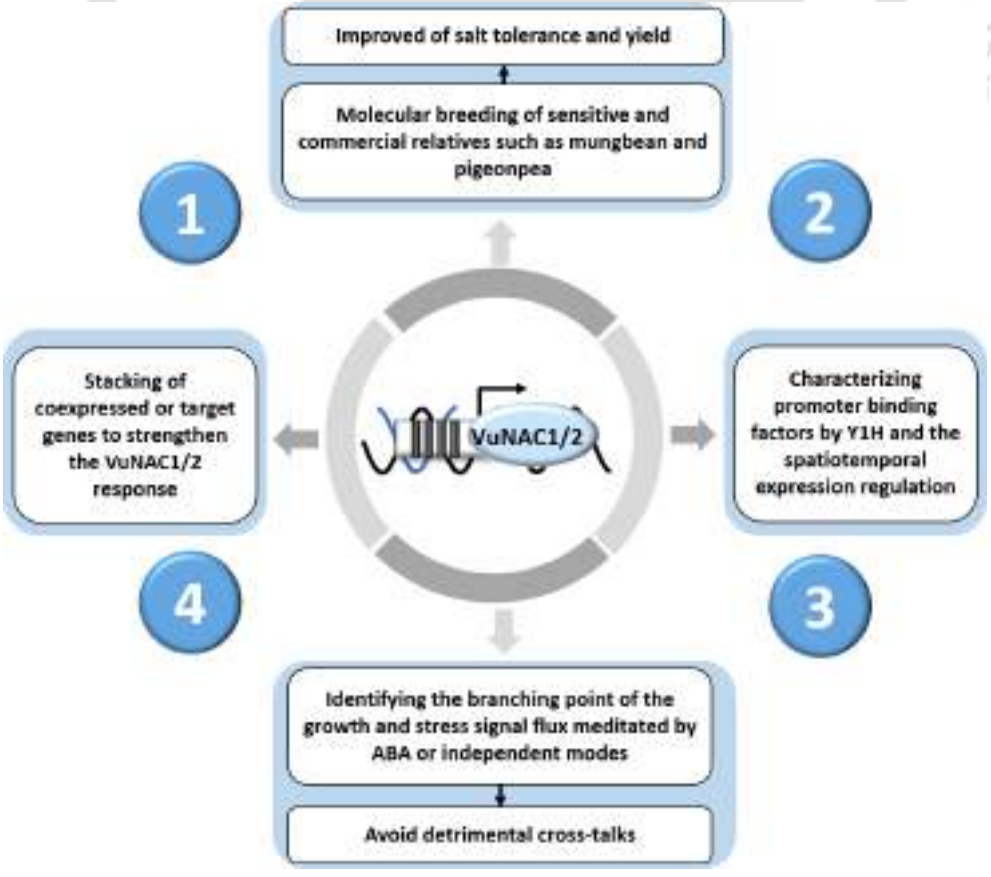

Fig. 7.4 Suggestions for future research perspectives.

7.2.1 Improvement of susceptible legume relatives

The exotic VuNAC1/2-mediated signaling harnessed from the stress-hardy cowpea genotype can be applied to improve the resilience and growth vigor of the sensitive but commercially valuable varieties of cash legumes like mung bean, pigeon pea, *etc*.

7.2.2 Co-expression of VuNAC1/2 with a key target or regulator

However, VuNAC1 and VuNAC2 are indispensable for growth and reproduction, as their homologs could not complement their function, indicating unique but coordinated operations. However, the signaling of TFs can be further strengthened by overexpressing both the TFs together or by co-expressing one of its prominent upstream regulators or downstream targets.

7.2.3 Elucidation of ABA-dependent and independent regulatory pathways

Various secondary ABA dependent and independent signals converge at NAC proteins. However, NAC itself may be the diversion point of the disparate growth and stress signaling. It is possible that NAC TF executes their role in stress signal transduction *via* ABA–mediated mode, but regulates growth through a ABA-insensitive pathway. Such unique feature can be useful for biotechnological exploitation to solve growth trade-off problem by branching out the signal flux of downstream effectors of growth and stress.

7.2.4 Native promoter characterization

The native of promoters of VuNAC1/2 have unique arrangement of regulatory elements that execute coordinated spatiotemporal expression during stress and growth-related responses. A reporter-based characterization of the promoter binding factors and gene expression pattern in normal growth and stressed conditions can provide insight of TF regulation.

7.2.5 Generating improved industrial yeast strains to add value to synthetic applications

Using the VuNAC1/2 TFs to design yeast strains for sustainable bioprocess applications can avoid poor productivity and metabolite overflow due to hampered growth in fluctuating fermentation conditions. Moreover, the TFs can be harnessed to enhance the commercial production of biomolecules. Thus, VuNAC1/2 TFs can be ideal for bioprocess engineering of stress-resilient yeast cell factories and other whole-cell applications, making them more suitable to survive harsh growth conditions without trading off the growth and fitness

8. APPENDIX

APPENDIX 1

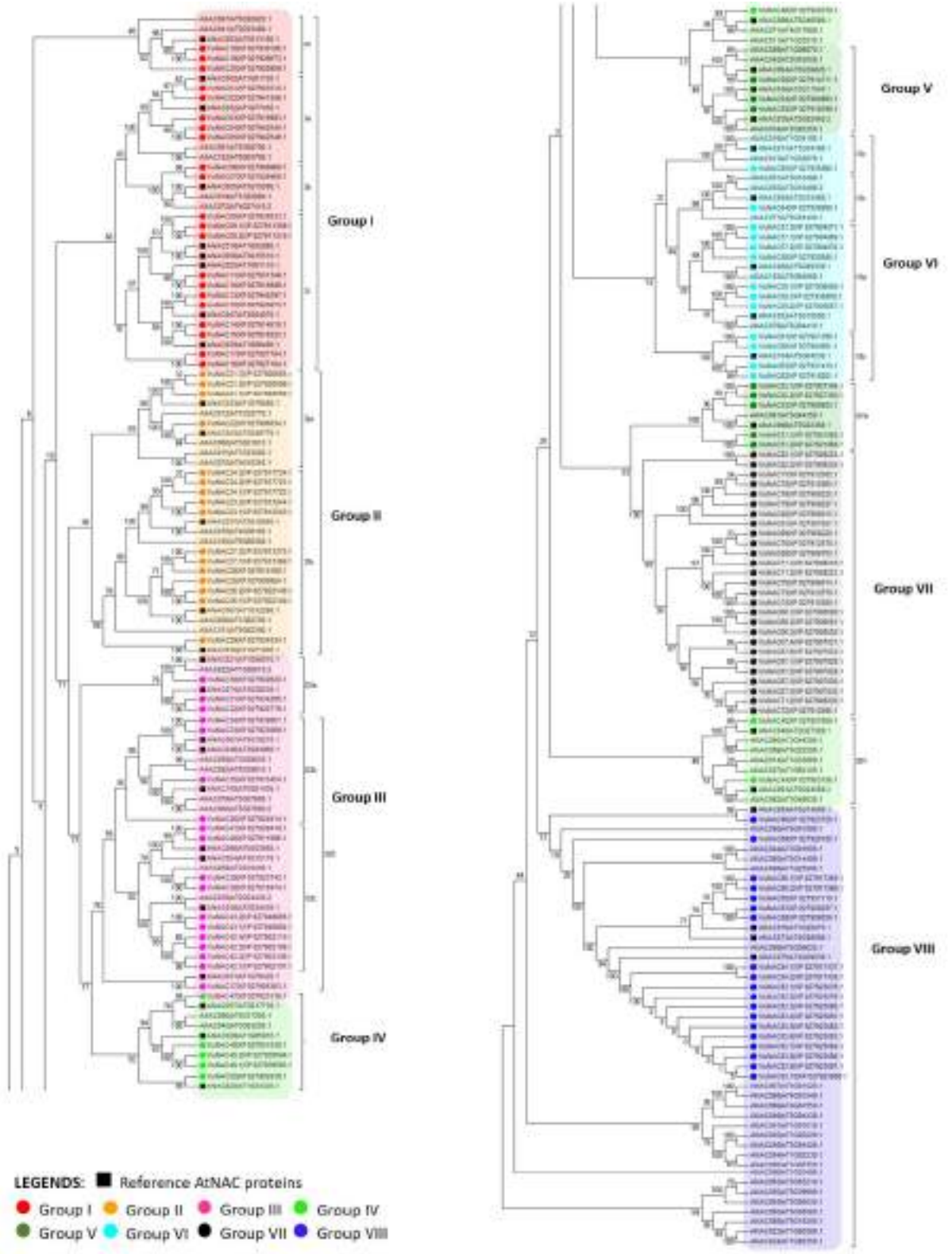

Fig. A1.1 Comparative phylogenetic clustering of VuNAC TFs based on Arabidopsis members. The VuNAC proteins were classified into eight major phylogenetic groups (I-VIII) based on the bootstrap support. The clustering was conducted by MEGA 6.0 using the Neighbour-Joining (NJ) method (1000 replicates) seeded by 75 ANAC proteins of Arabidopsis.

Table A1.2 VuNAC protein classification and distribution

Group	Subgroup	Group name		Bootstrap support (%)	Genes	Proteins
Group I	GIa	*Arabidopsis Transcription Activation Factor*	ATAF-like	100%	**5**	**5**
	GIb	-	AtNAC3-like	100%	**2**	**2**
	GIc	*NAC-like, Activated by AP3/ PI*	NAP-like	89%	**10**	**11**
	GId	*VND-Interacting2*	VNI2-like	98%	**3**	**3**
Group II	GIIa	*SOMBRERO/NAC Secondary Wall Thickening Promoting Factor*	SMB/NST-like	100%	**2**	**4**
	GIIb	*Vascular-related NAC Domains*	VND-like	89%	**7**	**12**
Group III	GIIIa	-	NAC1-like	76%	**3**	**3**
	GIIIb	*No Apical Meristem*	NAM-like	95%	**4**	**4**
	GIIIc	*Cup-shaped Cotyledon*	CUC-like	90%	**7**	**11**
Group IV	GIVa	*TCV-interacting protein*	TIP-like	NA*	**1**	**1**
	GIVb	*NAC with Transmembrane motif 1-Like*	NTL8-like	NA*	**1**	**1**
	GIVc	-	ANAC011-like	99%	**5**	**6**
Group V	GVa	*Tobacco Elicitor-Responsive NAC*	TERN-like	100%	**3**	**5**
	GVb	*FEZ/ Jungbrunnen1*	FEZ/JUB1-like	90%	**3**	**3**
Group VI	GVIa	*Xylem NAC domain*	XND1-like	28%	**3**	**7**
	GVIb		XND1-like	90%	**4**	**4**
	GVIc		XND1-like	NA*	**2**	**2**
Group VII	GVII	-	Cowpea-specific	100%	**17**	**27**
Group VIII	GVIIIa	*Secondary Wall-Associated NAC Domain Protein*	SND-like	100%	**2**	**12**
	GVIIIb		SND-like	98%	**4**	**5**
	GVIIc		SND-like	NA*	**2**	**2**
				Total	**90**	**130**

* Bootstrap values were not available for the subgroups consisting less than three members.

Table A1.3.1 Internal repeats and non-NAC protein domains of the chimeric VuNAC TFs

Protein	Domain family	Location	E-value	Sequence
VuNAC07	*V_ATPase_I*	275…329	0.049	NAWFHQNDFTQGYQNTVDTYG
VuNAC20	*DUF4562*	117…186	0.016	YRLANAETTACNSSHNYVNEIGdWVLCRLS-MKKRSLESGVDEK
VuNAC39	*TFIIA*	147…322	0.086	PCDTVSMVNEFGDVELPNLNSIANSSGHSFMnAdlsNNSVNTNMNLAMNWAVasEVQVQVPSLTSLPWPSGll
VuNAC41	*PT-VENN*	234…265	0.12	KEHVSCFSTIAAATAAVVSPNNFTNA
VuNAC45	*Oxidored_q4*	297…394	0.005	ISNSLVALLFLVFTLIFLVFVGWSQTSEMLrgckrTMSRPMLLVFLLIILIITSQFEWKQQ
	DUF4131	329…448	0.0094	SLVALLFLVFTLIFLVFVGWSqtsemlrgckrTMSRPMLLVFLLIILIITSQFEWKQQLVADVDSNPNVS
	ExbD	370…460	0.058	VFLLIILIITSQFEWKQQ
	VKOR	303…390	0.046	TIMQSSKSSFFaGISNSLVALLFLVFTLIFLVFVGwsqtsemlrgc
	DASH_Dad4	413…460	0.15	NIQRLNELVRHLQEQLQQCRGRNG
VuNAC49	*CEP19*	361…476	0.022	ADKAWEDANTRTIEIGDMDEEFKAERKVENLRWVGMSKEDLEKMEEQNIVPIEEISSfQTMMKENEVQESEQHSDMEHNNDF SLGFINDDEDPtDNFTEDGNK
VuNAC51.1	*Pdase_C33_assoc*	106…184	0.24	GAKTDWKMNEYTAI--KGEQPSQLQLRKEFSLCRVYKKSKC
VuNAC55	*BIRC6*	3…073	0.14	LSQSQSQEDVTTASTTNDNTNNSNNNNTTTDNKPDDHEHDM
VuNAC56	*RPEL*	33…050	0.13	LKRKIQQRPFTIELIK
VuNAC64	*GIT_CC*	432…458	0.45	LQESLESKESLALVKAPDFDAENLESSMSpsciKFIKDLQNEMHKIAVEKET--QAMINILQSRVDILSKENEDL
	HAUS6_N	364…461	0.11	HFLSALVEFSLQESLESKESlalvkapdfdaeNLESSMSPSCIKFIKDLQNEMHKIAVEKETMRFEIMSAQAMINILQSRVDILSKENED LKRMAQ
	bZIP_1	434…461	0.24	AMINILQSRVDILSKENEDLKR
	DUF5082	371…450	0.15	SMSPSCIKFIKDLQNEMHKIAVEKETMRFEIMSAQAMINILQSRVDIL
VuNAC68, VuNAC69, VuNAC70	*FH2*	266…368	0.0023	ETMQTLYETLQIPCETMQSSCESMQTPCETMQTSFESMQTPCETMQTSFESMQTPCETMQTSFESMQTPCETMQTPFESL
	FPP	214…409	0.058	ETMHTPYEIMQISCETMQTLYETLQIPCETMQSSCESMQTPCETMQTSFESMQTPCETMQTSFESMQTPCETMQTSFESMQ TPCETMQTPFESLQTPCEPVQTLCESMQISCESMQ
	SHE3	272…388	1.1	ESLQTPCEPVQTLCESMQISCESMQNPCEPMQISCETMQIS

	DUF1664	250…367	0.31	IMQIPYETMHTPCETMHTPYEIMQiscETMQTLYETLQIPCETMQSSCESMQTPCETMQTSFESMQTPCETMQTSFESMQTPCETMQTSFES
	THOC7	258…409	2.9	ETLQIPCETMQSSCESMQTPCETMQTSFESM
	YycC	276…304	0.36	QISCETMQTLYETLQIPCE
VuNAC71.1,2	*FPP*	190…395	0.0048	TMHTPCETIHTPYEIMQIPCETMQTLYETLQIPCETMQSSCESMQTPCETMQTSFESMQTPCETMQTSFESMQTPCETMQTPFESMHTPCEPVQTPCETMQISCESMQ
	CENP-F_leu_zip	281…408	0.087	ETMQSSCESMQTPCETMQTSFESMQTPCETMQTSFESMQTPCETMQTPFESMHTPCEPVQTPCETMQISCESMQ
VuNAC83	*Pex26*	293…360	0.47	EASTAREVVQASGSCEEvHERQRAQHVVHHHHHQQQ
	MutS_V	289…361	0.69	DEVGMGeASTAREVVQASGSCEEVHERQRAQHVVHHHHHQQQQHQQHQQHQQHAHHQIS
VuNAC85	*zinc_ribbon_4*	24…050	0.078	VTDVKLSEQIRTIRCPSCA
VuNAC86	*zf-ribbon_3*	34…051	0.0053	TITCPSCGHNIEFQ
VuNAC87	*RB_B*	151…253	0.4	sysaklngesvhevTNHKSTGFIEFYNNSF
VuNAC23.1	*signal peptide*	1-021	NA	MFFLQTFSIHFFFLFSQVSQT
VuNAC57.1	*Internal repeat*	234-307	0.0000191	ISIAKDIHPSTSGCAGLTSVSCVSELMPSCTEHHAIPNNNQVVSVSCVSELMPSCSAIPSSPNDALGSVSHLSK
	Internal repeat	326-410	0.0000191	VSCVSKLMPSSSAVSFGSNNEVDSISCVSKLMLSCLPLALAPNNVVEASSSVPELMPSCTTLPSASCPNHQDDDNVLSSLDYLKE
VuNAC57.2	*Internal repeat*	206-279	0.0000183	ISIAKDIHPSTSGCAGLTSVSCVSELMPSCTEHHAIPNNNQVVSVSCVSELMPSCSAIPSSPNDALGSVSHLSK
	Internal repeat	298-382	0.0000183	VSCVSKLMPSSSAVSFGSNNEVDSISCVSKLMLSCLPLALAPNNVVEASSSVPELMPSCTTLPSASCPNHQDDDNVLSSLDYLKE
VuNAC57.3	*Internal repeat*	155-228	0.0000249	ISIAKDIHPSTSGCAGLTSVSCVSELMPSCTEHHAIPNNNQVVSVSCVSELMPSCSAIPSSPNDALGSVSHLSK
	Internal repeat	247-331	0.0000249	VSCVSKLMPSSSAVSFGSNNEVDSISCVSKLMLSCLPLALAPNNVVEASSSVPELMPSCTTLPSASCPNHQDDDNVLSSLDYLKE
VuNAC68	*Internal repeat*	254-317	4.04E-13	RSPSEIMQIPYETMHTPCETMHTPYEIMQISCETMQTLYETLQIPCETMQSSCESMQTPCETMQ
	Internal repeat	338-433	4.04E-13	QTPCETMQTSFESMQTPCETMQTPFESLQTPCEPVQTLCESMQISCESMQNPCEPMQISCETMQISHETNQIPFEILQFLFET PFQTMQTPLETKQ
VuNAC69	*Internal repeat*	254-317	4.04E-13	RSPSEIMQIPYETMHTPCETMHTPYEIMQISCETMQTLYETLQIPCETMQSSCESMQTPCETMQ
	Internal repeat	338-433	4.04E-13	QTPCETMQTSFESMQTPCETMQTPFESLQTPCEPVQTLCESMQISCESMQNPCEPMQISCETMQISHETNQIPFEILQFLFET PFQTMQTPLETKQ
VuNAC70	*Internal repeat*	254-317	4.04E-13	RSPSEIMQIPYETMHTPCETMHTPYEIMQISCETMQTLYETLQIPCETMQSSCESMQTPCETMQ
	Internal repeat	338-433	4.04E-13	QTPCETMQTSFESMQTPCETMQTPFESLQTPCEPVQTLCESMQISCESMQNPCEPMQISCETMQISHETNQIPFEILQFLFET PFQTMQTPLETKQ
VuNAC71.1	*Internal repeat*	214-297	1.70E-09	METICQVTYQAEKCISPTEPSLIEIEQDDDAYFRNENNNGRSPSEIMQIPYETMHTPCETIHTPYEIMQIPCETMQTLYETLQI
	Internal repeat	358-437	1.70E-09	VQTPCETMQISCESMQNPCEPVQISCETMQISHETNQIPFEILQFPLETMQTPSQTTQIPFETIEVPFQTTQTPLETTQI
VuNAC71.2	*Internal repeat*	197-280	1.70E-09	METICQVTYQAEKCISPTEPSLIEIEQDDDAYFRNENNNGRSPSEIMQIPYETMHTPCETIHTPYEIMQIPCETMQTLYETLQI
	Internal repeat	341-420	1.70E-09	VQTPCETMQISCESMQNPCEPVQISCETMQISHETNQIPFEILQFPLETMQTPSQTTQIPFETIEVPFQTTQTPLETTQI

Table A1.3.2 Binding sites and functional protein motifs in the VuNAC proteins

MOTIF	Description*	Function	Occurrence
PS00006	*Casein kinase II phosphorylation site*	**Phosphorylation sites**	All groups
PS00004	*cAMP and cGMP dependent protein kinase phosphorylation*		All groups
PS00005	*Protein kinase C phosphorylation site*		All groups
PS00007	*Tyrosine kinase phosphorylation site 1*		All groups (except GII)
PS60007	*Tyrosine kinase phosphorylation site 2*		All groups (except GV, GVIII)
PS00001	*N-glycosylation site*	**Other modification**	All groups
PS00008	*N-myristoylation site*		All groups
PS00009	*Amidation site*		All groups
PS00017	*ATP/GTP-binding site motif A (P-loop)*	**ATP binding**	VuNAC66 (GVII)
PS51100	*PTS EIIB domain profiles and cysteine phosphorylation site*	**Carbohydrate transport**	VuNAC72 (GVII)
PS51612	*Class I SAM-dependent methyltransferases family profiles*	**Methyltransferase**	VuNAC61 (GVI)
PS51285	*AGC-kinase C-terminal domain profile*	**Phosphorylation sites**	VuNAC86 (GVIII)
PS51450	*Leucine-rich repeat profile*	**Immune response**	VuNAC66 (GVII)
PS00794	*7,8-dihydro-6-hydroxymethylpterin-pyrophosphokinase signature*	**Folate synthesis**	VuNAC24,VuNAC25 (GII)
PS51120	*LDL-receptor class B (LDLRB) repeat profile*	**Lipid signaling**	VuNAC34 (GIII),VuNAC47 (GIV), VuNAC55 (GV)
PS51181	*Phosphatase tensin-type domain profile*	**Lipid signaling**	VuNAC40 (III),VuNAC48 (GIV)
PS50128	*SURP motif repeat profile*	**RNA splicing**	VuNAC43 (GIII)
PS00016	*Cell attachment sequence*	**Cell-binding**	VuNAC44 (GIV), VuNAC51, VuNAC52 (GV)
PS51170	*Cell wall-binding repeat profile*	**Cell-wall binding**	VuNAC45 (GIV)
PS51293	*SANT domain profile*	**Chromatin remodelling**	VuNAC49 (GV), VuNAC81,VuNAC82 (GVII)
PS51224	*MVP (vault) repeat profile*	**Ribonucleoprotein**	VuNAC51 (GV)
PS51329	*C-CAP/cofactor C-like domain profile*	**Cytoskeleton protein**	VuNAC55 (GV), VuNAC67, VuNAC72 (GVII)
PS51125	*NHL repeat profile*	**Growth regulator**	VuNAC73, VuNAC74 (GVII)
PS51359	*Cytochrome c oxidase subunit Vb, zinc-binding domain profile*	**Electron transfer**	VuNAC87 (GVIII)

* **Source: ScanProsite**

Table A1.4 Gene location and duplication study

Type	S.N.	Gene ID	Group	Locus	Identity	Similarity	Coverage	Distance	Spacer genes
Gene Cluster	1	VuNAC13	Ic	Chr1:24039970...24041860	27.6%	36.4%	59.9%	61.7 kb	3
		VuNAC34	IIIb	Chr1:24102998...24104991					
	2	VuNAC02	Ia	Chr3:4945775...4947276	25.9%	39.9%	66.7%	189.3 kb	16
		VuNAC61	VIb	Chr3:5136355...5137852					
	3	VuNAC45	IVb	Chr5:42786452...42793889	16.1%	23.4%	39.5%	44.3 kb	6
		VuNAC52	Va	Chr5:42838225...42839587					
Tandem Duplication	1	VuNAC04	Ia	Chr9:26453906...26454919	**97.2%**	**97.9%**	**100.0%**	9.0 kb	0
		VuNAC03	Ia	Chr9:26464007...26465020					
	2	VuNAC07	Ib	Chr5:38122572...38123861	34.5%	45.5%	67.1%	46.0 kb	1
		VuNAC08	Ic	Chr5:38169866...38172210					
	3	VuNAC19	Id	Chr5:90905...92265	**94.4%**	**97.4%**	**100.0%**	5.6 kb	0
		VuNAC18	Id	Chr5:97829...99159					
	4	VuNAC61	VIb	Chr3:5136355...5137852	17.1%	26.6%	50.7%	90.4 kb	10
		VuNAC58	VIa	Chr3:5228252...5231490					
	5	VuNAC61	VIb	Chr3:5136355...5137852	49.8%	69.1%	-	-	-
		VuNAC62	VIb	Chr3:13165272...13166898					
	6	VuNAC64	VIc	Chr7:30718969...30728844	25.6%	36.2%	61.0%	4.9 kb	0
		VuNAC59	VIa	Chr7:30733818...30737355					
	7	VuNAC81	VII	Chr10:2396767...2398655	31.2%	39.7%	55.0%	2.6 kb	0
		VuNAC67	VII	Chr10:2401257...2417694					
	8	VuNAC66	VII	Chr10:37412180...37415600	48.0%	59.4%	81.2%	**5.4 kb**	0
		VuNAC68	VII	Chr10:37420985...37424727				34.0 kb	2
		VuNAC69	VII	Chr10:37458729...37462474	**85.0%**	**80.0%**	**80.0%**	2.2 kb	0
		VuNAC76	VII	Chr10:37464699...37466722				3.1 kb	0
		VuNAC75	VII	Chr10:37469895...37471753				1.7 kb	0
		VuNAC80	VII	Chr10:37473460...37475034				10.0 kb	0
		VuNAC79	VII	Chr10:37485056...37487114				9.3 kb	0
		VuNAC71	VII	Chr10:37477738...37492219					
Segmental Duplication	**1**	VuNAC01	Ia	Chr9::33300089...33302149	66.9	**75.8**	-	-	-
		VuNAC05	Ia	Chr8:13486162...13487724					
	2	VuNAC02	Ia	Chr3:4945775...4947276	66.0	73.9	-	-	-
		VuNAC03	Ia	Chr9:26464007...26465020					
		VuNAC03	Ia	Chr9:26464007...26465020					
	3	VuNAC06	Ib	Chr11:16461521...16463576	**63.1**	**75.1**	-	-	-
		VuNAC07	Ib	Chr5:38122572...38123861					
	4	VuNAC08	Ic	Chr5:38169866...38172210	68.5	**80.2**	-	-	-
		VuNAC09	Ic	Chr11:14743567...14745919					
	5	VuNAC10	Ic	Chr3:10221122...10223084	70.6	**78.2**	-	-	-
		VuNAC11	Ic	Chr6:31924177...31926042					
	6	VuNAC14	Ic	Chr2:20264548...20266034	70.0	**79.1**	-	-	-
		VuNAC15	Ic	Chr3:33676977...33678467					
	7	VuNAC23	IIb	Chr2:27622897...27627169	71.9	**81.4**	-	-	-
		VuNAC24	IIb	Chr3:42697313...42701453					
	8	VuNAC25	IIb	Chr11:41298448...41302298	71.5	**79.7**	-	-	-
		VuNAC26	IIb	Chr1:1000216...1005436					
	9	VuNAC27	IIb	Chr2:31205839...31208915	68.5	**76.5**	-	-	-
		VuNAC28	IIb	Chr3:49676234...49682116					
	10	VuNAC25	IIb	Chr11:41298448...41302298	59.0	72.6	-	-	-
		VuNAC27	IIb	Chr2:31205839...31208915					
	11	VuNAC31	IIIa	Chr7:18090097...18094361	71.6	**81.2**	-	-	-
		VuNAC32	IIIa	Chr1:32489855...32495432					
	12	VuNAC40	IIIb	Chr11:12643122...12645544	68.3	**76.2**	-	-	-
		VuNAC41	IIIb	Chr5:36963430...36966174					
	13	VuNAC48	IVc	Chr6:22802804...22806589	64.0	**76.1**	-	-	-
		VuNAC49	IVc	Chr8:31257369...31261040					
	14	VuNAC62	VIb	Chr3:13165272...13166898	81.7	**90.1**	-	-	-
		VuNAC63	VIb	Chr6:33442316...33443725					
	15	VuNAC60	VIb	Chr9:25352552...25353640	67.8	**77.6**	-	-	-
		VuNAC61	VIb	Chr3:5136355...5137852					-
	16	VuNAC83	VIIIa	Chr4:333751...338854	**87.6**	**90.2**	-	-	-
		VuNAC84	VIIIa	Chr3:2034088...2038887					
	17	VuNAC85	VIIIb	Chr6:31262634...31265962	**68.5**	**77.7**	-	-	-
		VuNAC86	VIIIb	Chr3:8920043...8923188					
	18	VuNAC87	VIIIb	Chr5:40313578...40315813	**80.0**	**88.1**	-	-	-

VuNAC88	VIIIb	Chr11:29140079…29143447	

Table A1.5 List of protein motifs detected by MEME analysis

Name	Group	Description	Length	Frequency	Motif Sequence
Motif 3	All	Subdomain A (Dimerization)	21	128	**PPGFRFHPTDEELVDHYLKKK**
Motif 4	GI	Subdomain B	15	110	**IPEIDLYKVEPWDLP**
Motif 23	GI	Subdomain C part	8	65	**AKFGEKEW**
Motif 1	GI	Subdomain C (DNA-binding)	35	105	**YFFSPRDRKYPNGKRTNRATKSGYWKATGKDREIY**
Motif 11	All	Subdomain D part (except GVIII)	11	125	**STNTLIGMKKT**
Motif 2	All	Subdomain D	21	127	**LVFYKGRAPKGEKTBWVMHEY**
Motif 5	All	Subdomain E(NLS)	21	124	**ESZDEWVLCRVFKKSGPTQKG**
Motif 31	GVII	AB junction	8	27	LLGDDPRV
Motif 19	GVII	BC Junction	15	24	**VILAKSRIRFKDPEW**
Motif 50	GVII	Subdomain D (end)	6	21	HAVTFH
Motif 6	GVIII	Subdomain B+C start	50	17	**HPLIDEFIPTIEGEDGICYTHPEKLPGVTRDGLSRHFFHRPSKAYTTGTR**
Motif 10	GVIII	Subdomain C end+ D start	41	12	**KRRKIQNECDLQGGETRWHKTGKTRPVMVNGKQKGCKKILV**
Motif 39	GI	C-terminal	41	5	HQHHPQSKCNPPTHHAATSVGTSAQKFPFHYLGCDTHDIMK
Motif 35	GII	C-terminal	29	6	EHDSPCWYDEQVSFMQDMDSPKQSSQPNA
Motif 21	GII	C-terminal	50	9	GPQNLLYKKETMADNLSDMHADGLMQLPQLESPSLPLVKKTTSVSLVSDN
Motif 20	GII	C-terminal	29	19	YLKEDSGTKQVTDWRALDKFVASQLSHEE
Motif 45	GII	C-terminal	29	7	LLQNSRERNKFNPFLSAGSSDCDIGICVF
Motif 40	GII	C-terminal	15	9	MFHSNYKHRVQCSPK
Motif 42	GII	C-terminal	21	8	AIGKEGTDIEMEGTHAKEETL
Motif 34	GIII	C-terminal	29	6	EIGQNIMQAPVMQMGDPAAHFLYGRNYMN
Motif 25	GIII	C-terminal	50	6	ARVLRGGGSTSSVNQPMQSQLGYPTSAGFTISGLNLNLGGATTTTQPVFR
Motif 41	GIII	C-terminal	29	4	PMQASSAPPVHTMGQVLDVNSSMMTTGSL
Motif 26	GIII	C-terminal	33	6	VGYGSEMSNMNSQGNRFMGMEHCMDLDNYWPSY
Motif 37	GVI	C-terminal	41	6	DEENDQKEADPLLPVGTPVPIPFSEIPPSIVKPPLPVTDGV
Motif 46	GVI	C-terminal	50	3	VSCVSELMPSCTEHHAIPNNNQVVSVSCVSELMPSCSAIPSSPNDALGSV
Motif 32	GVI	C-terminal	41	6	VSWIPKEMPDISAIPFGSNNEVDEISQISKEILQTLPKAJG
Motif 47	GVI	C-terminal	50	3	WDDIGAFLETNDLEGELDLSDMNGGVTFPSLNFHHGECSTYAENSQELIK
Motif 49	GVI	C-terminal	50	3	GISGPENGQPLDMAEQHDMGTGSVKDEDNGEQSEIENLLNFNDALDNMDL
Motif 48	GVI	C-terminal	41	6	DLYTGVTDILPSADDZDFLELNDLAGPNPGDLKEGDPGEBB
Motif 38	GVI	C-terminal	50	3	AFSVQNTEDAKLAAPGNTNPFVKQAYGWLASIPAAPAHAFEFPAKDITPG
Motif 36	GVI	C-terminal	50	3	ITTGMISITDITFRGNAMDWPMGKIGGFNTAMSTEFSQSDVNCAAFIPVS
Motif 13	GVII	C-terminal	50	20	ICDEGESSRIMVSDYENQAIGEGVPSGGTLTGVETICDATFQNEKNISPT
Motif 17	GVII	C-terminal	50	8	DAYFRNENNNGRSPSEIMQIPYETMHTPCETMHTPYEIMQISCETMQTLY
Motif 33	GVII	C-terminal	41	6	QPSPREEASFPNYPLNNVCFGNEKSFMQDEYLNRILADENL
Motif 15	GVII	C-terminal	50	8	ETLQIPCETMQSSCESMQTPCETMQTSFESMQTPCETMQTSFESMQTPC
Motif 18	GVII	C-terminal	50	7	QTPCEPVQTPCESMQISCESMQNPCEPMQISCETMQISHETNQIPFEILQ
Motif 44	GVII	C-terminal	29	5	PNSHESLTIDEENMFGFLNCFTQSESLKR
Motif 43	GVII	C-terminal	29	4	VHEGVCMPSPIHEKKQEKKKKKKSIFSFF
Motif 14	GVII	C-terminal	50	17	AYRESSCTDAEVVSZQDANIEDISTVYTKYLNSDEYHSSKRFKTSYDVGD
Motif 28	GVII	C-terminal	41	5	FLFETPFQTMQTPLETKQILPKLPNSLLADEYLVTQSKSLK
Motif 16	GVII	C-terminal	41	11	EASZEKKESIIQDDFWGMETSSCDSTTNKLVEINYSEISSF
Motif 29	GVII	C-terminal	29	6	EEFVNSFFVEDNYVNNEESTNTYFNTFTQ
Motif 30	GVIII	N-terminal	15	12	NLSSVSSSDLIDAKL
Motif 24	GVIII	N-terminal	15	12	PGCGHKFEGKPDWLG
Motif 27	GVIII	C-terminal	15	12	WSDRSATTGEGSGEP
Motif 12	GVIII	C-terminal	50	10	NNSSRRDSGSGSCSSKEIATHRDEMSAVVGVPPITTFTHHPLDIHHLKPD
Motif 8	GVIII	C-terminal	50	10	HFSFIPFRKSFDEVGMGEASTAREVVQASGSCEEVHERQRAQHVVHHHHH
Motif 7	GVIII	C-terminal	50	12	QQHQQHQQHQQHAHHQISNSAFHISRPSHPISTIISPPPLHHTSIILDDN
Motif 22	GVIII	C-terminal	15	12	YHVSRIMLQNENFQQ
Motif 9	GVIII	C-terminal	50	12	QQQHHHKLGGRSASGLEELIMGCTSTEIKEESSITNPQEAEWLKYSSYWP

Table A1.6 Multi-partite nuclear localisation signals (NLSs)

Protein	N-terminal multipartite NLS	C-terminal monopartite NLS
VuNAC01	68 - PRDRKYPNGSRPNRAAGTGYWKATGADKPIGHPKPVGIKKALVFYAGKAPKGDKSNWIMHEYRLADVDRTVRKKNSLR - 145	-
VuNAC02	68 - PRDRKYPNGSRPNRAAGTGYWKATGADKPIGKPEARGIKKALVFYAGKAPKGVKTNWI - 125	-
VuNAC03	68 - PRDRKYPNGSRPNRAAGSGYWKATGADKPIGKPKALGIKKALVFYSGKAPKGEKTNWI - 125	-
VuNAC04	68 - PRDRKYPNGSRPNRAAGSGYWKATGADKPIGKPKALGIKKALVFYSGKAPKGEKTNWI - 125	-
VuNAC05	70- PRDRKYPNGSRPNRSAGTGYWKATGADKPIGKPKPVGIKKALVFYSGKAPKGEKTNWIMHEYRLAEVDRSVRRKNSLRLDDWVLCRIY NKKGPVEKQP - 167	-
VuNAC06	75 - PRDRKYPNGSRPNRVAGSGYWKATGTDKVITTEGRKVGIKKALVFYVGKAPKGSKTN - 131	-
VuNAC07	76 - PRDRKYPNGSRPNRVAGSGYWKATGTDKIITTEGRKVGIKKALVFYVGKAPKGTKT - 131	-
VuNAC08	78 - RDRKYPNGARPNRAAT - 93	-
	113 - QKVGVKKALVFYGGKPPRGIKTNWIM - 138	-
	146 - NKPNNRP - 152	-
VuNAC09.1	78 - PRDRKYPNGARPNRAAT - 94	-
VuNAC09.2	113 - KVGVKKSLVFYGGKPPKGVKTDWI - 136	-
	143 - AETKPNNRPPG - 153	-
	157 - GHKKN - 161	-
VuNAC10	79 - RKYPNGVRPNR - 89	-
	111 - HQKVGVKKALVFYGGKPPKGVKTN - 134	-
	152 - KPPPLVPPNKKN - 163	-
VuNAC11	79 - PRDRKYPNGARPNRAASSGYWKATGTDRPILASHGHHKVGVKKALVFYGGKPPKGVKTN - 137	-
	162 - RSTKK - 166	-
VuNAC12	69 - SPRDRKYPNGARPNRAAASGYWK - 91	-
	105 - GGVRQHFGVKKALVFYKGKPPKGVKTNWIMHEYRL - 139	-
	142 - TNKPVRVK - 149	-
VuNAC13	105 - PRDRKYPNGARPNRAAAS - 122	-
	148 - GVKKALVFYKGRPPKGVKTNWIMHEYRLVDNNKPIKLKD - 186	-
VuNAC14	72 - ERKYPNGVRPNRA - 84	-
	96 - DKAIYSGSKHIGVKKALVFYKGKPPKGIKTDWIMHEYRLIGSRRQTNRQ - 144	-
	157 - RIYKKKNMGKS - 167	-
VuNAC15	102 - GSKLVGVKKSLVFYKGRPPKGDKTDWIMHEYRLAESKQSANRKIGSMRLDDWVLCRIYKKKNMGKTLEHKEAHPK - 176	-
VuNAC16	74 - RDRKYPNGLRPNRAAASGYWKATGTDKPILSSSGSKRIGVKKALVFYSGRPPKGSKTD - 131	-
VuNAC17	75 - RKYPNGVRPNRAA - 87	265 - KRKNIE - 270
	107 - MKNIGVKKALVFYKGRAPKGSKT - 129	-
VuNAC18	113 - KKTLVFYRGKPPHG - 126	-
	154 - RIFLKRRSGGRNGEEKEMESLRGGVENRKVRKSKMVFYNFLA - 195	-
VuNAC19	113 - KKTLVFYRGKPPHGS - 127	-
	154 - RIFLKRRSGGRNGEEKEMESLRGKVDSRKVRKLKMVF - 190	228 - VRRKP - 232
VuNAC20	170 - KKRSLESGVDEKQKGGSG - 187	-
VuNAC21	95 - KATGRDKAIYHTNSKRIGMRKT - 116	-
VuNAC22	88 - TRTNRATAAGFWKATGRDKVIYSNGKRIGMRKTLVFYKGRAPHGQ - 132	174 - KKKNNLKTLDSP - 185
VuNAC23.1	132 - GRDKA - 136	-
VuNAC23.2	140 - KTKLIGMRKTL - 150	-
VuNAC24	25 - RKKVASRK - 32	-
	102 - RTKLIGMRKT - 111	-
VuNAC25	26 - RKKVASRR - 33	-
	92 - KATGRDK - 98	-
VuNAC26	92 - KATGRDK - 98	-
VuNAC27.1	44 - HHYLKKKVASKRIDP - 58	-
	94 - KDKKYPTGTRTNRATKAGFWKATGRDK - 120	-
VuNAC27.2	24 - YLKKKVASKRIDP - 36	-
	72 - KDKKYPTGTRTNRATKAGFWKATGRDK - 98	-
VuNAC28	26 - RKKVASKR - 33	-
	72 - KDKKYPTGTRTNRATKAGFWKATGRDKA - 99	-
VuNAC29	91 - TRTNRATAAGFWKATGRDKAVMTKNRIIGMRKTLVFYKGRAPNGRKT - 137	-
VuNAC30	86 - ASGYWKATGKDRPILRKGTLVGMRKTLVFYQGRAPKGRKTEWVMHEFRIEGPHGPPKV - 143	-
VuNAC31	-	-
VuNAC32	-	-
VuNAC33	62 - LPKKAKMGEKDWYFFCQRDRKYPTGLR - 88	-
	98 - WKATGKDKEIFKGKNNLVGMKKTLVFYRGRAPKGEKTN - 135	-
VuNAC34	61 - LPKKAKIGEKEWYFFCQKDRKYPTGMRTNRA - 91	-
	95 - GYWKATGKDKEIYKGKGNLVGMKKTLVFYRGRAPKGEKTNW - 135	-
VuNAC35	96 - YWKATGKDKEIFRGKSLVGMKKTLVFYRGRAPKGEKSNWV - 135	-
VuNAC36	109 - WKATGKDKEIYKAKTLIGMKKTLVFYKGRAPS - 140	-
VuNAC37	121 - LGMKKTLVFYKGRAPRGEKTKWVM - 144	-
VuNAC38	113 - GRAPRGEK - 120	-
VuNAC39	103 - GMKKTLVFYRGRAPRGEKSNWVMHEYRLENKHHLRPSK - 140	-
VuNAC40	123 - MKKTLVFYRGRAPKGEKSN - 141	-
VuNAC41	116 - MKKTLVFYRGRAPKGEKSN - 134	-
VuNAC42.1	108 - GKAKMGEK - 115	-
VuNAC42.2	162 - MKKTLVFYKGRAPRGEKSNWVMHEYRIHSKSSFRTTRQDEWVVCRVFKKSGGAKKFPSSNHGR - 224	-
VuNAC42.3	74 - GKAKMGEK - 81	-
VuNAC42.4	128 - MKKTLVFYKGRAPRGEKSNWVMHEYRIHSKSSFRTTRQDEWVVCRVFKKSGGAKKFPSSNHGR - 190	-
VuNAC43.1	17 - MEEDKKK - 23	-
VuNAC43.2	75 - KAKMGAKE - 82	-
	89 - RDRK - 92	-
	129 - KKTLVFYKGRAPRGEKTNWVMHEYRNHSKSTFKITKQDEWVVCRVFRKSGGAKKFPSNP - 187	-
VuNAC44	91 - PNGHRLNRATSHGYWKATGKDRKIKSGMILIGMKKTLVFYTGRAPKGKRTNWVM - 144	470 - GTAHRRIRLAQKARNELSNKIVKKELDLK - 498
VuNAC45	79 - PRGRKYPNGSQSKRATECGYWKATGKERNVKSGSNVIGTKRTLVFHLGRAPKG - 131	294 - AQRRIRLRVGNSKRSSP - 310
VuNAC46	69 - PRDRKYPNGSRTNRATKAGYWKATGKDRK - 97	-
	155 - RVIKKNEKASATKGENKGKRAGSSSIN - 181	-
VuNAC47	69 - PRDRKYPNGFRTNRTRAGYWKSTGKDRRVSCQSRPIGMKKT - 109	-
VuNAC48	26 - LKRKINGRKIE - 36	-
	71 - PRDRKYPNGSRTNRATKSGYWKATGKDRKVNS - 102	-
VuNAC49	67 - SPRDRKYPNGSRTNRATKSGYWKATGKDRKVNSKARSVGMKKTLVYYRGRAPHGSR - 122	-
VuNAC50	70 - RDRKYPNGSRTNRATQAGYWKATGKDRPVHSQKKPVGMKKTLVYYRGRAPHGI - 122	-
VuNAC51	71 - RQESEARGGRPKRLTTTGYWKAT - 93	-
	147 - RKEFSLCRVYKKSKCLRAFDRRPPPRRNTVRHSI - 180	-
VuNAC52	75 - ETRGGRPNR - 83	-
	105 - KVIGMKKTMVFYEGKAPSGRKTKWKMHEYKAI - 136	-
VuNAC53	81 - ARGGRPSR - 88	-
	109 - NRVIGVKKSMVFYKGKAPMGRKTKWKMNEYRA - 140	-

VuNAC54	68 - REWYFFVPRDKKHGSGGRPNRTTEKGFWKATGSDRKIVTLSDPKRIIGLRKTLVFYMGRAPSGRK - 132	-
VuNAC55	74 - RRKVEGK - 80	-
	117 - RDRKYRNGDRPN - 128	-
	154 - GLKKTLVFYSGKAPKGI - 170	-
VuNAC56	78 - RDRKYRNSARPNRVT - 92	-
	116 - GLKKSLVFYKGRAAKGVK - 133	-
VuNAC57	3 - RRNSTPGFRFRPTDVELIEFFLKRKVRGKKIPSGIIAELDLYKY - 46	-
VuNAC58	24 - LKRKVMGKKFF - 34	-
	72 - KKYGSGSRMKRATEIGYWKATGRDRVVQHNHKTVGMIRTLIFHKGKSPKGERTNWV - 127	-
VuNAC59	103 - VGMKKTLVYHIGRAPHGRR - 121	-
VuNAC60	132 - ASCRSSRRRRKHDQSWSKWVLCRVYEKMR - 160	-
VuNAC61	139 - RGRRKSDQCRSKW - 151	-
VuNAC62	129 - DSASSSRSSRRRPQPKPDHSKW - 150	-
VuNAC63	126 - RLSDSASSTRSSKRKPQPKADYKKWVI - 152	-
VuNAC64	51 - KRKVSGKS - 58	305 - KPFSLIYKRRRHN - 317
	98 - KKYGNGGRMNRATNKGYWKATGNDRPVKHDQRTVGLKKTLVFHSGRAPDGKR - 149	457 - RMAQKP - 462
VuNAC65	38 - KRKICGKRLKL - 48	503 - RVKLRHTNIAAGKDTVTTKKAGRKGF - 528
	83 - RDRKYPNGARSNRATRHGYWKATGKDR - 109	-
	168 - KKSGPGPK - 175	-
VuNAC66	82 - SKRVNRRTKCGFWKPTGKDR - 101	-
	154 - RLIKKPGKI - 162	-
VuNAC67	70 - KLMSSNSKRFIRRTKSGFWKPTGKDRDVRSRDTNTVIGTKKTL - 112	-
VuNAC68	89 - KYSNSKRVNRKTEKGFWKATGKDRDIRS - 116	-
	166 - LIKKPEKKTEG - 176	-
VuNAC69	89 - KYSNSKRVNRKTEKGFWKATGKDRDIRS - 116	-
	166 - LIKKPEKKTEG - 176	-
VuNAC70	89 - KYSNSKRVNRKTEKGFWKATGKDRDIRS - 116	-
	166 - LIKKPEKKTEG - 176	-
VuNAC71.1	89 - KYSNSKRVNRKTEKGFWKATGKDRDIRS - 116	-
	166 - LIKKPEKKTEG - 176	-
VuNAC71.2	70 - KLMSSNSKRFNRRTKSGFWKPTGKDRDVRSRDTN - 103	-
	149 - LIKKPEKKTEG - 159	-
VuNAC71.3	89 - KYSNSKRVNRKTEKGFWKATGKDRDIRS - 116	-
	168 - RRKSG - 172	-
VuNAC72	70 - KLMSSNSKRFNRRTKSGFWKPTGKDRDVRSRDTN - 103	-
	149 - LIKKPEKKTEG - 159	-
VuNAC73	89 - KYSNSKRVNRKTEKGFWKATGKDR - 112	-
VuNAC74	89 - KYSNSKRVNRKTEKGFWKATGKDR - 112	-
VuNAC75	73 - KYSNSKRVNRKTEKGFWKATGKDR - 96	-
VuNAC76	91 - KPTGKDRE - 98	302 - EGVCMPSPIHEKKQEKKKKKKSIFSFF - 328
VuNAC77	91 - KPTGKDRE - 98	302 - EGVCMPSPIHEKKQEKKKKKKSIFSFF - 328
VuNAC78	91 - KPTGKDRE - 98	302 - EGVCMPSPIHEKKQEKKKKKKSIFSFF - 328
VuNAC79	76 - KPTGKDRE - 83	288 - GVCMSSPIHEKKQEKKKKKKSKFSFF - 313
VuNAC80	90 - KPTGKDR - 96	-
VuNAC81	88 - WKPTGKDR - 95	-
VuNAC82	98 - GNDRKIRIGGTN - 109	409 - KSEKDEKKAQN - 419
	112 - IGTKKTLVFHEGRVPRGAK - 130	-
	157 - KKFEKK - 162	-
VuNAC84	107 - GLSRHFFHRPSKAYTTGTRKRRKIQNECDLQGGETRWHKTGKTRPVMVNGKQKGCKKILVLYTNFGKNRKPEKT - 180	-
VuNAC85	118 - GVGKDGQIRHFFHRPSKAYTTGTRKRRKVESDEEGSETRWHKTGKTRAVFAGGGGAVKGFKKILVLYTNYGRKKKPEKTNWV - 199	-
VuNAC86	117 - KDGQIRHFFHRPSKAYTTGTRKRRKVHTDEEGSETRWHKTGKTRPVFVGGAVKGFKKILVLYTNYGRQKKPEK - 189	-
VuNAC87	104 - VGKDGLIRHFFHRPSKAYTTGTRKRRKVHTDADGSETRWHKTGKTRPVYISGKLKGYKKILVLYTNYRKQRKPEKTN - 180	-
VuNAC88	102 - KDGLIRHFFHRPSKAYTTGTRKRRKVHSDEDGSETRWHKTGKTRPVYNSAKLKGYKKILVLYTNYGKQRKPEKT - 175	-
VuNAC89	120 - WKSKGNSLAKTKWVMHEFRLALKSNPSKMSAMGVCRIFERKTSKRAKRARVSTEGVSN - 177	-
VuNAC90	150 - IFQKRKKTPKASQQRPFCSSKLQRV - 174	-

Table A1.7 Study of core elements and preferentially located motifs (PLMs) in the promoter

Protein	TATA box		Position		Promoter	TSS-YR	TC%	
	Type	Sequence	TATA	TC element	type		Core	5'-UTR
VuNAC01	Canonical	TATAAATA	**38**	**26**	**I**	**CA**	**57**	43.2
VuNAC02	TATAWA	TATAAA	8	51	**I**	**-**	51	38.5
VuNAC03	None	-	-	26	**III**	**CA**	72	40.9
VuNAC04	TATAWA	TATAAA	25	41	**I**	**-**	64	38.3
VuNAC05	TATAWA	TATAAA	9	25	**I**	**TG**	70	71
VuNAC06	Canonical	TATAAATA	31	-	**II**	**TG**	52	39.8
VuNAC07	Canonical	TATAAATA	24	-	**II**	**CG**	51	49.6
VuNAC08	TATAWA	TATAAA	40	-	**II**	**CA**	53	48.2
VuNAC09.1	TATA-variant	TATTAA	33	56	**I**	**CG**	50	53.5
VuNAC09.2	TATA-variant	TATTAA	33	56	**I**	**CG**	50	53.5
VuNAC10	None	-	-	40	**III**	**-**	74	56
VuNAC11	None	-	-	25	**III**	**CA**	68	67.5
VuNAC12	None	-	-	5	**III**	**CA**	68	75
VuNAC13	None	-	-	34	**III**	**CA**	71	69.2
VuNAC14	None	-	-	-	**IV**	**CA**	39	69.8
VuNAC15	None	-	-	50	**III**	**CA**	48	60.3
VuNAC16	Canonical	TATATATA	55	17	**I**	**CG**	51	63.8
VuNAC17	TATAWA	TATATA	14	-	**II**	**CG**	55	59.4
VuNAC18	None	-	-	-	**IV**	**TA**	54	64.5
VuNAC19	TATA-variant	ATATAA	52	-	**II**	**TG**	38	74.5
VuNAC20	Canonical	TATATATA	22	56	**I**	**CG**	62	60.3
VuNAC21.1	Canonical	TATATATA	50	33	**I**	**TG**	74.5	64.5
VuNAC21.2	None	-	-	37	**III**	**TG**	68	66
VuNAC21.3	None	-	-	37	**III**	**TG**	68	65
VuNAC22	Canonical	TATATATA	43	34	**I**	**CA**	69	72.3
VuNAC23.1	None	-	-	-	**IV**	**CA**	68	68
VuNAC23.2	TATA-variant	TATATT	26	43	**I**	**CA**	63	77.4
VuNAC24.1	None	-	-	-	**IV**	**-**	54	47.6
VuNAC24.2	Canonical	TATATATG	49	24	**I**	**CA**	54	58
VuNAC24.3	None	-	-	-	**IV**	**TG**	62	45.8
VuNAC25	None	-	-	36,19	**III**	**-**	66	62
VuNAC26.1	None	-	-	36	**III**	**TG**	61	66.5
VuNAC26.2	None	-	-	32	**III**	**-**	59	5.6
VuNAC27.1	TATAWA	TATAAA	31		**II**	**TG**	49	57.2
VuNAC27.2	TATA-variant	TATTTAA	55	25	**I**	**CA**	50	71
VuNAC28	TATAWA	TATATATG	38	-	**II**	**CA**	51	64.5
VuNAC29	Canonical	TATATATA	19	57	**I**	**-**	70	67.2
VuNAC30	Canonical	TATATATA	20	12	**I**	**-**	64	79.6
VuNAC31	Canonical	TATATATA	31	-	**II**	**TG**	52	66
VuNAC32	Canonical	TATATATA	26	-	**II**	**TG**	47	61.2
VuNAC33	None	-	-	-	**IV**	**CA**	40	73.5
VuNAC34	TATA-variant	TATTTAAA	52	36	**I**	**CA**	70	68.7
VuNAC35	None	-	-	-	**IV**	**TG**	29	64.8
VuNAC36	TATA-variant	TATTTAA	9	-	**II**	**-**	41	69
VuNAC37	TATAWA	TATATA	48	31	**I**	**TG**	73	50
VuNAC38	None	-		33	**III**	**TG**	64	46.5
VuNAC39	TATA-variant	TATATT	51	-	**II**	**TG**	42	46
VuNAC40	TATAWA	TATATA	56	-	**II**	**TG**	61	83.4
VuNAC41	None	-	-	25	**III**	**-**	86	72
VuNAC42.1	None	-	-	-	**IV**	**CA**	47	67.7
VuNAC42.2	None	-	-	-	**IV**	**TG**	45	68.3
VuNAC42.3	TATA-variant	TATTAAT	78	-	**II**	**TG**	41	58.2
VuNAC42.4	TATA-variant	TATTAAT	59	-	**II**	**TG**	40	60.3
VuNAC43.1	None	-	-	-	**IV**	**TG**	53	61.5
VuNAC43.2	None	-	-	-	**IV**	**TG**	53	61.5
VuNAC44	TATAWA	TATATA	61	-	**II**	**CA**	41	59
VuNAC45	TATAWA	TATAAA	55	-	**II**	**TG**	20	42
VuNAC46	Canonical	TATAAATA	20	36	**I**	**CA**	55	65
VuNAC47	None	-	-	54	**III**	**CA**	40	17.2
VuNAC48	TATA-variant	TATAATTA	50	-	**II**	**CA**	37	52.5
VuNAC49.1	None	-	-	49	**III**	**CA**	72	51.6
VuNAC49.2	None	-	-	45,17	**III**	**-**	75	55.7
VuNAC50	TATA-variant	ATATAA	36	-	**II**	**CA**	68	81.9
VuNAC51.1	TATAWA	TATATA	44	21	**I**	**CA**	46	50.5
VuNAC51.2	TATAWA	TATATA	44	21	**I**	**CA**	46	50.5
VuNAC52.1	None	-	-	53	**III**	**CA**	67	53
VuNAC52.2	None	-	-	53	**III**	**CA**	66	53.5
VuNAC53	None	-	-	36	**III**	**CA**	53	60.6
VuNAC54	TATA-variant	ATATAA	67	-	**II**	**CA**	50	30.3

VuNAC55	TATA-variant	TATTATA	47	-	**II**	**CA**	40	49.7
VuNAC56	None	-	-	-	**IV**	**CA**	59	66.5
VuNAC57.1	Canonical	TATATAAG	39	31,15	**I**	**CA**	49	54
VuNAC57.2	Canonical	TATATAAG	39	31,15	**I**	**CA**	49	54
VuNAC57.3	Canonical	TATATAAG	39	31,15	**I**	**CA**	49	54
VuNAC58	None	-	-	14	**III**	**CA**	58	66
VuNAC59.1	TATA-variant	TTATTT	28	-	**II**	**-**	63	69.8
VuNAC59.2	TATA-variant	TTATTT	30	-	**II**	**-**	62	70.6
VuNAC59.3	TATA-variant	TTATTT	28	-	**II**	**CA**	63	68.5
VuNAC60	TATA-variant	TTATATA	15	48	**I**	**CA**	65	37.2
VuNAC61	None	-	-	38	**III**	**CG**	59	56.3
VuNAC62	None	-	-	46	**III**	**TG**	58	63.5
VuNAC63	None	-	-	-	**IV**	**TG**	50	67.5
VuNAC64	TATA-variant	TTATTTTT	39	-	**II**	**CA**	39	48.5
VuNAC65	None	-	-	37	**III**	**CA**	59	66.5
VuNAC66.1	None	-	-	42	**III**	**CA**	67	0
VuNAC66.2	None	-	-	42	**III**	**CA**	67	0
VuNAC66.3	None	-	-	42	**III**	**CA**	67	0
VuNAC67.1	TATA-variant	ATTATA	17	-	**II**	**CG**	49	53.5
VuNAC67.2	TATA-variant	ATTATA	17	-	**II**	**CG**	49	53.5
VuNAC67.3	TATA-variant	ATTATA	17	-	**II**	**CG**	48	53.9
VuNAC67.4	TATA-variant	ATTATA	17	-	**II**	**CG**	49	53.5
VuNAC67.5	TATA-variant	ATTATA	17	-	**II**	**CG**	49	53.5
VuNAC67.6	TATA-variant	ATTATA	17	-	**II**	**CG**	48	53.9
VuNAC68	TATA-variant	ATTATA	17	-	**II**	**CG**	49	52
VuNAC69	TATAWA	TATAAA	14	-	**II**	**-**	49	52.5
VuNAC70	TATAWA	TATAAA	14	-	**II**	**CG**	49	52
VuNAC71.1	None	-	-	40,10	**III**	**TG**	61	54.9
VuNAC71.2	TATAWA	TATAAA	14		**II**	**CG**	49	52.5
VuNAC71.3	None	-	-	40,10	**III**	**TG**	61	54.9
VuNAC72	Canonical	TATATAAA	27	-	**II**	**CA**	48	56.6
VuNAC73	TATAWA	TATAAA	20	-	**II**	**CA**	57	67.1
VuNAC74	TATA-variant	TTATAAA	47	40	**I**	**CA**	66	67.1
VuNAC75	None	-	-	-	**IV**	**CA**	66	0
VuNAC76	TATAWA	TATAAA	14	-	**II**	**CG**	49	52.5
VuNAC77	TATAWA	TATAAA	46	-	**II**	**CA**	48	65.1
VuNAC78	TATAWA	TATAAA	46	-	**II**	**CA**	48	65.1
VuNAC79	TATAWA	TATAAA	46	36	**II**	**CA**	49	65.1
VuNAC80	None	-	-	53	**III**	**CA**	68	68
VuNAC81	None	-	-	41	**III**	**CA**	63	63
VuNAC82.1	None	-	-	-	**IV**	**-**	53	58.3
VuNAC82.2	None	-	-	-	**IV**	**CA**	53	58.3
VuNAC83.1	None	-	-	14	**III**	**-**	60	74
VuNAC83.2	TATA-variant	TTAAATTA	29	-	**II**	**TG**	70	57.5
VuNAC83.3	TATA-variant	TTAAATTA	29	-	**II**	**-**	70	60
VuNAC83.4	None	-	-	-	**IV**	**CA**	49	63
VuNAC83.5	TATA-variant	TTAAATTA	29	-	**II**	**-**	70	51.5
VuNAC83.6	None	-	-	14	**III**	**-**	59	74
VuNAC83.7	None	-	-	-	**IV**	**-**	48	51.5
VuNAC83.8	None	-	-	34	**III**	**-**	66	61.5
VuNAC83.9	TATA-variant	TTAAATTA	29	-	**II**	**TG**	70	53
VuNAC83.10	None	-	-	-	**IV**	**CA**	49	56
VuNAC84.1	TATA-variant	TATATTTA	41	-	**II**	**-**	39	57
VuNAC84.2	TATA-variant	TATTATTT	65	21	**I**	**-**	65	54.5
VuNAC85	TATA-variant	TATTTA	13	-	**II**	**CA**	53	50
VuNAC86.1	TATA-variant	TATTATA	70	63	**II**	**CA**	63	58
VuNAC86.2	TATA-variant	TATTATA	70	63	**II**	**CA**	63	58
VuNAC87	TATAWA	TATATA	34	25	**I**	**-**	58	57.5
VuNAC88	TATAWA	TATAAA	74	-	**II**	**CA**	45	59.5
VuNAC89	None	-	-	29	**III**	**-**	59	63.2
VuNAC90	Canonical	TATAAATG	10	47,31	**I**	**TG**	55	57.2

Table A1.8.1 Regulators predicted based on promoter analysis

Gene ID	Hormone	TF	Stress	Metabolism	Tissue
VuNAC01	MeJA, ABA, light	MYB, MYC	Drought, Cold, Hypoxia	-	-
VuNAC02	MeJA, ABA, light	MYB, MYC	Drought	-	-
VuNAC03	MeJA, ABA	MYB, MYC	-	-	-
VuNAC04	MeJA, ABA, auxin, light	MYB, MYC	Drought	-	-
VuNAC05	MeJA, light	MYB, MYC	Drought	-	-
VuNAC06	MeJA, ABA, light	MYB, MYC	-	-	-
VuNAC07	MeJA, ABA, light	MYB, MYC	-	-	-
VuNAC08	ABA, light	MYB, MYC	Pathogen	Zein metabolism	-
VuNAC09	Light	MYB, MYC	-	-	Seed
VuNAC10	ABA, light	MYB, MYC	Hypoxia, Pathogen	-	-
VuNAC11	ABA, light	MYB, MYC	Drought	-	-
VuNAC12	Auxin	MYB, MYC	Drought, Cold, Pathogen	Zein metabolism	Seed
VuNAC13	MeJA, ABA, GA, light	MYB, MYC	-	-	Seed
VuNAC14	Light	Circadian rhythm	-	-	-
VuNAC15	MeJA, ABA, auxin, light	MYB, MYC	Hypoxia	-	-
VuNAC16	ABA, light	MYB, MYC	Cold	Zein and flavonoid metabolism	Meristem
VuNAC17	Light	MYB, MYC	-	-	-
VuNAC18	Light	MYB, MYC, WRKY	Pathogen	Zein metabolism	Meristem
VuNAC19	Light	MYB, MYC	Hypoxia, Pathogen	Zein metabolism	Meristem
VuNAC20	-	MYB, MYC	Hypoxia, Pathogen	-	Seed
VuNAC21	Light	MYB, MYC	Hypoxia, Cold, Pathogen	Zein metabolism	Meristem
VuNAC22	ABA, light	MYB, MYC	Drought	-	-
VuNAC23	MeJA, light	-	Cold	Zein and flavonoid metabolism	-
VuNAC24	MeJA, GA, light	MYB, MYC	Drought, Hypoxia, Cold	Zein metabolism	-
VuNAC25	ABA, light	MYB, MYC	Hypoxia	-	-
VuNAC26	Light	MYB, MYC	Cold, Pathogen	-	-
VuNAC27	Light	MYB, MYC, WRKY	-	-	-
VuNAC28	Light	MYB, MYC	Drought	-	-
VuNAC29	Auxin, light	MYB, MYC	Hypoxia	-	Seed
VuNAC30	MeJA	MYB, MYC	-	Zein and flavonoid metabolism	Seed
VuNAC31	ABA, light	MYB, MYC	Cold, Pathogen	Zein and flavonoid metabolism	-
VuNAC32	MeJA, GA, light	MYB, MYC, circadian rhythm	-	-	-
VuNAC33	Light	MYB, MYC	Drought, Pathogen	-	-
VuNAC34	Light	MYB, MYC	Drought	-	-
VuNAC35	ABA, light	MYB, MYC	-	-	-
VuNAC36	Auxin, light	MYB, MYC, WRKY	Hypoxia	-	-
VuNAC37	ABA, light	MYB, MYC	-	Zein metabolism	-
VuNAC38	Light	MYB, MYC	Hypoxia	-	-
VuNAC39	Light	MYB, MYC	Hypoxia, Pathogen	-	-
VuNAC40	Light	-	Hypoxia	-	-
VuNAC41	-	MYB, MYC	-	-	-
VuNAC42	MeJA, ABA, light	MYB, MYC, WRKY, circadian rhythm	Hypoxia	-	-
VuNAC43	ABA, light	MYB, MYC, WRKY	-	Zein metabolism	-
VuNAC44	ABA, light	-	Hypoxia, Cold, Pathogen	-	Meristem
VuNAC45	ABA, light	MYB, MYC, WRKY	Drought	-	-
VuNAC46	ABA, light	MYB, MYC, WRKY	Cold, Pathogen	-	Meristem
VuNAC47	Light	MYB, MYC	Pathogen	-	-
VuNAC48	Light	MYB, MYC	Drought	-	Seed
VuNAC49	Light	MYB, MYC, WRKY	-	-	-
VuNAC50	-	MYB, MYC	Hypoxia, Pathogen	-	Meristem
VuNAC51	-	Circadian rhythm	-	-	-
VuNAC52	SA, light	MYB, MYC	Drought, Pathogen	Flavonoid metabolism	-
VuNAC53	Light	MYB, MYC	Hypoxia, Pathogen	-	-
VuNAC54	Light	MYB, MYC, WRKY	Drought, Pathogen	-	Seed
VuNAC55	GA, light	MYB, MYC	Drought	Flavonoid metabolism	-
VuNAC56	ABA, light	MYB, MYC, WRKY	Cold	-	-
VuNAC57	Light	MYB, MYC	Drought	-	-
VuNAC58	MeJA, GA	-	-	-	-
VuNAC59	MeJA, ABA, light	MYB, MYC	-	-	Seed
VuNAC60	ABA, auxin, light	MYB, MYC, WRKY	Drought, Pathogen	-	-
VuNAC61	Light	MYB, MYC, WRKY	Drought, Cold	-	-
VuNAC62	ABA, light	MYB, MYC	-	-	-
VuNAC63	ABA, light	MYB, MYC, WRKY	Pathogen	Zein metabolism	-
VuNAC64	Light	-	Pathogen	-	-
VuNAC65	GA, light	MYB, MYC, WRKY	-	-	Meristem
VuNAC66	Light	MYB, MYC, WRKY	Hypoxia	-	-
VuNAC68	Light	MYB, MYC	-	-	-
VuNAC69	Light	MYB, MYC	-	-	-
VuNAC70	Light	MYB, MYC	-	-	-
VuNAC71	ABA, light	MYB, MYC, WRKY	-	-	-

VuNAC72	Light	MYB, MYC	-	-	-
VuNAC73	MeJA, light	MYB, MYC, WRKY	-	Zein metabolism	Seed
VuNAC74	Light	MYB, MYC	-	-	-
VuNAC75	MeJA, light	MYB, MYC, WRKY	-	Zein metabolism	Seed
VuNAC76	Light	MYB, MYC	-	-	-
VuNAC77	Light	MYB, MYC	-	-	-
VuNAC78	Light	MYB, MYC	-	-	-
VuNAC79	Light	MYB, MYC	-	-	-
VuNAC80	Light	MYB, MYC	-	-	Meristem
VuNAC81	Light	MYB, MYC	Drought	-	Meristem
VuNAC82	Light	WRKY	-	-	-
VuNAC83	ABA, auxin, light	MYB, MYC	Hypoxia, Pathogen	Zein metabolism	-
VuNAC84	Light	MYB, MYC	Hypoxia	-	-
VuNAC85	VuNAC86	MYB, MYC	Drought	-	-
VuNAC86	MeJA, ABA, light	MYB, MYC	-	-	-
VuNAC87	ABA, light	MYB, MYC	Pathogen	-	-
VuNAC88	ABA, light	MYB, MYC	Drought	-	-
VuNAC89	MeJA, ABA, auxin, light	MYB, MYC, WRKY	-	Zein metabolism	-
VuNAC90	Light	MYB, MYC	Cold, Pathogen	-	-

Table A1.8.2 List of *cis*-elements identified by PlantCare tool

Regulators		Element	Sequence	Description
Hormonal	ABA	ABRE	**CACGTG**	ABA responsive element
		ABRE2	CACGTA/T**ACGTG**/C**CACGTG**G	
	Auxin	TGA-element	AACGAC	Auxin responsive element
		AuxRR-core	GGTCCAT	
		TGA-box	**TGACG**TAA	
	Jasmonate	CGTCA-motif	CGTCA/**TGACG**	Jasmonate responsive element
	Salicylate	TCA-element	CCATCTTTTT	Salicylic acid responsive element
	Gibberellin	GARE-motif	TCTGTTG	Gibberellin responsive element
		P-box	CCTTTTG	
		TATC-box	TATCCCA	
Transcription factor	MYB/MYC	MYB	CAACTG/TAACTG/ CAACCA/TAACCA	Involved in stress response
		MBSI	aaaAaaC(G/C)GTTA	Involved in flavonoid biosynthesis
		MRE	AACCTAA	Involved in light response
		MYC	CATTTG/CATGTG, TCTCTTA	Involved in stress response
	WRKY	W box	T**TGAC**C	Involved in stress response
	AP/ERF	AP-1	TGAGTTAG	Involved in stress response
	HD-zip	HD-Zip 1	CAAT(A/T)ATTG	Involved in differentiation of palisade mesophyll cells
Light		G-Box	CACGTG/TACGTG/ACACGTGT/ **GCCAC**GTGGA/ACACGTGGC	Light responsive element
		GT1-motif	**GGTTAA**	
		GATA-motif	AAG**GATA**AGG	
		TCT-motif	TCTTAC	
		TCCC-motif	TCTCCCT	
		Gap-box	CAAATGAA(A/G)A	
		Box 4	ATTAAT	
		LAMP-element	CTTTATCA	
Stress (abiotic, biotic, nutrition)	Dehydration	DRE core	**GCCGAC**	Drought responsive element
	Cold	LTR	CCGAAA	Low temperature responsive element
	Anoxia	ARE	**AAACCA**	Anaerobic responsive element
	Elicitor	TC-rich repeats	GTTTTCTTAC/ATTCTCTAAC	Defense and stress responsive element
		AT-rich sequence	TAAAATACT	High elicitor responsive element
Others	Circadian	circadian	**CAAAGATATC**	Involved in circadian control
	Meristem	CAT-box	GCCACT	Involved in meristem expression
	Endosperm	GCN4_motif	TGAGTCA	Involved in endosperm expression
	Seed	RY-element	CATGCATG	Involved in seed-specific regulation
	Zein metabolism	O2-site	GATGACATGG/GTTGACGTGA	Involved in zein metabolism regulation

Table A1.8.3 *cis*-elements identified by PLACE tool in ATAF-like subgroup in cowpea

Regulators		cis-element	Description	VuNAC1	VuNAC2	VuNAC3	VuNAC4	VuNAC5	SOGO ID
Hormone	**ABA**	ABREATRD22, ABREATCONSENSUS	ABA responsive element	**4**	**5**	1	2	2	S000013, S000406
	Auxin	ASF1MOTIFCAMV	Auxin/SA responsive element	**5**	**5**	2	5	9	S000024
		NTBBF1ARROLB, CATATGGMSAUR	Auxin responsive element						S000273, S000370
	Jasmonate	CGTCA-motif	JA responsive element	**2**	**3**	2	2	6	-
	Gibberellin	GADOWNAT	GA responsive element (negative)	**2**	**1**	0	0	2	S000438
	Ethylene	ERELEE4	Ethylene responsive element	**2**	**1**	1	0	1	S000037
Transcription factor	**MYB**	MYCCONSENSUSAT	Involved in water- stress	**15**	**18**	12	17	9	S000407
		MYB2CONSENSUSAT, MYBCORE, MYB1AT, MYBST1	Involved in water- stress						S000409, S000176,S000408, S000180
		MYBPZM	Involved in flavonoid biosynthesis	**1**	**2**	1	3	3	S000179
	WRKY	WRKY71OS	Involved in GA response	**12**	**22**	15	9	27	S000447
		WBOXATNPR1	Involved in SA response						S000390
		WBOXNTERF3	Involved in wounding						S000457
	CBF	CBFHV	Involved in dehydration-response	**2**	**3**	0	2	4	S000497
	EMBP	EMBP1TAEM	Involved in ABA-response	**1**	**2**	0	1	0	S000119
	NAC	NACRS	NAC binding site	**2**	**1**	1	1	1	-
Light		GT1CORE, SORLIP1AT, GATABOX	Light-responsive element	**28**	**30**	19	31	27	S000125, S000482, S000039
Stress (abiotic, biotic, nutrition)	**Dehydration**	ACGTATERD1, DRECRTCOREAT	Etiolation-induced expression of AtERD1	**5**	**8**	5	7	21	S000415, S000418
	Osmotic, salinity	TAAAGSTKST1	Regulating a K^+ influx channel in stomata	**5**	**5**	1	2	2	S000387
		ABRERATCAL	Ca^{2+} responsive genes	**5**	**3**	3	2	1	S000507
	Cold	LTRECOREATCOR15, CRTDREHVCBF2	Cold responsive element	**1**	**2**	0	2	8	S000153, S000411
	Oxygen	ANAERO2CONSENSUS	Involved in the fermentation	**1**	**1**	2	2	2	S000478
	Elicitor	GT1GMSCAM4	Pathogen and salt-responsive element	**21**	**26**	12	20	19	S000453
		EBOXBNNAPA, ARR1AT	RRE (R response element)						S000144, S000454
	Phosphate	P1BS	Phosphate-starvation response	**0**	**1**	0	1	0	S000459
	Sulphur	SURECOREATSULTR11	Sulfur-response	**0**	**3**	1	1	1	S000499
	Iron	IRO2OS	Iron deficiency response	**1**	**2**	1	2	1	S000505
	Copper	CURECORECR	Copper-response	**2**	**3**	2	0	3	S000493
	Sugar (repression)	PYRIMIDINEBOX-OSRAMY1A, SREATMSD, TATCCAYMOTIF-OSRAMY3D	Involved in sugar repression	**4**	**5**	4	7	4	S000259, S000470, S000256
Others	**Circadian**	CIACADIANLELHC	Involved in circadian expression	**1**	**0**	0	0	0	S000252
	Enhancer	EECCRCAH1	Enhancer element	**1**	**3**	5	1	1	S000494
	Root-hair	RHERPATEXPA7	Root hair-specific element	**1**	**2**	0	5	0	S000512
	Endosperm	AACACOREOSGLUB1	Endosperm-specific expression	**0**	**0**	1	1	0	S000353
	Mesophyll	CACTFTPPCA1	Mesophyll-specific expression	**4**	**17**	16	14	11	S000449
	Cytochrome	SITEIIATCYTC	Cytochrome expression	**4**	**0**	1	0	0	S000474

Table A1.9 VuNAC FPKM values of RNA seq analysis of shoot and root tissue

Group	Gene	Average FPKM values		Group	Gene	Average FPKM values	
		Mature Leaves	Seedling Root			Mature Leaves	Seedling Root
GI	VuNAC01	14.57	88.12		VuNAC46	0.41	11.06
	VuNAC02	5.15	16.73		VuNAC47	3.34	0.20
	VuNAC03	0.00	7.43		VuNAC48	0.23	0.39
	VuNAC04	27.45	7.62		VuNAC49	0.00	0.05
	VuNAC05	5.67	21.04		VuNAC50	1.04	0.41
	VuNAC06	2.82	4.86	GV	VuNAC51	0.47	3.72
	VuNAC07	6.07	25.32		VuNAC52	0.00	0.60
	VuNAC08	0.00	1.04		VuNAC53	0.00	2.36
	VuNAC09	2.91	19.30		VuNAC54	19.28	44.79
	VuNAC10	0.00	0.00		VuNAC55	2.79	3.73
	VuNAC11	2.02	2.00		VuNAC56	0.00	0.12
	VuNAC12	0.00	2.37	GVI	VuNAC57	7.54	37.61
	VuNAC13	1.60	40.03		VuNAC58	11.21	20.90
	VuNAC14	1.91	103.83		VuNAC59	12.50	35.40
	VuNAC15	1.39	18.59		VuNAC60	78.09	1.01
	VuNAC16	0.00	6.23		VuNAC61	1.26	1.06
	VuNAC17	0.00	0.91		VuNAC62	1.83	4.94
	VuNAC18	0.00	89.86		VuNAC63	21.90	8.09
	VuNAC19	3.63	64.44		VuNAC64	0.46	20.59
	VuNAC20	4.43	18.83		VuNAC65	9.48	63.63
GII	VuNAC21	0.00	1.57	GVII	VuNAC66	1.55	22.77
	VuNAC22	0.00	0.23		VuNAC67	0.00	0.18
	VuNAC23	1.51	0.30		VuNAC68	0.00	0.00
	VuNAC24	0.23	1.91		VuNAC69	0.00	2.39
	VuNAC25	0.13	0.30		VuNAC70	0.00	0.00
	VuNAC26	0.00	0.37		VuNAC71	9.36	38.64
	VuNAC27	0.22	0.15		VuNAC72	0.00	0.00
	VuNAC28	0.00	0.18		VuNAC73	0.00	0.00
	VuNAC29	0.19	5.36		VuNAC74	0.00	0.00
GIII	VuNAC30	7.71	110.84		VuNAC75	0.00	5.83
	VuNAC31	0.00	6.55		VuNAC76	0.00	0.12
	VuNAC32	0.22	5.62		VuNAC77	0.00	0.00
	VuNAC33	0.00	32.68		VuNAC78	0.00	0.00
	VuNAC34	1.49	51.77		VuNAC79	0.00	1.21
	VuNAC35	1.68	55.48		VuNAC80	0.00	0.30
	VuNAC36	0.23	0.21		VuNAC81	0.18	0.25
	VuNAC37	0.00	0.00		VuNAC82	1.83	10.72
	VuNAC38	0.35	7.60	GVIII	VuNAC83	1.16	4.43
	VuNAC39	0.00	8.98		VuNAC84	0.14	3.08
	VuNAC40	0.58	0.00		VuNAC85	3.63	3.15
	VuNAC41	0.00	1.96		VuNAC86	10.55	6.66
	VuNAC42	0.00	0.49		VuNAC87	0.53	1.44
	VuNAC43	0.00	0.49		VuNAC88	0.95	1.18
GIV	VuNAC44	19.36	37.29		VuNAC89	52.72	11.14
	VuNAC45	18.26	11.67		VuNAC90	30.21	3.09

APPENDIX 2

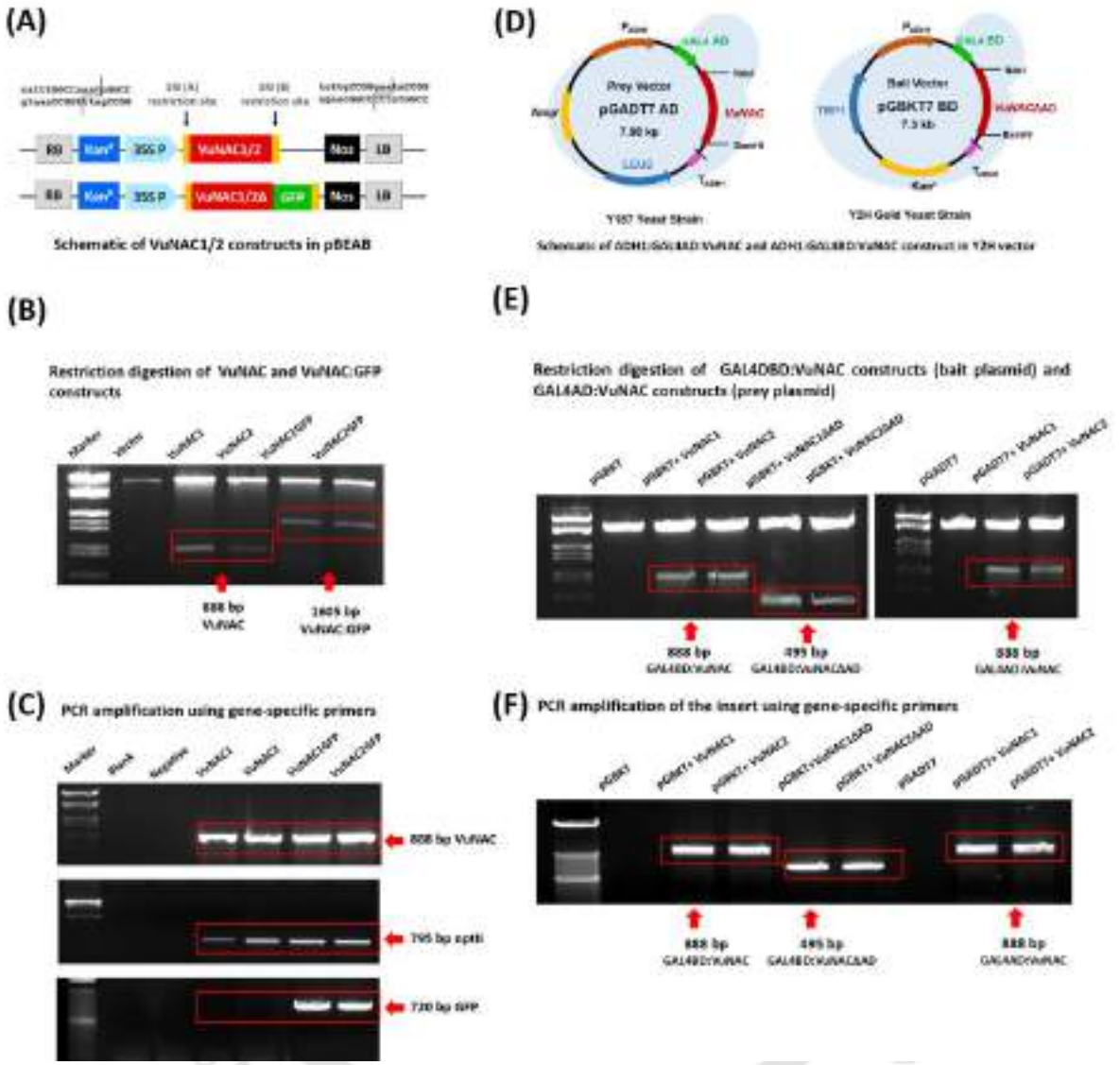

Fig. A2.1 Cloning of *VuNAC1* and *VuNAC2* genes in plant and yeast expression vector. (A) Schematic diagram of 35S:VuNAC1/2 and 35S:VuNAC1/2:GFP T-DNA gene constructs used for plant expression. **(B)** Molecular confirmation of the T-DNA vectors by restriction digestion. **(C)** Molecular confirmation of the T-DNA carrying agrobacterium strains by colony PCR. **(D)** Schematic diagram of the GAL4BD:VuNAC1/2 and GAL4BD:VuNAC1/2ΔAD gene constructs used for yeast-reporter assay and GAL4AD:VuNAC1/2 and GAL4BD:VuNAC1/2ΔAD used for Y2H assay. **(E)** Molecular confirmation of the yeast vectors by restriction digestion and **(F)** Molecular confirmation of the transformed yeast strains by colony PCR.

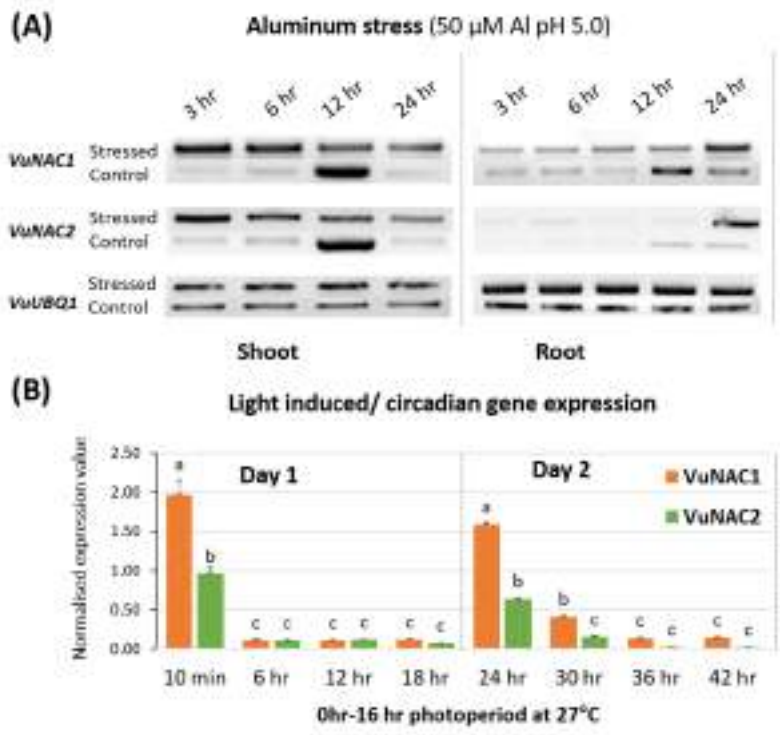

Fig. A2.2 Expression analysis in response to aluminum stress and light. (A) The VuNAC1/2 gene transcripts were accumulated in response to aluminium stress indicating early gene induction in shoot, and late response in the root tissue, suggesting different mode of signal transduction in shoot and root. **(B)** Gene expression profile in response to diurnal light exposure indicating circadian and/or light-mediated induction of *VuNAC1/2* genes.

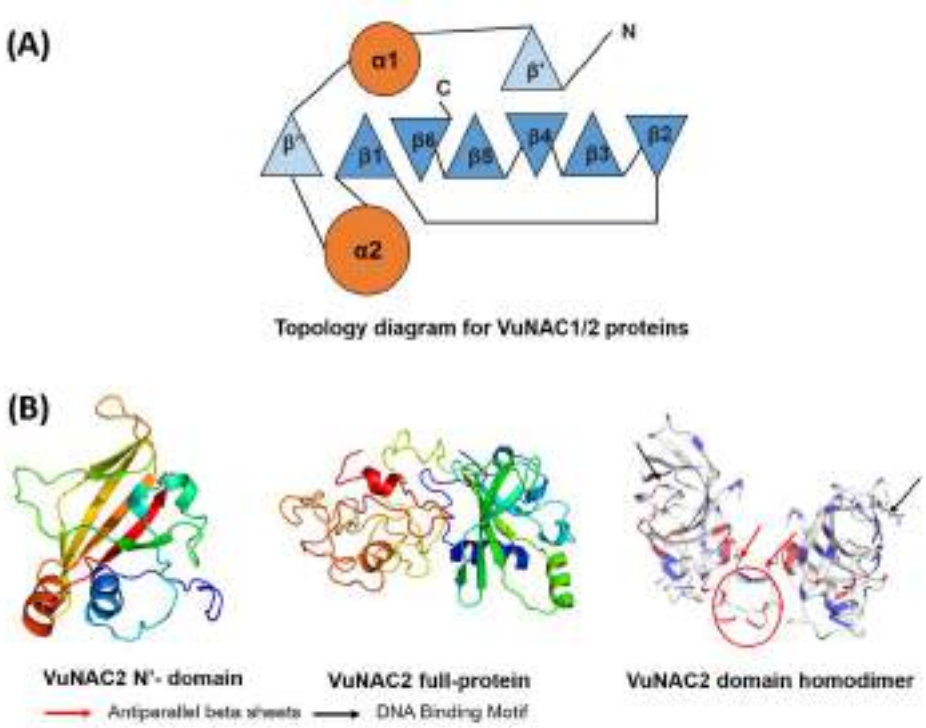

Fig. A2.3 Structure prediction. (A) Topology diagram of VuNAC1/2 proteins. **(B)** 3D folding of VuNAC2 protein.

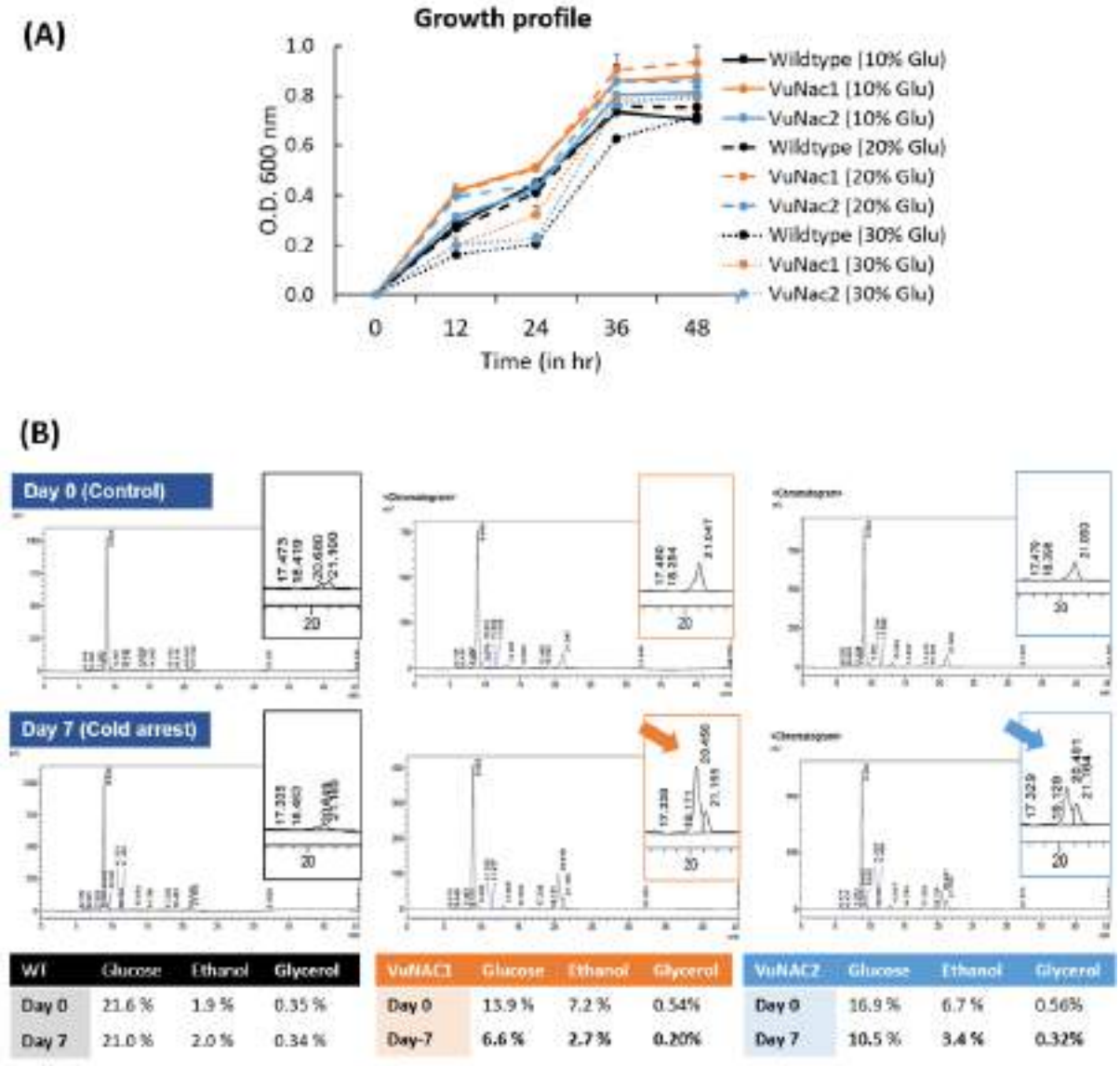

WT	Glucose	Ethanol	Glycerol
Day 0	21.6 %	1.9 %	0.35 %
Day 7	21.0 %	2.0 %	0.34 %

VuNAC1	Glucose	Ethanol	Glycerol
Day 0	13.9 %	7.2 %	0.54%
Day-7	6.6 %	2.7 %	0.20%

VuNAC2	Glucose	Ethanol	Glycerol
Day 0	16.9 %	6.7 %	0.56%
Day 7	10.5 %	3.4 %	0.32%

Fig. A2.4 Growth characterization. (A) Growth profile at different glucose concentrations (10%, 20%, and 30%) indicating increased growth of VuNAC1/2-expressing strains in high glucose levels. **(B)** The HPLC chromatogram showing the ethanol peaks (Day 0) and the peaks for ethanol and its esterified product (the two peaks indicated by the arrow) after a cold-arrest of 4°C (Day 7). The reduced glucose and ethanol level suggested active alcohol fermentation and metabolism in the transgenic strains, while the activity of wild type strain was halted due to freezing.

Table A2.5. Assignment of FTIR peaks detected in the yeast strains

Region no.	Assigned peaks (cm^{-1})*	Macromolecule	Functional group
I	3300 cm^{-1}	polysaccharide alcohol	-OH stretch
(3500-3000 cm^{-1})	3400-3300 cm^{-1}	aliphatic primary amine	-NH stretch
	3350-3310 cm^{-1}	secondary amine	-NH stretch
	3200-2700 cm^{-1}	alcohol	-OH stretch
	3000-2800 cm^{-1}	amine salt	-NH stretch
	3100 cm^{-1}	amide II	-C=O stretch
II	2960 cm-1, 2875 cm^{-1}	lipids	-CH2 stretch
(3000-2820 cm^{-1})	2920 cm-1, 2855 cm^{-1}	lipids	-CH3 stretch
	2890 cm^{-1}	lipids, proteins, and peptides	-CH deformation
III	2279-2250 cm^{-1}	isocyanate	-N=C=O stretch
(2820-1800 cm^{-1})	2239-2225 cm^{-1}	nitrile	-CΞN stretch
	2167-2200 cm^{-1}	thiocyanate	-S-CΞN stretch
	2148-2110 cm^{-1}	azide	-N=N=N stretch
IV	1747, 1620 cm^{-1}	pectin	-COOH stretch
(1800-1325 cm^{-1})	1749 cm^{-1}	lipid ester	-C=O stretch
	1652 cm^{-1}	amide I	-C=O strectch
	1620 cm^{-1}	amide I, polypeptides, mannoproteins	-C=O strectch
	1541 cm^{-1}	amide II	-C=O stretch
	1458 cm^{-1}	lipids and proteins	-CH2/CH3 bend
	1419 cm^{-1}	proteins	-COH plane bend
V	1250 cm^{-1}	DNA, RNA, and phospholipids	$-PO^{-2}$ stretch
(1325-750 cm^{-1})	1215 cm^{-1}	free nucleotides	-CO stretch
	1135 cm^{-1} ,802 cm^{-1}	mannans and β 1,3 glucans	-CO & -C-C stretch
	1001 cm^{-1}	β 1,3 glucans	-CO & -C-C stretch
	920 cm^{-1}	monosaccharides (glucose, mannose)	Pyranose ring
	879 cm^{-1}	polysaccharides (starch)	β-glycosidic link
	858 cm^{-1}	polysaccharides (starch)	α-glycosidic link

***Source: Burattini *et al.* 2008, Kochan *et al*. 2018**

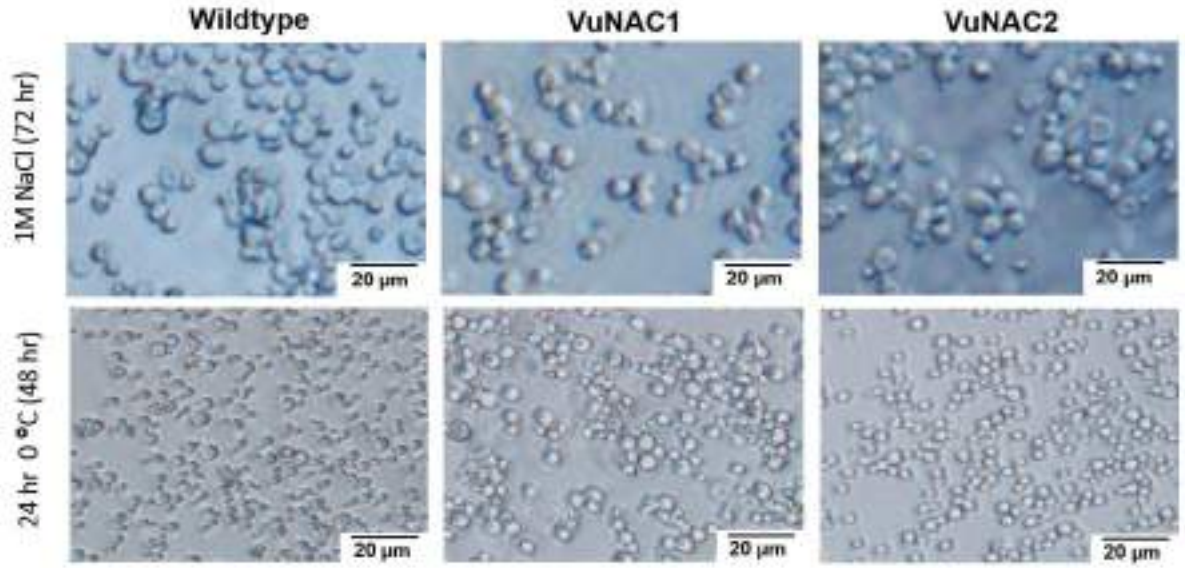

Fig. A2.6 Phenotypic analysis in response to salt and cold stress. The transgenic strains exhibited tolerance to NaCl and cold stress as indicated by the viable and dividing cells. Although, after NaCl treatment, the strains showed a reduction in cell size but retained the viability, unlike the wild type strain displaying severe cell death. Also, after the cold arrest, the transgenic strains displayed less cell shrinking than the wild type.

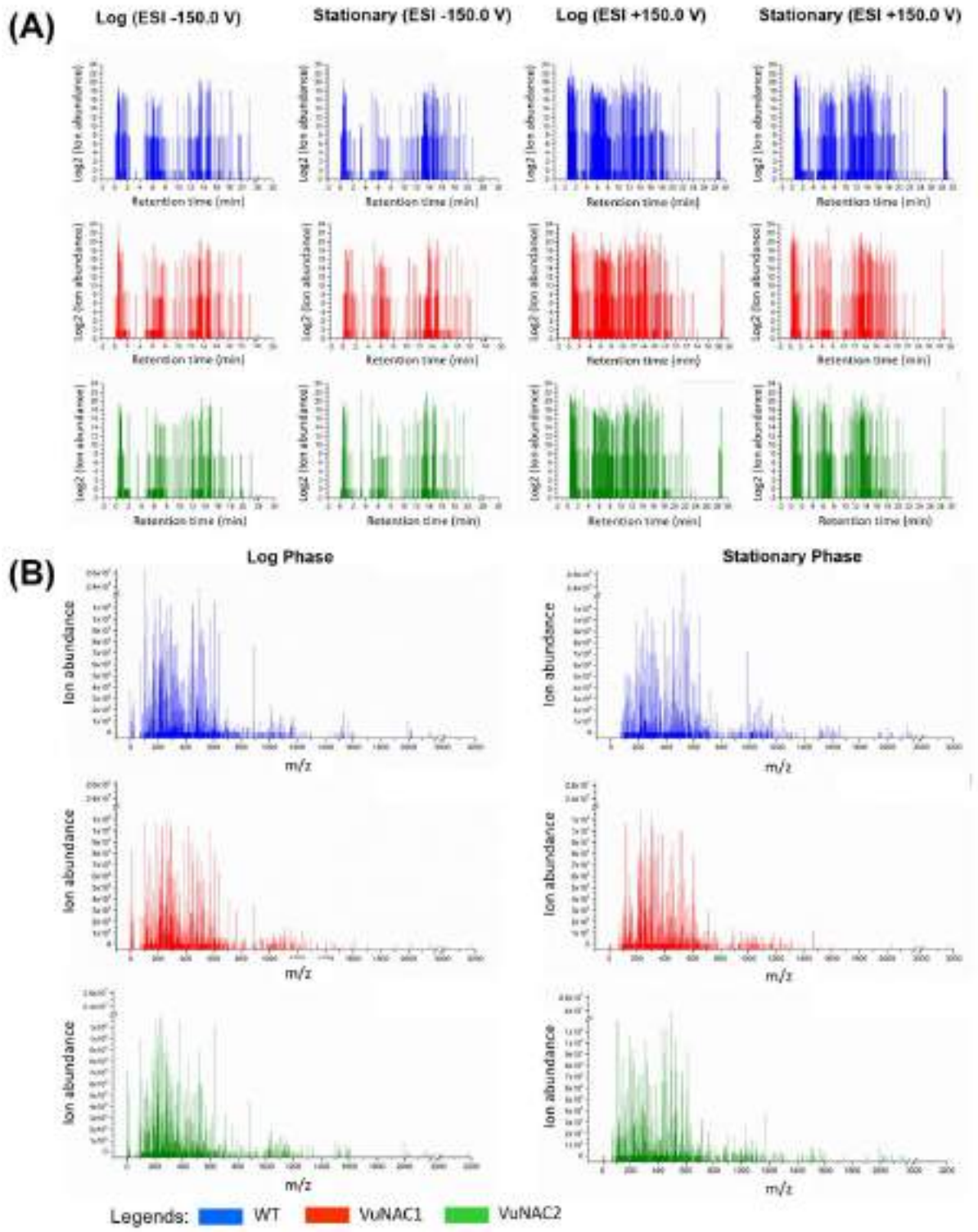

Fig. A2.7 LCMS Spectral Plot. (A) Ion abundance *vs.* retention time. **(B)** Ion abundance *vs.* m/z ratio.

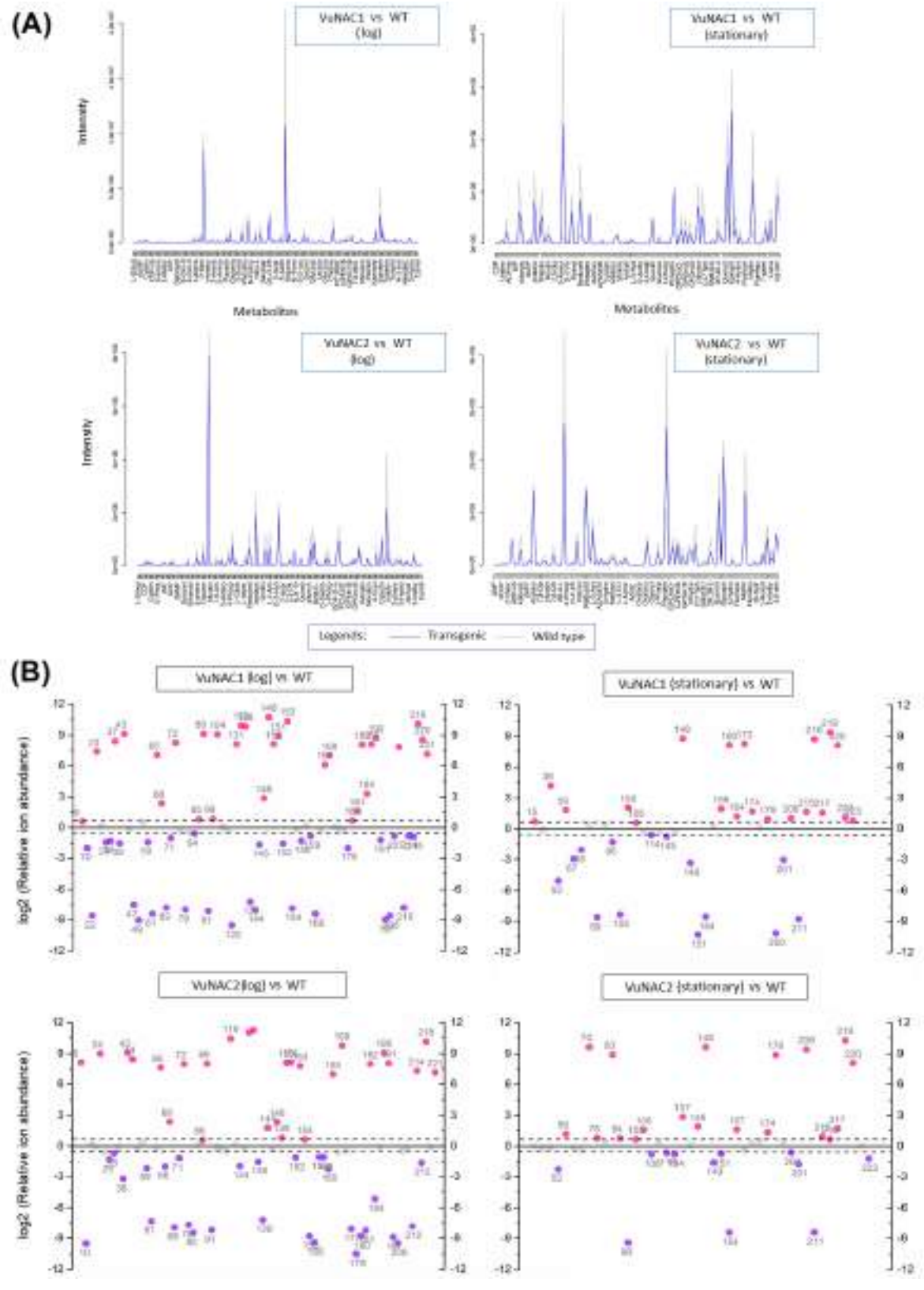

Fig. A2.8 Change in peak and fold change. (A) Overlaying LCMS spectra of transgenic and wild type strains indicating the change in metabolite content. **(B)** Normalized relative (transgenic vs. wild type) indicating increased (pink) and decreased (purple) metabolites in the order of retention time. The numeric labels correspond to the metabolites listed in Table A2.9.

Table A2.9 Metabolites identified by LCMS and their relative intensities

S.N.	Compounds	Description	m/z ratio	RT (min)	Fold-change (log phase)		Fold-change (stationary phase)	
					VuNAC1	VuNAC2	VuNAC1	VuNAC2
		PYRIMIDINE METABOLISM [530]						
1	L-Dihydroorotic acid	de novo pyrimidine precursors	218.1	0.5	-6.71	-6.71	-	-
2	Orotidylic acid		390.2	5.9	-7.74	-7.74	-	-
3	UMP	Salvage pyrimidine and RNA precursors	307.2	10.7	16.23	15.60	0.00	7.69
4	CMP	RNA precursors	345.0	0.7	0.00	7.64	-	-
5	2',3'-Cyclic CMP	Secondary messengers	343.1	0.8	8.22	0.00	-	-
6	CDP	DNA & RNA precursors	445.0	0.7	0.55	8.12	8.14	0.00
7	dUMP	Thymidine precursors	289.2	1.1	-17.80	-17.80	-	-
8	dUDP		388.2	6.5	-15.80	-15.80	7.04	6.95
9	dCDP	DNA precursors (Cytidine)	386.2	11.0	-	-	0.00	15.09
10	dTMP	DNA precursors (Thymidine)	342.2	0.7	-1.99	-9.51	15.68	0.00
11	dTDP		406.2	5.9	-8.02	-8.02	-	-
12	Cytidine	Salvage pyrimidine precursors	281.2	7.3	18.09	17.25	-	-
13	Deoxycytidine		231.1	5.2	7.57	0.00	-	-
14	2'-Deoxyuridine		270.2	14.4	-	-	15.52	7.87
15	Uridine		264.2	4.9	-17.00	-17.00	0.71	0.00
16	Thymidine		288.2	12.5	6.94	0.00	7.12	0.00
		PURINE METABOLISM [406, 531]						
17	ADP-D-ribose	Purine precursor	605.3	5.7	-7.70	-7.70	-	-
18	AIR	*de novo* purine precursor	333.1	2.9	-8.59	-8.59	-	-
18	AICAR		321.2	0.7	-7.16	-7.16	-	-
19	FAICAR[383]		317.2	6.7	-16.54	-16.54	15.15	0.00
20	Phosphoribosyl formamido carboxamide		404.2	5.9	-7.98	-7.98	15.12	0.00
21	IMP	Salvage purine precursor	408.2	13.7	16.75	15.19	7.83	0.00
22	Hypoxanthine		136.0	0.8	-8.60	0.23	-15.69	-15.69
23	XMP		363.2	14.9	7.35	-0.04	-	-
24	GDP	RNA precursor (Guanidine)	465.2	5.1	0.17	8.99	-	-
25	Adenosine	Salvage purine precursor	287.2	5.4	-8.25	-8.25	-	-
26	ATP	RNA precursor, energy currency	489.2	0.5	7.47	17.89	-9.00	-9.00
27	dATP	DNA precursor (Adenosine)	508.2	6.2	-7.75	-0.62	-7.35	-7.35
28	dADP		410.2	1.1	-8.08	-8.08	16.18	0.00
29	dAMP	Secondary messengers	333.2	2.9	-1.42	-1.31	-	-
		VITAMIN B6 [392]**, THIAMINE**[388] **& BIOTIN METABOLISM**						
30	2-Oxo-3-hydroxy-4-phosphobutanoic acid	Vitamin B6 precursor	214.1	1.4	-8.12	-8.12	-	-
31	Pyridoxine 5'-phosphate	Vitamin B6	269.1	9.6	7.76	14.90	-	-
32	Pyridoxamine 5'-phosphate		230.2	1.9	0.00	8.39	-0.07	-0.16
33	Pyridoxal 5'-phosphate (PLP) [392]		246.2	5.4	-16.47	-16.47	-	-
34	4-amino-2-methyl-5 phosphomethylpyrimidine	Thiamine precursor	218.1	1.2	-19.21	-19.21	16.84	0.00
35	Thiamine[388]	TPP co-enzyme precursor	264.1	0.5	-1.30	-0.72	-	-
36	Thiamine diphosphate	Thiamine derivative, Cofactor	423.3	11.6	15.49	16.55	-	-
37	Thiamine pyrophosphate	TPP co-enzyme	442.3	16.8	8.42	-0.09	-	-
38	Thiamine triphosphate	Thiamine derivative	505.3	5.1	-1.53	-3.23	4.21	-15.72
39	7,8-Diaminononanoate	Biotin precursor	234.2	14.7	-	-	15.76	7.83
40	D-Biotin	Cofactor in carboxylation	244.1	6.0	-7.75	-7.75	-16.98	-16.98
		FOLIC ACID METABOLISM[532]						
41	2,5-Diamino-6-(5'-phosphoribosylamino)-4-pyrimidineone	Biopterin & Flavin precursor	336.2	16.4	8.71	0.00	-7.41	-0.08
42	2,5-Diamino-4-hydroxy-6-(5-phosphoribosylamino) pyrimidine		335.2	12.5	0.00	14.14	-	-
43	7,8-Dihydroneopterin	Biopterin precursor	254.2	16.5	9.12	9.07	0.00	18.58
44	7,8-Dihydropteroic acid		352.3	18.0	-0.13	8.45	0.00	15.85
45	Tetrahydrofolic acid	Folate derivative	467.4	15.8	7.28	0.00	-	-
46	5,10-Methenyltetra-hydrofolic acid		460.4	18.3	-7.90	-7.90	-8.47	-8.47
		RIBOFLAVIN METABOLISM[389]						

47	5-Amino-6-(5'-phosphoribitylamino)uracil	Riboflavin precursor	338.2	17.8	-0.19	-0.62	-	-
48	2-Hydroxy-3-oxobutyl phosphate		166.1	5.5	-7.77	-7.77	-	-
49	6,7-Dimethyl-8-(1-D-ribityl) lumazine	Riboflavin intermediate	325.3	17.2	-9.04	-0.25	-	-
50	FMN	Cofactor, Riboflavin derivative	456.4	11.3	6.79	0.00	-	-
51	FMNH2		462.3	13.0	-	-	0.00	15.90
		PANTOTHENATE & COENZYME A METABOLISM[391]						
52	Pantothenic Acid[391]	Coenzyme A precursor	218.1	1.2	-19.21	-19.21	-5.05	-2.24
53	4-Phosphopantothenoyl cysteine	Coenzyme A intermediate	406.1	3.4	9.22	18.78	0.00	14.70
54	Pantetheine		278.1	6.2	18.31	16.71	0.00	8.46
		NAD/NADH BIOSYNTHESIS[390]						
55	NaMN	Vitamin B3/NAD precursor	374.2	5.3	-8.65	-8.65	18.39	0.00
56	NADH[390]	Cofactor	665.1	0.8	0.00	8.02	-17.38	-17.38
57	Nicotinate ribotide	NAD/B3 Salvage precursor	273.3	10.6	0.51	0.33	-7.80	-7.80
58	Nicotinamide	Vitamin B3	103.1	0.5	9.06	0.00	-	-
		OTHER VITAMINS						
59	Calcifediol	Involved in UV protection	357.4	14.4	-1.41	-2.15	1.80	1.16
60	Retinylphosphate mannose	Lipid-linked oligosaccharide synthesis	528.2	6.8	-	-	14.02	7.22
		GLUTAMATE, ASPARTATE & ALANINE METABOLISM						
61	Glutamate	TCA intermediate, nucleotides & amino acid precursor	147.1	0.6	-8.42	-7.32	-	-
62	L-Aspartic acid	TCA intermediate & nucleotide precursor	132.1	17.0	-8.88	-0.23	-	-
63	L-Aspartyl-4-phosphate	Aspartate derivative, amino acid precursor	273.1	0.5	7.53	0.00	-	-
64	L-aspartic 4-semialdehyde		137.1	2.8	0.00	8.60	-	-
65	Homoserine	Lysine, threonine & cysteine precursor	119.1	0.5	7.03	7.62	-8.76	-8.76
		GLUTATHIONE METABOLISM [393]						
66	Pyroglutamic acid	Glutathione precursor	167.1	0.8	-19.27	-2.00	-	-
67	Reduced Glutathione (GSH) [393]	Anti-oxidant	307.1	0.7	20.68	20.27	-2.96	-0.17
68	Oxidized Glutathione (GSSH) [393]		612.2	0.7	2.32	2.34	-2.06	-0.44
		HISTIDINE, ARGININE & LYSINE METABOLISM						
69	Phosphoribosyl-AMP	Amino acid & secondary metabolite precursor	559.3	12.2	-7.81	-7.93	14.83	0.00
70	Phosphoribulosylformimino-AICAR-P	Histidine Precursor	637.4	16.3	8.58	0.00	-7.24	9.64
71	Imidazole acetol-phosphate		201.1	1.5	-1.03	-1.18	-	-
72	2-(3-Carboxy-3-(methylammonio)propyl)-L-histidine	Histidine derivative	251.1	11.7	8.25	7.96	-	-
73	Ornithine	Arginine biosynthesis, NO	132.1	0.5	-8.81	-8.81	-	-
74	Citrulline	homeostatis	174.1	0.4	-20.16	-20.16	-	-
75	Nitro-L- Arginine[533]	Arginine derivative, NO inhibitor	236.1	1.9	8.30	0.00	-	-
76	L-Glutamic acid 5-phosphate	Proline precursor	228.1	1.5	-7.96	-7.96	-	-
77	1-Pyrroline-5-carboxylic acid	Proline & arginine precursor	117.1	0.7	-0.34	-9.61	-	-
78	L-2-Aminoadipic acid	Lysine precursor	143.1	0.7	20.65	20.32	0.29	0.78
79	Allysine	Lysine catabolism	145.1	0.7	-8.00	-7.69	-	-
80	Saccharopine	Lysine precursor	257.3	11.9	-0.50	-8.47	8.36	0.00
81	Lysine	Nitrogen nutrient, Histone component	146.1	0.5	7.46	8.44	-	-
82	Hydroxylysine	Lysine analog, collagen biosynthesis	222.1	10.9	-	-	7.20	14.44
83	Trimethyllysine[4]	Histone component, Carnitine biosynthesis	188.2	0.5	-	-	8.47	17.21
		LINEAR & BRANCHED AMINO ACID [395] **METABOLISM**						
84	Glycine	Thiamine & amino acid precursor	103.1	0.5	-0.59	0.05	-	-
85	DL-O-Phosphoserine	Serine intermediate, Cysteine Precursor	207.1	0.7	0.79	0.54	-	-
86	AZASERINE	Purine antagonist, glutamine analog	215.1	0.5	-	-	7.63	8.20
87	L-Threonine	Isoleucine precursor	157.1	1.4	16.94	0.00	-	-
88	Isoleucine[395]	Promote fermentation duration	113.1	2.7	18.61	9.24	-	-
89	Homolanthionine	Isoleucine precursor	250.1	0.7	9.11	7.99	-8.65	0.41
90	2-Isopropylmalic acid	Leucine precursor	204.1	0.5	-7.38	-7.38	-8.39	-8.39
91	3-Hydroxyisobutyric acid	Valine metabolite	86.0	0.6	-8.16	-8.20	0.00	16.50
		SULFUR AMINO ACID METABOLISM						
92	3-mercaptopyruvate	Cysteine metabolite	124.0	28.9	7.87	0.00	8.40	0.00
93	Methionine[396, 397]	Amino acid, Prolongs log phase	148.1	4.7	19.42	9.28	-8.50	8.91
94	Methionine sulfoxide[534]	Anti-oxidant, Effects life-span	165.1	0.7	-	-	0.41	0.75
95	Sulfate	Sulfur amino acid biosynthesis	98.0	0.6	24.34	0.00	-	-

96	Adenosine phosphosulfate	Sulfur reduction pathway	427.0	0.6	-	-	-1.28	-9.41
		AROMATIC AMINO ACID METABOLISM						
97	Shikimic acid	Aromatic amino acid precursor	173.1	1.4	-16.89	-16.89	8.77	0.00
98	Shikimate 3-phosphate		236.1	2.0	-7.62	-7.62	-	-
99	3-Methoxy-alpha-methyl-L-tyrosine	Phenylalanine derivative	225.1	6.5	0.81	-0.09	-	-
100	Levodopa[398]	Dopamine precursor Inhibition of respiratory growth and survival in yeast	243.1	0.5	-	-	-7.09	-7.09
101	Metyrosine	Tyrosine derivative	177.1	3.1	17.45	0.00	-	-
102	N-Formyl-L-tyrosine		231.2	9.0	0.00	14.01	-	-
103	L-3,5-Diiodotyrosine		432.9	0.2	-	-	-6.86	-6.86
104	N'-Formylkynurenine	Tryptophan catabolite	217.2	7.6	9.06	-0.16	-7.05	-7.05
105	L-Kynurenine		254.2	13.4	-	-	-8.38	0.64
106	L-3-Hydroxykynurenine		223.2	9.7	0.08	-0.51	2.03	1.57
107	Quinolinic acid	Folate and pterin precursor	187.1	0.5	16.21	8.35	-	-
108	4-(2-Aminophenyl)-2,4-dioxobutanoic acid	Tryptophan catabolite	189.0	3.9	-	-	0.56	-0.79
		PYRUVATE METABOLISM						
109	Pyruvaldehyde	Pyruvate intermediate	71.1	2.7	0.00	8.37	-	-
110	S-Lactoylglutathione		401.4	14.4	7.01	0.00	-	-
111	L-Lactic acid	Pyruvate metabolite	132.1	0.5	-8.81	-8.81	-	-
112	Acetic acid		102.1	6.2	-	-	-0.32	-7.88
113	S-Acetyldihydrolipoamide	Converts pyruvate into acetyl-CoA	248.1	0.6	16.24	0.00	7.98	7.56
		TCA & GLYOXYLATE CYCLE						
114	Oxalacetic acid	TCA cycle metabolite, Carboxylic acid derivatives	114.1	6.2	-	-	-0.59	0.34
115	trans-Aconitic acid		212.1	6.0	0.00	8.70	-9.29	-9.29
116	Isocitric acid		174.1	0.4	-20.16	-20.16	-	-
117	2-Oxoglutaric acid	TCA cycle metabolite, Keto acids derivatives	188.1	7.8	-	-	7.41	0.00
118	Oxalosuccinic acid	TCA cycle metabolite, Carboxylic acid derivatives	189.1	1.0	16.76	8.22	-16.83	-16.83
119	Succinic acid		117.1	0.6	-0.28	10.44	-0.39	-0.65
120	Fumaric acid		115.1	0.6	-9.52	0.13	-	-
121	4-hydroxy-2-oxoglutaric acid	Glyoxylate Precursor, Glutaric acid derivative	190.1	6.1	7.65	0.00	-6.91	-6.91
122	Glyoxylic acid	Glyoxalate	102.0	0.5	-	-	-7.92	-7.92
123	Glycolic acid	Glyoxalate derivative	118.1	1.9	9.34	0.00	-	-
		GLYCOLYSIS/ GLUCONEOGENESIS & PENTOSE PHOSPHATE PATHWAY						
124	Beta-D-Glucose	Hexose sugar	202.1	1.4	-9.11	-1.94	-	-
125	Glucose 6-phosphate	Hexose sugar derivative	260.1	0.8	-17.70	-17.70	17.54	0.00
126	D-fructose 1,6-bisphosphate		322.1	0.7	0.00	7.25	-	-
127	D-Glyceraldehyde 3-phosphate	Glycolsysis end product	151.0	5.1	-8.63	-8.63	-	-
128	L-Sorbose	Hexose sugar	222.2	12.0	7.50	7.26	-	-
129	D-Glucoside	Hexose sugar derivative	198.1	3.4	9.43	0.00	-	-
130	D-Sedoheptulose 7-phosphate	Heptose sugar derivative	328.0	12.0	0.00	7.93	-	-
131	Cellobiose	Disaccharides	342.3	11.2	8.10	-0.16	-	-
132	Lactulose	Disaccharides, Synthetic Sugar	342.1	0.5	9.92	11.01	-	-
133	D-Ribose 5-phosphate	Pentose sugar, Purine precursor	276.1	6.6	-7.16	-7.16	-	-
134	6-Phosphogluconic acid	Hexose sugar derivative	276.1	0.5	-	-	-7.76	-0.77
		GALACTOSE METABOLISM						
135	Melibitol	Disaccharide, Galactose metabolism	361.2	1.1	9.07	0.00	-	-
136	Epimelibiose		388.1	0.5	9.82	11.26	-9.69	-9.69
137	1-Phospho-alpha-D-galacturonate	Galactose derivative	216.1	0.6	9.41	18.29	-15.84	2.85
		AMINO SUGAR & NUCLEOTIDE SUGAR METABOLISM						
138	Glucosamine 6-phosphate	Lipid & Nucleoside sugar precursor	259.2	1.3	-10.10	-1.53	-	-
139	Glucosamine	Nucleoside sugar precursor	161.1	0.6	-7.22	-7.19	-	-
140	UDP-glucose	Glycogen precursor, cell-wall beta-glucan synthesis	583.3	6.4	7.37	0.00	15.68	0.00
141	UDP-GlcNAc	Cell-wall glycan synthesis, Coenzyme precursor	607.1	0.6	9.44	9.37	-	-
142	UDP-D-Xylose	Nucleoside sugar	596.1	0.7	-	-	7.67	0.00
143	UDP-N-acetyl-D-galactosamine	Nucleoside sugar, Cell wall precursor	653.1	0.7	-	-	0.00	16.57
		LIPID METABOLISM						
144	Choline	Phosphatidyl choline precursor	103.1	0.5	-8.01	1.74	-	-
145	Phosphocholine	Represses Phospholipid biosynthesis	183.1	13.0	-1.66	-0.25	-0.73	0.08

146	Glycerophosphocholine [400]	Membrane lipid homeostasis, salt tolerance	257.1	0.6	2.84	2.31	-0.26	1.89
147	PC(16:1(9Z)/18:0)	Glycerophosphocholines, C16, C18	761.1	0.7	18.15	17.87	-	-
148	GPCho(O-16:0/2:0)	C16, C2, Membrane phospholipid, activator	523.4	15.9	10.71	0.78	8.78	9.64
149	GPCho(16:0/0:0)	Glycerophosphocholines, C16	495.3	14.0	-	-	-3.36	-1.59
150	GPEtn(18:0/0:0)	Glycerophosphorylethanolamine, C18	541.3	14.4	8.11	8.08	-7.73	-7.73
151	GPEtn(16:0/0:0)	Glycerophosphorylethanolamine, C16	513.3	13.2	8.88	8.13	-10.30	-0.73
152	GPEtn(18:1(9Z)/0:0)	Glycerophosphorylethanolamine, C18	479.3	13.2	-1.56	-1.11	-9.27	-9.27
153	GPSer(16:0/0:0)	Glycerophosphoserine, C16	497.3	14.4	10.33	7.77	18.63	18.38
154	GPSer(18:1(9Z)/0:0)	Glycerophosphoserine, C18	523.3	14.9	-7.88	0.60	-8.58	-8.42
155	GPGro(18:0/0:0)	Gycerophosphoglycerol, C18	529.3	17.0	-0.19	-8.80	-7.24	-7.24
156	GPA(17:1(9Z)/0:0)	Glycerophospholipid, C17	485.3	11.6	-1.29	-9.42	-	-
157	GPA(21:4(6Z,9Z,12Z,15Z)/0:0)	Glycerophospholipid, C21	531.3	14.7	-	-	0.21	1.57
158	Dihydrosphingosine	Sphingolipid precursor	301.3	11.9	0.15	-1.06	1.92	-0.40
159	Phytosphingosine	Sphingolipid precursor	317.3	12.0	-0.82	-1.07	19.96	19.57
160	C17 Sphinganine	Sphingoid, toxic to growth	287.3	10.9	-8.43	-2.24	8.14	0.23
161	Ganglioside GM3 (d18:1/12:0)	Sphingolipid	1078.6	7.9	14.66	14.79	-	-
162	N-Acetyl-D-glucosaminyldiphosphodolichol	Glycan precursor, Prenol lipid	587.2	14.3	15.48	0.00	7.71	7.55
		SECONDARY METABOLITES						
163	N-Acetyl-D-mannosamine 6-phosphate	Sialic acid precursor	347.1	0.5	8.42	7.71	-	-
164	N-Acetyl-9-O-lactoyl neuraminic acid [401]	Sialic acid, protects from phagocytosis reduces cell-adhesion, Increases (-) charge	363.1	5.2	8.43	0.00	1.17	0.45
165	N-Acetyl-8-O-methyl-neuraminic acid		305.1	1.4	-0.29	6.96	-	-
166	Peonidin	Anthocyanin, Dephinidin derivative	305.2	9.3	-6.88	-6.88	16.49	8.37
167	Peonidin 3-O-glucoside	Anthocyanin	467.4	16.4	6.09	-9.66	-	-
168	4-Vinylguaiacol		172.2	9.8	6.98	-0.63	-	-
169	Petunidin		317.3	10.7	0.01	9.77	-	-
170	Alloxanthin	Carotenoid, Anti-oxidant & vitamin precursor	584.3	17.0	7.94	7.55	-	-
171	Engeletin	Flavononols, Inhbits ROS, NO & hypoxia signalling anti-inflammatory influence energy metabolism	456.4	11.5	15.12	0.00	-	-
172	Kaempferol [535]	Flavonols, anti-inflammatory and antioxidant	324.2	13.4	9.55	9.68	-	-
173	Quercetin	Flavonols, Anti-oxidant	285.2	14.3	0.00	7.94	8.27	-8.15
174	Catechin [536]	Flavanols, Alcohol tolerance, Toxin resistance	289.3	10.8	-0.07	-0.51	1.66	1.30
175	Piceatannol	Stilbenes	272.2	14.2	16.05	15.83	-	-
176	benzil		256.2	19.5	-	-	0.12	8.88
177	Resveratrol	Stilbenes, Promote lipid metabolism	227.3	11.2	-0.31	-8.08	-	-
178	Cucurbitacin E	Protects from autophagy & oxidative stress	598.3	15.1	-1.98	-10.51	-	-
179	Epinephrine-like	Hormone, promote glycogen break	165.1	1.2	22.23	22.02	0.90	0.42
180	Indole-3-carboxylic acid-like	Auxin, promotes sporulation	143.0	3.9	0.65	-8.80	18.18	8.20
181	1H-IAA, 5-[[(methylamino)sulfonyl]methyl]- glucuronide-like	Auxin derivative	440.1	0.6	1.56	-8.24	-	-
182	Kinetin riboside-like	Kinetin derivative promotes cell proliferation	347.1	5.9	8.06	7.97	-	-
183	Kinetin-like	Kinetin, promotes cell proliferation	215.1	3.7	-	-	19.02	8.30
184	Abscisic acid-like	ABA	246.1	1.0	3.29	-5.16	-	-
185	Tuberonic acid-like	JA derivative, defense and signaling	208.1	13.6	8.08	-0.10	-	-
186	2-phenylethanol	Aromatic compounds, Inhibits growth	142.1	1.3	-17.81	-17.81	-	-
187	Gallic acid	Gallic acid, Secondary-metabolite	192.1	1.4	-18.02	-18.02	-	-
188	4-Hydroxyphenylethanol	Aromatic compounds, Antioxidant	120.1	6.3	16.44	0.00	-	-
189	Indole-3-ethanol	Aromatic compounds, Quorum sensing	161.1	7.7	15.73	0.00	-	-
190	Terephthalic acid	Aromatic compounds, Fermentation product	148.0	11.3	8.72	9.06	-	-
191	Benzyl alcohol		90.1	1.1	-1.22	8.04	-	-
192	Benzanthrone	Aromatic compounds, Yellowish color	212.1	6.2	18.93	18.47	-	-
193	4-hydroxystyrene	Aromatic compounds, Fermentation product	102.1	1.2	-	-	11.33	8.71
194	P-hydroxycinnamaldehyde	Apoptosis inducer, NO synthase inhibitor	148.1	1.2	-	-	18.03	17.48
195	Cinnarizine	Drug, Anti-histamine, calcium signal blocker	410.2	14.8	-	-	7.86	7.91
196	Flumazenil	Drug, Benzodiazepine antagonist, inhibits GABA signaling by shifting carbon metabolism toward respiration, as calorie restriction does.	303.1	0.5	-	-	7.03	7.76
197	5-Hydroxydopamine [537]	Drug, Inhibits respiratory growth, counteracts with ascorbate and GSH	151.1	0.7	-8.99	-8.89	-	-

198	Dihydrolevobunolol glucuronide	Drug, beta-adrenergic signal blocker	469.2	13.3	-	-	7.25	14.70
199	Penbutolol glucuronide	Drug, beta-adrenergic signal blocker	509.3	13.8	-	-	16.13	7.50
200	Miglitol [399]	Drug, Inhibit breakdown of complex carbohydrate	189.1	1.2	-	-	-10.17	-0.63
201	Sulfasalazine	Drug, Inhibits biopterin biosynthesis	440.1	0.5	-	-	-3.05	-1.74
202	Sulfamerazine	Drug, Inhibits folic acid synthesis	246.1	0.5	-	-	-9.98	-9.98
203	Flumequine	Drug, Anti-lipase, growth inhibition	307.1	0.7	-	-	-8.14	-8.14
204	Methacholine	Drug, Inhibits autophagy, promotes log growth	141.1	1.0	7.83	7.94	-	-
205	N-(3-oxo-hexanoyl)-homoserine lactone[538]	Quorum sensing, Oxidative stress tolerance	212.1	0.7	8.35	16.27	-	-
206	Metergoline	Alkaloid, Induces cell death	423.2	1.9	-8.62	-9.48	-	-
		FATTY ACD METABOLISM						
207	13,14-dihydroxy-docosanoic acid	Hydroxy FA, C22, Behenic acid derivative	371.3	14.8	-0.83	-0.51	0.00	7.27
208	3-hydroxy behenic	Hydroxy FA, C22, Behenic acid derivative	373.4	11.1	-	-	1.01	9.42
209	18-hydroxy-9S,10R-dihydroxy-stearic acid	Hydroxy FA, C18, Membrane lipid precursor	314.3	16.9	7.83	-0.20	0.00	8.86
210	11-methyl-octadecanoic acid	Methyl FA, C18, membrane lipid precursor	297.3	20.1	-7.81	-7.83	-	-
211	13-hydroxy stearic acid	Hydroxy FA, C18	282.3	14.6	-	-	-8.81	-8.41
212	Hexadecanedioic acid	FA, C16, Membrane lipid precursor	285.2	13.8	8.40	8.74	-	-
213	7-palmitoleic acid	Unsaturated FA, C16	236.2	16.5	8.26	0.00	16.65	8.35
214	3-hydroxy-hexadecanoic acid	Hydroxy FA, C16, intermediate in FA synthesis	254.2	13.2	-0.82	7.28	-	-
215	1-Hexadecyl-2-O-methyl-glycerol	Methyl FA, C16, Inhibits growth	329.3	13.1	-0.89	-1.64	1.63	0.88
216	Isopentadecylic acid	FA derivative, C15	241.2	10.8	-	-	8.73	0.63
217	1-tetradecanol	FA alcohol, C14	213.3	11.1	-	-	1.54	1.67
218	2-methyl-tridecanedioic acid	Methyl FA, C13	257.2	12.1	10.07	10.15	0.00	15.35
219	13-amino-tridecanoic acid	Amino FA, C13	228.2	13.3	-	-	9.38	10.29
220	3-Hydroxydodecanedioic acid	Hydroxy FA, C12	268.1	13.6	8.56	-0.07	8.13	8.09
221	6-methyl-dodecanedioic acid	FA derivative, C12	226.2	10.0	7.13	7.13	-	-
222	4,8-dimethyl dodecanoic acid	Methyl FA, C12	245.2	9.3	-	-	1.08	0.02
223	4-hydroxy lauric acid	Hydroxy FA, C12	233.2	7.9	-	-	0.77	-1.21
224	4-hydroxy-undecanoic acid	Hydroxy FA, C11	224.1	11.0	-8.54	-8.54	-	-
225	3-Hydroxysuberic acid	Hydroxy FA, C8	232.1	0.5	-16.10	-16.10	-	-
226	a-hydroxybutyrate	Hydoxy acid, C4, Alternate energy source	104.1	0.5	8.77	0.00	-	-
227	Carnitine [399]	Carnitine, FA oxidation	143.1	1.0	7.81	8.62	-16.49	-16.49

Table A2.10. Full-length CDS sequences for VuNAC1 and VuNAC2 TFs.

VuNAC1	
NCBI Gene ID	**114163399**

>VuNAC01 [Vigna unguiculata] cultivar Kanannado NAC1 protein gene, complete mRNA

ATGGCATCAGAGCTTCAATTGCCCCCAGGCTTCAGATTCCATCCAACGGACGAGGAGCTCGTGATGCACTA
CCTCTGCCGCAAATGCGCGTCGCAGCCCATCGCCGTTCCCATCATCGCCGAAATCGACCTCTACAAATACGA
CCCTTGGGACCTCCCAGGATTGGCTTCTTATGGAGAGAAAGAGTGGTACTTCTTTTCACCACGGGACCGGA
AGTACCCTAACGGTTCGAGGCCGAACCGGGCGGCGGGAACCGGTTACTGGAAGGCAACCGGGGCGGATA
AGCCCATTGGTCACCCGAAACCGGTTGGGATCAAGAAAGCTTTGGTGTTTTACGCTGGGAAAGCTCCGAAA
GGGGACAAAAGCAATTGGATCATGCACGAGTATCGTCTGGCTGATGTAGATCGCACCGTTCGCAAAAAGA
ACAGCTTAAGGTTGGATGATTGGGTGCTGTGCCGTATCTACAACAAGAAGGGCACGATCGAGAAATTACA
ACCGACCAGCGACGTAGTCGTGAGCCGGAAAATCGAATCCCCGGAGATCGAAGAGAAGAAGCCGGAGAT
TCTGAAAAGCGGAGGAGTTCTTCCGCCGCCGCCGGCGATGACGGACTACATGTACTTCGATCCGTCGGATT
CAATCCCGAAGCTGCACACGGACTCGAGCTGTTCGGAGCAGGTGGTTTCGCCGGAATTCGCTAGCGAGGT
GCAGAGCGAGCCGAAGTGGAACGAGTGGGAGAAGAGCCTGGATTTTCCATTCTACATGGACACCACCACT
CTGAGCAACGGCTTCACCCAATTCGCGACCAATAACACCACCACCACCAATAATAATAATAATCAGATGTCG
CCGCTGCAGGACATGTTCATGTACTGGCCCAAGCCCTTTTGA

VuNAC2	
NCBI Gene ID	**114178342**

>VuNAC02 [Vigna unguiculata] cultivar Kanannado NAC2 protein gene, complete mRNA

ATGCAAGGAGAATTGGAATTACCACCCGGGTTTAGATTCCACCCCACTGACGATGAACTCGTGAATCACTA
CTTGTGTAGAAAGTGTGCTGCTCAATCCATTGCCGCTCCCATCATCAAAGAAATCGATTTGTATAAGTTTGA
TCCATGGCAGCTTCCAGACATGGCTCTTTACGGTGAGAAAGAGTGGTACTTTTTCTCCCCTCGTGACCGAAA
ATACCCTAACGGTTCACGACCGAACCGGGCCGCGGGAACCGGCTACTGGAAGGCCACCGGAGCGGATAAA
CCGATTGGAAAACCGGAAGCCCGTGGAATTAAGAAAGCCCTTGTGTTCTACGCGGGGAAAGCCCCGAAAG
GAGTCAAGACAAATTGGATCATGCACGAATATCGCTTGGCCAACGTCGATAGATCTGCCTCCAAGAAAAAC
AACAATTTGAGGCTTGATGATTGGGTGCTATGTCGGATTTACAACAAGAAAGGGAAGATTGAGAAGTACA
ATAATGTCGACGGGGTGGTGGAACAGAAACCGGCGAAATTACCGGAGGAGATTCTGTTCCAGCACGAGAT
GAAGCCTGAGATCCAGATGTACGACCACGATCATTTCAGGAACAACCAATTGTACATGGACACGTCGGATT
CGGTGCCGAGGTTAAACACGGACTCTAGCTGCTCCGAGCACGTGGTTTCGCCGGACGGCACCTGCGAGAA
GGAGGTGCAGAGCGAGCCCAAGTGGAACGACCTGGAGTTGGGCCCGGACCTGGTTTCGGGCTACGATTTT
AACTTCATGGAGCTATCAGCAGATGACGCTTTTGCTCCTCAGGCCCAATACCAAATGAACCAGCCCTCGACC
TGGCAAGATATGTTCGCGTACCTTCCGAAGACATTTTAA

Table A2.11 List of primers used in the study

Purpose		Name	Sequence
Gene isolation	Forward	NAC_Degenerate_1	5′-GGIGsIAsIGAIyTICAryTICCICC-3′
	Reverse	NAC_Degenerate_1	5′-TCIyTICwyTTIsGyTCIGwyTGIACyTC-3′
	Forward	NAC_Degenerate_2	5′-CCIGGITTymGITTyCAyCCIACIGAyGA-3′
	Reverse	NAC_Degenerate_2	5′-TTIsGyTCIGwyTGIACyTCrswrGCrAAITC-3′
3' RACE PCR	Reverse	Adapter primer	5′-CTGATCTAGAGGTACCGGATCCTTTTTTTTTTTTTTTTTTT-3′
	Forward	VuNAC1-partial-1	5′-CGTCTGGCTGATGTAGATCGCA5′-3′
	Forward	VuNAC1-partial-2	5′-TTGGTACCTCGCACCGTTCGCAAAAAGAAC-3′
5' RACE PCR	Forward	Universal primer	5′-CTGATCTAGAGGTACCGGATCC-3′
	Reverse	VuNAC2-partial	5′-CGGGTGGTAATTCCAATTCTCC-3′
	Reverse	VuNAC2-partial	5′-TTCCAATTCTCCTTGCATTCGC-3′
qRT-PCR	Forward	VuNAC1_RT	5′-GCCGGCGATGACGGACTACA-3′
	Reverse	VuNAC1_RT	5′-GAATTGGGTGAAGCCGTTGCTC-3′
	Forward	VuNAC2_RT	5′-GGAACAACCAATTGTACATGGACACG-3′
	Reverse	VuNAC2_RT	5′-CGTCATCTGCTGATAGCTCCATGAA-3′
	Forward	VuNAC3_RT	5′-ATACAACACGGGGGCACCGAAA-3′
	Reverse	VuNAC3_RT	5′-CCCTGAACCGCTCGACTCA-3′
	Forward	VuUBQ1_RT	5′-TCAGTTGAGCCCGAAGAAGA-3′
	Reverse	VuUBQ1_RT	5′-AAACCAGTCCCAGTCCCAAA-3′
Over-lapping PCR GFP fusion	Reverse	VuNAC1ΔstopGFP	5′-GCCCTTGCTCACCATAAAGGGCTTGGGCCAGTACA-3′
	Reverse	VuNAC2ΔstopGFP	5′-GCCCTTGCTCACCATAAATGTCTTCGGAAGGTACG-3′
	Forward	GFP-FL	5′-ATGGTGAGCAAGGGCGAGGAGC-3′
	Reverse	GFP-FL-SfiIB	5′-AGAACGGCCcttatGGCCTTACTTGTACAGCTCGTCCA-3′
Yeast expression	Forward	VuNAC1_Y2H_NdeI	5′-GGTGGTCATATGATGGCATCAGAGCTTCAATT-3′
	Reverse	VuNAC1_Y2H_BamHI	5′-TTATATGGATCCTCAAAAGGGCTTGGGCCAGTA-3′
	Forward	VuNAC2_Y2H_NdeI	5′-GGTGGTCATATGATGCAAGGAGAATTGGAATTACC-3′
	Reverse	VuNAC2_Y2H_BamHI	5′-GGTGGTGGATCCTTAAAATGTCTTCGGAAGGTAC-3′
	Reverse	VuNAC1Δ_Y2H_BamHI	5′-TTATATGGATCCTCATAATTTCTCGATCGTGCCCTT-3′
	Reverse	VuNAC2Δ_Y2H_BamHI	5′-GGTGGTGGATCCTTACTTCTCAATCTTCCCTTTCTTGT-3′
Protein expression	Forward	VuNAC1_pET_BamHI	5′-TTATATGGATCCATGGCATCAGAGCTTCAATT-3′
	Reverse	VuNAC1_pET_SalI	5′-TTATATGTCGACTCAAAAGGGCTTGGGCCAGTA-3′
	Forward	VuNAC2_pET_BamHI	5′-TTATAAGGATCCATGCAAGGAGAATTGGAATTACC-3′
	Reverse	VuNAC2_pET_XhoI	5′-TTATATCTCGAGTTAAAATGTCTTCGGAAGGTACG-3′

APPENDIX 3

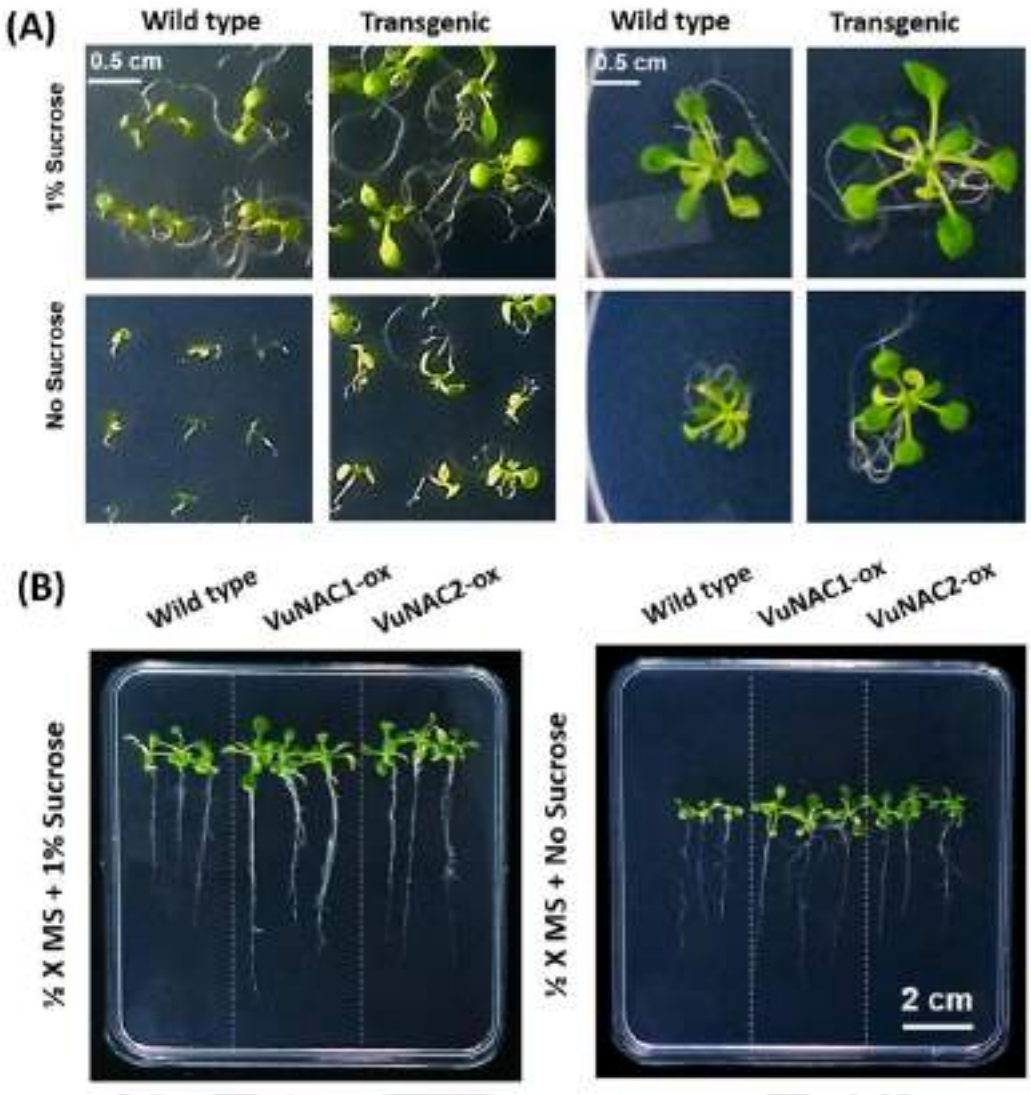

Fig. A3.1. Study of seedling growth phenotype. (A) **Representative post-embryonic and vegetative growth phenotype of one-week-old (left) and four-week-old (right) transgenic seedlings grown with/without sucrose supply.** (B) **The phenotype of t**hree independent **four-week-old** transgenic lines exhibiting improved growth compared to the wild type seedlings.

Table A3.2 List of orthologous genes in the ATAF-like network

Gene ID	AGI Code	Rank	Function	Reference	Gene ID	AGI Code	Rank	Function	Reference
HORMONE METABOLISM & SIGNALING									
AFP1	AT1G69260	4.68	ABA signaling	-	**IAA31**	AT3G17600	-	Auxin Signalling	-
HAB1	AT1G72770	3.97	Negative ABA sgnalling	[470]	**NAC047**	AT3G04070	-	Ethylene biosynthesis	[129]
PP2CG1	AT2G33700	3.61	ABA signaling, salt tolerance	[440]	**ACS2**	AT1G01480	3.1	Ethylene biosynthesis	[472]
PP2C49	AT3G62260	4.81	Negative ABA signaling, salt tolerance	[439]	**ACS6**	AT4G11280	4.12	Ethylene biosynthesis	[472]
PP2C63	AT4G33920	3.68	ABA signaling	-	**RAP2.4**	AT1G22190	3.93	Ethylene signalling	[539]
PP2C25	AT2G30020	3.67	ABA signaling	-	**Rap2.6L**	AT5G13330	3.22	Ethylene signaling	-
ABI1	AT4G26080	3.65	ABA signaling	[540]	**ERF1**	AT4G17500	4.98	Ethylene signalling	[442]
ABI2	AT5G57050	3.06	ABA signaling	-	**ERF4**	AT3G15210	4.46	Ethylene signaling	-
HAI1	AT5G59220	4.05	ABA signaling	[471]	**ERF6**	AT4G17490	3.24	Ethylene signalling	[541]
UGT74E2	AT1G05680	4.97	Auxin homeostasis	[542]	**GA2OX6**	AT1G02400	3.37	GA homeostasis	[424]
GH3.15	AT5G13370	3.42	Auxin homeostasis	-	**JAZ1**	AT1G19180	3.85	JA signaling	-
ZIFL1	AT5G13750	4.56	Auxin signaling	[441]	**JAZ12**	AT5G20900	-	JA-signalling	-
ABIOTIC STRESS RESPONSE									
NAC2	AT5G04410	3.55	Salt stress response	[148]	**DJ1A**	AT3G14990	4.74	Oxidative stress	[447]
ATAF1	AT1G01720	7.28	Drought response	[27]	**OPR1**	AT1G76680	4.62	Detoxification, JA synthesis	-
ATAF2	AT5G08790	5.12	Drought response	-	**DTX50**	AT5G52050	3.84	Detoxification	-
DREB2A	AT5G05410	4.74	Drought response	[437]	**ALF5**	AT3G23560	3.19	Detoxification	[450]
RD26	AT4G27410	3.38	Dessication	[299]	**HSFB1**	AT4G36990	3.84	Heat stress	-
GBF3	AT2G46270	3.93	Drought response	[438]	**HSFA2**	AT2G26150	3.29	Heat stress	-
RDUF1	AT3G46620	4.63	Drought response	-	**HSFB2A**	AT5G62020	4.4	Heat stress	-
RHA2A	AT1G15100	-	Drought response and early seed germination	-	**GFR**	AT5G45580	-	Cold and flavonoid regulation	[448]
LEA4-5	AT5G06760	3.02	Desiccation	-	**NAP**	AT1G69490	-	Senescence	[146]
DIV2	AT5G04760	4.54	Salt stress response	-	**MKK9**	AT1G73500	4.08	Apoptosis	[449]
MYB74	AT4G05100	3.43	Salt stress response	[443]	**SAG21**	AT4G02380	3.06	Senescence	-
STZ	AT1G27730	4.29	Salt stress response	-	**RHL41**	AT5G59820	5.77	Light stress	-
SZF1	AT3G55980	3.36	Salt stress response	-	**SAP9**	AT4G22820	4.33	Stress response	-
CCX2	AT5G17850	3.58	Salt stress response	[445]	**SAP6**	AT3G52800	3.49	Stress response	-
CZF1	AT2G40140	5.52	Salt stress response	[444]	**MBF1C**	AT3G24500	3.26	Stress response	-
BZIP60	AT1G42990	4.23	ER stress	-	**OCP3**	AT5G11270	-	Stress response	-
NAC062	AT3G49530	4.99	ER Stress tolerance	[446]	**CAMBP25**	AT2G41010	3.45	Stress response	-
NAC102	AT5G63790	8.15	Oxidative stress	[128]	**NRP**	AT5G42050	4.6	ABA-mediated stress response	-
NAC032	AT1G77450	6.92	Oxidative stress	[139]	**EDL3**	AT3G63060	4.3	Stress response	-

BIOTIC STRESS									
PUB17	AT1G29340	3.1	Pathogen response	-	**AT1G72940**	AT1G72940	3.25	Pathogen response	-
PGIP1	AT5G06860	3.92	Pathogen response	-	**RIPK**	AT2G05940	3.33	Pathogen response	-
BAP1	AT3G61190	3.64	Pathogen response	-	**AT5G54165**	AT5G54165	3.8	Pathogen response	-
BIK1	AT2G39660	3.42	Pathogen response	-	**WRKY15**	AT2G23320	3.75	Pathogen response	-
EXO70B1	AT5G58430	3.37	Pathogen response	-	**WRKY33**	AT2G38470	4.18	Pathogen response	-
NHL3	AT5G06320	3.47	Pathogen response	-	**WRKY40**	AT1G80840	4.37	Pathogen response	-
NPR3	AT5G45110	3.27	Pathogen response	-	**WRKY48**	AT5G49520	3.08	Pathogen response	-
PEPR1	AT1G73080	3.01	Pathogen response	-	**WRKY75**	AT5G13080	3.24	Pathogen response	-
TIP	AT5G24590	3.93	Pathogen response	-	**WRKY6**	AT1G62300	5.36	Pathogen response	-
AT1G72900	AT1G72900	4.16	Pathogen response	-	**CAD1**	AT1G29690	3.32	Programmed cell death	-
GROWTH AND DEVELOPMENT									
CNI1	AT5G27420	3.11	Post-germination growth	[451]	**ZF2**	AT3G19580	4.36	Flower abscission	-
ERF11	AT1G28370	3.19	Growth and stress	[453]	**AGL12**	AT1G71692	-	Flowering	[454]
FORMIN7	AT1G59910	3.18	Actin formation	-	**AGL16**	AT3G57230	-	Flowering	-
PLIM2a	AT2G45800	-	Cytoskeleton Formation	-	**CDF2**	AT5G39660	-	Flowering	[455]
ZAT6	AT5G04340	5.11	Growth, salt, and Cd tolerance	[452]	**CDF4**	AT2G34140	-	Flowering	-
CCR2	AT1G80820	3.16	Lignin Biosynthesis	[462]	**BBX18**	AT2G21320	-	Shade tolerance	[459]
CAD1	AT1G72680	3.56	Lignin Biosynthesis		**TCP15**	AT1G69690	-	Cell proliferation	[458]
CSLE1	AT1G55850	3.79	Cellulose Synthesis	-	**TCP14**	AT3G47620	-	Cell proliferation	-
FRK1	AT5G51830	3.13	Starch formation	-	**TCP7**	AT5G23280		Leaf development	[457]
BAM1	AT3G23920	3.49	Starch degradation	-	**TCP23**	AT1G35560		Leaf development	-
GAT6	AT5G62620	3.35	Cell differentiation	[461]	**BCS1**	AT3G50930	3.19	Electron transfer	-
AGP1	AT5G64310	3.54	Cell differentiation	-	**CYTC-2**	AT4G10040	3.07	Electron transfer	-
TET8	AT2G23810	3.45	Cell differentiation	-	**AOX1A**	AT3G22370	4.31	Respiration	[460]
METABOLITE BIOSYNTHESIS AND TRANSPORT									
BGLU11	AT1G02850	4.09	Glucose Metabolism	-	**PAP1**	AT1G56650	-	Anthocyanin metabolism	-
SUS3	AT4G02280	3.27	Sucrose metabolism	-	**ADT4**	AT3G44720	3.12	Anthocyanin metabolism	-
AT5G15870	AT5G15870	3.41	Glucose Metabolism	-	**ADT5**	AT5G22630	3.32	Anthocyanin metabolism	-
AT2G41640	AT2G41640	3.51	Glucose Metabolism	-	**TPK1**	AT1G02880	3.2	TPP for photosynthesis	[463]
ACX1	AT4G16760	3.23	FA oxidation	-	**DHAR2**	AT1G75270	3.61	Vitamin C metabolism	[464]
5PTASE11	AT1G47510	3.26	Lipid metabolism	-	**FC1**	AT5G26030	3.72	Heme biosynthesis	-
PI4K GAMMA 4	AT2G46500	3.38	Lipid metabolism	-	**GSTU1**	AT2G29490	5.39	Reseveratrol metabolism	[465]
LACS7	AT5G27600	3.58	Lipid metabolism	-	**GSTU7**	AT2G29420	7.11	Reseveratrol metabolism	-

GLTP	AT4G39670	4.33	Lipid transfer	-	**GSTU24**	AT1G17170	5.34	Reseveratrol metabolism	-
APR3	AT4G21990	3.55	Cysteine biosynthesis	-	**TPPG**	AT4G22590	3.07	Trehalose metabolism	-
SAT1	AT1G55920	5.06	Cysteine biosynthesis	-	**NUDT4**	AT1G18300	3.02	Amino acid transporter	[468]
ADC2	AT4G34710	3.9	Arginine metabolism	-	**OCT5**	AT1G79410	4.37	Solute transporter	[467]
PHL2	AT3G24120	-	Phosphate starvation	[466]	**AT1G79710**	AT1G79710	3.1	Folate transporter	-
					MAC9.6	AT5G61820	6.96	Stress-response	-
ENZYMES AND SIGNALLING PROTEINS									
CBL1	AT4G17615	3.67	Calcium signaling	[469]	**CYP81D11**	AT3G28740	5.31	Monoexygenases	-
CML37	AT5G42380	3.59	Calcium signaling	-	**CYP81D8**	AT4G37370	4.22	Monoexygenases	-
CMCU	AT5G66650	3.93	Calcium uptake	-	**CYP89A5**	AT1G64950	3.02	Monoexygenases	-
CPK32	AT3G57530	3.16	Calcium homeostasis	-	**MO1**	AT4G15760	3.7	Monoexygenases	-
CP1	AT5G49480	5.32	Cell signaling	-	**AT2G41380**	AT2G41380	4.1	Methylation	-
MAPKKK14	AT2G30040	3.62	Cell-signaling	-	**AT4G22530**	AT4G22530	4.1	Methylation	-
MAPKKK18	AT1G05100	3.92	Cell-signaling	-	**AT2G43320**	AT2G43320	3.65	Methylation	-
PBP1	AT5G54490	3.63	Signaling	-	**AT5G10830**	AT5G10830	3.11	Methylation	-
LYK5	AT2G33580	3.3	Signaling	-	**PMAT1**	AT5G39050	4.25	Detoxification	-
PERK9	AT1G68690	3.08	Signaling	-					-

APPENDIX 4

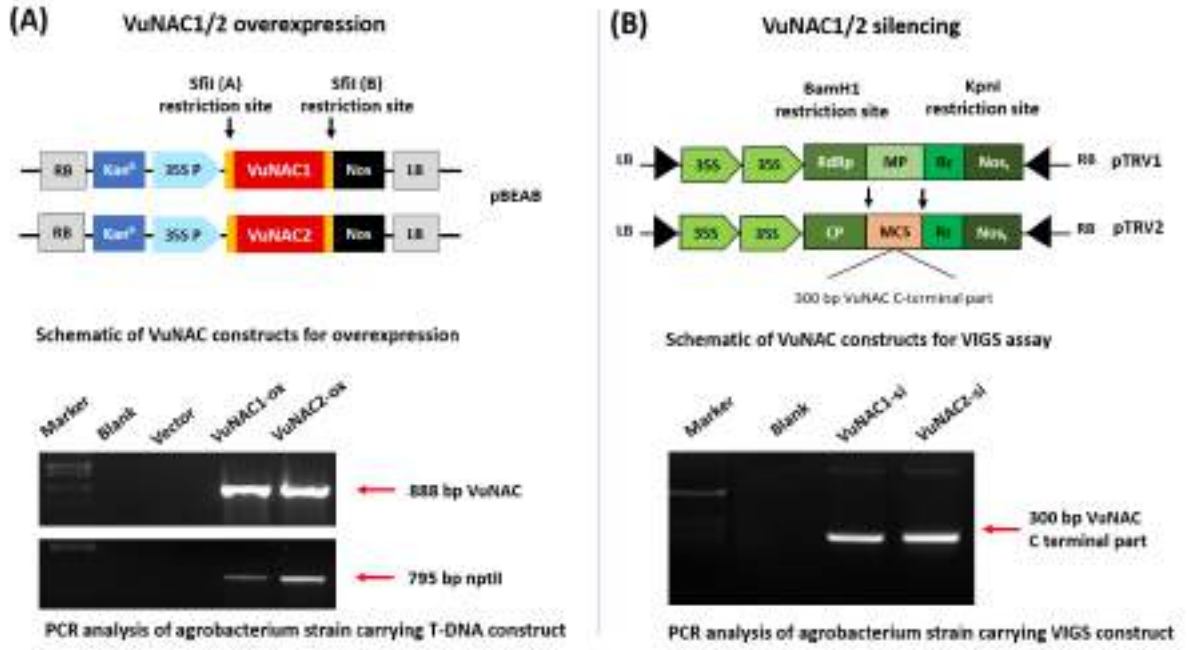

Fig. A4.1 T-DNA constructs used for genetic modification. (A) Schematic diagram of 35S: VuNAC1/2 construct in plant over-expression vector pBEAB (top) and PCR analysis of the Agrobacterium strains carrying the vectors (below). **(B)** Schematic diagram of the pTRV1/pTRV2 construct used for virus used gene silencing (top) and PCR analysis of the Agrobacterium strains carrying the vectors (below).

Table A4.2 List of primers used in the study.

Purpose		Name	Sequence
Overexpression construct preparation	Forward	VuNAC1-FL-SfiIA	5’-catttGGCCaaatcGGCCATGGCATCAGAGCTTCAATT-3’
	Reverse	VuNAC1-FL-SfiIB	5’-AGAACGGCCcttatGGCCTCAAAAGGGCTTGGGCCA-3’
	Forward	VuNAC2-FL-SfiIA	5’-catttGGCCaaatcGGCCATGCAAGGAGAATTGGAATTACC-3’
	Reverse	VuNAC2-FL-SfiIB	5’-AGAACGGCCcttatGGCCTTAAAATGTCTTCGGAAGGTACG-3’
	Forward	1026-BE5'	5'-CTATCCTTCGCAAGACCCTTCCTC-3'
	Reverse	1027-BE3'	5'-GATGTGCTGCAAGGCGATTAAGTTG-3'
VIGS-silencing	Forward	VuNAC1_VIGS_BamH1	5'-TTATATGGATCCTCGTGAGCCGGAAAATCGAATC-3’
	Reverse	VuNAC1_VIGS_KpnI	5'-TATTTAGGTACCTTGGTCGCGAATTGGGTGAAGC-3’
	Forward	VuNAC2_VIGS_BamH1	5'-TTATATGGATCCGAAGCCTGAGATCCAGATGTACG-3’
	Reverse	VuNAC2_VIGS_KpnI	5'-TATTTAGGTACCGAGGGCTGGTTCATTTGGTATTG-3’
	Forward	TRV1-specific	5'-GGTACGATTACGGACTTGGAGATGTG-3’
	Reverse	TRV1-specific	5'-CCTCTAGGAAACGCAATCAGTGAGTC-3’
	Forward	TRV2-specific	5'-GGGGTATGTCAGTGATCGCAGTAGAA-3’
	Reverse	TRV2-specific	5'-CCGCTAGTAACCCAGTGATCTCATCT-3’

Table A4.3 Differentially expressed (DE) genes in VuNAC expressing transgenic plants

(A) Growth and development associated genes

		VuNAC1-ox					VuNAC2-ox		
Gene name	**Gene ID**	**Predicted Function**	**log2_FC**	**p_value**	**Gene name**	**Gene ID**	**Predicted Function**	**log2_FC**	**p_value**
				CELL-WALL SYNTHESIS					
VuEXPA8-like	114163033	Cell wall elongation	3.84	0.00	**VuEXPA8**	114187014	Cell wall elongation	3.37	0.00
VuEXT-like	114190958	Cell wall elongation	2.78	0.04	**VuEXT-like**	114190958	Cell wall elongation	2.15	0.08
VuRWA2	114179119	Cell-wall metabolism	1.82	0.03	**VuRWA2**	114179119	Cell-wall metabolism	1.23	0.14
VuTBL39	114170605	Secondary cell-wall synthesis	2.21	0.01	**VuTBL39**	114170605	Secondary cell-wall synthesis	2.39	0.01
VuWAT1-like	114164012	Secondary cell-wall synthesis	1.96	0.03	**VuWAT1-like**	114194726	Secondary cell-wall synthesis	2.08	0.03
VuXET1	114164661	Primary cell-wall synthesis	2.55	0.01	**VuXETA**	114181348	Primary cell-wall synthesis	4.60	0.00
VuXET9	114184907	Primary cell-wall synthesis	4.15	0.01	**VuXET7**	114177311	Primary cell-wall synthesis	3.28	0.00
VuCESA1	114164006	Primary cell-wall synthesis	1.81	0.04	**VuCESA1**	114164006	Primary cell-wall synthesis	2.08	0.02
VuPRR4-like	114168952	Primary cell-wall synthesis	4.05	0.00	**VuPRR4-like**	114168952	Primary cell-wall synthesis	4.72	0.00
VuENG6	114177862	Cellulose & glucan metabolism	3.54	0.01	**VuENG17-like**	114190072	Cellulose & glucan metabolism	3.02	0.01
VuBGN4-like	114193978	Glucan metabolism	2.22	0.03	**VuBGN-like**	114176815	Glucan metabolism	2.17	0.02
VuPAE6-like	114191107	Pectin metabolism	1.98	0.03	**VuPAE6**	114175079	Pectin metabolism	1.79	0.05
VuPL5	114175680	Pectin metabolism	5.31	0.01	**VuPL5**	114175680	Pectin metabolism	3.51	0.02
VuCAD6	114195578	Lignin biosynthesis	2.93	0.00	**VuCAD6**	114195578	Lignin biosynthesis	1.88	0.04
VuCCR1	114185503	Lignin biosynthesis	6.66	0.00	**VuCSE-like**	114189660	Lignin biosynthesis	1.98	0.04
VuASD1-like	114187996	Arabinose metabolism	2.52	0.04	**VuCTL1-like**	114186268	Lignin degradation	1.85	0.03
VuCSLA2	114169202	Mannan biosynthesis	2.48	0.02	**VuASD1-like**	114187996	Arabinose metabolism	2.32	0.04
VuGMPPA-like	114162225	Mannan metabolism	1.58	0.06	**VuCSLA2**	114169202	Mannan biosynthesis	2.10	0.01
VuAXS2-like	114169802	Nucleotide sugar biosynthesis	2.12	0.02	**VuGMP1-like**	114191767	Mannan metabolism	1.57	0.10
VuMIOX1-like	114165702	Nucleotide sugar biosynthesis	1.77	0.03	**VuUGE4-like**	114176089	Nucleotide sugar biosynthesis	1.25	0.12
				ORGAN DEVELOPMENT					
VuSEOB-like	114191916	Phloem development	1.04	0.23	**VuSEOB-like**	114189737	Phloem development	1.76	0.09
VuROPGEF12	114185399	Root development	1.69	0.07	**VuROPGEF12**	114185399	Root development	2.68	0.02
VuGDI1-like	114176796	Root development	2.12	0.02	**VuROPGAP2**	114173132	Root development	1.77	0.09
VuLRP1	114168368	Root development	2.41	0.14	**VuLRP1**	114168368	Root development	1.58	0.24
VuEPFL1-like	114170724	Stomata development	4.09	0.09	-	-	-	-	-
VuDFC-like	114163951	Flowering	1.62	0.07	**VuDFC-like**	114163951	Flowering	1.71	0.04
VuLeguminV	114179944	Seed protein	4.85	0.00	**VuLeguminV**	114179944	Seed protein	3.32	0.00
VuSCPL26	114181186	Grain size	2.13	0.02	-	-	-	-	-
VuMARD1	114192255	Seed dormancy	-4.79	0.24	**VuMARD1**	114192255	Seed dormancy	-1.82	0.09

VuDRMH1	114188211	Dormancy	-2.54	0.01	**VuDRMH1**	114191933	Dormancy	-1.07	0.61
					CELL DIVISION AND EXPANSION				
VuTUBA3-like	114181014	Cytoskeleton formation	1.42	0.09	**VuTUBA3-like**	114181014	Cytoskeleton formation	2.24	0.01
VuTUBB-like	114196303	Cytoskeleton formation	1.89	0.03	**VuTUBB1-like**	114177857	Cytoskeleton formation	2.97	0.00
VuMAP651-like	114186601	Cytoskeleton formation	2.08	0.09	**VuMAP651-like**	114194735	Cytoskeleton formation	1.48	0.07
VuABIL5	114179352	Cytoskeleton formation	2.22	0.04	**VuAC97**	114173210	Cytoskeleton formation	1.68	0.05
VuADF	114174483	Cytoskeleton metabolism	-1.69	0.05	**VuABIL5**	114179352	Cytoskeleton formation	1.75	0.10
VuCYCD3-1-like	114193436	Germination	2.26	0.08	**VuADF**	114168644	Cytoskeleton metabolism	-1.67	0.04
VuCDC2-like	114193688	Cell-division	1.97	0.17	**VuCYCD1-1-like**	114177850	Germination	1.75	0.08
VuYAB1	114166456	Cell cycle signaling	5.20	0.14	**VuCNR13**	114174068	Cell-division	1.37	0.08
VuWDL1	114192665	Mitosis	2.40	0.07	**VuCDC2-like**	114193688	Cell-division	2.21	0.07
VuCYCLIN-1	114193337	Mitosis	2.82	0.04	**VuYAB1**	114166456	Cell-division	2.70	0.12
VuNFD4-like	114169477	Mitosis	1.86	0.07	**VuMAIL1**	114165526	Cell cycle signaling	2.63	0.05
VuAUR1	114162702	Mitosis	2.47	0.12	**VuWDL4**	114179125	Mitosis	2.46	0.04
VuBUB3.2	114191875	Anaphase	1.49	0.15	**VuCYCLIN-1**	114171554	Mitosis	2.22	0.15
VuMHK	114167158	Growth signaling	1.03	0.25	**VuNFD4-like**	114169477	Mitosis	3.13	0.01
VuH2AV1	114164475	Cell cycle control	4.44	0.09	**VuAUR1**	114162702	Mitosis	2.34	0.07
VuENDO2-like	114173247	DNA repair	4.98	0.01	**VuMHK**	114167158	Growth signaling	1.59	0.06
VuDTD	114188735	Protein translation	1.90	0.07	**VuERECTA**	114195362	Growth signaling	2.74	0.07
-	-	-	-	-	**VuH2A-like**	114183715	Cell cycle control	2.58	0.05
VuPCMPE-27	114179459	Gene expression	1.85	0.02	**VuPCMPE-27**	114179459	Gene-expression	2.91	0.00

(B) Chloroplastic and mitochondrial genes

		VuNAC1-ox					**VuNAC2-ox**		
Gene name	**Gene ID**	**Predicted Function**	**log2_FC**	**p_value**	**Gene name**	**Gene ID**	**Predicted Function**	**log2_FC**	**p_value**
					CHLOROPLASTIC GENE EXPRESSION AND TRANSLATION				
VuRPL24	114183442	Chromosomal translation	2.49	0.01	**VuRPL18**	114162427	Chromosomal translation	1.93	0.02
VuRPL13	114168309	Chromosomal translation	2.22	0.01	**VuRPL3**	114164345	Chromosomal translation	2.64	0.01
VuRPS5	114175291	Chromosomal translation	1.65	0.07	**VuRPL11**	114192464	Chromosomal translation	2.11	0.02
VuPTAC16	114169242	Chromosomal transcription	1.50	0.07	**VuRPS31**	114166432	Chromosomal translation	2.23	0.01
VuNTH1	114184586	Chromosomal DNA repair	2.01	0.07	**VuPTAC16**	114169242	Chromosomal transcription	2.54	0.01
VuRBCX2	114193949	Protein folding	1.76	0.05	**VuHSP70**	114186949	Protein folding	2.48	0.01
					PHOTOSYNTHESIS				
VuLHCA6	114162936	Photosynthesis	2.14	0.01	**VuPSAF3**	114176264	Photosynthesis	2.25	0.04
VuPSAF3	114176264	Photosynthesis	2.03	0.04	**VuPPL1**	114184111	Photosynthesis	2.13	0.02
VuPPL1	114184111	Photosynthesis	1.62	0.05	**VuRBCLA**	114169471	Photosynthesis	1.64	0.07
VuCYP38	114181336	Photosynthesis	2.50	0.01	**VuCYP38**	114181336	Photosynthesis	2.48	0.00

VuLHCB1-like	114181796	Photosynthesis	4.64	0.00	**VuLHCB1-like**	114181796	Photosynthesis	4.51	0.00
VuLIL3.2	114179027	Photosynthesis	1.44	0.10	**VuLIL3.2**	114179027	Photosynthesis	2.23	0.01
VuPSBO2	114186522	Photosynthesis	1.58	0.09	**VuPSBO1**	114173846	Photosynthesis	2.60	0.01
VuPNSB1	114166690	Electron transport	1.88	0.04	**VuPNSB3**	114184176	Electron transport	2.25	0.01
VuSTR4	114167404	Electron transport	1.84	0.04	**VuSTR4**	114167404	Electron transport	1.83	0.05
VuCAS	114176693	Stomatal regulation	1.28	0.12	**VuCAS**	114176693	Stomatal regulation	2.55	0.01
CHLOROPLAST DEVELOPMENT									
VuRER4	114168701	Leaf development	1.07	0.20	**VuEGY2**	114193051	Chloroplast development	1.88	0.02
VuCURT1C	114166301	Chloroplast development	1.94	0.04	**VuRER4**	114187319	Leaf development	1.77	0.05
VuTL17	114162574	Thylakoid protein	3.22	0.01	**VuTL17**	114162574	Thylakoid protein	3.77	0.00
VuFTSZ-like	114187024	Chloroplast division	1.32	0.28	**VuFTSZ-like**	114187024	Chloroplast division	2.18	0.04
VuPDV2	114169706	Chloroplast division	2.54	0.14	**VuSDR39U1**	114169903	Chloroplast division	2.13	0.01
CHLOROPHYLL BIOSYNTHESIS									
VuCHLI1	114187888	Chlorophyll biosynthesis	1.97	0.03	**VuCHLI1**	114187888	Chlorophyll biosynthesis	2.95	0.00
VuCHLP	114195668	Chlorophyll biosynthesis	2.77	0.00	**VuCHLP**	114178019	Chlorophyll biosynthesis	2.33	0.01
VuALAD	114163353	Chlorophyll biosynthesis	1.82	0.03	**VuALAD**	114163353	Chlorophyll biosynthesis	2.25	0.01
VuHEMA1	114193186	Chlorophyll biosynthesis	2.44	0.06	**VuHEMA1**	114193186	Chlorophyll biosynthesis	3.20	0.01
VuPBGD	114168924	Heme biosynthesis	3.87	0.05	**VuPBGD**	114168924	Heme biosynthesis	2.96	0.05
VuUROD	114164330	Heme biosynthesis	2.54	0.03	**VuUROD**	114164330	Heme biosynthesis	3.01	0.00
STRESS-RESPONSE									
VuBAS1	114186091	Oxidative-stress response	3.05	0.00	**VuPRXQ**	114176143	Oxidative-stress response	2.71	0.00
VuABC1-like	114176152	Oxidative-stress response	2.05	0.02	**VuABC1-like**	114176152	Oxidative-stress response	2.92	0.00
VuFSD1	114192036	Oxidative-stress response	3.50	0.01	**VuFSD1**	114170083	Oxidative-stress response	3.44	0.27
VuSEP2	114177963	Oxidative-stress response	1.72	0.12	**VuSEP2**	114177963	Oxidative-stress response	2.32	0.06
VuNQR	114179223	Detoxification	3.09	0.10	**-**	-	-	-	-
VuDHAR3	114173710	Glutathione metabolism	1.53	0.08	**VuHAGH**	114183734	Glutathione biosynthesis	1.40	0.09
VuFTSH2	114169808	Light stress response	1.32	0.28	**VuFTSH2**	114178388	Light stress response	1.63	0.06
VuLQY1	114193725	Light stress response	1.44	0.10	**VuLQY1**	114193725	Light stress response	1.79	0.06
PLASTID METABOLIC PATHWAYS									
VuPKP2	114189835	Seed development	3.61	0.01	**VuPKP2**	114189835	Seed development	2.01	0.04
VuPPDK	114175936	Pyruvate metabolism	-2.56	0.00	**VuGAPA1**	114162988	Calvin cycle	2.72	0.14
VuTKT	114190750	Pentose phosphate pathway	1.29	0.13	**VuPGK1**	114185042	Glycolysis, Calvin cycle	1.76	0.17
VuTKT2_1	114176963	MEP pathway	2.86	0.00	**VuCFBP1**	114175807	Ribulose synthesis	1.58	0.18
VuTKT2_2	114188652	MEP pathway	2.61	0.01	**VuFBA1**	114162136	Glycolysis	2.01	0.12
VuGLYR2	114185466	Glyoxylate cycle	1.26	0.13	**VuPYK**	114191699	TCA ycle	2.63	0.05
VuGBSS2	114192393	Starch biosynthesis	1.84	1.00	**VuTKT**	114190750	Pentose phosphate pathway	2.93	0.00
VuE1-BETA3	114164321	Acetyl-CoA synthesis	2.78	0.17	**VuTKT2_2**	114188652	MEP pathway	2.32	0.01
VuACP1	114177151	FA biosynthesis	3.69	0.00	**VuGLYR2**	114185466	Glyoxylate cycle	1.58	0.05
VuKAS1	114176177	FA biosynthesis	2.63	0.02	**VuGBSS2**	114185453	Starch biosynthesis	2.38	0.03
VuLOX2.1	114169189	FA metabolism	1.37	0.10	**VuE1-BETA3**	114187346	Acetyl-CoA synthesis	2.07	0.04

VuFAD7	114167372	FA metabolism	1.36	0.08	**VuACP1**	114177151	FA biosynthesis	3.51	0.00
VuRIDA	114193320	Isoleucine biosynthesis	1.54	0.05	**VuENRT2**	114169731	FA biosynthesis	1.60	0.06
VuEMB3004	114176253	Shikimate pathway	2.11	0.03	**VuLOX2.1**	114169189	FA metabolism	2.22	0.01
VuAKHSDH2	114195635	Amino acid biosynthesis	2.77	0.04	**VuFAD7**	114177711	FA metabolism	2.28	0.01
VuAEE14	114187026	Vitamin K1 bisynthesis	1.57	0.05	**VuPAP8**	114193135	Lipid metabolism	2.64	0.01
VuABA4	114183937	ABA biosynthesis	1.35	0.17	**VuAKHSDH2**	114195635	Amino acid biosynthesis	2.44	0.03
VuAOC	114182442	JA synthesis	2.22	0.02	**VuAEE14**	114187026	Vitamin K1 bisynthesis	1.46	0.09
VuWDR36	114182173	Circadian	2.92	0.04	**VuMBPQ**	114190003	Vitamin E synthesis	2.38	0.02
-	-	-	-	-	**VuTHI2**	114192234	Thiamine biosynthesis	1.49	0.09
VuWDR44	114196278	Circadian	2.16	0.06	**VuWDR44**	114196278	Circadian	3.72	0.02
				PLASTID TRANSPORTERS					
VuGPT2	114187952	Sugar transport	2.49	0.06	**VuDIT2.1**	114189035	Carbohydrate transport	2.50	0.03
VuPLGG1	114178781	Glycerate transport	1.62	0.07	**VuGPT2**	114187952	Sugar transport	1.44	0.23
VuBT1	114195430	Amino acid transport	1.54	0.09	**VuPLGG1**	114178781	Glycerate transport	1.50	0.09
				MITOCHONDIAL GENES					
VuNDUFAF6-like	114190910	Electron transport	1.93	0.05	**VuNDUFAF6**	114168289	Electron transport	1.21	0.14
VuCYB5R1	114194647	Electron transport	1.82	0.04	**VuNDA1**	114189132	Electron transport	1.37	0.10
VuCYTB5	114165829	Electron transport	1.48	0.09	**VuCYTB5**	114196256	Electron transport	1.44	0.13
VuME3	114162179	Pyruvate synthesis	1.98	0.03	**VuME3**	114162179	Pyruvate synthesis	1.56	0.08
VuGCSH	114173111	Glycine degradation	2.03	0.07	**VuAMT**	114178290	Glycine degradation	2.87	0.00
VuNUDT16	114180297	Nucleotide metabolism	2.85	0.04	**VuNUDT16**	114180297	Nucleotide metabolism	2.85	0.04
VuFQR1-like	114185669	Oxidative stress	1.03	0.23	**VuFQR1-like**	114189080	Oxidative stress	1.88	0.04
VuNQR	114179223	Detoxification	3.09	0.10	**VuNQR**	114179223	Detoxification	3.68	0.06
VuMYG1	114164508	Mitochondrial translation	1.12	0.19	**VuMYG1**	114164508	Mitochondrial translation	1.71	0.04

(C) Hormone and Stress signaling genes

		VuNAC1-ox					**VuNAC2-ox**		
Gene name	**Gene ID**	**Predicted Function**	**log2_FC**	**p_value**	**Gene name**	**Gene ID**	**Predicted Function**	**log2_FC**	**p_value**
				HORMONE RESPONSE					
VuABI5-2	114188149	ABA signaling	-2.22	0.17	**VuABI5-2**	114188149	ABA signaling	-2.42	0.13
VuSnRK2E	114177059	ABA signaling	-1.49	0.09	**VuSnRK2E**	114177059	ABA signaling	-3.40	0.00
VuRGLG5	114173026	ABA signaling	-1.59	0.05	**VuRGLG5**	114173026	ABA signaling	-1.34	0.09
VuSDIR1-like	114168659	ABA and salt response	2.14	0.03	**VuCAR11-like**	114178678	ABA signaling	-1.88	0.08
VuTAR4-like	114181525	Auxin biosynthesis	7.29	0.01	**VuTAR4-like**	114181525	Auxin biosynthesis	3.25	0.01
VuDAO-like	114181607	Auxin metabolism	3.57	0.00	**VuPILS3-like**	114176353	Auxin metabolsim	1.52	0.13
VuNDL2-like	114164667	Auxin signaling	2.32	0.05	**VuZIFL1**	114175493	Auxin transport	2.21	0.08
VuZIFL1	114175493	Auxin transport	3.34	0.02	**VuAUX22A**	114167429	Negative auxin signaling	2.54	0.02
VuAUX22A	114167429	Negative auxin signaling	3.83	0.01	**VuAUX22B**	114189786	Negative auxin signaling	1.53	0.05

VuLOG3	114176978	Cytokinin Signaling	1.77	0.04	**VuLOG3**	114195618	Cytokinin Signaling	1.86	0.07
VuAHP1	114192329	Cytokinin Signaling	-4.91	0.06	**VuAHP1**	114162884	Cytokinin Signaling	-2.96	0.00
VuARR17	114176983	Negative Cytokinin Signaling	1.98	0.04	**VuARR17**	114162105	Negative Cytokinin Signaling	3.53	0.13
VuGASA4	114186156	GA signaling	1.68	0.05	**VuGASA6**	114162260	GA signaling	3.66	0.00
VuGASA6	114162260	GA signaling	3.05	0.00	**VuGA2OX1**	114186714	GA signaling	2.00	0.06
VuACO-like	114179148	Ethylene synthesis	1.65	0.08	**VuACO-like**	114187947	Ethylene synthesis	1.20	0.17
VuCTR1	114196337	Negative ethylene signaling	-2.01	0.06	**VuCTR1**	114196337	Negative ethylene signaling	-3.83	0.01
VuTIFY10B	114167367	Negative JA signaling	1.31	0.09	**VuTIFY10B**	114180419	Negative JA signaling	2.03	0.09
VuRGLG4	114168390	JA signaling	-1.50	0.13	**VuRGLG4**	114168390	JA signaling	-1.26	0.17
				ABIOTIC STRESS					
VuLTL1-like	114187414	Salt stress response	5.81	0.00	**VuLTL1-like**	114187414	Salt stress response	3.72	0.00
VuRSS3-like	114162706	Salt stress response	4.24	0.01	**VuRSS3-like**	114162706	Salt stress response	3.36	0.01
VuTTL1-like	114169701	Osmotic stress response	1.99	0.09	**VuC3H29**	114194571	Salt stress response	2.47	0.05
VuPRXE5	114188722	Oxidative stress	2.56	0.01	**VuPRXE5**	114188722	Oxidative stress	2.88	0.01
VuMRSA2	114163162	Oxidative stress	-1.69	0.09	**VuMRSA2**	114186539	Oxidative stress	1.34	0.13
VuRBOPB-like	114187879	ROS	1.53	0.09	**VuRBOPB-like**	114187879	ROS	1.64	0.07
VuLOL1-like	114174628	ROS-mediated cell death	-2.71	0.02	**VuLOL1-like**	114174628	ROS-mediated cell death	-1.81	0.03
VuGST23	114176697	Detoxification	2.28	0.07	**VuGSTU18**	114172532	Detoxification	1.56	0.07
VuHSC70-2	114173774	Heat response	1.52	0.14	**VuHSC70-2**	114169933	Heat response	2.40	0.01
VuDJA6	114194380	-	1.94	0.11	**VuDJA6**	114194380	-	1.77	0.09
VuMPH1	114191780	Light response	1.36	0.11	**VuHSP17.3**	114176828	Heat response	2.65	0.01
VuSAP12-like	114181269	Stress response	1.91	0.30	**VuLTD**	114186775	Light response	1.54	0.05
VuPRR4-like	114168952	Stress response	4.05	0.00	**VuMPH1**	114191780	Light response	2.60	0.01
VuSRABDP	114183808	Stress response	4.54	0.09	**VuPRR4-like**	114168952	Stress response	4.72	0.00
VuLEA5-like	114179814	Dessication stress	-5.18	0.00	**VuSAP12-like**	114181269	Stress response	4.05	0.10
VuPHOS32	114193570	Stress response	-4.23	0.00	**VuLEA5-like**	114179814	Dessication stress	-3.91	0.00
				BIOTIC STRESS					
VuPLP1	114166318	Nutrient-reservoir and pathogen resistance	4.81	0.00	**VuPLP3**	114165692	Nutrient-reservoir and pathogen resistance	1.05	0.51
VuMLO4	114173170	Defense	2.10	0.03	**VuMLO6**	114189887	Defense	1.26	0.10
VuERG1	114193445	Defense	1.92	0.02	**VuNTMV**	114181896	Defense	-2.40	0.10
VuNIK1-like	114185476	Defense	2.04	0.03	**VuHIR1**	114179021	HR response	-2.05	0.07

(D) Metabolic pathway regulating genes

		VuNAC1-ox					VuNAC2-ox		
Gene name	**Gene ID**	**Predicted Function**	**log2_FC**	**p_value**	**Gene name**	**Gene ID**	**Predicted Function**	**log2_FC**	**p_value**
			CARBOHYDRATE METABOLISM						
VuPFP-BETA	114186927	Glycolysis	2.13	0.03	**VuPGM**	114177838	Glycolysis	1.30	0.12
VuPGAM-like	114173019	Glycolysis, Calvin cycle	-2.17	0.01	**VuALDC**	114195199	Glycolysis	1.71	0.05
VuSETH3	114174535	Ribulose-Arabinose metabolism	1.65	0.07	**VuPGAM-like**	114193173	Glycolysis, Calvin cycle	1.36	0.13
VuCCR4-3	114177204	Carbohydrate metabolism	1.28	0.16	**VuPK**	114189621	Glycolysis	1.37	0.10
VuBGL18-like	114186321	Carbohydrate degradation	2.37	0.01	**VuPPC**	114169911	TCA cycle	1.70	0.06
VuSUS5-like	114185026	Sucrose metabolism	-2.40	0.01	**VuCCR4-3**	114177204	Carbohydrate metabolism	1.38	0.11
VuAGAL1	114183116	Galactose metabolism	1.30	0.09	**VuBGL44**	114182410	Carbohydrate degradation	2.68	0.00
VuBGAL5-like	114194163	Galactose metabolism	3.26	0.00	**VuSUS5-like**	114186592	Sucrose metabolism	-2.24	0.02
VuRFS2	114162572	Raffinose synthesis	-1.95	0.02	**VuAGAL1**	114189904	Carbohydrate metabolism	2.64	0.05
VuTPS1	114185194	Trehalose synthesis	1.37	0.27	**VuBGAL5-like**	114194163	Galactose metabolism	1.77	0.03
VuMTD	114177536	Mannitol metabolism	2.68	0.00	**VuCA1P**	114187431	Arabinose metabolism	1.43	0.09
VuMSR1	114194653	Mannan biosynthesis	2.21	0.02	**VuTPPA**	114170658	Trehalose synthesis	1.36	0.09
			LIPID METABOLISM						
VuWSD1-like	114181636	Wax synthesis	3.90	0.00	**VuFAR3-like**	114184085	FA metabolism	1.70	0.08
VuFAR3-like	114168315	FA metabolism	2.00	0.03	**VuFAD3**	114186845	Polyunsaturated FA synthesis	3.50	0.01
VuFAD3	114186845	Polyunsaturated FA synthesis	2.70	0.04	**VuLACS2-like**	114168391	Long FA synthesis	1.75	0.04
VuLACS2-like	114167599	Long FA synthesis	3.00	0.00	**VuGLIP**	114187609	Lipid metabolism	3.46	0.01
VuEXL3-like	114194002	Lipid metabolism	2.49	0.01	**VuEXL3-like**	114194002	Lipid metabolism	2.49	0.01
VuEBP	114180987	Mevalonate synthesis	2.09	0.02	**VuGDPL1**	114194638	Lipid hydrolysis	2.15	0.08
VuSMO2-2	114170147	Sterol synthesis	1.93	0.06	**VuSTE-like**	114175722	Sterol biosynthesis	1.84	0.04
VuSDC1-like	114176701	Ethanolamine synthesis	2.09	0.04	**VuVEP1**	114164335	Steroid biosynthesis	2.04	0.09
VuPEAMT	114175128	Phosphoethanolamine metabolism	1.39	0.09					
			NUCLEOTIDE METABOLISM						
VuURH2	114174665	Pyrimidine metabolism	-1.21	0.19	**VuURH2**	114174665	Pyrimidine metabolism	-1.53	0.08
VuGK2	114189732	Purine metabolism	2.97	0.10	**VuAPT5**	114162385	Purine biosynthesis	1.24	0.15
VuGDA	114196027	Purine metabolism	-3.31	0.01	**VuGDA**	114196027	Purine metabolism	-2.22	0.01
			AMINO ACID METABOLISM						
VuGAD1-like	114188225	GABA synthesis	1.86	0.04	**VuGAD1-like**	114188225	GABA synthesis	2.36	0.01
VuQCT-like	114181657	Glutathione synthesis	5.34	0.06	**VuACR11-like**	114184102	Glutamine metabolism	1.89	0.04
VuASN1	114194393	Asparagine biosynthesis	-9.20	0.08	**VuASN1**	114194393	Asparagine biosynthesis	-2.58	0.02
VuP5CS	114165791	Proline biosynthesis	-2.42	0.01	**VuP5CS**	114165791	Proline biosynthesis	-2.24	0.01
VuAHCY	114178710	Cysteine synthesis	1.79	0.04	**VuAHCY**	114178710	Cysteine synthesis	1.73	0.05
VuMET	114179267	Methionine biosynthesis	1.65	0.04	**VuMET**	114179267	Methionine biosynthesis	2.24	0.01
			VITAMIN & COFACTOR METABOLISM						
VuGGH	114183810	Folic acid synthesis	5.43	0.00	**VuGGH**	114183810	Folic acid synthesis	3.37	0.00

VuAAO	114170096	Vitamin C metabolism	4.48	0.02	**VuAAO**	114170096	Vitamin C metabolism	2.95	0.03
VuDHNAT1-like	114183635	Vitamin K synthesis	1.66	0.09	**VuMDAR4**	114185184	Vitamin C metabolism	2.51	0.01
					VuACL5	114190212	Thermospermidine synthesis	1.76	0.04
SECONDARY METABOLISM									
VuACL5	114190212	Thermospermidine synthesis	2.14	0.04	**VuTR-like**	114183604	Alkaloid metabolism	2.24	0.01
VuFLS	114193841	Flavonol Synthesis	2.46	0.01	**VuBAS**	114167020	Triterpene synthesis	-3.11	0.00
VuTR-like	114184261	Alkaloid metabolism	3.81	0.00	**VuNIA2**	114195673	Nitrogen assimilation	2.09	0.03

(E) Tranporters, transcription factors and signalling genes

		VuNAC1-ox					**VuNAC2-ox**		
Gene name	**Gene ID**	**Predicted Function**	**log2_FC**	**p_value**	**Gene name**	**Gene ID**	**Predicted Function**	**log2_FC**	**p_value**
METABOLITE TRANSPORTER									
VuORP3C	114183572	Sterol transport	2.74	0.04	**VuLTP8**	114177487	Lipid transport	3.67	0.00
VuSTARTD10	114177097	Lipid transport	1.79	0.05	**VuLTP1**	114166255	Lipid transport	-4.57	0.00
VuLTP8	114177487	Lipid transport	3.98	0.01	**VuPITPNM3**	114162962	Membrane lipid transport	-4.45	0.08
VuLTP1	114184178	Lipid transport	-5.42	0.00	**VuHEX6-like**	114179530	Glucose transport	1.47	0.16
VuPITPNM3	114162962	Membrane lipid transport	-2.66	0.04	**VuSUC8**	114181582	Sugar-transport	-2.66	0.05
VuHEX6-like	114179530	Glucose transport	1.82	0.08	**VuN3-like**	114177517	Sugar-transport	-3.70	0.02
VuSUC4	114194682	Sucrose transport	-2.47	0.01	**VuSWEET6**	114181426	Sugar-transport	-3.45	0.01
VuSWEET3	114162130	Sugar transport	-2.61	0.00	**VuURGT6**	114173567	Aminosugar transport	1.12	0.14
VuURGT6	114180402	Aminosugar transport	1.04	0.26	**VuYPQ3**	114177092	Amino acid transport	1.78	0.03
VuPROT2	114176001	Proline transport	1.89	0.08	**VuNAT6**	114163363	Ascorbate transporter	1.50	0.06
VuMSL10-like	114176272	Mechanical stress	1.88	0.04	**VuNPF6.4**	114194514	Nitrate transporter	1.85	0.06
SOLUTE/ION TRANSPORTER									
VuNPF6.4	114194514	Nitrate transporter	1.16	0.25	**VuMFSD5**	114163754	Micronutrient-uptake	1.72	0.04
VuMFSD5	114163754	Micronutrient-uptake	1.40	0.07	**VuCSC1**	114187339	Calcium transport	1.69	0.07
VuNOD26-like	114187000	Solute transport	3.87	0.09	**VuSULTR2.1**	114194873	Sulfur transport	2.50	0.01
VuKAT1-like	114168892	Stomata opening	-3.19	0.00	**VuNOD26-like**	114187000	Solute transport	3.96	0.06
VuPIP1-4	114165137	Solute transport	1.52	0.08	**VuKAT1-like**	114168892	Stomata opening	-2.24	0.01
VuTIP-like	114175546	Solute transport	1.66	0.06	**VuTIP2-1**	114183327	Solute transport	2.70	0.00
VuNIP6-1-like	114185354	Solute transport	-2.56	0.00	**VuTIP-like**	114175546	Solute transport	2.91	0.00
VuALMT12-like	114173215	Anion-transporter	-2.65	0.00	**VuNIP6-1-like**	114185354	Solute transport	-2.57	0.01
VuPCR2-like	114175914	Zinc and heavy metal response	-3.82	0.00	**VuALMT12**	114173215	Anion-transporter	-3.64	0.00
VuCAX3	114187660	Cation transport	-2.46	0.01	**VuPCR2-like**	114175914	Zinc & heavy metal response	-3.82	0.00
VuCCH	114193649	Copper transport	1.65	0.05	**VuPOT1**	114193023	Potassium transporter	1.68	0.09
VuHIPP07	114187538	Heavy metal homesostasis	2.92	0.01	**VuDTX40**	114183373	Multi-drug transporter	-2.05	0.01
VuHIPP31	114181665	Heavy metal homesostasis	3.78	0.06	**VuDTX35**	114181458	Multi-drug transporter	-1.88	0.04
VuDTX35	114192689	Multi-drug transporter	1.83	0.05	**VuABCG15**	114169537	Growth	2.01	0.02
GROWTH-ASSOCIATED TRANSCRIPTION FACTORS									

VuNAC83-like	114178462	Negative xylem development	-2.19	0.03	**VuNAC83-like**	114181461	Negative xylem development	-2.43	0.03
VuNAC104-like	114164463	Negative cell-wall & PCD regulation	-4.40	0.02	**VuNAC104**	114164463	Negative cell-wall & PCD regulation	-1.74	0.04
VuHBI-1	114162414	Cell expansion	2.00	0.04	**VuHBI-1**	114162414	Cell expansion	1.89	0.04
VuPRE5	114181382	Cell expansion	2.27	0.01	**VuMYB2-like**	114183791	Cell cycle	1.55	0.09
VubHLH74-like	114194107	Cell expansion	1.51	0.08	**VubHLH63-like**	114168601	Flowering	1.47	0.07
VuMYB2-like	114183791	Cell cycle	1.32	0.17	**VuHHO5-like**	114167386	Flowering	1.62	0.08
VuMUTE	114189182	Stomata formation	2.23	0.08	**VuMUTE**	114189182	Stomata formation	2.23	0.08
-	-	-	-	-	**VuGATA22**	114164431	Choloroplast development	3.02	0.03
-	-	-	-	-	**VuGLK1**	114183872	Choloroplast development	2.25	0.01
STRESS-RESPONSIVE TRANSCRIPTION FACTORS									
VuDREB2C-like	114193153	Cold response	1.21	0.28	-	-	-	-	-
VuICE1-like	114162308	Cold response	1.72	0.04	**VuICE1-like**	114162308	Cold response	1.46	0.06
VuNAC2-like_2	114196184	Stress-response	1.34	0.22	**VuNAC2-like_2**	114196184	Stress-response	1.45	0.11
VuNACP-like	114194335	Senescence	1.27	0.32	**VuHHO2-like**	114179563	Phosphate balance	1.48	0.08
VuPHR1-like	114190599	Phosphate response	-1.50	0.10	**VuATHB12-like**	114165996	Drought response	-2.25	0.01
VuATHB12-like	114165996	Drought response	-3.17	0.01	-	-	-	-	-
OTHER TRANSCRIPTION FACTORS									
VubHLH162-like	114179389	Transcription	1.97	0.07	**VuMYB1R1-like**	114164218	Trancription	2.22	0.08
VuELOF1	114179086	Transcription	2.93	0.01	**VubHLH089**	114176620	Trancription	2.35	0.04
VuNFYA9-like	114168407	Trancription	-2.12	0.03	**VuMED22-like**	114175119	Trancription	-2.04	0.09
VuCALFD-like	114181616	Trancription	-5.36	0.01	**VuCALFD-like**	114181616	Trancription	-6.30	0.01
SIGNALING GENES									
VuAGP20	114187529	Cell-signaling	3.13	0.00	**VuAGP20**	114174036	Cell-signaling	4.05	0.07
VuCML11	114190353	Calcium signaling	2.89	0.01	**VuSNF1-like**	114194595	Energy metabolism	1.13	0.2
VuSNF1-like	114194595	Energy metabolism	1.45	0.10	**VuNARS2**	114166216	Defense	-2.75	0.01
VuPIX13	114173242	Defense	-1.85	0.07	**VuFEI-1**	114173278	Cell-wall synthesis	1.49	0.10
VuGsSRK-like	114168195	Signaling	-1.75	0.08	**VuPBL3**	114173573	Defense	1.40	0.07
VuPP2C38	114195391	Signaling	-3.19	0.01	**VuRIPK**	114178134	Defense	1.63	0.08
VuCOT44-like	114179029	Protein metabolism	-2.02	0.04	**VuGsSRK-like**	114177877	Signaling	-1.99	0.05
VuSCPL34	114168917	Protein metabolism	3.39	0.07	**VuPP2C43**	114189680	Signaling	-1.89	0.02
VuPRCP-like	114174242	Protein metabolism	2.42	0.03	**VuCOT44-like**	114179029	Protein metabolism	-1.84	0.03
VuZP1-like	114187241	Protein metabolism	2.28	0.02	**VuZP1-like**	114187241	Protein metabolism	2.53	0.01
-	-	-	-	-	**VuPSMD3**	114163168	Protein-metabolism	2.25	0.03

Table A4.4 Orthologous genes associated with the differentially expressed VuNAC members in the transgenic lines

	Gene name/ID	Description	Function
Cell-wall & xylem biosynthesis	CESA4	cellulose synthase A4	Cellulose biosynthesis
	IRX1	cellulose synthase family protein	Cellulose biosynthesis
	IRX3	Cellulose synthase family protein	Cellulose biosynthesis
	CTL2	chitinase-like protein	Cellulose biosynthesis
	RFK1	Leucine-rich repeat transmembrane protein kinase	Cellulose biosynthesis
	IRX15	IRREGULAR XYLEM protein (DUF579)	Xylan Biosynthesis
	NAC007	NAC domain containing protein 7	Xylem biosynthesis
	PME44	pectin methylesterase 44	Pectin metabolism
	FRA8	Exostosin family protein	Secondary cell wall biosynthesis
	AT5G25820	Exostosin family protein	Secondary cell wall biosynthesis
	GAUT12	galacturonosyltransferase 12	Secondary cell wall biosynthesis
	TBL45	TRICHOME BIREFRINGENCE-LIKE 45	Secondary cell wall modification
	AT2G31110	trichome birefringence-like protein (DUF828)	Secondary cell wall modification
	ESK1	trichome birefringence-like protein (DUF828)	Secondary cell wall modification
	TBL3	trichome birefringence-like protein (DUF828)	Secondary cell wall modification
	PGSIP1	plant glycogenin-like starch initiation protein 1	Cell-wall biogenesis
	IRX6	COBRA-like extracellular glycosyl-phosphatidyl inositol-anchored protein family	Cell-wall biogenesis
	AT3G26910	hydroxyproline-rich glycoprotein family protein	Cell-wall biogenesis
	ELF7	hydroxyproline-rich glycoprotein family protein	Cell-wall biogenesis
	LAC10	laccase 10	Oxidation reaction
	IRX12	Laccase/Diphenol oxidase family protein	Oxidation reaction
Growth	VRLK1	Leucine-rich repeat protein kinase family protein	Cell elongation & cell-wall thickening
	MYB1	myb domain protein 1	Cell-cycle regulation
	LAZY 1	regulator of nonsense transcript protein	Growth
	PHO1	phosphate 1	Phosphate assimilation
	CDF2	cycling DOF factor 2	Photoperiodic flowering
	CEP1	Cysteine proteinases superfamily protein	PCD, pollen development
	NAC052	NAC domain containing protein 52	Flowering time
	QRT3	Pectin lyase-like superfamily protein	Pollen development
	Oct-01	organic cation/carnitine transporter1	Lateral root development
	Oct-05	organic cation/carnitine transporter5	Lateral root development
	AT1G32410	Vacuolar protein sorting 55 (VPS55) family protein	Cell-trafficking
	VSR7	VACUOLAR SORTING RECEPTOR 7	Cell-trafficking
	ARFB1A	ADP-ribosylation factor B1A	Cell-trafficking
	GAMMA-VPE	gamma vacuolar processing enzyme	Cell-trafficking
	ASG1	ATP-dependent DNA helicase	DNA helicase
	AT1G24575	DEAD-box ATP-dependent RNA helicase-like protein	DNA helicase
	CEN2	centrin 2	DNA repair
	ATL15	RING/U-box superfamily protein	Protein modification
	UBC29	ubiquitin-conjugating enzyme 29	Protein modification
	UBP24	ubiquitin-specific protease 24	Protein modification
	UBP25	ubiquitin-specific protease 25	Protein modification
Abiotic Stress	AT2G35585	cystic fibrosis transmembrane conductance regulator	Salt homeostasis
	RAB1C	RAB GTPase homolog 1C	Salt stress
	AT3G22160	VQ motif-containing protein	Seed development, abiotic stress
	OM47	beta-galactosidase	Senescence
	MKK9	MAP kinase kinase 9	Senescence
	DRA2	Nucleoporin autopeptidase	Shade response
	MYB59	myb domain protein 59	Stress and Growth Regulation
	SAP7	A20/AN1-like zinc finger family protein	Stress response
	SAP9	A20/AN1-like zinc finger family protein	Stress response
	SIBP1	BTB/POZ domain-containing protein	Stress response
	ATHCYSTM12	cysteine-rich TM module stress tolerance protein	Stress response
	AT1G69450	Early-responsive to dehydration stress protein (ERD4)	Stress response
	UGT73B3	UDP-glucosyl transferase 73B3	Stress response

	UGT73B5	UDP-glucosyl transferase 73B5	Stress response
	UGT73B2	UDP-glucosyltransferase 73B2	Stress response
	UGT73B4	UDP-glycosyltransferase 73B4	Stress response
	EGM1	G-type lectin S-receptor-like Serine/Threonine-kinase	Stress signaling
	AT1G11303	G-type lectin S-receptor-like Serine/Threonine-kinase	Stress signaling
	HSP21.7	HSP20-like chaperones superfamily protein	Heat response
	AT1G44160	HSP40/DnaJ peptide-binding protein	Heat response
	NAC062	NAC domain containing protein 62	ER Stress tolerance
	SRO1	similar to RCD one 1	Oxidative stress
	AT2G37130	Peroxidase superfamily protein	Redox reaction
	AT2G03850	Late embryogenesis abundant protein (LEA) family protein	Desiccation
	AT4G19880	Glutathione S-transferase family protein	Detoxification
	AT3G62040	Haloacid dehalogenase-like hydrolase (HAD) superfamily protein	Detoxification
	HIPP46	Heavy metal transport/detoxification superfamily protein	Detoxification
	GATA3	GATA transcription factor 3	Light response
Biotic Stress	TGA1	bZIP transcription factor family protein	Pathogen resistance
	TGA4	TGACG motif-binding factor 4	Pathogen resistance
	RIN13	RPM1 interacting protein 13	Disease signaling
	SD1-13	S-domain-1 13	Disease signaling
	AT5G54165	Avr9/Cf-9 rapidly elicited protein	Pathogen resistance
	WRKY33	WRKY DNA-binding protein 33	Pathogen resistance
	WRKY6	WRKY family transcription factor	Pathogen resistance
Metabolism	NRT1.5	nitrate transporter 1.5	Nitrogen assimilation
	NRT2.5	nitrate transporter2.5	Nitrogen assimilation
	SNRK2.7	SNF1-related protein kinase 2.7	Energy production
	AT3G16370	GDSL-like Lipase/Acylhydrolase superfamily protein	FA metabolism
	GDSL1	GDSL-like Lipase/Acylhydrolase superfamily protein	FA metabolism
	AT1G09740	Adenine nucleotide alpha hydrolases-like superfamily protein	Amino acid metabolism
	GLN1;4	glutamine synthetase 1;4	Glutamine Synthesis
	AT3G14280	LL-diaminopimelate aminotransferase	Lysine biosynthesis
	ADC2	arginine decarboxylase 2	Arginine metabolism
	SUS3	sucrose synthase 3	Sucrose metabolism
	BGLU10	beta glucosidase 10	Sugar metabolism
	SERAT2;1	serine acetyltransferase 2;1	Cysteine biosynthesis
	MYB48	myb domain protein 48	Flavonol Biosynthesis
	MYB7	myb domain protein 7	Flavonol Biosynthesis
	AGAL3	Melibiase family protein	Galactose Metabolism
	PYD2	pyrimidine 2	Pyrimidine degradation
	GSTU24	glutathione S-transferase TAU 24	Reseveratrol metabolism
	GSTU7	glutathione S-transferase tau 7	Reseveratrol metabolism
	GPX2	glutathione peroxidase 2	Glutathione metabolism
	GPAT8	glycerol-3-phosphate acyltransferase 8	Glycerolipid Biosynthesis
	ALN	allantoinase	Allantoin degradation
	CCH	copper chaperone	Copper homeostasis
	AT5G60720	electron transporter, putative (Protein of unknown function, DUF547)	Electron transporter
Enzymes	ROT3	Cytochrome P450 superfamily protein	Monoexygenases
	CYP71B7	cytochrome P450, family 71 subfamily B, polypeptide 7	Monoexygenases
	CYP72A15	cytochrome P450, family 72, subfamily A, polypeptide 15	Monoexygenases
	CYP89A5	cytochrome P450, family 89, subfamily A, polypeptide 5	Monoexygenases
	MXA21.9	alpha/beta-Hydrolases superfamily protein	Hydrolase
	TAR4	Pyridoxal phosphate (PLP)-dependent transferases superfamily protein	Transferase
Hormone	CKL2	casein kinase 1-like protein 2	ABA signaling
	PP2CG1	Protein phosphatase 2C family protein	ABA signaling
	SAUR36	SAUR-like auxin-responsive protein family	Auxin metabolism
	AT2G46690	SAUR-like auxin-responsive protein family	Auxin metabolism
	AT3G12830	SAUR-like auxin-responsive protein family	Auxin metabolism
	AT3G60690	SAUR-like auxin-responsive protein family	Auxin metabolism
	DFL2	Auxin-responsive GH3 family protein	Auxin signaling
	ERF-1	ethylene-responsive element-binding factor 1	Ethylene signaling

	ERF2	ethylene-responsive element-binding factor 2	Ethylene signaling
	ERF5	ethylene-responsive element-binding factor 5	Ethylene signaling
	ERF6	ethylene-responsive element-binding factor 6	Ethylene signaling
	MES9	methyl esterase 9	Hormone Signalling
Cell-signalling	AT1G73630	EF-hand calcium-binding protein family C2 calcium/lipid-binding plant	Calcium signaling
	MCPT9	phosphoribosyltransferase family protein	Calcium signaling
	CP1	Ca2+-binding protein 1	Calcium signaling
	AT3G07940	Calcium-dependent ARF-type GTPase activating protein family	Calcium signaling
	AT1G13830	Carbohydrate-binding X8 domain superfamily protein	Cell signaling
	AT4G19110	Protein kinase superfamily protein	Signaling
	WNK7	Protein kinase superfamily protein	Signaling
	PAP20	Purple acid phosphatases superfamily protein	Signaling
Transporters	GLR1.1	glutamate receptor 1.1	Ion transport, Growth
	AAP4	amino acid permease 4	Amino acid transport
	UMAMIT14	nodulin MtN21 /EamA-like transporter family protein	Amino acid transport
	UMAMIT29	nodulin MtN21 /EamA-like transporter family protein	Amino acid transport
	UMAMIT25	nodulin MtN21 /EamA-like transporter family protein	Amino acid transport
	AVT6A	Transmembrane amino acid transporter family protein	Amino acid transport
	AT1G05030	Major facilitator superfamily protein	Plastid Glucose Transporter
	UXT1	Nucleotide/sugar transporter family protein	Sugar transport
	AT5G55950	Nucleotide/sugar transporter family protein	Sugar transport
	IRX9	Nucleotide-diphospho-sugar transferases superfamily protein	Sugar transport
	STP7	sugar transporter protein 7	Sugar transport
	AT4G18220	Drug/metabolite transporter superfamily protein	Transporter
	AT2G28780	P-hydroxybenzoic acid efflux pump subunit	Transporter
	UPS1	ureide permease 1	Transporter
	ZIP1	zinc transporter 1 precursor	Zinc transporter
	ALIS5	ALA-interacting subunit 5	Lipid transport

9. References

9. REFERENCES

1. Francini, A. and L. Sebastiani, *Abiotic stress effects on performance of horticultural crops*. 2019: Multidisciplinary Digital Publishing Institute.
2. Velásquez, A.C., C.D.M. Castroverde, and S.Y. He, *Plant–pathogen warfare under changing climate conditions.* Current Biology, 2018. **28**(10): p. R619-R634.
3. Horn, L.N. and H. Shimelis, *Production constraints and breeding approaches for cowpea improvement for drought prone agro-ecologies in Sub-Saharan Africa.* Annals of Agricultural Sciences, 2020.
4. Rana, D., et al., *Biotic and abiotic stress management in pulses.* Indian J Agron, 2016. **61**: p. S238-S248.
5. van Zonneveld, M., et al., *Mapping patterns of abiotic and biotic stress resilience uncovers conservation gaps and breeding potential of Vigna wild relatives.* Scientific reports, 2020. **10**(1): p. 1-11.
6. Araujo, S.S., et al., *Abiotic stress responses in legumes: strategies used to cope with environmental challenges.* Critical Reviews in Plant Sciences, 2015. **34**(1-3): p. 237-280.
7. Hossain, A., et al., *Nutrient Management for Improving Abiotic Stress Tolerance in Legumes of the Family Fabaceae*, in *The Plant Family Fabaceae*. 2020, Springer. p. 393-415.
8. Bal, S.K. and P.S. Minhas, *Atmospheric stressors: challenges and coping strategies*, in *Abiotic Stress Management for Resilient Agriculture*. 2017, Springer. p. 9-50.
9. Schlenker, W. and M.J. Roberts, *Nonlinear temperature effects indicate severe damages to US crop yields under climate change.* Proceedings of the National Academy of sciences, 2009. **106**(37): p. 15594-15598.
10. Morales, F., et al., *Photosynthetic metabolism under stressful growth conditions as a bases for crop breeding and yield improvement.* Plants, 2020. **9**(1): p. 88.
11. Farooq, M., et al., *Drought stress in grain legumes during reproduction and grain filling.* Journal of Agronomy Crop Science, 2017. **203**(2): p. 81-102.
12. Dietterich, L.H., et al., *Increasing CO2 threatens human nutrition.* Scientific Data, 2014. **2**: p. 150036.
13. Yadav, S.S., et al., *Climate change and management of cool season grain legume crops*. 2010, Springer Science and Business Media: Springer Science and Business Media.
14. Foyer, C.H., et al., *Neglecting legumes has compromised human health and sustainable food production.* Nature plants, 2016. **2**(8): p. 1-10.
15. Bhatia, V., et al., *Yield Gap Analysis of Soybean, Groundnut, Pigeonpea and Chickpea in India Using Simulation Modeling: Global Theme on Agroecosystems Report No. 31.* 2006.
16. Lakshmi, S.R., P. Patra, and K. Gummagolmath, *Impact of Doubling Farmers' Income on Area, Production and Productivity of Pulses in India.* Current Journal of Applied Science Technology, 2020: p. 73-86.
17. Abraham, M. and P. Pingali, *Shortage of pulses in India: Understanding how markets incentivize supply response.* Journal of Agribusiness in Developing Emerging Economies, 2021.
18. Agbicodo, E., et al., *Breeding drought tolerant cowpea: constraints, accomplishments, and future prospects.* Euphytica, 2009. **167**(3): p. 353-370.
19. Mickelbart, M.V., P.M. Hasegawa, and J. Bailey-Serres, *Genetic mechanisms of abiotic stress tolerance that translate to crop yield stability.* Nature Reviews Genetics, 2015. **16**(4): p. 237-251.
20. Mahalingam, R., *Consideration of combined stress: a crucial paradigm for improving multiple stress tolerance in plants*, in *Combined stresses in plants*. 2015, Springer. p. 1-25.
21. Mittler, R., *Abiotic stress, the field environment and stress combination.* Trends in plant science, 2006. **11**(1): p. 15-19.

22. Kudo, M., et al., *A gene-stacking approach to overcome the trade-off between drought stress tolerance and growth in Arabidopsis.* The Plant Journal, 2019. **97**(2): p. 240-256.
23. Kaufmann, K., A. Pajoro, and G.C. Angenent, *Regulation of transcription in plants: mechanisms controlling developmental switches.* Nature Reviews Genetics, 2010. **11**(12): p. 830-842.
24. Manna, M., et al., *Transcription factors as key molecular target to strengthen the drought stress tolerance in plants.* Physiologia Plantarum, 2020.
25. Shahzad, R., et al., *Harnessing the Potential of Plant Transcription Factors in Developing Climate-Smart Crops: Future Prospects, Challenges, and Opportunities.* Saudi Journal of Biological Sciences, 2020.
26. Bian, Z., H. Gao, and C. Wang, *NAC Transcription Factors as Positive or Negative Regulators during Ongoing Battle between Pathogens and Our Food Crops.* International Journal of Molecular Sciences, 2021. **22**(1): p. 81.
27. Wu, Y., et al., *Dual function of Arabidopsis ATAF1 in abiotic and biotic stress responses.* Cell research, 2009. **19**(11): p. 1279-1290.
28. Liu, Y., J. Sun, and Y. Wu, *Arabidopsis ATAF1 enhances the tolerance to salt stress and ABA in transgenic rice.* Journal of plant research, 2016. **129**(5): p. 955-962.
29. Peng, H., J. Zhao, and M.M. Neff, *ATAF2 integrates Arabidopsis brassinosteroid inactivation and seedling photomorphogenesis.* Development, 2015. **142**(23): p. 4129-4138.
30. Takasaki, H., et al., *The abiotic stress-responsive NAC-type transcription factor OsNAC5 regulates stress-inducible genes and stress tolerance in rice.* Molecular Genetics Genomics, 2010. **284**(3): p. 173-183.
31. Jeong, J.S., et al., *OsNAC5 overexpression enlarges root diameter in rice plants leading to enhanced drought tolerance and increased grain yield in the field.* Plant Biotechnology Journal, 2013. **11**(1): p. 101-114.
32. Nakashima, K., et al., *Functional analysis of a NAC-type transcription factor OsNAC6 involved in abiotic and biotic stress-responsive gene expression in rice.* The Plant Journal, 2007. **51**(4): p. 617-630.
33. Jin, H., et al., *Overexpression of the GmNAC2 gene, an NAC transcription factor, reduces abiotic stress tolerance in tobacco.* Plant Molecular Biology Reporter, 2013. **31**(2): p. 435-442.
34. Singh, B., *Cowpea: the food legume of the 21st century*. Vol. 164. 2020, John Wiley & Sons: John Wiley & Sons.
35. Vasconcelos, M.W., et al., *The Biology of Legumes and Their Agronomic, Economic, and Social Impact*, in *The Plant Family Fabaceae*. 2020, Springer. p. 3-25.
36. Raza, A., et al., *Nitrogen Fixation of Legumes: Biology and Physiology*, in *The Plant Family Fabaceae*. 2020, Springer. p. 43-74.
37. Mudryj, A.N., N. Yu, and H.M. Aukema, *Nutritional and health benefits of pulses.* Applied Physiology, Nutrition, Metabolism, 2014. **39**(11): p. 1197-1204.
38. Jayathilake, C., et al., *Cowpea: an overview on its nutritional facts and health benefits.* Journal of the Science of Food Agriculture, 2018. **98**(13): p. 4793-4806.
39. Carvalho, M., et al., *Cowpea: a legume crop for a challenging environment.* Journal of the Science of Food Agriculture, 2017. **97**(13): p. 4273-4284.
40. Boukar, O., et al., *Cowpea (Vigna unguiculata): Genetics, genomics and breeding.* Plant Breeding, 2019. **138**(4): p. 415-424.
41. Singh, B., *Improved Cowpea Cultivation and Seed Production*, in *Cowpea: The Food Legume of the 21st Century*. 2014. p. 87-123.
42. Ashkani, S., et al., *Molecular breeding strategy and challenges towards improvement of blast disease resistance in rice crop.* Frontiers in plant science, 2015. **6**: p. 886.
43. Tuteja, N., *Abscisic acid and abiotic stress signaling.* Plant signaling behavior, 2007. **2**(3): p. 135-138.

44. Liu, X. and X. Hou, *Antagonistic regulation of ABA and GA in metabolism and signaling pathways.* Frontiers in plant science, 2018. **9**: p. 251.
45. Mudgal, V., N. Madaan, and A. Mudgal, *Biochemical mechanisms of salt tolerance in plants: a review.* International Journal of Botany, 2010. **6**(2): p. 136-143.
46. Seiler, C., et al., *Abscisic acid flux alterations result in differential abscisic acid signaling responses and impact assimilation efficiency in barley under terminal drought stress.* Plant physiology, 2014. **164**(4): p. 1677-1696.
47. Agarwal, P.K., et al., *Role of DREB transcription factors in abiotic and biotic stress tolerance in plants.* Plant cell reports, 2006. **25**(12): p. 1263-1274.
48. Magome, H., et al., *The DDF1 transcriptional activator upregulates expression of a gibberellin-deactivating gene, GA2ox7, under high-salinity stress in Arabidopsis.* The Plant Journal 2008. **56**(4): p. 613-626.
49. Todaka, D., K. Shinozaki, and K. Yamaguchi-Shinozaki, *Recent advances in the dissection of drought-stress regulatory networks and strategies for development of drought-tolerant transgenic rice plants.* Frontiers in plant science, 2015. **6**: p. 84.
50. Jensen, M.K., et al., *NAC genes: time-specific regulators of hormonal signaling in Arabidopsis.* Plant signaling behavior, 2010. **5**(7): p. 907-910.
51. Baillo, E.H., et al., *Transcription factors associated with abiotic and biotic stress tolerance and their potential for crops improvement.* Genes, 2019. **10**(10): p. 771.
52. Jin, J., et al., *PlantTFDB 4.0: toward a central hub for transcription factors and regulatory interactions in plants.* Nucleic acids research, 2016: p. gkw982.
53. Wang, Z. and F. Dane, *NAC (NAM/ATAF/CUC) transcription factors in different stresses and their signaling pathway.* Acta Physiologiae Plantarum, 2013. **35**(5): p. 1397-1408.
54. Udvardi, M.K., et al., *Legume transcription factors: global regulators of plant development and response to the environment.* Plant Physiology, 2007. **144**(2): p. 538-549.
55. Singh, S., et al., *The biotechnological importance of the plant-specific NAC transcription factor family in crop improvement.* Journal of plant research, 2021: p. 1-21.
56. Jensen, M.K., et al., *ATAF1 transcription factor directly regulates abscisic acid biosynthetic gene NCED3 in Arabidopsis thaliana.* FEBS open bio, 2013. **3**: p. 321-327.
57. Garapati, P., et al., *Transcription factor ATAF1 in Arabidopsis promotes senescence by direct regulation of key chloroplast maintenance and senescence transcriptional cascades.* Plant Physiology, 2015. **168**(3): p. 1122-1139.
58. Kleinow, T., et al., *NAC domain transcription factor ATAF1 interacts with SNF1-related kinases and silencing of its subfamily causes severe developmental defects in Arabidopsis.* Plant Science, 2009. **177**(4): p. 360-370.
59. Lonardi, S., et al., *The genome of cowpea (Vigna unguiculata [L.] Walp.).* The Plant Journal, 2019. **98**(5): p. 767-782.
60. Souer, E., et al., *The no apical meristem gene of Petunia is required for pattern formation in embryos and flowers and is expressed at meristem and primordia boundaries.* Cell, 1996. **85**(2): p. 159-170.
61. Aida, M., et al., *Genes involved in organ separation in Arabidopsis: an analysis of the cup-shaped cotyledon mutant.* The plant cell, 1997. **9**(6): p. 841-857.
62. Maugarny-Calès, A., et al., *Apparition of the NAC transcription factors predates the emergence of land plants.* Molecular plant, 2016. **9**(9): p. 1345-1348.
63. Xu, B., et al., *Contribution of NAC transcription factors to plant adaptation to land.* Science, 2014. **343**(6178): p. 1505-1508.
64. Mathew, I.E. and P. Agarwal, *May the Fittest Protein Evolve: Favoring the Plant-Specific Origin and Expansion of NAC Transcription Factors.* BioEssays, 2018. **40**(8): p. 1800018.
65. Jin, X., et al., *Divergent evolutionary patterns of NAC transcription factors are associated with diversification and gene duplications in angiosperm.* Frontiers in plant science, 2017. **8**: p. 1156.

66. Pereira-Santana, A., et al., *Comparative genomics of NAC transcriptional factors in angiosperms: implications for the adaptation and diversification of flowering plants.* PloS one, 2015. **10**(11): p. e0141866.
67. Ooka, H., et al., *Comprehensive analysis of NAC family genes in Oryza sativa and Arabidopsis thaliana.* DNA research, 2003. **10**(6): p. 239-247.
68. Nuruzzaman, M., et al., *Genome-wide analysis of NAC transcription factor family in rice.* Gene, 2010. **465**(1-2): p. 30-44.
69. Rushton, P.J., et al., *Tobacco transcription factors: novel insights into transcriptional regulation in the Solanaceae.* Plant physiology, 2008. **147**(1): p. 280-295.
70. Ling, L., et al., *Genome-wide analysis and expression patterns of the NAC transcription factor family in Medicago truncatula.* Physiology Molecular Biology of Plants, 2017. **23**(2): p. 343-356.
71. Melo, B.P., et al., *Revisiting the soybean GmNAC superfamily.* Frontiers in plant science, 2018. **9**: p. 1864.
72. Wu, J., L. Wang, and S. Wang, *Comprehensive analysis and discovery of drought-related NAC transcription factors in common bean.* BMC plant biology, 2016. **16**(1): p. 1-13.
73. Van Ha, C., et al., *Genome-wide identification and expression analysis of the CaNAC family members in chickpea during development, dehydration and ABA treatments.* PLoS One, 2014. **9**(12): p. e114107.
74. Satheesh, V., et al., *NAC transcription factor genes: genome-wide identification, phylogenetic, motif and cis-regulatory element analysis in pigeonpea (Cajanus cajan (L.) Millsp.).* Molecular biology reports, 2014. **41**(12): p. 7763-7773.
75. Li, P., et al., *Genome-Wide Identification of NAC Transcription Factors and Their Functional Prediction of Abiotic Stress Response in Peanut.* Frontiers in Genetics, 2021. **12**: p. 240.
76. Shiriga, K., et al., *Genome-wide identification and expression pattern of drought-responsive members of the NAC family in maize.* Meta gene, 2014. **2**: p. 407-417.
77. Guérin, C., et al., *Genome-wide analysis, expansion and expression of the NAC family under drought and heat stresses in bread wheat (T. aestivum L.).* PLoS One, 2019. **14**(3): p. e0213390.
78. Puranik, S., et al., *Comprehensive genome-wide survey, genomic constitution and expression profiling of the NAC transcription factor family in foxtail millet (Setaria italica L.).* PloS one, 2013. **8**(5): p. e64594.
79. Murozuka, E., et al., *Genome wide characterization of barley NAC transcription factors enables the identification of grain-specific transcription factors exclusive for the Poaceae family of monocotyledonous plants.* PloS one, 2018. **13**(12): p. e0209769.
80. Kadier, Y., et al., *Genome-wide identification, classification and expression analysis of NAC family of genes in sorghum [Sorghum bicolor (L.) Moench].* Plant Growth Regulation, 2017. **83**(2): p. 301-312.
81. Dudhate, A., et al., *Comprehensive analysis of NAC transcription factor family uncovers drought and salinity stress response in pearl millet (Pennisetum glaucum).* BMC genomics, 2021. **22**(1): p. 1-15.
82. Liu, M., et al., *Genome-wide analysis of the NAC transcription factor family in Tartary buckwheat (Fagopyrum tataricum).* BMC genomics, 2019. **20**(1): p. 1-16.
83. Liu, T., et al., *Genome-wide analysis and expression patterns of NAC transcription factor family under different developmental stages and abiotic stresses in Chinese cabbage.* Plant Molecular Biology Reporter, 2014. **32**(5): p. 1041-1056.
84. Hu, W., et al., *Genome-wide identification and expression analysis of the NAC transcription factor family in cassava.* PLoS One, 2015. **10**(8): p. e0136993.
85. Singh, A.K., et al., *Genome-wide organization and expression profiling of the NAC transcription factor family in potato (Solanum tuberosum L.).* DNA research, 2013. **20**(4): p. 403-423.

86. Karanja, B.K., et al., *Genome-wide characterization and expression profiling of NAC transcription factor genes under abiotic stresses in radish (Raphanus sativus L.).* PeerJ, 2017. **5**: p. e4172.
87. Su, H., et al., *Genome-wide analysis of NAM-ATAF1, 2-CUC2 transcription factor family in Solanum lycopersicum.* Journal of plant biochemistry biotechnology, 2015. **24**(2): p. 176-183.
88. Lv, X., et al., *Global expressions landscape of NAC transcription factor family and their responses to abiotic stresses in Citrullus lanatus.* Scientific reports, 2016. **6**(1): p. 1-14.
89. Liu, X., et al., *Comprehensive analysis of NAC transcription factors and their expression during fruit spine development in cucumber (Cucumis sativus L.).* Horticulture research, 2018. **5**(1): p. 1-14.
90. Li, B., et al., *Genome-wide identification and characterization of the NAC transcription factor family in Musa Acuminata and expression analysis during fruit ripening.* International journal of molecular sciences, 2020. **21**(2): p. 634.
91. Su, H., et al., *Genome-wide analysis and identification of stress-responsive genes of the NAM–ATAF1, 2–CUC2 transcription factor family in apple.* Plant Physiology Biochemistry, 2013. **71**: p. 11-21.
92. Olsen, A.N., et al., *NAC transcription factors: structurally distinct, functionally diverse.* Trends in plant science, 2005. **10**(2): p. 79-87.
93. Puranik, S., et al., *NAC proteins: regulation and role in stress tolerance.* Trends in plant science, 2012. **17**(6): p. 369-381.
94. Tran, L.S.P., et al., *Co-expression of the stress-inducible zinc finger homeodomain ZFHD1 and NAC transcription factors enhances expression of the ERD1 gene in Arabidopsis.* The Plant Journal, 2007. **49**(1): p. 46-63.
95. Yamaguchi, M., et al., *VND-INTERACTING2, a NAC domain transcription factor, negatively regulates xylem vessel formation in Arabidopsis.* The Plant Cell, 2010. **22**(4): p. 1249-1263.
96. Jensen, M.K., et al., *The Arabidopsis thaliana NAC transcription factor family: structure–function relationships and determinants of ANAC019 stress signalling.* Biochemical Journal, 2010. **426**(2): p. 183-196.
97. Ernst, H.A., et al., *Structure of the conserved domain of ANAC, a member of the NAC family of transcription factors.* EMBO reports, 2004. **5**(3): p. 297-303.
98. Chen, Q., et al., *A structural view of the conserved domain of rice stress-responsive NAC1.* Protein cell, 2011. **2**(1): p. 55-63.
99. Welner, D.H., et al., *NAC transcription factors: from structure to function in stress-associated networks*, in *Plant Transcription Factors*. 2016, Elsevier. p. 199-212.
100. Lindemose, S., et al., *A DNA-binding-site landscape and regulatory network analysis for NAC transcription factors in Arabidopsis thaliana.* Nucleic acids research, 2014. **42**(12): p. 7681-7693.
101. Hao, Y.-J., et al., *Plant NAC-type transcription factor proteins contain a NARD domain for repression of transcriptional activation.* Planta, 2010. **232**(5): p. 1033-1043.
102. Shao, H., H. Wang, and X. Tang, *NAC transcription factors in plant multiple abiotic stress responses: progress and prospects.* Frontiers in plant science, 2015. **6**: p. 902.
103. Nuruzzaman, M., A.M. Sharoni, and S. Kikuchi, *Roles of NAC transcription factors in the regulation of biotic and abiotic stress responses in plants.* Frontiers in microbiology, 2013. **4**: p. 248.
104. Kunieda, T., et al., *NAC family proteins NARS1/NAC2 and NARS2/NAM in the outer integument regulate embryogenesis in Arabidopsis.* The Plant Cell, 2008. **20**(10): p. 2631-2642.
105. Sánchez-Montesino, R., et al., *A regulatory module controlling GA-mediated endosperm cell expansion is critical for seed germination in Arabidopsis.* Molecular plant, 2019. **12**(1): p. 71-85.

106. Maugarny, A., et al., *CUC transcription factors: to the meristem and beyond*, in *Plant Transcription Factors*. 2016, Elsevier. p. 229-247.
107. Willemsen, V., et al., *The NAC domain transcription factors FEZ and SOMBRERO control the orientation of cell division plane in Arabidopsis root stem cells.* Developmental cell, 2008. **15**(6): p. 913-922.
108. Kim, Y.-S., et al., *A membrane-bound NAC transcription factor regulates cell division in Arabidopsis.* The Plant Cell, 2006. **18**(11): p. 3132-3144.
109. Zhou, Y., et al., *Identification and functional characterization of a rice NAC gene involved in the regulation of leaf senescence.* BMC Plant Biology, 2013. **13**(1): p. 1-13.
110. Kim, H.J., H.G. Nam, and P.O. Lim, *Regulatory network of NAC transcription factors in leaf senescence.* Current opinion in plant biology, 2016. **33**: p. 48-56.
111. Hickman, R., et al., *A local regulatory network around three NAC transcription factors in stress responses and senescence in A rabidopsis leaves.* The Plant Journal, 2013. **75**(1): p. 26-39.
112. Yamaguchi, M., et al., *VASCULAR-RELATED NAC-DOMAIN 7 directly regulates the expression of a broad range of genes for xylem vessel formation.* The Plant Journal, 2011. **66**(4): p. 579-590.
113. Sakamoto, S., et al., *Wood reinforcement of poplar by rice NAC transcription factor.* Scientific reports, 2016. **6**(1): p. 1-11.
114. Hussey, S.G., et al., *SND2, a NAC transcription factor gene, regulates genes involved in secondary cell wall development in Arabidopsis fibres and increases fibre cell area in Eucalyptus.* BMC plant biology, 2011. **11**(1): p. 1-17.
115. Johnsson, C., et al., *The plant hormone auxin directs timing of xylem development by inhibition of secondary cell wall deposition through repression of secondary wall NAC-domain transcription factors.* Physiologia plantarum, 2019. **165**(4): p. 673-689.
116. Yang, X., et al., *Overexpression of the soybean NAC gene GmNAC109 increases lateral root formation and abiotic stress tolerance in transgenic Arabidopsis plants.* Frontiers in plant science, 2019. **10**: p. 1036.
117. Chen, X., et al., *Auxin-independent NAC pathway acts in response to explant-specific wounding and promotes root tip emergence during de novo root organogenesis in Arabidopsis.* Plant Physiology, 2016. **170**(4): p. 2136-2145.
118. Kim, S.-G., S.-Y. Kim, and C.-M. Park, *A membrane-associated NAC transcription factor regulates salt-responsive flowering via FLOWERING LOCUS T in Arabidopsis.* Planta, 2007. **226**(3): p. 647-654.
119. Zhao, C., et al., *XND1, a member of the NAC domain family in Arabidopsis thaliana, negatively regulates lignocellulose synthesis and programmed cell death in xylem.* The Plant Journal, 2008. **53**(3): p. 425-436.
120. Zhao, D., et al., *Overexpression of a NAC transcription factor delays leaf senescence and increases grain nitrogen concentration in wheat.* Plant Biology, 2015. **17**(4): p. 904-913.
121. Yuan, X., et al., *NAC transcription factors in plant immunity.* Phytopathology Research, 2019. **1**(1): p. 1-13.
122. Tweneboah, S. and S.-K. Oh, *Biological roles of NAC transcription factors in the regulation of biotic and abiotic stress responses in solanaceous crops.* Journal of Plant Biotechnology, 2017. **44**(1): p. 1-11.
123. Hussain, R.M., et al., *The essence of NAC gene family to the cultivation of drought-resistant soybean (Glycine max L. Merr.) cultivars.* BMC plant biology, 2017. **17**(1): p. 1-11.
124. Nguyen, K.H., et al., *The soybean transcription factor GmNAC085 enhances drought tolerance in Arabidopsis.* Environmental Experimental Botany, 2018. **151**: p. 12-20.
125. Jiang, D., et al., *Overexpression of a microRNA-targeted NAC transcription factor improves drought and salt tolerance in Rice via ABA-mediated pathways.* Rice, 2019. **12**(1): p. 1-11.

126. Yuan, X., et al., *Rice NAC transcription factor ONAC066 functions as a positive regulator of drought and oxidative stress response.* BMC plant biology, 2019. **19**(1): p. 1-19.
127. Liu, X.H., et al., *A membrane-associated NAC transcription factor OsNTL3 is involved in thermotolerance in rice.* Plant biotechnology journal, 2020. **18**(5): p. 1317-1329.
128. Christianson, J.A., et al., *The low-oxygen-induced NAC domain transcription factor ANAC102 affects viability of Arabidopsis seeds following low-oxygen treatment.* Plant physiology, 2009. **149**(4): p. 1724-1738.
129. Rauf, M., et al., *NAC transcription factor speedy hyponastic growth regulates flooding-induced leaf movement in Arabidopsis.* The Plant Cell, 2013. **25**(12): p. 4941-4955.
130. Jin, J.F., et al., *Genome-wide identification and expression analysis of the NAC transcription factor family in tomato (Solanum lycopersicum) during aluminum stress.* BMC genomics, 2020. **21**: p. 1-14.
131. Moreno-Alvarado, M., et al., *Aluminum enhances growth and sugar concentration, alters macronutrient status and regulates the expression of NAC transcription factors in rice.* Frontiers in plant science, 2017. **8**: p. 73.
132. Ochiai, K., et al., *Suppression of a NAC-like transcription factor gene improves boron-toxicity tolerance in rice.* Plant physiology, 2011. **156**(3): p. 1457-1463.
133. Nilsson, L., R. Müller, and T.H. Nielsen, *Dissecting the plant transcriptome and the regulatory responses to phosphate deprivation.* Physiologia plantarum, 2010. **139**(2): p. 129-143.
134. Sahito, J.H., et al., *Identification, association, and expression analysis of ZmNAC134 gene response to phosphorus deficiency tolerance traits in maize at seedling stage.* Euphytica, 2020. **216**: p. 1-19.
135. Lee, M.H., et al., *An Arabidopsis NAC transcription factor NAC4 promotes pathogen-induced cell death under negative regulation by microRNA164.* New Phytologist, 2017. **214**(1): p. 343-360.
136. Kim, S.-Y., et al., *Exploring membrane-associated NAC transcription factors in Arabidopsis: implications for membrane biology in genome regulation.* Nucleic acids research, 2007. **35**(1): p. 203-213.
137. Nagahage, I.S.P., et al., *An Arabidopsis NAC domain transcription factor, ATAF2, promotes age-dependent and dark-induced leaf senescence.* Physiologia Plantarum, 2020. **170**(2): p. 299-308.
138. Mahmood, K., et al., *ANAC032 positively regulates age-dependent and stress-induced senescence in Arabidopsis thaliana.* Plant Cell Physiology, 2016. **57**(10): p. 2029-2046.
139. Mahmood, K., et al., *The Arabidopsis transcription factor ANAC032 represses anthocyanin biosynthesis in response to high sucrose and oxidative and abiotic stresses.* Frontiers in plant science, 2016. **7**: p. 1548.
140. Tran, L.-S.P., et al., *Isolation and functional analysis of Arabidopsis stress-inducible NAC transcription factors that bind to a drought-responsive cis-element in the early responsive to dehydration stress 1 promoter.* The Plant Cell, 2004. **16**(9): p. 2481-2498.
141. Sukiran, N.L., et al., *ANAC019 is required for recovery of reproductive development under drought stress in Arabidopsis.* Plant molecular biology, 2019. **99**(1-2): p. 161-174.
142. Xu, Z.-Y., et al., *The Arabidopsis NAC transcription factor ANAC096 cooperates with bZIP-type transcription factors in dehydration and osmotic stress responses.* The Plant Cell, 2013. **25**(11): p. 4708-4724.
143. Kim, Y.-S., et al., *Mutation of the Arabidopsis NAC016 transcription factor delays leaf senescence.* Plant Cell Physiology, 2013. **54**(10): p. 1660-1672.
144. Sakuraba, Y., et al., *The Arabidopsis transcription factor NAC016 promotes drought stress responses by repressing AREB1 transcription through a trifurcate feed-forward regulatory loop involving NAP.* The Plant Cell, 2015. **27**(6): p. 1771-1787.
145. Kou, X., C.B. Watkins, and S.-S.J.J.o.e.b. Gan, *Arabidopsis AtNAP regulates fruit senescence.* Journal of experimental botany, 2012. **63**(17): p. 6139-6147.

146. Guo, Y. and S. Gan, *AtNAP, a NAC family transcription factor, has an important role in leaf senescence.* The Plant Journal, 2006. **46**(4): p. 601-612.
147. Seok, H.-Y., et al., *Arabidopsis AtNAP functions as a negative regulator via repression of AREB1 in salt stress response.* Planta, 2017. **245**(2): p. 329-341.
148. He, X.J., et al., *AtNAC2, a transcription factor downstream of ethylene and auxin signaling pathways, is involved in salt stress response and lateral root development.* The Plant Journal, 2005. **44**(6): p. 903-916.
149. Patil, M., et al., *Overexpression of AtNAC2 (ANAC092) in groundnut (Arachis hypogaea L.) improves abiotic stress tolerance.* Plant biotechnology reports, 2014. **8**(2): p. 161-169.
150. Balazadeh, S., et al., *A gene regulatory network controlled by the NAC transcription factor ANAC092/AtNAC2/ORE1 during salt-promoted senescence.* The Plant Journal, 2010. **62**(2): p. 250-264.
151. Oda-Yamamizo, C., et al., *The NAC transcription factor ANAC046 is a positive regulator of chlorophyll degradation and senescence in Arabidopsis leaves.* Scientific Reports, 2016. **6**(1): p. 1-13.
152. Yoon, H.-K., et al., *Regulation of leaf senescence by NTL9-mediated osmotic stress signaling in Arabidopsis.* Molecules Cells, 2008. **25**(3).
153. Wu, A., et al., *JUNGBRUNNEN1, a reactive oxygen species–responsive NAC transcription factor, regulates longevity in Arabidopsis.* The Plant Cell, 2012. **24**(2): p. 482-506.
154. Shahnejat-Bushehri, S., B. Mueller-Roeber, and S. Balazadeh, *Arabidopsis NAC transcription factor JUNGBRUNNEN1 affects thermomemory-associated genes and enhances heat stress tolerance in primed and unprimed conditions.* Plant Signaling Behavior, 2012. **7**(12): p. 1518-1521.
155. Shim, J.S., et al., *Overexpression of OsNAC14 improves drought tolerance in rice.* Frontiers in plant science, 2018. **9**: p. 310.
156. Huang, L., et al., *Rice NAC transcription factor ONAC095 plays opposite roles in drought and cold stress tolerance.* BMC plant biology, 2016. **16**(1): p. 1-18.
157. Kang, K., et al., *Mutation of ONAC096 enhances grain yield by increasing panicle number and delaying leaf senescence during grain filling in rice.* International journal of molecular sciences, 2019. **20**(20): p. 5241.
158. Hong, Y., et al., *Overexpression of a stress-responsive NAC transcription factor gene ONAC022 improves drought and salt tolerance in rice.* Frontiers in plant science, 2016. **7**: p. 4.
159. Sakuraba, Y., et al., *Rice ONAC106 inhibits leaf senescence and increases salt tolerance and tiller angle.* Plant Cell Physiology, 2015. **56**(12): p. 2325-2339.
160. El Mannai, Y., et al., *The NAC transcription factor gene OsY37 (ONAC011) promotes leaf senescence and accelerates heading time in rice.* International journal of molecular sciences, 2017. **18**(10): p. 2165.
161. Zhang, X., et al., *OsNAC45 is Involved in ABA Response and Salt Tolerance in Rice.* Rice, 2020. **13**(1): p. 1-13.
162. Zheng, X., et al., *Overexpression of a NAC transcription factor enhances rice drought and salt tolerance.* Biochemical biophysical research communications, 2009. **379**(4): p. 985-989.
163. Shen, J., et al., *The NAC-type transcription factor OsNAC2 regulates ABA-dependent genes and abiotic stress tolerance in rice.* Scientific reports, 2017. **7**(1): p. 1-16.
164. Mao, C., et al., *OsNAC2 positively affects salt-induced cell death and binds to the OsAP37 and OsCOX11 promoters.* The Plant Journal, 2018. **94**(3): p. 454-468.
165. Fang, Y., et al., *A stress-responsive NAC transcription factor SNAC3 confers heat and drought tolerance through modulation of reactive oxygen species in rice.* Journal of experimental botany, 2015. **66**(21): p. 6803-6817.
166. Hao, Y.J., et al., *Soybean NAC transcription factors promote abiotic stress tolerance and lateral root formation in transgenic plants.* The Plant Journal, 2011. **68**(2): p. 302-313.

167. Jeong, J.S., et al., *Root-specific expression of OsNAC10 improves drought tolerance and grain yield in rice under field drought conditions.* Plant physiology, 2010. **153**(1): p. 185-197.
168. Hu, H., et al., *Characterization of transcription factor gene SNAC2 conferring cold and salt tolerance in rice.* Plant molecular biology, 2008. **67**(1-2): p. 169-181.
169. Hu, H., et al., *Overexpressing a NAM, ATAF, and CUC (NAC) transcription factor enhances drought resistance and salt tolerance in rice.* Proceedings of the National Academy of Sciences, 2006. **103**(35): p. 12987-12992.
170. Saad, A.S.I., et al., *A rice stress-responsive NAC gene enhances tolerance of transgenic wheat to drought and salt stresses.* Plant Science, 2013. **203**: p. 33-40.
171. Liu, G., et al., *Overexpression of rice NAC gene SNAC1 improves drought and salt tolerance by enhancing root development and reducing transpiration rate in transgenic cotton.* PLoS One, 2014. **9**(1): p. e86895.
172. Chen, D., et al., *Overexpression of a predominantly root-expressed NAC transcription factor in wheat roots enhances root length, biomass and drought tolerance.* Plant cell reports, 2018. **37**(2): p. 225-237.
173. Zhang, L., et al., *The novel wheat transcription factor TaNAC47 enhances multiple abiotic stress tolerances in transgenic plants.* Frontiers in plant science, 2016. **6**: p. 1174.
174. Huang, Q., et al., *TaNAC29, a NAC transcription factor from wheat, enhances salt and drought tolerance in transgenic Arabidopsis.* BMC plant biology, 2015. **15**(1): p. 1-15.
175. Xu, Z., et al., *Wheat NAC transcription factor TaNAC29 is involved in response to salt stress.* Plant Physiology Biochemistry, 2015. **96**: p. 356-363.
176. Guo, W., et al., *The wheat NAC transcription factor TaNAC2L is regulated at the transcriptional and post-translational levels and promotes heat stress tolerance in transgenic Arabidopsis.* PLoS One, 2015. **10**(8): p. e0135667.
177. Tang, Y., et al., *Molecular characterization of novel TaNAC genes in wheat and overexpression of TaNAC2a confers drought tolerance in tobacco.* Physiologia plantarum, 2012. **144**(3): p. 210-224.
178. Mao, X., et al., *TaNAC2, a NAC-type wheat transcription factor conferring enhanced multiple abiotic stress tolerances in Arabidopsis.* Journal of Experimental Botany, 2012. **63**(8): p. 2933-2946.
179. Nazari, M., et al., *Expression changes in the TaNAC2 and TaNAC69-1 transcription factors in drought stress tolerant and susceptible.* Plant Genetic Resources: Characterization Utilization, 2019. **1**: p. 9.
180. Xue, G.-P., et al., *Overexpression of TaNAC69 leads to enhanced transcript levels of stress up-regulated genes and dehydration tolerance in bread wheat.* Molecular Plant, 2011. **4**(4): p. 697-712.
181. Mao, H., et al., *ZmNAC55, a maize stress-responsive NAC transcription factor, confers drought resistance in transgenic Arabidopsis.* Plant physiology biochemistry, 2016. **105**: p. 55-66.
182. Mao, H., et al., *A transposable element in a NAC gene is associated with drought tolerance in maize seedlings.* Nature communications, 2015. **6**(1): p. 1-13.
183. Lu, M., et al., *A maize stress-responsive NAC transcription factor, ZmSNAC1, confers enhanced tolerance to dehydration in transgenic Arabidopsis.* Plant cell reports, 2012. **31**(9): p. 1701-1711.
184. Shinde, H., et al., *Pearl millet stress-responsive NAC transcription factor PgNAC21 enhances salinity stress tolerance in Arabidopsis.* Plant Physiology Biochemistry, 2019. **135**: p. 546-553.
185. Rahman, H., et al., *Over-expression of a NAC67 transcription factor from finger millet (Eleusine coracana L.) confers tolerance against salinity and drought stress in rice.* BMC biotechnology, 2016. **16**(1): p. 7-20.
186. Al Abdallat, A., et al., *Overexpression of the transcription factor HvSNAC1 improves drought tolerance in barley (Hordeum vulgare L.).* Molecular breeding, 2014. **33**(2): p. 401-414.

187. Christiansen, M.W., et al., *Barley plants over-expressing the NAC transcription factor gene HvNAC005 show stunting and delay in development combined with early senescence.* Journal of experimental botany, 2016. **67**(17): p. 5259-5273.
188. Nguyen, N.C., et al., *Ectopic expression of Glycine max GmNAC109 enhances drought tolerance and ABA sensitivity in Arabidopsis.* Biomolecules, 2019. **9**(11): p. 714.
189. Hoang, X.L.T., et al., *The soybean GmNAC019 transcription factor mediates drought tolerance in Arabidopsis in an abscisic acid-dependent manner.* International journal of molecular sciences, 2020. **21**(1): p. 286.
190. So, H.-A. and J.-H. Lee, *NAC transcription factors from soybean (Glycine max L.) differentially regulated by abiotic stress.* Journal of Plant Biology, 2019. **62**(2): p. 147-160.
191. Nguyen, K.H., et al., *Overexpression of GmNAC085 enhances drought tolerance in Arabidopsis by regulating glutathione biosynthesis, redox balance and glutathione-dependent detoxification of reactive oxygen species and methylglyoxal.* Environmental Experimental Botany, 2019. **161**: p. 242-254.
192. Li, S., et al., *Evolutionary and functional analysis of membrane-bound NAC transcription factor genes in soybean.* Plant Physiology, 2016. **172**(3): p. 1804-1820.
193. Pinheiro, G.L., et al., *Complete inventory of soybean NAC transcription factors: sequence conservation and expression analysis uncover their distinct roles in stress response.* Gene, 2009. **444**(1-2): p. 10-23.
194. Liu, X., et al., *Improved drought and salt tolerance in transgenic Arabidopsis overexpressing a NAC transcriptional factor from Arachis hypogaea.* Bioscience, biotechnology, biochemistry, 2011. **75**(3): p. 443-450.
195. Liu, X., et al., *Overexpression of Arachis hypogaea NAC3 in tobacco enhances dehydration and drought tolerance by increasing superoxide scavenging.* Plant physiology biochemistry, 2013. **70**: p. 354-359.
196. Tang, G., et al., *Overexpression of a peanut NAC gene, AhNAC4, confers enhanced drought tolerance in tobacco.* Russian Journal of Plant Physiology, 2017. **64**(4): p. 525-535.
197. Pandurangaiah, M., et al., *Cloning and expression analysis of MuNAC4 transcription factor protein from horsegram (Macrotyloma uniflorum (Lam.) Verdc.) conferred salt stress tolerance in Escherichia coli.* Acta physiologiae plantarum, 2013. **35**(1): p. 139-146.
198. Liu, Y., et al., *A chickpea NAC-type transcription factor, CarNAC6, confers enhanced dehydration tolerance in Arabidopsis.* Plant molecular biology reporter, 2017. **35**(1): p. 83-96.
199. Yu, X., et al., *CarNAC4, a NAC-type chickpea transcription factor conferring enhanced drought and salt stress tolerances in Arabidopsis.* Plant cell reports, 2016. **35**(3): p. 613-627.
200. Movahedi, A., et al., *Expression of the chickpea CarNAC3 gene enhances salinity and drought tolerance in transgenic poplars.* Plant Cell, Tissue Organ Culture, 2015. **120**(1): p. 141-154.
201. Wang, L., et al., *The abiotic stress-responsive NAC transcription factor SlNAC11 is involved in drought and salt response in tomato (Solanum lycopersicum L.).* Plant Cell, Tissue Organ Culture, 2017. **129**(1): p. 161-174.
202. Li, X.-D., et al., *Overexpression of a novel NAC-type tomato transcription factor, SlNAM1, enhances the chilling stress tolerance of transgenic tobacco.* Journal of plant physiology, 2016. **204**: p. 54-65.
203. Thirumalaikumar, V.P., et al., *NAC transcription factor JUNGBRUNNEN 1 enhances drought tolerance in tomato.* Plant Biotechnology Journal, 2018. **16**(2): p. 354-366.
204. Delessert, C., et al., *The transcription factor ATAF2 represses the expression of pathogenesis-related genes in Arabidopsis.* The Plant Journal, 2005. **43**(5): p. 745-757.
205. Huh, S.U., et al., *ATAF2, a NAC transcription factor, binds to the promoter and regulates NIT2 gene expression involved in auxin biosynthesis.* Molecules cells, 2012. **34**(3): p. 305-313.

206. Peng, H. and M.M. Neff, *CIRCADIAN CLOCK ASSOCIATED 1 and ATAF2 differentially suppress cytochrome P450-mediated brassinosteroid inactivation.* Journal of experimental botany, 2020. **71**(3): p. 970-985.
207. Maki, H., et al., *ANAC032 regulates root growth through the MYB30 gene regulatory network.* Scientific reports, 2019. **9**(1): p. 1-13.
208. Sun, L., et al., *The SNAC-A transcription factor ANAC032 reprograms metabolism in Arabidopsis.* Plant Cell Physiology, 2019. **60**(5): p. 999-1010.
209. Zhu, X., et al., *Jasmonic acid promotes degreening via MYC 2/3/4-and ANAC 019/055/072-mediated regulation of major chlorophyll catabolic genes.* The Plant Journal, 2015. **84**(3): p. 597-610.
210. Fang, Y., et al., *Systematic sequence analysis and identification of tissue-specific or stress-responsive genes of NAC transcription factor family in rice.* Molecular Genetics Genomics, 2008. **280**(6): p. 547-563.
211. Redillas, M.C., et al., *The overexpression of OsNAC9 alters the root architecture of rice plants enhancing drought resistance and grain yield under field conditions.* Plant Biotechnology Journal, 2012. **10**(7): p. 792-805.
212. Chen, X., et al., *The NAC family transcription factor OsNAP confers abiotic stress response through the ABA pathway.* Plant Cell Physiology, 2014. **55**(3): p. 604-619.
213. Lu, M., et al., *Expression of SbSNAC1, a NAC transcription factor from sorghum, confers drought tolerance to transgenic Arabidopsis.* Plant Cell, Tissue Organ Culture, 2013. **115**(3): p. 443-455.
214. Tran, L.-S.P., et al., *Molecular characterization of stress-inducible GmNAC genes in soybean.* Molecular Genetics Genomics, 2009. **281**(6): p. 647-664.
215. He, X., et al., *The nitrate-inducible NAC transcription factor TaNAC2-5A controls nitrate response and increases wheat yield.* Plant Physiology, 2015. **169**(3): p. 1991-2005.
216. Wang, J., et al., *The NAC transcription factors OsNAC20 and OsNAC26 regulate starch and storage protein synthesis.* Plant Physiology, 2020. **184**(4): p. 1775-1791.
217. Vidal, E.A., J.M. Álvarez, and R.A. Gutiérrez, *Nitrate regulation of AFB3 and NAC4 gene expression in Arabidopsis roots depends on NRT1. 1 nitrate transport function.* Plant signaling behavior, 2014. **9**(6): p. e28501.
218. Peng, H. and M.M. Neff, *Two ATAF transcription factors ANAC102 and ATAF1 contribute to the suppression of cytochrome P450-mediated brassinosteroid catabolism in Arabidopsis.* Physiologia Plantarum, 2021.
219. Ko, J.H., et al., *ANAC012, a member of the plant-specific NAC transcription factor family, negatively regulates xylary fiber development in Arabidopsis thaliana.* The Plant Journal, 2007. **50**(6): p. 1035-1048.
220. Meng, X., et al., *ANAC017 coordinates organellar functions and stress responses by reprogramming retrograde signaling.* Plant physiology, 2019. **180**(1): p. 634-653.
221. Xie, Q., et al., *Arabidopsis NAC1 transduces auxin signal downstream of TIR1 to promote lateral root development.* Genes development, 2000. **14**(23): p. 3024-3036.
222. Yoo, S.Y., et al., *Control of flowering time and cold response by a NAC-domain protein in Arabidopsis.* PloS one, 2007. **2**(7): p. e642.
223. Mitsuda, N., et al., *NAC transcription factors, NST1 and NST3, are key regulators of the formation of secondary walls in woody tissues of Arabidopsis.* The Plant Cell, 2007. **19**(1): p. 270-280.
224. Mathew, I.E., et al., *Three rice NAC transcription factors heteromerize and are associated with seed size.* Frontiers in plant science, 2016. **7**: p. 1638.
225. Chen, X., et al., *OsNAC2 encoding a NAC transcription factor that affects plant height through mediating the gibberellic acid pathway in rice.* The Plant Journal, 2015. **82**(2): p. 302-314.

226. Jiang, D., et al., *Overexpression of miR164b-resistant OsNAC2 improves plant architecture and grain yield in rice.* Journal of experimental botany, 2018. **69**(7): p. 1533-1543.
227. Li, W., et al., *A wheat transcription factor positively sets seed vigour by regulating the grain nitrate signal.* New Phytologist, 2020. **225**(4): p. 1667-1680.
228. Chen, D., et al., *Drought-up-regulated TaNAC69-1 is a transcriptional repressor of TaSHY2 and TaIAA7, and enhances root length and biomass in wheat.* Plant Cell Physiology, 2016. **57**(10): p. 2076-2090.
229. Peng, X., et al., *A maize NAC transcription factor, ZmNAC34, negatively regulates starch synthesis in rice.* Plant cell reports, 2019. **38**(12): p. 1473-1484.
230. Xiao, Q., et al., *Transcription factor ZmNAC126 plays an important role in transcriptional regulation of maize starch synthesis-related genes.* The Crop Journal, 2021. **9**(1): p. 192-203.
231. Li, J., et al., *miRNA164-directed cleavage of ZmNAC1 confers lateral root development in maize (Zea mays L.).* BMC plant biology, 2012. **12**(1): p. 1-14.
232. Liang, C., et al., *OsNAP connects abscisic acid and leaf senescence by fine-tuning abscisic acid biosynthesis and directly targeting senescence-associated genes in rice.* Proceedings of the National Academy of Sciences, 2014. **111**(27): p. 10013-10018.
233. Uauy, C., et al., *A NAC gene regulating senescence improves grain protein, zinc, and iron content in wheat.* Science, 2006. **314**(5803): p. 1298-1301.
234. Sablowski, R.W. and E.M. Meyerowitz, *A homolog of NO APICAL MERISTEM is an immediate target of the floral homeotic genes APETALA3/PISTILLATA.* Cell, 1998. **92**(1): p. 93-103.
235. Tang, Y., et al., *Arabidopsis type II phosphatidylinositol 4-kinase PI4Kγ5 regulates auxin biosynthesis and leaf margin development through interacting with membrane-bound transcription factor ANAC078.* PLoS genetics, 2016. **12**(8): p. e1006252.
236. Kim, S.G., et al., *A membrane-bound NAC transcription factor NTL8 regulates gibberellic acid-mediated salt signaling in Arabidopsis seed germination.* The Plant Journal, 2008. **55**(1): p. 77-88.
237. Zhou, J., R. Zhong, and Z.-H. Ye, *Arabidopsis NAC domain proteins, VND1 to VND5, are transcriptional regulators of secondary wall biosynthesis in vessels.* PloS one, 2014. **9**(8): p. e105726.
238. Ye, Y., et al., *OsSND2, a NAC family transcription factor, is involved in secondary cell wall biosynthesis through regulating MYBs expression in rice.* Rice, 2018. **11**(1): p. 1-14.
239. Quach, T.N., et al., *Functional analysis of water stress-responsive soybean GmNAC003 and GmNAC004 transcription factors in lateral root development in Arabidopsis.* PLoS One, 2014. **9**(1): p. e84886.
240. Balazadeh, S., et al., *ORS1, an H2O2-responsive NAC transcription factor, controls senescence in Arabidopsis thaliana.* Molecular plant, 2011. **4**(2): p. 346-360.
241. Yang, S.-D., et al., *The Arabidopsis NAC transcription factor VNI2 integrates abscisic acid signals into leaf senescence via the COR/RD genes.* The Plant Cell, 2011. **23**(6): p. 2155-2168.
242. Matallana-Ramirez, L.P., et al., *NAC transcription factor ORE1 and senescence-induced BIFUNCTIONAL NUCLEASE1 (BFN1) constitute a regulatory cascade in Arabidopsis.* Molecular plant, 2013. **6**(5): p. 1438-1452.
243. Mao, C., et al., *A rice NAC transcription factor promotes leaf senescence via ABA biosynthesis.* Plant Physiology, 2017. **174**(3): p. 1747-1763.
244. Ren, T., et al., *Involvement of NAC transcription factor SiNAC1 in a positive feedback loop via ABA biosynthesis and leaf senescence in foxtail millet.* Planta, 2018. **247**(1): p. 53-68.
245. Lee, S., et al., *The Arabidopsis NAC transcription factor NTL4 participates in a positive feedback loop that induces programmed cell death under heat stress conditions.* Plant Science, 2014. **227**: p. 76-83.
246. Pimenta, M.R., et al., *The stress-induced soybean NAC transcription factor GmNAC81 plays a positive role in developmentally programmed leaf senescence.* Plant Cell Physiology, 2016. **57**(5): p. 1098-1114.

247. Zhang, K. and S.-S. Gan, *An abscisic acid-AtNAP transcription factor-SAG113 protein phosphatase 2C regulatory chain for controlling dehydration in senescing Arabidopsis leaves.* Plant Physiology, 2012. **158**(2): p. 961-969.
248. Shinozaki, K. and K. Yamaguchi-Shinozaki, *Gene networks involved in drought stress response and tolerance.* Journal of Experimental Botany, 2006. **58**(2): p. 221-227.
249. Cai, W., et al., *Pepper NAC-type transcription factor NAC2c Balances the Trade-off Between Growth and Defense Responses.* Plant Physiology, 2021.
250. Boukar, O., et al., *Genomic tools in cowpea breeding programs: status and perspectives.* Frontiers in plant science, 2016. **7**: p. 757.
251. Langyintuo, A., et al., *Cowpea supply and demand in West and Central Africa.* Field crops research, 2003. **82**(2-3): p. 215-231.
252. Ishiyaku, M. and H. Aliyu, *Field evaluation of cowpea genotypes for drought tolerance and Striga resistance in the dry savanna of the North-West Nigeria.* International Journal of Plant Breeding and Genetics, 2013. **7**(1): p. 47-56.
253. Dadson, R.B., et al., *Effect of water stress on the yield of cowpea (Vigna unguiculata L. Walp.) genotypes in the Delmarva region of the United States.* Journal of Agronomy Crop Science, 2005. **191**(3): p. 210-217.
254. Fery, R.L., *The cowpea: production, utilization, and research in the United States.* Horticultural Reviews, 1990. **12**: p. 197-222.
255. Martins, L., et al., *Contribution of biological nitrogen fixation to cowpea: a strategy for improving grain yield in the semi-arid region of Brazil.* Biology fertility of soils, 2003. **38**(6): p. 333-339.
256. Abayomi, Y., E. Afolabi, and M. Aderolu, *Effects of water stress at different stages on growth, grain yield and seed quality of cowpea genotypes.* NISEB Journal, 2019. **1**(1).
257. Maas, E. and J. Poss, *Salt sensitivity of cowpea at various growth stages.* Irrigation Science, 1989. **10**(4): p. 313-320.
258. Ismail, A.M. and A.E. Hall, *Reproductive-stage heat tolerance, leaf membrane thermostability and plant morphology in cowpea.* Crop Science, 1999. **39**(6): p. 1762-1768.
259. Dolferus, R., *To grow or not to grow: a stressful decision for plants.* Plant Science, 2014. **229**: p. 247-261.
260. Gupta, A., A. Rico-Medina, and A.I. Caño-Delgado, *The physiology of plant responses to drought.* Science, 2020. **368**(6488): p. 266-269.
261. Isayenkov, S.V. and F.J. Maathuis, *Plant salinity stress: many unanswered questions remain.* Frontiers in Plant Science, 2019. **10**: p. 80.
262. Monakhova, O. and I. Chernyad'Ev, *Effects of cytokinin preparations on the stability of the photosynthetic apparatus of two wheat cultivars experiencing water deficiency.* Applied Biochemistry Microbiology, 2004. **40**(6): p. 573-580.
263. Golding, A.J. and G.N. Johnson, *Down-regulation of linear and activation of cyclic electron transport during drought.* Planta, 2003. **218**(1): p. 107-114.
264. Asch, F., et al., *Drought-induced changes in rooting patterns and assimilate partitioning between root and shoot in upland rice.* Field Crops Research, 2005. **93**(2-3): p. 223-236.
265. Reddy, A.R., K.V. Chaitanya, and M. Vivekanandan, *Drought-induced responses of photosynthesis and antioxidant metabolism in higher plants.* Journal of plant physiology, 2004. **161**(11): p. 1189-1202.
266. Shavrukov, Y., et al., *Early flowering as a drought escape mechanism in plants: How can it aid wheat production?* Frontiers in plant science, 2017. **8**: p. 1950.
267. Hall, A.E., *Breeding for adaptation to drought and heat in cowpea.* European Journal of Agronomy, 2004. **21**(4): p. 447-454.
268. EGASHIRA, C., et al., *Physiological responses of cowpea (Vigna unguiculata (L.) Walp) to drought stress during the pod-filling stage.* Cryobiology Cryotechnology, 2016. **62**(1): p. 69-75.

269. Ogbonnaya, C., et al., *Selection of cowpea genotypes in hydroponics, pots, and field for drought tolerance.* Crop Science, 2003. **43**(3): p. 1114-1120.
270. Ismail, A.M. and A.E. Hall, *Variation in traits associated with chilling tolerance during emergence in cowpea germplasm.* Field crops research, 2002. **77**(2-3): p. 99-113.
271. Ismail, A., A. Hall, and T. Close, *Chilling tolerance during emergence of cowpea associated with a dehydrin and slow electrolyte leakage.* Crop Science, 1997. **37**(4): p. 1270-1277.
272. Gwathmey, C.O., A.E. Hall, and M.A. Madore, *Adaptive attributes of cowpea genotypes with delayed monocarpic leaf senescence.* Crop Science, 1992. **32**(3): p. 765-772.
273. Manchanda, G. and N. Garg, *Salinity and its effects on the functional biology of legumes.* Acta Physiologiae Plantarum, 2008. **30**(5): p. 595-618.
274. Murillo-Amador, B., et al., *Effect of NaCl salinity in the genotypic variation of cowpea (Vigna unguiculata) during early vegetative growth.* Scientia Horticulturae, 2006. **108**(4): p. 423-431.
275. Thiam, M., et al., *NaCl effects on in vitro germination and growth of some senegalese cowpea (Vigna unguiculata (L.) Walp.) cultivars.* International Scholarly Research Notices, 2013. **2013**.
276. Munns, R. and M. Tester, *Mechanisms of salinity tolerance.* Annu. Rev. Plant Biol., 2008. **59**: p. 651-681.
277. Ahmad, I. and F.J. Maathuis, *Cellular and tissue distribution of potassium: physiological relevance, mechanisms and regulation.* Journal of plant physiology, 2014. **171**(9): p. 708-714.
278. Vašák, M. and J. Schnabl, *Sodium and potassium ions in proteins and enzyme catalysis*, in *The Alkali Metal Ions: Their Role for Life*. 2016, Springer. p. 259-290.
279. Burssens, S., et al., *Expression of cell cycle regulatory genes and morphological alterations in response to salt stress in Arabidopsis thaliana.* Planta, 2000. **211**(5): p. 632-640.
280. Navarro, J.M., et al., *Phosphorus uptake and translocation in salt-stressed melon plants.* Journal of plant physiology, 2001. **158**(3): p. 375-381.
281. Fageria, N., H. Gheyi, and A. Moreira, *Nutrient bioavailability in salt affected soils.* Journal of Plant Nutrition, 2011. **34**(7): p. 945-962.
282. Chaves, M.M., J.M. Costa, and N.J.M. Saibo, *Recent advances in photosynthesis under drought and salinity.* Advances in botanical research, 2011. **57**: p. 49-104.
283. Shrivastava, P. and R. Kumar, *Soil salinity: A serious environmental issue and plant growth promoting bacteria as one of the tools for its alleviation.* Saudi journal of biological sciences, 2015. **22**(2): p. 123-131.
284. Sun, K., K. Hunt, and B.A. Hauser, *Ovule abortion in Arabidopsis triggered by stress.* Plant Physiology, 2004. **135**(4): p. 2358-2367.
285. Huang, H., et al., *Mechanisms of ROS regulation of plant development and stress responses.* Frontiers in Plant Science, 2019. **10**: p. 800.
286. Gowda, V.R., et al., *Root biology and genetic improvement for drought avoidance in rice.* Field Crops Research, 2011. **122**(1): p. 1-13.
287. Amede, T., S. Schubert, and K. Stahr, *Mechanisms of drought resistance in grain legumes I: Osmotic adjustment.* SINET: Ethiopian Journal of Science, 2003. **26**(1): p. 37-46.
288. Al-Yasi, H., et al., *Impact of drought on growth, photosynthesis, osmotic adjustment, and cell wall elasticity in Damask rose.* Plant Physiology Biochemistry, 2020. **150**: p. 133-139.
289. Verbruggen, N. and C. Hermans, *Proline accumulation in plants: a review.* Amino acids, 2008. **35**(4): p. 753-759.
290. Weyers, J.D. and N.W. Paterson, *Plant hormones and the control of physiological processes.* New Phytologist, 2001. **152**(3): p. 375-407.
291. Bielach, A., M. Hrtyan, and V.B. Tognetti, *Plants under stress: involvement of auxin and cytokinin.* International journal of molecular sciences, 2017. **18**(7): p. 1427.

292. Brossa, R., et al., *Interplay between abscisic acid and jasmonic acid and its role in water-oxidative stress in wild-type, ABA-deficient, JA-deficient, and ascorbate-deficient Arabidopsis plants.* Journal of Plant Growth Regulation, 2011. **30**(3): p. 322-333.
293. Fernando, V.D. and D.F. Schroeder, *Role of ABA in Arabidopsis salt, drought, and desiccation tolerance*, in *Abiotic and biotic stress in plants-recent advances and future perspectives*. 2016, IntechOpen.
294. Pierik, R., R. Sasidharan, and L.A. Voesenek, *Growth control by ethylene: adjusting phenotypes to the environment.* Journal of Plant Growth Regulation, 2007. **26**(2): p. 188-200.
295. Gomes, D., et al., *Aquaporins are multifunctional water and solute transporters highly divergent in living organisms.* Biochimica et Biophysica Acta -Biomembranes, 2009. **1788**(6): p. 1213-1228.
296. Kuwagata, T., et al., *Influence of low air humidity and low root temperature on water uptake, growth and aquaporin expression in rice plants.* Plant Cell Physiology, 2012. **53**(8): p. 1418-1431.
297. Liu, Y., et al., *Multifunctional roles of plant dehydrins in response to environmental stresses.* Frontiers in plant science, 2017. **8**: p. 1018.
298. Al-Whaibi, M.H., *Plant heat-shock proteins: a mini review.* Journal of King Saud University-Science, 2011. **23**(2): p. 139-150.
299. Fujita, M., et al., *A dehydration-induced NAC protein, RD26, is involved in a novel ABA-dependent stress-signaling pathway.* The Plant Journal, 2004. **39**(6): p. 863-876.
300. Abe, H., et al., *Arabidopsis AtMYC2 (bHLH) and AtMYB2 (MYB) function as transcriptional activators in abscisic acid signaling.* The Plant Cell, 2003. **15**(1): p. 63-78.
301. Tiwari, P., et al., *Over-expression of rice R1-type MYB transcription factor confers different abiotic stress tolerance in transgenic Arabidopsis.* Ecotoxicology Environmental Safety, 2020. **206**: p. 111361.
302. Wang, Y., et al., *Overexpression of a maize MYB48 gene confers drought tolerance in transgenic arabidopsis plants.* Journal of Plant Biology, 2017. **60**(6): p. 612-621.
303. Sarkar, T., et al., *Advances in the development and use of DREB for improved abiotic stress tolerance in transgenic crop plants.* Physiology Molecular Biology of Plants, 2019. **25**(6): p. 1323-1334.
304. Yang, Y., et al., *DREB/CBF expression in wheat and barley using the stress-inducible promoters of HD-Zip I genes: impact on plant development, stress tolerance and yield.* Plant biotechnology journal, 2020. **18**(3): p. 829-844.
305. Singh, B., et al., *Improving the production and utilization of cowpea as food and fodder.* Field Crops Research, 2003. **84**(1-2): p. 169-177.
306. Wang, G., et al., *Competitiveness of erect, semierect, and prostrate cowpea genotypes with sunflower (Helianthus annuus) and purslane (Portulaca oleracea).* Weed science, 2004. **52**(5): p. 815-820.
307. Buleti, S.I., E.G. Mamati, and M.O. Abukutsa-Onyango, *Potential of cowpea improvement from a collection of farmers crop, Gene Bank and advanced lines.* Journal of Medicinally Active Plants, 2020. **9**(2): p. 47-59.
308. Ramamoorthy, P., et al., *Root traits confer grain yield advantages under terminal drought in chickpea (Cicer arietinum L.).* Field crops research, 2017. **201**: p. 146-161.
309. Duc, G., et al., *Breeding annual grain legumes for sustainable agriculture: new methods to approach complex traits and target new cultivar ideotypes.* Critical Reviews in Plant Sciences, 2015. **34**(1-3): p. 381-411.
310. Fried, H.G., S. Narayanan, and B. Fallen, *Evaluation of soybean [Glycine max (L.) Merr.] genotypes for yield, water use efficiency, and root traits.* PloS one, 2019. **14**(2): p. e0212700.
311. Prince, S.J., et al., *Evaluation of high yielding soybean germplasm under water limitation.* Journal of integrative plant biology, 2016. **58**(5): p. 475-491.

312. Ghanbari, A.A., et al., *Morpho-physiological responses of common bean leaf to water deficit stress.* European Journal of Experimental Biology, 2013. **3**(1): p. 487-492.
313. Polania, J., et al., *Shoot and root traits contribute to drought resistance in recombinant inbred lines of MD 23–24× SEA 5 of common bean.* Frontiers in Plant Science, 2017. **8**: p. 296.
314. Ramamoorthy, P., et al., *Shoot traits and their relevance in terminal drought tolerance of chickpea (Cicer arietinum L.).* Field Crops Research, 2016. **197**: p. 10-27.
315. Hossain, M., A. Hamid, and M. Khaliq, *Evaluation of mungbean (Vigna radiata (L.) Wilczek) genotypes on the basis of photosynthesis and dry matter accumulation.* Journal of Agriculture Rural Development, 2009: p. 1-8.
316. Hall, A., *Phenotyping cowpeas for adaptation to drought.* Frontiers in physiology, 2012. **3**: p. 155.
317. Smitchger, J. and N.F. Weeden, *The ideotype for seed size: a model examining the relationship between seed size and actual yield in pea.* International Journal of Agronomy, 2018. **2018**.
318. Beebe, S., et al., *Phenotyping common beans for adaptation to drought.* Frontiers in physiology, 2013. **4**: p. 35.
319. Takada, S., et al., *The CUP-SHAPED COTYLEDON1 gene of Arabidopsis regulates shoot apical meristem formation.* Development, 2001. **128**(7): p. 1127-1135.
320. Herniter, I.A., M. Muñoz-Amatriaín, and T. Close, *Genetic, textual, and archeological evidence of the historical global spread of cowpea (Vigna unguiculata [L.] Walp.).* Legume Science, 2020. **2**(4): p. e57.
321. El-Gebali, S., et al., *The Pfam protein families database in 2019.* Nucleic acids research, 2019. **47**(D1): p. D427-D432.
322. Letunic, I., T. Doerks, and P. Bork, *SMART: recent updates, new developments and status in 2015.* Nucleic acids research, 2015. **43**(D1): p. D257-D260.
323. Muñoz-Amatriaín, M., et al., *Genome resources for climate-resilient cowpea, an essential crop for food security.* The Plant Journal, 2017. **89**(5): p. 1042-1054.
324. Gasteiger, E., et al., *Protein identification and analysis tools on the ExPASy server*, in *The proteomics protocols handbook*. 2005, Springer. p. 571-607.
325. Tamura, K., et al., *MEGA6: molecular evolutionary genetics analysis version 6.0.* Molecular biology evolution, 2013. **30**(12): p. 2725-2729.
326. Bailey, T.L., et al., *MEME SUITE: tools for motif discovery and searching.* Nucleic acids research, 2009. **37**(suppl_2): p. W202-W208.
327. Ba, A.N.N., et al., *NLStradamus: a simple Hidden Markov Model for nuclear localization signal prediction.* BMC bioinformatics, 2009. **10**(1): p. 202.
328. Krogh, A., et al., *Predicting transmembrane protein topology with a hidden Markov model: application to complete genomes.* Journal of molecular biology, 2001. **305**(3): p. 567-580.
329. Hu, B., et al., *GSDS 2.0: an upgraded gene feature visualization server.* Bioinformatics, 2015. **31**(8): p. 1296-1297.
330. Srivastava, R., et al., *Comparative genome-wide analysis of WRKY transcription factors in two Asian legume crops: Adzuki bean and Mung bean.* Scientific reports, 2018. **8**(1): p. 1-19.
331. Lescot, M., et al., *PlantCARE, a database of plant cis-acting regulatory elements and a portal to tools for in silico analysis of promoter sequences.* Nucleic acids research, 2002. **30**(1): p. 325-327.
332. Higo, K., et al., *Plant cis-acting regulatory DNA elements (PLACE) database: 1999.* Nucleic acids research, 1999. **27**(1): p. 297-300.
333. Hoagland, D.R. and D.I. Arnon, *The water-culture method for growing plants without soil.* Circular. California agricultural experiment station, 1950. **347**(2nd edit).
334. Simon, A., *FastQC: a quality control tool for high throughput sequence data.* Cambridge, UK: Babraham Institute, 2011.

335. Patel, R.K. and M. Jain, *NGS QC Toolkit: a toolkit for quality control of next generation sequencing data.* PloS one, 2012. **7**(2): p. e30619.
336. Sirén, J., N. Välimäki, and V. Mäkinen, *HISAT2-fast and sensitive alignment against general human population.* IEEE/ACM Trans Comput Biol Bioinforma, 2014. **11**: p. 375-88.
337. Pertea, M., et al., *StringTie enables improved reconstruction of a transcriptome from RNA-seq reads.* Nature biotechnology, 2015. **33**(3): p. 290-295.
338. Obayashi, T., et al., *ATTED-II in 2018: a plant coexpression database based on investigation of the statistical property of the mutual rank index.* Plant Cell Physiology, 2018. **59**(1): p. e3-e3.
339. Mi, H., et al., *PANTHER version 16: a revised family classification, tree-based classification tool, enhancer regions and extensive API.* Nucleic Acids Research, 2021. **49**(D1): p. D394-D403.
340. Mohanta, T.K., Y.-H. Park, and H.J.S.r. Bae, *Novel genomic and evolutionary insight of WRKY transcription factors in plant lineage.* 2016. **6**(1): p. 1-22.
341. Zhang, Q., et al., *Modulation of NAC transcription factor NST1 activity by XYLEM NAC DOMAIN1 regulates secondary cell wall formation in Arabidopsis.* Journal of Experimental Botany, 2020. **71**(4): p. 1449-1458.
342. Hoppe, T., et al., *Activation of a membrane-bound transcription factor by regulated ubiquitin/proteasome-dependent processing.* Cell, 2000. **102**(5): p. 577-586.
343. Shahmuradov, I.A., R.K. Umarov, and V.V. Solovyev, *TSSPlant: a new tool for prediction of plant Pol II promoters.* Nucleic acids research, 2017. **45**(8): p. e65-e65.
344. Porto, M.S., et al., *Plant promoters: an approach of structure and function.* Molecular biotechnology, 2014. **56**(1): p. 38-49.
345. Mohanty, B., et al., *Detection and preliminary analysis of motifs in promoters of anaerobically induced genes of different plant species.* Annals of Botany, 2005. **96**(4): p. 669-681.
346. Chen, Y.-J., et al., *The barley HvNAC6 transcription factor affects ABA accumulation and promotes basal resistance against powdery mildew.* Plant Molecular Biology Reporter, 2013. **83**(6): p. 577-590.
347. He, X., et al., *GhATAF1, a NAC transcription factor, confers abiotic and biotic stress responses by regulating phytohormonal signaling networks.* Plant Cell Reports, 2016. **35**(10): p. 2167-2179.
348. Nakano, Y., et al., *NAC-MYB-based transcriptional regulation of secondary cell wall biosynthesis in land plants.* Frontiers in plant science, 2015. **6**: p. 288.
349. Ohtani, M., et al., *A NAC domain protein family contributing to the regulation of wood formation in poplar.* The Plant Journal, 2011. **67**(3): p. 499-512.
350. Gao, Z., et al., *KIRA1 and ORESARA1 terminate flower receptivity by promoting cell death in the stigma of Arabidopsis.* Nature Plants, 2018. **4**(6): p. 365-375.
351. Huysmans, M., et al., *NAC transcription factors ANAC087 and ANAC046 control distinct aspects of programmed cell death in the Arabidopsis columella and lateral root cap.* The Plant Cell, 2018. **30**(9): p. 2197-2213.
352. Shahnejat-Bushehri, S., et al., *Arabidopsis NAC transcription factor JUB1 regulates GA/BR metabolism and signalling.* Nature plants, 2016. **2**(3): p. 1-9.
353. Ohbayashi, I., et al., *Evidence for a role of ANAC082 as a ribosomal stress response mediator leading to growth defects and developmental alterations in Arabidopsis.* The Plant Cell, 2017. **29**(10): p. 2644-2660.
354. Shih, C.-F., et al., *The NAC-like gene ANTHER INDEHISCENCE FACTOR acts as a repressor that controls anther dehiscence by regulating genes in the jasmonate biosynthesis pathway in Arabidopsis.* Journal of experimental botany, 2014. **65**(2): p. 621-639.
355. Fujiwara, S. and N. Mitsuda, *ANAC075, a putative regulator of VASCULAR-RELATED NAC-DOMAIN7, is a repressor of flowering.* Plant Biotechnology, 2016: p. 16.0215 b.

356. Kamiya, M., et al., *Control of root cap maturation and cell detachment by BEARSKIN transcription factors in Arabidopsis.* Development, 2016. **143**(21): p. 4063-4072.
357. Kato, H., et al., *Overexpression of the NAC transcription factor family gene ANAC036 results in a dwarf phenotype in Arabidopsis thaliana.* Journal of plant physiology, 2010. **167**(7): p. 571-577.
358. Moore, R.C. and M.D. Purugganan, *The early stages of duplicate gene evolution.* Proceedings of the National Academy of Sciences, 2003. **100**(26): p. 15682-15687.
359. Seo, P.J., C.-M.J.P.s. Park, and behavior, *A membrane-bound NAC transcription factor as an integrator of biotic and abiotic stress signals.* Plant signaling behavior, 2010. **5**(5): p. 481-483.
360. Wingler, A., et al., *Trehalose 6-phosphate is required for the onset of leaf senescence associated with high carbon availability.* Plant Physiology, 2012. **158**(3): p. 1241-1251.
361. Dube, E. and M. Fanadzo, *Maximising yield benefits from dual-purpose cowpea.* Food security, 2013. **5**(6): p. 769-779.
362. IITA, I., *Applied and adaptive research on cowpea in semi-arid zones of West Africa.* Executive Board-69th session, 2000: p. 18-20.
363. Zhu, J.-K., *Abiotic stress signaling and responses in plants.* Cell, 2016. **167**(2): p. 313-324.
364. Crozet, P., et al., *Mechanisms of regulation of SNF1/AMPK/SnRK1 protein kinases.* Frontiers in plant science, 2014. **5**: p. 190.
365. Dahiya, P., D.S. Bhat, and J.K. Thakur, *Expression of AtMed15 of Arabidopsis in yeast causes flocculation and increases ethanol production in yeast culture.* Scientific reports, 2016. **6**: p. 27967.
366. Bu, Y., et al., *Overexpression of AtOxR gene improves abiotic stresses tolerance and vitamin C content in Arabidopsis thaliana.* BMC biotechnology, 2016. **16**(1): p. 69.
367. Quintero, F.J., et al., *Reconstitution in yeast of the Arabidopsis SOS signaling pathway for Na+ homeostasis.* Proceedings of the National Academy of Sciences, 2002. **99**(13): p. 9061-9066.
368. Naseri, G., et al., *Plant-derived transcription factors for orthologous regulation of gene expression in the yeast Saccharomyces cerevisiae.* ACS Synthetic Biology, 2017. **6**(9): p. 1742-1756.
369. Puranik, S., et al., *Electrophoretic mobility shift assay reveals a novel recognition sequence for Setaria italica NAC protein.* Signaling Behavior, 2011. **6**(10): p. 1588-1590.
370. Tang, S.-Y., et al., *High resolution scanning electron microscopy of cells using dielectrophoresis.* PloS one, 2014. **9**(8): p. e104109.
371. Jenkins, S., S.M. Fischer, and T.R. Sana, *Nontargeted, Discovery-Based Profiling of the Yeast Metabolome Using QTOF LC-MS and LC-MS-MS.* LC GC NORTH AMERICA, 2013: p. 41-45.
372. Srivastava, R. and L. Sahoo, *Cowpea NAC Transcription Factors Positively Regulate Cellular Stress Response and Balance Energy Metabolism in Yeast via Reprogramming of Biosynthetic Pathways.* ACS Synthetic Biology, 2021.
373. Kang, M., et al., *The C-domain of the NAC transcription factor ANAC019 is necessary for pH-tuned DNA binding through a histidine switch in the N-domain.* Cell reports, 2018. **22**(5): p. 1141-1150.
374. Olsen, A.N., et al., *DNA-binding specificity and molecular functions of NAC transcription factors.* Plant Science, 2005. **169**(4): p. 785-797.
375. Duval, M., et al., *Molecular characterization of AtNAM: a member of theArabidopsis NAC domain superfamily.* Plant molecular biology, 2002. **50**(2): p. 237-248.
376. Garcia-Gimeno, M.A. and K. Struhl, *Aca1 and Aca2, ATF/CREB activators in Saccharomyces cerevisiae, are important for carbon source utilization but not the response to stress.* Molecular and Cellular Biology, 2000. **20**(12): p. 4340-4349.

377. Rep, M., et al., *The Saccharomyces cerevisiae Sko1p transcription factor mediates HOG pathway-dependent osmotic regulation of a set of genes encoding enzymes implicated in protection from oxidative damage.* Molecular microbiology, 2001. **40**(5): p. 1067-1083.
378. Miyahara, K., D. Hirata, and T. Miyakawa, *yAP-1-and yAP-2-mediated, heat shock-induced transcriptional activation of the multidrug resistance ABC transporter genes in Saccharomyces cerevisiae.* Current genetics, 1996. **29**(2): p. 103-105.
379. Hanlon, S.E., et al., *The stress response factors Yap6, Cin5, Phd1, and Skn7 direct targeting of the conserved co-repressor Tup1-Ssn6 in S. cerevisiae.* PloS one, 2011. **6**(4): p. e19060.
380. Hinnebusch, A.G. and K. Natarajan, *Gcn4p, a master regulator of gene expression, is controlled at multiple levels by diverse signals of starvation and stress.* Eukaryotic cell, 2002. **1**(1): p. 22-32.
381. Hartwell, L.H. and M.W. Unger, *Unequal division in Saccharomyces cerevisiae and its implications for the control of cell division.* The Journal of cell biology, 1977. **75**(2): p. 422-435.
382. Palková, Z., D. Wilkinson, and L. Váchová, *Aging and differentiation in yeast populations: elders with different properties and functions.* FEMS Yeast Research, 2014. **14**(1): p. 96-108.
383. Bharathi, V., et al., *Use of ade1 and ade2 mutations for development of a versatile red/white colour assay of amyloid-induced oxidative stress in saccharomyces cerevisiae.* Yeast, 2016. **33**(12): p. 607-620.
384. Pfeiffer, T. and A. Morley, *An evolutionary perspective on the Crabtree effect.* Frontiers in molecular biosciences, 2014. **1**: p. 17.
385. Chang, Y.-H., et al., *Enhancement of the efficiency of bioethanol production by Saccharomyces cerevisiae via gradually batch-wise and fed-batch increasing the glucose concentration.* Fermentation, 2018. **4**(2): p. 45.
386. Burattini, E., et al., *A FTIR microspectroscopy study of autolysis in cells of the wine yeast Saccharomyces cerevisiae.* Vibrational Spectroscopy, 2008. **47**(2): p. 139-147.
387. Kochan, K., et al., *Single cell assessment of yeast metabolic engineering for enhanced lipid production using Raman and AFM-IR imaging.* Biotechnology for biofuels, 2018. **11**(1): p. 106.
388. Wolak, N., et al., *Thiamine increases the resistance of baker's yeast Saccharomyces cerevisiae against oxidative, osmotic and thermal stress, through mechanisms partly independent of thiamine diphosphate-bound enzymes.* FEMS yeast research, 2014. **14**(8): p. 1249-1262.
389. Abbas, C.A. and A.A. Sibirny, *Genetic control of biosynthesis and transport of riboflavin and flavin nucleotides and construction of robust biotechnological producers.* Microbiology and Molecular Biology Reviews, 2011. **75**(2): p. 321-360.
390. Lin, S.-J., P.-A. Defossez, and L. Guarente, *Requirement of NAD and SIR2 for life-span extension by calorie restriction in Saccharomyces cerevisiae.* Science, 2000. **289**(5487): p. 2126-2128.
391. White, W.H., P.L. Gunyuzlu, and J.H. Toyn, *Saccharomyces cerevisiae is capable of de novo pantothenic acid biosynthesis involving a novel pathway of β-alanine production from spermine.* Journal of biological chemistry, 2001. **276**(14): p. 10794-10800.
392. Perli, T., et al., *Vitamin requirements and biosynthesis in Saccharomyces cerevisiae.* Yeast, 2020. **37**(4): p. 283-304.
393. Zhang, Y., *Role of glutathione in the accumulation of anticarcinogenic isothiocyanates and their glutathione conjugates by murine hepatoma cells.* Carcinogenesis, 2000. **21**(6): p. 1175-1182.
394. Swiegers, J.H., et al., *Carnitine biosynthesis in Neurospora crassa: identification of a cDNA coding for ε-N-trimethyllysine hydroxylase and its functional expression in Saccharomyces cerevisiae.* FEMS microbiology letters, 2002. **210**(1): p. 19-23.

395. Li, Z.-L., et al., *Effect of branched-chain amino acids, valine, isoleucine and leucine on the biosynthesis of bitespiramycin 4"-O-acylspiramycins.* Brazilian Journal of Microbiology, 2009. **40**(4): p. 734-746.
396. Laxman, S., B.M. Sutter, and B.P. Tu, *Methionine is a signal of amino acid sufficiency that inhibits autophagy through the methylation of PP2A.* Autophagy 2014. **10**(2): p. 386-387.
397. Zou, K., et al., *Life span extension by glucose restriction is abrogated by methionine supplementation: Cross-talk between glucose and methionine and implication of methionine as a key regulator of life span.* Science advances, 2020. **6**(32): p. eaba1306.
398. Iriarte, C.E. and I.G. Macreadie, *Comparison of Cytocidal Activities of L-DOPA and Dopamine in S. cerevisiae and C. glabrata.* Current Bioactive Compounds, 2020. **16**(1): p. 90-93.
399. Franken, J., et al., *Carnitine and carnitine acetyltransferases in the yeast Saccharomyces cerevisiae: a role for carnitine in stress protection.* Current genetics, 2008. **53**(6): p. 347.
400. Kiewietdejonge, A., et al., *Hypersaline stress induces the turnover of phosphatidylcholine and results in the synthesis of the renal osmoprotectant glycerophosphocholine in Saccharomyces cerevisiae.* FEMS yeast research, 2006. **6**(2): p. 205-217.
401. Varki, A., *Sialic acids in human health and disease.* Trens in molecular medicine, 2008. **14**(8): p. 351-360.
402. Park, H.C., et al., *Pathogen-and NaCl-induced expression of the SCaM-4 promoter is mediated in part by a GT-1 box that interacts with a GT-1-like transcription factor.* Plant physiology, 2004. **135**(4): p. 2150-2161.
403. Sakai, H., T. Aoyama, and A. Oka, *Arabidopsis ARR1 and ARR2 response regulators operate as transcriptional activators.* The Plant Journal, 2000. **24**(6): p. 703-711.
404. Stålberg, K., et al., *Disruption of an overlapping E-box/ABRE motif abolished high transcription of the napA storage-protein promoter in transgenic Brassica napus seeds.* Planta, 1996. **199**(4): p. 515-519.
405. Garapati, P., et al., *Transcription factor Arabidopsis Activating Factor1 integrates carbon starvation responses with trehalose metabolism.* Plant Physiology, 2015. **169**(1): p. 379-390.
406. Pinson, B., et al., *Metabolic intermediates selectively stimulate transcription factor interaction and modulate phosphate and purine pathways.* Genes Development, 2009. **23**(12): p. 1399-1407.
407. Sadhukhan, A., et al., *Synergistic and antagonistic pleiotropy of STOP1 in stress tolerance.* Trends in Plant Science, 2021.
408. Enomoto, T., et al., *STOP1 regulates the expression of HsfA2 and GDH s that are critical for low-oxygen tolerance in Arabidopsis.* Journal of experimental botany, 2019. **70**(12): p. 3297-3311.
409. Das, P., et al., *A unique bZIP transcription factor imparting multiple stress tolerance in Rice.* Rice, 2019. **12**(1): p. 1-16.
410. Kulkarni, K.P., et al., *Harnessing the potential of forage legumes, alfalfa, soybean, and cowpea for sustainable agriculture and global food security.* Frontiers in plant science, 2018. **9**: p. 1314.
411. Zhang, X., et al., *Agrobacterium-mediated transformation of Arabidopsis thaliana using the floral dip method.* Nature protocols, 2006. **1**(2): p. 641.
412. Kingsbury, R.W., E. Epstein, and R.W. Pearcy, *Physiological responses to salinity in selected lines of wheat.* Plant physiology, 1984. **74**(2): p. 417-423.
413. Dionisio-Sese, M.L. and S. Tobita, *Antioxidant responses of rice seedlings to salinity stress.* Plant science, 1998. **135**(1): p. 1-9.
414. Heath, R.L. and L. Packer, *Photoperoxidation in isolated chloroplasts: I. Kinetics and stoichiometry of fatty acid peroxidation.* Archives of biochemistry biophysics, 1968. **125**(1): p. 189-198.
415. Bates, L.S., et al., *Rapid determination of free proline for water-stress studies.* Plant soil, 1973. **39**(1): p. 205-207.

416. Griffith, O.W., *Determination of glutathione and glutathione disulfide using glutathione reductase and 2-vinylpyridine.* Analytical biochemistry, 1980. **106**(1): p. 207-212.
417. Oser, B.L. and P.B. Hawk, *Hawk's physiological chemistry*. 1965: McGraw-hill.
418. Zheng, Z.-L., *Carbon and nitrogen nutrient balance signaling in plants.* Plant signaling behavior, 2009. **4**(7): p. 584-591.
419. Podgórska, A., et al., *Efficient photosynthetic functioning of Arabidopsis thaliana through electron dissipation in chloroplasts and electron export to mitochondria under ammonium nutrition.* Frontiers in plant science, 2020. **11**: p. 103.
420. Lawlor, D.W., *Carbon and nitrogen assimilation in relation to yield: mechanisms are the key to understanding production systems.* Journal of experimental botany, 2002. **53**(370): p. 773-787.
421. Simkin, A.J., P.E. López-Calcagno, and C.A.J.J.o.E.B. Raines, *Feeding the world: improving photosynthetic efficiency for sustainable crop production.* Journal of Experimental Botany, 2019. **70**(4): p. 1119-1140.
422. Kermode, A.R., *Role of abscisic acid in seed dormancy.* Journal of Plant Growth Regulation, 2005. **24**(4): p. 319-344.
423. Shu, K., et al., *Abscisic acid and gibberellins antagonistically mediate plant development and abiotic stress responses.* Frontiers in Plant Science, 2018. **9**: p. 416.
424. Alarcón, M., J. Salguero, and P.G. Lloret, *Auxin modulated initiation of lateral roots is linked to pericycle cell length in maize.* Frontiers in plant science, 2019. **10**: p. 11.
425. Sakoda, K., et al., *Higher stomatal density improves photosynthetic induction and biomass production in Arabidopsis under fluctuating light.* Frontiers in Plant Science, 2020. **11**: p. 1609.
426. Xiang, Y., et al., *The transcription factor ZmNAC49 reduces stomatal density and improves drought tolerance in maize.* Journal of Experimental Botany, 2021. **72**(4): p. 1399-1410.
427. Ju, Y.-l., et al., *VvNAC17, a novel stress-responsive grapevine (Vitis vinifera L.) NAC transcription factor, increases sensitivity to abscisic acid and enhances salinity, freezing, and drought tolerance in transgenic Arabidopsis.* Plant Physiology and Biochemistry, 2020. **146**: p. 98-111.
428. Bertolino, L.T., R.S. Caine, and J.E. Gray, *Impact of stomatal density and morphology on water-use efficiency in a changing world.* Frontiers in plant science, 2019. **10**: p. 225.
429. Lawson, T. and M.R.J.P.p. Blatt, *Stomatal size, speed, and responsiveness impact on photosynthesis and water use efficiency.* Plant physiology, 2014. **164**(4): p. 1556-1570.
430. De Clercq, I., et al., *Integrative inference of transcriptional networks in Arabidopsis yields novel ROS signalling regulators.* Nature Plants, 2021. **7**(4): p. 500-513.
431. Nishizawa, A., et al., *Arabidopsis heat shock transcription factor A2 as a key regulator in response to several types of environmental stress.* The Plant Journal, 2006. **48**(4): p. 535-547.
432. Matsuo, M., et al., *High REDOX RESPONSIVE TRANSCRIPTION FACTOR1 levels result in accumulation of reactive oxygen species in Arabidopsis thaliana shoots and roots.* Molecular Plant, 2015. **8**(8): p. 1253-1273.
433. Mara, C.D. and V.F. Irish, *Two GATA transcription factors are downstream effectors of floral homeotic gene action in Arabidopsis.* Plant Physiology, 2008. **147**(2): p. 707-718.
434. Wu, C., et al., *HRS1 acts as a negative regulator of abscisic acid signaling to promote timely germination of Arabidopsis seeds.* PLoS One, 2012. **7**(4): p. e35764.
435. Medici, A., et al., *AtNIGT1/HRS1 integrates nitrate and phosphate signals at the Arabidopsis root tip.* Nature communications, 2015. **6**(1): p. 1-11.
436. Bournier, M., et al., *Arabidopsis ferritin 1 (AtFer1) gene regulation by the phosphate starvation response 1 (AtPHR1) transcription factor reveals a direct molecular link between iron and phosphate homeostasis.* Journal of Biological Chemistry, 2013. **288**(31): p. 22670-22680.

437. Sakuma, Y., et al., *Functional analysis of an Arabidopsis transcription factor, DREB2A, involved in drought-responsive gene expression.* The Plant Cell, 2006. **18**(5): p. 1292-1309.
438. Ramegowda, V., et al., *GBF3 transcription factor imparts drought tolerance in Arabidopsis thaliana.* Scientific reports, 2017. **7**(1): p. 1-13.
439. Chu, M., et al., *The Arabidopsis phosphatase PP2C49 negatively regulates salt tolerance through inhibition of AtHKT1; 1.* Journal of Integrative Plant Biology, 2020.
440. Liu, X., et al., *AtPP2CG1, a protein phosphatase 2C, positively regulates salt tolerance of Arabidopsis in abscisic acid-dependent manner.* Biochemical Biophysical Research Communications, 2012. **422**(4): p. 710-715.
441. Remy, E., et al., *A major facilitator superfamily transporter plays a dual role in polar auxin transport and drought stress tolerance in Arabidopsis.* The Plant Cell, 2013. **25**(3): p. 901-926.
442. Mao, J.-L., et al., *Arabidopsis ERF1 mediates cross-talk between ethylene and auxin biosynthesis during primary root elongation by regulating ASA1 expression.* PLoS genetics, 2016. **12**(1): p. e1005760.
443. Xu, R., et al., *Salt-induced transcription factor MYB74 is regulated by the RNA-directed DNA methylation pathway in Arabidopsis.* Journal of experimental botany, 2015. **66**(19): p. 5997-6008.
444. Sun, J., et al., *The CCCH-type zinc finger proteins AtSZF1 and AtSZF2 regulate salt stress responses in Arabidopsis.* Plant Cell Physiology, 2007. **48**(8): p. 1148-1158.
445. Corso, M., et al., *Endoplasmic reticulum-localized CCX2 is required for osmotolerance by regulating ER and cytosolic Ca2+ dynamics in Arabidopsis.* Proceedings of the National Academy of Sciences, 2018. **115**(15): p. 3966-3971.
446. Yang, Z.T., et al., *A plasma membrane-tethered transcription factor, NAC062/ANAC062/NTL6, mediates the unfolded protein response in Arabidopsis.* The Plant Journal, 2014. **79**(6): p. 1033-1043.
447. Xu, X.M., et al., *The Arabidopsis DJ-1a protein confers stress protection through cytosolic SOD activation.* Journal of cell science, 2010. **123**(10): p. 1644-1651.
448. Petridis, A., et al., *Arabidopsis thaliana G2-LIKE FLAVONOID REGULATOR and BRASSINOSTEROID ENHANCED EXPRESSION1 are low-temperature regulators of flavonoid accumulation.* New Phytologist, 2016. **211**(3): p. 912-925.
449. Zhou, C., et al., *An Arabidopsis mitogen-activated protein kinase cascade, MKK9-MPK6, plays a role in leaf senescence.* Plant physiology, 2009. **150**(1): p. 167-177.
450. Diener, A.C., R.A. Gaxiola, and G.R. Fink, *Arabidopsis ALF5, a multidrug efflux transporter gene family member, confers resistance to toxins.* The Plant Cell, 2001. **13**(7): p. 1625-1638.
451. Sato, T., et al., *CNI1/ATL31, a RING-type ubiquitin ligase that functions in the carbon/nitrogen response for growth phase transition in Arabidopsis seedlings.* The Plant Journal, 2009. **60**(5): p. 852-864.
452. Liu, X.-M., et al., *Phosphorylation of the zinc finger transcriptional regulator ZAT6 by MPK6 regulates Arabidopsis seed germination under salt and osmotic stress.* Biochemical Biophysical Research Communications, 2013. **430**(3): p. 1054-1059.
453. Zhou, X., et al., *The ERF11 transcription factor promotes internode elongation by activating gibberellin biosynthesis and signaling.* Plant physiology, 2016. **171**(4): p. 2760-2770.
454. Tapia-López, R., et al., *An AGAMOUS-related MADS-box gene, XAL1 (AGL12), regulates root meristem cell proliferation and flowering transition in Arabidopsis.* Plant physiology, 2008. **146**(3): p. 1182-1192.
455. Fornara, F., et al., *Arabidopsis DOF transcription factors act redundantly to reduce CONSTANS expression and are essential for a photoperiodic flowering response.* Developmental cell, 2009. **17**(1): p. 75-86.
456. Danisman, S.J.F.i.p.s., *TCP transcription factors at the interface between environmental challenges and the plant's growth responses.* Frontiers in plant science, 2016. **7**: p. 1930.

457. Aguilar Martinez, J.A. and N.R. Sinha, *Analysis of the role of Arabidopsis class I TCP genes AtTCP7, AtTCP8, AtTCP22, and AtTCP23 in leaf development.* Frontiers in plant science, 2013. **4**: p. 406.
458. Nicolas, M. and P. Cubas, *TCP factors: new kids on the signaling block.* Current opinion in plant biology, 2016. **33**: p. 33-41.
459. Wang, Q., et al., *DBB1a, involved in gibberellin homeostasis, functions as a negative regulator of blue light-mediated hypocotyl elongation in Arabidopsis.* Planta, 2011. **233**(1): p. 13-23.
460. Vishwakarma, A., et al., *Physiological role of AOX1a in photosynthesis and maintenance of cellular redox homeostasis under high light in Arabidopsis thaliana.* Plant Physiology Biochemistry, 2014. **81**: p. 44-53.
461. Basu, D., et al., *A small multigene hydroxyproline-O-galactosyltransferase family functions in arabinogalactan-protein glycosylation, growth and development in Arabidopsis.* BMC plant biology, 2015. **15**(1): p. 1-23.
462. Pan, H., et al., *Structural studies of cinnamoyl-CoA reductase and cinnamyl-alcohol dehydrogenase, key enzymes of monolignol biosynthesis.* The Plant Cell, 2014. **26**(9): p. 3709-3727.
463. Ajjawi, I., et al., *Thiamin pyrophosphokinase is required for thiamin cofactor activation in Arabidopsis.* Plant molecular biology, 2007. **65**(1): p. 151-162.
464. Yoshida, S., et al., *Cytosolic dehydroascorbate reductase is important for ozone tolerance in Arabidopsis thaliana.* Plant cell physiology, 2006. **47**(2): p. 304-308.
465. Sharma, R., et al., *Over-expression of a rice tau class glutathione s-transferase gene improves tolerance to salinity and oxidative stresses in Arabidopsis.* PloS one, 2014. **9**(3): p. e92900.
466. Sun, L., et al., *Arabidopsis PHL2 and PHR1 act redundantly as the key components of the central regulatory system controlling transcriptional responses to phosphate starvation.* Plant Physiology, 2016. **170**(1): p. 499-514.
467. Eggen, T. and C. Lillo, *Role of transporters for organic cations in plants for environmental cycling of pharmaceutical residues*, in *Organic Cation Transporters*. 2016, Springer. p. 243-256.
468. Ogawa, T., et al., *Comprehensive analysis of cytosolic Nudix hydrolases in Arabidopsis thaliana.* Journal of Biological Chemistry, 2005. **280**(26): p. 25277-25283.
469. Cheong, Y.H., et al., *CBL1, a calcium sensor that differentially regulates salt, drought, and cold responses in Arabidopsis.* The Plant Cell, 2003. **15**(8): p. 1833-1845.
470. Saez, A., et al., *Gain-of-function and loss-of-function phenotypes of the protein phosphatase 2C HAB1 reveal its role as a negative regulator of abscisic acid signalling.* The Plant Journal, 2004. **37**(3): p. 354-369.
471. Chong, G.L., et al., *Highly ABA-Induced 1 (HAI1)-Interacting protein HIN1 and drought acclimation-enhanced splicing efficiency at intron retention sites.* Proceedings of the National Academy of Sciences, 2019. **116**(44): p. 22376-22385.
472. Peng, H.-P., et al., *Differential expression of genes encoding 1-aminocyclopropane-1-carboxylate synthase in Arabidopsis during hypoxia.* Plant molecular biology, 2005. **58**(1): p. 15-25.
473. Liu, C., et al., *Heterologous expression of the transcription factor EsNAC1 in Arabidopsis enhances abiotic stress resistance and retards growth by regulating the expression of different target genes.* Frontiers in plant science, 2018. **9**: p. 1495.
474. Liu, C., et al., *TsNAC1 is a key transcription factor in abiotic stress resistance and growth.* Plant physiology, 2018. **176**(1): p. 742-756.
475. Des Marais, D.L. and T.E. Juenger, *Pleiotropy, plasticity, and the evolution of plant abiotic stress tolerance.* Annals of the New York Academy of Sciences, 2010. **1206**(1): p. 56-79.
476. Singh, Y., et al., *Short durartion cowpea varieties for cultivation as a niche crop in various cropping systems for enhanced pulse production.* Agricultural Science Digest, 2017. **37**(3).

477. Lichtenthaler, H.K. and Welburn, A.R., *Determinations of total carotenoids and chlorophyll a and b of leaf extracts in different solvents.* Biochem. Soc. Trans., 1983. **11**: p. 591-593.
478. Trapnell, C., et al., *Differential analysis of gene regulation at transcript resolution with RNA-seq.* Nature biotechnology, 2013. **31**(1): p. 46-53.
479. Staden, R., D.P. Judge, and J.K. Bonfield, *Analyzing sequences using the Staden Package and EMBOSS*, in *Introduction to bioinformatics*. 2003, Springer. p. 393-410.
480. Tatusov, R.L., et al., *The COG database: an updated version includes eukaryotes.* BMC bioinformatics, 2003. **4**(1): p. 1-14.
481. Powell, S., et al., *eggNOG v3. 0: orthologous groups covering 1133 organisms at 41 different taxonomic ranges.* Nucleic acids research, 2012. **40**(D1): p. D284-D289.
482. Ramegowda, V., K.S. Mysore, and M. Senthil-Kumar, *Virus-induced gene silencing is a versatile tool for unraveling the functional relevance of multiple abiotic-stress-responsive genes in crop plants.* Frontiers in plant science, 2014. **5**: p. 323.
483. Reeves, P.H. and G. Coupland, *Analysis of flowering time control in Arabidopsis by comparison of double and triple mutants.* Plant Physiology, 2001. **126**(3): p. 1085-1091.
484. Bagnall, D. and R. King, *Temperature and irradiance effects on yield in cowpea (Vigna unguiculata).* Field Crops Research, 1987. **16**(3): p. 217-229.
485. Ookawara, R., et al., *Expression of α-expansin and xyloglucan endotransglucosylase/hydrolase genes associated with shoot elongation enhanced by anoxia, ethylene and carbon dioxide in arrowhead (Sagittaria pygmaea Miq.) tubers.* Annals of Botany, 2005. **96**(4): p. 693-702.
486. Bischoff, V., et al., *TRICHOME BIREFRINGENCE and its homolog AT5G01360 encode plant-specific DUF231 proteins required for cellulose biosynthesis in Arabidopsis.* Plant Physiology, 2010. **153**(2): p. 590-602.
487. Philippe, F., J. Pelloux, and C. Rayon, *Plant pectin acetylesterase structure and function: new insights from bioinformatic analysis.* BMC genomics, 2017. **18**(1): p. 1-18.
488. Lukowitz, W., et al., *Arabidopsis cyt1 mutants are deficient in a mannose-1-phosphate guanylyltransferase and point to a requirement of N-linked glycosylation for cellulose biosynthesis.* 2001. **98**(5): p. 2262-2267.
489. Gendre, D., et al., *Rho-of-plant activated root hair formation requires Arabidopsis YIP4a/b gene function.* Development, 2019. **146**(5).
490. Žárský, V. and J. Fowler, *ROP (Rho-related protein from plants) GTPases for spatial control of root hair morphogenesis.* 2008.
491. He, Y. and S. Gan, *A novel zinc-finger protein with a proline-rich domain mediates ABA-regulated seed dormancy in Arabidopsis.* Plant molecular biology, 2004. **54**(1): p. 1-9.
492. Li, Y., et al., *Natural variation in GS5 plays an important role in regulating grain size and yield in rice.* Nature genetics, 2011. **43**(12): p. 1266-1269.
493. Shpak, E.D., et al., *Synergistic interaction of three ERECTA-family receptor-like kinases controls Arabidopsis organ growth and flower development by promoting cell proliferation.* Development, 2004. **131**(7): p. 1491-1501.
494. Menges, M., et al., *The D-type cyclin CYCD3; 1 is limiting for the G1-to-S-phase transition in Arabidopsis.* The Plant Cell, 2006. **18**(4): p. 893-906.
495. Kolesiński, P., J. Piechota, and A. Szczepaniak, *Initial characteristics of RbcX proteins from Arabidopsis thaliana.* Plant molecular biology, 2011. **77**(4): p. 447-459.
496. Zhang, J.-Y., Z. Cun, and J.-W. Chen, *Photosynthetic performance and photosynthesis-related gene expression coordinated in a shade-tolerant species Panax notoginseng under nitrogen regimes.* BMC plant biology, 2020. **20**(1): p. 1-19.
497. Kong, F., et al., *Identification of light-harvesting chlorophyll a/b-binding protein genes of Zostera marina L. and their expression under different environmental conditions.* Journal of Ocean University of China, 2016. **15**(1): p. 152-162.

498. Lu, Y., *Identification and roles of photosystem II assembly, stability, and repair factors in Arabidopsis.* Frontiers in plant science, 2016. **7**: p. 168.
499. Basak, I. and S.G. Møller, *Emerging facets of plastid division regulation.* Planta, 2013. **237**(2): p. 389-398.
500. Tanaka, R., K. Kobayashi, and T. Masuda, *Tetrapyrrole metabolism in Arabidopsis thaliana.* The Arabidopsis book/American Society of Plant Biologists, 2011. **9**.
501. Manara, A., et al., *At SIA 1 AND At OSA 1: two Abc1 proteins involved in oxidative stress responses and iron distribution within chloroplasts.* New Phytologist, 2014. **201**(2): p. 452-465.
502. Broin, M., et al., *The plastidic 2-cysteine peroxiredoxin is a target for a thioredoxin involved in the protection of the photosynthetic apparatus against oxidative damage.* The Plant Cell, 2002. **14**(6): p. 1417-1432.
503. Gazzarrini, S. and A.Y.-L. Tsai, *Trehalose-6-phosphate and SnRK1 kinases in plant development and signaling: the emerging picture.* Frontiers in plant science, 2014. **5**: p. 119.
504. Zhang, H., et al., *The RING finger ubiquitin E3 ligase SDIR1 targets SDIR1-INTERACTING PROTEIN1 for degradation to modulate the salt stress response and ABA signaling in Arabidopsis.* The Plant Cell, 2015. **27**(1): p. 214-227.
505. Wang, Y., et al., *Cytokinin antagonizes ABA suppression to seed germination of Arabidopsis by downregulating ABI5 expression.* The Plant Journal, 2011. **68**(2): p. 249-261.
506. Wu, Q., et al., *Ubiquitin ligases RGLG1 and RGLG5 regulate abscisic acid signaling by controlling the turnover of phosphatase PP2CA.* The Plant Cell, 2016. **28**(9): p. 2178-2196.
507. Zhao, Z., et al., *A role for a dioxygenase in auxin metabolism and reproductive development in rice.* Developmental Cell, 2013. **27**(1): p. 113-122.
508. Mudgil, Y., et al., *Arabidopsis N-MYC DOWNREGULATED-LIKE1, a positive regulator of auxin transport in a G protein–mediated pathway.* The Plant Cell, 2009. **21**(11): p. 3591-3609.
509. Thomas, S.G., A.L. Phillips, and P. Hedden, *Molecular cloning and functional expression of gibberellin 2-oxidases, multifunctional enzymes involved in gibberellin deactivation.* Proceedings of the National Academy of Sciences, 1999. **96**(8): p. 4698-4703.
510. Naranjo, M.A., et al., *Overexpression of Arabidopsis thaliana LTL1, a salt-induced gene encoding a GDSL-motif lipase, increases salt tolerance in yeast and transgenic plants.* Plant, cell environment, 2006. **29**(10): p. 1890-1900.
511. Toda, Y., et al., *RICE SALT SENSITIVE3 forms a ternary complex with JAZ and class-C bHLH factors and regulates jasmonate-induced gene expression and root cell elongation.* The Plant Cell, 2013. **25**(5): p. 1709-1725.
512. Rosado, A., et al., *The Arabidopsis tetratricopeptide repeat-containing protein TTL1 is required for osmotic stress responses and abscisic acid sensitivity.* Plant Physiology, 2006. **142**(3): p. 1113-1126.
513. Gustavsson, N., et al., *A peptide methionine sulfoxide reductase highly expressed in photosynthetic tissue in Arabidopsis thaliana can protect the chaperone-like activity of a chloroplast-localized small heat shock protein.* The Plant Journal, 2002. **29**(5): p. 545-553.
514. Epple, P., et al., *Antagonistic control of oxidative stress-induced cell death in Arabidopsis by two related, plant-specific zinc finger proteins.* Proceedings of the National Academy of Sciences, 2003. **100**(11): p. 6831-6836.
515. Reuscher, S., et al., *The sugar transporter inventory of tomato: genome-wide identification and expression analysis.* Plant Cell Physiology, 2014. **55**(6): p. 1123-1141.
516. Chen, L.Q., *SWEET sugar transporters for phloem transport and pathogen nutrition.* New Phytologist, 2014. **201**(4): p. 1150-1155.
517. Rentsch, D., et al., *Salt stress-induced proline transporters and salt stress-repressed broad specificity amino acid permeases identified by suppression of a yeast amino acid permease-targeting mutant.* The Plant Cell, 1996. **8**(8): p. 1437-1446.

518. Hou, C., et al., *DUF221 proteins are a family of osmosensitive calcium-permeable cation channels conserved across eukaryotes.* Cell research, 2014. **24**(5): p. 632-635.
519. Kim, E.J., et al., *AtKUP1: an Arabidopsis gene encoding high-affinity potassium transport activity.* The Plant Cell, 1998. **10**(1): p. 51-62.
520. Takahashi, H., et al., *The roles of three functional sulphate transporters involved in uptake and translocation of sulphate in Arabidopsis thaliana.* The Plant Journal, 2000. **23**(2): p. 171-182.
521. Shin, L.-J., J.-C. Lo, and K.-C. Yeh, *Copper chaperone antioxidant protein1 is essential for copper homeostasis.* Plant Physiology, 2012. **159**(3): p. 1099-1110.
522. de Abreu-Neto, J.B., et al., *Heavy metal-associated isoprenylated plant protein (HIPP): characterization of a family of proteins exclusive to plants.* The FEBS journal, 2013. **280**(7): p. 1604-1616.
523. Bai, M.-Y., et al., *A triple helix-loop-helix/basic helix-loop-helix cascade controls cell elongation downstream of multiple hormonal and environmental signaling pathways in Arabidopsis.* The Plant Cell, 2012. **24**(12): p. 4917-4929.
524. Lee, S., et al., *Overexpression of PRE1 and its homologous genes activates Gibberellin-dependent responses in Arabidopsis thaliana.* Plant cell physiology, 2006. **47**(5): p. 591-600.
525. Ikeda, M., et al., *A triantagonistic basic helix-loop-helix system regulates cell elongation in Arabidopsis.* The Plant Cell, 2012. **24**(11): p. 4483-4497.
526. Miura, K., et al., *SIZ1-mediated sumoylation of ICE1 controls CBF3/DREB1A expression and freezing tolerance in Arabidopsis.* he Plant Cell, 2007. **19**(4): p. 1403-1414.
527. MacAlister, C.A., K. Ohashi-Ito, and D. Bergmann, *Transcription factor control of asymmetric cell divisions that establish the stomatal lineage.* Nature, 2007. **445**(7127): p. 537-540.
528. Eckardt, N.A., *The role of flavonoids in root nodule development and auxin transport in Medicago truncatula*. 2006, Am Soc Plant Biol.
529. Nagata, M. and A.J.T.O. Suzuki, *Effects of phytohormones on nodulation and nitrogen fixation in leguminous plants.* 2014: p. 111-128.
530. Hermansen, R.A., et al., *Characterizing selective pressures on the pathway for de novo biosynthesis of pyrimidines in yeast.* BMC evolutionary biology, 2015. **15**(1): p. 232.
531. Rolfes, R.J., *Regulation of purine nucleotide biosynthesis: in yeast and beyond.* Biochemical Society Transactions, 2006. **34**(5): p. 786-790.
532. Irby, R.B. and W.L. Adair, *Intermediates in the folic acid biosynthetic pathway are incorporated into molybdopterin the yeast, Pichia canadensis.* Journal of Biological Chemistry, 1994. **269**(39): p. 23981-23987.
533. Almeida, B., et al., *NO-mediated apoptosis in yeast.* Journal of cell science, 2007. **120**(18): p. 3279-3288.
534. Koc, A., et al., *Methionine sulfoxide reductase regulation of yeast lifespan reveals reactive oxygen species-dependent and-independent components of aging.* Proceedings of the National Academy of Sciences, 2004. **101**(21): p. 7999-8004.
535. González-Gallego, J., et al., *Anti-inflammatory and immunomodulatory properties of dietary flavonoids*, in *Polyphenols in human health and disease*. 2014, Elsevier. p. 435-452.
536. Caridi, A., *Effect of protectants on the fermentation performance of wine yeasts subjected to osmotic stress.* Food Technology and Biotechnology, 2003. **41**(2): p. 145-148.
537. Macreadie, I.G., N. Bartone, and L. Sparrow, *Inhibition of respiratory growth and survival in yeast by dopamine and counteraction with ascorbate or glutathione.* Journal of biomolecular screening, 2010. **15**(3): p. 297-301.
538. Zhao, Q., et al., *N-3-oxo-hexanoyl-homoserine lactone, a bacterial quorum sensing signal, enhances salt tolerance in Arabidopsis and wheat.* Botanical studies, 2020. **61**(1): p. 1-12.
539. Lin, R.-C., H.-J. Park, and H.-Y. Wang, *Role of Arabidopsis RAP2. 4 in regulating light-and ethylene-mediated developmental processes and drought stress tolerance.* Molecular plant, 2008. **1**(1): p. 42-57.

540. Rodrigues, A., et al., *ABI1 and PP2CA phosphatases are negative regulators of Snf1-related protein kinase1 signaling in Arabidopsis.* The Plant Cell, 2013. **25**(10): p. 3871-3884.
541. Dubois, M., et al., *ETHYLENE RESPONSE FACTOR6 acts as a central regulator of leaf growth under water-limiting conditions in Arabidopsis.* Plant physiology, 2013. **162**(1): p. 319-332.
542. Tognetti, V.B., et al., *Perturbation of indole-3-butyric acid homeostasis by the UDP-glucosyltransferase UGT74E2 modulates Arabidopsis architecture and water stress tolerance.* The Plant Cell, 2010. **22**(8): p. 2660-2679.

10. RESEARCH OUTPUT

PUBLICATIONS:

- ✓ **Srivastava R.** and Sahoo L., (2021), Cowpea NAC transcription factors positively regulate cellular stress response and balance energy metabolism in yeast *via* reprogramming of biosynthetic pathways**.** ***ACS Synthetic Biology,*** 10, 2286-2307
- ✓ **Srivastava R.** and Sahoo L., (2021), Genome-wide analysis of NAC transcription factor family to elucidate genetic & molecular relationships unraveling their role in stress and growth in Cowpea. ***Genomics*** (Under Review)
- ✓ **Srivastava R.**, Kobayashi Y., Koyama H., and Sahoo L., (2021), Ectopic expression of ATAF-like Cowpea NAC transcription factors confer drought tolerance of Arabidopsis without growth penalty**.** ***Plant Cell Reports*** (Under Review)
- ✓ **Srivastava R.**, Kobayashi Y., Koyama H., and Sahoo L., (2021), Overexpression of VuNAC1/2 transcription factors improved yield and tolerance to multiple abiotic stresses in cowpea by regulating chloroplast genes. ***Journal of Integrative Plant Biology*** (Under Review)
- ✓ **Srivastava R.**, Sahoo, L., (2021), Balancing yield trade-off in legumes during multiple stress tolerance via strategic crosstalk by native NAC transcription factors. ***Journal of Plant Biochemistry and Biotechnology*** (Under Review)
- ✓ **Srivastava R.,** Kumar S., Kobayashi Y., Kusunoki K., Tripathi P., Kobayashi Y., Koyama H., and Sahoo L. (2018), Comparative genome-wide analysis of WRKY transcription factors in two Asian legume crops: Adzuki bean and Mung bean. ***Scientific Reports***, 8, 16971
- ✓ Kumar S., Kalita A., **Srivastava R.**, and Sahoo L., (2017), Co-expression of Arabidopsis NHX1 and bar improves the tolerance to salinity, oxidative stress, and herbicide in transgenic Mungbean. ***Frontier in Plant Sciences***, 8, 1896
- ✓ Sharma P. K., Saharia M., **Srivastava R**., Kumar S., and Sahoo L. (2018), Tailoring microalgae for efficient biofuel production. ***Frontiers in Marine Science***, *5*, 382

CONFERENCES, SEMINARS, AND WORKSHOPS:

- ✓ S**rivastava, R.**, J, Muthuvel J., Kumar, S., Sahoo, L. (2016), Overexpression of Arabidopsis PYL9 in Indian mustard enhances drought and salinity tolerance by modulating ABA signaling, At National Seminar on "***Plant Genomics and Biotechnology*: *Challenges and Opportunities in 21st Century****"*, (pp 54), OUAT, Bhubaneswar
- ✓ **Srivastava, R.** (2017), Seminar on *"Research activity and Convention on Biological Diversity and its Protocols"*, UGSAS, Gifu University, Japan
- ✓ **Srivastava, R.** (2017), Seminar on *"Special Lecture on Agriculture II"*, At UGSAS, Gifu University, Japan
- ✓ **Srivastava, R.**, Kalita, A., Kumar, S., Sahoo, L. (2017), Manipulation of vacuolar sequestration of Na^+ and salt- responsive NAC transcription factor for salt tolerance, At National Symposium on *"Pulses for Nutritional Security and Agricultural Sustainability"*, (pp 87), IIPR, Kanpur
- ✓ **Srivastava, R.** (2018), Hands On Workshop on *'Gene Expression and Functional Analysis for Crop Improvement"*, IIT Guwahati
- ✓ **Srivastava, R.**, Koyama A., S., Sahoo, L. (2018), Exploring novel NAC mediated mechanisms integrating multiple abiotic stress tolerance and aluminum toxicity in legume crops, At *International Plant Physiology Congress*, (pp 109), NBRI, Lucknow
- ✓ **Srivastava, R.**, Koyama A., S., Sahoo, L. (2019), Exploring novel NAC transcription factor mediated mechanism regulating abiotic stresses in Cowpea, At *International Plant Physiology Congress*, (pp 208), IIT Guwahati
- ✓ **Srivastava, R.** (2019), Indo-US flow Cytometry Workshop on application on "*Applications of flow cytometry in Biotechnology*", IIT Guwahati
- ✓ **Srivastava, R.** (2019), Exploring novel NAC-mediated signaling in Cowpea in response to multiple abiotic stress , At National Workshop on *"Frontiers in Plant Biology*", IIT Guwahati
- ✓ **Srivastava, R.** (2019), International GIAN Lecture Series on "*RNA interference & epigenetic regulation of gene expression in plants"*, IIT Guwahati